



Status of liquid metal cooled fast reactor technology



INTERNATIONAL ATOMIC ENERGY AGENCY

IAEA

30 - 22

D

April 1999

The originating Section of this publication in the IAEA was
Nuclear Power Technology Development Section
International Atomic Energy Agency
Wagramer Strasse 5
P O Box 100
A-1400 Vienna, Austria

The IAEA does not normally maintain stocks of reports in this series
However, copies of these reports on microfiche or in electronic form can be obtained from

INIS Clearinghouse
International Atomic Energy Agency
Wagramer Strasse 5
PO Box 100
A-1400 Vienna, Austria
E-mail: CHOUSE@IAEA.ORG
URL <http://www.iaea.org/programmes/inis/inis.htm>

Orders should be accompanied by prepayment of Austrian Schillings 100,—
in the form of a cheque or in the form of IAEA microfiche service coupons
which may be ordered separately from the INIS Clearinghouse

STATUS OF LIQUID METAL COOLED FAST REACTOR TECHNOLOGY
IAEA, VIENNA, 1999
IAEA-TECDOC-1083
ISSN 1011-4289

© IAEA, 1999
Printed by the IAEA in Austria
April 1999

FOREWORD

In 1985 the International Atomic Energy Agency published a report entitled "Status of Liquid Metal Cooled Fast Breeder Reactors" (Technical Reports Series No. 246). It was a general review of the status of fast reactor development at that time, covering some aspects of design and operation and reviewing experience from the earliest days. It summarized the programmes and plans in all countries which were pursuing the development of fast reactors.

During the period 1985–1998, there have been substantial advances in fast reactor technology development. Chief among these has been the demonstration of reliable operation by several prototypes and experimental reactors, the reliable operation of fuel at a high burnup (BN-600, BN-350, Phenix, PFR BOR-60, FFTF). Some additional countries, such as China, India and the Republic of Korea have launched new fast reactor programmes. At the IAEA meetings on liquid metal cooled fast reactor (LMFR) technology, it became evident that there have been significant technological advances as well as changes in the economic and regulatory environment since 1985. Therefore, the International Working Group on Fast Reactors (IWGFR) has recommended the preparation of a new status report on fast reactor technology.

The present status report intends to provide comprehensive and detailed information on LMFR technology. The focus is on practical issues that are useful to engineers, scientists, managers, university students and professors, on the following topics: experience in construction and operation, reactor physics and safety, core structural material and fuel technology, fast reactor engineering and activities in progress on LMFR plants.

This report has been prepared with contributions from China, France, Germany, India, Japan, the Russian Federation, the United Kingdom and the United States of America. The responsible IAEA officer was A. Rinejski of the Division of Nuclear Power.

The IAEA expresses its appreciation to all those who have participated in the preparation of this reference compilation and also to the Member States that have made available experts to assist and participate in this work.

EDITORIAL NOTE

In preparing this publication for press, staff of the IAEA have made up the pages from the original manuscript(s). The views expressed do not necessarily reflect those of the IAEA, the governments of the nominating Member States or the nominating organizations.

Throughout the text names of Member States are retained as they were when the text was compiled.

The use of particular designations of countries or territories does not imply any judgement by the publisher, the IAEA, as to the legal status of such countries or territories, of their authorities and institutions or of the delimitation of their boundaries.

The mention of names of specific companies or products (whether or not indicated as registered) does not imply any intention to infringe proprietary rights, nor should it be construed as an endorsement or recommendation on the part of the IAEA.

CONTENTS

CHAPTER 1.	BACKGROUND AND OVERVIEW	1
1.1.	Progress within the period 1985–1998	1
1.1.1.	Demonstration reactor operation	1
1.1.2.	Prototype reactor operation	1
1.1.3.	Technical achievements	2
1.1.4.	Design advances	3
1.2.	Contents of this report	4
CHAPTER 2.	OPERATION EXPERIENCE WITH PROTOTYPE AND DEMONSTRATION LMFRs	5
2.1.	BN-350 operating experience	5
2.1.1.	Design features	5
2.1.2.	Operating experience	7
2.1.3.	Safety enhancement and equipment life extension	21
2.1.4.	Review of experimental programme	22
2.2.	Phenix operating experience	23
2.2.1.	Design features	23
2.2.2.	Operating experience	25
2.2.3.	Statutory inspection - Spring 1989	26
2.2.4.	Inspections and maintenance during the test period (1991–1993)	28
2.2.5.	Negative reactivity shutdown	29
2.2.6.	Plant statistics	29
2.2.7.	Radiological safety	30
2.3.	PFR operational experience	30
2.3.1.	Design features	30
2.3.2.	Review of operating history	34
2.3.3.	Advanced technology developments	52
2.3.4.	PFR safety and licensing	53
2.3.5.	PFR and the fuel cycle	55
2.3.6.	The future	58
2.3.7.	PFR in perspective	58
2.4.	Super Phenix 1 operating experience	59
2.4.1.	Design features	59
2.4.2.	Operating experience	62
2.4.3.	The present situation	71
2.5.	BN-600 operation experience	72
2.5.1.	Design features	72
2.5.2.	Operating experience	78
2.5.3.	Radiological safety	87
2.5.4.	Fire safety, sodium leaks	88
2.5.5.	BN-600 operating safety enhancement	89
2.5.6.	Experimental programmes	91
	Bibliography	92
CHAPTER 3.	EXPERIENCE IN CONSTRUCTION AND PRE-OPERATIONAL TESTING OF THE PROTOTYPE LMFRs	95
3.1.	Construction and pre-operational testing of the LMFR SNR-300	95
3.1.1.	Introduction	95
3.1.2.	Description	95
3.1.3.	Construction and pre-operational testing	99
3.1.4.	Unexpected occurrences and their remedy	106
3.1.5.	Achievements	109
3.1.6.	Epilogue	115
3.2.	Construction and pre-operational testing of the prototype LMFR “Monju”	117
3.2.1.	Overview of project	117
3.2.2.	Research and development	118

3.2.3. Design and construction of monju	120
3.2.4. Pre-operational tests.....	128
References	133
 CHAPTER 4. LMFR PHYSICS	 135
4.1. Production of nuclear data for reactor neutronics calculations	137
4.1.1. Measurement and the use of nuclear theory	137
4.1.2. Analysis.....	138
4.1.3. Compilation.....	138
4.1.4. Evaluation	138
4.1.5. Nuclear data uncertainty information	139
4.1.6. Integral measurements	140
4.1.7. Fission spectrum average.....	140
4.1.8. Dosimetry cross-sections	140
4.1.9. Nuclear data processing codes and group cross section data sets	141
4.1.10. Validation.....	143
4.1.11. Uncertainties in reactor parameters caused by nuclear data uncertainties	143
4.2. Energy production, radiation emission, induced radioactivity and irradiation damage	144
4.2.1. Heating.....	145
4.2.2. The radioactivity of irradiated fuel	147
4.2.3. Activation of structural and coolant materials	147
4.2.4. Irradiation damage effects and dosimetry.....	148
4.3. Neutronics calculation methods.....	149
4.3.1. Forms of heterogeneity	150
4.3.2. Methods for treating heterogeneity.....	151
4.3.3. Control rod homogenisation	152
4.3.4. Derivation of broad group cross-sections	152
4.3.5. Whole reactor calculation methods	152
4.3.6. The sub-group treatment of resonance shielding.....	153
4.3.7. Perturbation theory methods.....	155
4.3.8. Methods of adjustment of cross-sections to fit integral measurements	155
4.3.9. Kinetics calculations	156
4.4. Computer codes used in fast reactor neutronics	157
4.4.1. Codes based on diffusion theory.....	157
4.4.2. Transport theory and codes.....	158
4.4.3. Codes based on the Monte Carlo method.....	159
4.4.4. Application of code systems to fast reactor calculations	161
4.5. Validation of methods and data	164
4.5.1. Effective multiplication of a core at start-up	165
4.5.2. Variation of reactivity with burn-up	166
4.5.3. Incineration of fission products	166
4.5.4. Power distributions	167
4.5.5. Control rod reactivity worths	168
4.6. Reactivity coefficients.....	169
4.6.1. Doppler effects.....	170
4.6.2. Sodium voiding and sodium density coefficients	173
4.7. Shielding studies	174
References	175
Bibliography.....	180
 CHAPTER 5. LMFR SAFETY: NEW TRENDS AND FINDINGS.....	 185
5.1. New trends in safety principles and goals.....	185
5.1.1. LMFRs and main recent nuclear safety trends	185
5.1.2. Safety fundamentals	185
5.1.3. Risk minimization and accident analysis approaches consequences for LMFRs	186
5.1.4. Local subassembly faults	194
5.1.5. Sodium fires	200
5.2. Emergency heat removal by natural and forced convection.....	205
5.2.1. Safety objectives of emergency heat removal systems (EHRS).....	205

5.2.2.	Main design concepts.....	205
5.2.3.	Status of international R&D activities and future needs.....	219
5.2.4.	General conclusions.....	220
	References.....	221
CHAPTER 6. SOME ASPECTS OF INSTRUMENTATION AND INSPECTION OF MAIN LMFR COMPONENTS		225
6.1.	Steam generator: designs, instrumentation and protection	225
6.1.1.	Configuration	225
6.1.2.	Construction.....	232
6.1.3.	Design details.....	235
6.1.4.	Protection	237
6.1.5.	Sodium-water reactions in steam generators.....	239
6.2.	Reactor core with other components: acoustic instrumentation	249
6.2.1.	Detection of boiling	249
6.2.2.	Plant monitoring.....	252
6.3.	Ultrasonic instrumentation.....	255
6.3.1.	Ultrasonic imaging.....	256
6.3.2.	Ultrasonic monitoring.....	256
6.3.3.	Ultrasonic measurement of temperature.....	259
6.3.4.	Ultrasonic systems	259
6.4.	In-service inspection and repair	259
6.4.1.	Background	262
6.4.2.	Operational in-service inspection components.....	262
6.4.3.	Research and development in France	264
	References	270
CHAPTER 7. CORE STRUCTURAL MATERIAL AND FUEL TECHNOLOGY FOR HIGH BURN-UP		273
7.1.	Introduction.....	273
7.2.	Behaviour of materials for fuel pin cladding and subassembly duct (wrapper).....	273
7.2.1.	Pin cladding materials.....	273
7.2.2.	Wrapper-tube (duct) materials.....	279
7.3.	Irradiation performance of oxide fuel elements.....	280
7.3.1.	Fuel and fission product behaviour.....	283
7.3.2.	Mechanical interaction between fuel and cladding (FCMI).....	286
7.3.3.	Chemical interaction between fuel and cladding (FCCI)	286
7.3.4.	Behaviour under off-normal conditions.....	288
7.3.5.	Failed pin behaviour	290
7.3.6.	Modelling of oxide fuel performances	291
7.3.7.	Achievable burn-up.....	291
7.4.	Irradiation performance of metallic fuel elements.....	292
7.5.	Irradiation performance of advanced fuel elements	294
7.5.1.	Carbide fuel elements.....	295
7.5.2.	Nitride fuel elements.....	299
7.5.3.	Fuel for high plutonium burning.....	300
7.6.	Irradiation performance of absorber elements.....	307
	References	313
CHAPTER 8. LMFR ENGINEERING.....		317
8.1.	Sodium pumps.....	317
8.1.1.	Design basis	317
8.1.2.	Sodium pump design features.....	319
8.1.3.	Pump testing techniques.....	336
8.1.4.	Pump operating experience.....	337
8.1.5.	Cavitation in sodium pump impellers.....	340
8.1.6.	Structural improvements in new sodium pump designs	343
8.2.	Thermal-hydraulics of the primary circuit.....	351

8.2.1.	Introduction.....	351
8.2.2.	Objectives of the thermal-hydraulic studies	351
8.2.3.	Steady state studies of the hot pools of pool-type reactors.....	352
8.2.4.	Transient studies of hot pools	362
8.2.5.	Studies of the cold pool of a pool-type reactor.....	363
8.2.6.	Strongback	364
8.2.7.	Diagrid	364
8.2.8.	Gas entrainment at the free surface.....	365
8.2.9.	Cover gas thermal-hydraulics	366
8.2.10.	Thermal stripping studies.....	366
8.2.11.	Conclusions.....	369
8.3.	Decommissioning of the experimental liquid-metal fast reactor Rapsodie.....	370
8.3.1.	Introduction.....	370
8.3.2.	Main features of the installation.....	370
8.3.3.	Pre-decommissioning operations (1983–1985).....	372
8.3.4.	Decommissioning operations (1986–1994).....	373
8.3.5.	Conclusions	378
	References	381
CHAPTER 9. ACTIVITIES IN PROGRESS ON LMFR PLANTS.....		385
9.1.	European fast reactor	385
9.1.1.	Introduction.....	385
9.1.2.	Organizational structure of the European fast reactor cooperation	385
9.1.3.	EFR programme status.....	386
9.1.4.	Main design features	388
9.1.5.	R&D support of the design	406
9.1.6.	Concept validation phase achievements	408
9.1.7.	The success of the EFR project	415
9.2.	BN-1600M	415
9.2.1.	Stages of development and design concept evolution	415
9.2.2.	Basic parameters and design optimization	416
9.2.3.	Reactor unit design.....	420
9.2.4.	Reactor plant safety.....	429
9.3.	BN-800 reactor plant.....	431
9.3.1.	Design status	431
9.3.2.	Reactor design basis.....	431
9.3.3.	Reactor design concept	431
9.3.4.	Main design improvements and reactor plant features.....	433
9.4.	BN-600M advanced LMFR.....	445
9.4.1.	Design status	445
9.4.2.	Design basis	449
9.4.3.	Reactor design concept and main data.....	449
9.4.4.	Safety features.....	451
9.4.5.	Improvement of economic performance.....	452
9.5.	The demonstration fast breeder reactor	453
9.5.1.	Introduction.....	453
9.5.2.	DFBR plant design.....	453
9.5.3.	Technical and economic evaluation.....	463
9.5.4.	Prospects for FBR commercialization.....	468
9.5.5.	Conclusion	469
9.6.	Prototype fast breeder reactor-design description	469
9.6.1.	Introduction.....	469
9.6.2.	Reactor assembly	469
9.6.3.	Primary sodium system	475
9.6.4.	Secondary sodium systems	476
9.6.5.	Fuel handling.....	476
9.6.6.	Decay heat removal.....	476
9.6.7.	Materials.....	476
9.6.8.	Instrumentation and control	478
9.6.9.	Fire protection.....	478

9.6.10. Containment	479
9.6.11. Emergency control room	479
9.6.12. Balance of plant (BOP).....	479
9.6.13. Present status.....	479
9.7. ALMR technology development.....	479
9.7.1. Introduction.....	479
9.7.2. ALMR plant design.....	484
9.7.3. Integral fast reactor concept development.....	501
9.8. BMN-170 modular fast nuclear reactor.....	510
9.8.1. Design goals and status.....	510
9.8.2. Design basis	512
9.8.3. Reactor safety features	515
9.8.4. Radiological safety.....	517
9.8.5. Economics.....	517
9.9. Experimental fast reactor CEFR-25.....	518
9.9.1. Introduction.....	518
9.9.2. History and achievements	518
9.9.3. Trends of experimental reactors	522
9.9.4. CEFR-25 design.....	522
9.9.5. Site work	528
9.9.6. Nuclear licensing system in China.....	529
9.9.7. Safety features	529
Bibliography.....	531
CHAPTER 10. SUMMARY AND FUTURE TRENDS.....	533
10.1. Introduction.....	533
10.2. Technology trends.....	533
10.2.1. Fast reactors as burners of plutonium.....	533
10.2.2. Fast reactors as incinerators of nuclear waste.....	536
10.2.3. Design styles	538
10.2.4. Safety.....	539
10.3. The programme	540
10.4. Conclusion.....	541
Contributors to drafting and review.....	543

Chapter 1

BACKGROUND AND OVERVIEW

1.1. PROGRESS WITHIN THE PERIOD 1985 - 1998

1.1.1. Demonstration reactor operation

The outstanding success of the decade has undoubtedly been the reliable operation of the BN-600 plant at Belojarsk in Russia. It has been in operation since 1980, and has an overall lifetime load factor of 72 %. In 1992 it achieved a load factor of 83.5 %. The success was achieved in spite of a number of incidents including sodium fires. The effectiveness of the protective and remedial measures clearly demonstrates that a sodium-cooled fast reactor is capable of sustained reliable contribution to an electricity supply system.

In France the Super Phenix plant at Creys-Malville was successfully commissioned and operated, but not without difficulty. Three incidents marked the commissioning procedure and caused lengthy delays. In 1987 there was a sodium leak from the used fuel storage drum, in 1990 there was an air leak into an auxiliary circuit which caused extensive pollution of the primary sodium, and also in 1990 an exceptional snow fall caused the collapse of the roof of the turbine hall with extensive damage to the steam plant. Partly as a result of this experience the safety of the plant was thoroughly reviewed and modifications to improve the response to secondary sodium fires were made. A public enquiry on renewal of the operating license was held and reported positively, and in 1994 the plant was ready for restart. This was further delayed by a small leak of argon from the sealing bell surrounding one of the intermediate heat exchangers. Corrective action was taken and in the latter part of 1995 and through 1996 power was gradually raised to the full-power level. Later political changes called future operation into question and in February 1998 the French Government finally confirmed to discontinue its operation.

1.1.2. Prototype reactor operation

In Germany construction of SNR-300 was completed and commissioning was successfully taken to an advanced stage. A small leak in a ferritic steel sodium dump tank was found, and there was some pollution of the primary sodium by moisture released from shielding material. Effective technical provisions to meet the extensive criticism of the safety of the plant were successfully put into place, but the project was eventually terminated for political reasons.

The earlier problems of steam leaks in the evaporators of the PFR plant in Scotland were successfully solved, but in 1987 there was a large leak in one of the superheaters. This gave rise to a major review of the protection against large sodium-water reactions. In 1991 the primary sodium was polluted by oil from one of the sodium pumps. These technical problems were overcome successfully, and in addition in 1990 an operating license (which hitherto had not been a legal necessity) was obtained from the safety authority after a review against the same criteria applied to commercial thermal reactors. When it was finally shut down in 1994 PFR was operating with good reliability.

The BN-350 plant in Kazakhstan has operated for over 20 years, and a case for future operation has been made. Means of improving the protection of the plant against the effects of

earthquakes have been identified. In 1989 there were failures in the two modular steam generators, which were repaired and returned to operation in 1993. These steam generators provide an important emergency decay heat rejection capability.

There are similarities between BN-350 and the Phenix plant in France, which is of a similar age. Phenix also has been operating for more than 20 years, and has been subject to a review of the requirements for future operation which has revealed the need to improve the ability of parts of the auxiliary systems to withstand seismic damage. There have been leaks on the secondary side of some of the intermediate heat exchangers and as a result they are all to be replaced. Inspection in the period 1991 - 1993 revealed cracks in some of the secondary circuit components made of 321 stainless steel, and repairs have been made. In 1989 and 1990 a series of fleeting negative reactivity transients were experienced, but in spite of intense investigation the cause has not been identified.

In Japan construction of the MONJU reactor was completed in 1991. Since then extensive start-up tests have been completed leading to criticality in 1994 and connection to the grid in 1995. Completion of commissioning has been delayed by a secondary sodium leak in December 1995.

1.1.3. Technical achievements

The period 1985 - 1998 has seen substantial technical advances. Chief among these has been the demonstration of reliable operation by the BN-600 plant, and the reliable operation of fuel at high burnup. In PFR large numbers of mixed-oxide fuel pins reached more than 15 % burnup without failure, and several reached 20 % burnup with an irradiation dose in excess of 130 displacements per atom (dpa) in the cladding. These results have been confirmed and surpassed by irradiations in Phenix to more than 160 dpa. The fuel cycle, based on mixed oxide fuel and PUREX reprocessing, has been closed in that plutonium from irradiated fuel has been separated, fabricated into new fuel and recycled to the reactor for further use. In the USA burnup of up to 20 % has been achieved in ternary alloy U - Pu - Zr metal fuel. The basic technology of the use of fast reactors to breed and recycle plutonium in a commercially acceptable manner has thus been demonstrated.

If a coolant loss occurs by boiling or gas intrusion, large LMFR cores show a significant reactivity increase. According to some experts, an increase of coolant temperature causes expansion of the absorber-rod guide structure, of fuel in the axial direction, and of the core grid plate in the radial direction, leading to negative reactivity coefficients that counteract a positive sodium-void coefficient in large LMFRs. Since cooling disruptions and sodium boiling may occur in a much shorter time than passive negative feedback, there was a strong incentive to reduce the positive sodium-void coefficient in large LMFRs. An IAEA/EC project assessed the capability of reducing the sodium-voiding feedback reactivity of the core by introducing a sodium plenum above the core in place of the upper axial blanket. The analysis showed that the overall void effect for the reference BN-800 MOX-fuel reactor might be close to zero. Further investigations were needed to determine differences in severe accident responses in order to estimate the improvement in overall safety that could be achieved from a reduction in the sodium-void value for a reactor core. It has been established by analyses done in various countries in the framework of the IAEA/EC 1994-1998 project that the upper sodium layer above the fissile core region instead of the upper axial blanket is quite an efficient design measure to prevent the net reactivity to approach prompt criticality in the severe reactor accidents.

An important theme of the decade has been that of protection against sodium fires. The concern started with a non-nuclear event, a fire in a solar power facility at Almeria in Spain in 1986, in which structural steelwork suffered significant damage. Partly as a result of this experience, with detailed experimental support, extensive modifications were made to the Super Phenix secondary circuit cells to improve sodium leak detection, and to mitigate the consequences and secondary damage in the event of a major sodium leak. The fire protection systems at Phenix have also been improved.

There have been significant sodium leaks and fires from the BN-600 primary (1993) and secondary (1994) circuits. In both cases the protective systems were effective, the damage was not extensive and repairs were effected quickly. Nevertheless the protective systems have been improved. A secondary sodium leak and fire at the MONJU plant in late 1995 has caused a longer operational delay, and plant modifications will be made. The finding of cracks and defects in stainless steel components of older reactors such as PFR and Phenix has contributed to the general concern to provide adequate sodium fire protection measures.

Reactor safety experience has been good and sodium-cooled fast reactors have continued to give particularly low radiation doses to operating personnel and low releases of radioactive material to the environment, even in the cases of the sodium fires mentioned above. Safety has been examined closely by the licensing authorities in some countries, in all cases with satisfactory results. Super Phenix was subjected to a major public safety review, which made a positive recommendation. PFR was licensed to modern safety standards applicable to commercial thermal reactor plants. The EFR design has been reviewed and shown to meet safety standards comparable with those of future PWRs.

Good progress with the decommissioning of the Rapsodie reactor has been made, although the success was marred by a fatal accident. Decommissioning of PFR has also been started.

1.1.4. Design advances

Major steps towards commercial reactor designs have been made. In Western Europe the European Fast Reactor (EFR) design has been completed. This synthesises the extensive experience from France, Germany and the United Kingdom of large pool-type oxide-fuelled reactors. One of the outstanding achievements of the EFR programme has been to make firm and reliable cost estimates. Although the construction of a reactor to the EFR design may not be commercially possible in the near future, but a well-validated way forward to commercial utilisation of fast reactors has been established.

Oxide fuel and sodium coolant have been chosen in several other countries. In Russia several designs for future power plants have been produced. These apply the experience from BN-350 and BN-600, together with modern safety and commercial standards, to a range of potential applications. In India the PFBR design is based on construction and commissioning experience with FBTR. The Japanese DFBR design follows a similar trend except that it utilises the loop layout of the primary circuit with separate vessels for the reactor, the primary pumps and the intermediate heat exchangers.

In the USA GE continue to follow a different line by making use of metal fuel in their ALMR design. This has good safety characteristics for many accident situations, and also allows use of the IFR integral pyrometallurgical reprocessing and waste handling technology. The

ALMR, in common with the Russian BMN-170 design, is a relatively low-power reactor which can be utilised either singly to meet small electrical loads in remote locations, or as one of several modules making up a large power station, depending on the economic circumstances.

1.2. CONTENTS OF THIS REPORT

Chapter 2 details operating experience from the world's prototype and demonstration fast reactors, BN-350 and BN-600 in the former Soviet Union, Phenix and Super Phenix in France, and PFR in the United Kingdom. Smaller test reactors such as FBTR, JOYO, BOR-60, EBR-II, FFTF and Rapsodie are not covered. Chapter 3 describes pre-operational testing of SNR-300 and MONJU. Between them these two chapters give a complete account of the decade's technical progress on fast reactors of greater than 250 MW(e) capacity.

Chapters 4 to 8 survey the areas where major technical advances have been made. Chapter 4 is an account of the neutron physics of large oxide-fuelled breeder cores, the calculation methods available for assessing the performance of these cores, and the state of validation of the methods. Chapter 5 is an account of new developments in reactor safety, with particular attention to design methods for the minimisation of risks, and to the question of the reliable removal of decay heat. Chapter 6 covers developments in instrumentation and inspection techniques, with particular reference to steam generators and to in-service inspection and repair. Ultrasonic and acoustic techniques are dealt with in some detail. Chapter 7 surveys advances in the understanding of the performance of fuel and core materials at high burnup and high radiation dose. Chapter 8 surveys some of the engineering fields in which there have been notable advances, particularly in thermal-hydraulics and the design of sodium pumps. It also covers the experience of decommissioning the Rapsodie reactor plant.

Chapters 9 and 10 look towards the future. Chapter 9 describes the substantial advances in reactor design which have been made, covering the EFR design, the Russian BN-1600M, BN-800, BN-600M and BMN-170 options, the American ALMR, the Japanese DFBR and the Indian PFBR (all of which are in the category of prototype or demonstration reactors), and concludes with an important account of the design of the smaller Chinese CEFR-25 test reactor. Finally Chapter 10 reviews the prospects for development of fast reactors in the future.

Chapter 2

OPERATION EXPERIENCE WITH PROTOTYPE AND DEMONSTRATION LMFRs

2.1. BN-350 OPERATING EXPERIENCE

2.1.1. Design features

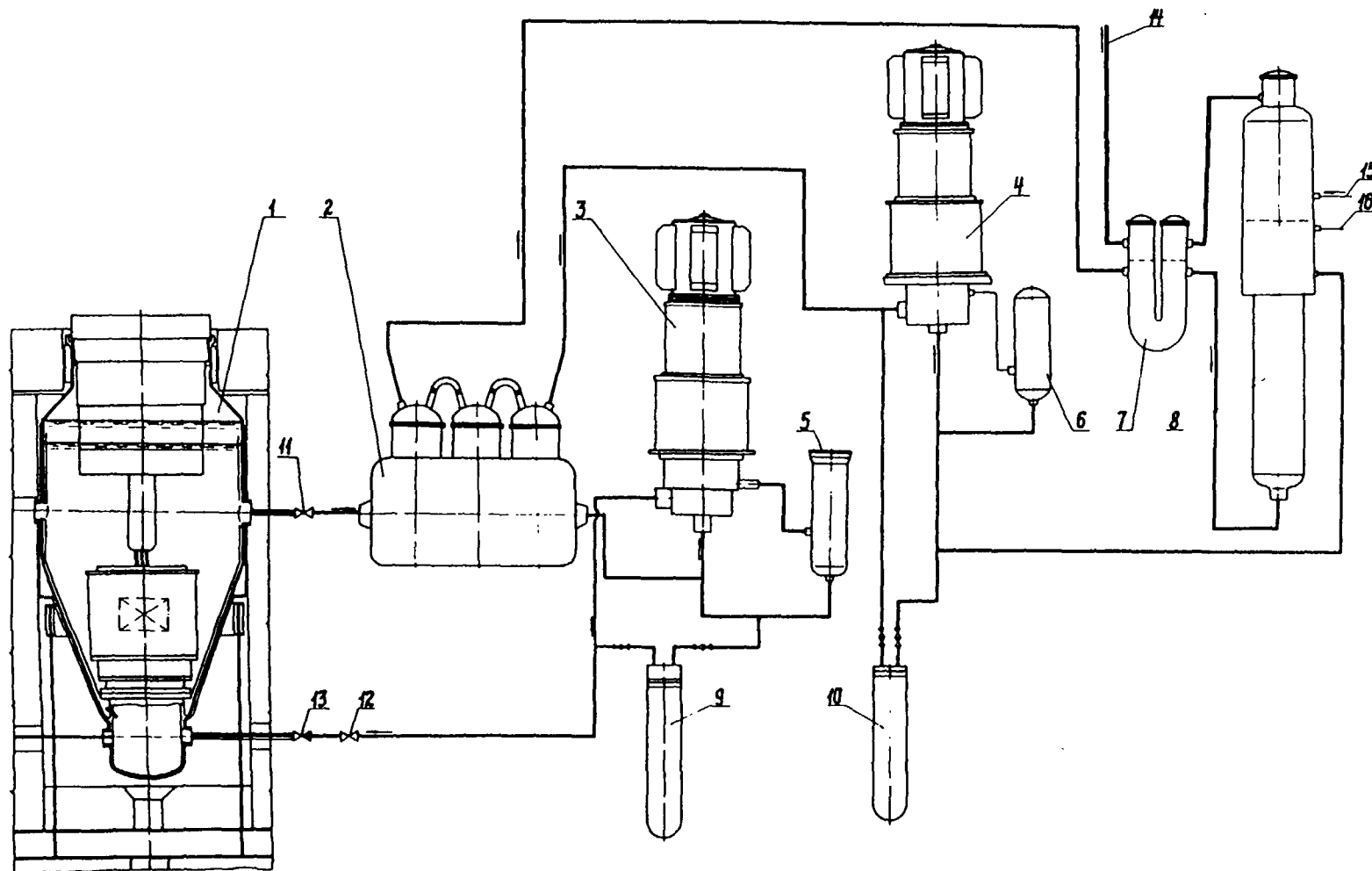
The BN-350 reactor plant is a constituent of Mangyshlak energy integrated works 10 km away from Aktau (former Shevchenko), Mangistauskaya Region of Republic of Kazakhstan on the shore of the Caspian Sea (Mangyshlak peninsula). It was designed and constructed as a two-purpose pilot-industrial power plant for electricity generation and heat production for seawater desalination. On July 16, 1993, twenty years has passed since the start of the reactor. Throughout that time BN-350 has been operated as a part of the industrial complex including the large capacity co-generation power plant and the distillate production works providing electricity and fresh water for Aktau and the adjoining industrial region, which is completely devoid of natural fresh water resources.

BN-350 has a dispersed (loop) arrangement of the primary circuit components, i.e. the primary sodium pumps, intermediate heat exchangers, and valves are disposed in separate compartments (cells) and are connected with the reactor and interconnected by pipelines. The temperature expansions of the pipelines are accommodated by the bends.

The BN-350 reactor plant includes the following main components: (1) fast sodium-cooled reactor, (2) six primary loops, (3) six intermediate (secondary) loops, (4) steam generators, (5) refuelling complex (integrated mechanical system), (6) primary and secondary sodium purification system, and (7) automated process control system, including the reactor control and protection system (CPS) and diagnostic systems for monitoring the operating state of the safety-related components and systems.

During power operation core heat removal and transport to the working medium (steam-water) are provided by a three-circuit flow scheme (Fig.2.1). The primary circuit is composed of six IHXs, six PSPs, and sodium pipelines with gate and non-return valves. The pressure chamber with the core diagrid and the upper mixing plenum above the core are the common sections of primary sodium flow path. Sodium flow is distributed from the diagrid into the core and the radial blanket fuel assemblies. A portion of the primary sodium (250t/h) is removed from the pressure chamber through throttles and utilised for cooling the reactor vessel and its outlet nozzles.

There is a capability to isolate each primary loop from the reactor using two gate valves on the suction and pressure pipelines of the circuit. On the pressure pipeline of each loop downstream of the PSP a flap-type check valve is provided eliminating coolant backflow in the event of a PSP trip in one loop when the other PSPs are operative. The secondary sodium circuits comprise: IHX heat transfer tubes, pipelines, secondary sodium pumps and steam generators. Due to utilization of the reactor energy for fresh water production the steam-water system has some specific features. Steam from the SG is supplied to turbines of two types: a condensing turbine (K-100-45) and a back-pressure turbine (K-50-45). Exhaust steam flows from the back-pressure turbine and from intermediate bleeds of K-100-45 turbine are supplied to the water desalination facilities. At a heat output of 750 MW the reactor produces ~



1 - reactor, 2 - intermediate heat exchanger, 3 - reactor coolant pump,
 4 - secondary coolant pump, 5,6 - pump leakage drain tanks, 7 - steam
 superheater, 8 - evaporator, 9,10 - filter-traps, 11 - ND 600 gate valve,
 12 - ND 500 gate valve, 13 - check valve, 14 - main steam line, 15 - feed
 water, 16 - gas system line

Fig. 2.1. BN-350 Principal Flow Diagram

100,000 t per day of desalinated water and generates ~ 135 MWe. Basic data for the BN-350 reactor plant are given in Table 2.1. for a nominal power of 750 MW.

The BN-350 reactor (Figs. 2.2, 2.3.) includes: the reactor vessel which contains the core diagrid with neutron reflector and a set of core and blanket fuel assemblies; the reactor refuelling system; the above core structure with CPS drive mechanisms and in-core instrumentation guides. The diameter of the cylindrical part of the reactor vessel is 6000 mm, and the wall thickness is 30 mm. In the middle section of the vessel there is a support belt by

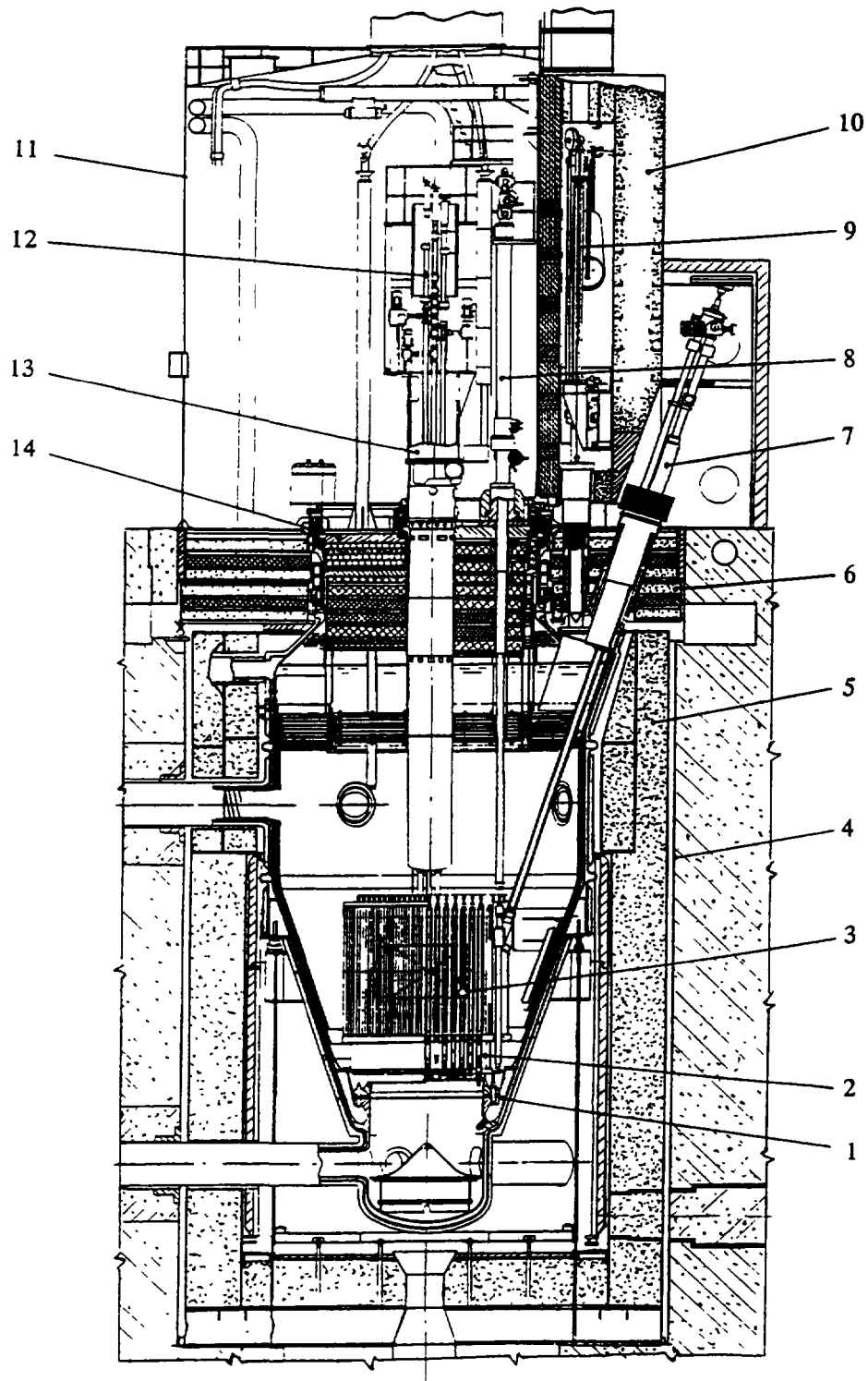
TABLE 2.1. BN-350 BASIC OPERATING PARAMETERS

Characteristics	Value
1. Reactor thermal output, MW	750
2. Primary sodium temperature, C	
- at reactor inlet	288
- at reactor outlet	437
3. Sodium flow through reactor, t/h	14,100
4. Secondary coolant temperature, C	
- at SG inlet	420
- at SG outlet	260
5. Sodium flow in secondary loop, t/h	3,400
6. Number of operating loops	5
7. Main steam parameters:	
- temperature, C	405
- pressure, MPa	4.5
8. Steam flow, t/h	1070
9. Volume of primary sodium, m ³	500
10. Maximum electric output of power unit, MW	125-150
11. Distilled water output per day, t	100,000
12. Maximum neutron flux in core, n-cm ⁻² s ⁻¹	6 10 ¹⁵
13. Design service life, year	20

which the reactor is located on 16 roller bearings arranged on a support shell of 5850 mm diameter transmitting the reactor weight load onto the foundations. The reactor vessel is enclosed in a guard vessel. The reactor unit is set in a concrete well covered by the upper stationary shield which is composed of steel shot and serpentinite concrete layers. Between the reactor and the wall of the well is a radiation shield consisting of an iron ore concentrate-filled cage. Six cells enclosing the primary circuit thermo-mechanical equipment are adjoined to the reactor well.

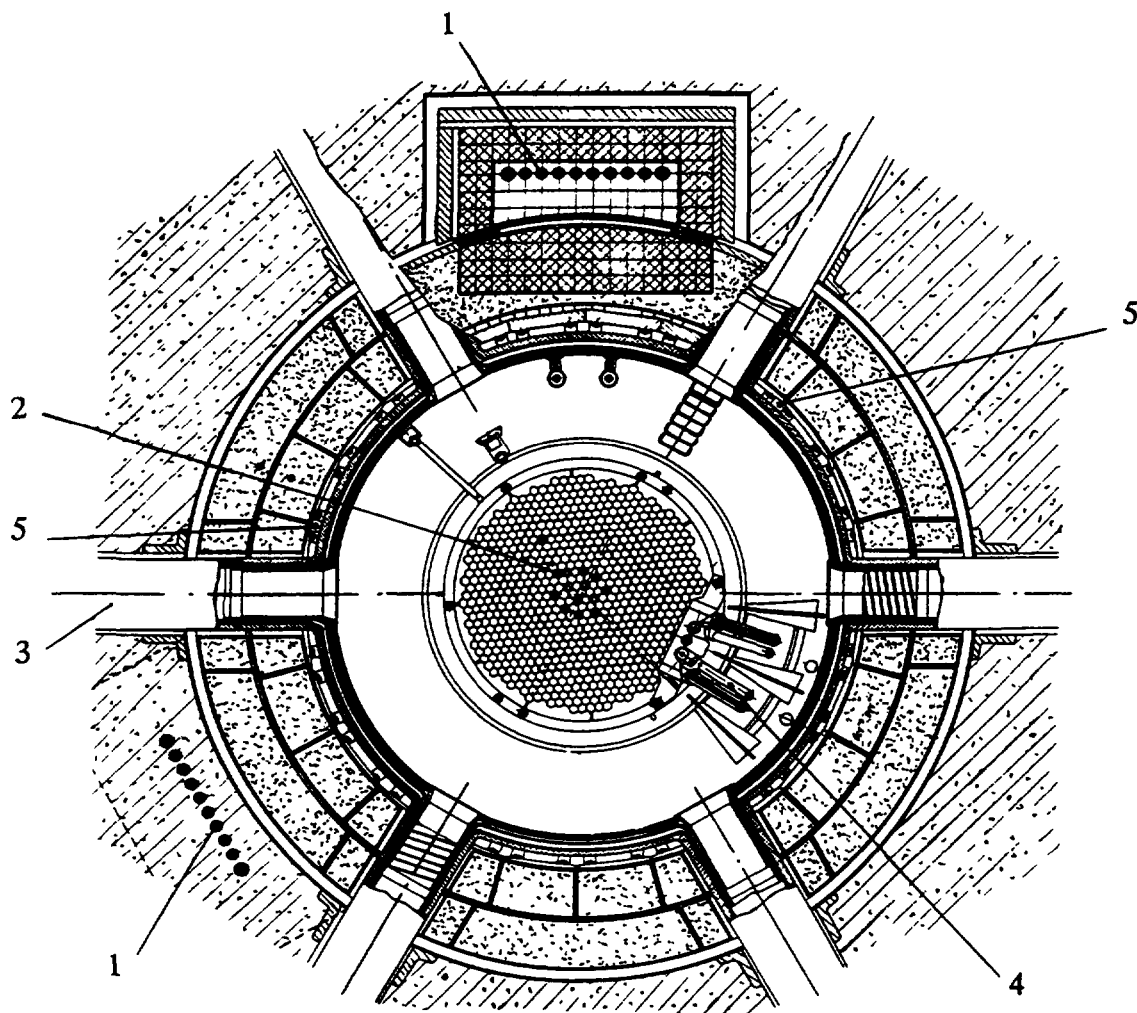
2.1.2. Operating experience

General results of operation. More than twenty year of operation of the power unit associated with the BN-350 reactor have promoted the exploration of the new industrial region of Kazakhstan which is rather rich in natural resources. The reactor first criticality date was Nov. 29, 1972, and power startup was carried out on July 16, 1973. The extended startup was explained by loss-of-integrity events in four evaporators (detected by the appearance of hydrogen in the gas plenum) when the SGs were filled with water. For that reason the power startup was carried out with three loops available at a superheated steam pressure of 3.0 MPa



1 - reactor vessel; 2 - core diagrid; 3 - reactor core; 4 - reactor well liner; 5 - lateral shield; 6 - upper-stationary shield; 7 - elevator, 8 - refuelling mechanism; 9 - FAs transfer mechanism; 10 - fuel transfer cell; 11 - protective dome; 12 - control rod drive mechanism; 13 - above core structure; 14 - rotating plugs.

Fig. 2.2. BN-350 Nuclear Reactor



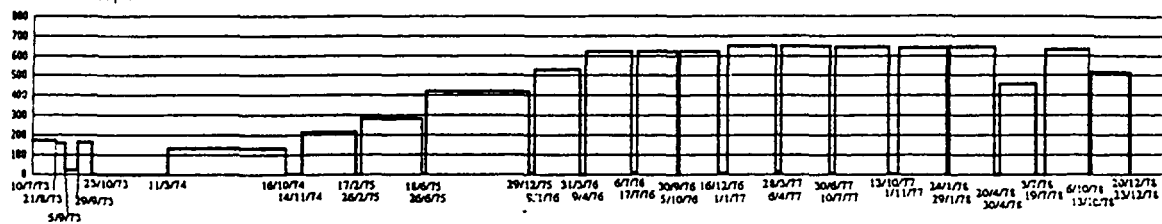
1 - set of ionization chambers; 2 - reactor core; 3 - sodium outlet pipeline; 4 - elevator; 5 - channels for additional ionization chambers.

Fig. 2.3. BN-350 Reactor Plan View (cross section)

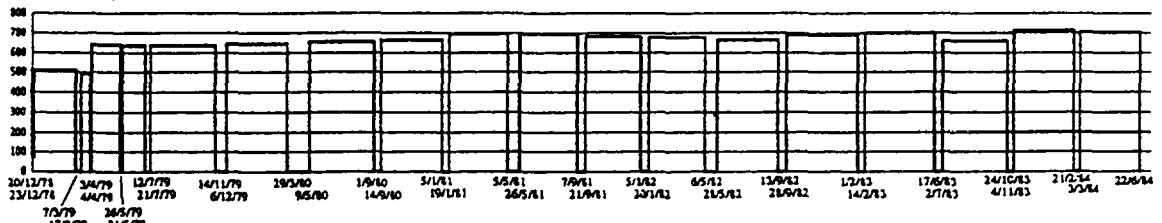
(compared with the design value of 5.0 MPa), the reactor thermal power attained being approx. 200 MW. The reactor was designed for thermal output of 1000 MW, but in the first stages of operation its power level was limited by unsatisfactory operation of the steam generators. To give of less demanding conditions for the operation of evaporators with field tubes a maximum power of 130 MW was specified for each SG. For the Czech-produced SGs "Nadjozhnost" the allowable power level was set somewhat higher - at 200 Mwe. In addition, from an experiment carried out in 1976 on plant emergency cooling with loss-of-normal power it was found that the available capacity of the steam-water system under these conditions allows normal development of the residual heat removal process at reactor power levels not higher than 750 MWth. Therefore, in further operation this power level was not exceeded, taking into account the power limitations imposed by the SGs as well.

During its operating life the reactor has operated at various power levels (Fig. 2.4). The average load factor in respect to allowed power levels was 85%. Reduction in the load factor was caused basically by outages for refuelling and planned maintenance of the equipment. The

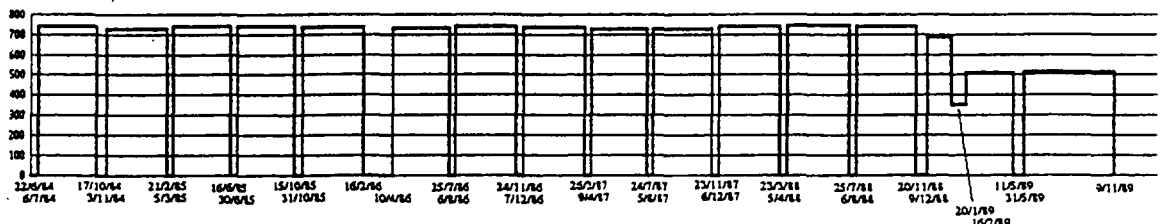
Thermal Power, MW



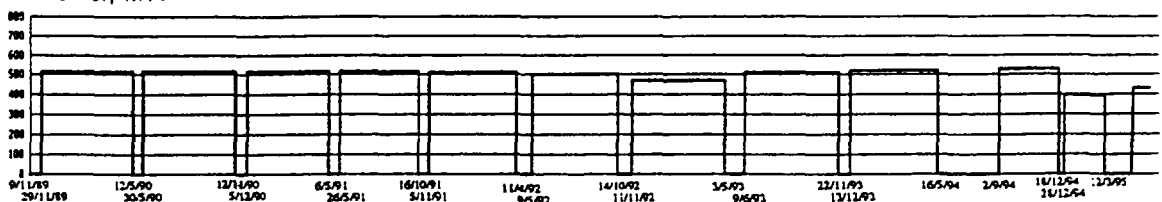
Thermal Power, MW



Thermal Power, MW



Thermal Power, MW



From Jan.1996
(to present time)

Operation at 420 MWth, 50 MWe, and producing ~ 45000 tonnes
of distilled water per day..

Fig. 2.4. BN-350 Specified Power Variation During Operation Life

reactor was shutdown for scheduled refuelling and maintenance two or three times a year (as a rule) with outage durations of 20-30 days. The main factor limiting the reactor power level were failures of the steam generators. At the same time, the reactor components and main circulating pumps have demonstrated stable fault-free operation.

In the first years of plant operation the reactor core posed certain problems due to the excessive heat rating of the fuel rods and considerable shape variation of the core structural items. Modernization of the core and changing to new structural materials allowed these problems to be solved.

The availability of stand-by components (six loops) and the ability to operate with different numbers of loops (from three to five) provided for stable operation of the reactor plant and production of electricity and fresh water. As a result, repair and replacement work on the steam generators (if necessary) were carried out without shutting down the reactor.

Simultaneously with solving the paramount economic and social problems of provision of fresh water and electric energy for the prospective industrial regions of Kazakhstan, much experience was obtained from the construction and long-term operation of the power unit and BN-350 reactor, which was valuable for the further development of sodium cooled fast reactors. Among the results obtained the following can be highlighted:

1. Construction and long-term testing in the power reactor environment of such equipment as refuelling mechanisms and the main reactor components such as coolant pumps and CPS drive mechanisms, filter-traps, etc. which were then used without changes or with minor modifications in the next fast nuclear reactors - BN-600, BN-800, BN-600M.
2. Construction and improvement of the main fast reactor core components: fuel assemblies (FAs), fuel rods, control rods and guide sleeves, which have the same dimensions as similar components of BN-600, BN-800 and BN-600M reactors.
3. Development of sodium coolant technology and associated equipment for utilization in fast power reactors, providing safe operation of sodium systems, in particular fire safety.
4. Investigation of safety-related physical and thermal-hydraulic characteristics of fast reactor cores.
5. Investigation of hydrodynamics and heat transfer in sodium circuits under various operating conditions.
6. Experience in construction and operation of heat-exchange equipment with systems for inter-circuit boundary integrity control.

BN-350 construction and operation experience became a reliable scientific and engineering basis for creation of the next fast nuclear power reactor BN-600.

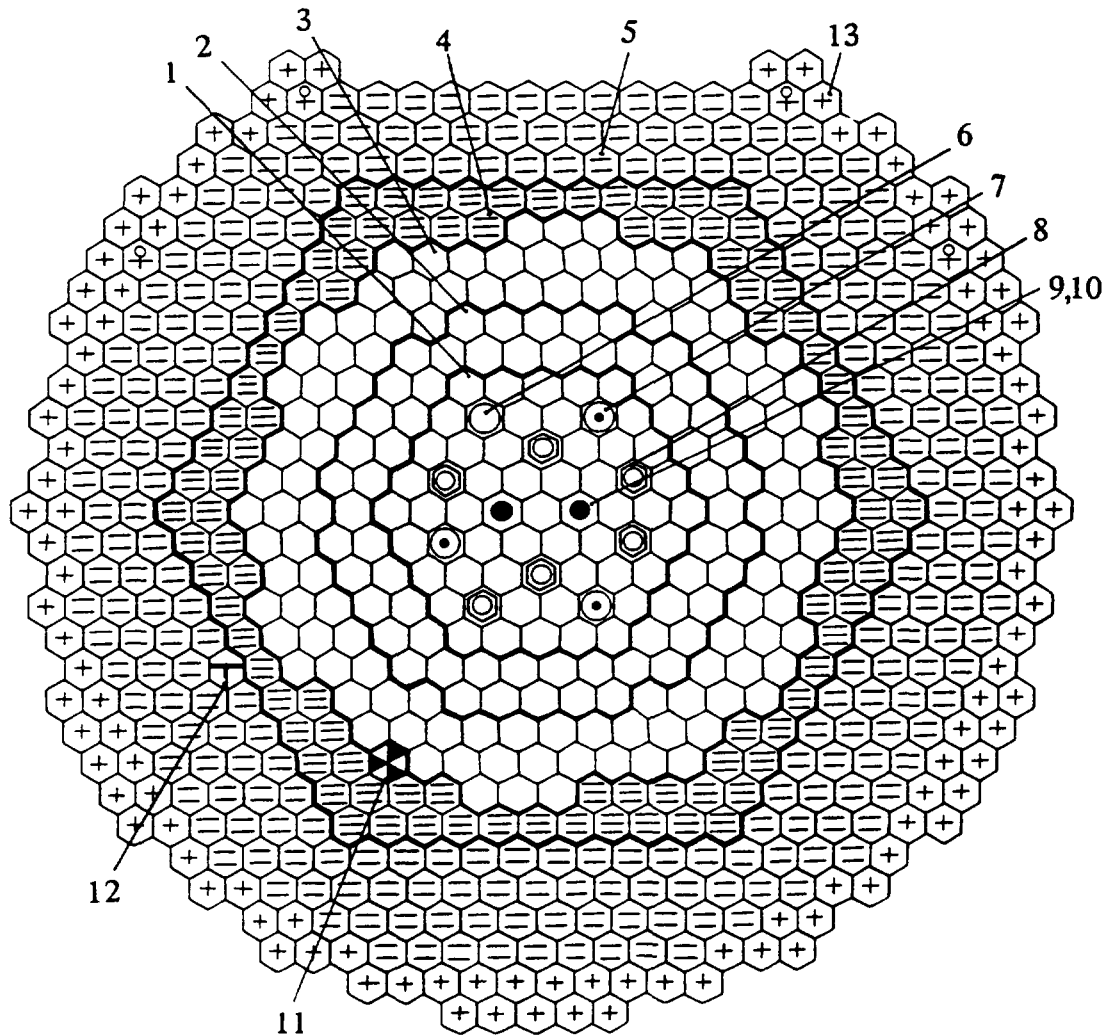
Radiological safety. Radiation doses to the BN-350 personnel have been associated mainly with repair and maintenance activities for sodium components in the primary circuit boxes. Radiation conditions in the rooms (except the reactor well) depended substantially on the state of fuel rods in the core. In the initial period of the reactor plant operation when the first type core was used numerous cladding failures caused a significant rise of fission fragment activity in the primary system. In 1979 the gamma-radiation dose rate on the surface of the sodium equipment at reactor shutdown reached $8.90 \mu\text{Sv/s}$, 80% of which was attributed to caesium nuclides. Radiological conditions were improved significantly after completion (in 1979) of the core change over to the second type fuel design. It was promoted not only by reduction in the number of failed fuel rods, but also by clean-up of caesium from the primary coolant using a special trap with a graphite absorber. Since 1984 the gamma-radiation dose rate in the primary circuit rooms during outages did not exceed of $1.5 \mu\text{Sv/s}$.

Due to the loop design of the reactor primary system the reactor well is virtually inaccessible even at outages because of high radiation-induced activity of the reactor vessel structures. Transport of gaseous fission fragments into the upper part of the CRDMs and to the oil system of the reactor coolant pumps turned out to be one of the reactor operating peculiarities which degraded radiological conditions in the reactor servicing zones.

The major source of the reactor radiological impact to the environment was gaseous discharges from the equipment air cooling system and from the reactor plant rooms through the vent stack. Resulting from the improvements in the fuel design and associated reduction in the number of failed fuel rods in the core to single events (which have become quite rare lately)

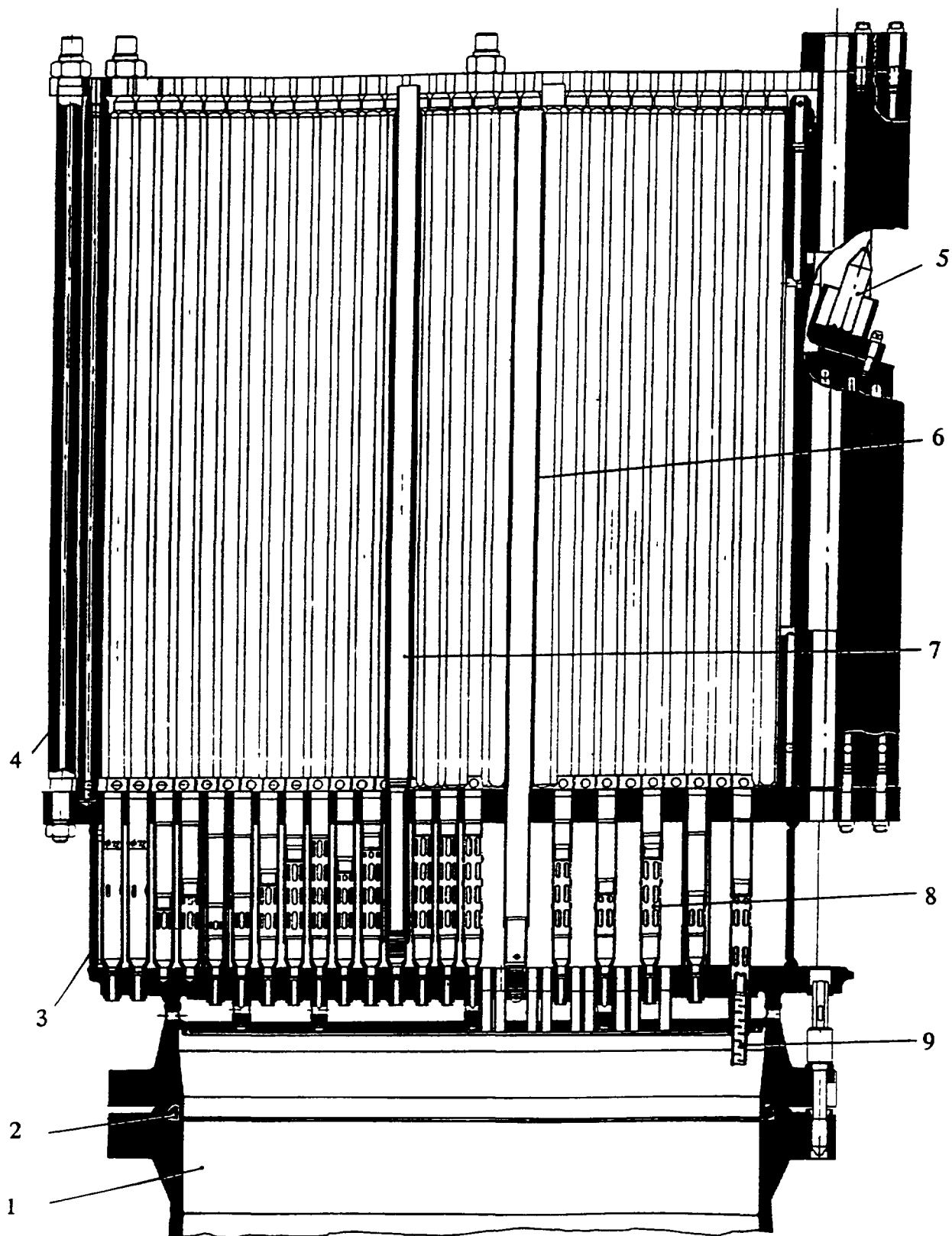
radioactivity of the plant discharges to the atmosphere determined by the radiation-induced activation of air in the reactor well cooling system. Daily release of gaseous nuclides was 0.55-0.74 TBq while that for aerosols was $1.9 \cdot 10^{-6}$ TBq. Observations over many years of radioactivity of the flora and fauna, and radiological conditions in the local populated areas and in the sanitary restricted zone around the NPP, showed that those characteristics affected by natural and man-induced radiation sources correspond to background radiation levels.

Reactor core. The central part of the reactor contains a set of core and blanket FAs, guide sleeves for CPS rods and neutron reflectors installed in the diagrid (Fig.2.5). The diagrid is attached to the sodium pressure chamber (Fig.2.6). The internal plenum of the diagrid is divided into two chambers: high and low pressure. The sodium from the high pressure chamber is distributed for cooling the core FAs, control rods and FAs of the inner blanket. From the low pressure chamber the coolant goes for cooling FAs of the outer blanket. Core FAs arranged in the internal store around the outer blanket periphery are cooled by natural convection of coolant in the reactor vessel.



1 -LEZ-core FAs; 2 - MEZ-core FAs; 3 - HEZ-core FAs; 4 - inner blanket FAs; 5 - outer blanket FAs; 6 - temperature effect compensator rod; 7 - emergency protection rod and its guiding sleeve; 8 -reactivity compensation rod and its guiding sleeve; 9,10 - automatic control rod; 11 - neutron source; 12 -technological assembly; 13 - core FAs in-reactor store.

Fig. 2.5. BN-350 Reactor Core and Blanket Layout



1 - sodium pressure chamber; 2 - sealing ring; 3 - diagrid; 4 - neutron reflector; 5 - elevator lower support; 6 - emergency protection rod sleeve; 7 - reactivity compensation rod sleeve; 8 - throttling sleeves for FAs installation; 9 - throttling devices for supplying sodium into low pressure chamber.

Fig. 2.6. BN-350 Core Diagrid

Coolant flowrate profiling in the core and in the radial blanket according to power distribution is provided by overlap of a certain portion of the orifices in the FA end fittings with throttling sleeves into which the FAs are inserted. To flatten the power distribution along the core radius for the initial reactor core FAs of two enrichment values (in uranium 235) were used: 17 and 26%. First-type core FAs had 169 fuel rods with cladding of 6.1 mm diameter and wall thickness of 0.35 mm. The fuel rod length was 1140 mm and the core height was 1060 mm, so the height of the gas plenum was very small - 50 mm which caused high stresses in the cladding from gaseous fission products. In the upper and lower parts of the core FA bundles of axial blanket rods were placed: 37 fuel rods of 12 mm diameter.

During the initial period of the reactor operation until 1979, when the first type core (fuel rod of 6.1 mm OD) was used, large number of fuel failures (loss-of-clad integrity events) occurred that caused a significant increase in fission fragment activity in the primary circuit and consequently resulted in deterioration of radiation conditions in the reactor plant rooms. Therefore the second type core design was developed with fuel rods of 6.9 mm OD. This advanced core provided for increased fuel burn-up and more reliable operation of the fuel rods, mainly due to the following improvements:

1. The gas plenum height in the fuel rod was increased at the expense of integration in one clad tube (6.9x0.4 mm) of core and axial blankets material (fissile and fertile) and reduction of the lower blanket height.
2. The fuel assembly duct material Cr18Ni10Ti (austenitic steel) was replaced by stabilized austenitic steel Cr16Ni11Mo3 in a heat-treated state.
3. The coolant pressure in the middle plane inside the duct was diminished by approx. 35% resulting in a decrease in duct deformation by radiation-induced creep.
4. The power distribution over the core radius was flattened by the incorporation of a medium fuel enrichment (21%) zone between the existing core zones with "low" (17%) and "high" (26%) enrichment of fuel, resulting in a decrease of the fuel rod specific heat rating.

The above measures and reactor operation under derated power conditions resulted in a significant reduction in the number of defective fuel rods in the core. Further increase in fuel burn-up is planned through utilization of the ferritic steel EP-450 for ducts and improved austenitic steel in cold-worked state for cladding. The basic parameters for different cores used in the reactor are given in Table 2.2. Simultaneously with the improvement of the core fuel operating performances, modifications have been introduced in the design of the control rods and guide sleeves by the use of radiation-resistant structural materials.

Control rod drive mechanisms. Ionization chamber suspensions. There are twelve CPS elements in the reactor: two power control rods, three emergency protection rods and seven reactivity compensating rods. For the entire period of operation the CRDMs have functioned without any significant abnormalities.

In 1979 and 1980, there were difficulties in disconnecting the control rods from their drive lines before refuelling the reactor. Analysis revealed a potential for seizing the CRDM moving items in the guide tubes in the sodium-to gas transition zone by solidified sodium if coolant temperature were to diminish. To eliminate such events the sodium temperature in the refuelling mode was set at a higher level (230-240 C). After that minor modification there were no problems with movement of the control rods. The CRDMs service life has been extended periodically with replacement (if necessary) of individual items on the basis of planned inspection results.

TABLE 2.2 BN-350 REACTOR CORE DESIGN EVOLUTION

Parameter	1	Core 2	Type 3
1. Reactor heat output(max), MW		650	
2. Core dimensions, mm			
-active height		1060	
-equivalent diameter		1550	
3. Axial blankets height, mm:			
-upper		600	
-lower		600	
4. Radial blanket thickness,mm		450	
5. Number of different of fuel enrichment (in U-235), %	2		3
6. Fuel enrichment (in U-235), %			
LEZ*	17	17	17
MEZ	---	---	21
HEZ	26	26	26
7. Number of fuel assemblies			
LEZ	109	109	61
MEZ	---	---	48
HEZ	108	120	114
8. Cladding outer diameter and wall thickness, mm:			
-core fuel rod	6.1x0.35	6.9x0.4	6.9x0.4
-lower axial blanket rod	12x0.4	6.9x0.4	6.9x0.4
-upper axial blanket rod	12x0.4	12x0.4	6.9x0.4
-radial blanket rod	14.1x0.4	14.1x0.4	14.1x0.4
9. Length of fuel rod, mm	1140	1800	2400
10. Length of gas plenum in fuel rod,mm			
-upper	50	50	380
-lower	---	250	310
11. Number of fuel rods in fuel assembly:			
-core fuel assembly	169	127	127
-blanket fuel assembly	37	37	37
12. Duct width across flats and thickness, mm	96x2	96x2	96x2
13. Structural material			
-cladding**	EI-847	ChS-68	
-duct	Cr18Ni10Ti	Cr16Ni11Mo3	
14. Fuel rod maximum linear rating, kW/m	28	40	43
15. Fuel rod cladding temperature (max), °C	550	570	600
16. Maximum fuel burnup, %h.a.	5.7	9.0	10.0
17. Maximum radiation dose, dpa	46	60	65
18. Core fuel life ed	332-498	424-636	400-600
19. Refuelling interval, ed	83	106	100
20. UO ₂ inventory in core, kg	7400	7800	7000
21. Aver. fuel burnup, MW day/kgU	38	54	58

Abbreviations: *LEZ- "low" enrichment zone
 *HEZ- "high" enrichment zone
 *MEZ- "medium" enrichment zone

**EI-847 - Cr16Ni15Mo3Nb
 **ChS-68 - Cr16Ni15Mo2Mn2TiB

There are two sets of ionization chambers (10 chambers in each set) for neutron flux monitoring which are located in a concrete wall of the reactor well. Two additional ionization chamber suspensions were introduced (1976) in the immediate vicinity of the guard vessel wall, that significantly enhanced reactor subcriticality control during refuelling operations.

Refuelling equipment. The BN-350 refuelling system consists of two components:

- complex of in-reactor refuelling mechanisms,
- complex of out-of-reactor refuelling mechanisms.

The first complex is a constituent of the reactor and includes: two rotating plugs (large and small), refuelling mechanisms and loading-unloading elevators. This complex provides for loading and unloading of the main core items and their re-arrangement inside the reactor. The rotating plugs are disposed eccentrically to each other. On the small rotating plug the refuelling mechanisms are mounted eccentrically. By rotating the plugs the refuelling mechanism is guided to any position in the core, radial blanket and in-vessel store, or to any control rod. The refuelling mechanism (Fig.2.7.) simultaneously with reshuffling of FAs rotates them for alignment with the hexagonal cells in the core.

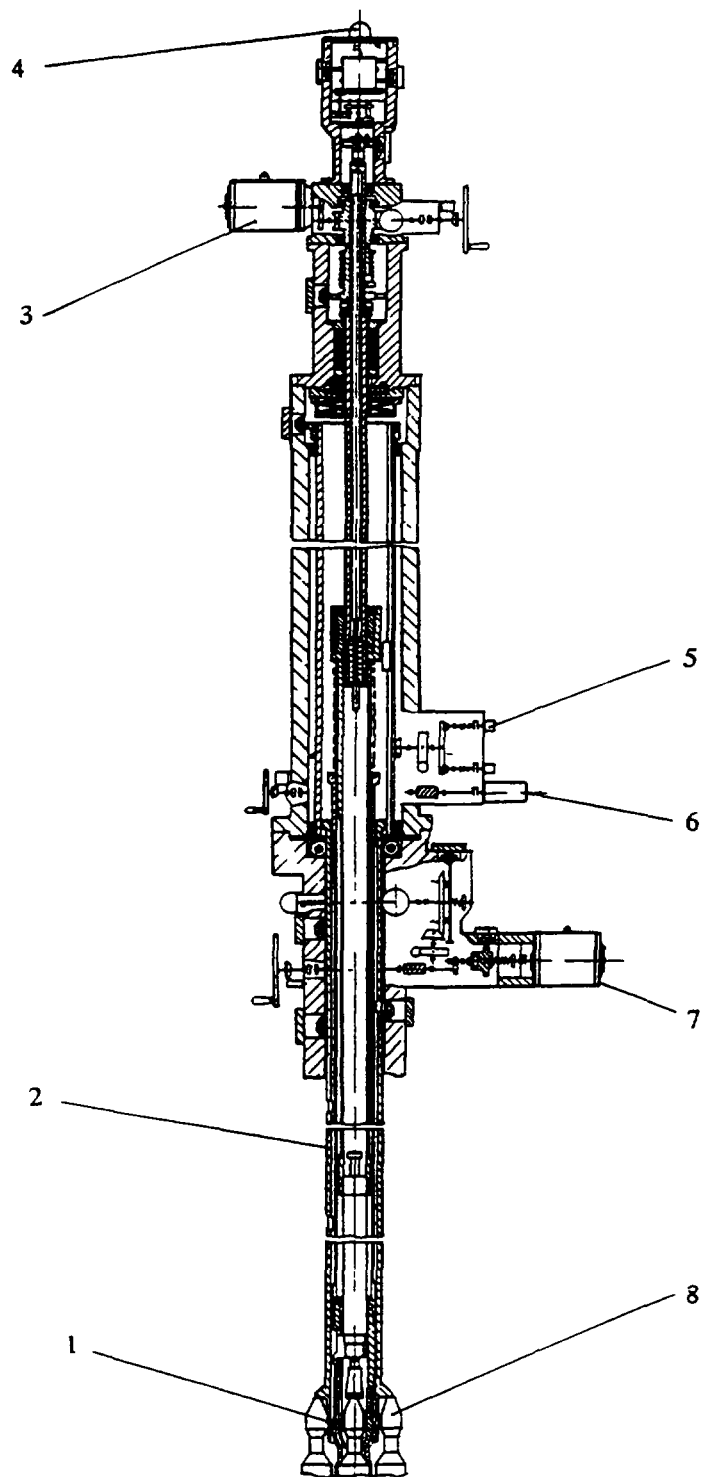
The complex of out-of-reactor refuelling mechanisms includes:

- fresh FAs drums,
- fuel transfer cell transfer mechanism,
- spent fuel drum,
- washing cell fuel transfer mechanism,
- loading-unloading elevator plug lifting mechanism.

Spent FAs and other items are transported into sockets in the washing cell and then transferred into the spent fuel water pool for decaying. The fuel transfer cell with its transfer mechanism and the washing cell adjoin the reactor (Fig.2.8). New fuel assemblies are loaded into the reactor from the new fuel storage drum located beneath the refuelling cell. New fuel loading operations have not posed any difficulties during the reactor operating life.

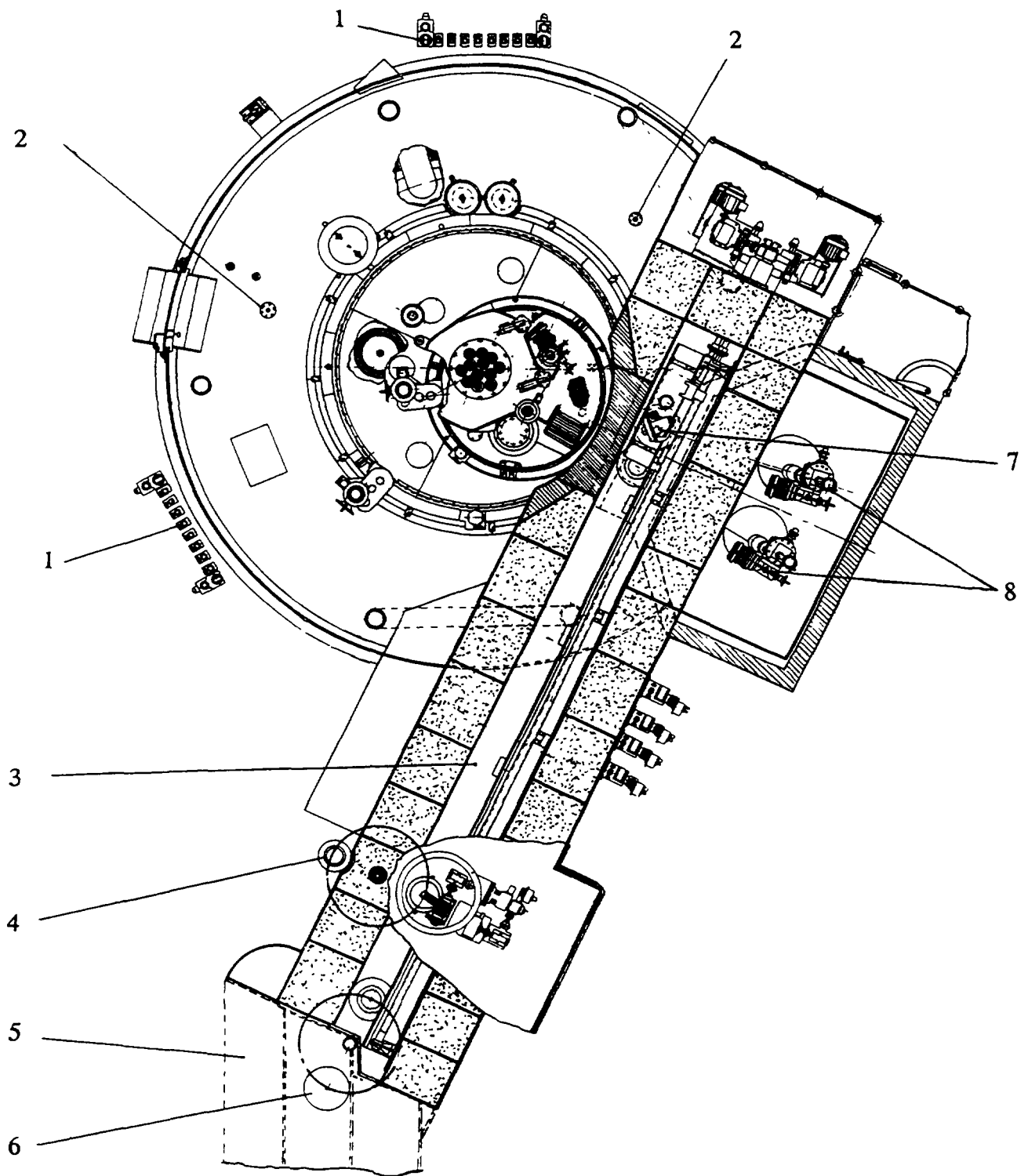
According to the design, irradiated fuel assemblies were to be transported from the fuel transfer cell to the washing cell through the spent fuel storage drum located in a tank filled with Na-K alloy beneath the junction between the cells. Due to failure of the spent fuel storage drum (1976) a special lead-shielded flask was designed and manufactured for transporting spent fuel assemblies from the transfer cell to the washing cell.

It was noticed during operation that increased forces were required for rotation of the shield plugs. Probable causes were sodium vapour condensation in gaps or non-uniform heating of the hydraulic seals. Plug operation became normal after increasing the Pb-Bi eutectic working temperature to 200°C and temporary interruption of the plug air cooling system in the process of heating up the hydraulic seals. The refuelling mechanisms, elevators and fuel transfer mechanisms in the cells have been operated without significant disturbances. Minor disturbances were remedied through replacement and modernization of individual items. To improve the reliability of the mechanisms a system to control installation and withdrawal forces was incorporated. During the entire period of reactor operation (till Oct. 1995) 56 planned refuelling cycles have been fulfilled. The time spent for one fuel assembly replacement was one hour. The total number of loading-unloading operating cycles of the elevators and fuel transfer mechanisms is ~ 3200.



1 - gripping device; 2 - guide tube; 3 - gripping device drive motor;
 4 - gripping device synchro-pickup; 5 - gripping device swing position pickup;
 6 - gripping device swing stepping motor; 7 - guide tube drive motor; 8 - fuel
 assembly heads.

Fig. 2.7. BN-350 Refuelling Mechanism Kinematic Scheme



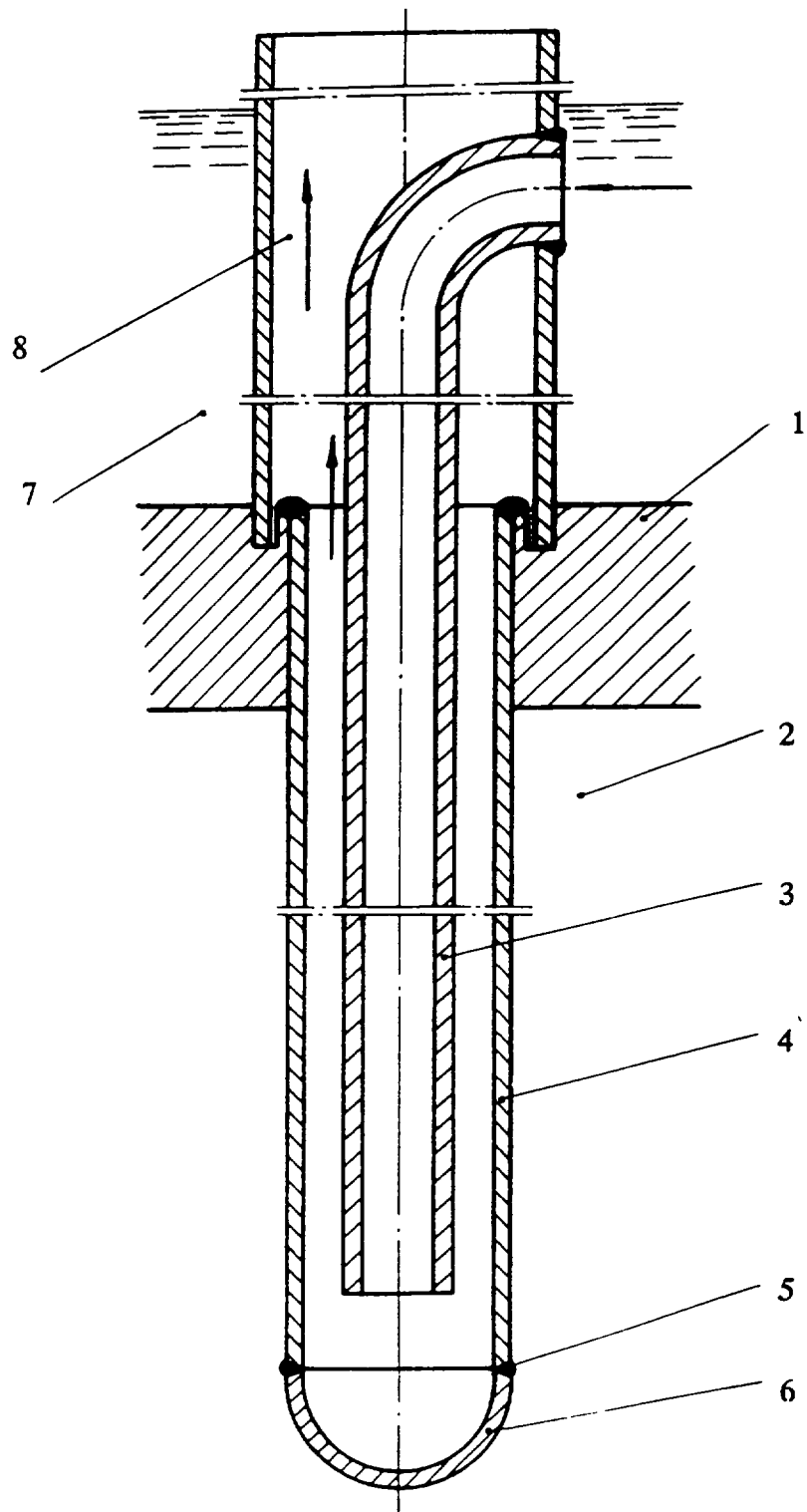
1 - ionization chambers in reactor concrete well; 2 - installation of additional chambers; 3 - fuel transfer cell; 4 - seat for FAs installation in new fuel drum; 5 - washing cell; 6 - seat for transfer spent FAs to washing cell; 7 - FAs transfer mechanism; 8 - FAs loading-unloading elevator.

Fig. 2.8. BN-350 Reactor Plan View

Steam generators. The BN-350 steam generators consist of two super-heaters with U-shaped tubes and two evaporators with Field-type tubes inside which water flows under natural convection and partial evaporation conditions. The initial period of reactor plant operation was characterized by unreliable operation of the SGs. Numerous loss-of-integrity events occurred in the Field tubes of the evaporators. Metallographic examination of a great number of Field tubes (Fig. 2.9.) showed the presence of microcracks in the tube-to-bottom weld joints. Mechanical deformation of the tube bottoms during cold stamping were acknowledged as the most probable cause of the microcracks. Growth of the microcracks could occur under the effect of internal stresses arising during welding the bottoms to the tubes and under cyclic thermal loads during evaporator operation. After repair of the Field-tube evaporators when outer tubes of 32x2 mm (OD x wall thickness) were replaced by 33x3 mm tubes with machined bottoms reactor plant operation was continued with five loops at thermal power of 650 MW. One of the repaired SGs failed later due to a large leak of water to sodium. It was dismantled and replaced with the micromodular SG "Nadjozhnost-1" of Czech fabrication (1980). Another SG of the same type "Nadjozhnost-2" was put into operation in 1982 instead of one of the Field-tube SGs which had been operated reliably since the reactor start up. In general, the plant operation demonstrated the reliability and high operating performances of the Field-tube SG design taking into account particularly their behavior in water-to-sodium leak events. At the same time, the thermal-hydraulic disadvantage of the design was revealed by natural convection flow instability during emergency residual heat removal. The use of "Nadjozhnost"-type steam generator eliminates this disadvantage and in addition allows the removal of heat from the SG by air flowing outside the modules under forced or natural convection conditions. In January 1989, both these SGs failed due to stress-induced corrosion on the steam-water side of the tubes promoted by non-uniform thermal-hydraulic conditions in the tube bundles. After repair the SGs were put again into operation in 1993.

Intermediate heat exchangers. Horizontal tube-and-shell IHXs with three modules connected in series, made of U-shaped tubes are used in the BN-350. The IHX of each loop consists of two sections connected in parallel both for primary and secondary coolant flows. The IHX is located in a suction loop upstream of the primary coolant pump, while in the secondary circuit it is in a pressure loop downstream of the circulating pump. The IHX tube bundles can be removed if necessary and replaced with new ones. The most stressed units in the IHX are the fixing joints for the tube module covers and for the frame which stiffens the flat walls of the IHX body. Measurements of temperatures and stresses in various items of the IHX were carried out during reactor plant operation. On this basis requirements were formulated to limit the rate of the IHX heating-up in steps of 10% specified power with delays of 5-10 h in each step. By 1995 the IHXs have operated more than 160000 h at various power levels without any disturbances and failures.

Gate and check valves. Double-disk wedge gate valves with freezing seals of OD 500 mm and OD 600 mm (12 items) are used in the reactor plant. They are remotely operated and provide for disconnection of the primary circuit loops from the reactor. The total operating time of the primary circuit gate valves by January 1996 was approx. 180,000 h; the number of "closed-open" cycles for each OD 600 valve from the beginning of operation amounts to approx. 140. The operability and reliability of the valves has been proved during the reactor plant operation. Check valves are installed downstream of the reactor coolant pumps. The operation of these valves could not be checked on the pump test rigs. In the course of adjustment and commissioning on the reactor plant considerable displacements of primary pipelines were detected on the occasion of a trip of one of the pumps operating at maximum speed followed by check valve closure. The displacements were caused by a large backflow as



1 -tube sheet; 2 - sodium; 3 - downcomer tube; 4 - heated outer tube;
 5 - lower weld seam; 6 - bottom of Field tube; 7 - boiler water; 8 -steam-
 water mixture outlet.

Fig. 2.9. BN-350 Evaporator Field Tube

the valve closed. A new design of check valve was developed which differs in that the mass of the gate member and the backflow on valve closure are smaller. The advanced valves are operating satisfactorily, which has made it possible to dispense with the reactor shutdown when a primary loop is switched off, thus realizing the design algorithm of loss of a single loop without scram.

2.1.3. Safety enhancement and equipment life extension

The reactor was developed on the basis of codes valid in the 1960s and therefore does not meet the up-to-date safety requirements fully. The possibility of further operation of BN-350 depends primarily on reactor safety enhancement.

In 1992, the design institutions together with the plant operator completed a review of the conformity of the reactor to the requirements of safety codes currently valid in this country. Resulting from the analysis a list of deviations was compiled and the necessary measures for reactor plant upgrading were developed, part of which has been realized. The most important among those measures performed recently in the framework of reactor safety enhancement are as follows:

1. From 1990, efforts have been under way to ensure safety under external dynamic loading, such as an earthquake. All necessary investigations have been completed to refine the parameters of the maximum design seismic impact. Calculations have been carried out to assess the building structures, pipelines, heat exchange equipment and the reactor main and guard vessels. Work has started on the reinforcement of individual equipment items and pipelines and provision of additional restraints. Analysis of the consequences of seismic impact on the reactor plant building structures, equipment and pipelines showed that the existing safety system such as the reliable power supply system, the feed water system and the reliable service water supply to components important to safety would be destroyed completely or partially under seismic impact of 6 units magnitude (MSK-64 scale) - the Maximum Design Earthquake accepted for the BN-350. Taking this fact into account a design was developed providing for the arrangement of safety equipment in the seismically robust part of the reactor building to ensure reactor residual heat removal under seismic impact conditions. A design was developed and is currently being realized providing for reactor seismic protection by triggering the shutdown system in response to signals from seismic sensors.
2. Analysis of the influence on the reactor of explosion-hazardous industrial facilities situated in the vicinity of the site is complete and the corresponding measures for ensuring reactor safety have been developed.
3. The control and protection system is being upgraded by renovation of its components and optimization of transient control algorithms.
4. A core residual heat removal system for the event of coolant level lowering in the reactor below the outlet nozzles has been installed.
5. An independent feedwater system for the SGs has been mounted and put into operation, as well as the air-cooling system for the micromodular SGs "Nadjozhnost -1 and -2". The electric valve drives are powered from a reliable power source.
6. A diagnostic system for checking the state of the primary circuit pipeline metal is under development.

Lifetime extension implies analysis of the current state of main systems and components, determination of their residual lifetime, finding the items with expired lifetime and

replacing them, and validation of the plant lifetime extension. The preliminary findings resulting from this activity proved that such components as the reactor vessel, guard vessel, reactor support system, internal structures of the reactor, reactor coolant pump casings, and the bodies of the primary circuit check and gate valves still have a considerable lifetime reserve. The reactor operating record confirmed that its technical and economic performances during the entire period of service life, including recent years, are quite satisfactory. There are no symptoms of the reactor plant operating performance indicating deterioration. Based on the results of the ongoing work, a decision will be made on the possibility of continuing reactor operation.

2.1.4. Review of experimental programme

The BN-350 reactor plant has been used from the very beginning for tests and research activity aimed at enhancing safety and economic efficiency of reactor operation. The results of a considerable part of the experiments performed were used in the development of advanced fast nuclear reactor designs. Among the research work carried out the following can be noted:

1. Testing of structural materials for cladding and ducts of FAs with increased fuel burnup using the normal, experimental and special test fuel assemblies. The development and fabrication (1980) of a FA dimensional check system made it possible to obtain the required information on the deformation of core items associated with radiation-induced damage of structural materials.
2. Testing of FAs with mixed uranium-plutonium oxide fuel and other types of nuclear fuel.
3. Testing and post-irradiation investigation of absorber elements for control rods of enhanced efficiency and with extended service life.
4. Testing of new control rods guide sleeves made of more radiation-resistant structural materials to improve reliability and to extend service life.
5. Experiments with a special sodium boiling generator movable along the core height involving recording of boiling initiation by acoustic and neutron sensors. The experiment confirmed the possibility of detecting sodium boiling and locating FAs in which the coolant is boiling.
6. Investigation of reactivity effects and power distribution in the reactor core using indicators placed in capillary tubes integrated into the FAs and using a gamma-scanning technique.
7. Experiments on the reactor plant emergency cooling using active and passive heat removal methods including natural convection of sodium in the circuits and cooling of the "Nadjozhnost" steam generators by air.
8. Development and test of more effective systems for hydrogen monitoring and detection of leaks in both types of steam generators.
9. Development and installation into the reactor of a small-size graphite absorber for removal of caesium nuclides from the reactor coolant and investigation of the efficiency of this technique.
10. Investigation and perfection of reactor plant operation modes, modernization of the CPS and installation of additional sensors for control of reactor parameters.
11. Experiments with large sodium fires and development of fire extinguishing techniques.
12. Checking of new designs of advanced equipment and systems and substantiation of their utilization in other BN-type nuclear reactors.

2.2. PHENIX OPERATING EXPERIENCE

2.2.1. Design features

Reactor core. The reactor block is of an integrated design (pool) except for a few auxiliary circuits. The entire primary sodium system, containing 800 tons of radioactive sodium, is enclosed in the main reactor vessel, which is 11.8 m in diameter (Fig. 2.10).

The fissile core, in which most of the reactor power is generated, is surrounded by a fertile blanket and neutron shielding to prevent activation of the secondary sodium flowing through the intermediate exchangers.

The fuel is uranium dioxide mixed with plutonium dioxide (UO₂ - PuO₂). It is contained in 103 subassemblies, each containing 217 pins, which in turn consist of a stack of sintered oxide pellets, 5.5 mm in diameter, in stainless steel cladding. The pins are assembled in clusters in a stainless steel outer shell, which also contains the upper and lower fertile blanket pins (depleted uranium oxide) and the upper neutron shielding.

The radial blanket is composed of depleted uranium dioxide pellets measuring 12.15 mm in diameter, in 90 assemblies of 61 pins each. The structural components of these subassemblies are identical with those of the fissile subassemblies, with sodium flow through the spike inserted into the diagrid.

Vessel. The sodium in the main vessel is separated into two zones:

- hot pool at the core outlet where the hot sodium flows into the intermediate heat exchangers,
- cold pool taken from a peripheral annular space between the primary tank and the wall of the main reactor vessel, which contains the three main circuit circulating pumps and six heat exchangers, suspended from the upper slab.

A number of other devices are located in the main vessel: the fuel transfer arm, the six control rods, neutron flux detectors, thermocouples, failed fuel detection and location devices, the core acoustic detection system components, etc.

An argon gas atmosphere is maintained above the sodium surface to prevent any contact with air.

The main vessel is closed at the top by a flat roof with openings for pump and heat exchanger pipes. It is associated with the cylindrical seating of a rotating plug in the slab penetrations forming the top of the reactor block.

An outer guard vessel surrounds the main vessel. It has the double function of containing any sodium escaping by leakage, and preventing a drop in the sodium level of the main vessel which might affect core cooling.

Finally, an outer leak jacket aims at containing any radioactive products that might escape from the main vessel in the event of an accident. This containment is cooled by a water circuit which maintains the concrete of the reactor block at a low temperature, and which is

capable of acting as a standby cooling circuit for decay heat removal after shutdown, should all the secondary sodium circuits be out of service

Heat transfer circuit. The three primary sodium pumps are variable speed units (150 to 970 rpm) delivering about 950kg/s at 825 rpm, which is their normal service speed. The circulating sodium enters the core at 400°C and moves from there, at 560°C, to six intermediate heat exchangers which are connected in pairs with three independent secondary loops

Sodium must be kept very pure to prevent corrosion of the steel piping and plugging of circuit components. It is purified by cold traps operating on the principle of precipitation of any oxide in the sodium at low temperature

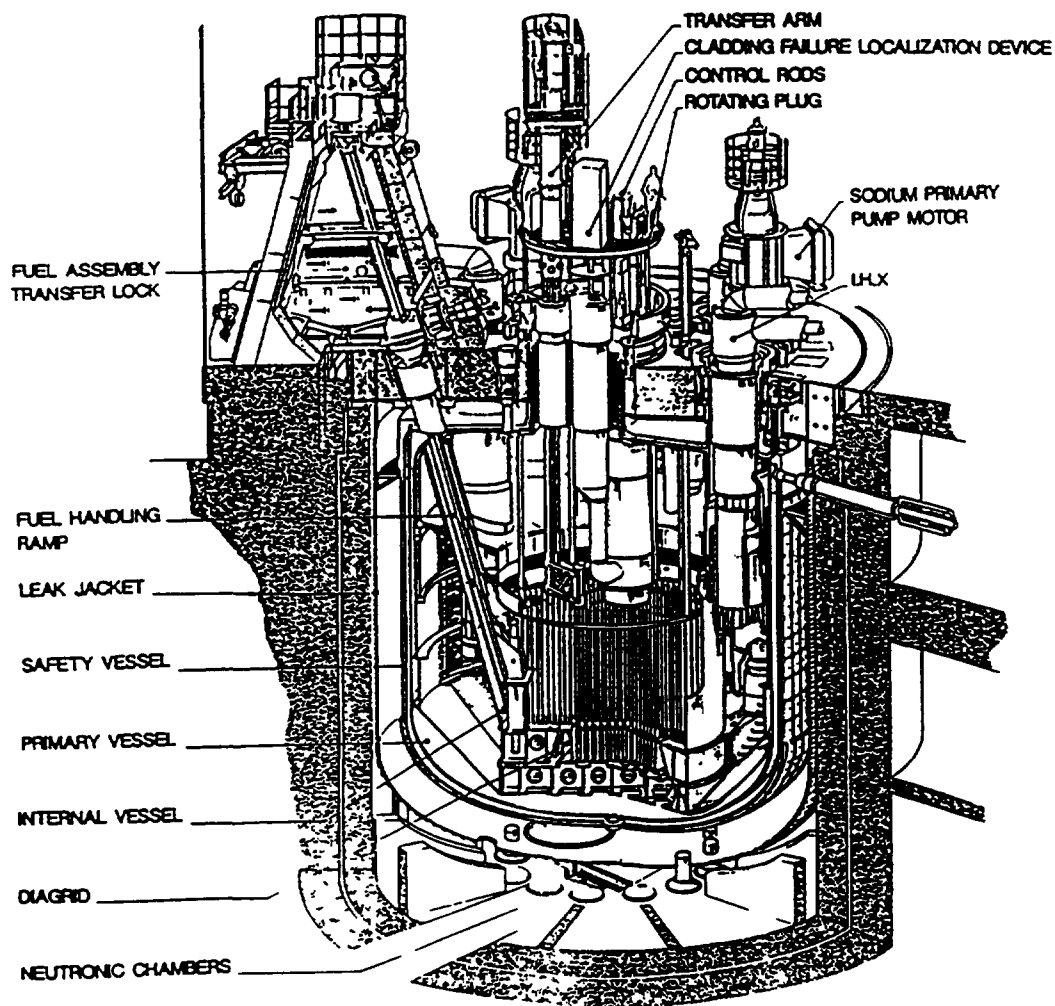


FIG 2 10 Phenix cut-away view

Secondary sodium, which is not radioactive, is circulated by a mechanical pump with a flow delivery of 700 kg/s. It enters the Intermediate Heat Exchangers (IHX) at 350 C and leaves at 550 C.

Each secondary loop is connected to a steam generator consisting of an evaporator, superheater, and reheater, in 12 modules for each stage.

2.2.2. Operating experience

The following table shows the main events with their chronology, and the number of EFPD per year.

Reactor core. During these ten years, the behaviour of the subassemblies was strongly improved by the choice of specific steels, for wrapper and cladding, with low swelling properties. The maximum burnup achieved was 136 000 MWd/t of oxide.

Main events	84	85	86	87	88	89	90	91	92	93
IHX leak	□ □				□					
Secondary circuit leak			□							
Statutory inspection						□				
Negative reactivity						□	□			
Tests 350 MWth										□
EFPD by year	262	217	278	285	272	113	184	Test period 7		

Eight cladding failures, with delayed neutron emission, occurred during these ten years. Consequences on reactor operation were small, failed subassembly identification being fast and replacement often shorter than three days. This short time of radioactive element emission allowed both primary sodium and argon cover gas to be kept at very low level of activity.

An unusual event appeared in 1989, shown as a quick decrease and rise of core reactivity, involving automatic reactor scram by reaching the "negative reactivity" threshold. A specific chapter (2.2.5.) presents this phenomenon and its consequences on plant operation.

In spring 1990, the power of the reactor was limited to 500 MWth, because of a safety request: to check the decay heat removal ability, in case of failure of the normal decay heat removal circuits.

Over the operating period, the irradiation programme was continued: for example, wrapper and cladding materials.

Recently, two new trends of politics appeared: plutonium burning and long lived waste incineration. In this context, one of the three radial breeder rows of the core was replaced by steel subassemblies and the replacement of the two other rows is planned for the next few years. An extensive irradiation programme of minor actinides is being defined.

Non-nuclear component behaviour. During these ten years, some problems have resulted in limited periods of operation at two third full power, operating on two secondary circuits.

In May 1984, a new secondary sodium leak occurred in an IHX: sodium was detected in the annular space between cold and hot secondary sodium. The leak was small enough to continue operation until the end of the cycle (July), when the IHX was replaced by a spare. The same defect reappeared in December on this IHX. Then the plant had to operate for nine months at two third of full power, until repair was completed. It was concluded that these two successive leaks were not generic defects, but the result of two repairs made in 1977 after the first IHX leaks.

In May 1986, a leak occurred on secondary circuit n° 3. It was detected by the leak detection device, at the inlet of the main pipe feeding the superheater. Around 50 kg of sodium leaked and froze in the thermal insulation casing surrounding the pipe. Two months, during which the plant operated on two secondary circuits, were necessary to replace the affected part of this pipe.

In January 1987, vibrations appeared on secondary pump n° 1, which forced a shutdown some days later. Radiography showed that the shaft bush of the hydraulic bearing had slid down on the shaft. The same problem appeared again some years ago on the primary pumps, which were modified. Having no spare, the plant had to run on two circuits for the six weeks needed for the secondary pump repair.

In October 1988, a leak of secondary sodium was detected into the annular interspace of an IHX. The IHX was removed and replaced by a new one, instrumented with 66 thermocouples.

Between 1984 and 1990, the evaporators of the three steam generators have been successfully chemically washed.

2.2.3. Statutory inspection - Spring 1989

French law requires hydraulic tests to be conducted at least once every ten years on equipment subject to gas or vapour pressure. The last tests were carried out in 1980. A complete inspection of the turbogenerator set was also required.

The whole operation was scheduled to be completed during a general overhaul of 13 weeks from April to June 1989. It was prolonged by five weeks due to an unexpected need to change a turbine rotor after inspection.

The main plant parts concerned were the fuel storage drum, the reactor unit, the secondary coolant circuits and steam generators, the turbogenerator set, and the high pressure steam pipes. A large part of these operations consisted of non-destructive testing in compliance with the utility company's wish to get in-depth knowledge of the condition of the equipment and to evaluate any possible aging.

Fuel storage drum. Major welds of this 5.40 m high drum, made of A 42 grade steel, selected for their mechanical load and/or geometry, were inspected. An ultrasonic method was used. The inspection showed no significant faults.

Reactor unit. Dismantling of parts for replacement or inspection was not required. The only operations involved were testing and inspection. They were performed on the following parts; no significant faults were detected:

- Vessel leak test

Leak tests using helium injection were conducted at the following locations:

- between the double-wall vessel and the primary containment vessel,
- between the upper part of the main vessel and the double-wall vessel,
- on component penetrations in the reactor slab.

-Weld inspections on the main vessel

Ultrasonic inspection was carried out on around 60% of the length of the connection welds between the roof and the main vessel and between the main vessel and the double safety wall vessel.

-Other inspections

- connection weld between a hanger and the main vessel,
- thermal insulation of the double-wall,
- sodium and argon primary coolant auxiliary circuits.

Secondary sodium circuits. The main pipe work had 185 welds inspected. Five welds showed unacceptable defects and were replaced.

Steam generator. The position of the steam tubes inside the sodium pipe was checked on modules by gamma radiography. No fault was detected. In the superheater and reheater stages, a hydraulic test was carried out in water at a pressure 1.5 times greater than the nominal pressure. During testing of the reheater of steam generator N°2, a leak appeared on the connection welds of five modules (out of twelve). The reason of this well-known defect is explained by microcracks in the weld between steam collector (ferritic steel) and the modules (austenitic steel), and some sodium traces remaining around the welds, despite cleaning, after the first sodium/water reaction in 1982.

- *Turbogenerator set*. An extensive inspection was performed:
- *condenser*: the condenser was completely retubed,
- *low-pressure rotor*: it was replaced, because of significant cracks revealed by magnetic particle testing. They were thought to come from intergranular stress corrosion in the presence of caustic coming from a sodium/water reaction in 1982,
- *alternator rotor*: it was replaced by a spare, because of short-circuit detected on four windings.

2.2.4. Inspections and maintenance during the test period (1991 - 1993)

Secondary circuit welds. During this period, many checks were performed. Faults were detected, involving important works.

- *AISI 321 steel lines*

Around thirty suspicious welds were replaced. The opportunity was taken to improve sodium leak detection by the addition of detection wires near the circumferential welds.

It was demonstrated that the cracking was related to aging of the 321 stainless steel. An R and D programme was undertaken to improve the understanding of the cracking phenomenon.

- *Buffer tanks*

In August 1991, a defect was detected on buffer tank n 2, penetrating the wall above the sodium level. In consequence the examination programme was increased and the tank was removed for repair. Finally, on the recommendation of the safety authorities, it was decided to fit the circuits with new tanks instead of repaired.

- *Expansion tanks*

In June 1993, faults were detected on expansion tank n 3 on welds subject to thermal fatigue. After careful examination and removal of the secondary pumps and thermal insulation, similar faults were found on the other tanks. Replacement (under argon atmosphere) of the connection flange to the inlet pipe and parts of the sphere wall were undertaken and are still in progress.

A reassessment of the zones potentially affected by thermal fatigue on all the sodium circuits was undertaken.

Subassembly transfer arm. Rotation and upward and downward movements of this arm become more and more difficult over several months. This was caused by sodium deposits, probably increasing with the present low temperature of the reactor.

During Spring 1993, the arm was cleaned. More than 10 kg of sodium were taken out, allowing arm movements to return to normal.

2.2.5. Negative reactivity shutdown

On three occasions in Summer 1989, the reactor was stopped by automatic emergency shutdown, the negative reactivity threshold (-10 pcm) being exceeded. This reactivity variation was very fast: first a minimum after 50 ms followed by an increasing oscillation, and then a decrease, caused by the control rod drop, 200 ms after the start of the transient. The first two events were thought to be spurious (a neutronic chamber fault) and the reactor was restarted. The normal plant instrumentation did not allow proper recording of the transient so following the second trip special instrumentation was installed. After the third trip, the reactor was shut down in order to identify the cause of the events.

It was found that the phenomenon could be explained by gas entrainment through the core, after accumulation under the diagrid. The void coefficient explained the transient loss of reactivity. After some reactor improvements related to this explanation, the reactor was allowed to restart at the end of 1989, but the event occurred again in September 1990, after 182 EFPD of operation.

An expert committee was then set up, and an extensive study of all the possible phenomena was started. Also it was decided to fit the plant with special monitoring equipment including fast recording systems, and to perform tests. Around 200 data were concerned. Tests on vessel and component mock-up were also planned.

The tests were performed with the reactor shut down, critical at zero power (since October 1991) and at 350 MWth power (for around 12 days - February 1993). In the same time, checks were performed on the plant, especially on the reactor, its components and auxiliaries. Reactor tests were very satisfactory: they proved the good behaviour of the instrumentation, and data are now stored as reference of steady state power and emergency shutdown conditions.

By the end of 1993, studies had not led to a clear explanation of the phenomenon: "false" reactivity variations (a "neutronic mask" between core and neutronic chambers, or a spurious signal) are thought to be impossible. Among "real" reactivity variations, a sodium void effect or variation of the relative displacement of fuel and control rods are also thought to be impossible. There remains only a radial core volume variation, the origin of which (a "pressure wave") has not been found.

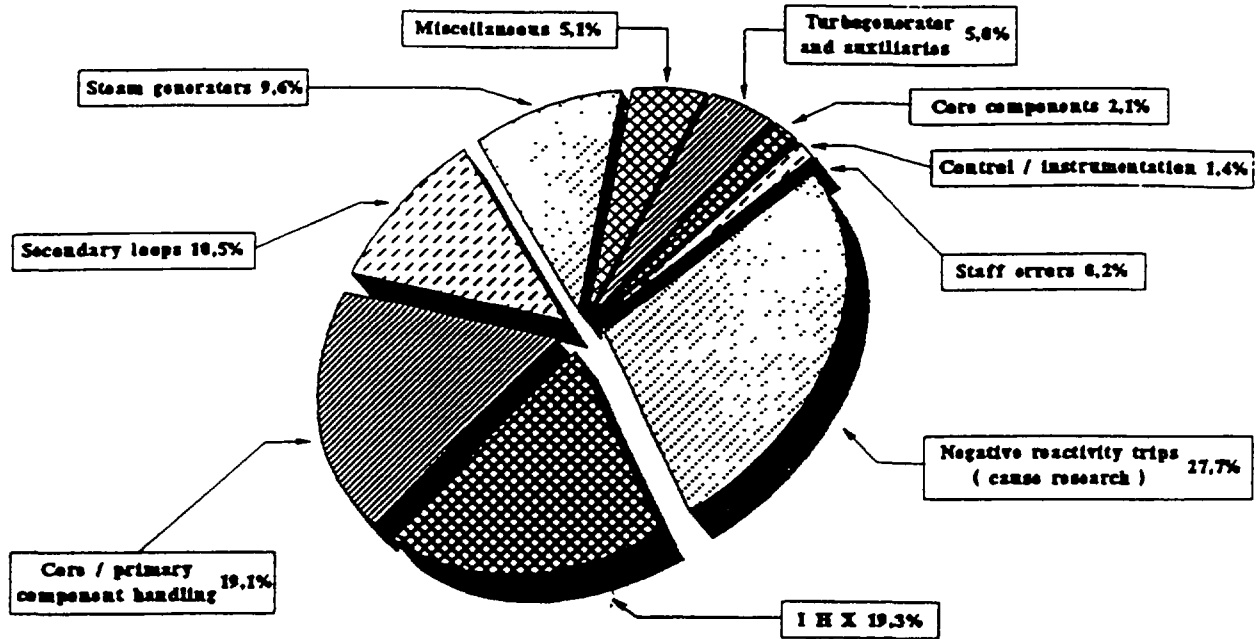
These studies confirm that the reactor safety was not affected. Operation with special instrumentation seems to be the only way to understand the origin of these negative reactivity trips.

2.2.6. Plant statistics

By 31 December 1993, the main production data of PHENIX were as follows:

-	Equivalent full power days	3 675 EFPD
-	Gross electrical energy production	21 484 GWh
-	Load factor (since commissioning in July, 1974)	50,36%
-	Number of irradiated subassemblies	829
-	Number of irradiated pins	176 521
-	Burn-up (maximal)	136 000 MWd/t oxide

The causes of loss of production are as follows. The largest is now the plant shutdown for investigation of the cause of the negative reactivity trips.



2.2.7. Radiological safety

Staff radiation exposure The radioactivity level to which the staff is exposed is very low for several reasons: the pool design of the reactor which confine the primary circuit, the near absence of fission products because of the small number of cladding failures and early detection, identification and extraction from the core; good protection conditions for handling not only fuel but also components like pumps or IHXs. The main dose exposures result from specific inspections (storage drum, reactor vessel, ...) or maintenance operations (fuel transfer device, primary circuit, IHX, ...) Since 1974, the total dose equivalent integrated by the plant staff and contractors is 1,33 manSv (133 man.rem).

Radioactive wastes. These are also very low. (1) solid waste, essentially parts of fuel subassembly frames after dismantling, (2) liquid waste coming from subassembly pump and IHX cleaning (these are not released directly from the plant but are transported to and treated at the COGEMA MARCOULE Center nearby), and (3) gaseous waste which follows the activity released from cladding failures, and so is very low. Most of the time, the activity is at background level.

Since 1974, the total activity of these wastes are about (a) solid $741 \cdot 10^{15}$ Bq ($20 \cdot 10^6$ Ci), (b) liquid $54 \cdot 10^{12}$ Bq (1470 Ci), and (c) gaseous $114 \cdot 10^{12}$ Bq (3080 Ci) equivalent Xe135

2.3. PFR OPERATIONAL EXPERIENCE

2.3.1. Design features

The Prototype Fast Reactor, PFR, was built and operated at the United Kingdom Atomic Energy Authority's site at Dounreay in Scotland to validate and provide operational experience of a large pool-type fast reactor and as a test bed for the fuel, components, materials and instrumentation needed for an eventual commercial-sized station. It represented

the climax of a programme which began in the early 1950s to ensure long-term security of the nuclear component of the UK's electricity supplies, should eventual shortages of new supplies of uranium limit the deployment of thermal reactor stations.

As an initial experimental stage in this programme, a decision was made in 1954 to build the 60MW(th), 15MW(e) Dounreay Fast Reactor (DFR), which subsequently operated from 1959 to 1977. The information and experience gained from DFR provided the necessary confidence that a commercial-sized fast reactor could be successfully built and operated. However, because a large increase in size between DFR and a commercial plant was necessary, the need for an intermediate plant incorporating the major steps in concept and scale was identified.

Thus, in 1966, approval was given for the building of PFR on land adjacent to DFR. PFR was designed to produce 250MW(e) from 600MW(th) core power and its design incorporated lessons learnt from the operation of DFR. DFR had used a 70-30 sodium-potassium alloy as coolant; PFR would use sodium which was cheaper and easier to handle. Coolant flow would be upwards through the core (in DFR the flow was downwards) to avoid gas entrainment. The fuel would be a ceramic - a mixed plutonium-uranium oxide in sealed stainless steel clad pins (in DFR the driver fuel was a vented enriched uranium method alloy) to achieve higher burn-up and to keep the coolant relatively clean. The sodium pumps would be mechanical centrifugal pumps (electromagnetic pumps were used in DFR) to obtain higher capacity in compact units. Finally, the steam generators would be of an advanced highly-rated tube-in-shell design (whereas those in DFR were of a low-rated, double-walled matrix design).

First criticality was achieved on 3 March 1974 and operations continued until 31 March 1994. During this period, PFR contributed considerably to the UK's and latterly to the Western European partnership's experience on fast reactors, and the purpose of this paper is to review this contribution.

A description of PFR has been given in an earlier IAEA publication and a comprehensive listing of design and operational parameters is presented in another. It is not, therefore, proposed to give an extended description of the plant here, Figure 2.11. shows the general arrangement of the reactor and the stern raising plant and Figure 2.12. shows a cross-section of the primary circuit. Heat from the 600MW(th)-rated core was transported to six intermediate heat exchangers within the primary vessel by sodium primary coolant pumped by three electrically-driven (1MW) mechanical pumps. Sodium entered the core at a temperature of 400-430 C; the core temperature differential was about 160 C. The 900 tones of primary sodium were contained in a primary vessel of 18/8/1 stainless steel, 12.2m in diameter and 14.0m deep, surrounded by a guard vessel made from medium carbon boiler grade steel.

Secondary sodium flowed through the shell side of each IHX and transported heat to the steam generators. There were three secondary circuits, each containing about 75 tones of sodium which was circulated by a mechanical pump similar to the primary sodium pumps and each coupling a pair of IHXs to a set of steam generators consisting of an evaporator, a superheater and a reheater.

Each steam generator was of single-wall tube-in-shell design. The evaporators were of the forced-circulation type, with each of the three circuits having a steam drum and a boiler circulating pump. Superheated steam from the three circuits flowed to a common header to drive a 300MW turbo-alternator. The main feed was via a 100% duty steam-driven pump with

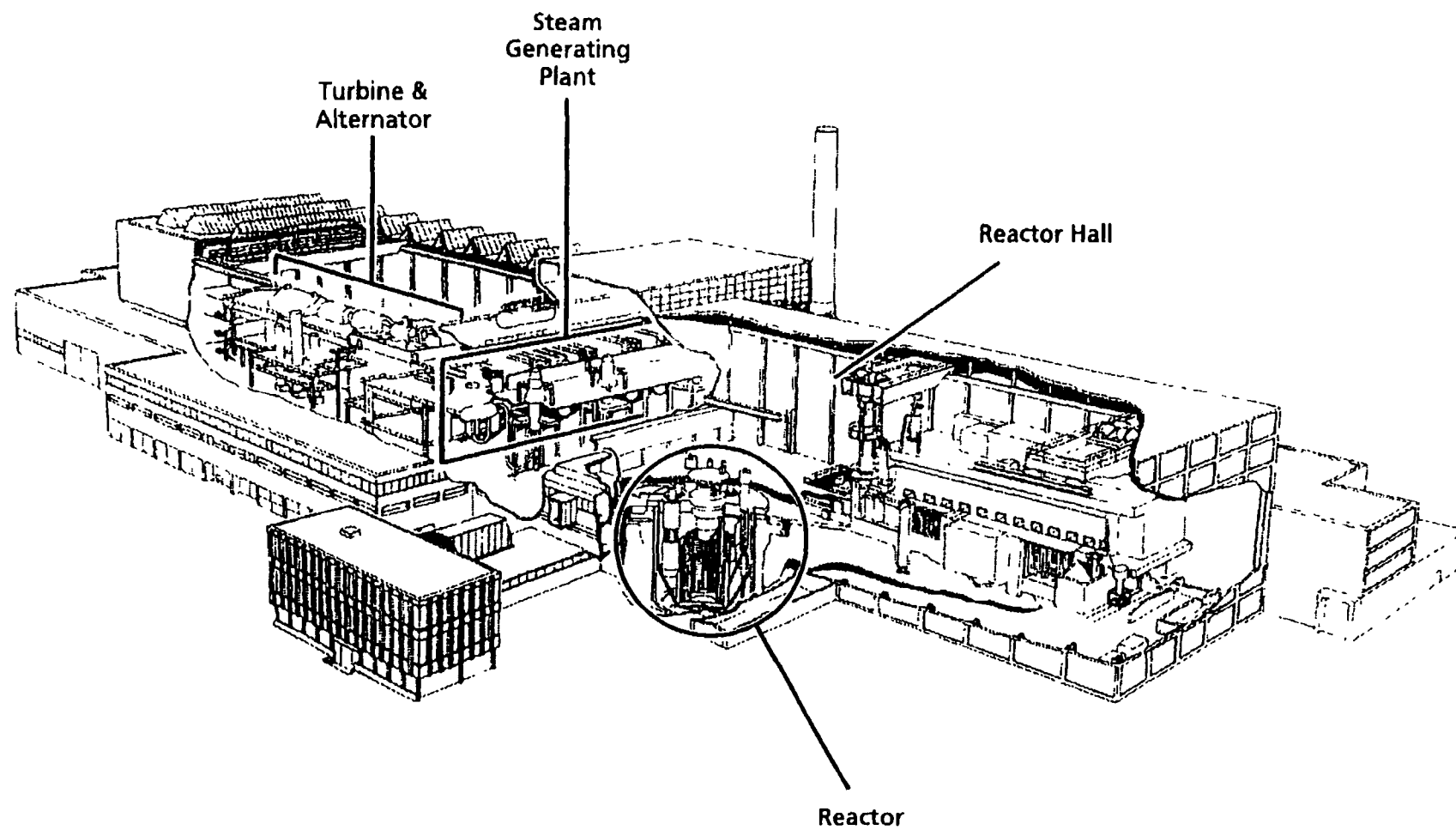


FIG. 2.11. PFR: General arrangement of the reactor and steam generating plant

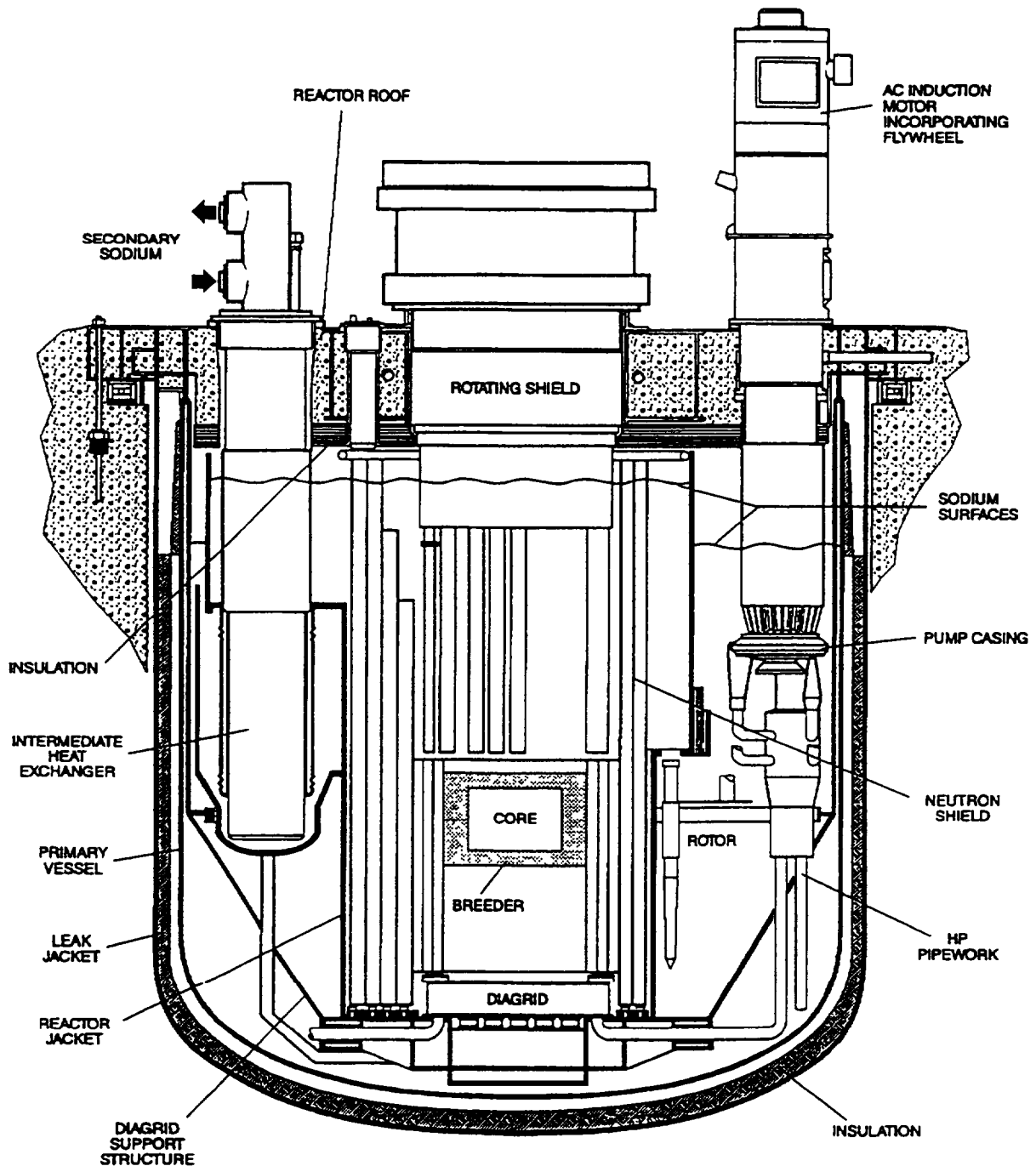


Figure 2.12 PFR: cross-section of the primary circuit

10% electric- and 10% steam-driven pumps for start-up and post-trip use. (Later, a 50% capacity auxiliary electrically-driven pump was installed as back-up). Appropriate water conditions were provided by a full-flow polishing plant, and the feed-heating by sets of low pressure direct contact and high pressure tube units. The underslung condenser was cooled by seawater.

The reactor core and its surrounding blanket was made up from an array of hexagonal sub-assemblies, 142mm across flats. The assemblies were of a size appropriate to a full-scale

commercial reactor, and provided a core 910mm high and about 1550mm in diameter. Control was exercised through five boron carbide absorber rods, and a further five similar rods were available to shut-down the reactor. A radial breeder (blanket) surrounded the core and was itself bounded by stainless steel reflector assemblies to improve neutron economy. Outboard of the core and blanket was a graphite shield which essentially eliminated neutron activation of major removable components such as the primary pumps, valves and the IHXs, the secondary sodium, and the primary vessel itself. Special loops filled with eutectic sodium-potassium alloy (liquid at room temperature) as coolant were provided to reject decay heat from the primary coolant via air-cooled heat exchangers to the atmosphere after reactor shut-down if the steam generators were not available for this purpose.

Fuel could be transferred from an adjacent preparation facility, the irradiated fuel cave (IFC), to a storage rotor within the primary vessel while the reactor was operating. This rotor reduced the time required for refuelling operations and, when irradiated fuel was discharged from the rotor to the IFC, reduced the number and complexity of the transfer flask movements because irradiated fuel removed from the core could be left to cool in the rotor before being moved to the IFC after the reactor had resumed operation. Transfers between the core and the storage rotor used a vertical lift pantograph charge machine working through a single rotating plug in the reactor roof; for such moves the reactor had to be shut down to allow the charge machine to be installed. Fuel discharged from the rotor after irradiation was first stored under sodium in the IFC until either it had been examined and returned to the reactor for further irradiation or was cool enough to be prepared for reprocessing (including steam cleaning to remove all traces of sodium) and then moved to a buffer store to await transfer to a reprocessing plant, also located on the Dounreay site (see Section 2.3.5 below).

2.3.2. Review of operating history

The review of the operating history of PFR which follows is, of necessity, selective. There have, however, been earlier reviews in journals and conference papers, and activities relating to PFR and its associated reprocessing plant have regularly been reported at Annual Meetings of the IWGFR.

The operating history of PFR can be conveniently divided into two phases. For the first ten years, electrical output was limited, mainly because of a series of leaks in the tube-to-tube plate welds of the steam generator units, and the highest load factor in any year was 12% (in 1978). After 1984, with the steam generator weld problems dealt with, plant performance improved [Fig. 2.13.]. In the final year of operation the load factor was 56.5%. In this second decade of operation there was one major outage, in 1991/92. In contrast to experience with the steam generators, until 1991 the reactor and primary circuit were responsible for only a very small fraction of unplanned outage time; however, in mid-1991, a leakage of oil from a bearing of one of the primary pumps into the primary sodium led to suspension of reactor operation for 18 months. Fig. 2.13. shows a histogram of annual load factors; Table 2.3. shows the annual operating statistics and Table 2.4. shows the statistics for each run.

2.3.2.1. The first decade, 1974-1984

The approach to criticality began in February 1974. The time from start of construction to filling of the primary circuit had been seven years compared with the four years planned, the delay being due principally to difficulties experienced in the welding of the reactor vessel roof. Nevertheless, the reactor was delivered at a cost of about £40M, with an additional £5M for

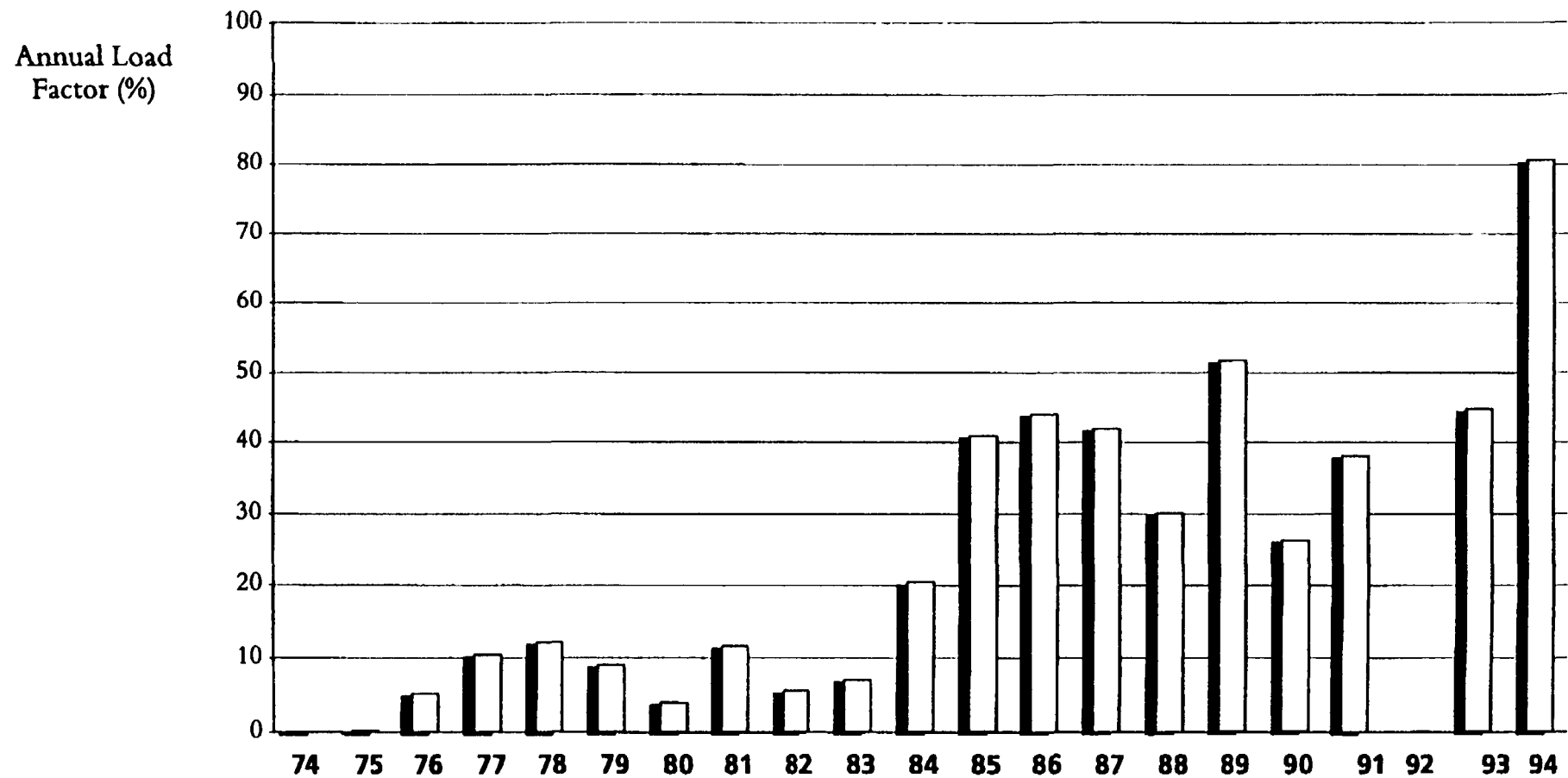


Figure 2.13. PFR: annual load factors (1994 for three months' operation only)

TABLE 2.3.

ANNUAL OPERATING STATISTICS: 1974 to 1994

Year	GROSS ELECTRICAL GENERATION		Net Electrical Generation (MW-days)	GENERATOR AVAILABILITY		Reactor Thermal Energy		Reactor Availability	
	MW-days	Load Factor %		Hours on line	%	MW-days	Load Factor %	Hours Critical	%
1974	—	—	—	—	—	932	1.3	2,673	40.5
1975	141	0.2	79	372	0.4	4,864	2.2	7,716	88.1
1976	4,711	5.1	3,890	1,616	18.4	22,172	10.1	7,306	83.2
1977	9,380	10.3	7,308	3,682	42.0	43,087	19.7	6,987	79.8
1978	11,159	12.2	9,678	2,538	29.0	41,286	18.9	4,781	54.6
1979	8,231	9.0	6,585	2,855	32.6	35,607	16.3	4,960	56.5
1980	3,560	3.9	2,927	1,219	13.9	17,815	8.1	7,455	84.9
1981	10,513	11.5	8,939	3,225	36.8	40,837	18.6	7,005	80.0
1982	5,058	5.5	3,958	2,971	33.9	23,024	10.5	4,100	46.8
1983	6,413	7.0	5,325	3,542	40.4	27,062	12.4	5,664	64.7
1984	18,586	20.3	16,991	3,097	35.3	54,335	24.7	5,835	66.4
1985	37,217	40.8	34,401	4,466	51.0	101,283	46.2	6,256	71.4
1986	40,022	43.9	37,058	4,669	53.3	108,420	49.5	6,023	68.8
1987	38,170	41.8	35,076	4,804	54.8	104,472	47.7	6,790	77.5
1988	27,423	30.0	25,440	2,906	33.1	74,072	33.7	3,884	44.2
1989	47,231	51.8	43,439	5,526	63.1	131,673	60.1	6,385	72.9
1990	23,937	26.2	22,253	2,600	29.7	65,611	30.0	3,447	39.3
1991	34,767	38.1	32,383	3,599	41.1	93,486	42.7	3,753	42.8
1992	-	-	-	-	-	-	-	46	0.5
1993	40,663	44.6	37,606	4,826	55.1	113,034	51.6	6,246	71.3
1994 *	18,160	80.7	16,926	1,826	84.5	47,800	88.5	1,870	86.6

* to 31 March

Declared Thermal Capacity of Reactor: 600 MWt

Declared Electrical Output of Station: 250 MWe

TABLE 2.4.

RUN STATISTICS from Reactor Critical

RUN N°	DATES	REACTOR			TURBINE		
		elpd (600MW nominal)	Load Factor %	Availability %	Electrical Generation MWd gross	Load Factor %	Availability %
0	03/03/74 - 03/03/77	63.08	6	73	7038	3	10
1	13/05/77 - 23/02/78	68.66	24	96	9940	14	49
2	18/06/78 - 16/10/78	39.99	33	97	6913	23	53
3	09/11/78 - 07/02/79	25.12	28	77	3983	18	49
4	17/02/79 - 06/09/79	43.15	21	87	5908	12	46
5	23/02/80 - 05/09/81	93.05	17	97	13570	10	32
6	01/11/81 - 09/03/82	24.79	19	97	3204	10	59
7	27/07/82 - 02/09/83	63.38	16	78	8742	9	51
8	28/12/83 - 07/11/84	90.56	29	76	18587	24	41
9	04/01/85 - 31/05/85	65.51	45	84	14580	40	52
10	04/07/85 - 24/11/85	99.63	69	91	21898	61	71
11	19/12/85 - 31/05/86	94.89	58	82	20997	52	62
12	09/08/86 - 04/12/86	83.10	71	97	18374	63	77
13	18/12/86 - 17/08/87	98.94	41	81	21474	36	52
14	*						
15	05/09/87 - 17/10/87	21.61	52	75	4547	44	60
16	22/10/87 - 07/07/88	178.55	69	75	40043	62	67
17	27/11/88 - 09/04/89	72.05	54	70	15370	46	60
18	*						
19	23/04/89 - 21/07/89	72.14	81	87	15639	70	81
20	27/08/89 - 12/02/90	121.29	72	77	26294	63	73
21	26/02/90 - 28/05/90	45.19	50	71	9861	43	50
22	24/11/90 - 16/04/91	129.9	90	98	28928	81	87
23	*						
24	06/05/91 - 12/07/91	48.74	72	77	10766	64	70
25	*						
26	*						
27	*						
28	*						
29	30/12/92 - 11/07/93	119.5	61	87	25706	53	66
30	15/09/93 - 27/12/93	69.0	67	90	14955	58	70
31	12/01/94 - 31/03/94	79.7	102	100	18160	93	98

* Runs deleted to maintain allocated numbers of major annual shutdowns.

the installation of a 170 km long high voltage transmission line to connect with the main Scottish grid at Beaulieu.

Commissioning had proceeded without major problems though a water test of the sodium side of Circuit 3 had revealed a gas entrainment problem requiring modification of all shut-off circuits, and bearing problems on one of the primary pumps and two of the secondary pumps had needed attention.

Criticality was first achieved on 3 March 1974. Physics parameters for the core and for the reactivity effectiveness of, and interactions between, the control and shut-off rods agreed with prediction within the expected uncertainties. The hot dynamic test was completed in June, when a small sodium leak was detected at a butt-joint of piping in a leak-jacketed section of one of the secondary circuits. It was found to be due to a poor quality repair of a construction weld defect and was satisfactorily repaired *in situ*.

In October 1974, during early steam commissioning, a leak was detected in Superheater 3. This was found to have occurred in a tube-to-tube plate weld and was the first of 43 similar events - 2 in the superheaters, 1 in a reheater and 41 in the evaporators - which were to have a major influence on operations in the next seven years, with the highest incidence (11 leaks in the evaporators) in 1981. Thereafter, apart from a small leak in a tube-to-tube plate weld of Superheater 3 in 1986, there were to be no more problems in this area, principally as a result of a major programme of sleeving carried out on the evaporator units.

The steam generator problems and their alleviation were thus to be the dominant influence on reactor operations in the first decade.

Steam generators. As has been observed, the first leak in a steam generator was experienced in a superheater, and though leaks in the ferritic steel evaporators were eventually to have most impact, experience with the superheater and reheater units, fabricated from stainless steel, will be reviewed first.

Superheaters and reheaters. The October 1974 leak in Superheater 3 was followed three months later by a similar leak in the tube-to-tube plate weld of Superheater 2. In both cases, repair was effected by explosively plugging both ends of the faulty tube. Inspection of Superheater 3 revealed cracks in the tubeplate which were sufficiently accessible for removal by machining. After machining, the tubeplate thickness was adjudged to be sufficient for continued service. Inspection of Superheater 2 unit also revealed some tubeplate cracking, but in a region more difficult of access and machining was not possible. For this unit, a case for continued service was made, based upon plugging of tubes surrounding the failed one, passivation by sodium washing, a leak-before-break argument and the scheduling of periodic ultrasonic inspections of major shutdowns. No significant crack growth was observed in these inspections.

Early in 1976, a leak occurred in Reheater 3. Inspection showed that a significant amount of sodium had entered the tubes. Further examination showed that the tubeplate was irretrievably damaged. The tube bundle was replaced by a flow restrictor in the sodium circuit to allow the associated evaporator and superheater to continue to be used. The reactor operated without a reheater in this circuit until 1984 when a replacement tube bundle was installed.

The original tube bundles of the superheaters and reheaters were fabricated, as has been observed earlier, in austenitic stainless steel, a design choice made to facilitate the achievement of the high temperature steam conditions being specified at the time by the UK electrical utilities. This steel is prone to chloride- and caustic-induced stress-corrosion cracking. This susceptibility was compounded in the superheaters and reheaters by an inability to stress relieve the tube-to-tubeplate welds after fabrication. Thus, when a leak occurred, secondary cracking was always a risk; moreover, crack propagation could be rapid.

This unfavorable experience, so early in the operating life of the steam generating plant, led to a decision to order a complete replacement set of superheater and reheater tube bundles of modified design to be fabricated in 9Cr1Mo ferritic steel. As in the original units, the new units were to have no under-sodium welds in the steam tubes, but, in addition, the need for difficult tube-to-tubeplate welds, and, indeed, for any welds separating the steam and sodium environments, was eliminated by passing the steam tube through a sleeve projecting above the tubeplate, removing the joint to the steam header from the sodium environment. Each sleeve was brazed to the steam tube and welded to a seal plate [Fig. 2.14.]. The new design also incorporated improvements to reduce flow-induced vibration of the tube bundles. These units were delivered to site in 1984, at which time it became possible to replace the missing reheated and thereby restore the full complement of steam generator units.

The two remaining replacement reheaters and the three replacement superheaters were stored as strategic spares. One of the latter was used to replace Superheater 3 after the 1986 leak event and all of the others were deployed in 1987.

Evaporators. The operating conditions for the evaporators were less demanding than those of the superheaters and reheaters and these units were constructed from 2¼ Cr1Mo steel. The tubeplate and vessel material was unstabilised. However, a niobium-stabilised variant was used for the tubes to reduce the risk of adverse effects due to decarburisation during service life.

A leak occurred after a tube-to-tubeplate weld failure in Evaporator 2 only a few days after the first superheater leak (in the same circuit), discussed in the previous section, had occurred. The unit was returned to service by plugging both ends of the defective tube. Further leaks occurred in the same evaporator and in Evaporator 3 early in 1976. Whilst the steam generator unit leaks occurring in 1974 had tentatively been ascribed to weld defects undetected by the radiographic and visual inspections and the leak testing after fabrication, the occurrence of further leaks after nearly two years of service prompted closer examination and a technique was developed to remove a sample of the failed weld for examination before the tube was plugged. This was first applied to one of the early 1976 failures. Metallography indicated cracks on the water side. The welds were extremely hard. Up to that time such water-side cracking had not been observed in the laboratory, but subsequent experiments showed that hard, highly-stressed weld material could, in fact, develop cracks in good quality water. The phenomenon was described as "pure water stress corrosion cracking". The hard highly-stressed welds were a consequence of the style of the tube-to-tubeplate junction - a direct face weld joining a tube with 3mm wall thickness to a 400mm thick tubeplate.

There were further evaporator leaks later in 1976 and in the first half of 1977, then none for a period of about eighteen months, followed by a further low level of incidence in 1979 (one of these leaks being in Evaporator 1 which had hitherto been fault-free). Fig. 2.15. shows the incidence of leaks.

Examination of weld samples taken in 1977 showed some partially penetrating sodium-side cracking. The significance of this was not understood at the time. The discovery, however, prompted a major programme to develop non-destructive methods of detecting partially-penetrating cracks.

Throughout this time, consideration had been given to methods of heat-treating or otherwise stress-relieving the welds. Bulk stress relief was considered but rejected because of difficulties in ensuring that there would be no distortion of the tubeplate. Local methods,

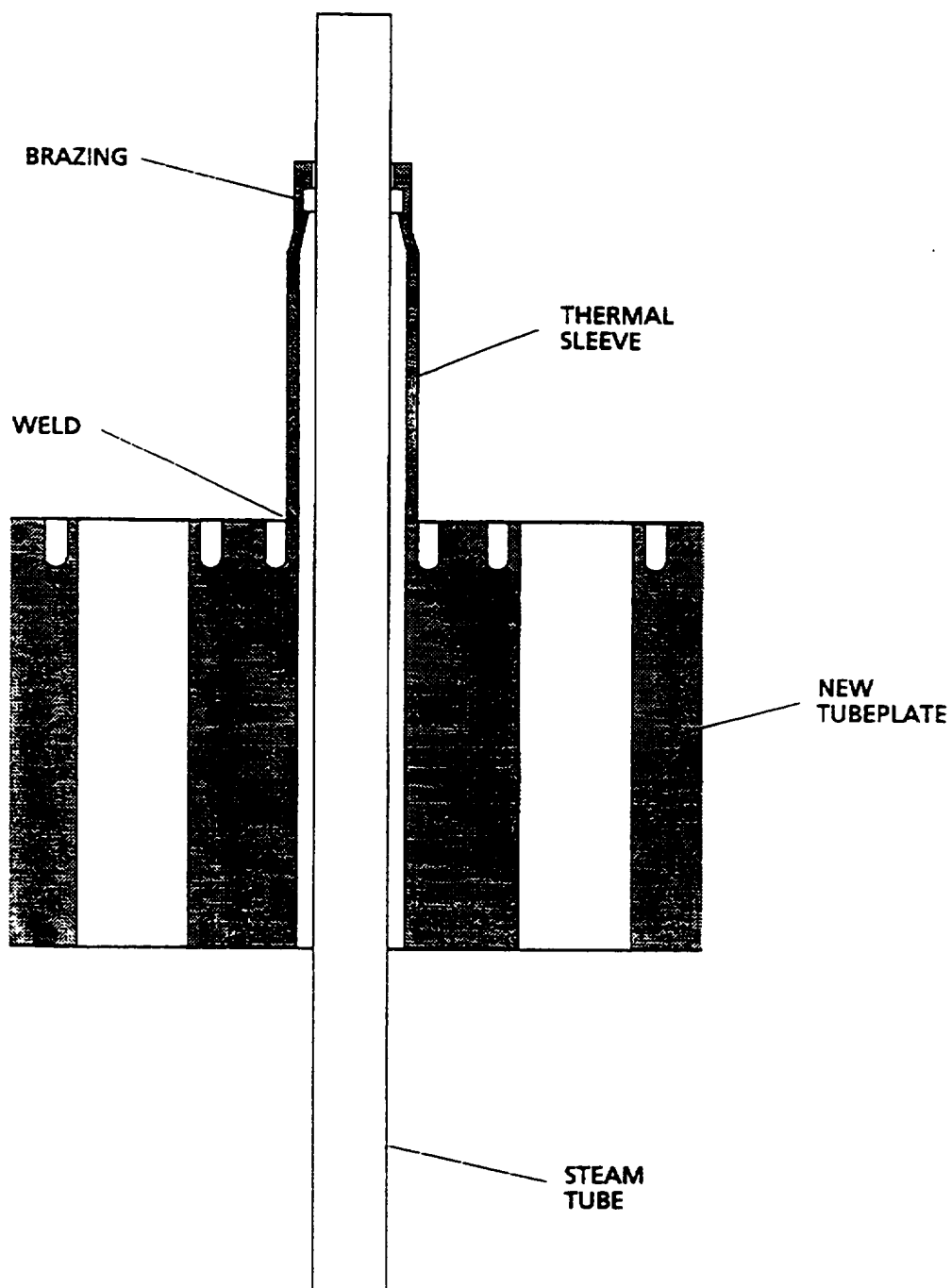


Figure 2.14. Tube/tubeplate junction of the replacement superheater and reheater tube bundles

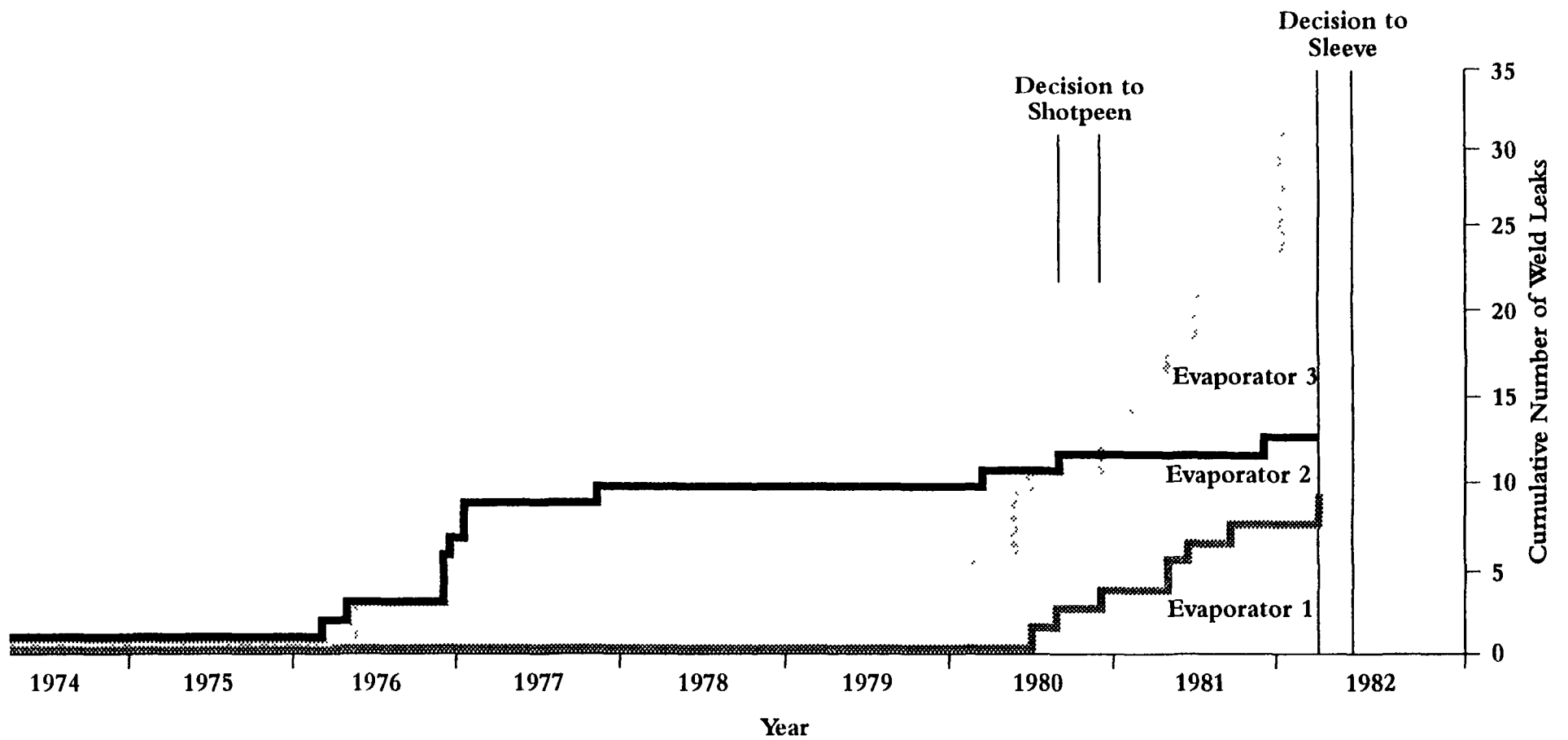


Figure 2.15. Incidence of evaporator leaks

including heat treatment of individual welds by glow discharge and elimination of tensile stresses in the surface layer by shot-peening, were therefore pursued. In the autumn of 1980, when it had become apparent that the rate of incidence of leaks was increasing, it was decided, after trials on a spare evaporator tube bundle, to shot-peen the bores of all of the 3000 tube-to-tubeplate welds in the operating units as a means of protecting them against pure water stress corrosion cracking. The possible benefit of shot-peening the sodium side of the welds was considered but adjudged to be not practicable. All of the evaporator units were shot-peened during the winter of 1980/81. Each unit was out of service for about two months. Most of the time was for preparation, inspection and reinstatement, the peening work itself taking only about a week

Experience following this treatment was variable. One unit (Evaporator 2) operated for a year after shot-peening before developing another leak. In the others the incidence continued to increase. Again defective welds were extracted for metallographic examination. These showed extensive sodium-side cracking. A survey using newly developed eddy current and ultrasonic methods, supported by selective radiography for validation and calibration, was initiated for the two units continuing to develop leaks. This found over 100 welds with sodium-side cracking in one unit, and about 20 in the other. This led to a major review of the tube-to-tubeplate weld problem

With leaks having occurred in all three evaporators and a sodium-side origin of cracking in evidence, it was decided that the most practicable solution was to by-pass the suspect tube-to-tubeplate welds by using a sleeve. Each sleeve was a precisely machined cylindrical tube of a 9Cr1Mo steel inserted into the tubeplate and extending downwards into the top 75mm of the tube. The upper end of the sleeve was explosively welded to the tubeplate and the lower end was braised into the inside of the tube [Fig. 2.16].

Following extensive laboratory trials, four experimental sleeves were first fitted to operational evaporators towards the end of 1980. A further 11 evaporator weld leaks occurred in 1981 and a further 41 sleeves were fitted to by-pass defective and suspect welds. In parallel, work was in progress to examine whether the sleeving technique could be applied on a routine basis. A trial installation of 200 sleeves was conducted on the spare evaporator tube bundle in the latter part of 1982. A decision was then made to sleeve all the 3000 tube-to-tubeplate junctions in the three evaporators. Work on two of the units was completed in 1983 and the third unit was sleeved by March 1984. It was installed in the summer and PFR operated for the first time with three fully-sleeved evaporators in August 1984.

From then, until operations ended in March 1994, there were no further problems with the evaporators.

Temperature profiles in the reactor vessel. The vertical temperature profile up the wall of the primary vessel was required to be free from steep gradients to ensure that normal plant manoeuvring or trip action did not give rise to unacceptable thermal stresses as the sodium level in the vessel changed. The top of the vessel was at roof temperature, about 50 C, and the vessel wall at and below the sodium level was at the outer pool sodium temperature, about 400 C. The shape of the temperature profile in the section of the primary vessel (the "top strake") between these steady values was determined by the combined effect of the tapered external thermal insulation and the forced cooling by the roof cooling argon supply. During commissioning of the reactor, the temperature profile was found to have an unacceptably steep gradient in the region just above the sodium level, and this would result in unacceptable cyclic

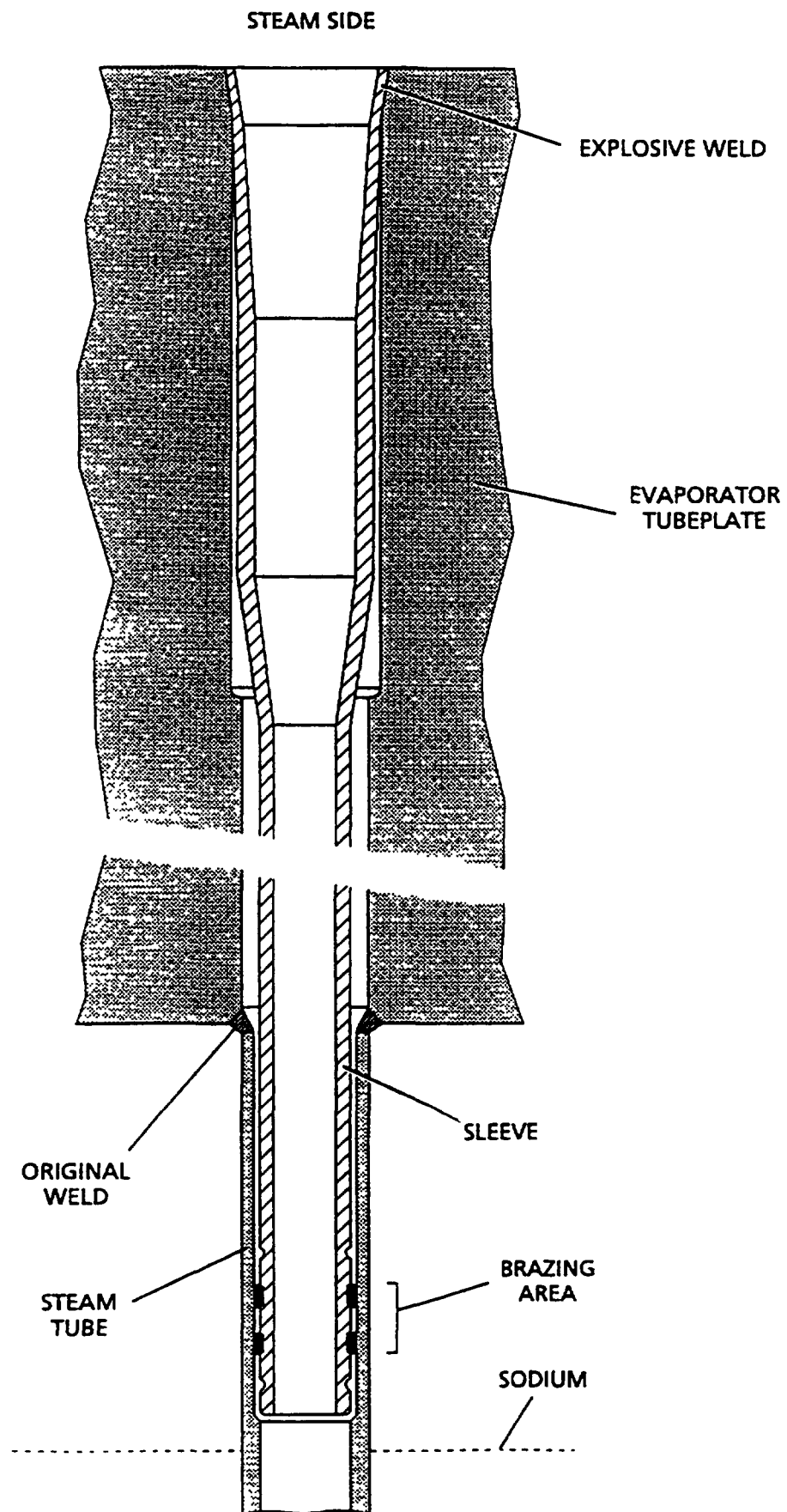


Figure 2.16. Sleeving to repair the evaporators

thermal stressing as the sodium level changed. The roof cooling system was modified to deal with this; a more positive control of the cooling gas flow was achieved by installing independent diverter valves around the vessel circumference to reduce the cooling flow over the vessel. Structural analysis suggested possible creep ratchetting of the vessel in an inward radial direction and though, at the time when it was decided to introduce the remedial measures, no distortion of the vessel could be perceived, linear displacement transducers were fitted at five locations around the tank and at thirteen vertical positions to monitor the situation. In ten years of monitoring (1975-1985) no significant changes were detected in the surveys and monitoring was then discontinued.

Flow-mixing phenomena. PFR was fitted with extensive primary circuit instrumentation for use during the commissioning and operation of the plant. This instrumentation, supplemented by special rigs, proved to be invaluable, in association with laboratory facilities, in providing information on primary circuit performance, and, in particular, on flow-mixing phenomena. In the above-core plenum of PFR, temperature fluctuations arose in regions where the flows from core and breeder assemblies mixed. This subjected the above-core structure and its supports to thermal striping. Extensive studies concluded that there were no constraints on operation which would restrict output at design power. In circumstances where steam generator leaks led to operation on less than three secondary circuits, a small flow of sodium at core outlet temperature past nominally-shut sleeve isolation valves in the IHXs which were not in service provided a potential for mixing of sodium flows at core inlet and core outlet temperatures and hence to possible thermal striping damage to the IHXs and their containment pods. These effects were extensively studied in laboratory rigs and resulted in the setting of limits on the core temperature rise when PFR was operating on less than three circuits.

Core distortions. PFR was designed before one of the two irradiation-induced phenomena affecting the dimensional stability of reactor core structural materials exposed to a high fast neutron flux had been discovered (void swelling) and before the other had been characterized (irradiation-induced creep). By the time operations began, however, the possible impact of both phenomena on the major core components (fuel assembly wrappers, pin cladding, and control rods and their guide tubes) had been evaluated. The guide tubes had been designed to be replaceable, but work was initiated to develop special tools to rotate the guide tubes during refuelling in order to extend their life.

In addition, development work to identify the swelling and creep-resistant alloys which would be necessary to tolerate these phenomena in a core designed to accommodate neither had proceeded sufficiently far to indicate that the austenitic steels chosen for the core components for PFR were far from optimum choices. It was decided, therefore, that major core components should be regularly monitored by measuring dimensional changes and curvatures as they were removed from the core and transferred to the fuel cave, and by using the charge machine at shutdowns to monitor length changes of fuel assemblies in situ. In addition, free movement of the control rods in their guide tubes was regularly monitored during operations. To guide the schedule of measurements, a predictive code, CRAMP, which modelled the core distortions due to void swelling, calculated the resultant stresses arising from swelling-induced interactions between components, and then estimated the creep-induced responses to these stresses, was developed.

The in-core life of some sub-assemblies, particularly those with solution treated austenitic stainless steel wrappers, was determined more by the irradiation-induced distortions

than by the performance of the fuel itself. It was, however, possible in some cases to extend in-core life by rotating the assemblies so that bowing due to irradiation in a neutron flux gradient would be offset by further irradiation and the amount of bowing would not exceed that acceptable for extraction through the fuel discharge route. The risk of severe core component distortions thus needed continuous attention in the early years of operation but, in later years, the definition of management procedures based on earlier experience and the increasing use of swelling-resistant alloys (ferritic steels or high-nickel alloys) in fabricating wrappers, guide tubes and other components effectively eliminated the problems.

Conventional plant. Although this paper is concerned primarily with experience of operation of the nuclear island, it is relevant to note that several improvements were made to the conventional plant during the first decade of operations, to increase availability and to reduce plant outages arising in this area. Early bearing failures on the turboalternator were remedied. The plant as originally designed had only a single steam-turbine driven feed pump, and a 50% capacity auxiliary electrically-driven pump was installed as back-up. Following trips initiated by the direct-contact feed heaters, improvements were made to their protection systems. Considerable work was undertaken to increase the capacity of the water treatment plants and the capacity for storing treated water. Ingresses of seaweed, restricting the seawater cooling flow to the main condenser and to other key plant ancillaries, caused reactor trips and significant loss of availability in the early years. Improvements to plant in the seawater pump house only partly alleviated the problem and in 1980 it was decided that a more radical solution should be sought. Modelling trials by a hydraulics consultancy led to a decision to construct a barrier with a low-tide by-pass channel on the foreshore at the seawater inlet. Construction was completed in 1987, and subsequent experience proved its effectiveness.

Station operations. Though the load factor of the station in the first ten years of operation never exceeded 12%, the first decade was also marked by many significant achievements. The primary circuit, the primary and secondary sodium pumps and the intermediate heat exchangers all proved to be very reliable in operation. Reactor availability figures of 80% and over were recorded in five of the years. The station was synchronised to the grid for the first time in January 1975 and in early February, with the reactor at 200MW(th), 40MWe was exported from the site. In July 1976, operation at 500MW(th) generated 150MWe and full core power of 600MW(th) was reached on 25 February 1977; electrical generation was limited to 200MWe, however, because of the absence of Reheater 3 and operation of the steam plant outside its design conditions because of feed heating problems. Generation throughout the period up to 1983 was, however, intermittent, for reasons already discussed, and the maximum net generation in any one year was 9,678 MW days in 1978 at a load factor of 12.2%.

Fuel development. Major advances were made during the first decade of operation in the development of fuel, and PFR's Demountable Sub-Assembly (DMSA) facilities, in which independent clusters of up to 19 fuel pins could be irradiated to test both materials and design variants and to explore operational limits, provided a capability to mount a major fuel development programme. The initial target burn-up for the PFR driver fuel was 7.5% (heavy atoms) and by the end of 1983 it was evident that this could be raised since, by that time, approaching 10,000 pins had exceeded the limit without failure and a significant number of pins had either exceeded or were approaching 10% burn-up. It was, however, recognised that the variability in the swelling behaviour of the specified M316 austenitic stainless steel cladding (caused by minor variations in composition which could not be reliably controlled in the manufacturing process), the absolute magnitude of the swelling in the most susceptible batches,

and doubts on the ability of the material to withstand fission gas plenum pressures at higher burn-ups without exceeding creep design criteria, would never allow the achievement of the burn-up targets then being contemplated for commercial stations (12.5 to 15%). However, the swelling resistance of the high nickel alloy, Nimonic PE16, had been recognised ever since the first experimental studies of void swelling at Dounreay in the mid-1960s and Nimonic PE16 was replacing the austenitic stainless steel as cladding in new batches of fuel.

Though there had been no fuel pin failures in the driver charge fuel, there had been a handful of failures in experimental fuels. These were not an operational problem. As has been noted, PFR's predecessor, the Dounreay Fast Reactor (DFR), was successfully operated for 18 years with metallic fuel in fully vented cladding. However, in designing PFR and switching to oxide fuel, it had been decided that the reference fuel would have hermetically sealed cans, though reservation of an option to include a partial loading (as much as one-third of the core) of vented fuel had led to the incorporation in the cover gas circuit of facilities to monitor and, if necessary, to deal with the presence of fission product gases. Equipment to locate fuel failures in the core was also provided. Experience in the oxide fuel development programme in DFR had shown that the normal failure mode of a hermetically-sealed oxide fuel pin is the development of a thin crack in the cladding, releasing fission product gas into the coolant. Later - as much as 70 days or more later - the defect may develop to bring fuel into contact with sodium. PFR was provided with delayed neutron signal instrumentation to detect this development and DFR experience indicated that this was the stage at which removal of the fuel became advisable; until this stage, the "gas leakers" were not an impediment to continued reactor operation. PFR experience with the failed experimental pins confirmed this strategy, and showed that the bulk delayed neutron detection system, located in the intermediate heat exchangers, provided adequate protection against a large rapidly developing failure.

PFR after ten years. With 10 years of operations completed in March 1984, it was appropriate to review the situation and to speculate on the future. The major impediment to sustained high power operation in the early years - the defective tube-to-tubeplate welds of the evaporators - was being dealt with by an engineering solution (the sleeving of every tube-to-tube plate junction to by-pass the suspect welds) and three fully sleeved units would be available for service later in the year. After initial problems, which led to the removal of one of the reheaters, the superheaters and reheaters had been kept in service after plugging the tubes with defective welds and devising a technique for removing all traces of caustic from the undersides of the tube plates by washing with hot sodium. Replacement tube bundles for the superheaters and reheaters were due to be delivered to the site within the new few months and this would allow reheater 3 to be brought back into service. Several parts of the conventional plant - valves, the dump system, the feed pump and the condenser coolant inlet channel - had all been modified to improve plant flexibility and the reliability of operations. All of the major components of the primary circuit - the pumps, the intermediate heat exchangers and the reactor control systems and instrumentation - had performed without problems. Most significantly, PFR was already showing excellent fuel performance with the prospect of even more significant advances as early choices of cladding and wrapper alloys, selected only for compatibility, fabricability and mechanical property qualities, were replaced by new materials more resistant to the endurance-limiting effects of void swelling and irradiation creep. The prospects in mid-1984 seemed good.

2.3.2.2. The second decade 1984-1994

The second decade of operations were to see these prospects largely fulfilled.

Station operations. The annual operating statistics [Table 2.3.] and the histogram derived from them [Fig. 2.13.] show the marked improvement in load factors. For most of 1984, only two secondary circuits, with sleeved evaporators, were available and this was the major factor reducing output. A sodium pump bearing seizure caused an extended shutdown as did a fire in a secondary circuit cell, resulting from a leak of some tens of kilogrammes of sodium after a small-bore pipe failure in the gas space hydrogen detection system of Superheater 1. A leak in one of the decay heat rejections loops (actually the fourth such leak, but the first to impede reactor operations) led to a decision to order new ones of modified design.

In 1985, PFR was able to operate, for the first time since the commissioning period, with a full set of steam generator units. A reload-to-reload run of 135 days duration, generating 486,000MWh at a turbine load factor of 65%, was achieved during the year. This was a particularly bad year for seaweed ingress, with the new mid-tide barrier being not yet completed. It was estimated that 125,000MWh of generation was lost to this cause during the year. In 1986, a continuous turbine run from 23 August to 11 October generated 276,000 MWh of electricity at a load factor of 92.5%. A fuel assembly still in serviceable condition at 15.9% (heavy atoms) burn-up was discharged from the core for examination.

In 1987, a major tube failure in Superheater 2 led to PFR being off-line for 6½ months while the aftermath was dealt with and the replacement tube bundles were deployed. There was also the first sodium leak from a reheater vessel. However, in spite of these problems, PFR returned a very creditable gross annual load factor of 41.8% during the year. In 1988, there were further problems with a reheated vessel leak, but the year saw a continuous high-power run of 41 days from 19 March to 29 April in which 230,100MWh of electricity were generated at a load factor of 94%.

PFR's best full calendar year of operation was 1989, with gross generation of 47,231MWd of electricity at an annual load factor of 51.8%. The station operated for 230 days. The major achievement of 1990 was the licensing of the station by the UK Nuclear Installations Inspectorate. Prior to this the station had been licensed by its owner-operator's internal procedures, and independent licensing of the 16 year old plant was both a major achievement and a vindication of the standards previously used.

Operations in 1991 and 1992 were severely affected by a leakage of bearing oil from one of the primary pumps into the primary sodium coolant which took PFR out of service from 29 June 1991 until 30 December 1992. Operations then continued until 11 July 1993 - 119.5 effective full-power days in which 25,706MWd (gross) of electricity was generated at a load factor of 53%. A second run later in the year generated 14,955 MWd (gross) of electricity at a load factor of 58%.

PFR was started up for the last time on 14 January 1994. An output of 240MWe was achieved on 16 January and operation continued at this level until the final shutdown on 31 March. In this period, 18,160MWd (gross) of electricity was generated at a load factor of 93%. So, in its final weeks of operation, PFR achieved its highest ever load factor for a single run. The continuous turbo alternator output of 18,160MWd exceeded the previous record of 13,570MW set in March 1991. The total electricity generation in the last year of operation (April 1993 to March 1994) was 51,546MWd with a load factor of 56.5%. The previous best in any twelve-month period was 48,170MWd with a load factor of 52.8% achieved in 1989/90.

Fuel performance. One of the principal tasks of PFR was to demonstrate a reliable, safe and robust fuel capable of routinely achieving a high burn-up target. Successful completion of this task is one of PFR's major achievements.

The major advances made in the second decade of PFR operations resulted from the introduction of Nimonic PE16 as the reference cladding alloy. The fuel assembly discharged at 15.9% burn-up in 1986, mentioned earlier, gave the first indications of the benefit of this change. The pins showed maximum diametral increases of only 1%, with uniformly low diametral change profiles showing little pin-to-pin variability, compared with the 5-8% (maximum) diametral changes and highly peaked profiles showed by earlier examinations of pins clad in cold-worked M316 steel and irradiated to half the exposure. Destructive examination of the pins indicated that the fuel column was stable, that internal corrosion was low and that there was no evidence of any fuel/clad mechanical interaction resulting from containment of a high burn-up swelling fuel in a non-distending cladding tube. This confirmed that higher burn-ups were probably feasible. Measurements of the PE16 wrapper showed trivial length increase, across-flats distension and bowing, and revealed no potentially life-limiting changes.

By 1990, irradiations of PE16 clad fuel pins in driver assemblies and in DMSAs had achieved more than 17% and 21% burn-up respectively. Even with displacement doses of the order of 130 displacements per atom no life-limiting features could be identified in either the wrappers or the cladding.

Meanwhile materials irradiation experiments had shown ferritic/martensitic steels to be particularly resistant to void swelling, and while the high temperature mechanical strength of these materials seemed to preclude their use as pin cladding, application as wrapper materials seemed to be practicable. Accordingly, in the late 1980s driver fuel assemblies with wrappers of the ferritic/martensitic steel FV448 and pins clad in Nimonic PE16 were introduced into PFR. By the end of the reactor's working life, over 20 such assemblies had been loaded and seven of these had exceeded the 15% burn-up (110dpa) target; one had achieved the then world record, for a mixed-oxide driver charge assembly, of 19.8% burn-up (155dpa).

The fuel in all of these high burn-up assemblies was high intrinsic density annular pelleted mixed oxide, and this was the reference variant in the UK fast reactor fuel development programme. It was, however, recognised that vibrocompacted fuel offers advantages with respect to fuel fabrication costs and this variant also featured in the programme. Almost 3000 pins containing vibrocompacted fuel were irradiated in PFR but failures in several pins due to fuel column instability at burn-ups in the range 1-10% confirmed the wisdom of concentrating on annular fuel and studies of vibrocompacted fuel ended in the mid-1980s.

In the drive for better commercial fast reactor station economics the possibility of annual refuelling became a design option. This led to consideration of lower mass-rated, larger diameter pins. PFR, with the capability to accept both DMSA and full assembly irradiations, was ideally suited to parallel testing of pin design variants of different diameters and a programme covering the range 5.84 to 8.5 mm was developed over the final few years of operation. Unfortunately the target burn-ups for the largest diameter pins (20%) could not be reached before the reactor operations ended, and the maximum attained was 10%.

Statistics illustrate the undoubted success of the fuels development programme in PFR. Approximately 98,000 pins were irradiated and, of these, over 40,000 exceeded the original 7.5% target burn-up. The introduction of PE16 as cladding allowed over 2,400 pins to attain burn-ups in excess of 15% with about 320 of these having successfully exceeded 20% at the end of operations. The peak burn-up achieved (in lead pins irradiated in a DMSA) was 23.2% (135dpa).

The overall failure rate of PFR fuel pins was remarkably low, considering the number of experimental variants examined in the programme. Of the 23 failure events which occurred in the 20 years of reactor operation, the majority could be linked either to experimental design features or to the less-stable vibrocompacted fuel form. In statistical terms, the failure rate for the vibrocompacted fuel pins irradiated in PFR was 7.4 in 1000 while for all annular variants the rate was 0.2 in 1000. It should be noted, in comparing these figures, that the burn-ups experienced by vibrocompacted fuel pins were significantly lower than those achieved by annular fuel pins. The failure rate for pins clad in Nimonic PE16 was 0.21 in 1000. Four Nimonic PE16 clad driver fuel pins actually failed. Three of the failures were in pins which had exceeded 17.5% burn-up. The fourth failure, which occurred at a burn-up of 11.5%, arose from a suspected fabrication defect. In all four cases, the rate of development of the failures allowed adequate time for the reactor operators to observe the slow development of the failure, and in one case, irradiation was continued for 45 days after the leakage of fission product gas was detected. In no case was there any significant loss of fuel from the failed pin and there was no evidence of pin-to-pin failure propagation.

Breeder assembly operating conditions differ substantially from those experienced by the fuel assemblies. Breeder pins operate initially at a mass rating which is approximately one-tenth of that of fuel pins, but this rating increases as burn-up proceeds. As the breeder assembly flow is set prior to irradiation to give acceptable pin cladding temperatures at end-of-life ratings, the pins are therefore overcooled at start-of-life and this, and the lower neutron fluxes experienced in the breeder zone, combine to increase the risk of mechanical interaction between the breeder pellets and the cladding. The target burn-up for the PFR breeder was therefore set at a conservative 1%. More than 4,250 breeder pins exceeded this target in PFR, with apparently no failures. Examination of breeder pins clad in Nimonic PE16 and irradiated to burn-ups close to 3% showed no evidence of excessive plastic straining of the cladding. PFR experience therefore suggests that a burn-up target of around 2% would be a reasonable initial aim in future reactors.

Specific aspects of operational experience. The performance of the steam generators which had so affected reactor operations in the first decade was to give little cause for concern in the second. The sleeved evaporators operated throughout the period without problems. There was, however, a failure in Superheater 2 on 27 February 1987 which led to a major leakage of steam into the secondary circuit sodium. Examination of this austenitic steel unit after the leak event revealed a fretting failure of a single tube which had been subjected to unexpected flow-induced vibration. In the sodium/water reaction event which followed, 39 neighbouring tubes also failed. This event rendered the unit unserviceable and it was decided to install one of the replacement tube bundles, stored on site as strategic spares since 1984, in its place. Consideration of the location of the fretting suggested that the possibility of a similar problem arising in the other original units could not be ruled out and it was decided to replace all of them. This led to a 6½ months outage for the station. Observations of damage due to vibration in the units after removal indicated the wisdom of the decision.

The under-sodium leak in Superheater 2 was important for a number of reasons. It involved 40 tubes, yet the automatic protection system coped with the incident despite the severity being beyond that for which the system had been designed. In addition, analysis of data led to a complete reappraisal of the consequences of sodium/water reactions in steam generators. It also revealed the problems caused by not being able, in PFR, to clean up the intermediate heat exchangers independently of the contaminated secondary circuit - problems which took two months to circumvent. (Dump tanks of greater capacity would have eased the clean-up work). The main lesson for the future is that great care is needed in steam generator design to avoid tube vibration and that the earliest possible indication of a leak is essential if tube-to-tube failure progression is to be avoided.

The only other problem with the steam generators in the second decade was the observation of deteriorating welds in the stainless steel outer vessels of the superheaters and reheaters. Leaks in reheater vessels in 1987 and 1988 revealed cracks (in one case over 100mm long) in the original interplate welds. Subsequent inspections of the other vessels revealed large but non-penetrating cracks, similarly located in two of the superheater vessels. All of the cracks were in welds which had been reworked during fabrication or where fabrication welds had overlapped. It was decided that the defects should be cut out after dumping the sodium and that the vessels should be repaired. However, one of the non-penetrating cracks in the Superheater 3 vessel was left in situ after assessment indicated low likelihood of rapid propagation. Strain gauges were fitted to the crack region as monitors. Two repair methods were used. In the earlier one, the excised region was filled with weld metal against a backing plate. One of these repairs was to be the cause of a further leak in 1990. In the later repair technique, a circular stub surrounding the defect area was welded on, the defect was then removed and the vessel was re-sealed by welding a cap on to the stub end. In subsequent years this method was evolved into a "stood off" patch, with the crack being left in situ with holes drilled at both ends to act as crack stoppers.

Investigation of the problem indicated that the cracks were initiated by delayed reheat cracking and grew by a high temperature brittle intergranular mechanism driven by the residual stress field.

The condition of the vessels became of increasing concern in the final years of operation and the need for regular examination significantly extended shutdown times. The basic problem was one of choice of material; a problem of availability of material during fabrication led to the use of a stabilised stainless steel and this resulted in a susceptibility to delayed reheat cracking.

Oil in sodium. The only primary circuit event ever to affect plant performance significantly occurred on 29 June 1991, when the reactor was manually tripped, following observations of overheating on the top bearing of a primary sodium pump. Remedial work was expected to take more than a week and, with a scheduled annual maintenance shutdown only two weeks away, it was decided to advance the shutdown and to begin preparatory work for the planned refuelling and maintenance.

It soon became clear that a significant quantity of oil (possibly up to 35 litres) had been lost from a primary pump upper bearing and had entered the primary sodium circuit. Replacement of the pump bearing and cleaning the primary sodium would be required before the reactor could return to power. To clean the primary sodium, it was necessary to rebuild the cold trap loop, which required procurement of a new basket, which was installed early in

November. The impurity burden in the primary circuit could be monitored through the plugging temperature of coolant within the cold trap. When clean-up began this was 225 C but reduced steadily to below 170 C by the end of the year, when the primary circuit was temperature cycled up to 420 C and then back to 310 C. This caused the plugging temperature to rise to 180 C, but a further phase of clean-up which reduced the plugging temperature to 150 C was completed by the end of January 1992.

The top bearing of the primary sodium pump concerned was replaced in September and the pump was successfully run-in at half speed in early November, but when full speed tests were attempted, these had to be stopped as a result of high pressure in the oil drains tank - over five times the corresponding pressure on one of the other primary pumps. Further tests showed that the flow route from the bottom bearing and out through the pump case was restricted. Variations in pump speed cleared the blockage, which is believed to have been caused by oil degradation products.

Further suspicions of deposition of oil degradation products arose from observations that, just before the shutdown on 29 June, there had been indications of temperature increases in a number of core sub-assemblies, suggesting reduction of coolant flow through the inlet filters.

Attention therefore turned to the primary pump filters and it was decided, as a precautionary measure, to examine all three of these, as well as some of the core sub-assembly filters, to check their condition. Removal of the pump filters was a major task never before attempted.

Work to recover from the oil ingress problem, most particularly work to install new primary pump filters, occupied almost the whole of 1992.

Deposits incorporating some carbon were found on all three filters removed. Some difficulty was experienced in fitting new filters because of the distortion of some thermocouple guide tubes and it was necessary to cut these away to complete the task.

Examination of a number of fuel assemblies also showed deposits on the inlet filters of those which had shown temperature increases prior to shutdown, but none on assemblies which had shown no increases. However, the deposits were sparse (about 0.5g) and mainly of sodium. It was thought improbable that these were sufficient (even allowing for the possibility of some loss during handling) to cause the observed temperature rises and contamination of the cladding surfaces by adsorption of oil degradation products was postulated to be a contributory factor.

Work on the reactor was supported by laboratory studies to examine the effects of temperature, sodium and irradiation on both new and degraded oil. These included cooperative work with the Institute of Physics and Engineering at Obninsk to replicate in a rig the introduction of PFR pump bearing oil into flowing sodium upstream of a PFR subassembly filter.

The totality of information acquired was submitted to the UK Nuclear Installations Inspectorate, the licensing authority, and consent to restart operations was given on 23 December. Criticality was achieved on 30 December 1992.

The outage of just over 18 months indicated the importance of designing to avoid any possibility of spillage of oil from pump bearings into the sodium coolant. There is, however, also a more general inference of the desirability of designing for easy removal of major circuit components to cope with unforeseen eventualities.

Decay heat removal loops. The normal route for the removal of decay heat in a fast reactor is via the secondary sodium circuits and the steam plant. Should this route not be available, decay heat in PFR could be rejected by one or more of three thermal syphon loops, each filled with eutectic sodium/potassium alloy. Each loop extracted heat through an immersed coil, intercepting some of the primary sodium as it flowed from the core towards an intermediate heat exchanger, and delivered the heat by natural convection to the outside atmosphere through a sodium-potassium/air heat exchanger built into the wall of the secondary containment building.

In March 1975, a leak occurred as a result of failure in a welded pulled-tee connection between one of the forty parallel cooling tubes and the header in one of these heat exchangers; the failure was attributed to a cold tear which developed during manufacture and a repair was effected by fitting a replacement tee. Similar leaks occurred in 1981 and 1982. Strain gauges and thermocouple were fitted to one of the loops and these revealed considerable temperature anomalies in a number of the tubes.

Measurements on the original heat exchangers and on a laboratory simulation suggested that the temperature differences between the tubes were caused by a reduction of sodium-potassium alloy flow, caused by gas locking in the bank of parallel cooling tubes, some of which were horizontal. In some cases, the flow reduction was compounded by deposition of impurities in places where the flow, and hence the temperature, was low. The temperature differences were sufficient to induce low frequency high strain fatigue as a consequence of normal plant manoeuvring. Vacuum filling of the heat exchangers and batch cold-trapping of the coolant improved but did not eliminate the problem.

Specimen pulled tees were subjected to cyclic strain and a stress versus cycles-to-failure curve was established. From this an allowable operating curve was derived, using measured plant data to define the strain history, and a damage account was maintained. Non-contacting displacement transducers were fitted to 240 positions on the heat exchangers to provide strain measurements to define fatigue development.

With these precautions, operation of the reactor was continued with visual examination of all the tube-to-header connections after specified fatigue damage increments. This, however, could only be an interim measure as it did not remove the underlying cause of the problem. In 1985, therefore, new heat exchangers for the decay heat removal loops were designed with this aim in mind. These new units incorporated heavier gauge headers, a modified geometry of the entry and exit connections of the tubes, a reduced-constraint tube support arrangement, and a slope (2° to the horizontal) in the tubes to reduce the possibility of gas locking. Two of the new heat exchangers were installed in 1986 and a third in 1988. All three were heavily instrumented and performed as designed for the remainder of PFR's operating life.

2.3.3. Advanced technology developments

PFR was also used to test advanced technology developments of potential interest in future fast reactors. Thus, as an example, in 1982, an under-sodium viewer, specially

developed for PFR by the AEA's Risley Nuclear Laboratories, was installed in the reactor during the long maintenance shut-down. Echoes of ultrasonic pulses were detected and stored in a computer for processing into a colour image, showing detail of the top of the core, which was submerged under 5 meters of sodium at 250 C. The viewer could be mounted in three positions on the top rotating plug and rotation then allowed an annular scan from each position. The total viewing area covered about 60% of the top of the core. The computer-generated images were of excellent quality, and the orientation bars and code rings on individual assemblies could be clearly seen. Colour imaging allowed differentiation of the heights of the tops of the assemblies. Comparison of data from the viewer with data obtained by using the charge machine to measure the assembly heights showed excellent agreement, and though the under sodium viewer was not used again in the reactor this comparison gave considerable confidence in the practice of using the charge machine to monitor wrapper growth. The viewer images also provided information on the lateral displacements of the tops of the assemblies due to bowing.

A single channel trip system was developed for CDFR to detect abnormal behaviour in a single fuel assembly and to shut down the reactor, if necessary. It was installed in PFR on a test basis to demonstrate its ability to detect circumstances needing shut-down action. This technology was subsequently applied to Nuclear Electric's Dungeness B Advanced Gas Cooled Reactors which because of problems in ensuring the integrity of coolant flow gags had been operating at low power for many years. The single channel trip system - known as ISAT - which was installed in the Dungeness B reactors allowed Nuclear Electric to satisfy the licensors that the reactors had the necessary protection system to allow them to be operated at the design power.

The early problems with the steam generators highlighted a need to improve non-destructive methods of detecting small flaws in relatively inaccessible welds. A major programme of development work led to major refinements, particularly in ultrasonic techniques.

2.3.4. PFR safety and licensing

The design of the PFR was intended to minimise the frequency and severity of accidental releases of radioactivity. This was achieved by "defence in depth" incorporating: (a) sound engineering design coupled with a high standard of material specification, fabrication and pre-service inspection; (b) the provision of instrumentation to detect divergences from normal operation and, if necessary, to initiate reactor shutdown using the fail safe shutdown system provided; (c) the provision of multiple containment barriers between fuel and the environment, including a high pressure capability plant containment; (although the primary circuit is little above atmospheric pressure) and an overall building containment, both aimed at defence against very low probability accident situations; (d) the provision of a reliable decay heat removal capability, and (e) the use of redundancy, diversity, segregation and emergency power supplies to achieve a high degree of reliability for the operation of the engineered safeguards in (b) - (d) above.

The achievement of this policy was quantified in a probabilistic risk assessment (PRA) for the plant, judged against the frequency/severity criterion recommended for a prototype reactor at a remote location. PRA was used throughout PFR's history to improve the quality of the safety arguments. The 1974 risk assessment was revised in 1984, and again in 1990 as part of the preparations for licensing of the AEA by the Nuclear Installations Inspectorate (NII).

Engineered safeguards. PFR was protected by an automatic protection system (APS) to detect abnormal conditions and to shut down the reactor automatically if necessary. The APS was designed to be fail safe, to be robust and to provide redundancy and diversity. For example, there were two completely independent sub-systems with separate power supplies operated from separate parameters, constructed from different hardware and feeding separate groups of control and shut-off rods. Of the total of ten rods, the insertion of any three would shut the reactor down. Both sets of absorbers were exercised routinely to demonstrate their availability. Exercising was seen originally as providing an early warning of swelling, through neutron-induced voidage, restricting rod movement. Experience showed this concern to be unfounded, but it also showed the value of continued routine rod exercising to limit the effect of sodium deposition on the rod internals from sodium aerosol in the cover gas blanket. The total number of rod drops was well over 3000 and on no occasion did any rod fail to reduce reactivity on demand.

There were multiple barriers between fuel and the environment. The fuel in each fuel pin was hermetically sealed within a strong stainless steel clad; the fuel pins were immersed in a sodium pool able to retain chemically a number of important fission products, should a fuel pin fail; the coolant was contained within the primary containment (the reactor vessel, the biological shield roof and, surrounding the reactor vessel, the leak jacket); over the biological shield roof was the secondary containment building which incorporated a post-incident clean-up plant. The latter ensured that any radioactive release to the environment, even following a major incident would be kept to a minimum.

There must be a highly reliable means of removing decay heat from the primary circuit. To insure against non-availability of the secondary circuits and steam plant, PFR was provided with the three independent decay heat rejection loops.

Inherent safety properties. PFR possessed inherent safety features which would allow it to survive a range of very improbable incidents, even in the highly unlikely circumstances of failure of the engineering safeguards. The major inherent safety features were natural circulation (within the NaK filled decay heat rejection loops and of the primary sodium coolant) and the reactor's negative temperature and power coefficients.

Loss of electrical supplies to the PFR would result in a trip of the reactor and the run down of the main coolant pumps. Because of flywheels the primary pump speed halving time was 10 seconds, and the pumps would stop after approximately 200 seconds but for the clutching-in of the continuously running pony motors which maintained a pump speed of 10%. Should all three pony motors or their clutches fail to operate, reactor experiments demonstrated that natural circulation of the hot sodium in the core would transfer the core decay heat to the 900 tonnes of primary coolant. The decay heat could then be transferred to the atmosphere via the naturally circulating decay heat rejection system without the sub-assembly outlet temperatures exceeding normal operating levels.

When the temperature of the PFR primary circuit changed there was a consequential change in the reactor power, which arose from a combination of structural and neutronic effects, the overall result of which was that an increase in temperature caused a decrease in power; that is, PFR had negative temperature and power coefficients. Negative power and temperature coefficients represented a potentially powerful safety feature in the highly unlikely case of a failure of the engineered safeguards, making the reactor remarkably robust against a loss of cooling event.

It is also an inherent safety feature of pool type fast reactors that the personnel radiation dose is low, between one and two orders of magnitude lower than for light water reactors. Table 2.5. summarises the average dose to operators since 1981.

Licensing. For the early years of PFR operations, the station was licensed to operate by internal UKAEA procedures. Because of the wide range of its activities, the AEA had been exempted from the provisions of the Nuclear Installations Act of 1965, which set up a governmental organization, the Nuclear Installations Inspectorate, NII, with national responsibility for licensing activities involving operations with nuclear materials. The AEA set up an internal system, supervised by its Safety and Reliability Directorate and independent of the Divisions operating the nuclear facilities, to ensure comparable standards to those of the NII. In 1990, however, the UK government decided that, to ensure a publically demonstrable consistency of standards, the AEA's exemption should be ended, and all of its nuclear facilities became subject to NII licensing. After a thorough examination of the design of the plant, a review of the operating procedures and an assessment of experience from 16 years of reactor operations, PFR was given an NII license to continue operations in 1990.

The successful licensing of a 16-year-old plant was a major achievement and confirmed the validity of the internal AEA practices previously in operation, and the soundness of the original design.

2.3.5. PFR and the fuel cycle

Fast reactors, through their ability to extend uranium resources by breeding plutonium, require parallel development of fuel cycle facilities. Thus, in the UK, when the decision was made by the UKAEA in 1954 to build the metal-fuelled DFR, it was also decided that dedicated fuel fabrication and reprocessing plants would be located with the reactor at Dounreay. A third fast reactor-oriented fuel plant to make small batches of, initially cermet, and, later, oxide and carbide fuels for the test programme in DFR, was also built at Dounreay.

TABLE 2.5.

Average Dose (mSv) to PFR Operators

Year	Average Dose (mSv)
1981	1.5
1982	2.0
1983	0.2
1984	0.3
1985	2.1
1986	0.9
1987	0.9
1988	1.9
1989	1.0
1990	1.2
1991	1.2
1992	0.8
1993	0.6

For the larger oxide-fuelled PFR, collocation of the reactor and its associated fuel plants was not practicable. The larger quantities of fuel involved favoured the industrial scale involvement of British Nuclear Fuels, whose Magnox reactor fuel reprocessing plant at Sellafield would provide the initial plutonium inventory. It was, therefore, decided that the PFR oxide fuel fabrication plant would be built and operated by BNFL at Sellafield and that fuel would then be transported to Dounreay as completed assemblies ready, after inspection and adjustment of the coolant flow control gags, for irradiation. The small experimental fast reactor fuel fabrication plant was moved from Dounreay to the AEA's Windscale Laboratory, adjacent to BNFL Sellafield, to provide R&D support to the main fuel fabrication plant and to supply small batches of experimental variants for incorporation by BNFL into DMSA clusters and driver fuel assemblies.

In the late 1980s, with UK partnership in the European Fast Reactor Programme, it was decided, for economic reasons, to close the Sellafield fabrication plant which, because of the high burn-up levels being achieved in the PFR driver fuel, had for some years been operated at well below its design throughput, and to take advantage of spare capacity on the Commissariat à l'Energie Atomique's fast reactor fuel fabrication plant at Cadarache to provide fuel for the remainder of PFR's operating life.

A decision had been made in 1972, however, that PFR fuel would be reprocessed at Dounreay and studies of modifications to the existing DFR fuel reprocessing plant were begun. A need to increase plutonium throughput by a factor of 1000, and a factor of 10 increase in fission product activity, demonstrated the need for an extensive change to the plant and the construction of additional waste management facilities for the treatment and storage of plutonium contaminated waste.

In outline, reprocessing was based on disassembly of the fuel assemblies to individual pins, single pin cropping, dissolution in nitric acid and operation of a Purex-type flowsheet in a chemical separation plant equipped with pulsed mixer settlers. The modified dissolver cell and solvent extraction plant were recommissioned late in 1979 and were tested in reprocessing of the final batches of DFR fuel. The new head-end facility, to disassemble the PFR fuel assemblies and to crop the pins, and the new waste treatment facilities were commissioned in 1980; reprocessing of the first batches of PFR fuel began later that year.

After removal from the reactor rotor, the fuel assemblies were retained in the reactor fuel handling cave - initially under sodium coolant to allow fission product heat decay. The handling and location features were removed by laser cutting and the fuel section of the subassembly was exposed to a moist inert gas stream (steam cleaning) to remove residual sodium, the bulk of the sodium already having been drained. The fuel subassembly was finally washed with demineralised water and soaking for three to four hours. The system was drained and the fuel subassembly allowed to dry. The fuel subassembly was sealed in a nitrogen-filled transfer can for transfer to the reprocessing plant or to the water cooled irradiated fuel store at the reactor.

Steam cleaning proved to be a most effective operation and very little residual sodium was observed in the reprocessing cave during fuel disassembly.

Following transfer to the reprocessing plant, the fuel assembly transfer can was opened. A section of the wrapper was then removed using laser cutting to expose the fuel pin ends. (A 400 watt laser was originally used but was found to be working close to its limit and was

replaced by a 1200 watt unit in 1988). The pins were withdrawn by gripping each in turn with a collet chuck. Over 83,600 pins had been pulled from irradiated assemblies at the time PFR operations ended in March 1994. Breakages were less than 0.1%. Maximum pulling forces were of the order of 50kg. When all the pins had been removed the wrapper was cut into sections using the laser to allow monitoring for any fissile material and eventual storage.

The laser proved to be a reliable cutting tool in remote operation and was a very flexible piece of equipment. Some fine solids were generated by laser cutting but most of these remained with the slag on the underside of the cut.

After pulling from the fuel assembly the fuel pins were fed in pairs to a small air-driven cropper. The irradiated cladding materials were found to shear very easily, allowing maximum exposure of fuel to the dissolver acid. The head-end cell could deal with one fuel assembly per day if required.

The sheared fuel was transferred as a 30kg batch to the dissolver - a 24 hour cycle time being allowed for charging, fuel dissolution in nitric acid, washing of the stainless steel fuel cladding (fuel hulls) and clarification of the dissolver solution. (This dissolver cycle time is the rate determining operation, limiting plant throughput to a maximum of about 5kg of oxide fuel per day). It is important that the feed to the solvent extraction plant should contain the minimum amount of particulate material, so it was clarified using a high speed centrifuge. An air-turbine-driven centrifuge was designed and developed, paying particular attention to active remote maintenance. This meant designing all moving parts as easily replaced modules. The centrifuge proved to be very efficient, as demonstrated by the trouble-free operation of the mixer settlers in the extraction plant and the clarity of liquor samples taken from the extraction plant feed and active waste streams. After clarification, the dissolver solution was conditioned and adjustments made, as required, to both the acidity and plutonium valency before feeding to the three cycle solvent extraction plant. The solvent extraction process operated entirely as expected from both development laboratory tests and theoretical predictions.

The pure plutonium nitrate product from the solvent extraction process was concentrated in a titanium evaporator and conditioned with respect to nitric acid concentration and the plutonium IV valency state to reduce radiolytic off-gas production before loading to the transport flask for shipment to BNFL Sellafield.

The first fuel assemblies containing plutonium from PFR recycled into new oxide were loaded into PFR in June 1982, thereby closing the reactor fuel cycle.

In March 1994, the reprocessing plant had treated a total of over 23 tones of oxide fuel, recovering more than 3.5 tones of plutonium, from 239 fuel assemblies, 144 mixer breeders and 10 radial breeder assemblies. The highest burn-up in the fuel was 17.6%.

Typical cooling times were 270-360 days, but the shortest cooling time was 136 days when some short-cooled fuel was reprocessing experimentally to study movements of iodine species.

The plant has been operated since 1980 in campaigns to keep pace with fuel discharges from PFR. The highest throughput in any year so far was 4.79 tones in the period from April 1993 to March 1994.

The PFR fuel reprocessing plant proved the technical feasibility of oxide fuel reprocessing via a Purex-cycle, with recovery of over 99.5% of the plutonium. This high recovery was also reflected in the low amounts of plutonium in the liquid and solid waste streams from the plant. The amount of radioactivity discharged to the environment was always about an order of magnitude less than the licensed limits. The plant is subject to IAEA and Euratom safeguards.

Based on the approach adopted for the PFR plant, and taking experience of its operation into account, a design study was completed in 1984 for a larger plant (60 tonnes per annum). Cost evaluations indicated the capital cost for such a plant (and its associated fuel fabrication and waste treatment plants) to be less than 10% of the capital cost of the three 1500MWe fast reactors it would service.

2.3.6. The future

As described in this Chapter, PFR was shut down for the last time late in the evening of 31 March 1994. Stage 1. of a decommissioning schedule, described as "storage with surveillance", began the following day. Storage with surveillance has three sub-stages. In the first the reactor is being rendered inoperative, the potential hazards are being reduced and the station is being defuelled. This is expected to take about two years. The second sub-stage will involve activities to achieve a care-and-maintenance condition, which is the third substage and will be sustained for the medium or long term.

2.3.7. PFR in perspective

PFR proved, as expected, to be very stable in operation. The 1000 tonnes of sodium in the primary and secondary circuits needed less attention in normal operation than the circuits carrying water for steam generation and cooling. The large mechanical sodium pumps proved to be exceptionally reliable. The only major problem in this area of the plant, which affected performance, resulted from the ingress of oil from a pump bearing into the primary sodium in 1991. The products produced by this caused reductions in flow, requiring the removal and replacement of filters between the primary pump and the core inlet. This task, involving operations deep in the sodium pool, demanded much ingenuity and persistence to solve the engineering problems posed, but demonstrated clearly that, given such ingenuity and a refusal to be beaten, a skilled operations team will not find the opacity of sodium a problem.

Many judgements were made during the design of PFR with a much more limited data base than is available to those viewing the plant retrospectively. With the exception of the choice of tube-to-tubeplate weld for the steam generators, these judgements were generally vindicated by subsequent experience. In the first decade of operations, the failure of these welds in both the ferritic steel evaporators and the stainless steel superheaters and reheaters greatly affected the plant's performance. Following the fitting of 3000 sleeves to bypass the welds in the evaporators, these units operated uneventfully for the last ten years of operations. With concern about stress corrosion cracking of the welds in the superheater and reheaters extending into the tubeplate material, new superheater and reheater tube bundles were fabricated in ferritic steel and installed in 1984-87. They too operated without problems. All of this experience made it clear that the choice of a weld geometry which could not be stress relieved after fabrication was inappropriate.

One other important incident with the steam generators in 1987 also contributed greatly to understanding and to the development of future fast reactors. Vibration in one of the

original stainless steel superheaters led, through tube-wall fretting under sodium, to a sodium-water reaction event with the resulting failure of many tubes. The unit was rendered unserviceable. Through the analysis of this event, supported by tests in laboratory rigs, improved methods are now available for the design of protection systems to deal with any sodium/water reaction event in future fast reactors. The replacement tube bundles which were deployed after this event were of a design which would not be prone to such vibration. Even so, it was thought to be worthwhile to develop systems for monitoring vibration in all the steam generators. In 1992, these systems revealed evidence of a vibration problem in two of the evaporators which investigation showed needed corrective action. This technology, used to advantage in PFR, is now being developed to monitor the performance of steam generators in light-water reactors.

A major purpose of PFR was to prove the fuel design and to study the irradiation performance of advanced designs, with the aim of increasing burn-up and reducing fuel cycle costs. The complete fuel cycle was the subject of attention with fuel reprocessed in a dedicated plant at Dounreay and new fuel fabricated at Sellafield by BNFL, and later at Cadarache by CEA. The original burn-up target for PFR fuel was 7.5% heavy atoms. This was surpassed and raised progressively with design and materials improvements. As a result largely of PFR work, the designers of future fast reactors can be assured of achieving 15% burn-up and, from PFR pilot studies, 20% is a reasonable prospect. Great understanding of the irradiation-induced swelling and creep performance of structural materials was a concomitant of the fuel development programme. About 93,000 fuel pins were irradiated with only a handful of failures, most of them in developmental variants exploring performance limits.

The fuel cycle of PFR was closed in 1982, when fuel was returned to the reactor for irradiation after reprocessing and refabrication.

Throughout the operating life of PFR, the UK's, and subsequently the EFR partnership's, design teams were involved in reviewing experience and assisting in providing solutions to problems which arose, both large and small. By such means there has been an effective transfer of knowledge to the benefit of future plant designs.

PFR operational experience had considerable influence on NNC's follow-up reactor design for a Commercial Demonstration Fast Reactor, CDFR. Many features of this design were subsequently incorporated in the design of the European Fast Reactor, EFR, and the success of this design project in developing a plant potentially competitive with future light water reactors rests in part on PFR pioneering improvements in the technology. PFR contributions continue as it provides the first experience of decommissioning a commercial-scale plant.

2.4. SUPER PHENIX 1 OPERATING EXPERIENCE

2.4.1. Design features

The Creys-Malville plant which is derived from Phenix is of the pool type. Primary sodium coolant is entirely enclosed in the main stainless steel vessel which contains the core, and in which are installed four primary pumps and 8 intermediate heat exchangers.

The reactor core is made up of 364 fissile subassemblies, in the form of uranium - 15% plutonium mixed oxide pellets stacked in 271 stainless steel cladding pins, with upper and

lower depleted uranium oxide blankets. The fissile subassemblies are surrounded by 3 rows of fertile subassemblies of similar design containing only depleted uranium oxide, and by several rows of steel subassemblies.

The main vessel is closed above the free level of sodium and argon cover gas by the slab which contains in its central section two eccentric rotating plugs and the core cover plug which supports the control rod drive mechanisms and the core instrumentation. It is surrounded by the safety vessel, welded to the slab, which is itself topped by a metallic dome. This dome can resist a pressure of 3 bar at a temperature of 180 C. The safety vessel and the dome make up the primary boundary, and the reactor building in reinforced concrete constitutes the secondary boundary.

Thermal power extracted from the core by primary sodium is transferred by the 8 intermediate heat exchangers to 4 secondary loops which in turn supply the steam generators, housed in four buildings around the outside of the reactor building. The steam produced spins two turbogenerator sets of 620 MWe each, at 3000 rpm.

Since the end of construction in 1984, the plant has seen three different stages of evolution:

- in 1984, with the building of the fuel storage pool building (APEC),
- in 1988, with the replacing of the storage drum by an argon-filled Fuel Transfer Station (PTC),
- in 1993, with the modifications to improve means of prevention and handling of secondary sodium fires in the reactor building and the steam generator buildings.

The APEC and PTC. In the initial plant project, it was envisaged to remove the fuel subassemblies to a reprocessing plant after a period of one year in the sodium-filled storage drum. It was also planned to renew 50% of the core after a half-cycle of 320 EFPD. The storage drum could receive 409 subassemblies with a decay heat of up to 28 kW. Removal of the subassemblies was carried out when the decay heat was less than 7,5 kW.

In 1982 the necessity for fast reactors was less acute and therefore there was less need for a dedicated reprocessing centre. This led NERSA to decide on the on-site construction of temporary storage for several spent cores. This is referred to as the APEC (Atelier Pour l'Evacuation du Combustible).

Then in 1988, when repair of the storage drum turned out to be impossible, NERSA chose to eliminate it altogether and replace it with a gas-filled transfer chamber. This modification, which was made possible through the existence of the APEC, in turn led to modification of the management mode of the core which is now based on frequency 1. The core is renewed entirely after a cycle of 2 to 3 years (640 EFPD). Replacing the subassemblies at a later stage requires 7 to 8 months delay, including an initial period of 2 months, for decay of the first subassemblies to a level of 7,5 kW.

The APEC and the PTC make up two links of the handling line shown in Figure 2.17. Construction of the APEC covered the period 1984 to 1989, and that of the PTC lasted two years (1990/91).

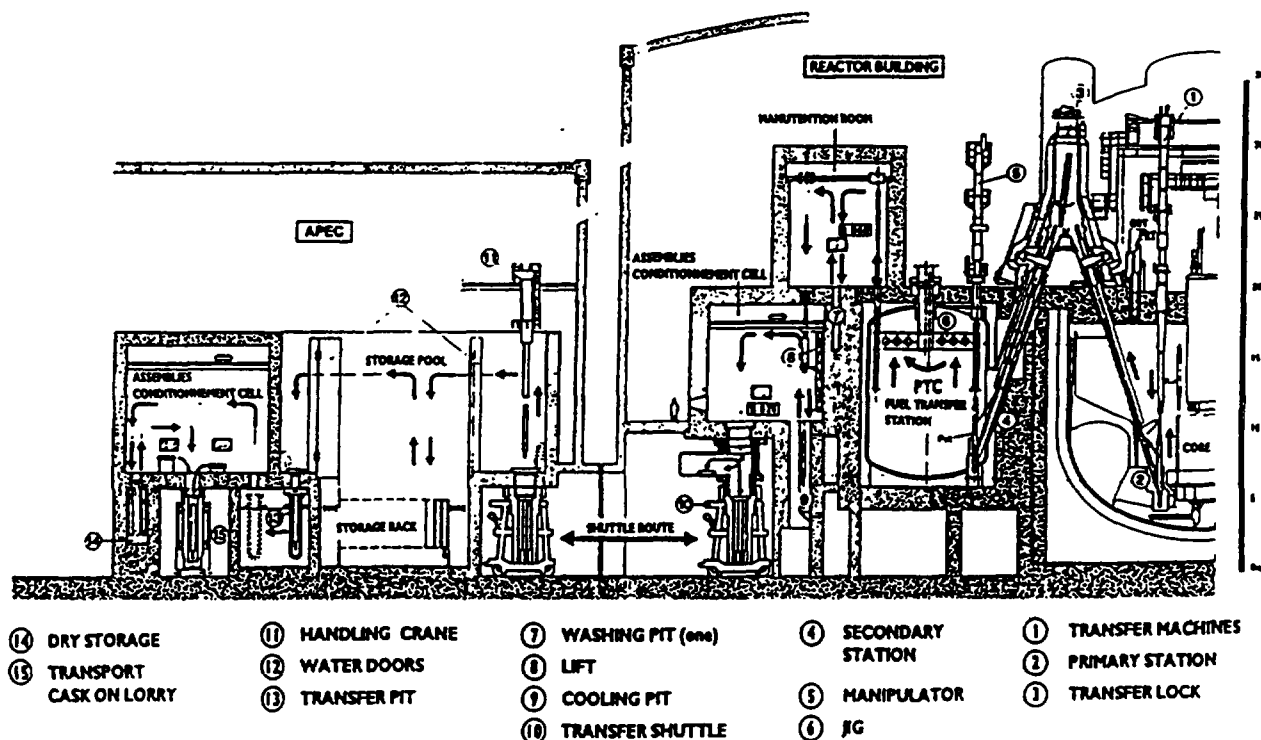


FIG. 2.17. Super-phenix - evacuation line for fuel subassemblies.

The subassemblies are placed by the transfer machine in a sodium-filled container which is carried by the pot in the A-frame. In the PTC, under argon, the container carrying the subassembly is placed on a pivot arm which transfers it to the handling line. The pivot arm has a third position to receive the new subassemblies to be loaded.

After washing, the subassemblies are placed in a transfer shuttle which can receive three subassemblies. The APEC offers storage for approximately 1,700 subassemblies between the pool with a capacity of about 1,400 subassemblies and a hall which can house about 300 subassemblies in casks under gas atmosphere. Unloading capacity of the handling line is about four to five subassemblies per day.

Sodium fire modifications. Initially the type of secondary sodium fire taken into account for safety resulted from a clean break of the largest piping (1 metre diameter), supposing that the sodium would spread in pool form. In 1986 an important sodium spray fire (about 10 tones at 225 C) occurred in the solar plant at Almeria (Spain), destroying the major part of the installation. It was then decided to undertake the necessary work with the view, on the one hand, to improving prevention of such a fire risk, and on the other hand to guaranteeing safety in the hypothetical event of a spray fire resulting from the same clean pipe break.

As far as prevention is concerned, the improvements have involved mainly an extension of leak detection by wire on the auxiliary piping, and placing of nearly 600 new detectors called "sandwich detectors" to cover the welds on the large piping (diameter exceeding 200mm).

As far as consideration of consequences is concerned, the main modifications carried out in the four large areas (1,000 m³) of secondary loops have been the installation of partitions creating 100 m³ zones to limit build-up of pressure upon outbreak of fire; the piercing in the wall of the containment building of 4 outlets equipped with valves set at 10 mbar to evacuate the hot gases outside the reactor building; and the insulation of the concrete walls with stainless steel sheeting to contain the secondary sodium in the event of leak, to avoid reactions with sodium (see Figure 2.18).

In the four steam generator buildings improvements involved civil engineering resistance, metallic partitions, and better reliability of the dump valves to avoid any increase in the consequences of a fire due to their failure.

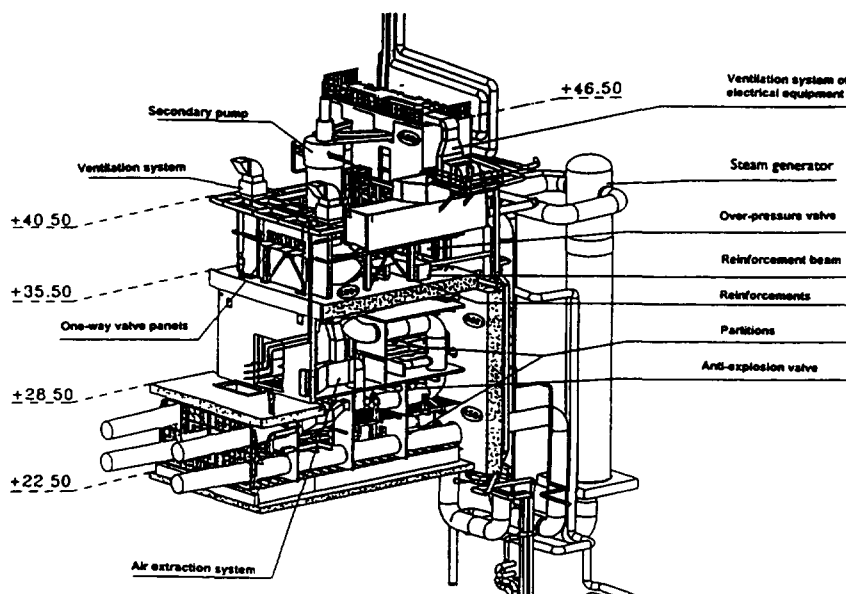


FIG. 2.18. Super-phenix - disposition on secondary loop for sodium fire risk prevention.

2.4.2. Operating experience

Sodium fill and isothermal testing. Successive filling of the storage drum, two secondary loops, the reactor block and lastly the two remaining secondary loops, took from June to December 1984. Filling the reactor block took 2 months, from 23rd August to 31st October, after prior heating to about 150 C by circulation of hot nitrogen.

These filling operations were preceded by:

- supply and on-site storage of 5650 tones of sodium, transported by 291 tankers,
- testing of the handling line under air,
- tightness checks of the intermediary containment (main vessel and slab), the primary containment (safety vessel and the dome), and the storage drum under air,
- biological shielding checks by means of an 18 000 Ci source.

Isothermal tests started in January 1985 with an initial build-up in temperature limited to 395 C following the appearance of a phenomenon of oscillation of the thermal shield in the main vessel during increased primary pump speed. Investigations on this problem, carried out both on the reactor (visual examination by camera and displacement measurements through the

"MIR" reactor inspection robot) and by mock-up under water, rapidly attributed this phenomenon to a hydrodynamic coupling of the fluid and the structures, caused by vessel coolant sodium flow through the spillway (see Figure 2.19). This problem was later resolved by a 50% increase in coolant flow thanks to slight modification in the foot of 19 subassemblies in order to reduce the height of the fall. Efficiency of the modifications was successfully tested in the course of a second temperature build-up to 425 C in June 1985. The interval between the two temperature build-ups was used to advantage for carrying out handling-line testing in sodium, and loading of the special device for introducing a neutronic chamber into the centre of the core. At the same time, testing of the turbines by auxiliary steam was carried out, as were tests on the feedwater plant and steam generators with sodium drained.

Core loading and physics testing. The dummy subassemblies were replaced by fissile subassemblies based on an original method called checkerboard pattern which allowed criticality by loading the core in 4 batches. The first subassembly was loaded on 20th July and first criticality was achieved on 7th September 1985, with a core made up of 325 fissile subassemblies, as planned.

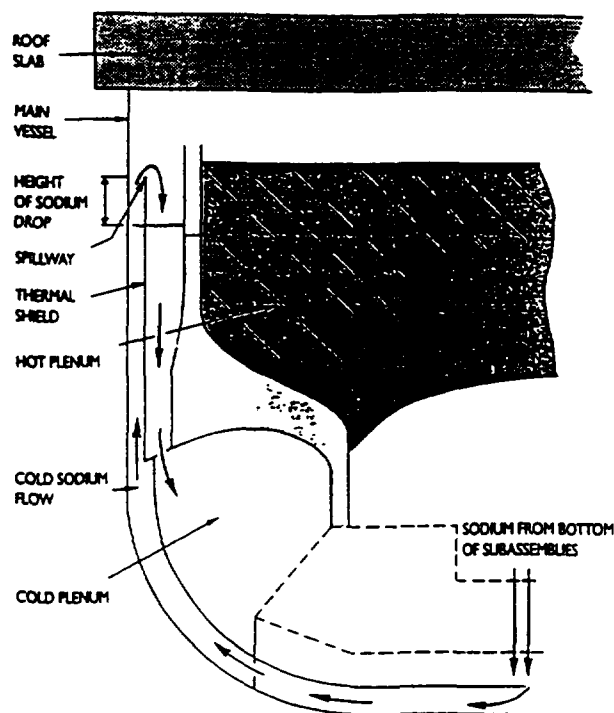


FIG. 2.19. Super-phenix - thermal shield oscillation.

In October 1985, 33 fuel subassemblies were added to constitute the core for power build-up; it was with this core that zero power testing was carried out at no more than 30 MWt:

- control rod worth,
- neutron flux distribution and fission rates,
- calibration of neutron channels,
- measurements of reactivity and feedback coefficients.

Build-up of power. After obtaining the "first nuclear" steam on 31st December 1985, plant operation was managed by stages as is shown in the diagram in Figure 2.20.

Start of power build-up was made on B turbine, as the A turbine was unavailable as a result of modifications in progress on the bypass circuit (experience feedback from PWR reactors).

1. B turbogenerator testing - build up to 30% of nominal power
2. Zero power physics testing
3. Full power operation of B turbogenerator
4. Clad rupture detection systems testing
5. A turbogenerator testing and running both turbogenerator sets
6. Build-up to nominal power by stages
7. Maintenance work
8. Half-power operation due to unavailability of B turbogenerator

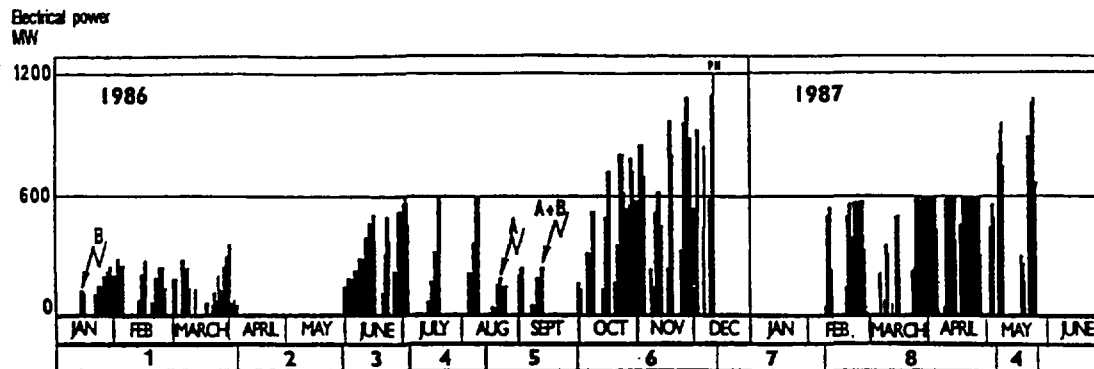


FIG 2.20. Super-phenix - commissioning steps after link-up.

After initial link-up on 14th January, build-up was soon interrupted, first by abnormal heating of a fuel subassembly that had to be replaced (a plug in the foot had been overlooked), then by several technical problems concerning the feedwater plant. Build-up was then interrupted in April and May to carry out necessary modification work and to complete the zero power physics testing programme.

B turbine reached full power (620 MWe) on 30th June, and this first build-up to 50% of nominal power was completed in July/August by calibration tests on the clad rupture detection and localization systems.

When A turbine was available again, it was linked up to the grid on 22nd August 1986, then nominal power build-up was achieved on both turbines on 12th September, full power being reached on 9th December 1986.

After various maintenance work, plant operation started again at the beginning of February 1987 but was again hampered successively by water hammer on the A auxiliary feedwater plant piping, putting it out of action for three months, then at the end of March by the detection of a sodium leak on the storage drum. This led to reactor shutdown at the end of May 1987, after a second calibration test on the clad rupture detection systems at 90% of nominal power.

2.4.2.1 First shutdown period

The two main activities of this shutdown period, which lasted from May 1987 until January 1989, were on the one hand, investigations on the storage drum which led to its

replacement by the fuel transfer station (PTC), and on the other hand to the preparation of the reactor with a view to its resumption without the storage drum.

Investigations on the storage drum. Following detection, on 8th March, of the leak in its main drum by detectors situated at the bottom of the safety drum, several actions were immediately envisaged:

- pinpointing the leak where flow was assessed at approximately 20 litres/hour,
- installation of means of prevention in the event of a leak on the safety drum,
- installation of a draining circuit on the safety drum to limit the quantity of sodium contained in it. The first draining occurred on 12th May and was repeated several times,
- unloading the storage drum which was carried through between April and July 1987.

290 non-radioactive dummy fuel subassemblies were stored on-site, 73 low radioactive steel subassemblies were stored in a cask in the APEC, and 49 various subassemblies were transferred into the reactor as a provision for operation without the storage drum.

The cause of the sodium incident was determined at the beginning of September, and the storage drum was then definitively drained on 9th September. At the beginning of October, gamma radiography examination revealed that a crack had developed at the base of a weld on a support plate of the cooling circuits (see Figure 2.21).

At the beginning of 1988, gamma radiographies showed up that other indications of cracks existed in several zones of the main drum made of 15 D3 ferritic steel and the first assessments of a sample, which were later on confirmed, showed that cracking by hydrogen, affecting these zones, was highly intense.

The drum therefore appeared irreparable, and in March 1988 it was decided to replace the storage drum by a single fuel transfer station (PTC) while keeping the safety drum made of the same ferritic steel. Finally, the decision to construct a new tank in stainless steel was taken in March 1989, after dismantling the internal structures and the storage drum.

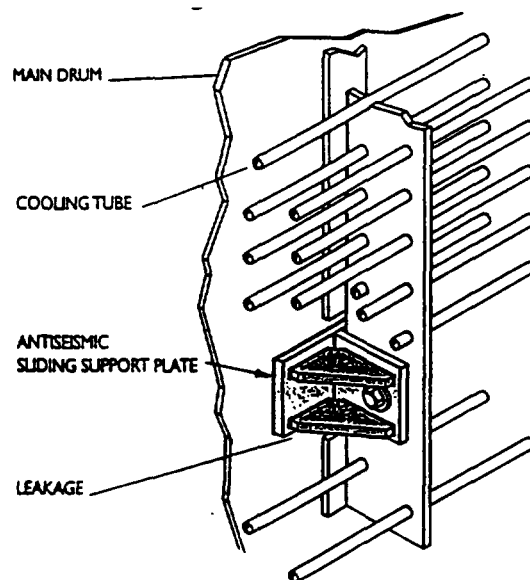


FIG. 2.21. Super-phenix fuel storage drum leak localization.

Preparation of the reactor. As a preparation for resumption of power, a considerable programme of study and work was undertaken at the request of the Safety Authorities; this mainly concerned:

- re-examination of the design and fabrication of the reactor vessels, the secondary circuits, the decay heat removal circuits and inspection of the welds of the main vessel with the MIR inspection robot,
- re-examination of accidental conditions and drawing up of procedures to define necessary actions for handling a highly hypothetical situation resulting from a leak on the main vessel, followed later by a leak on the safety vessel. Simultaneously a flask to unload fuel in the absence of the storage drum, while awaiting the PTC, was studied and then manufactured.

At the same time, a campaign of work and modification devoted to improving the operation and availability of the installation was launched.

Examination of the main reactor vessel welds by the MIR robot travelling in the space between the vessels took place in the course of the summer 1988 and confirmed the sound quality of manufacture. On 29th November, examination of the overall status allowed concluding that the plant was fit for service, and on 12th January 1989 approval for resumption of power was granted by the Ministers concerned.

2.4.2.2. Resumption of operation

After criticality, on 14th January, following a neutronic and isothermal tests phase made necessary by the long shutdown of the installation, the plant was linked up to the grid on 21st April, and reached full power on 16th June, i.e. in about 2 months as is shown in the diagram in Fig. 2.22.

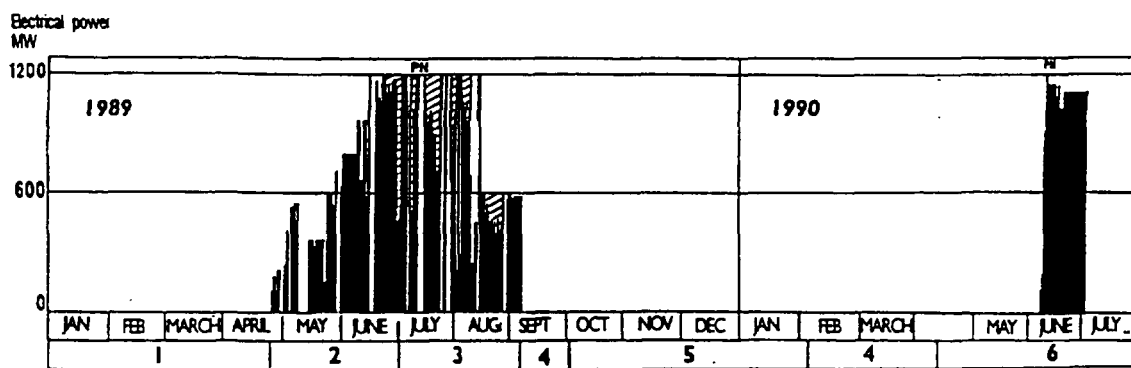


FIG. 2.22. Super-phenix - plant operation after fuel storage drum shutdown period.

1. Neutronic and isothermal testing
2. Power build-up
3. Limited power operation due to Rhône temperature and flow and A turbogenerator unavailable
4. Safety-related tests

5. Maintenance work and PTC civil work
6. Resumption of power

The power build-up was disturbed by several incidents on equipment in the balance of plant, certain adjustments and a spurious sodium leak alarm on a steam generator.

Power operation then continued but had to be reduced in respect of the regulation on thermal releases because of a particularly unfavourable flow rate in the Rhône. After 17th August, operation continued with a single turbine, as the other had to be shut down following abnormal vibrations. There again, the main difficulties are attributable to the balance of plant: electric generator (hydrogen tightness), feedwater regulation valves and purge valves and fittings.

This period of operation ended on 7th September 1989 for a scheduled shutdown which was necessary for:

- core rearrangement in order to recover a sufficient level of reactivity. 12 diluent subassemblies were shifted to the outside of the core and replaced by 18 fuel subassemblies,
- assembly works linked to the PTC and not compatible with reactor operation.

This shutdown was preceded by two safety tests in September which allowed, on the one hand, to confirm the ability of Superphenix to evacuate decay heat by natural convection of the primary circuit and the secondary loops after reactor shutdown, and on the other hand, to demonstrate the absence of risk of a reactivity accident, caused by a passage of argon gas in the core following depressurization of an intermediate heat exchanger argon-filled bell.

The shutdown was used advantageously to carry out other preventive maintenance operations, and in particular:

- replacing two tanks of the reactor argon circuit, constructed in the same ferritic steel as the storage drum, by two tanks in austenitic steel,
- repair on the turbine which had shown vibrations.

This shutdown was later considerably prolonged in order to carry through a test imposed by the Safety Authorities, following the incident experienced at the Phenix plant, consisting of injections of radioactive gas into the diagrid to demonstrate that the purge subassemblies were able to evacuate the gas that could accumulate in it.

Plant operation then resumed on 14th April. Link-up to the grid, which was delayed by a sodium leak of a few litres on an auxiliary secondary loop circuit, took place on 8th June and nominal power was reached 3 days later.

On 3rd July, operation had to be interrupted following detection of an untimely air intake in the reactor argon circuit which caused impermissible oxidation of the primary sodium.

2.4.2.3. *Second shutdown period*

As soon as reactor shutdown took place, all actions needed to find the causes and consequences of the pollution incident were undertaken as follows:

- investigations to identify the cause of the air inlet which, on 23rd July, led to the incrimination of the faulty compressor membranes on the primary argon activity measurement bypass,
- sodium purification carried out in two campaigns, during which 3 sets of two purification cartridges were extracted from the reactor block. In January 1991, the sodium recovered a level at least equal to the purity prior to the incident,
- repair of the installation and verification of the innocuous nature of the incident to components, which were completed in March 1991, following, notably, endoscopic inspections.

But this incident also led the Safety Authorities to demand, at the end of October 1990, a general re-examination of the organization of plant operation and further safety studies, in particular of the sodium fire risk in the secondary galleries, and feedback of experience from the Phenix incident.

Moreover on 27th May 1991 the Conseil d'Etat (Council of State) announced the partial cancellation of the Order of January 1989 approving plant operation without the Storage Drum; this led NERSA to accelerate work for completion of the PTC for commissioning as soon as possible. At the beginning of 1992, all the installation allowing evacuation of spent fuel from the reactor to APEC was available.

This period in other respects was marked, on 13th December 1990, by the collapse of half the roof of the turbine hall due to an exceptionally heavy fall of snow, causing unavailability of one of the turbogenerator sets. Reconstruction work was undertaken rapidly on the turbine hall and repair of equipment was completed in October 1992.

In June 1992, the Safety Authorities concluded that an eventual restarting of Creys-Malville was possible subject to limitations and precautions, but on 29th June, the Prime Minister decided to defer the approval and requested a prior Public Enquiry and the immediate application of improvements to the prevention and handling of the sodium fire risk. In other respects he requested a Report on the possible contribution of Creys-Malville to the problem of fuel cycle-end from the Minister of Research.

NERSA then committed the necessary work which concluded with the handing over, on 28th October 1992, of a new request for operational approval to the Ministry of Industry, backed up by a Dossier of 900 pages designed to support the Public Enquiry.

2.4.2.4. *Operational characteristics*

Availability. Since the first link-up, the accumulated gross energy amounts to 4½ billion kWh, and the energy extracted from the fuel represents 174 EFPD.

Except for periods of unavailability specifically due to incidents of the storage drum, pollution and gas injection tests in the diagrid, the reactor has been operating or under tests over about 26 months, which can be broken down as follows:

- 7 months of test without link-up,

- 19½ months with link-up, in the course of which the plant was effectively linked for 7410 hours, i.e. availability of more than 50% during this period.

In other respects, successive periods of production show up a regular and considerable reduction in spurious shutdowns during operation.

Incidents. Since July 1985, 80 incidents have been declared "significant incidents for safety", with the annual breakdown shown in the following table:

Year	1985	1986	1987	1988	1989	1990	1991	1992	1993
N° of significant incidents	15	22	12	1	7	6	10	5	2

The yearly frequency of incidents reached 10.1, but outside this period of startup, it has been established since 1989 at about 7.1 significant incidents a year, similar to that recorded by the French park of PWR reactors.

The application of classification criteria on the severity scale has led to the following:

- 2 incidents classed level 2 (both because of plant unavailability duration criteria),
- storage drum leak (March 1987),
- primary sodium pollution (July 1990),
- 6 incidents classed level 1,
- overheating of a subassembly (January 1986),
- fall of a handling device (October 1989),
- sodium leak on auxiliary circuit (April 1990),
- collapse of turbine hall roof (December 1990),
- involuntary evacuation from site of low-radioactivity small components (March 1989),
- unavailability of 2 diesel emergency groups of the same train (December 1992),
- 72 incidents unclassified on the scale.

Breakdown according to type of incident or cause of the fault is therefore shown as follows:

Type of incident		Cause of failure	
-automatic shutdown	35%	- mechanical	21%
-startup of emergency system	18%	- electrical	24%
-non respect of operating rules	37%	- instrumentation	18%
- other causes	10%	- human	37%

Thanks to analysis of these incidents, it appears that about:

- half the incidents are attributable to faults in design or fabrication which have been since corrected;
- a quarter are associated with methods of organization in reactor operation. They nevertheless have mostly occurred during shutdown;
- 1/8 can be attributed to faults in equipment or human error;
- the remaining 1/8 are due to methods and organization of commissioning.

Health physics. Plant operating results since fuel loading and particularly during reactor operating periods have confirmed a feature specific to fast reactors, i.e. a low exposure to radiation of personnel who run and maintain the installations as shown in the following table:

Year	1985	1986	1987	1988	1989	1990	1991	1992	1993
Total dose (man. mSv)	0,5*	15	18	11	11	29	20	7,5	13

* over 5 months

There are about 1000 to 1200 people (plant staff and contractors) working on Superphenix. The total dose received in 1987 is mainly due to investigations on the storage drum while that in 1990 corresponds to replacement of primary purification cartridges.

2.4.2.5 Experience

Core. Sub-critical approach, criticality and the different core rearrangements have shown very similar measurement results to initial calculations.

Operational features of the core stabilized by feedback coefficients (Doppler, temperature, etc.) were confirmed. This neutronic stability together with important thermal inertia make reactor control trouble-free. Particularly at low power uncoupling followed by recoupling of a turbogenerator set is performed without affecting the reactor.

However, larger variations than expected in measured sodium temperatures at subassembly outlets, particularly from fertile and fissile subassemblies on the core periphery, due to sodium recirculation in the hot plenum called for specific measurement campaigns and the adaptation of monitoring methods for these subassemblies.

Reactor block:

The behaviour of the reactor block was on the whole in line with estimates. The main problem was the appearance of oscillations in the internal structures during the first build-up in speed of the pumps: this gave feedback for further theoretical knowledge on the questions of fluid-structure coupling.

The use on two occasions of the MIR robot and the excellent correlation between the measurements carried out during fabrication (1979) and those taken by the MIR showed the feasibility of reactor vessel in-service inspection.

Numerous primary circuit components were handled with special flasks within the framework of tests or maintenance operations, thus confirming the maintainability of components in the sodium environment of the primary circuit.

Knowledge of primary circuit behaviour has in fact been improved on the one hand thanks to natural convection tests which showed that it was established in the core in about 5 minutes, and on the other hand in relation to the risk of gas ingress thanks to tests carried out on the reactor and on several water mock-ups including one simulating the whole diagrid at 0,36 scale (SUPERPANORAMIX).

Lastly, the primary sodium pollution incident led to the installation of a chromatograph on the reactor argon circuit to monitor chemical purity of the primary argon. Besides, this incident gave the opportunity of further knowledge on the chemistry of sodium (new tests on the Cadarache loop), on the behaviour of integrated cold traps and on the workings of plugging indicators.

Large components. Experience feedback on large components remains significant in spite of the short operating period. Primary and secondary pumps total more than 50,000 hours on main motor, and the continuous improvement of maintenance operations has allowed an increase in reliability and availability. As far as the steam generators are concerned, the sodium/water reaction detection systems have been improved on the basis of validated calculation codes through experience. The startup tests have led to review of the SG decompression-isolation sequences with a view to reinforcing the safety criteria applied.

Circuits. Numerous draining and filling operations (more than 30 for the secondary loops and more than 20 for the decay heat removal emergency circuits (RUR)) have allowed validation of the corresponding procedures.

Monitoring of sodium circuit piping displacements has only shown up abnormal behaviour on the RUR circuits where displacements, considering its considerable flexibility, differed from predictions and for which a specific follow-up has been implemented.

Sodium leak wire-detection has shown problems of spurious earthing, and embrittlement of the nickel wire in the long run; this has meant several interventions with, notably, a change from nickel to stainless steel. This wire detection system has been further reinforced on secondary piping of over 200 mm diameter by sandwich-type detectors.

Apart from the storage drum leak of no external consequence, three sodium leaks which did not cause fires, have occurred in the last ten years:

- in 1985 a leak of a few cubic centimetres on the weld of a secondary loop thermocouple support due to vibration,
- in 1990 a leak of about 10 litres on a T-connection weld on a secondary loop auxiliary circuit due to thermal fatigue,
- in 1991 a small leak on a temperature measurement thimble on a secondary loop plugging indicator due to inadequate preheating procedure.

These incidents gave irreplaceable experience concerning monitoring techniques, interventions on sodium circuits and the dismantling of sodium installations.

The storage drum incident has, on the one hand, considerably increased knowledge of 15 D3 ferritic steel. In addition practical consideration of sodium spray fires in the secondary loop rooms has led to progress in modelling the phenomena involved in the event of sodium leak. Spray fire tests with and without partitioning have been carried out with flows reaching 230 kg/s.

2.4.3. The present situation

A Public Enquiry, concerning the renewal of the plant licence, which was announced on 23rd December 1992 by a Press Release from the Prime Minister, referring to the handing-over

of a dossier from NERSA and positive conclusions of the Report submitted on 17th December by the Minister of Research and Space Affairs, Hubert Curien, took place from 30th March to 14th June 1993. There was no notable incident, and in a report of 29th September 1993, the Enquiry Committee expressed positive opinion on plant resumption of power on condition of a favourable decision from the Safety Authorities.

At the same time, improvement work for the prevention and handling of sodium fire on the secondary loops was launched as from the end of 1992, in the four secondary galleries of the reactor building, then from the middle of 1993 in the steam generator buildings. All this work needed secondary loop draining, and was completed at the beginning of May 1994. In the latter part of 1995 and through 1996, power was gradually rised to full-power level.

The situation was changed with the governmental decision to abandon Superphenix (announced in June 1997 and confirmed in February 1998). It was made very clear that the reason of the shutdown was in no way associated with safety problems, but with economy: the government said that when uranium appears now durably cheap there is no need today to operate an industrial FR prototype which "cost more than expected". The French Government confirmed that FR in France is considered as a promising solution for the future of nuclear energy and transmutation. As a whole, the final operating experience of SPX was incomplete but not as negative as sometimes reported: over eleven years of existence it has been operating during four and a half years producing 7.9 billion kWh (half in 1996), it has been shutdown two years for technical reasons and four and a half years for administrative reasons (public inquiries, authorizations, etc.)

2.5. BN-600 OPERATION EXPERIENCE

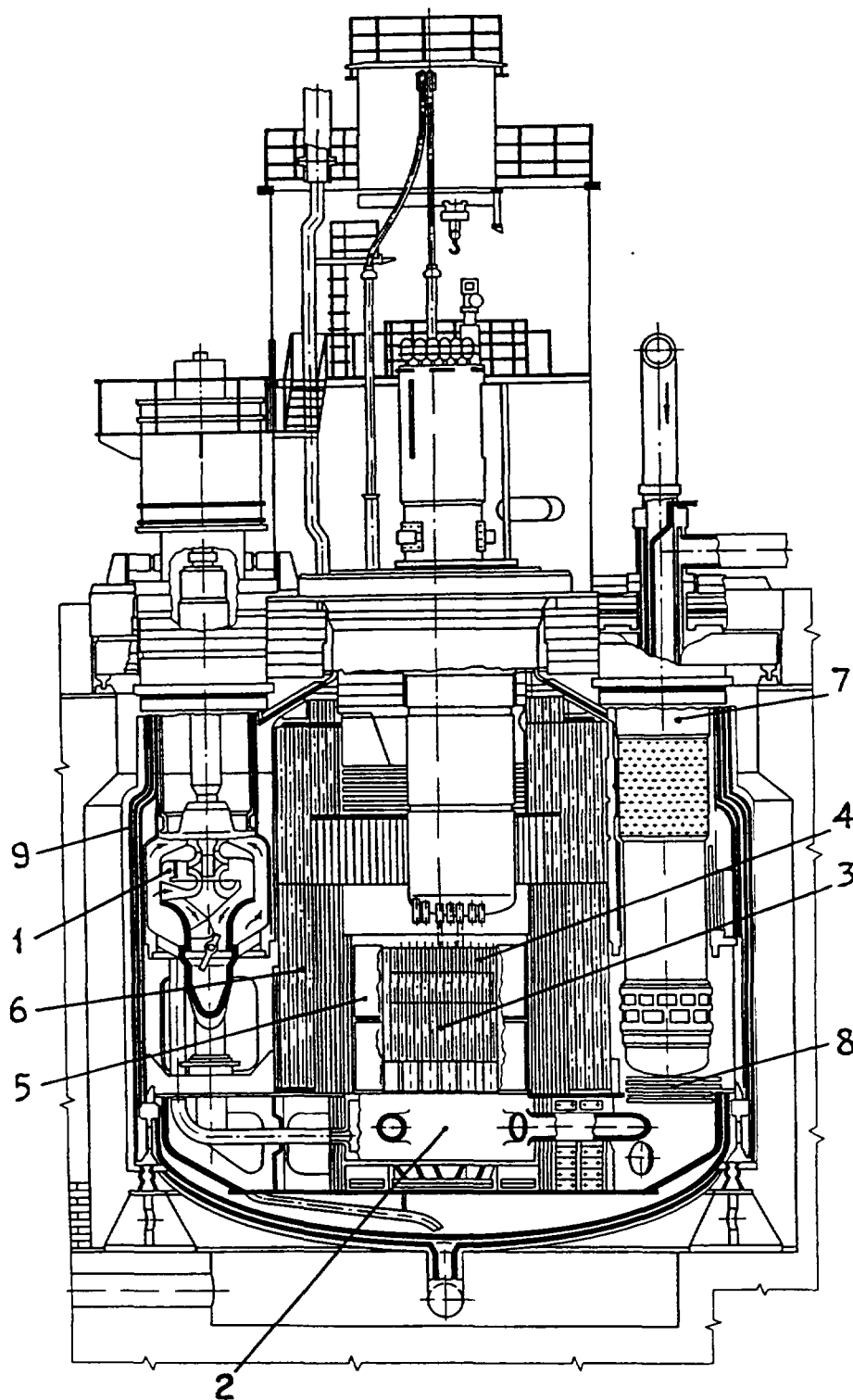
2.5.1. Design features

The reactor plant BN-600 has been operating since 1980 as Belojarsk-3 power plant. The power unit comprises the fast nuclear reactor BN-600 of 1470 MW(th) power, three steam generators PGN-220M and three steam turbine plants K-200-130-3 (Fig.2.24., Table 2.6.)

The primary, secondary and tertiary (steam-water) circuits each have three loops. Each secondary circuit loop includes two intermediate heat exchangers (enclosed in the reactor vessel), steam generator, sodium expansion tank, main circulating pump and pipes. The once-through steam generator consists of eight sections, each comprising three modules: evaporator, superheater and reheater. Every section can be isolated (if necessary) by valves.

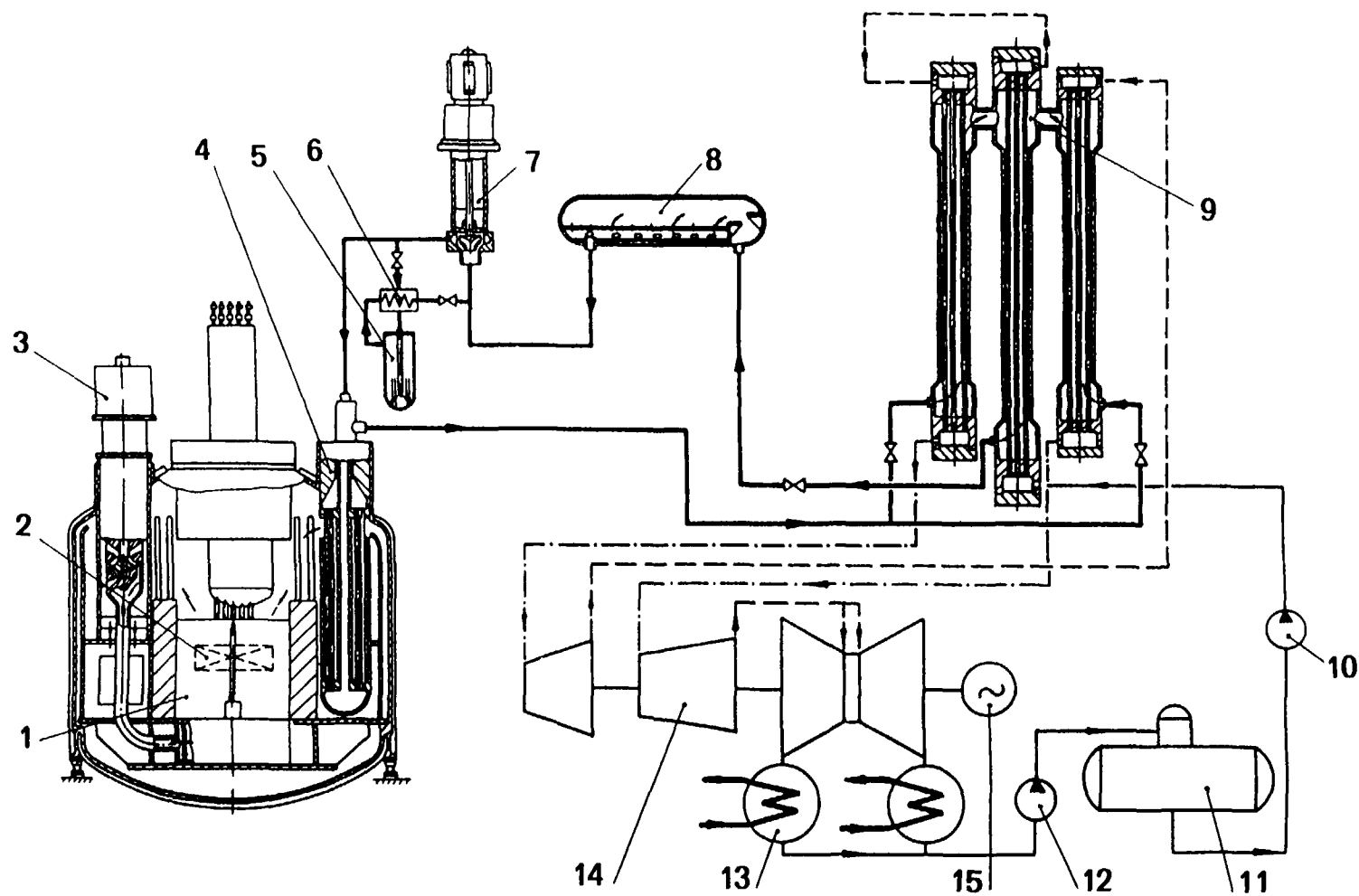
Each tertiary loop includes the modular steam generator, the turbine plant with related auxiliary equipment, 0.6 MPa deaerator, three feedwater pumps and one emergency feedwater pump. The circuit flow scheme and equipment are similar to those used in fossil-fuelled power plants. The reactor plant is capable of operating with two loops at a power up to 70% of the rated level.

The reactor uses an integral layout of the primary circuit components: the reactor core, intermediate heat exchangers and reactor coolant pumps are contained in the common reactor



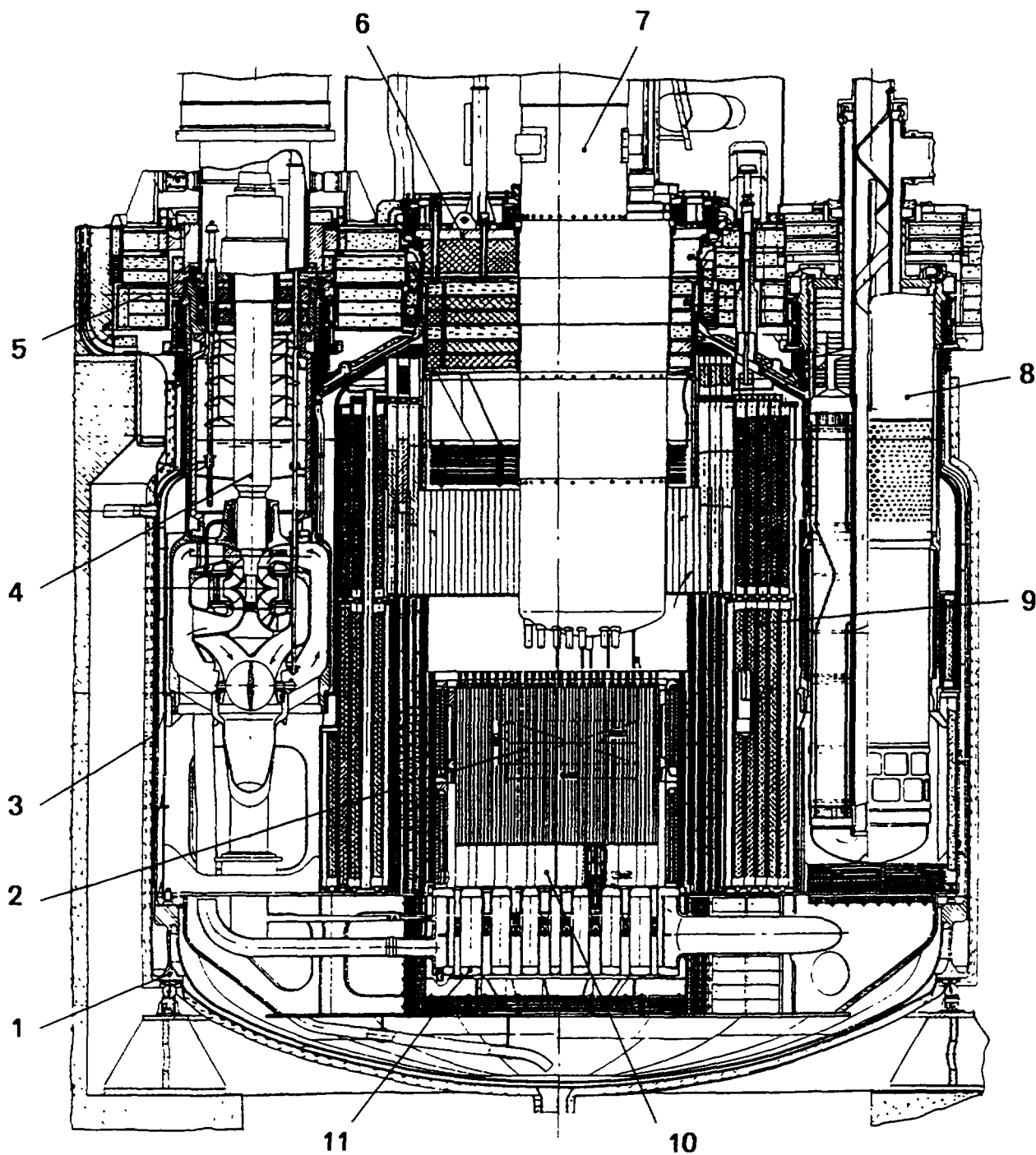
1 - pumps, 2- high pressure header,
3 - core, 4 - blanket zone, 5 - spent
assemblies storage, 6- in-vessel neu-
tron shield, 7- heat exchanger,
8 - dumps, 9- reactor vessel.

FIG. 2.23 BN-600 Reactor



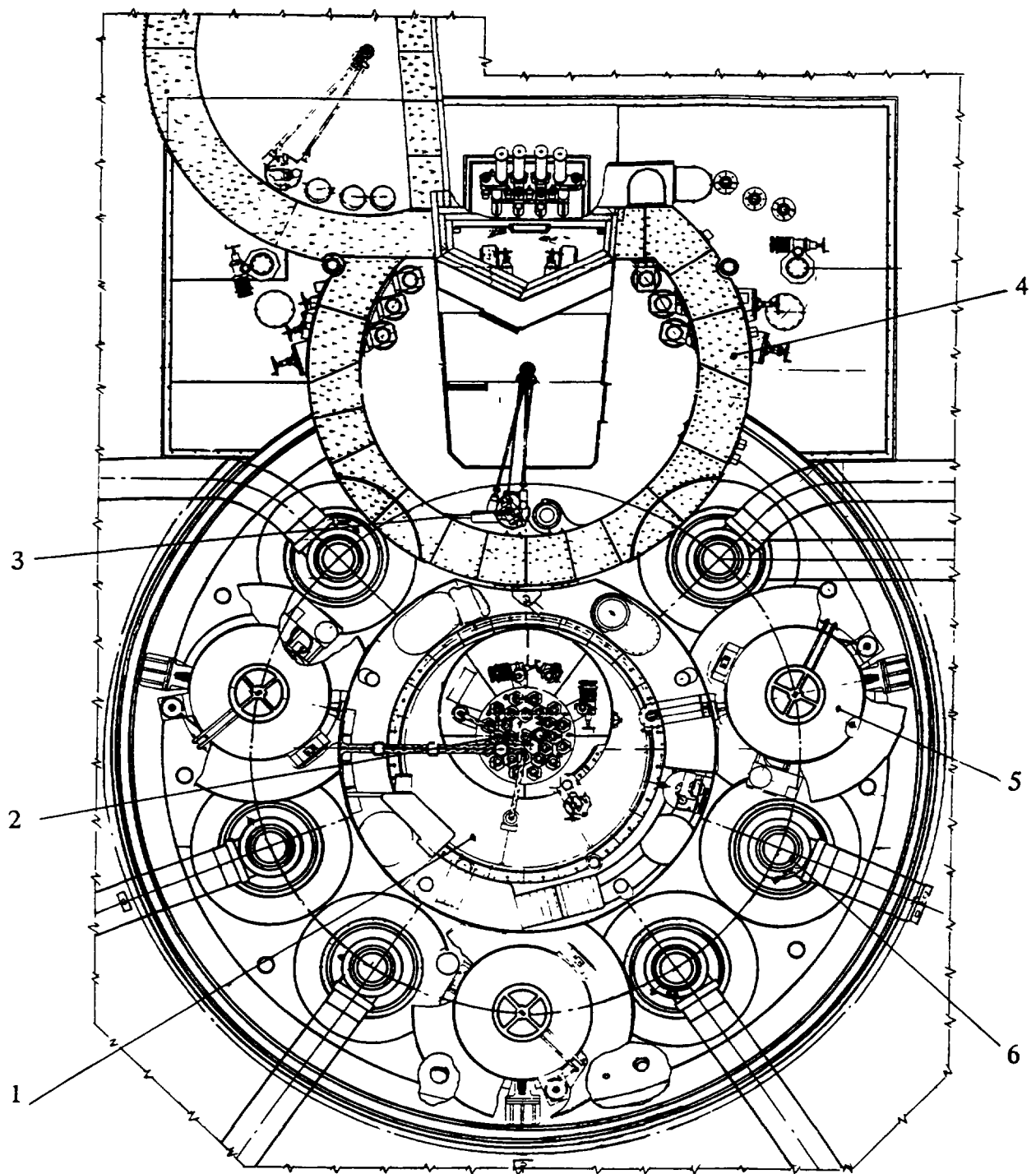
1 - reactor, 2 - reactor core, 3 - reactor coolant pump, 4 - intermediate heat exchanger, 5 - filter-trap, 6 - recuperator, 7 - secondary coolant pump, 8 - sodium expansion tank, 9 - steam generator, 10 - feedwater pump, 11 - deaerator, 12 - condensate pump, 13 - condenser, 14 - turbine plant, 15 - turbogenerator.

Fig. 2.24. BN-600 Power Unit Flow Diagram



1 - reactor support, 2 - reactor core, 3 - reactor vessel, 4 - reactor coolant pump, 5 - upper radiation shield, 6 - rotating plug, 7 - above core structure, 8 - intermediate heat exchanger, 9 - in-vessel radiation shield, 10 - core diagrid, 11 - sodium pressure chamber.

Fig. 2.25. BN-600 Reactor Cut-Away View



1-large rotation plug, 2 - above core structure head, 3 - fuel transfer mechanisms, 4 - refuelling cell, 5- reactor coolant pump, 6 - intermediate heat exchanger.

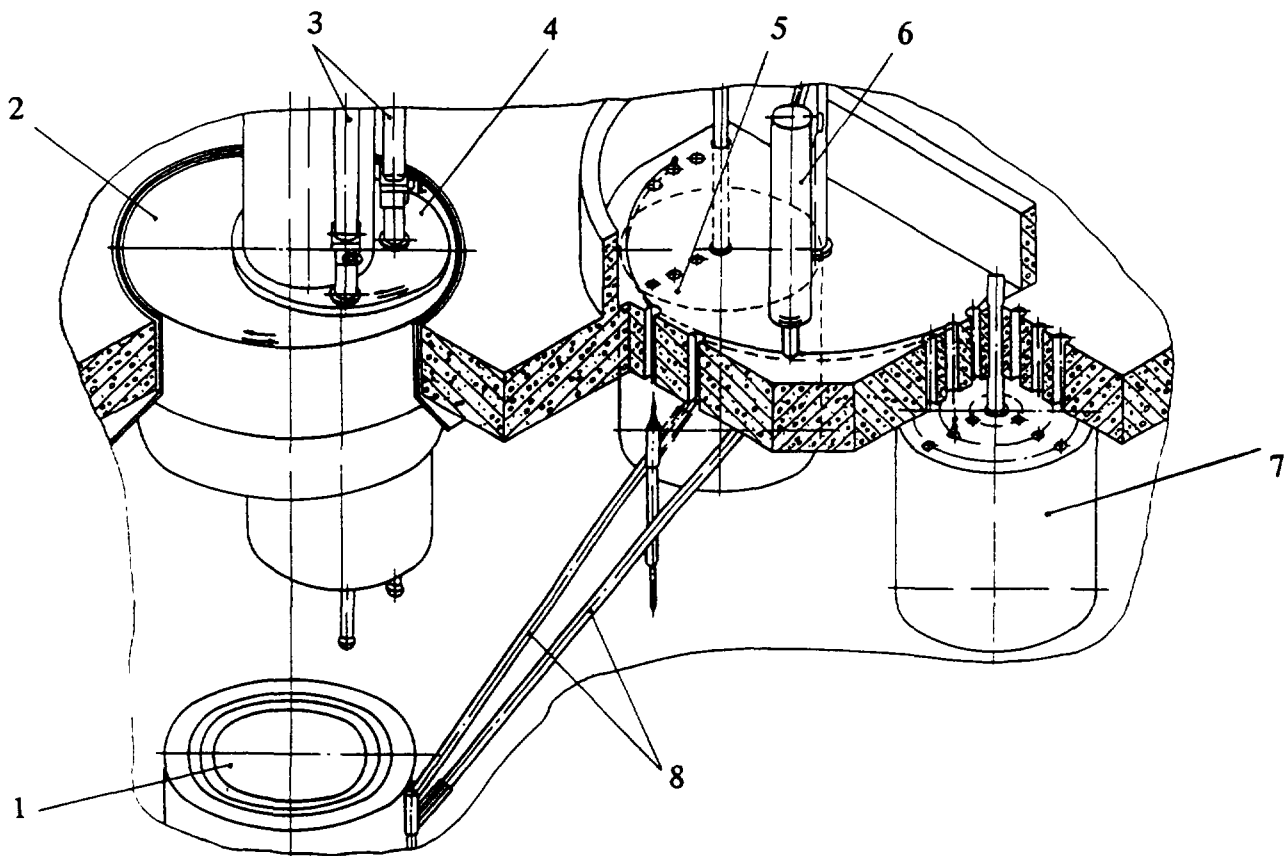
Fig. 2.26. BN-600 Reactor Plan View

vessel enclosed by the external guard vessel (Fig.2.25, 2.26). The distinctive feature of the BN-600 reactor is bottom support of the reactor vessel which gives, in the designers' opinion, certain structural and technological advantages compared with alternative option of top-suspended reactors.

Under refuelling conditions the reactor is cooled by two reactor coolant pumps operating at reduced speed 280 rpm. Primary coolant temperature is maintained during the reactor refuelling outage in the range of 220-250 C.

In abnormal reactor operating conditions and during planned outages the core residual heat is removed using the main components of the reactor heat-transport loops. Power supply for the reactor coolant pumps and the feedwater pumps can be provided from three sources: main, stand-by and reliable. If the main and stand-by power sources were lost the core residual heat would be removed via the steam generators by energizing the primary and secondary pumps and the emergency feedwater pumps from the reliable power source which is the diesel-generator plant.

Reactor refuelling is carried out by an integrated mechanical system providing for loading and unloading of fuel assemblies and transportation in sodium or noble gas environments (Fig.2.27).



1 - reactor core, 2 - large rotation plug, 3 - refuelling mechanisms, 4 - above core rotation structure, 5 - spent fuel drum, 6 - fuel transfer mechanism, 7 - new fuel drum, 8 - loading-unloading elevators.

Fig. 2.27. BN-600 Reactor Refuelling Scheme

The refuelling system comprises:

- two rotating plugs with close and distant (relative to the reactor core axis) refuelling mechanisms installed on the small plug, - two inclined elevators for loading new fuel assemblies and unloading spent ones from the reactor,
- two drums for new and spent fuel assemblies,
- a fuel transfer mechanism for transportation of new fuel assemblies from the respective drum to the loading elevator and spent fuel assemblies from the unloading elevator to the spent fuel drum, - a spent fuel-to-washing cell transfer mechanism, - fuel transfer and washing cells.

The reactor has two independent reactivity control systems, each ensuring the reactor can be shut down and maintained in a subcritical state.

The reactor and all the related systems are regulated from the main control room and from local control boards. There is a capability to shut down the reactor and control its state from a separate room remote from the main control room.

2.5.2. Operating experience

General results. The average load factor for the whole period of the reactor plant operation on full power equals to 72%. The maximum value of load factor (83.5%) was reached in 1992. As to reliability indicators the BN-600 power unit is among the best NPPs in Russia. The power histogram for the unit operation life beginning from the date of its power startup is given in Fig. 2.28.

Up to June 1, 1995 the reactor plant total on-power operation time amounted to 102,139 h, and 53.62 GWh of electricity was generated.

The cost of electricity produced by the power unit is approx. 20% lower than from fossil fuelled power plants operating in the same region.

The number and causes of unplanned full and partial (loss of one loop) outages of the power unit are given in Tables 2.7. and 2.8. The contribution of reactor equipment failures to the energy loss due to unplanned outages and to rated power reduction was 28%, including human-factor related causes. The main contributors to the reactor plant unavailability were: core fuel, reactor coolant and secondary coolant pumps, steam generator faults.

Reactor core. The core of the first type (original design) was designed for quite high performance. However, as the initial operating experience showed, it turned out to be unreliable. Even during the first fuel cycles cladding loss-of-integrity events started, increased swelling of fuel assembly ducts and some control rod items was observed, as well as loss of ductility of the control rod guide tube material. Due to the core fuel failures in the period from 1983 till 1987 the reactor was shut down six times for unplanned refuelling. Core design improvement became essential to provide operating reliability and safety of the reactor plant.

Examination of the failed fuel revealed stress-induced corrosion of the annealed austenitic steel cladding as one of the main causes of early failure. The cladding was damaged

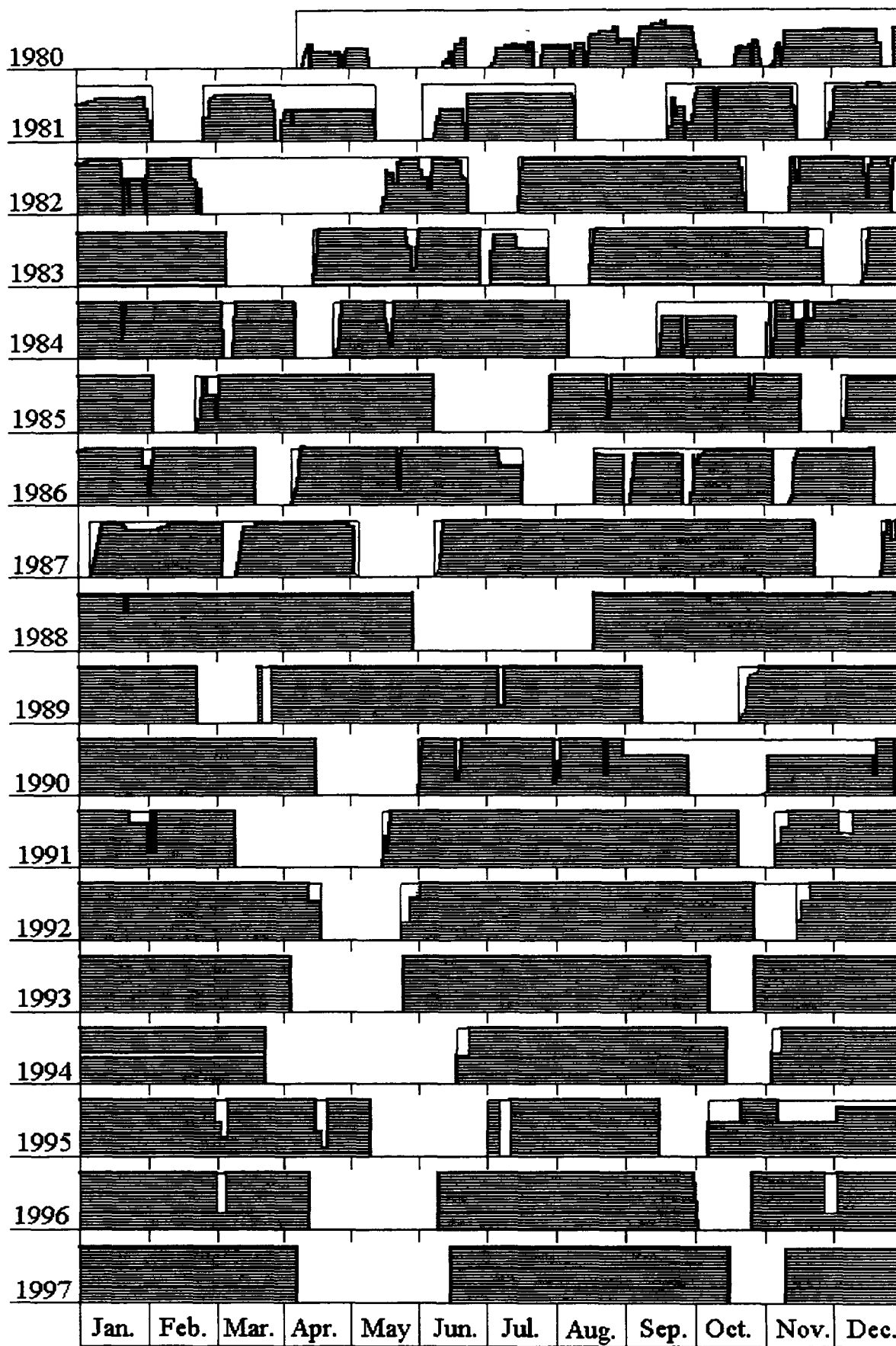


Fig. 2.28. BN-600 NPP operating histogram.

TABLE 2.6. BN-600 BASIC TECHNICAL DATA

Parameter	Value
1. Reactor thermal output, MW	1470
2. Service life, year	30
3. Primary system:	
- core inlet sodium temperature, C	377
- core outlet sodium temperature, C	550
- pressure in protective gas plenum, MPa	0.04
- gas plenum volume, including expansion tank, m ³	135
- coolant volume, m ³	820
- coolant flowrate, kg/s	6945
- pump delivery head, m	97
4. Secondary system:	
- steam generator inlet sodium temperature, C	518
- steam generator outlet sodium temperature, C	328
- pressure in gas plenum, MPa	0.2
- coolant flow in one loop, kg/s	2030
5. Steam-water system:	
- steam pressure, MPa	13.5
- feed water temperature, C	240
- steam temperature, C	505
6. Reactor vessel:	
- inner diameter, m	12.86
- total height, m	13.85
- structural material	09Cr18Ni9
7. Reactor total mass (empty), t	3660

mainly in the peripheral region of the core. It was due to the very unfavourable operating conditions for peripheral fuel assemblies. Because of reshuffling and rotation in the course of operation the fuel rod linear heat rating and cladding temperature rose to 54 kW/m and 710 C respectively at the end of a fuel cycle.

In the advanced core M-design (the first core modification) the following changes had been implemented to improve conditions for fuel operation:

- the core active height was increased from 75 to 100 cm, decreasing the fuel rod maximum linear heat rating to 47.2 kW/m,
- reshuffling and rotation of the fuel assemblies were eliminated,
- swelling-proof cold-worked austenitic steel was used for the cladding and for the fuel assembly ducts.

By the end of 1987 the reactor core was completely assembled with advanced FAs. Loss-of-cladding integrity events virtually terminated resulting in substantial reduction in fission product activity in the reactor gas plenum. The increase of caesium nuclide concentration in the primary system had also stopped.

TABLE 2.7. BN-600 REACTOR UNPLANNED OUTAGES

Outage Cause	Total number of outages													
	Total	1981	82	83	84	85	86	87	88	89	90	91	92	1993
Failure of reactor coolant pumps and related systems	5	--	3	--	2	--	--	--	--	--	--	--	--	--
Failure of reactor control and protection systems	1	--	--	--	1	--	--	--	--	--	--	--	--	--
Claddings lose of integrity	6	--	--	1	1	--	3	1	--	--	--	--	--	--
Failure of turbine-generator and related systems	3	--	--	--	1	--	--	--	--	--	2	--	--	--
Failure of tertiary system equipment items	1	--	--	--	--	--	--	--	--	1	--	--	--	--
Supply system	1	--	1	--	--	--	--	--	--	--	--	--	--	--

TABLE 2.8. BN-600 REACTOR PLANT POWER REDUCTION CAUSED BY LOOP ISOLATION

Cause (Failure)	Number of Outages													
	Total	1981	82	83	84	85	86	87	88	89	90	91	92	1993
Reactor coolant pumps and related systems	13	--	7	2	3	1	--	--	--	--	--	--	--	--
Secondary coolant pumps	4	--	--	--	1	1	2	--	--	--	--	--	--	--
Steam generator	2	--	1	--	--	--	--	--	--	--	--	1	--	--
Secondary system equipment	1	--	--	--	--	--	--	--	--	--	--	1	--	--
Turbine-generator and related systems	21	1	1	2	3	5	1	1	1	--	2	3	1	--
Tertiary system equipment	10	--	2	1	2	--	--	--	--	1	4	--	--	--

In 1990-1992 the reactor core was changed to the advanced M1-design (the second core modification). Ferritic steel was used in the new duct design and boron-modified cold-worked austenitic steel for cladding. Fuel burn-up in the core has reached 10% h.a. with a fuel cycle length of 160 full-power days. Basic design features and characteristics of the BN-600 reactor cores are given in Table 2.9.

TABLE 2.9. BN-600 REACTOR CORE DESIGNS EVOLUTION

Performances		Reactor core type		
		1	M	M1
1.	Reactor thermal output (max.), MW	1470	1470	1470
2.	Reactor core diameter, mm	2058	2058	2058
3.	Active core height, mm	750	1000	1030
4.	Axial blankets height, mm			
-	upper	400	300	300
-	lower	400	380	350
5.	Number of different fuel enrichment zones	2	3	3
6.	Fuel enrichment in U-235, %			
-	LEZ	21	17	17
-	MEZ	--	21	21
-	HEZ	33	26	26
7.	Number of FA in core zones:			
-	LEZ	209	136	136
-	MEZ	--	94	94
-	HEZ	160	139	139
8.	Core fuel cladding OD x wall thickness, mm	6.9x0.4	6.9x0.4	6.9x0.4
9.	Fuel rod length, mm	2400	2400	2400
10.	Fuel rod gas plenum length, mm	808	653	653
11.	Number of fuel rods in FA	127	127	127
12.	Duct width across flats x wall thickness, mm	96x2	96x2	96x2
13.	Core structural materials:			
-	cladding*	EI-847	EI-847	ChS-68
-	duct	Cr16Ni11Mo3	Cr16Ni11Mo3Ti	**
14.	Fuel rod maximum linear heat rating, kw/m	54.0	47.2	47.1
15.	Fuel rod cladding peak temperature, °C	700	700	700
16.	Maximum fuel burnup, % h.a.	7.2	8.3	10
17.	Maximum radiation dose to cladding, dpa	43.5	53.9	75.0
18.	Fuel operating life, fpd	200/300	300/495	480
19.	Core fuel cycle, fpd	100	165	160
20.	Fuel inventory in core, kg	8260	11630	12090
21.	Average fuel burnup, MW.d/kg U	42.5	44.5	60.0
22.	Temp.-power reactivity effect, % $\Delta k/k$	-1.4	-1.3	-1.3

* EI-847 - Cr16Ni15Mo3Nb - austenitic steel, Chs-68 - Cr16Ni15Mo2Mn2TiB - austenitic steel;

** Cr12MoBnVB - ferritic-martensitic steel.

Development of advanced radiation-resistant steels is the main problem now in the attainment of higher fuel burn up. Considering the present status of this problem, a fuel burn up of 12% h.a. (90 dpa) is believed to be quite realistic for an advanced reactor core. This would give two options for the core refuelling pattern: to increase the refuelling interval from 160 to 190 efpd, or to change to a refuelling pattern replacing 114 FAs at a refuelling interval of 145 efpd. In either case the core reactivity margin will have to be increased, e.g. through expansion of the "medium" fuel-enrichment zone at the expense of the adjacent FAs of the "low" enrichment zone. If the medium enrichment core zone were to be expanded to the limit of one FA row the heat rating of the fuel rods would remain at an acceptable level - approx. 48 kW/m.

In the course of reactor operation other components of the core have also been improved (e.g. the control and protection system guide tubes and rods, and the neutron source) through the use of advanced structural materials and optimization of the structure of the items to mitigate the influence of temperature and radiation effects, which resulted in improvements to reliability and service life.

Control rod drive mechanisms. For majority of the CRDMs the total operating time since the date of first criticality until 1 June, 1995 amounts to 105,000 h, and the time in a sodium environment is 132,000 h. In the course of commissioning tests a structural disadvantage of the CRDM design was revealed which caused damage each time the movable member of a CRDM reached one of its extreme positions without being noticed by the operator. After minor modification the CRDMs have been operating reliably, without difficulty.

Sodium pumps. Problems with the pumps resulting in unplanned energy losses occurred in 1981-1985, and were caused by unstable operation of the pump speed control system. Impulses from the electric motors caused failures of the pump-motor couplings, and increased vibration and fatigue cracks in the pump shafts. The use of advanced shafts and couplings and changing to a steady mode of pump operation after attaining the preset reactor power level have eliminated any failures of the reactor coolant pumps since 1985.

The secondary coolant pumps have been operating virtually without failures and their maximum operating age amounts to 103,000 h (Oct. 1993).

Steam generators and heat exchangers. The sectional-modular SGs (Fig. 2.29.) have demonstrated high operating robustness in the event of inter-circuit leaks. During the entire period of SG operation there have been twelve water/steam-to-sodium leak events, half of which occurred in the first year of operation and were caused by development of latent manufacturing defects. Inter-circuit leaks were mainly in the superheater modules (six events) and in the reheaters (five events), while in the evaporators there was only one leak event (Table 2.10).

Total operating time of the evaporator modules amounts to 100,000 h. During the planned outage for the reactor plant maintenance in Spring 1993 the evaporators in one of the loops were replaced because their design lifetime had expired. The specified design lifetime of the superheater and reheater modules corresponds to the reactor plant operation life of $200 \cdot 10^3$ h.

The intermediate shell-and-tube sodium/sodium heat exchangers which have tubes with expansion bends have been operated for 13 years without faults or troubles (Fig. 2.30). Preparations are currently being made to remove one of the IHXs from the reactor for inspection to determine the residual life before the specified service life of 20 years expires.

Refuelling mechanisms. Operating experience of the reactor refuelling mechanisms has been satisfactory. The refuelling concept which relies on the utilization of simple mechanisms for each individual part of the fuel transportation route has been proved to be reliable and safe.

The total operating age in terms of double strokes of the in-reactor refuelling mechanism amounts to 36,100, for the elevators to 9,060 and for the ex-reactor fuel transfer mechanism to 29,200. These exceed the respective design values. Based on results of audits of the refuelling mechanisms their operating life has been extended.

Reactor maintainability. The reactor plant operating experience has demonstrated quite acceptable maintainability of the integral LMFR. There have been no additional difficulties in repairing primary system components on BN-600 compared with BN-350. Repairs of the reactor equipment items and sodium systems, including such complicated operations as replacement of the reactor coolant pumps and SG modules, re-arrangement and jacketing of primary sodium systems, extraction of distorted items from the reactor core, etc. had virtually no influence on the duration of planned outages, which were defined, as a rule, by inspections and preventive maintenance of the steam-water system components.

Conclusion. When assessing the reliability of the reactor equipment in general, it is necessary to take into account the fact that BN-600 is a pilot power unit and most of the failures occurred in the initial period of plant operation. Later, feedback of operating equipment items (leak in a SG, secondary sodium leak in a gate valve, primary sodium leak from an external pipe). The reliability of the reactor equipment demonstrated during BN-600 operation testifies to the high quality of the design, structural materials, equipment manufacture, and operating culture, which undoubtedly influences the safety of the nuclear power plant operations.

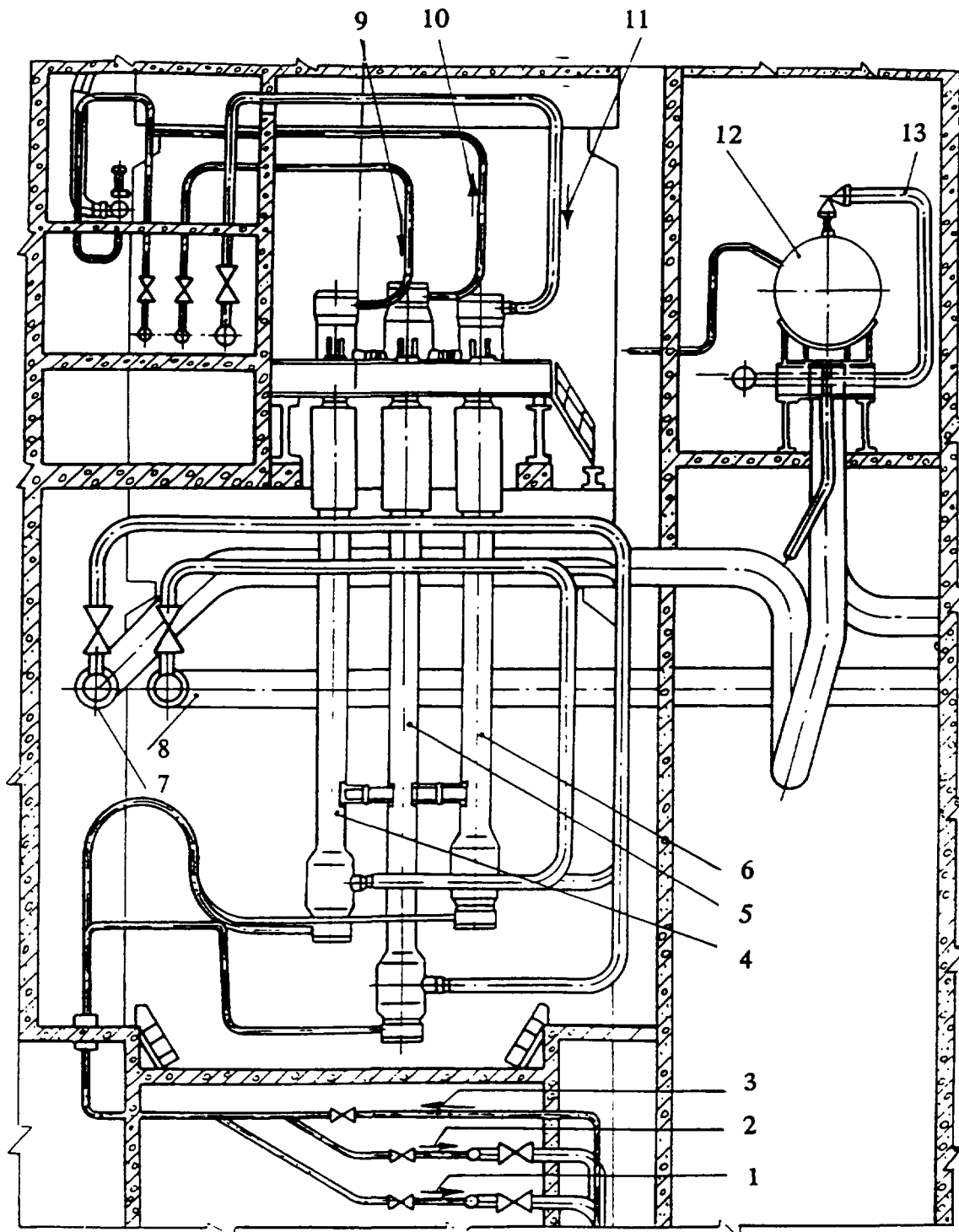
TABLE 2.10. BN-600 SG LOSS-OF-TUBES INTEGRITY EVENTS

Date	24.06 1980	04.07 1980	24.08 1980	08.09 1980	20.10 1980	09.06 1981	19.01 1982	22.08 1983	06.11 1984	10.11 1984	24.02 1985	24.01 1991
Leak place	RH	SH	RH	SH	SH	RH	SH	SH	E	RH	SH	RH
Leak size	L	L	S	S	S	S	L	S	S	S	S	S

Abbreviations: RH - reheater, SH - main superheater, E - evaporator, L - large leak, S - small leak

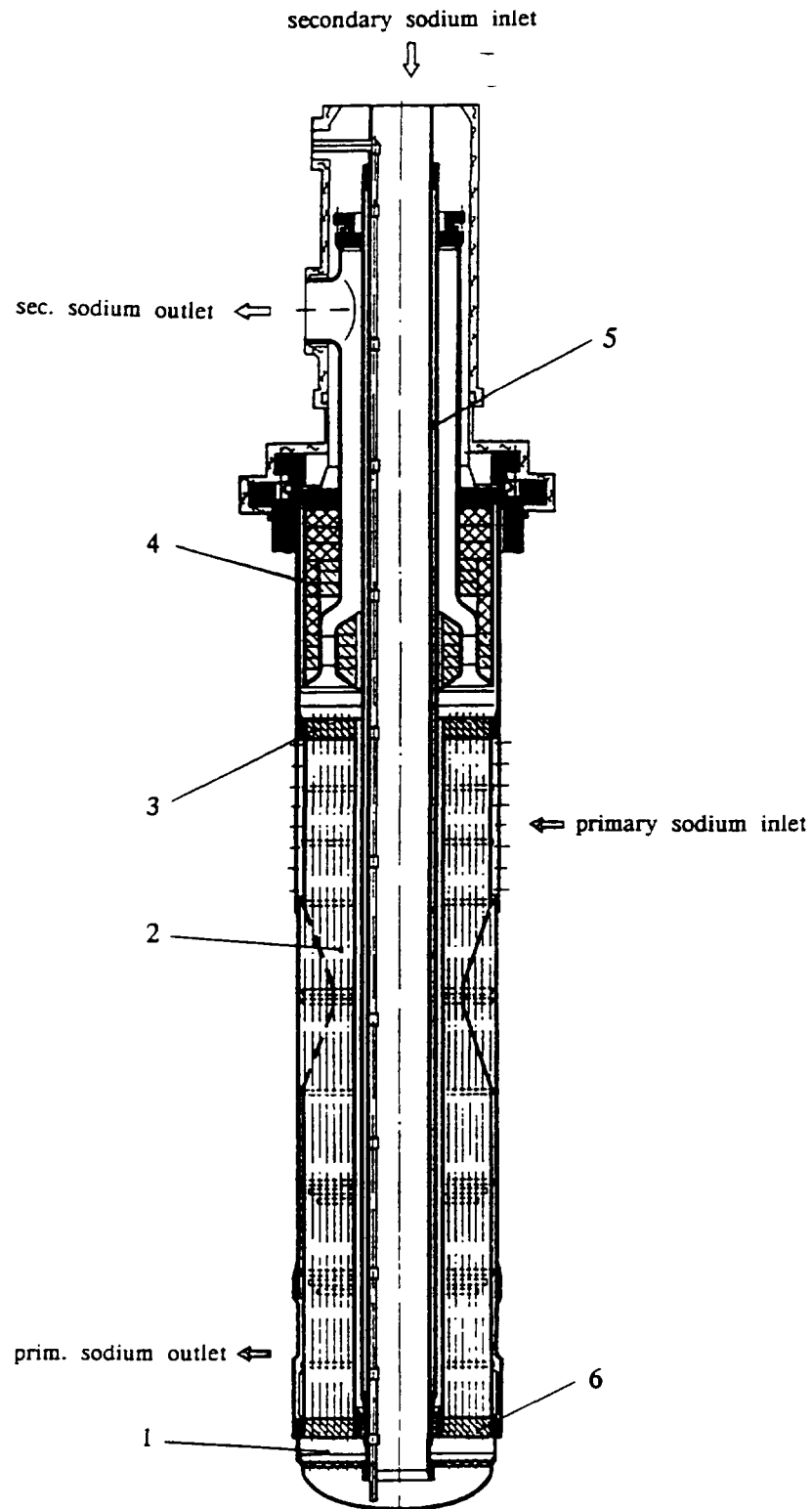
Note: Large leak is characterized by changes in integral parameters of a secondary loop (sodium and gas pressure in expansion tank).

The reactor equipment failures which took place did not violate safe operating limits and according to the International Nuclear Event Scale were assigned to levels 0 or 1.



1 -main steam removal, 2 - reheated steam removal, 3 -feedwater supply, 4 - superheater, 5 evaporator, 6 - reheater, 7 - sodium removal, 8 - sodium supply, 9 - steam supply to superheater, 10 - steam removal from evaporators, 11 - steam supply to reheater, 12 - sodium expansion tank, 13 - steam- sodium reaction products dump line.

Fig. 2.29. BN-600 Steam Generator Layout In Compartment



1 - sodium pressure chamber, 2 - tubing system, 3 - upper tube sheet,
4 - shielding unit, 5 - central downcomer tube, 6 - lower tube sheet

Fig. 2.30. BN-600 Intermediate Heat Exchanger

2.5.3. Radiological safety

Exposure of the reactor unit personnel was associated mainly with maintenance and repair work performed in the primary equipment rooms during reactor outages. Gamma-radiation dose rates in these rooms amounted to 0.05-0.4 $\mu\text{Sv/s}$ being defined by induced radioactivity of the primary sodium (Na-22). The contribution of fission products from leaky fuel rods did not exceed 15%.

Average annual doses to the plant personnel in the last 5 years ranged from 1 to 2.7 mSv. The collective dose to personnel in the same period was 0.65 to 1.8 man.Sv per year. Maximum values of the collective dose were associated with modernization of the primary circuit external sodium systems in 1991-1992.

Gaseous discharges from the equipment air-cooling system and from the reactor plant rooms through the vent stack were the major source of radiological impact on the environment. Aerosol-retaining filters provided in the gas-discharge system mitigate the plant radioactive releases effectively. The activity is caused by leaks in the reactor gas system equipment, by planned gas blow-off from the reactor, particularly at refuelling, and by repair or research work. Data on external releases of radioactivity from the reactor unit are summarized in Table 2.11.

TABLE 2.11. BN-600 RADIOACTIVE RELEASES

Year	1988	1989	1990	1991	1992
Annual release, TBq	33.3	19.3	12.8	10.4	9.0
Average daily release, TBq	0.091	0.053	0.053	0.0285	0.025
Release in TBq per MWe•year	0.072	0.042	0.033	0.025	0.018

In the period of 1988-95 radioactive releases from the power unit to the atmosphere were less than 0.092 TBq/day (compare with the permissible limit of 18.5 TBq/day). In those years upgrading of the fuel design had reduced the number of fuel failure events to single figures. The plant releases consisted mainly of noble radioactive gases - Xe, Kr, Ar. The release of long-lived radioactive aerosols (Ce-137, Sr-90, Mn-54, Co-60, -active nuclides of Pu and Po) was negligible - not more than 1% of the permissible limits. Such radiologically hazardous nuclides as I-131 were absent from the releases because of the high iodine-retaining ability of sodium. The average annual normalized release of radioactivity from the power unit for the last five years was to 0.037 TBq/MWe.

The following constituents of the off-site environment are under continuous surveillance within a 35 km radius area: near-ground layer of air, atmospheric precipitations, snow, soil, water, grass, water-plants, bottom sediments in ponds, local fish, vegetables and fruits. Monitoring data show that in the residential areas and the majority of the sanitary-restricted zone around the station the actual radiological characteristics of flora and fauna are determined by natural sources of radioactivity and are comparable with the natural radiation background. The gamma-radiation dose rate in the satellite town of Zarechny (3 km away from the site) ranges from 0.04 to 0.1 $\mu\text{Sv/h}$. The annual dose to individuals in the local population does not exceed 1.3mSv.

There is a difference between the actual radiation level and the normal background only in the region of the Olikhovskoe bog which is inside the sanitary restricted zone. Several investigations have shown that the bog's radiation conditions were formed during the operation of the first and second uranium-graphite reactor units before the commissioning of BN-600 in 1980. The activity accumulated in the bog is approx. 80 Ci and is attributed mainly to Cs-137. The gamma-radiation dose rate at several points on the edge of the bog reached 2.4 $\mu\text{Sv/h}$. In recent years the gamma-radiation background in this area has shown a tendency to gradual reduction.

2.5.4. Fire safety, sodium leaks

The risk of fire in the power unit is associated with the presence of electrical cables and equipment, and the oil and hydrogen necessary for operation of the pumps and tertiary circuit equipment. Provisions in the power unit for fire safety of these items are traditional for conventional power stations and have been proved by long-term operation.

Particular attention was paid to fire safety for the primary and secondary sodium equipment and pipelines. Technical measures are provided to limit the scope of sodium leaks and fires. Thus all reactor-related auxiliary sodium system pipes leaving the reactor vessel are jacketed up to a second isolation valve (including the valve casings) and are located in partially leak-tight rooms.

Several methods are used for fighting sodium fires: self-extinguishing in partially leak-tight rooms with or without nitrogen supply, extinguishing in trays with hydraulic seals, draining of sodium into emergency catch tanks, and extinguishing by powder compositions.

In partially leak-tight rooms sodium fires are extinguished by actuation of a filtered fire-fighting rarefaction vent system which reduces the oxygen concentration. To promote extinguishing nitrogen can be supplied to the room from special gas receivers.

Non-radioactive sodium fires are extinguished using trays with hydraulic seals covering the entire surface of the floor of respective rooms. Escaped sodium extinguishes itself as a tray is filled. In the steam generator rooms sodium leakage is removed to emergency catch tanks where the fire is extinguished by limitation of air inleakage. In rooms where small sodium leaks are probable systems are provided for the supply of extinguishing powder. In addition in certain places the powder is stored for manual use if a small fire should arise.

During thirteen and a half years of operation of the BN-600 reactor there have been 28 events with sodium leakage out of primary and secondary equipment. The main causes of sodium leakages were:

- defects caused by poor-quality repair - 9 events,
- latent defects of manufacturing and mounting - 6 events,
- depletion of equipment lifetime due to inadequacy of the design - 7 events,
- equipment design imperfections - 4 events,
- human errors during operation - 2 events.

There have been four emergencies with primary sodium leaks, three of which occurred on the pipeline for removal of sodium from the cold-trap. Recently (Oct. 7, 1993) the largest happened in the same place. The total amount of sodium escaped during the event was assessed to be approximately 1000 kg.

The first symptoms of the emergency were short circuits in the main and stand-by electric heating systems. Following actuation of the automatic alarm system by rising radioactivity in the exhaust ventilation air duct from the primary sodium purification system pipeline room, the supposed leaky section was isolated by the valves and the fire-ventilation system was activated. These operated normally. Despite these measures a buildup of radioactive releases from the ventstack was registered as well as a deterioration of radiation conditions in the reactor building rooms, including the main control room. As a result the primary sodium purification system was isolated completely and the reactor was shut down and put into the scheduled maintenance outage state a week earlier the assigned date.

There was no overexposure of the plant personnel and no contamination on or off the site was registered. All this gave grounds for classification of the event as an anomaly, i.e. level 1 to the International Nuclear Event Scale. After completion of the scheduled refuelling and the necessary repair the reactor was returned to power on Oct.24, 1993.

The probable cause of a through hole in the joint between tubes with sodium flows of different temperatures could be high thermal stresses in combination with stresses caused by thermal expansion of the tubes.

Despite the negligible radiological consequences it was concluded from analysis of the event that in the next BN-type reactors external primary sodium pipework systems have to be excluded by arranging them inside the reactor vessel, or (if impossible) by providing complete jacketing in order to have two leak-tight protective barriers.

The largest leakage of secondary sodium happened in May 1994 in a drain pipeline (ID 48 mm). Approximately 1000 kg of sodium were lost, but only about thirty kilograms burned. The remaining sodium was retained and smothered with extinguishing powder in the catch system.

The complex of means used in BN-600 to detect sodium leaks, to localize them and to fight sodium fires allowed serious fire incidents to be avoided during reactor operation.

2.5.5. BN-600 operating safety enhancement

While the reactor has been in operation more stringent regulatory codes and rules for nuclear reactor safety have been adopted. In this connection a special review was carried out to assess the compliance of safety-related systems and components with the up-to-date regulatory requirements. Discrepancies were identified and corrective measures were developed.

The major discrepancy, elimination of which will be most expensive in labour and cost is an inconsistency of the seismostability of individual buildings, structures, systems and devices with the revised requirements for stability against external impacts. According to the new code for NPP seismostability the following levels of seismicity are defined for the site of Belojarsk NPP: design basis earthquake of magnitude 5 to MSK-64 scale, maximum design earthquake magnitude 6. The existing buildings, structures, components and pipelines of the reactor plant were designed, manufactured and erected for the magnitude 5 earthquake in compliance with the regulatory documents currently valid.

Analysis carried out to assess the actual seismic stability of the plant buildings, structures and systems showed that under seismic impact of magnitude 6 destruction of parts

of the SG supports and the turbine building is to be anticipated. Structures of the reactor building, the primary equipment items and the reactor itself would be practically undamaged.

A design has been developed which enhances the seismostability of the reactor building and the SG supports and provides a 3-channel DHRS incorporating air coolers. The DHRS is assumed to operate by natural convection of primary coolant and air in the coolers. In the DHRS intermediate circuit, which is connected to the secondary system pipelines, electromagnetic pumps will be used for initial operation. After experimental study this circuit might be put into a passive mode of operation as well. To promote implementation of this design the technical choices were based on the DHRS previously developed for the advanced reactor BN-800. The main design data for one DHR channel are given below:

Heat removal capacity, MW	13
Sodium flow, kg/s	54
Air flow, kg/s	45
Sodium temperature, C	
- inlet	518
- outlet	328
Air temperature, C	
- inlet	- 46.+ 40
- outlet	317
Time for system actuation, s	25

A special building will be built for the DHRS air coolers. The system is planned to be commissioned in 1998. The DHRS eliminate the need for seismic upgrading of the reactor tertiary system and other systems participating in emergency residual heat removal (power supply system, diesel-generator plant, electric motors of the primary and secondary coolant pumps, etc.). Creation of the seismic protection system (in 1991) for the reactor automatic trip at magnitude 5 earthquake was the first step in implementation of this programme.

Installation of a stand-by control board in the DHR air cooler building is planned. From it the reactor could be shut down and cooled under reliable control if the main control room were to be lost. Pending realization of this modification a procedure has been developed for cooling the reactor down from the local control panels, and for controlling the reactor in a subcritical state from a room which functions temporarily as a stand-by control board.

According to the design the reactor vessel was provided with leak tightness detectors of induction and contact types which are capable of detecting large leaks of sodium from the main vessel to the guard cavity. To detect small sodium leaks an advanced monitoring system based on registration of radioactive aerosols in the argon-filled inter-vessel cavity was tested and commissioned in 1990.

To limit the scope of possible leaks of sodium from the external primary coolant systems additional jacketing was provided for pipelines to the second isolation valves including the valve casings. Similar measures with installation of an additional valve are planned for the spent fuel drum cooling system to prevent failure due to faults or leaks in the isolation valves. Passive safety devices (hydraulic seals) are installed for overpressure protection of the drum's main and guard casings.

Replacement of equipment and instruments from the reactor control and protection system is planned to be carried out in 1993-1996, due to expiration of their design lifetimes. The system will be upgraded to ensure fulfillment (to a feasible extent) of the up-to-date requirements for such systems.

2.5.6. Experimental programmes

Many research programmes have been carried out during reactor operation aiming at the study and perfection of reactor plant performance, development of fast nuclear reactor technology in general, and obtaining experience necessary for construction of the next generation of BN-type reactors. The following experimental programmes might be pointed out:

1. Investigation of power and temperature distribution skewing in the core due to movement of control rods.
2. Investigation of the stress-strain state of the reactor vessel (during plant commissioning and the initial period of operation).
3. Measurement of torsional vibrations of the reactor coolant pump shafts.
4. Investigation for optimization of a high-temperature chemical flushing procedure for the steam-water system.
5. A comprehensive research programme on structural materials for reactor core items (fuel cladding, duct, etc.), and SG tube sheets and tubes.
6. Investigation of reactor core dynamics (transients and response to various perturbations in reactivity and thermal-hydraulic parameters).
7. Investigation of the natural convection capability of the primary and secondary circuits at various levels of initial power up to 50% nominal.
8. Optimization of the procedure for reconnection of one loop to the reactor while it is operating at a power of 20-35% nominal.
9. Investigation of the capability to remove the reactor residual heat in the event of loss of water from the station cooling pond.
10. Experimental determination of the content of various radionuclides in the sodium coolant and in the pipeline materials, and investigation of the behaviour of fission products in the primary circuit.
11. Testing and evaluation of the efficiency of various water/steam-to-sodium leak control systems.
12. Assessment of the sensitivity of the primary sodium boiling detection system using a neutron noise technique.
13. Testing and perfection of the failed fuel monitoring systems.
14. Investigation of the efficiency of systems for the monitoring and control of sodium impurities.

BIBLIOGRAPHY

BN-350 and BN-600

Usynin, G.B., Kusmartsev, E.V., Fast Reactors, Energoatomizdat, Moscow, 1985 (in Russian).

Kochetkov, L.A., et al., Main Results of Operation of Nuclear Power Stations with BN-350 and BN-600 Fast Reactors, Int. Symp. on Fast Breeder Reactors - Experience and Future Trends, Lyon, France, July 22-26, 1985.

Kochetkov, L.A., et al., Operating Experience on Fast Breeder Reactors in the USSR, Int. Conf. on Fast Reactors and Related Fuel Cycles, 28 October - 1 November, 1991, Kyoto, Japan.

Bolgarin, V.I., et al., Experience and Organization and Performing Repair Works on Main Equipment of BN-350 Reactor, Int. Symp. on Fast Breeder Reactors and Future Trends, Lyon, France, July 22-26, 1985.

Mitenkov, F.M., et al., Control Rod Drivers for Sodium Fast Reactor Control and Protection Systems. Atomizdat, Moscow, 1980 (in Russian).

Stekolnikov, V.V., et al., Operation Experience of Sodium-Water Steam Generators in the USSR and Prospects for Their Development, Int. Symp. on Fast Breeder Reactors - Experience and Future Trends, Lyon, France, July 22-26, 1985.

Makovsky, A.A., et al., Comparative Analysis of the Arrangement and Design Features of the BN-350 and BN-600 Reactors, Int. Symp. on Design, Construction and Operating Experience of Demonstration Liquid Metal Fast Breeder Reactors, Bologna, Italy, April 10-14, 1978.

Kirushin, A.I., et al., Experience of BN-600 Reactor Plant Safe Operation as a Part of the 3rd Power Unit of Belayarok NPP, the 4th Annual Scientific & Technical Conf. of the Nuclear Society "Nuclear Energy and Human Safety", June 28-July 2, 1993, Nizhny Novgorod, Russia (in Russian).

Kirushin, A.I., et al., Evolution of BN-600 Reactor Core, the 4th Annual Scientific & Technical Conf. of the Nuclear Society. Ibid.

Rineiskii, A.A., Comparison of Technical and Economic Characteristics of NPPs with Modern Thermal and Fast Reactors, Atomnaya Energiya, V. 53, pp. 360-367, 1982 (in Russian).

Budov, V.M., et al., Intermediate Heat Exchangers Design and Experimental Testing, Int. Symp. on Design, Construction and Operating Experience of Demonstration Liquid Metal Fast Breeder Reactors, Bologna, Italy, April 10-14, 1978.

Osipov, S.L., et al., Radiation Influence of BN-600 Fast Reactor Power Unit on the Environment, the 4th Annual Scientific & Technical Conf. of the Nuclear Society "Nuclear Energy and Human Safety", June 28-July 2, 1993, Nizhny Novgorod, Russia (in Russian).

Kamanin, Yu. L., et al., BN-600 Reactor Plant Safety Insuring. Considering its Operating Experience, Int. Fast Reactor Safety Meeting, Snowbird, Utah, USA, Aug. 12-16, 1990.

PFR

"Status of Liquid Metal Cooled Fast Breeder Reactors". Chapter III - 8.2. IAEA Technical Reports Series No 246 (1985).

"Fast Reactor Data Base", IAEA-TECDOC-866, (1996).

Broomfield A.M., Nucl. Energy 25(2), 73-84, (1986).

Gregory C.V.G., Nucl. Energy 31(3), 173-183, (1992).

Adam E.R. and Gregory C.V.G., The Nuclear Engineer, 35(4), 112-117, (1994).

Gregory C.V.G., Proc. Int. Conf. "Fast Reactors and Related Fuel Cycles".

PHENIX and SUPER PHENIX

Chevrier, C., et al., Les surgénérateurs, Rev. Gen. Nucl. RGN (6-1979) 569-670.

Creys-Malville, Nuclear Power Station, Construction of the World's First Full Scale Fast Breeder Reactor, Nucl. Eng. Int. 43-60 (1978) .

Superphenix, Nucl. Europe, Journal of ENS, 18-36 (1985).

Tarby, S. et al., L'atelier pour l'évacuation du combustible de la centrale de Creys-Malville Proc. Int. Symp., Lyon, 1985.

Perotto, G., et al., Repair of the Creys-Malville fuel Storage Drum Proc. Int. Conf., Kyoto, Japan, 28 October - 1 November, 1991.

Pesteil, J.M., et al., Consequences of External Storage Barrel Leakage on Fuel Management Trans. ANS Win. Meet., Washington, 1990.

Montane, C. et al., Nachrüstarbeiten im Superphenix, Atomwirtschaft, December, 1993.

Barberger, M., et al., The Creys-Malville Plant Fast Breeder Station; Test and Start-up, Proc. Am. Pow. Conf., Chicago, 1986.

Saitcevsy, B. et al., Le démarrage de Superphénix et la filière des réacteurs à neutrons rapides, Rev. Gen. Nucl. RGN (2-1987).

Mergyu, A., Commissioning of the World's First Commercial Scale FBR at Creys-Malville, Nucl. Eng. Int. 20-24 (1988).

Gourdon, J., et al., Superphénix Physics, Nucl. Sc. and Eng. (September, 1990).

Asty, M., et al., MIR Inspects Superphenix, Nucl. Eng. Int.38 (1986).5

Mergui, A., et al., Experience of the 1200 MWe Superphenix FBR Operation, Proc. Am., Pow. Conf., Chicago, 1990.

-
-

Sauvage, M., et al., Overview on European Fast Reactor Operating Experience., Proc. Int. Conf., Fast Reactors and Related Fuel Cycles, Kyoto, Japan, 28 October - 1 November 1, 1991.

Lacroix, A., et al., Experience Gained from 1200 MWe Superphenix FBR Operation. Ibid.

Elie, X., Chaumont, J.M., Operation Experience with the Phenix Prototype Fast Reactor. Ibid.

Coulon, P., Martin, L., Phenix Operating Experience; Fuel Management and Fuel Cycle. Ibid.

Gregory, C.V., Acket, C., Repair in Fast Breeder Reactors; Experience to date Prospects for the Future. Ibid.

Hennies. H.H., Development of Fast Reactor in Europe. Ibid.

Chapter 3

EXPERIENCE IN CONSTRUCTION AND PRE-OPERATIONAL TESTING OF THE PROTOTYPE LMFRs

3.1. CONSTRUCTION AND PRE-OPERATIONAL TESTING OF THE LMFR SNR-300

3.1.1. Introduction

After the respective R&D preliminaries, the nucleus of the fast reactor prototype SNR-300 developed towards realization in 1972, when international groupings of utilities and manufacturers of Belgium, the Netherlands, and Germany were founded in order to build the plant as Kalkar Nuclear Power Plant on the Rhine river banks close to the border with the Netherlands. Construction began early in 1973 after the concept and first erection license was granted in December 1972. In March 1991, the German Federal Minister of Research and Development announced the unconditional abandonment of the project after a thorough evaluation of the overall situation.

It was clear at that time that a final operating license was not achievable under the prevailing political circumstances, at least not in a foreseeable future. This again meant a further incalculable increase in costs. Neither the industry involved in the project (utilities and manufacturers) nor the Federal Minister of Research and Development were prepared to carry the additional financial burden related to the nuclear commissioning still to come. Moreover a financial risk-sharing contract related to operation of the plant had still to be agreed in the absence of a clear positive perspective. The costs had already increased by a factor of 5, of which about 50% could be attributed to price escalation because of the delays of the project, and another 50% to additional engineering and R&D work and installations required by the licensing authority. Both factors were clearly licensing-related. The degree of price escalation and the final cessation of the project were definitely politically motivated.

The adverse political influence started in Germany as early as the late seventies, when the usefulness and the safety standards of nuclear power in general and SNR-300 in particular were questioned more and more by the Social Democratic Party, the initiator and until then strong supporter of this research project.

So, besides the tremendous amount of money already spent, all the valuable experience gained so far with international cooperation, with design work, erection, construction, and pre-operational testing, particularly with trouble-shooting under extraordinarily difficult conditions, with safety-related tests of decay heat removal operation by natural convection, and with completely passive plant behaviour (e.g. after a long-lasting station black-out) have been wasted, in so far as this experience is plant-specific. This has led finally to the fact that the development of fast reactor technology as a potential future source of electricity generation has been suspended in Germany.

3.1.2. Description

Classification of SNR-300: The nuclear power plant SNR-300 was a prototype reactor project comparable to PHENIX in France, to the Prototype Fast Reactor PFR in Great Britain, and MONJU in Japan. PHENIX and PFR went into operation in 1974, and MONJU reached

criticality in 1994. A similar project in the United States of America, the Clinch River Breeder Reactor CRBR, was cancelled in 1983 after site preparation and main component manufacturing had already started. Construction of SNR-300 began early 1973. Start of power operation was originally scheduled for 1978/79.

All these projects were designed for a power output of 250-300 MWe. They were supposed to form an important intermediate step on the way to fast breeder reactor power plants with a power output of 1000-1500 MWe. Such a power plant has been built in France already, SUPERPHENIX (SPX 1).

PHENIX, SUPERPHENIX and PFR are so-called pool reactors, whereas the other three projects are loop reactors. In a pool reactor, the whole primary heat transfer system including main pumps and intermediate heat exchangers is integrated into the reactor vessel (pool), while the loop reactors have parallel primary sodium heat transfer circuits (loops) with the main heat transfer components external to the reactor vessel. The secondary heat transfer system, installed between primary system and water/steam system for safety reasons, is practically identical in both cases. It also consists of three parallel circuits. Live steam conditions and the achievable efficiency are very similar in all plants: 500°C, 165 bar, 40%. These are close to the conditions of coal-fired stations.

Highlights of the pre-construction period: SNR-300 was planned as an international project from the very beginning, i.e. about 1966. The final arrangement consisted of a three-country cooperation comprising Germany, Belgium, and the Netherlands, involving the manufacturers, the utilities, and the R&D organizations. The project was shared 70% for Germany, 30% for Belgium and the Netherlands, i.e. 15% for each. The main highlights of the project development until start of construction in 1973 are listed in Table 3.1. For more details of the origin and design of the plant reference can be made to [3.1, 3.2, 3.3].

The first nuclear license of SNR-300, which was necessary for the beginning of construction, was granted in December 1972 after a 2-year safety assessment and licensing process. Based on 16 further licensing steps, which were spread over 13 years altogether (the last one was granted in 1985), construction of the plant and pre-operational testing were completed by 1986 and early 1987. A survey on the most important licensing steps is given in Table 3.2.

The German licensing procedure is usually a step-wise approach as indicated in Table 3.2. It means that the first step generally comprises an overall approval of the safety design concept of the plant, and is required for excavation of the pit, erection of a certain part of the main buildings, essentially the base mat and the walls up to zero level, and a so-called "preliminary positive overall appraisal" of construction, erection, and operation of the whole plant. This appraisal is explicitly required by the Atomic Energy Act.

On this basis, the further course of the project on the site can be divided into steps according to the progress of work. In these steps, the construction and erection of individual technical items (buildings, systems, components, etc.) are licensed after respective safety assessment processes, and the "preliminary positive overall appraisal" is developed further until the last licensing step, namely operation, by which time the appraisal is finalised.

This procedure must be kept in mind in understanding the tremendous time delays mentioned later from one erection step to the next, since each licensing decision offers the

opportunity to licensing authorities, if they are not basically in support of the project, to bring in various kinds of disturbances, e.g. new design rules, new general thinking on safety issues, and even politically-motivated influences. Today, many nuclear projects are in the situation where a licensing authority is practising a "cessation-orientated execution of the law", which is illegal. The most important factors in this respect are outlined later.

TABLE 3.1. HIGHLIGHTS OF THE SNR-300 PRE-CONSTRUCTION PERIOD

Time	Highlights
09.11.1966	Approval to go ahead with the SNR-300 project issued by the then Federal Ministry of Scientific Research (BMwF)
January 1968	Establishment of consortia relations on the manufacturer's side between Siemens/Interatom (Germany), Belgonucléaire (Belgium), and Neratoom (The Netherlands)
December 1969	First issue of Safety Analysis Report (SAR)
06.03.1970/23.10.1970	Licensing application by the then utility customer Projektgesellschaft Schneller Brüter (PSB)
May 1970/December 1971	Revised SAR
14.07.1971	Memo of understanding between manufacturers
January 1972	Founding of the utility grouping Schnell- Brüter-Kernkraftwerksgesellschaft mbH (SBK), the successor of PSB
20.03.1972	Public hearing at Kleve
May 1972	Preliminary safety assessment
June 1972	Positive vote of the Reactor Safety Commission (RSK)
Summer 1972	Tender placed to SBK
12.10.1972	Founding of International Natrium-Brutreaktor-Bau GmbH (INB), the successor of the manufacturer consortium
10.11.1972	Power station contract signed by SBK and INB
23.11.1972	Notification of granting of public funding as a contribution to the overall costs by the then Federal Minister of Education and Science (BMBW)
18.12.1972	Concept and first partial construction license granted
April 1973	Start of construction

TABLE 3.2.: SURVEY OF IMPORTANT LICENSING STEPS FOR SNR-300

Time	Licensed Construction and Erection Step
18.12.1972	Basic concept, reactor building up to +/-0.00m, basemat of steel shell
22.05.1974	Reactor building, remainder of steel shell, steam generator building D2, ancillary systems building
01.08.1975	Steam generator buildings D0 and D4, switchgear building, cooling water extraction and return building, auxiliary cooling water line, cavities, catch pans, cranes
15.04.1976	Emergency core cooling system stack, cooling water pumps building
15.12.1977	Biological shield, redundant diesel air intake channel
20.12.1978	N ₂ -inertization systems, fuel store and handling (partly) including related instrumentation and control, electrical power distribution system, main control room, reactor cell cover
10.06.1980	Sodium auxiliary systems, cover gas systems, fuel store and handling systems (remainder), cooling water and supply systems, waste treatment and disposal systems, communication and data handling, reactor cell internals (vessel support structure, reactor safety tank)
09.10.1981	Ventilation systems (except reactor building), floor cooling device (core catcher), decay heat removal systems and cooling water system, emergency core cooling system
30.04.1982	Modification of steel shell of containment
30.07.1982	Well building, ventilation systems (reactor building), radiation protection instrumentation
22.09.1982	Reventing system, emergency power supply, reactor vessel including internals, rotating reactor shield plug, primary and secondary heat transfer systems, plant protection system
20.06.1984/03.10.1985	Various plant and system modifications

Plant cost evolution: The original cost estimates of November 1972 of 1,535 Billion DM already included a provision of 248 Million DM for escalation. This price was considered high in comparison to other projects of similar nature.

In October 1975, the estimates already resulted in a cost increase of 50%, assuming a project delay of about 16 months. This increase was attributed mainly to an inflationary price development in the rather long delay period. Also the fact that the plant had to be considerably modified as a result of the first licensing step in order to comply with important additional safety design requirements led to a cost increase.

In April 1978, the new cost estimates had to take into account an overall project delay already of 75 months caused mainly by licensing-related delays. Additional engineering and R&D efforts as well as further originally unplanned installations due to the escalating licensing requirements became necessary. This was due to the general attitude starting in the seventies to demand more safety-related measures, to take into account accidents which were more improbable, e.g. aircraft crashes, and the increasing tendency to go into much more detail in the proofs to be furnished. This process was a dynamic one and did not stabilize over the years. The result was an enormous escalation of costs.

In the estimate of 1982, the prospective total costs had now increased by 300% based on a project delay of 7.5 years. This was attributable 50% to inflation-related price escalation during the time delay and 50% to licensing-related refurbishment and design extensions.

At the time of the abandonment of the project in April 1991, the overall costs had increased to almost 7 Billion DM, almost 5 times the original estimate, 4.9 Billion of which was public funding, and the rest was from both sides of industry, the utility and the manufacturer.

This development of costs triggered dwindling political support. And an additional costs increase could already been foreseen for the nuclear commissioning phase still to come, for the financial risk-sharing contract to be agreed on by the Federal Ministry of Research and Development and the utilities for the later plant operation. The operating costs were planned to be recovered by selling the electricity.

3.1.3. Construction and pre-operational testing

Construction of SNR-300 began in April 1973 and was essentially finished in mid 1985, when the leak and pressure tests of buildings and systems were successfully completed. During the period until about 1979 only the buildings could be erected in the main, since licensing of systems and components was already seriously delayed. This was also the reason for the rather long erection process for the buildings. It resulted from the fact that the respective licenses were depending on the safety evaluation of the Hypothetical Core Disruptive Accident (HCDA), which determined respective mechanical and thermal loads for the structures in the reactor vessel system surrounding the core, the vessel support structures, and the containment building itself.

Another problem was posed by the requirement for redundancy, diversity and overall reliability of the decay heat removal scheme for an unusual spectrum of operating and accident situations including the already mentioned hypothetical core disruptive accident, and various external events, especially large earthquakes and airplane crashes.

These licensing problems, however, were not only related to the buildings and their arrangement on the site, but also - and even more so - to the respective systems and components.

After completion of civil work to the greatest possible degree, the erection of the mechanical and electrical components and systems commenced very late, and only in small steps, due to the long licensing process from the end of 1978 until the end of 1982. The number of personnel on site, as shown in Figure 3.1, a real indicator of the work actually going on, could therefore be increased only very slowly during this period, i.e. from about 300 to

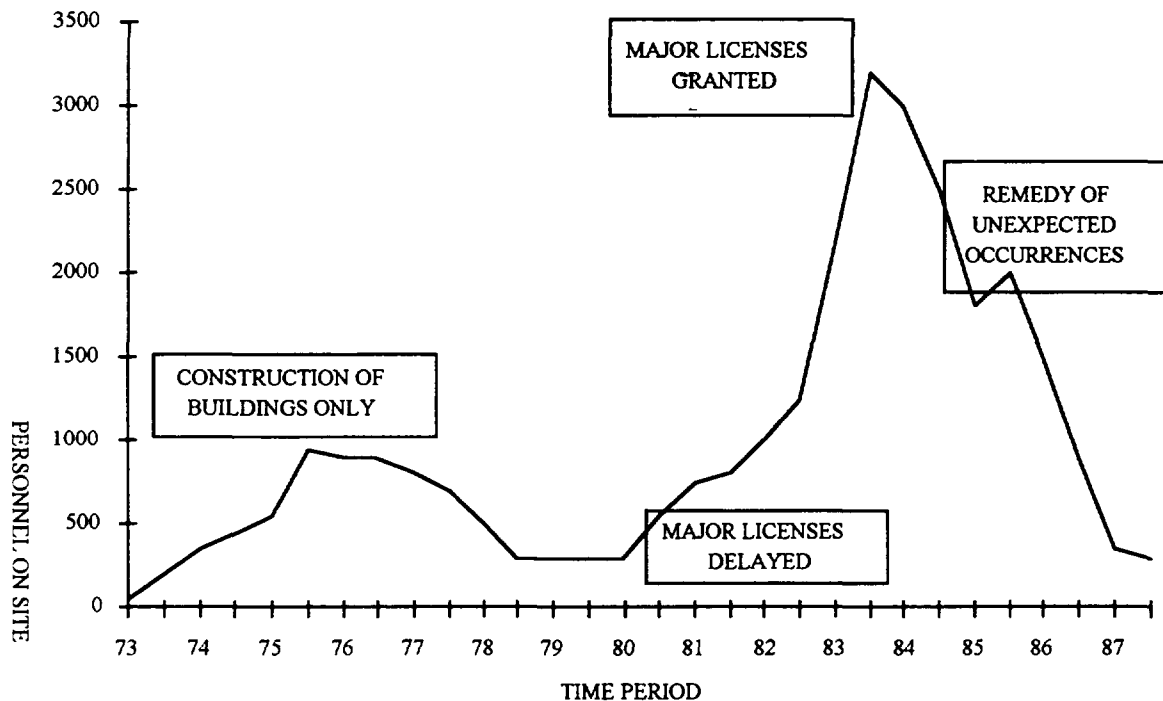


FIG 3 1 Development of plant personnel during construction and pre-operational testing

about 1250. A sharp increase up to about 3200 was then realized within roughly 18 months after granting of a major license in September 1982. The systems and components concerned are listed in Table 3 2.

The large increase of the work force in this short period required far-reaching organizational measures including accommodation, site access regulations, and especially a detailed work schedule to assure effective working on the site.

The following numbers may create a feeling of the volume of erection work to be accomplished: around 70 km of pipe work with 3000 supports, 21000 valves, 1100 pumps and blowers, 1500 vessels and heat exchangers had to be installed. This included also the drilling of about 300000 plug holes, 5000 km of cables to supply 8700 pieces of equipment and measuring circuits had to be routed. Some milestones of this period are listed in Table 3 3.

Since SNR-300 was built in Germany, all design and safety requirements had to be orientated on German regulations, which meant continuous adjustment to the developing state of science and technology. This was a significant burden, especially for the partners from Belgium and the Netherlands.

A large part of the existing regulations were of a conventional nature and posed no serious problems apart from their interaction with the nuclear regulations. The latter, which were developed only after 1974, raised many serious difficulties, mainly for two reasons:

- 1) The development of nuclear regulations proceeded only very slowly during the detailed planning and erection phase, and was finished in many cases only after its completion.
- 2) These regulations were exclusively orientated to Pressurized Water Reactors and required interpretation for other licensing cases as, e.g. SNR-300.

TABLE 3.3. IMPORTANT MILESTONES OF ERECTION WORK OF SNR-300

Time	Erection Event
January 1981	Start of erection of components of mechanical and electrical auxiliary systems
Autumn 1981	Erection of reactor safety vessel
September 1982	Erection of reactor vessel
July 1983	Completion of radial breeder assembly fabrication
November 1983	Delivery of reactor cover plug, erection of primary pipe work
March 1984	Completion of erection of reactor vessel system (installation of cover plug)
September until November 1984	Delivery of helical tube steam generators
March 1985	Completion of fuel assembly fabrication

Since there were no specific regulations available for fast breeder reactors, this resulted in the necessity to at first clarify their applicability to a completely different reactor concept. After many iterations and interpretations, the respective component or system design had to be adjusted. Due to the large discretionary powers of the licensing authorities, this was always an extensive source for delays and, as a consequence, cost increases. It was only in 1980, in the light of similar plants being already in operation or in a late state of erection in other countries, that it was realised that the specific character of this prototype plant had to be given more consideration. By then, however, most of the design and fabrication work had been practically completely adjusted to the often inadequate requirements so that SNR-300 could no longer take advantage of the change of approach sufficiently to simplify the remaining work.

On the other hand in many areas new design rules and methods had to be developed for the new technology. This was particularly true in the following fields:

- 1) Creation of design criteria and methods for furnishing proof of the mastering of the Hypothetical Core Disruptive Accident (HCDA) in the following main areas:
 - codes for the description of dynamic hydraulic/structural integrity behaviour;
 - criteria for the respective material strength;
 - codes for the evaluation of the energetics of the accident;
 - verification of the developed codes;
 - containment dynamics taking due account of aerosol behaviour and radiology.
- 2) Creation of applicable rules for the calculation of stress and strain in the domain of high temperatures taking due account of creep and fatigue phenomena.
- 3) Creation of design criteria and methods for loading due to large earthquakes and airplane crashes.

- 4) Fulfilling strong demands for the reliability of shutdown, decay heat removal and electrical energy supply systems in order to maintain the HCDA in the regime of hypotheticality.
- 5) Creation of design criteria and methods for furnishing proof of the mastering of the highly dynamical steam generator accident loads due to a large sodium/water reaction.

After what was undoubtedly the most important partial license according to the Atomic Energy Act was delivered in September 1982, erection and pre-operational testing of a large number of components and systems were possible. Both erection and pre-operational testing were no longer depending on further licenses, but only on the so-called releases by the supervisory authority. This had, however, only a negligible effect on the erection and pre-operational testing according to a time schedule prepared in 1983 [3.4-3.7].

Construction and pre-operational testing of a system were formally licensed together. However, construction and pre-operational testing were subject to a thorough supervision programme, which meant that individual erection and pre-operational testing events required a formal release. This, of course, was dependent on the fulfillment of many prerequisites defined and agreed in advance between the supervisory authority, the inspectors and, naturally, the plant manufacturer. Last but not least, it was dependent on the preparation of the huge amount of obligatory documents.

The prerequisites for the release of the pre-operational testing events of a system can be described quite generally as verification of successful completion of construction, the design review (including stress analyses), functional tests of the system, and the fulfillment of special requirements set in the preceding licenses.

Pressure and leak tests were defined as the start of the pre-operational testing of the plant. They and the erection events marked the transition from pure construction to pre-operational testing. Numerous pressure and leak tests were performed on subsections of these systems before the first integral pressure and leak tests were carried out. More than 900 of these partial and integral tests were completed from summer 1983 to about April 1985.

The most striking single events of this period, which were specified in the revised October 1983 schedule, were the pressure and leak tests of the:

- 1) Primary system including the reactor vessel in December 1983
- 2) Secondary systems in February/March 1984 and January 1985
- 3) Containment system in October 1984.

It was possible to complete all tests without any significant corrections within the specified values and within the given time. In this respect, the pressure and leak tests of the relatively complex and large-volume low-pressure containment system and the reventing system were outstanding highlights. The leak-rates were much lower than specified.

The second striking step towards readiness for operation was the delivery of the sodium to the site, final filling of the respective systems (which had been preheated electrically or by the gas heating system), circulation of the sodium and operation of the purification plant. According to the schedule, this period was to commence in August 1984. It contained the contractually important key point "Plant Construction Completed", scheduled for August 1985. It was defined as the filling of the primary system and the reactor vessel with sodium, and high temperature purification operation scheduled to last from begin of October until begin of November 1985.

In practice, this period lasted only from July 1984 until August 1985, whereby the most important key point "Plant Construction Completed" was attained in April 1985, which was 4 months earlier than scheduled. This meant that the work was 7 months ahead of the contractual schedule.

Approximately 1070 t of sodium were loaded into the dump tanks of the primary and secondary systems in 4 steps from July 1984 to February 1985.

Purification of the sodium in the dump tanks via the primary and secondary purification systems began in late September and December 1984, respectively. At the start of the measurements, the plugging temperatures were around 200°C, and it was possible to lower them to 130-120°C within a short time.

Pre-heating, filling, and operation of the systems at higher temperatures were carried out in compliance with specific temperature and temperature difference criteria, which were stress analysis.

The impurities in the sodium were well below the specified values. High temperature purification operation commenced in June 1985 instead of October as indicated in the revised schedule. The following targets were pursued during this testing phase:

- 1) Increasing temperatures in approximately 30 K steps from around 200°C to 420°C and a subsequent temperature setback to 200°C; duration of this operation was about 30 days.
- 2) Measurement of the quality of the sodium and the cover gas.
- 3) Determination of the change of volume in the level holding tank (primary system) and in the secondary surge tanks caused by temperature changes in the main heat transfer loops during operation.
- 4) Measurement of various hydraulic data.
- 5) Measurements of heat losses from the systems (via the insulation for example), and plant room temperatures.
- 6) Vibration measurements on the pipe work, and inspection of support and guidance structures.
- 7) Temperature measurements at penetrations and temperature reduction sections of the pipe work.

In the primary system the plugging temperature increased with the system temperature. A value of 200°C was measured for about 2 weeks, but it was then possible to lower it to 160°C and subsequently to 120°C. The hydrogen content in the cover gas of the primary system was reduced from 5000 to approximately 600 vpm by way of continued purification of the sodium.

In the secondary system, a comparable plugging temperature variation resulted from similar changes in the system temperature. The final value here was also around 120°C. But in this case it was achieved within a few days. Although the plant room temperature and system heat loss measurements performed during the high temperature purification phase confirmed the design values in wide areas, it was necessary to rework the insulation in some regions (e.g. in the area around the main heat transfer systems), and to increase the flow-rates in subsections of the ventilation and nitrogen inertization systems using booster blowers to be installed at a later date.

Hot flushing operation on the water/steam side was performed for the main heat transfer system at the beginning of April 1985, and for the decay heat removal systems in May 1985. Good conductivity and iron values were obtained in the cooling water relatively quickly.

Power testing of the decay heat removal systems commenced with the filling a steam generator group of one loop on the water side. To start with it was impossible to continue the test at 420°C due to the repair of the dump and leakage hold-up tanks, described later. As a result of the temporarily insufficient dump tank capacity, the possible necessity of a dumping event was avoided by cautious operation of the main heat transfer systems at approximately 300°C with a main pump speed of about 30%.

Especially in a loop-type reactor, the behaviour of the pipe work is of significant importance. Tests showed the following:

- 1) After reference measurements with the hangers locked, the procedure included unlocking, increasing the pipework temperatures sodium filling and temperature variation. Calculated and measured displacements were in quite good agreement. Only a few spring or constant hanger forces had to be re-adjusted by less than 12%. Insulation weight tolerances were the reason for this deviation.
- 2) Vertical movement of the pipework followed the temperature steps with a time lag due to friction in the insulation.
- 3) The deviation in vertical displacement between calculation and measurement was within the specified tolerances.
- 4) Low mass flow-rates in the circuits sometimes led to some stratification effects in the coolant.
- 5) In very flexible parts of the pipework the sliding support bearings with a friction coefficient of ~ 0.1 had to be replaced by ball bearings with a friction coefficient of ~ 0.01 in order to reduce the number of earthquake shock absorbers and snubbers. A larger number of sliding support bearings than would otherwise have been necessary had to be installed.
- 6) The auxiliary sodium service systems were checked, too, but to a lesser extent. The principal results were the same as for the main system.
- 7) There were no significant vibrations of the primary and secondary pipework. During the start-up period before the core was in place, butterfly valves in the primary circuits served as throttle valves. This induced some vibration in the adjacent down-stream line, but it was judged not to be relevant for operating conditions with the core installed.

In the phase described from autumn 1983 until December 1985, around 95% of the overall pre-operational testing was completed. This was only slightly below the target and was an exceptional accomplishment for a prototype reactor. Table 3.4. summarizes the milestones of the pre-operational testing phase up-to early 1986.

Further pre-operational testing was considerably impeded and delayed from the second half of 1985 until late 1986 by special unexpected events described later. Rectification of these events made it necessary to repeat various testing steps already carried out. Nevertheless, it was possible to inert the primary cell areas in December 1985. The 95% completion already mentioned included approximately 3040 single system and approximately 200 interconnected system tests. Thus in spring 1986, the plant was ready to accept the breeder and fuel

TABLE 3.4. MILESTONES IN THE PRE-OPERATIONAL TESTING PHASE OF SNR-300 UP TO JANUARY 1987

Milestones	Time/Period
Approximately 900 partial and whole system pressure tests	June 1983 - April 1985
Single pressure and leak tests	
- Primary system (closure of reactor plug)	12.83/(01.84)
- Secondary systems 1/2/3	02.84/03.84/12.84
- Containment system	28.09.84 - 01.10.84
- Steel shell and containment building	05.04.85 - 06.04.85/
- 1a area/1b area	08.02.85 - 09.02.85
Sodium delivery to the site	15.07.84 - 13.05.85
Sodium filling into the dump tanks and start of purification operation in the primary/secondary systems	11.12.85/29.09.85
Sodium filling into the systems and start of circulation operation	
- Primary system	28.04.85
- Reactor tank and loop 1 (i.e. construction completed)	02.05.85/09.05.85
- loop 2/loop 3	24.11.84/07.02.85/
-Secondary system loop 1/loop 2/loop 3	28.02.85
-Emergency core cooling system	15./19.06.85
-Na-cooled fuel store and cooling system	30.03.85-05.05.85
High temperature purification operation (Primary and secondary systems)	28.06.85-15.09.85
NaK delivery and filling into floor cooling device (core catcher), circulation operation	10.09.85-21.11.85
Water/steam side	
- water flushing operation	April/May 1985
- steam generator filling and testing of a leg-specific decay heat removal system	interrupted on 13.08.85 until after dump tank repair
Inertization of Na-systems area	from 20.12.85 onwards
Natural circulation tests	12.85 until 01.87

assemblies which were available in the fabrication plants, despite the remedial work for the unexpected occurrences.

These negative influences were, however, reflected in the staff development on the site: a relatively sharp decrease in the number of site personnel from the end of 1983 from a temporary peak of approximately 3200 to about 1200 people in the summer of 1985, which was largely planned. The problems described later, made it necessary, however, to increase the number to 1900 people by the turn of the year 1985/86 (Figure 3.1). In the middle of 1986, the work force was again roughly up to schedule. In May 1987, only about 350-400 people were still working on the site, almost exclusively commissioning personnel of the manufacturer and the customer.

3.1.4. Unexpected occurrences and their remedy

In the following section, three occurrences which caused serious delays in the non-nuclear start-up schedule are described: repair of the sodium dump and leakage hold-up tanks; recovery of fragments of a broken vibration measurement lance; and increased hydrogen concentration in the reactor vessel and the sodium-cooled fuel store inert gas plenum.

Repair of sodium dump and leakage hold-up tanks: Ten sodium dump and leakage hold-up tanks made of ferritic material with the designation 15Mo3 were installed in the primary and secondary systems area. In August 1985 a small sodium leak in one of the dump tanks was discovered visually during a routine inspection walk. Due to the very small leak-rate no alarm was triggered by the smoke detectors. Thorough inspection showed that all ten tanks revealed transverse microcracks which penetrated the walls in the area of the weld seams. More detailed investigation showed that they had originated from the inside.

All parties concerned (manufacturer, safety experts, authorities) finally came to the conclusion that the cause was the adverse coincidence of the following parameters, which had led to the formation of cracks and their propagation through the wall about a year after filling with sodium:

- 1) Microscopic cracks and geometric inhomogeneities as a result of the welding process
- 2) A rather high level of residual stresses after welding without subsequent heat treatment
- 3) Formation of iron hydroxide, especially $\text{FeO}(\text{OH})$, being the only corrosion product relevant for this question, during hydraulic pressure tests and the subsequent long storage times on the plant despite inert atmosphere.
- 4) Formation of atomic hydrogen due to the reaction of the sodium with the iron hydroxide.

After the cause was identified, all welding seams, not only those directly affected, were removed on site under extremely difficult confined conditions and rewelded using improved welding parameters. This process took approximately 4.5 months, and was completed in accordance with a schedule drawn up for the operation. Ultrasonic tests shortly after repair and recharging with sodium and one year later showed no evidence of cracks. An examination of the complete plant for similar evidence showed that the cold trap vessels were also affected. However repair work on these was very much easier as disassembly and reassembly were relatively simple and repairs could be carried out in the workshop.

Salvage of debris from a broken vibration measurement lance: At the beginning of 1986, a vibration measurement lance, which had been installed for trial purpose in the central position of the core (which had not yet been loaded) had to be disassembled because the measuring signals indicated a fault. The lance had two inductive pick-ups, one for connection to the bottom of the gas bubble separator and one for connection to a special central grid plate insert.

When removal was attempted the lance jammed in the grid plate area. The reason was that the retention springs were not able to pull the coupling jaws of the inductive pick-up back into the original position. This was due to a sodium leakage in the pneumatic system with which the jaws were to be activated. During the attempt to free the lance by rotating it and increasing the tensile pull, it broke in the region of the upper inductive pick-up, roughly 2.5 m above the bottom. The 2.5 m long piece and some small parts remained in the reactor vessel and had to be salvaged. Fortunately, six dummy assemblies were positioned around the central

position, which meant that the search for the parts could be limited to this small area. Apart from a very small eyelet, which posed no risk to safety, it was possible to remove all the missing parts from the vessel using plastic bags to retain an inert atmosphere. For this purpose, the sodium level was lowered to the level of the grid plate, the argon was kept under a slight overpressure and the temperature was maintained at approximately 200°C.

The grab and lighting equipment were tested and optimized in an Interatom (now SIEMENS) test plant before being used in the reactor vessel. Use was made of valuable experience from the UK and France. The salvage process took approximately 2 months, and was completed to time according to the special work schedule drawn up for the purpose.

Penetration of moisture into the inert gas plenum of the reactor vessel: Handling tests carried out at the same time with the shutdown systems showed a certain sluggishness of the centering tube shifting device. The centering tube moves when resetting the reactor to handling operation. During this period the hydrogen content in the gas plenum of the reactor vessel behaved remarkably and seemed to increase continuously.

Detailed and systematic investigations finally clarified the cause for these unusually high hydrogen concentrations in the inert gas: a relatively high amount of moisture was penetrating from the venting apertures in the boxes attached to the rotating cover plug lid and the fixed cover ring containing basalt granulate shielding material. A number of very important constructional reasons had emphasized the need for venting into the plenum, e.g. to avoid being subject to pressure vessel regulations and to provide for thermal expansion. It must be admitted, however, that the rate at which the moisture was released from the basalt granulate and the total amount of water were definitely underestimated at the time of design and fabrication.

When disassembling three shutdown rod supports, thick deposits became obvious on the exterior, which, although they had impeded the movement of the centering tube, probably had no adverse effect on the shutdown function. Visual inspection of the inert gas plenum area showed that there were also thick deposits on other internals. The primary task was now to dry the basalt granulate in such a way that no more moisture could enter the plenum. For this purpose a system was installed by which fresh argon was forced through the basalt by applying pressure cycles and, after absorbing the moisture, was drained off in a controlled manner to the exterior. The basalt temperature was steadily increased during this operation by increasing the sodium temperature and partly heating the boxes.

The system was in operation with short interruptions from August 1986 until January 1987 when an adequate degree of dryness was obtained. Laboratory and simulation tests with basalt and basalt fills carried out in parallel permitted a quantitative evaluation of the drying process. The deposits were mostly concentrated in the area directly above the sodium level. It was therefore possible to dissolve them to a large extent by raising the level of sodium by about 500 mm and increasing the temperature to approximately 420°C. Above this area the deposits were mainly dissolved by hot sodium aerosols.

This occurrence had raised some fundamental questions, on the authority's side, not only with regard to elementary operational considerations but above all with a view to safety. Priority in the following discussions was given to the integrity of the heterogeneous weld seam in the upper area of the vessel and to the functioning of the shutdown systems.

Whereas the thick parts of the deposits on the internals adhered firmly and had to be removed mechanically from the disassembled parts, in the region of the heterogeneous weld seam of the tank, which was situated well above the sodium level in the vicinity of the cover, and accessible from the inside through six small in-service inspection apertures on the circumference, only flake-like aerosols were found. They could easily be removed by suction, blowing or scraping. This was done through the apertures. Specimens of the deposits were also taken from six points and were thoroughly examined chemically and spectroscopically. The heterogeneous welding seam was also inspected through the apertures by cameras and endoscopes.

From the optical, metallurgical, chemical, and spectroscopic tests carried out with the deposits and the internal structures, there was no evidence at all of any actual damage at that time or to be expected later during operation. Careful attention was paid especially to indications of selective corrosion.

The deposits, which consisted of sodium, sodium oxides, and sodium hydroxides had apparently affected the surface of the structures to a certain degree by pitting: partly by general oxidation and partly by attacking the grain boundaries of the base material and the δ -ferritic phase of the welds. A specific observation and materials testing programme was set up by agreement between the relevant experts and the authority in order to find out what long-term effect this attack could possibly have and how it could be kept under control.

The fast shutdown functions were not impeded to any measurable extent. This was proved by comparative measurements taken in April 1986 and February 1987. A basic inspection and functional testing programme for the shutdown systems and other internals was carried out in the framework of other functional tests on the reactor in order to corroborate the recent findings.

The permissible moisture and hydrogen levels during operation were investigated as a result, because the residual moisture from the basalt boxes and the fixed cover ring could not be completely removed either during the pre-operational testing phase (temperature too low) or during nuclear operation (asymptotic behaviour).

The conclusion of these investigations was that approximately 1000 vpm of H_2 in the inert gas plenum would not present any serious problem (actual value at that time: 350 vpm H_2). This corresponded to a moisture penetration-rate of about 400 g/day. The plugging temperature range from 120 to 150°C specified for continuous operation corresponded to much more than this ingress rate at a adequately available cold trap capacity. This meant that it could easily be controlled by cold trap operation. The same was true for the Na-cooled spent fuel storage vessel.

Although these significant unpredicted events caused strong setbacks to the pre-operational testing, the overall satisfactory completion must be emphasized. It must also be stressed that the remedies would not have been successful without the massive support of the R&D laboratories especially in the fields of chemistry and metallurgy. Positive results - in particular with respect to safety concerns - were obtained from, among others, the natural circulation tests via the main sodium heat transfer loops and via the emergency core cooling system, on which information is given below.

3.1.5. Achievements

Besides the valuable experience gathered during the pre-operational testing phase described above, the safety-related achievements should be emphasised, because they were finally able to demonstrate the tremendous potential of an LMFBR system with respect to passive decay heat removal by natural convection.

Decay heat removal via the emergency core cooling system: For removal of decay heat, SNR-300 was equipped with 5 redundant systems, the 3 redundant legs of the primary, secondary, and tertiary heat transfer system, and the 2 redundant systems (i.e. 2 times 6 individual loops) of the emergency core cooling system. The emergency core cooling system was intended for use specifically on the very rare accidental occasions when the 3 parallel loops of the main heat transfer system were simultaneously inoperable, e.g. because of airplane crashes or large earthquakes [3.8]. Initial non-nuclear experiments, which were performed of course without nuclear heat, confirmed the respective design calculations for 2 operating modes: Emergency core cooling system (all active components operational) and Passive decay heat removal (no active components operational).

The primary, secondary and tertiary heat transfer system, and the emergency core cooling system were set to 400°C isothermal, the primary coolant loop dampers to minimum opening and the main pumps with the pony motors to 5% nominal speed. The flow-rate in the emergency core cooling system was raised by means of the electromagnetic pumps to 100%, but the air side dampers were closed and the blowers were switched off. For reasons of materials strength (to protect the components involved), another limit condition was that the sodium outlet temperature at the air cooler should not drop below 200°C. The experiment was started by opening the air outlet dampers after the blowers were switched on. The air inlet dampers were opened step by step. The cooling range was about 100 K and the core outlet temperature dropped by 40 K. With vessel temperatures of approximately 600°C and air dampers completely open, the overall design capacity of the emergency core cooling system was 12 MW, or 2 MW per individual loop. With these performance data and given a temperature of 400°C during the experiment, the cooling system removed 73% of the power, whereas a figure of only 67% was expected. When extrapolating to a vessel temperature of 600°C, the heat removal capacity was significantly beyond 100%.

As was reported in [3.9], SNR-300 had the potential for passive decay heat removal: even in the case of complete and unlimited failure of all active systems (station black-out) and without any supporting actions by the operating staff, none of the radioactivity barriers (cladding, primary system boundary, containment) would have been jeopardized. This passive decay heat potential was based essentially on three principles:

- 1) The high heat capacity of the sodium and the structural masses of the circuits, which were coupled thermodynamically to the core via natural circulation;
- 2) The good natural circulation capability of the sodium circuits by provision of appropriate level differences between the heat exchanging components with respect to the heat source;
- 3) Sufficiently high insulation heat losses from the sodium loops, which increased more than proportionally to the temperature increase.

The capacity of the concrete and steel of the reactor building to accumulate large quantities of heat and to discharge them to the environment slowly was of further importance.

While principle 1 was determined by design, principles 2 and 3 had to be verified during pre-operational testing:

Significant natural convection flow-rates caused by temperature differences of only some 10°C, consistent with the theoretical estimates, were observed in the primary and secondary circuits.

The heat losses, mainly via the insulation of the heat transfer system, were measured using two different methods:

- 1) The power input from the main pumps at various levels, the relevant equilibrium temperatures were measured.
- 2) The systems were heated to 420°C, the heat sources were switched off, the temperature decay function was measured taking account of calculated heat losses and heat capacities.

The previous analysis of passive decay heat removal had been based conservatively (for safety reasons) on theoretically-determined heat losses assuming ideal manufacturing and installation of the insulation and neglecting any penetrations, disturbances and other irregularities. It predicted a maximum temperature of 740°C. Later analyses utilizing the actual heat losses gave an upper temperature of 570°C after about 20 hours.

During pre-operational testing the natural convection capacity of the emergency core cooling system was also demonstrated. It was of particular interest in the R&D frame with regard to the follow-on project at that time, SNR2, for which passive decay heat removal via immersion coolers had been demanded by the customer.

The initial conditions of the experiments were the same as in the case of the emergency core cooling system tests described above. The EM-pumps were switched off. The dampers were opened partially to avoid sodium temperatures falling below 200°C in the cold legs. The heat removed by natural convection at the air side and at the Na-side amounted to 1.1 MW. This value was consistent with predictions of the given boundary conditions. The dampers of the air coolers, opened by simple manual operation, were introduced as an additional heat sink into the analysis of passive decay heat removal. A maximum temperature of 530°C was then reached after about 10 hours. The demonstrated temperatures lay very close to the normal operating temperatures (Figure 3.2).

Natural circulation in the sodium loops of the main heat transfer system: The natural circulation potential of SNR-300 resulted from the system arrangement, and was determined analytically. As an important part of the pre-operational testing, natural circulation operations were first evaluated in the secondary loop. Primary and overall system tests were carried out and evaluated later. Natural circulation in the secondary system started under two different boundary conditions: switching off the secondary pump while operating the decay heat removal systems on the water side, and after draining the water side of the steam generator. In the first case, the flow-rate increased from 18 kg/s with a difference in temperature on the intermediate heat exchanger of 15 K, to 34 kg/s with a difference in temperature of 34 K. During this process, the temperature increased continuously due to the heat supply from the primary pumps, and then decreased because of the heat transfer to the water/steam side. On reaching a temperature difference of 34 K as mentioned above, the water/steam side was switched off so that the evaporator outlet temperature increased again. A stable natural

circulation flow-rate of slightly more than 1 kg/s/DT resulted. Calculations predicted approximately 0.5 kg/s/DT. Thus the design calculations were confirmed.

In the second case, the flow-rate increased to 30 kg/s with 60 K on the intermediate heat exchanger, and stabilized to 8 kg/s.

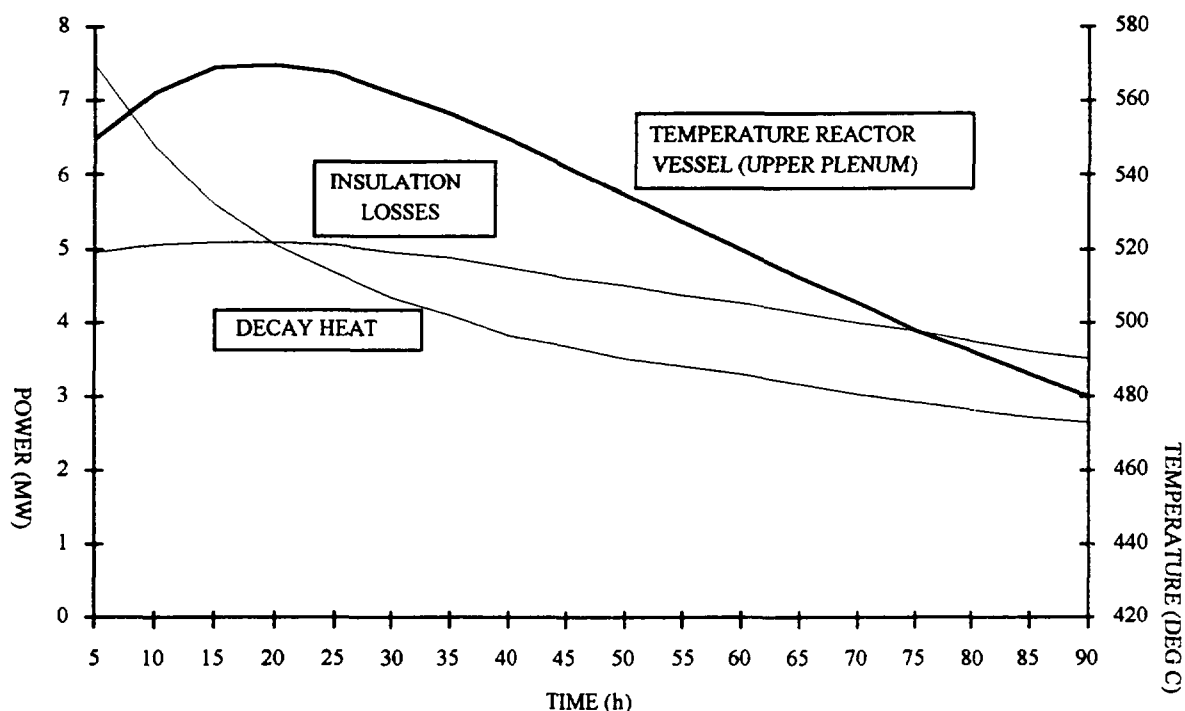


FIG 3.2. Temperature variation in the reactor vessel upper plenum with natural circulation cooling

Evaluation of the overall "passive" safety behaviour of the plant in case of decay heat removal: The tests on the safety potential of the plant described above, several of which exceeded the design and licensing basis, gave confidence in the plant safety, which until then had been only theoretically determined. This applied not only to the main heat transfer system in conjunction with the immersion coolers of the emergency core cooling system; it was also valid for other plant installations such as the sodium-cooled and gas-cooled fuel storage facilities, where significant amounts of decay heat would have been released. This was an important factor in the then current evaluations of accident management measures in the aftermath of the Chernobyl accident [3 9]. Under extremely unfavourable loading conditions component failure limits were reached after more than 40 hours for the sodium-cooled fuel store and after more than 100 hours for the gas-cooled store. Failure limits for the main heat transfer system components including the reactor vessel and the emergency core cooling system would not have been reached at all. The temperatures here would have decreased quite quickly (Figure 3.3). The main reason for this was the relatively large sodium volume in the reactor vessel and the adjoining primary and secondary systems which participated in the flow circulation to remove the heat, and the large system surfaces via which the heat dissipated into the surrounding rooms. The heat would have been stored in the steel and concrete masses of the building, and from there dissipated into the environment.

In this respect, it is important to recall that in Germany a total station black-out of at least 2 hours, during which absolutely no externally and internally produced energy is available apart from batteries. Battery energy is only used to monitor important plant operating parameters during the station black-out period (i.e. ± 24 V DC power) and to re-establish the

grid connection when the grid becomes available again (220 V DC). Without being specifically designed for this purpose, the battery capacity of SNR-300 was sufficient for approximately 5 hours. From this, it was concluded that the available battery power would have a limited operating period to monitor plant parameters and re-establish the grid connection, but could not contribute to the decay heat removal function itself.

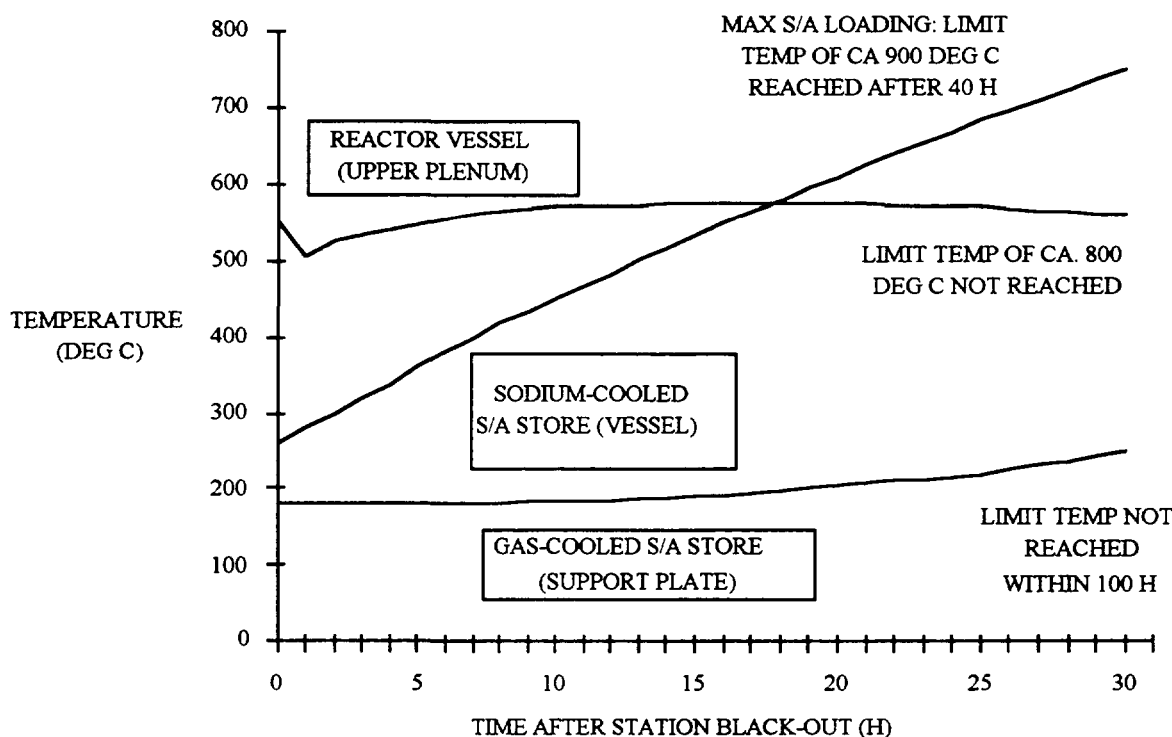


FIG.3.3. Relevant temperatures after station black-out.

Reassessment of safety design aspects in the light of important safety related events in other facilities: It is legally mandatory and usual practice in a licensing process in Germany to evaluate events in other facilities in the world which are obviously relevant to safety with respect to their possible implications for the facility which is the subject of the licensing process. This can possibly lead to a re-assessment of the safety design basis or even backfitting measures. Three events in particular are worth reporting in this context: the sodium fire accident at the solar test power station at Almeria, Spain, in August 1986, the steam generator accident at the Prototype Fast Reactor, PFR, at Dounreay, Scotland in February 1987, and, quite naturally, the serious accident at Chernobyl in the then USSR, in April 1986.

At the solar test power station at Almeria, Spain, sodium was ejected from the main heat transfer system in the course of an obviously inexperienced repair action, which resulted in tremendous damage to the whole facility. Sodium under unexpectedly high pressure in an apparently empty pipe was released and sprayed violently onto a valve flange over the leak. This resulted in the formation of very small droplets with large reacting surface. The reaction with the ambient air led to very high temperatures. The resulting damage was compatible with observations from recent experiments on mixed pool/spray fires. A generally-applicable analytical description was however not possible at the time. A similar accident would have been extremely improbable at SNR-300. In other operating facilities no leakage larger than a few kilograms per hour had ever occurred. Therefore, such an accident was not considered in the design basis either in operating plants or in plants in the design stage. The calculated course of accidents for design considerations is basically a maximum or limit estimate, firstly

because, contrary to expectations, they start spontaneously from large pipe breaks (leak-before break behaviour not being accounted for), or secondly because an ideal spray cone which maximises the consequences can form only at a very few locations. An inexperienced repair procedure such as at Almeria could be excluded for SNR-300, was shown by detailed comparison.

Contrary to the procedure adopted at Almeria, at SNR-300 the following steps had to be performed before commencing repair action.

- 1) The system had to be depressurised, the sodium dumped, and the affected area doubly isolated.
- 2) A sodium section had to be frozen in a controlled manner as an isolation measure (the cool-down curve, temperature holding point, and system internal pressure being recorded).
- 3) A written and verified repair procedure had to be prescribed.

The phenomenological application of the Almeria fire results the SNR-300 steam generator building was supported and confirmed by applying a physical spray cone model validated with respect to the findings of the Almeria fire and experiments. By this means the original design basis was proved to be still valid. Not only was the overriding goal of protection achieved by demonstrating the stability of the steam generator buildings, but also the mechanical and electrical installations necessary for mastering leakage were shown to remain fully functional.

In applying the spray cone model to the inertization area of the plant, the reaction of the sprayed sodium with oxygen was the decisive factor. Only a limited amount of oxygen is available, but the heat transfer area of the total sodium droplet surface to the ambient nitrogen atmosphere is much larger than that of the previously-assumed pool. This led - as calculations revealed - to higher gas temperatures compared with previous calculations, and as a consequence to higher room pressures. An evaluation of the dimensions of the concrete walls enclosing the rooms fortunately showed that the design requirements for these walls could be fulfilled for the higher pressures.

Re-examinations of the aerosol physics showed that the aerosol mass was higher than previous expectation. However, the containment of radioactivity was still guaranteed. With respect to environmental impact the change of data proved to be irrelevant.

The accident in a PFR superheater unit, a power plant of similar size to SNR-300 but of pool design resulted in breach of 40 bundle tubes. A larger number were damaged to a certain extent, as post-accident evaluations revealed. The containment boundary of the intermediate heat exchanger, however, was not affected. Subsequent calculations showed that there was a sufficient safety margin, so that nuclear safety was not impaired.

In the absence of detailed information about the accident, its origin and course had to be reconstructed and derived from post-accident evaluations. Both could be put down to the choice of material, specific design features of the apparatus, and to incomplete monitoring of important operational parameters.

Because of these factors, immediate application to SNR-300 was not appropriate: the tubes consisted of ferritic steel which was practically insensitive to intercrystalline corrosion,

and in addition the bundles were probably not sensitive to flow-induced vibrations so that the basic cause for the origin of the accident could be excluded. The monitoring instrumentation (H_2 in the coolant) was more reliable, since it was designed with redundancy and would have undergone regular maintenance. Limit estimates in connection with the recent licensing process for SNR-300 had also demonstrated that all the bundle tubes could fail simultaneously without endangering the containment boundary in the intermediate heat exchanger.

One essential finding from the course of the accident at PFR, however, was new, namely that under specific circumstances the bundle tubes could be damaged if they were heated up by a long-lasting and locally stable sodium/water reaction to the point of bursting. Until this accident at PFR, all experimental evidence had led to the assumption that the damage mechanism was local material erosion due to the impact of the reaction flame. The flame was assumed to originate at the location of the steam/water leak by reaction with sodium, and to impinge on the neighbouring tubes.

This new insight resulted in a specific analytical and experimental programme on behalf of SNR-300 at the R&D organizations. It finally led to the conclusion that also the loads produced by tube damage caused by overheating would not go beyond the design basis loads. This was basically due to the existence of bursting disks at both ends of the apparatus, a design feature not present at PFR. By this means the sodium would be expelled very quickly from the component so that the sodium/water reaction would close. Therefore, no adjustment or modification of the design measures to prevent and master a steam generator accident was necessary.

The very serious accident at Chernobyl brought up a series of important safety related technical questions, which obviously had and still have to be answered by all those building and operating nuclear facilities. More than that, the accident and its consequences are still having a considerable negative influence on public opinion and the political attitude towards nuclear energy in the whole world and especially so in Germany. Both factors played an important, if not decisive role, in the SNR-300 case. The Chernobyl case was taken by the licensing authority as an argument for a complete re-assessment of the overall safety design of SNR-300. This attitude in 1986 was the real starting point of the last act in the attempt to deal the deathblow to the project. It finally led to the consequences outlined under section 3.1.6. Three phenomena were of prime concern: the positive void coefficient of reactivity during normal operation and in case of accidents, breach of radioactivity containment after core disruption accidents, and possible exothermal chemical reactions in the case of core disruption. Whereas the Reactor Safety Commission (RSK) came to the conclusion that the points of concern were reliably protected by preventive and mitigative measures, the licensing authority demanded a complete re-assessment of the overall safety design. From a technical point of view, a comparison of the specific features which had most aggravated the course of the accident with the respective safety features of the SNR-300 led to the following conclusions [3.9]: (1) Stable reactivity behaviour and good controllability characterize SNR-300, in contrast with unstable behaviour and complex spatial dependencies in the core of the RBMK-1000. (2) Design deficiencies in the protection and emergency shutdown systems were - among other things - responsible for the accident at Chernobyl. All SNR-300 safety features, such as, for instance, redundancy, diversity, degree of automation, separation of operational and safety tasks within the control system, security against uncontrolled access, efficiency and safety margins of the protection and fast acting shutdown systems, were far superior to those of RBMK-1000. For this reason reactivity excursion accidents could be classified hypothetical in SNR-300. (3) Because of elementary physical properties the possible energy release in the case of a nuclear excursion were in principal much lower than in RBMK-1000. (4) In addition to these far-

reaching safety features, the primary circuit and the containment system including a so-called floor cooling device (core catcher) of SNR-300 were designed in such a way that even the consequences of a very unfavourable excursion accident could be mastered. At RBMK-1000 no mitigating features were installed. (5) At RBMK-1000, exothermal chemical processes had escalated the accident consequences. In particular the protracted graphite fire had increased the radiological releases greatly, and (6) In SNR-300, the radioactivity enclosure (containment) was protected by inertization with nitrogen, steel cladding, and catch pans against large sodium leaks from pipe breaks or brought about by the consequences of a hypothetical power excursion accident, so that no exothermal reaction of any significance could have occurred. All in all, the re-assessment of various safety design features by the safety experts, and a review of events in other facilities, were about to converge to positive results when the decision to terminate the project was taken, since the licensing authority did not seem to follow the findings of the experts. The re-assessment had taken too long, and had led to further considerable delay and therefore to an increase of costs.

3.1.6. Epilogue

On March 20th, 1991, the Federal Minister of Research and Technology announced after consultations with the industrial partners involved, who had already participated by contributing 30% of the funding for the project, that the German-Dutch-Belgian sodium-cooled fast breeder reactor prototype SNR-300 should not proceed to commence operation. He offered as a reason for this the politically-motivated delaying of the licensing process [3.10]. At the time of the cessation of the project, not even an estimated date for granting the operating licence was available. This was the definitive reason for abandoning the project. A process leading to successful completion of the project within a reasonable period of time could not be foreseen since the licensing problems raised by the authority appeared insurmountable. This, however, was absolutely necessary for the residual costs and their distribution amongst the potential financiers to be estimated. An assessment of the current project situation had been fixed contractually for 1988, when for the second time since 1986 a decision on interim funding was due. On this occasion it was to cover a period of 3 years: 1989 to 1991. With this funding, a project waiting phase was to be supported, during which the plant would have run in a stand-by mode at lowest possible costs, and all conceivable attempts would have been taken to get the licensing process moving again and successfully completed [3.11]. The Federal Minister of Research and Technology, the utilities, and Siemens AG have to provide this funding equally in 3 annual shares. However, the main targets, namely to make progress in licensing and, as a minimum, to be granted a partial license for fuel storage on site and to develop a clear perspective for the power operation license, could not be achieved [3.12]. There were essentially 2 basic reasons:

- (1) The Social Democratic Party, which was in power in the state in which SNR-300 was being built with an absolute majority, and was responsible for licensing SNR-300, decided at the federal level to abandon nuclear power and in particular to prevent nuclear commissioning of SNR-300 by any means.

According to the German Basic Law and other relevant regulations, the Atomic Energy Act has to be executed by the government of the State in which the respective facility is to be built and operated. However, on the other hand the state government executes the licensing process on behalf of the federal government (administration by commission), represented at that time and still today by the Federal Minister of the Environment, Protection of Nature, and Reactor Safety (BMU). In case of differing opinions, the state authority has to ask BMU, the

supreme authority, for instructions before a license can be granted. Conflicts are obviously likely if the authorities are of different political opinions.)

- (2) Administrative action by the state licensing authority in executing the licensing process of SNR-300 had led to tremendous delays in making decisions.

Faced with the funding bottlenecks, which the licensing authority was also very well aware of, it was obvious that acting in this way could lead to the death of the project. The action was formally still in accordance with the letter of the law, which concedes to the authority a practically unlimited scope of administrative discretion in the process of decision making.

In case of SNR-300, however, it was not at all justified in the light of the previous 17 licenses and the related thorough assessment work as well as recent experience. This and the differing opinions on the interpretation of procedural aspects finally led to instructions on the various relevant matters by BMU to the state licensing authority in April 1988. The state authority filed an appeal against this act with the Federal Constitutional Court. In spring 1990, the highest German court dismissed this appeal as baseless in all respects. With this decision, one would have expected a green light for further progress with the project.

That was, as it turned out in the following months, not at all the case. The licensing authority did not change procedures, which had been described as "kalkarisation" by a German weekly newspaper. In recognition of the fact that the decision of the Federal Constitutional Court had not led to constructive administrative action, and that the BMU as the supreme authority had de facto no means to translate the powers, given to it by the court, into action, an evaluation of the chances of success of the project was launched late 1990. The decision - as already stated - was made against the continuation of the project, even though the foreign partners in Belgium and the Netherlands at first did not agree.

With this, a project which was launched in 1970/71 with great enthusiasm and clear objectives and was supported by all relevant parties in Germany and in the partner countries, had come to an end. Only in the late seventies did the project enter into serious political turbulence. Nevertheless 17 construction and erection licenses had been granted up to autumn 1985. In this context more than 100 expert opinions had been issued. Only 19, for which positive conclusions were expected, were still outstanding at that time. The project had been evaluated several times and in different ways in the political arena. Even the Federal Parliament had installed an Enquête Commission to advise whether the parliamentary reservation against nuclear commissioning of the plant, expressed in 1978, could be repealed. All evaluations came to positive results for the project.

All other court proceedings were in favour of the project and became non-appealable early in 1986. Even the Federal Constitutional Court was appealed to, twice. The judgements were both in support of SNR-300. With this, SNR-300 was undoubtedly the mostly checked and re-checked project in the world. The results were always positive. However, neither this fact nor the fact that this project had already cost the taxpayer a considerable amount of money (about 5 Billion DM) had led to its successful completion, and this primarily because the political parties involved had differing opinions on the final research benefits of a technology with such an incomparable potential as a future energy source.

3.2. CONSTRUCTION AND PRE-OPERATIONAL TESTING OF THE PROTOTYPE LMFBR "MONJU"

3.2.1. Overview of project

The construction of Monju, the prototype fast breeder reactor (FBR) which PNC has built as part of the Japanese FBR development programme, was completed in April 1991, and system start-up tests are presently underway. Monju is a loop-type sodium-cooled fast breeder reactor with U-Pu mixed oxide fuel. It supplies 280 MWe to the grid and is situated on the Tsuruga Peninsula facing the Sea of Japan, about 400 km west of Tokyo.

Work on the preliminary design of Monju was begun before the final design of the Joyo experimental FBR was completed in 1968, and the conceptual design began in 1969. Safety evaluations were conducted from 1980 to 1983, and the construction permit granted by the Prime Minister in May 1983. Construction proper then began in 1985, and was completed in April 1991. The pre-operational tests started in May 1991 and initial criticality was achieved in April 1994.

The FBR in Japan: The development of nuclear power in Japan is based on the premise that the FBR will become a major component of future nuclear capacity, alongside the LWR. In 1966, the Japan Atomic Energy Commission decided to go ahead with a national project to develop the FBR involving the government, universities and the private sector. The following steps were then taken:

- basic research on plutonium fuel, sodium coolant, etc.;
- R&D, including industrial development to bring components up to the point of practical application;
- the construction of an experimental reactor to confirm that the basic FBR technologies were ready for application;
- the construction of a prototype reactor to confirm the FBR's performance and to provide the basis for future commercialization.

The Power Reactor and Nuclear Fuel Development Corporation (PNC) was established in October 1967 as the central development organization, and the Oarai Engineering Center, which consists of large-scale test and research facilities, was built.

The role of Monju: The purposes of the Monju development programme are to:

- develop an intermediate-scale reactor as a step towards to a large-scale commercial reactor;
- get experience with an FBR plant;
- determine the feasibility of solutions to technical issues associated with a large-scale reactor through experience with design, fabrication, construction and operation of a prototype reactor.

Monju will also be a source of basic data on possible economies, as well as playing a role in the irradiation of fuels and materials for demonstration and commercial reactors and in the training of reactor operators.

Development work on Monju has mainly involved a scaling-up of the Joyo plant, including performance upgrading, with the application of new technologies and the addition of a steam/water system and a power generation facility. -

Monju is firmly based on:

- guides and criteria (e.g. a high temperature structural design guide, a design evaluation guide and material design criteria using structural strength data and material testing);
- computer codes taking into account partial, small-scale, or full-scale mockup tests, their detailed evaluation and determination of design formula;
- the development and verification of computer codes for analyzing plant system characteristics using large-scale test facilities.
- the establishment of safety design guides and design methods reflecting safety test results.

3.2.2. Research and development

The R&D for Monju covered system design, core and fuel, heat transfer and fluid dynamics, structures and materials, instrumentation and safety. Research projects were started in the early years, in concert with design studies, so that the results could be applied to Monju. The R&D aimed to:

- introduce a "design by analysis" method instead of "design by test", and use partial- and reduced-scale models instead of full-scale models for verification tests as far as possible, based on Joyo experience.;
- develop steam generator technology and other systems not used in Joyo (such as a decay heat removal system) via a research programme going from basic research to performance with larger scale models;
- prepare design codes and standards applicable to FBRs in general;- actively promote international co-operation in research and development (for instance, in the areas of fuel irradiation and core safety), and promote technical information exchange on systems and components with the USA and European countries;
- summarize data and information on design and construction, and establish a method for carrying out effective R&D leading to commercial FBRs.

Reactor physics: PNC developed a nuclear design analysis method which consists of nuclear data and reactor constants, calculation models, computer codes and methods for interpolation and extrapolation (Bondarenko-type 26 group constants, computer codes for 2D or 3D diffusion calculations, etc.). In addition, PNC performed a full size mockup test (the MOZART project) in the ZEBRA fast critical test facility at Winfrith in the UK, and a partial mockup test at the FCA (JAERI) in Japan, to help understand the nuclear characteristics of the Monju core and confirm the validity and accuracy of the nuclear design.

As for shielding research, PNC developed a shielding design analysis method for Monju and confirmed its accuracy and reliability via shielding characteristics tests at Joyo and FFTF in the USA, and by using shielding experimental data from the fast neutron source reactor Yayoi in Japan. An improved version of this method was applied to shielding design research for large-scale FBRs.

Fuel development: The aim of the fuel development for Monju was to develop core materials which would guarantee performance to 130,000 MWd/t burn-up (pellet peak) and to

a neutron fluence of $2.3 \times 10^{23} \text{ cm}^{-2}$ ($E > 0.1 \text{ MeV}$). The programme includes verification tests to prove the integrity of fuel pins and large fuel assemblies under irradiation.

PNC also developed a type of 316 stainless steel with significantly increased high temperature creep strength and low swelling properties by adding small amounts of phosphorus, boron, titanium and niobium to conventional SUS 316 stainless steel. The low-swelling PNC 316 steel used in Monju will be applicable to 90,000 MWd/t in the initial core and 130,000 MWd/t in a high burn-up core. It is a top performer compared with similar materials that have been developed around the world. A fuel pin behavior analysis code (CEDAR) was also developed by PNC to evaluate the behavior of the fuel pins in Monju.

Initial fuel irradiation tests (accelerated fuel burn-up) were conducted in PFR (UK) and Rapsodie (France). Subsequently Joyo and EBR-II (USA) were used for various irradiation tests. These facilitated understanding of the behaviour of Monju fuel at high burn-up. In addition, irradiation tests to confirm high burn-up properties were performed on full-scale fuel assemblies in FFTF and Phenix (France). The results showed that Monju fuel can meet the specified requirements with both high reliability and safety.

Components and systems: R&D on the components and systems was conducted with small-scale models or partial models, based on the R&D done for Joyo components.

A design analysis code (COPD) was developed for the system dynamics of the cooling systems. In-core instrumentation, some process instrumentation, sodium leak detectors and steam generator water leak detectors were also developed.

Tests on in-service inspection machines for the reactor vessel and enclosure, the primary main cooling piping and heat transfer tubes in the steam generator, were also carried out.

The steam generator R&D examined:

- fundamentals such as heat transfer, fluid dynamics and materials;
- heat transfer and fluid dynamics characteristics (POPAI analytical code) using a 1 MWt model and a 50 MWt model;
- reliability of the structure;
- cooling system instability (BOST analytical model);
- cooling system control characteristics (including the auxiliary cooling system);
- maintenance techniques;
- sodium-water reactions (SWACS analytical code);
- leak detection;
- techniques for removing sodium-water reaction products.

Structure and material: A high temperature structural design guide was provided for structural design of Monju components and piping and for evaluation of integrity, with material tests, structure tests and analyses.

Five structural materials for components and piping, types SUS 304, SUS 316, SUS 321, 2.25 Cr-1 Mo and alloy 718, were tested to establish design rules, in particular for creep characteristics at high temperatures, and for evaluating the influence of neutron irradiation and sodium and steam environments.

In structural tests relating to Monju components, evaluation methods for creep-fatigue rupture, creep ratchetting, plasticity, rupture, creep buckling and thermal transient/creep fatigue were developed and improved. In this connection full-scale mockup tests of elbows and tees in the main cooling system, welded joints of dissimilar materials, and reactor vessel welds were conducted.

A widely used non-linear structural analysis code (FINAS) was developed for structural analysis. It allowed static and dynamic structural analysis under a range of temperatures, inelasticity, large deformation, buckling, and fluid-mechanical vibrations, and also analysis of non-linear fracture mechanics of Monju components. In addition the possibility of leak-before-break of the primary main piping was proved with an evaluation method based on fracture mechanics.

In aseismic R&D, a dynamic analysis method was developed including aseismic structural tests.

Safety research: Safety research was carried out on:

- the thermal transient fluid dynamics of the plant, including evaluation of natural circulation characteristics;
- accidents such as sodium leakage and burning;
- steam generator water leakage;
- phenomena in the containment vessel (from events such as core disruption due to a local fault, anticipated transient without scram, loss of the heat removal system, etc., to fission product transport and PSA).

To promote this research effectively, PNC has participated in several international collaborations, for instance, the CABRI and SCARABEE projects (with European countries), and the setting up of a database for component reliability and development of the CONTAIN code (with the USA).

Evaluation of natural circulation characteristics was carried out using out-of-pile tests (sodium and water) and by means of an in-pile test in Joyo. In parallel with these tests, an analytical code (NATURAL) was introduced and improved, and verified against test data.

3.2.3. Design and construction of MONJU

Design features: Compared with the experimental reactor Joyo, the prototype reactor Monju has about seven times the thermal capacity - (Joyo 100 MWt; Monju: 714 MWt)- and a provision for power generation.

The principal design and performance data of Monju are shown in Table 3.5.

Monju was designed in accordance with the same laws, regulations and standards which are applied to LWRs in Japan, but with the addition of new standards peculiar to sodium-cooled FBRs, for example those relating to high-temperature structural design.

Core and fuel. The hexagonal core consists of fuel assemblies, control rods and blanket assemblies, and a neutron shield which surrounds the blanket.

TABLE 3.5. PRINCIPAL DESIGN AND PERFORMANCE DATA OF MONJU

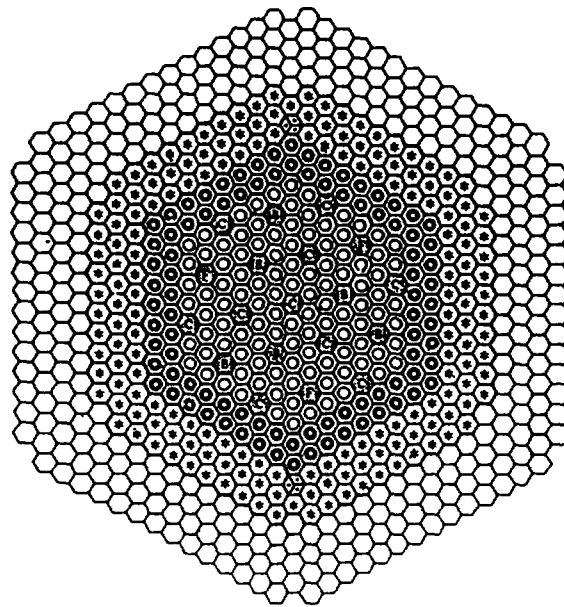
Reactor type	- Sodium-cooled loop-type
Thermal power (MW)	714
Electrical power (MW)	~ 280
Fuel material	PuO ₂ -UO ₂
Core	
Equivalent diameter (mm)	1790
Height (mm)	930
Volume (l)	2335
Plutonium enrichment (inner core/outer core) (% fissile plutonium)	
Initial core	15/20
Equilibrium core	16/21
Fuel inventory	
Core (uranium + plutonium metal) (t)	5.9
Blanket (uranium metal) (t)	17.5
Average burnup (MWd/t)	80 000
Cladding material	Type 316 stainless steel
Cladding outside diameter/thickness (mm)	6.5/0.47
Permissible cladding temperature (mid-wall) (°C)	675
Power density (kW/l)	283
Blanket thickness	
Upper (mm)	300
Lower (mm)	350
Radial (mm)	300
Breeding ratio	1.2
Reactor inlet/outlet sodium temperature (°C)	397/529
Secondary sodium temperature (IHX outlet/inlet) (°C)	505/325
Reactor vessel (height/diameter) (m)	17.8/7.1
Number of loops	3
Pump position (primary and secondary loop)	cold leg
Type of steam generator	Helical coil, once-through
Steam pressure (turbine inlet) (MPa)	12.7
Steam temperature (turbine inlet) (°C)	483
Refuelling system	Single rotating plug with fixed-arm fuel-handling machine
Refueling interval (months)	6

It contains two kinds of fuel assemblies with different plutonium enrichments, the more highly enriched core fuel assemblies being located on the outside to levelize the output power (Fig. 3.4). The initial burn-up will be 80,000 MWd/t (average for discharged fuel assemblies).

Refueling is to be done every six months or so, with about one-fifth of the core and blanket fuel assemblies exchanged each cycle.

Several sorts of radioisotope had to be accounted for in the design of the plutonium fuel assemblies. The amounts of the various radioisotopes in the plutonium feed material vary depending upon the reactor type in which the radioisotopes have been produced, the fuel burnups and the time elapsed to reprocessing

The concept of equivalent enrichment was introduced to keep the reactivity worth of fuel constant, even when feed materials with different radioisotope composition ratios are used. Using this method, and under the assumption that the reactivity worth of plutonium 239 is equal to unity, the reactivity worths (equivalent coefficients) of other radioisotopes are calculated and the ratio of the mixed oxides is controlled to keep the reactivity worth constant.



Core Zone	Inner Core		108
	Outer core		90
Radial Blanket			172
Control Rod	Fine Control Rod		3
	Coarse Control Rod		10
	Backup Control Rod		6
Neutron Source			2
Neutron Shield			324

FIG. 3.4. Core Configuration

Heat transport system. The stainless steel reactor vessel contains the core and core internals. The shield plug contains a single rotating plug in which the upper core structure is installed, near its center (Fig. 3.5).

The upper core structure contains control rod drive mechanisms which position control rods consisting of three fine regulating rods and ten coarse regulating rods, plus six back-up safety rods.

The heat generated in the reactor is removed by a loop-type sodium cooling system composed of three independent loops. It is transferred to a steam/water system through the primary and secondary sodium systems (Fig. 3.6).

The sodium inventory (total quantity of the primary, secondary and ex-vessel storage tank systems) is about 1,700 t.

The primary sodium, at a temperature of 397°C, is fed to the reactor vessel through bottom inlets, and, after being heated in the core, flows out of the upper cylindrical part of the vessel at 529°C.

The sodium in the secondary loop takes heat from the primary sodium via an intermediate heat exchanger, in it is heated to a temperature of 505°C from an inlet temperature of 325°C. Next, heat from the secondary loop is transferred to water in a helical coil-type steam generator system which consists of an evaporator and a superheater. Superheated steam with a pressure of 12.7 MPa and a temperature of 483°C is injected to a turbine directly connected to a generator. The thermal output of the reactor is 714 MWt and the electrical output 280 MWe.

Most of the piping which connects the primary system components is installed at high level, and guard vessels are provided for the reactor vessel, the primary main circulation pumps, the intermediate heat exchangers and the connecting piping. With this design, sufficient coolant for core cooling is guaranteed even if coolant leakage occurs. Moreover, compartments which confine systems with radioactive sodium contain a nitrogen atmosphere and their walls are lined with steel so that leaked sodium cannot ignite.

In addition to the main cooling system there is an auxiliary cooling system to remove decay heat from the core when the reactor is shut down for refueling, or in an emergency. The auxiliary cooling system which is separated from the secondary sodium system, has an air cooler in parallel with the steam generator. When it is operating, the primary and secondary sodium are circulated by the primary and secondary main circulation pumps driven by pony motors.

Spent fuel handling. Spent fuel is taken from the core and transferred to a tank in the lower part of an in-vessel transfer machine. This is done by a fuel handling machine of the pantograph fixed-arm type. After the fuel has been removed from the reactor vessel with an ex-vessel transfer machine, it is transferred through a containment equipment hatch. Later it is stored in a fuel cooling pond after sodium cleaning.

Instrumentation and control. The normal start-up and shutdown of the reactor is achieved with regulating rods. A reactor shutdown system for emergency scram has been designed using the so-called "independent two" systems in which regulating rods and back-up safety rods are inserted.

Monju's I&C is similar to that of a LWR, but with specific considerations for a sodium cooled fast breeder reactor:

- the temperature difference between the reactor inlet and outlet is large;
- the main cooling systems have a large heat capacity and transport delay time;

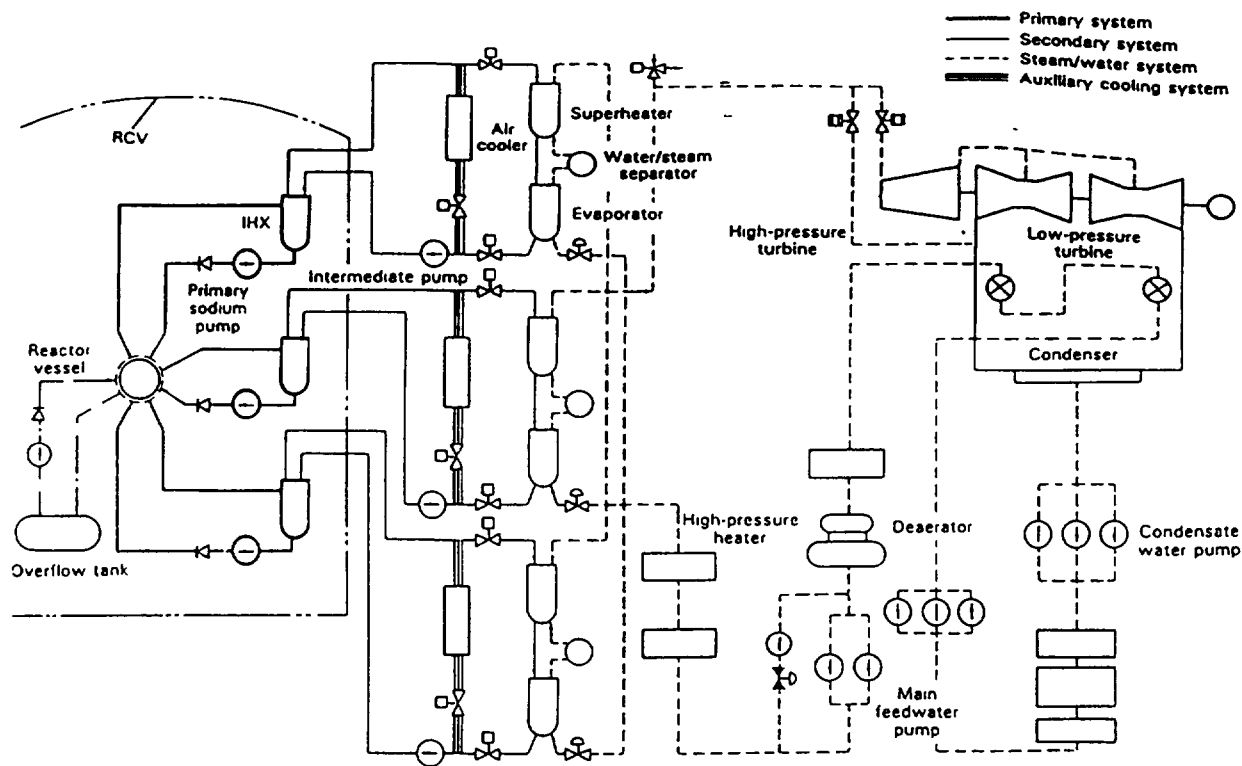


FIG. 3.5. Heat transport system

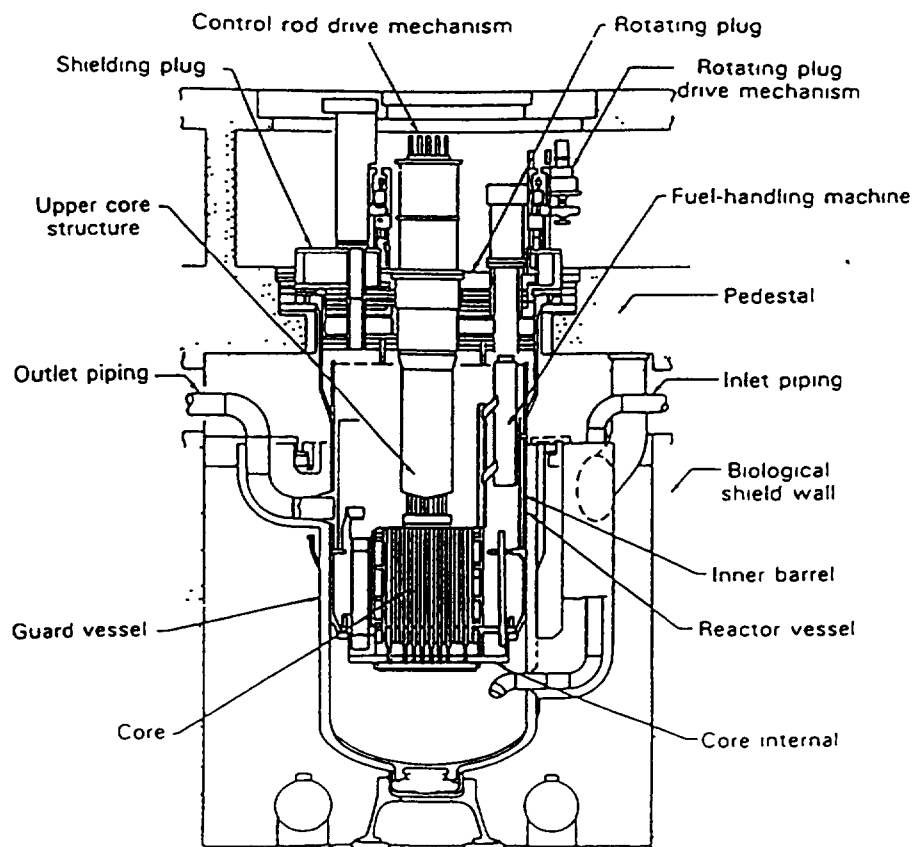


FIG 3 6 Monju reactor system

- as a superheated steam turbine is used, the main steam temperature and pressure in the steam/water system have to be kept constant. For this reason, the main cooling system flow rate is controlled so that it is more-or-less proportional to the overall plant output power demand; at the same time, reactor power is controlled to follow the turbine/generator output power.

Reactivity changes from a cold condition to about 30% of rated power, and reactivity changes related to fuel burn-up, are controlled mainly with coarse regulating rods. Reactivity changes during power operation are mostly regulated with the fine regulating rods. The power is controlled manually below 40% of rated power, and automatically with set points from 40% to 100% of rated power.

A delayed neutron method, a cover gas method and a tagging gas method are used to detect and locate fuel failure.

Digital control technology, multiple system technology and automatic operation are incorporated in the control, monitoring and safety protection systems.

Structure, materials and aseismic design. PNC 316 steel (developed by PNC, as already noted) is used as fuel cladding.

SUS 304 steel is the main structural material, but 2.25 Cr-1 Mo steel and SUS 321 steel have been adopted for the evaporator and superheater sections of the steam generator, respectively.

The structural design was done in accordance with the High Temperature Structural Design Guide for Monju, based on PNC R&D results.

Aseismic design was based primarily on the design considerations for LWRs i.e. the foundation should be directly on a rock bed and the buildings should all be based on a rigid structure.

Aseismic considerations have led to any thin, long piping being supported by mechanical snubbers (primary system) or oil snubbers (secondary system).

The containment vessel is reinforced and can sustain depressurization inside.

FABRICATION: Main components fabrication. The cylindrical reactor vessel is made of austenitic stainless steel about 7 m in diameter, 18 m high and 50 mm thick. To improve the structural reliability by reducing the number of welded parts, the vessel is composed of 12 pieces of ring forged metal and has only circumferential welds.

The shield plug had to be firm enough to support the components installed on it and to keep them properly aligned with the core internals. For this reason, the plug was manufactured with a proven thick rib structure.

Because the main circulation pump in the primary system is vertical with a thin shaft about 6 m long, much consideration was given to the fabrication of rotating parts to ensure a highly controlled rotating balance. The balance of the shaft was tested under the same high temperature conditions as exist in actual operation.

But welds were used for both the tube-to-tube and the tube-to-tube sheet joints of the steam generator. An automated welding machine was developed, principally for the tube sheet welds.

The shield plug, fuel handling machine, ex-vessel storage tank and other major components were assembled in advance at the factory, and assembly tests were conducted to confirm the performance of system prior to assembly on site.

Electromagnetic flow meters and level gauges, etc. were tested for calibration with actual flowing sodium before delivery to the site.

Fuel fabrication. In parallel with the construction of Monju, construction of the Plutonium Fuel Production Facility (PFPP, PNC's Tokai Works, 5 t MOX/y) started in July 1982. It was designed to develop fuel fabrication technologies as well as to fabricate fuels for Monju and Joyo. The construction was completed in October 1987. After test operation, production of Joyo fuel started in October 1988 as the first production campaign at PFPP. Production of the initial core fuel of Monju started in October 1989 and was completed in January 1994.

When expanded, the PFPP will be able to produce 15t MOX/y. Instead of using the existing fabrication method, which depends upon manual work in glove boxes, a fabrication process with automatic remote operation techniques has been applied in the PFPP to improve productivity and reduce external exposure. The main process consists of pellet fabrication, fuel element fabrication and assembling. Each process involves remote handling controlled by a computer.

Construction: After Shiraki was chosen as the construction site in 1970, design, R&D and licensing for the construction of Monju went ahead. Preparation work started in 1983 and construction work proper began in October 1985. The installation of equipment was completed in April 1991 (Fig. 3.7).

Because the organization of the construction work was complicated and included many related groups, a careful schedule was established with emphasis on harmony rather than on getting the job done more quickly. In the event the construction work was carried out on schedule.

On-site work on buildings. Construction work started in the spring of 1986 with the foundation work for the reactor building and reactor auxiliary building, which are located at the center of the plant (Fig. 3.8).

A great deal of reinforcement and many anchor bolts for components were installed in the reactor building, which has a complicated shape and contains the reactor vessel and other major components. Prior to construction, models of the reinforcement arrangement were built to see how the reinforcement would interact with the component basement structures and whether the fabrication sequence could be improved.

The reactor cavity wall around the reactor vessel is made of serpentine concrete covered with steel plates. This steel cover is a structural member, being the support for the reactor vessel. It had to be installed with extreme precision, particularly with regard to remote refueling requirements. For this reason, each segment was fabricated in the factory and had its

dimensions confirmed by temporary assembly before being finally assembled on site, maintaining tolerances of 1 mm or less.

In the busiest period of construction, about ten cranes (controlled by computers to avoid mutual interference) were operated simultaneously.

Reactor construction. The reactor vessel and internals were constructed in this order: the guard vessel for the reactor vessel, the reactor vessel, the core internals, the shield plug, the upper core structure and then the control rod drive mechanism.

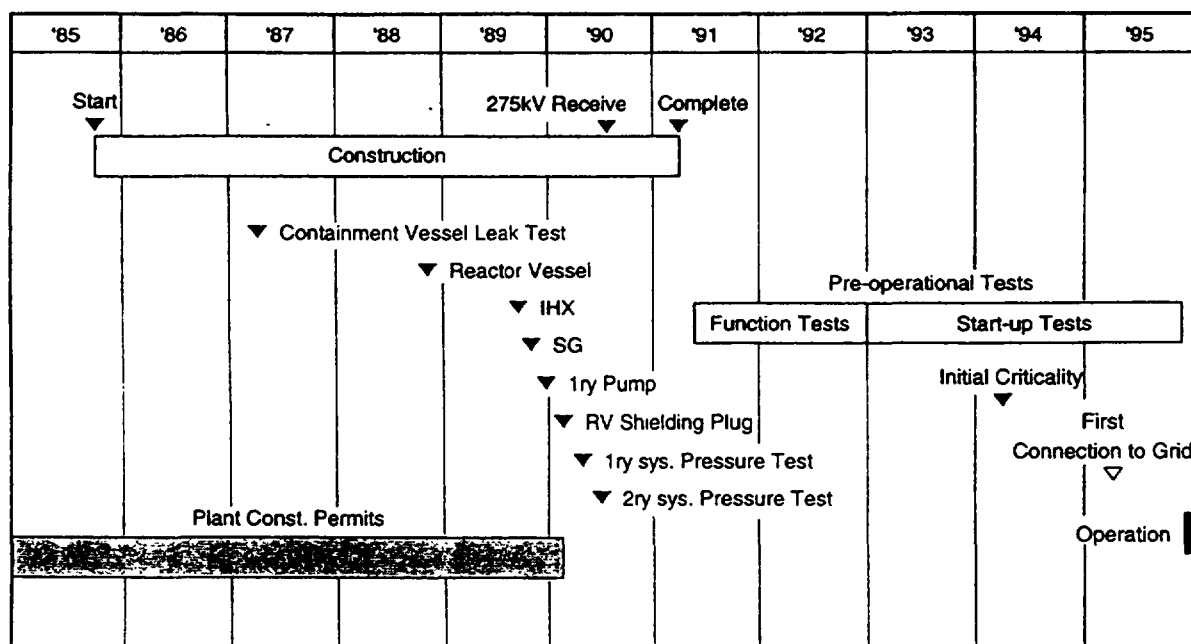


FIG. 3.7. Monju Construction & Tests Schedule

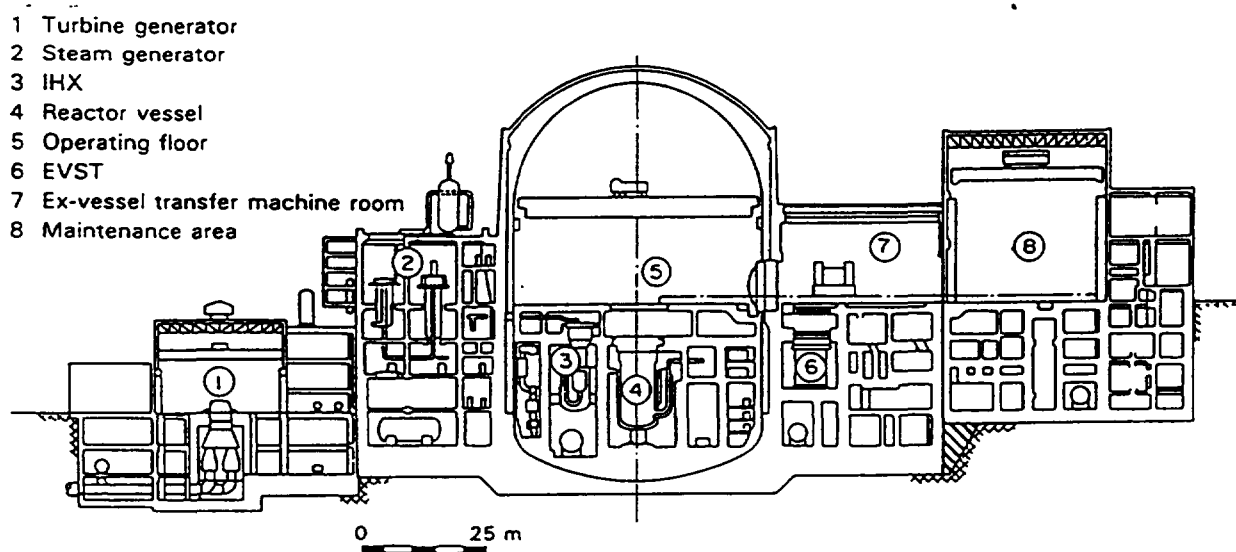


FIG. 3.8. Sectional view of main building

In transportation, the guard vessel and the reactor vessel weighed about 500 t. Both were shipped to the site and moved with rollers from the wharf to the reactor vessel compartment over a period of five days. Installation work then proceeded with special attention being paid to assure both accurate installation and cleanliness of the components.

Pieces of the main cooling pipework were manufactured in the factory; the piping supports and the main cooling piping connections to the components were then welded at site. The same automatic welding technique was usually applied at the site as had been used in the factory to keep the quality level constant.

On-site tests and inspections. Looking at the numbers of tests done on materials, structures, strength and leakage, two peaks, similar to those in LWR testing, were observed in the distribution curve. Most of the tests in the first peak occurred in the factory; the second peak is related to tests at the construction site. The reason why factory tests occupied a large portion of the first peak is that sodium components are welded structures usually incorporating internal structures. Accordingly tests were required in the course of fabrication.

Research and development reactors are monitored by the Science and Technology Agency, and commercial reactors are controlled by the Ministry of International Trade and Industry. However, Monju has power generation facilities, so it had to be reviewed independently by both governmental organizations.

Organization. Many large Japanese companies, including those in the civil, electrical and component manufacturing areas, were involved in the construction of Monju, so it was truly a national project. There were about 20 main contractors and around 300 associated companies. The daily number of workers peaked at about 2700 in the busiest period of construction. Responsibilities for the construction of the main components and electrical facilities were shared as follows (these also apply for design and fabrication):

- reactor structure - Mitsubishi Heavy Industries;
- primary sodium system - Hitachi;
- secondary sodium system - Toshiba;
- fuel handling and storage facilities - Fuji;
- civil works and buildings - five consortia composed of construction companies.

The FBR Engineering Company, established by the above four companies, acted as technical co-ordinator. On behalf of PNC, the overall construction manager, the Japan Atomic Power Company (JAPC) took responsibility for direct management of construction under the supervision of PNC. This allowed the project to benefit from the extensive experience of the Japanese electric power companies, which are joint shareholders in JAPC.

3.2.4. Pre-operational tests

There were five main objectives of the pre-operational tests:

- to confirm the functions and verify the safety and reliability required by the design of the systems and components in the plant;
- to verify the designs and evaluate the design margins based on pre-operational test data;

- to provide data from actual systems and components for, the general FBR development effort;
- to ensure operators master operational techniques;
- to advance FBR technologies substantially.

Functional and performance testing of Monju components and systems was done in the following order: factory tests, installation tests, component function tests, system function tests and then system start-up tests. System function and start-up tests (classified as pre-operational tests) were begun in May, 1991.

Because Monju is the first FBR to generate electricity in Japan, tests and inspections are conducted by the appropriate governmental organizations on the basis of the laws for nuclear power stations. Tests also are included for evaluating design margins. In addition, the opportunity will be taken to conduct general FBR R&D with the benefit of an actual plant. In particular, research will be undertaken into the design of future demonstration reactors.

System function tests. System function tests were conducted to confirm the function and performance of the plant systems, following various tests and inspections during fabrication and installation of the components in Monju. They were completed prior to fuel loading.

The tests were divided into three phases:

- testing the fuel handling system and control rod drive mechanism in air at room temperature prior to sodium charging;
- tests in argon gas before loading sodium into the systems. Argon was used for preheating and heat-up;
- testing the cooling systems, control systems, fuel handling systems, etc. after sodium loading.

There were about 300 system function tests, of which 240 are specific to the FBR. Included in this were:

- the configuration of a dummy core;
- confirmation of the operation of fuel handling components in gases and sodium;
- confirmation of the movement of in-service inspection and pre-service inspection equipment;
- preheating of the system components and sodium charging;
- leak rate measurement of the reactor containment vessel after loading the sodium.

System start-up tests. System start-up tests, aimed at confirming and evaluating the performance of the core, each system of the plant, and the plant as a whole, started with fuel loading. They are being conducted along with various phases of criticality tests, reactor physics tests, nuclear heating tests and power operation tests, somewhat similar to the phase for an LWR (Fig. 3.9). Safe operation of the plant in accordance with the design will be confirmed at full power.

After the leak rate test of the reactor containment vessel, which was the final system function test, a criticality approach test was performed as the first performance test. The minimum critical mass was measured, replacing dummy elements with core fuel stored in the

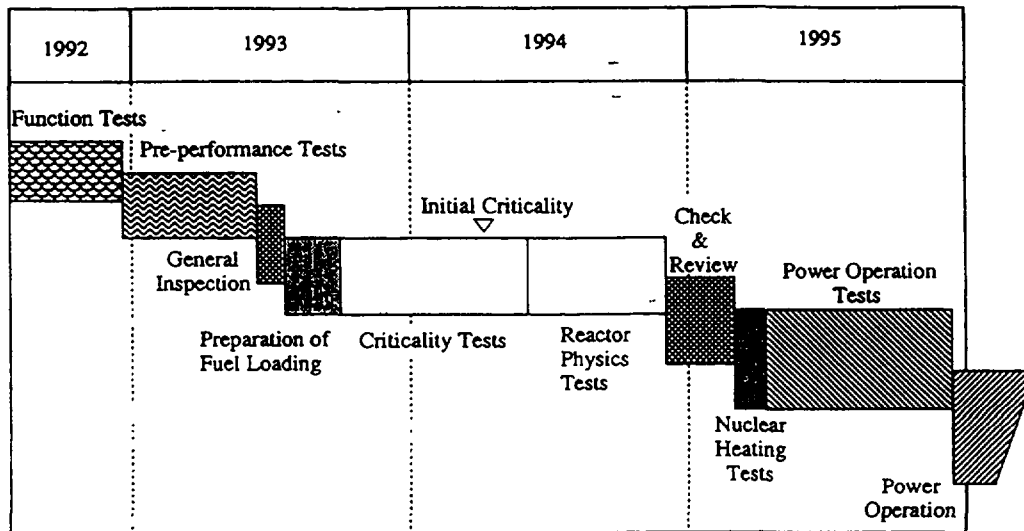


FIG. 3.9. Monju Start-up Tests Schedule

ex-vessel storage tank one by one using the fuel handling system (whose function had already been verified in the course of the system function test).

Initial criticality was achieved with 168 fuel assemblies in April 1994 (Fig. 3.10). After the criticality test, reactor physics tests were performed and the core reactivity worth, core reaction rate distribution, core flow rate distribution, etc., were measured.

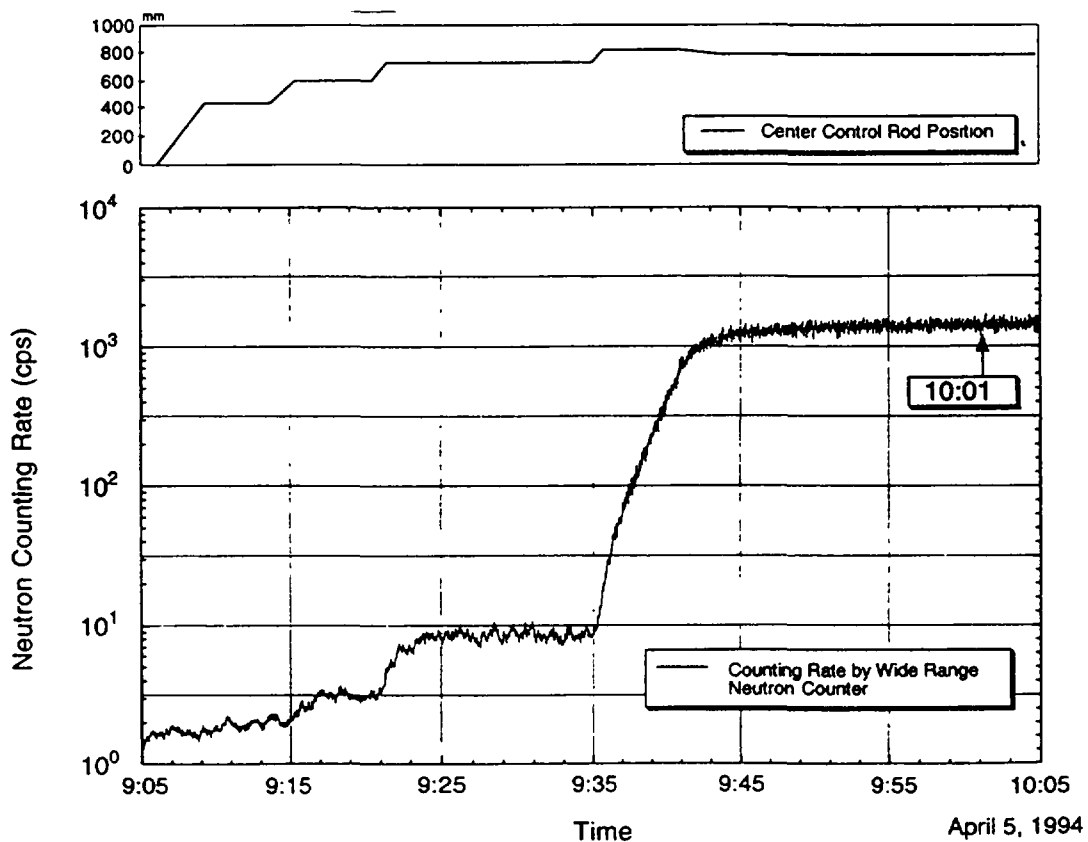


FIG. 3.10. Critical loading experiment in Monju
Neutron Counting Rate at Initial Criticality

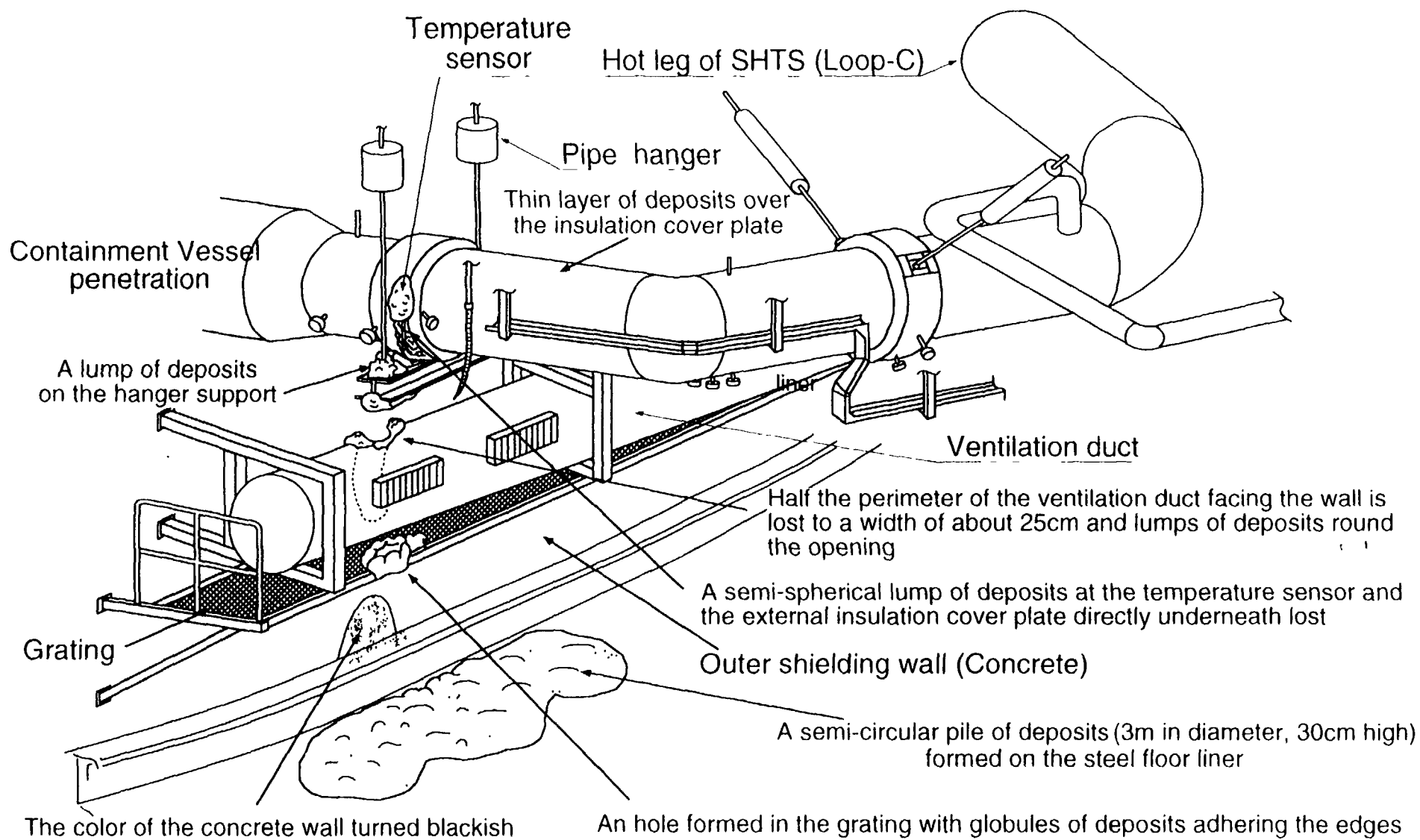


FIG. 3.11 Place of the leak and sketh of the affected area

The nuclear heating test was started on February 1995 and the reactor power was increased gradually. Monju was connected to the grid in August and the power-raising testing was started. In the power-raising tests plant characteristics under power operation and transient conditions were confirmed up to 40% power.

When power was being increased for the plant trip test as part of the 40% power tests, a sodium leak occurred in the Secondary Heat Transport System (SHTS), loop C, on 8 December 1995. The leak was near the outlet of the secondary side of the intermediate heat exchanger (IHX) (Fig. 3.11). The reactor was shut down manually to the cold shutdown state and the sodium in the affected primary and secondary loops C was drained. The secondary sodium had leaked through a temperature sensor. The tip of the well tube of the sensor installed near the outlet of the intermediate exchanger in loop C had broken away. Cooling of the reactor core was maintained so that, from the point of view of radiological hazards, the safety of the reactor was secured. There were no adverse effects for operating personnel or the surrounding environment. The total mass of leaked sodium was estimated to be 640 +/- 42 kg on the basis of plant data by comparing sodium levels with other loops. The cause of the failure of the well tube is considered to be high-cycle fatigue due to flow-induced vibration. Delay in draining the sodium from the leaking loop increased the consequential effects from sodium combustion products.

REFERENCES

- [3.1] Nuclear Engineering International, 21, 246, 39 (1976), SNR-300, Liquid Metal Fast Breeder Reactor Prototype Plant.
- [3.2] Nuclear Technology, September, 1987-Vol. 78, No. 3, p. 227-294.
- [3.3] Marth, W., Der Schnelle Brüter SNR-300 im Auf und Ab seiner Geschichte, KfK 4666, March, 1992.
- [3.4] Morgenstern, F. H., Commissioning and Related Licensing of SNR-300, European Nuclear Conference '86, Geneva, Switzerland, 1-6 June, 1986.
- [3.5] Morgenstern, F. H., Bürkle, W., Hendl, G., Most Recent Experience in Non-Nuclear Commissioning and Efforts to Obtain an Operating License for the SNR 300 Reactor, International Conference on Nuclear Power Performance and Safety, IAEA, Vienna, Austria, 28 September, 1987.
- [3.6] Morgenstern, F.H., Bürkle, W., Hendl, G., Experience Gained During Commissioning and Related Licensing Phase of the SNR-300, International Conference on Fast Breeder Systems, in Richland, WA, USA, September 13-17.
- [3.7] Bürkle, W., Eitz, A. W., Construction of SNR-300, International Conference on Fast Breeder Systems, in Richland, WA, USA, September 13-17, 1987.
- [3.8] Morgenstern, F.H. et al., The Decay Heat Removal Plan for SNR-300. A Licensed Concept, ANS/ENS International Meeting on Fast Reactor Safety and Related Physics, Chicago, Ill, USA, 5-8 October, 1976, Conf. 761001.
- [3.9] Vossebrecker, H. et al., Evaluation of Special Safety Features of the SNR-300 in View of the Chernobyl Accident, INTERATOM-Report 35.02468.5, 5. March, 1987.
- [3.10] Eitz, A. W., Vogel, J., Riethmüller, R., Aktueller Stand des Projektes SNR 300 (Nukleare Inbetriebnahme nicht in Sicht), Energiewirtschaftliche Tagesfragen, 37. Jg. (1987) Heft 10.
- [3.11] Rasche, G., Hendl, G., Morgenstern, F. H., Das Kernkraftwerk Kalkar -Seit 3 Jahren in aufgezwungener Warteposition, Jahrestagung Kerntechnik, Düsseldorf, Germany, 9.-11. May, 1989.
- [3.12] Vogel, J., Morgenstern, F. H., Atomrechtliches Genehmigungsverfahren SNR-300, Jahrestagung Kerntechnik, Düsseldorf, Germany, 9-11 May 1989.
- [3.13] "Building Monju - Japan's Prototype FBR", Nuclear Engineering International, October, 1991.
- [3.14] "A Review of Fast Reactor Program in Japan", PNC TN1410 94-033, April, 1994.

**NEXT PAGE(S)
left BLANK**

Chapter 4

LMFR PHYSICS

Neutronics calculations are made for three different types of application: conceptual design studies, detailed design calculations and for planning reactor operations. Conceptual design studies are made to assess the potential benefits of improved types of reactor or the potential effectiveness of new components. Reactor designs with improved safety characteristics, better economic performance and with new objectives, such as reducing the stocks of plutonium, and for incineration of minor actinides and fission products, are being investigated. For evaluating such design concepts a high accuracy in the calculations is often not required. For example, it isn't important to know the fuel enrichment and control rod performance accurately. However, new materials can be involved and it is necessary to have sufficiently accurate nuclear data for these. If the geometrical arrangement of the reactor or the new component is markedly different from those already studied some mock-up experiments can be required. The irradiation endurance of the materials and components must also be evaluated and this can require irradiation experiments. At the detailed design stage a high accuracy is required. The safety must be demonstrated. This requires the calculation of the kinetic characteristics of the reactor - the changes of reactivity resulting from changes in the temperatures, densities and geometries of components, associated with changes in reactor power or coolant flow and inlet temperature. Accurate estimates must be made of the required fissile enrichment of the fuel. An underestimation will result in the necessity to replace the fuel earlier than would be the economic residence time because the loss of reactivity with burnup prevents criticality being achieved. An overestimation of the critical enrichment results in the reactor reaching criticality with fewer fuel assemblies loaded than desired, or a greater control rod insertion, and a consequent loss of power output. When fuel of different enrichments is available, for example an outer core zone of higher enrichment, there is some greater flexibility for meeting the reactivity requirements, by interchanging high and low enrichment assemblies, but with some loss of economy in the power output. Control rods are expensive items. They occupy space in the core and so affect reactor size. The control rod mechanisms and replacement rods are also costly. Highly enriched boron rods must be replaced frequently as the boron-10 is burnt up. The control rod requirements to meet the variation of reactivity with fuel burn-up, and to ensure that the reactor can be safely shut down at any stage of operation (and with some redundancy to cover possible failures of mechanisms) must be predicted accurately. This requires an accurate prediction of the anti-reactivity of control rods, of the variation of reactor reactivity with burn-up, and of the variation of reactor reactivity with coolant inlet temperature and reactor power, so that the requirements which the control rods must satisfy are accurately known.

For reactor operation it is necessary to predict the power output and temperatures of each sub-assembly to ensure that none are being operated above the acceptable level. Fuel burn-up and the associated loss of reactivity, and the irradiation induced swelling and distortion of components must be predicted so that the optimum time to replace them can be decided. Effects of irradiation on control rods and other reactor components must also be predicted. The prediction of these various properties requires the calculation of the interaction probabilities for neutrons of different energies with the nuclei of the various materials of the reactor. For the calculation of heating, the energy spectra of gamma rays produced in nuclear reactions and their interaction probabilities must also be calculated. For the design of reactor shielding the attenuation of both neutrons and gamma rays must be calculated.

When a reactor is shut down radioactive decay of fission products, the actinide isotopes (produced by capture reactions in the fuel) and structural material activation products continues to generate heat (the decay heat) and this must be accurately predicted so that adequate cooling can be provided. It is also necessary to predict the heating and radioactive emissions associated with the transfer, storage and reprocessing of fuel.

For studies on both fast and thermal reactors data are required for the interaction of neutrons having energies between thermal energies, with a lower energy limit of 10^{-5} electron volts (eV), and 20 million electron volts (MeV). This is the energy range covered in the libraries of evaluated nuclear data. The mean energy of neutrons produced in fission is about 2 MeV (depending on the nucleus being fissioned and also slightly on the energy of the neutron causing fission) and the energy distribution of fission neutrons is approximately Maxwellian. The fraction produced above 10 MeV is small (less than 0.1%) but there are some reactions occurring at these high energies which produce radioactive products of importance in waste management, in particular (n,2n) and (n,3n) reactions in uranium and plutonium isotopes which result in the production of additional actinide isotopes.

Studies of accelerator driven, or hybrid, reactors are now being made. These have a source of neutrons in the core, produced by a proton beam striking a suitable target, the neutrons being produced in spallation reactions. These extra neutrons can help to improve the neutron economy, this being helpful for incineration of minor actinide and fission product isotopes. For these studies the reactions of interest and the energy ranges are wider than for conventional reactors.

In a conventional fast reactor the mean energy of neutron absorption is about 100 kilo electron volts (keV). However energies down to about 100 eV are of importance in the calculation of reactor core properties, and a lower energy range can be of importance in some types of accident study (in particular to calculate the effect of the entry of hydrogenous substances into the core).

The materials of primary interest are:

- I. the light elements, C, N and O, which occur in the fuel in the case of carbide, nitride or oxide fuel;
- II. the coolant, Na (K was also used in the past in combination with Na, and alternative coolants, such as Pb, are under study);
- III. structural materials, in particular, Cr, Fe and Ni but also the elements which occur as trace elements, Mn, Mo; alternative structural materials which are considered are Nb, Ti and Zr;
- IV. primary actinide isotopes of current interest are Th-232, U-233 (for the thorium fuel cycle) and U-235, U-238, Pu-239, Pu-240, Pu-241, Pu-242 (for the uranium/plutonium fuel cycle);
- VI. secondary actinide isotopes, including, for example, for the uranium/plutonium cycle, U-236, Np-237, 239, Am-241, 242, 243, Cm-242, 244;
- VII. absorber materials, in particular B-10 and B-11.

Structural materials are used as fuel cladding and assembly wrappers, and also as fuel stabilisers. In connection with fast reactors designed as plutonium burners there is an interest in fuels which are a dispersion of plutonium oxide particles in a ceramic, such as MgO or MgAl_2O_4 (a CERCER fuel) or in a metallic matrix such as Cr, or Cr-W alloy (a CERMET

fuel). Structural materials, primarily steels, are also used for shielding the core of a reactor.

4.1 PRODUCTION OF NUCLEAR DATA FOR REACTOR NEUTRONICS CALCULATIONS

Several stages are involved in obtaining the nuclear data sets used in reactor calculations:

- I. nuclear data measurements are made;
- II. the raw measurements are analysed to correct for resolution broadening and other limitations of the experimental techniques;
- III. the measured data are compiled at one of the Four Data Centres and then transmitted to the other three. The four centres are the IAEA Nuclear Data Section in Vienna, the OECD NEA Data Bank in Paris and the Centres at Brookhaven, USA (for North America) and at Obninsk in Russia. These centres distribute the data to the users;
- IV. an evaluation is made of all the measured data for a substance to produce a single 'best' set of data. This involves examination of all the measured data for consistency and, following this, by statistical averaging. Nuclear theory is used to fit the measurements and extend their range;
- V. processing to produce the data sets used in reactor neutronics programs, and
- VI. validation of the recommended data by analysis of integral measurements made in experimental facilities and on reactors.

4.1.1. Measurement and the use of nuclear theory

The first step in the production of nuclear data for applied purposes is measurement. Nuclear theory cannot provide accurate nuclear data. Nevertheless theory plays an important part in the interpretation of measurements, and is used for interpolation and extrapolation of measured data. Theory also provides much of the data for reactions of lesser importance, such as secondary energy and angular distributions of inelastically scattered neutrons, and also capture cross-sections for materials which are difficult to measure, such as radioactive fission products and minor actinide isotopes. If the resonance structure of a cross-section needs to be known, when

shielding effects are important, measurements must be made, unless the effects can be treated in an average way.

Theory is also used to predict the half-lives and the mean energies of the beta and gamma rays emitted in the beta decay of short-lived fission products (with half-lives of the order of 1 sec.). These are required for decay heat predictions. However, measured data form the major part of the decay data even at short decay times.

For the measurement of the resonance structure of cross-sections the pulsed white neutron source, time of flight technique is used. A target is bombarded with a pulse of charged particles which produces a pulse of neutrons having a wide energy range. These neutrons impinge on a sample of the material being studied and the energy dependence of the response is measured by measuring the time dependence of the response at the end of a long neutron flight path. The time between the initiation of the pulse and the detector response determines the energy of the neutron interaction. The electron linear accelerators, GELINA at IRMM, Geel (a laboratory of the Joint Research Centre of the European Community in Belgium), and

ORELA at Oak Ridge National Laboratory, are examples of the facilities used for high resolution measurements in the energy range from a fraction of an eV up to several MeV. The proton beams produced by the LAMPF facility at Los Alamos National Laboratory are used to produce pulsed white neutron sources by nuclear spallation. This facility is primarily used for measurements at MeV energies. There are a number of facilities which can be used for monoenergetic neutron measurements. An example is the Van der Graaff machine at IRMM, Geel. There are also a number of low-resolution measurement facilities which can be used to measure the broad features of cross-sections.

Measurements of fission product yields and decay properties are made, for example at the reactor of the Studsvik Neutron Research Laboratory of the University of Uppsala, in Sweden. This has a facility called OSIRIS for the rapid transfer and analysis of irradiated samples.

4.1.2. Analysis

Following measurement the data must be analysed to take into account the corrections needed for sample size effects (multiple scattering) and resolution broadening, in the case of cross-section measurements. At this stage theory is used. For example, resonance region data are analysed using a standard resonance formalism to obtain the parameters.

4.1.3. Compilation

The data are then sent to one of the four Data Centres where all measured data are stored in a computer data bank in an internationally agreed exchange format, EXFOR. The Data Centres are:

- (1) the NEA Data Bank in Paris, which serves OECD countries other than those which have their own centres such as the USA and Canada (or choose not to be a participating country);
- (2) the National Nuclear Data Center, NNDC, at Brookhaven National Laboratory, USA, which serves North America (the USA and Canada);
- (3) the Russian Nuclear Data Centre at Obninsk, Russia, and
- (4) the IAEA Nuclear Data Section, NDS, which serves countries not covered by the other three centres and provides a coordinating role.

Japan also has its National Data Centre at JAERI but Japan also participates fully in the NEA Data Bank. All the centres use the same computer systems and Data Base systems. An index to the literature and the computer files on microscopic neutron data, called CINDA, is issued periodically by the IAEA NDS.

4.1.4. Evaluation

An evaluation of the available measured nuclear data is necessary to produce a recommended file of cross-section data for a nuclide, or an evaluation of fission product yields or the radioactive decay data for a nuclide. This is because there are often several sets of measurements or gaps in the measured data which must be filled using theory. Inconsistent data must be examined and a best estimate made, taking into account any theoretical constraints. There are several evaluation projects which coordinate the efforts of the scientists working in the field and make plans to meet the data requirements. All cross-section

evaluation projects now use the ENDF/B format to store their data [4.1]. The IAEA Nuclear Data Section periodically issues an Index of Nuclear Data Libraries in the IAEA-NDS-7 series, and this should be consulted for information about the current status. Below is a summary of the status in 1998.

ENDF/B is the North American evaluation project coordinated by the Cross-section Evaluation Working Group, CSEWG, and compiled and distributed by the National Nuclear Data Center, NNDC, at Brookhaven National Laboratory. The current version of the library is ENDF/B-VI-version 4.

JEF, the Joint Evaluated File Project, is a Western European Cooperation, coordinated by a Working Group of the OECD NEA Nuclear Science Committee and compiled by the NEA Data Bank in Paris. The current version of the library is JEF-2.2. EFF, the European Fusion File, is also a Western European evaluation activity closely related to the JEF Project with a particular emphasis on higher energy data (MeV energies) and the materials of importance in Fusion Reactor Technology (Be, Li, Pb and structural materials). The current version is EFF-2.4. There is also EAF, the European Activation file, a compilation of activation cross-sections and decay data. The JEF and EFF Projects now cooperate to produce a single library, JEFF-3, and the EAF activation library is also part of this combined project.

JENDL is the Japanese Evaluated Nuclear Data Library coordinated by the Japanese Nuclear Data Committee, JNDC, and compiled at the JAERI Nuclear Data Center. The current version is JENDL-3.2.

BROND is the Russian Evaluated Nuclear Data Library Project, compiled at the Nuclear Data Centre, Obninsk. The current version is BROND-2.2. There are also the "Maslov" updates for a number of actinide isotopes. In addition there is a proton interaction data library, MENDL-2P.

CENDL is the Chinese Evaluated Nuclear Data Library Project, compiled at the Chinese Nuclear Data Centre, Beijing. The current version is CENDL-2.1R.

FENDL is a Fusion Reactor Technology Evaluated Nuclear Data Library Project coordinated by the IAEA Nuclear Data Section specifically for the ITER Fusion Project. Files are selected from the available libraries following validation studies.

IRDF is the International Reactor Dosimetry File Project coordinated by the IAEA Nuclear Data Section.

4.1.5 Nuclear data uncertainty information

The assessment of the uncertainties in the prediction of reactor properties is an important requirement, both for economic and safety reasons. Allowances must be made in the design and operation of reactors to cover uncertainties by introducing suitable margins. A very high level of confidence in the safety aspects of reactors must be achieved. Uncertainties in nuclear data contribute to the overall uncertainty. Consequently the uncertainties in the data and the sensitivity of calculated reactor parameters to these uncertainties must be estimated. The estimation and representation of uncertainties in evaluated differential cross-sections is a complex problem. However, since the required information is the uncertainty in reactor neutron spectrum averaged values of cross-sections, or in ratios of such averages, the required

information can take a simpler form in many cases. For example, when the cross-section does not influence the spectrum the requirement is for the uncertainty in the average value of the cross-section in a specified spectrum and its correlation with the uncertainty in other averaged cross-sections entering into the calculations. In other cases, for example, when resonance shielding effects are important, the effect of the uncertainties on the calculated spectrum must also be taken into account. Integral measurements can help to provide a normalisation which reduces the uncertainty in predictions and improve confidence in predictions.

4.1.6. Integral measurements

This is the name given to nuclear data related measurements made in reactor spectra. The information obtained depends on reactor spectrum averaged values of cross-sections. Measurements of the neutron spectrum itself have also been made in some facilities. There have been extensive programs of measurements made in zero power critical facilities, and neutron source driven assemblies, which have been designed to provide a test of nuclear data. When integral measurements are taken into account the uncertainties in the nuclear data used in reactor calculations and, consequently, in the accuracy of predictions of reactor properties can be reduced. The types of measurement made include the determination of the size of a critical assembly having a particular composition, measurements of reaction rate ratios and distributions, and measurements of the reactivity effects of samples of materials. Irradiations of samples of isotopically pure materials provide information on capture rates (or transmutations of different types). Measurements of changes in reactivity, made on operating power reactors, resulting from changes in temperature, power or fuel burn-up also provide valuable information. Measurements of the transmission of neutrons and gamma rays through blocks of materials also provide a valuable test of the nuclear data and calculation methods, in particular for shielding applications. Integral measurements provide a better basis for the assessment of uncertainties in neutronics calculations.

4.1.7. Fission spectrum averages

The reactor neutron flux spectrum above about 3 MeV is approximately proportional to the fission neutron spectrum. For reactions with an effective threshold energy above about 3 MeV the reactor spectrum averaged value of the cross-section can be related approximately to the fission spectrum averaged value by applying a scaling factor which is appropriate for the reactor region. Many (n,α) , (n,a) and $(n,2n)$ reactions have effective thresholds above about 3 MeV and so approximate values of the reaction rates can be obtained in this way. Many of these reactions are of interest because they result in radioactive products (which present handling and disposal problems) and the (n,α) reactions contribute to structural material radiation damage effects. Measurements of fission spectrum averaged cross-sections and cross-section ratios also provide a useful test of the differential cross-sections.

4.1.8. Dosimetry cross-sections

For monitoring neutron fluence (the time integrated flux) and irradiation damage fluence (the time integrated flux weighted with the energy dependent materials damage function) selected time integrated reaction rates are used. These integrated reaction rates can be correlated with measured materials irradiation damage effects. The chosen reactions are those which result in radioactive products which have a sufficiently long half-life and an easily measured mode of decay. The energy dependence of the cross-section must also be approximately correlated with materials irradiation damage effects.

The International Reactor Dosimetry File, IRDF, produced by a cooperative effort organised by the IAEA Nuclear Data Section, contains a set of recommended cross-sections and associated uncertainty data. The current version is described in IAEA-NDS-141 Rev. 2 (1993). There is also a dosimetry file produced at Obninsk.

4.1.9. Nuclear data processing codes and group cross section data sets

Reactor codes cannot use evaluated nuclear data libraries directly because these data are usually of large volume and have a complicated structure. Therefore special code systems are used to process the evaluated nuclear data into more compact and simple form.

Most reactor neutronics codes use group cross-section data sets, the exception being some Monte Carlo codes which use continuous energy nuclear data. The group cross section sets (or group constants libraries) contain energy group averaged cross sections, resonance self-shielding parameters, transfer matrices and other auxiliary data. For routine reactor calculations few group (less than 10 group) and broad group (10 - 100 group) cross sections are usually used. The number of groups depends upon the complexity of the code (more complex codes, such as 3D transport codes, normally use few group data) and the parameters being calculated (accurate perturbation theory calculations of effects such as sodium voiding need at least 30 groups). In addition to the broad group data sets used for routine calculations there are the fine group (about 2000 group) libraries which permit an accurate treatment of resonance shielding in heterogeneous geometries. Resonance shielding is treated using either the f-factor method or the subgroup method, these being parametrisations of the resonance structure from which effective cross-sections can be calculated for particular compositions.

The most widely used computer code to process evaluated nuclear data into group cross section libraries is the NJOY code [4.2]. In addition, a code may be needed to convert the data produced by NJOY into the form required by a particular code scheme. For the treatment of resonance shielding auxiliary codes can be required to produce the appropriate parameters (e.g. the CALENDF code [4.6] for subgroup parameter calculations). There are other processing codes, such as GRUCON [4.3], AMPX [4.4] and ETOE [4.5] which are used mainly in the nuclear research centres where they were originated.

Deterministic neutron transport calculations are usually made in two stages, the first stage being the production of group cross-sections for regions of the reactor, such as the core and blanket regions of subassemblies. In this first stage resonance shielding effects are treated and flux fine structure effects allowed for. This involves a "cell calculation" for each region followed by flux averaging of the cross-sections. The whole reactor calculation is then made using these equivalent homogeneous cross-sections.

The space-averaging of group cross sections for a fast reactor fuel subassembly may sometimes be done simply by treating the assembly on a radial plane as a homogeneous mixture of fuel, coolant and steel materials, not taking into account heterogeneity effects. This is because for fast reactors these effects are in many cases of minor importance compared with their significance for thermal reactors. This is essentially due to the fact that the dimensions of the substructures (e.g. the pin diameter of about 6 or 8 mm) are small compared with the mean free path of fast neutrons of about 3 or 5 cm. However, the heterogeneity cannot be completely neglected and cell codes are then used to treat the effects more accurately. Special care has to be taken in the determination of anisotropic diffusion constants, especially for

"voided" conditions, i.e. for cases when coolant is removed or has been lost from regions of the core. Then, neutron streaming along preferential flight paths in low-density channels becomes possible. The accurate treatment of the heterogeneity of subassemblies is of most importance for calculations of reactivity effects such as control rod worths, and sodium void and Doppler reactivity effects. Heterogeneity effects are also more important in calculations for critical assembly geometries, particularly for those assembled from plates. Some examples of cross section preparation systems are the given in the following paragraphs.

The main Russian fast reactor group cross section preparation system is based on the 26-group ABBN library. For design calculations the ABBN-78 [4.7] version of this library is used as a standard tool together with the ARAMACO [4.8] processing code. The latest version of the ABBN library, based on BROND-2, ENDF/B-6 and JENDL-3 data, processed by the GRUCON code, has still not fully replaced ABBN-78, but some projects are already using it [4.9]. Both f-factor and subgroup data are included. For the most important isotopes this library contains fine group data (about 300 groups) in addition to the 26 group library. These are used to calculate fine group fundamental mode spectra, and then they are condensed to 26 groups. In the standard procedure, effective 26-group cross sections are calculated for homogeneous fast reactor subassemblies. Cell calculations to estimate heterogeneity effects are usually performed using the collision probability code FFCP [4.10] or the Monte Carlo code MMC FK [4.11]. A special treatment is also used to analyse experimental results [4.12].

The Japanese fast reactor group cross section sets are usually in 70 group form [4.13]. Now data sets based on the JENDL-2 and JENDL-3 libraries are in use. Cell calculations [4.14] are usually a standard option in the preparation of effective cross sections. Recently homogenisation techniques for control rods based on "reaction rate preservation" have been implemented in the cross section preparation scheme [4.15]. The effective 70 group cross sections are usually collapsed to 6-18 groups using 2D RZ spectra for use in 3-dimensional calculations.

For fast reactor calculations in the USA several group cross section libraries and corresponding processing codes have been developed. Perhaps the best known tool for fast reactor analysis is the MC**2-II/SDX scheme [4.5]. The main steps in this scheme are the following:

- (1) the MC**2-II fine group library (about 2000 groups) is produced from ENDF/B format files using the ETOE code. Following a fundamental mode calculation the cross-sections are condensed to an intermediate library of 230 groups. This 230 group library is tailored to treat the narrow resonances in diluent materials;
- (2) cell heterogeneity calculations are made using this intermediate library which is then collapsed to the working library in 28 groups or 21 groups. Earlier calculations used a buckling search (to give unit k-infinity) in the cell flux calculations used for group condensation. More recent calculations use bucklings recycled from one-dimensional diffusion theory reactor calculations;
- (3) special cell calculations in 28 or 21 groups to generate anisotropic diffusion coefficients by the Benoist method, and
- (4) further condensation to 8-9 energy groups using 2D and 3D diffusion theory spectra.

In the past in France, Germany and the UK had their own fast reactor group cross section data libraries and corresponding processing codes [4.16-4.18], and these are still in use for some project studies. As part of the European Fast Reactor Project these national systems

have been replaced by the ECCO cell code and its library [4.19]. The ECCO library contains cross-sections in 1968 fine groups, together with sub-group data to represent within fine group resonance structure. The ECCO library has been derived from JEF-2.2 using NJOY and CALENDF. The code can perform cell fine group calculations using collision probability methods for a large range of geometries and thus treat various types of heterogeneity effects. Alternatively broad group calculations can be performed in which the fine group library is condensed using collision densities and fluxes calculated for a typical fast reactor.

4.1.10. Validation

Validation of the nuclear data and calculational methods involves comparing values of reactor parameters calculated using the evaluated data with values measured in experimental reactor facilities or on operating reactors. The data can be adjusted, within the uncertainty margins, to improve the agreement with these measured values. An important result of the validation work is the estimation of the uncertainties in calculated values. Several nuclear data sets currently in use have been adjusted to fit a wide range of integral measurements. The adjustment procedure provides a covariance matrix for the adjusted cross-sections. However, more extensive validation studies are required to validate the calculational methods because these also involve approximation and uncertainties. Examples are control rod reactivity worths, coolant voiding effects and reaction rate distributions near interfaces.

4.1.11. Uncertainties in reactor parameters caused by nuclear data uncertainties.

The uncertainties of calculated reactor parameters calculated may be divided into two components, the first resulting from uncertainties in the nuclear data, and the second from approximations made in the nuclear data processing and the reactor calculations.

The main source of uncertainty for the majority of reactor parameters (such as k-eff) is the nuclear data used. However, calculational errors can be of large magnitude if appropriate numerical analysis is not done, for example if the diffusion approximation is used to analyse the sodium void effect in sodium plena [4.20].

TABLE 4.1. TARGET AND ACHIEVED UNCERTAINTIES IN SOME FAST BREEDER REACTOR PARAMETERS DUE TO UNCERTAINTIES OF NUCLEAR DATA (%)

Parameters	Target Uncertainties	Acheived Uncertainties
Criticality	0,5%	0,7%
Doppler effect	10%	10%
Burnup reactivity swing per 1% burnup	0,07%	0,10%
Control rod worths	5%	5%
Sodium void effect	0,3	0,3
Power spatial distribution	2%	2%
Breeding gain	0,03	0,03

The nuclear data libraries used in different countries result in different uncertainties in reactor parameters caused by nuclear data. But the magnitudes of these uncertainties are to some extent similar for most current nuclear data libraries because they are based on similar experimental information. So the comparison of target accuracies and uncertainties, provided by the ABBN data set, is of general interest. Some results of an analysis based on ABBN [4.21] are given in Table 4.1.

4.2. ENERGY PRODUCTION, RADIATION EMISSION, INDUCED RADIOACTIVITY AND IRRADIATION DAMAGE

Important products of nuclear interactions are the energy release, the radiation emissions, the reaction products (some of which are radioactive) and the irradiation damage of materials. The major sources of energy are fission reactions but the contributions from other reactions are also significant. The majority of the energy released in fission is in the form of fission product recoil energy and this is deposited close to the point of fission (within about 10 microns). The kinetic energy of the fission neutrons and the energy of the γ -rays can be deposited over a wide region (1 m). Not all of the fission energy is emitted promptly; a significant proportion is emitted as α and β energy resulting from the radioactive decay of fission products (predominantly by β decay). This is called fission product decay heat. This component of heating is important in connection with emergency core cooling, heat removal in the shut-down reactor and the design of fuel transfer and transport flasks. A knowledge of the energy transferred to materials by neutron scattering and γ ray interactions is required in the design of cooling for control elements, reflector regions, breeder regions and experimental rigs in reactors. Shielding must be provided for biological protection from neutrons and γ -rays and also to protect components from irradiation damage. Materials damage mechanisms include atomic displacements resulting from nuclear recoils, primarily in scattering reactions and in β -emission, and helium production in (n, α) reactions. Shielding is also required when handling radioactive materials.

Dosimetry is the measurement of neutron dose or fluence, the time (and energy spectrum) integrated flux. The dose is sometimes considered in terms of the damage flux or flux above 100 keV. Dosimetry monitoring reactions are those which result in a suitable radioactive product, the suitability depending on the half-life, detectability and the energy range of the neutron spectrum to which they are sensitive. Threshold reactions and reactions with prominent resonances have the advantage that they give a measure of the integral flux above the threshold energy or the flux at the resonance energy. By using a set of dosimetry reactions both the total fluence and its energy spectrum can be derived, and hence the damage effects predicted. Dosimetry is used to monitor the doses that irradiated components have experienced.

The radioactive decay of transactinium isotopes makes a contribution to the decay heat following reactor shut-down and in fuel transport. Spontaneous fission and (α ,n) reactions provide a source in a shut-down reactor which can be used when monitoring the reactivity of the core. If the source is known and the flux is measured then the reactivity can be derived and the approach to critical monitored. The radioactive decay must also be allowed for in the design of transport flasks and in reprocessing plant studies. The α -decay of the curium isotopes, Cm242 and Cm244, and associated neutron emissions from (α ,n) reactions are important in fuel which has undergone a long irradiation.

4.2.1. Heating

The accuracy of the total energy released in fission is higher than $\pm 0.5\%$ and the accuracy of the gamma component is higher than $\pm 10\%$. Although the accuracies assessed for the total delayed gamma and beta components are high ($\sim 1\%$) the time dependence of the decay heat is not so accurately known, this accuracy being, typically, $\pm 5\%$. In addition to the total gamma energies the gamma spectra are required. This is because the energies of individual gamma rays determine the migration distances and also the probabilities for (γ, n) and (γ, f) reactions. Gamma spectra are stored in nuclear data libraries and converted into group form for reactor calculations. Coupled neutron-gamma cross-section sets are produced and used in coupled neutron-gamma flux and energy deposition calculations.

Fission product decay heat. Heat generated by fission product decay is calculated by summing the contributions from individual fission products. Summation codes, such as ORIGEN [4.22], and the many similar codes, are used for these calculations. The data libraries they require contain fission product yields, and decay data (the half-lives, beta and gamma total energy yields and gamma energy spectra). Fission product capture reactions can have a significant effect on decay heat in some reactors and the above codes are capable of treating these effects in a simple way, using few group cross-sections and fluxes. These reactions tend to increase the total decay heat by a few percent. For applications where fission product capture effects can be neglected (or treated by means of a small correction factor) the decay heat can be represented by a sum of exponentials. About 20 exponentials are required to give a fitted accuracy of 1% over the time range of interest in reactor operations (this being more accurate than the actual accuracy of predictions).

The accuracy of fission product decay heat data has been assessed in two ways. The sensitivity of the summation calculations to changes in yield and decay data have been calculated and combined with estimates of the uncertainties in these [4.23]. The uncertainties estimated for $M(t)$, the decay heat following a long irradiation, are about $\pm 3\%$ for U-235 and Pu-239. The uncertainties in $m(t)$, the decay heat following a single fission, are larger, particularly at short times following the fission. They are then in the range $\pm 5\%$ to $\pm 10\%$ for times less than 100 secs. There are larger uncertainties for these short decay times because of the uncertainties in the beta and gamma energy yields of short lived fission products. Nuclear theory is used to provide some of these data, an example being the Gross Theory of Beta Decay [4.24] and the work of Klapdor and Metzinger [4.25]. The accuracies of the data are also assessed by comparing with microcalorimetric measurements of total heat as a function of time and also with measurements of the separate total beta and total gamma heating components by means of β and γ ray detection [4.26-4.28]. The agreement between these measurements and the calculations is not as good as the summation calculation sensitivity studies suggest. The summation calculations tend to be about 5% to 10% lower than the total heat measurements at short cooling times, but there are also significant discrepancies between the different total heat measurements. Work is in progress in several countries to try to resolve these discrepancies, in particular the decay data measurements on short lived fission products being made at Studsvik. The differences between fission product decay heat for fission in thermal and fast reactors are calculated to be small ($<2\%$). The differences in fission product yields between thermal and fast reactor spectra are small but not well known. However, this source of uncertainty is not considered to be important and it is not unusual to use thermal neutron fission yields in fast reactor decay heat calculations. At times of

the order of 10^7 secs (116 days), when fast reactor fuel might be transported for reprocessing, just a few fission products contribute to the total decay heat, in particular the following:

Rh-106 + Ru-106	30%
Zr-95 + Nb-95	30%
Ce-144 + Pr-144	24%
Ru-103	5%
Sr-89	1%
Remainder	6%

Actinide decay heat. The actinide decay heat at short times following the shut-down of a power reactor arises predominantly from the decay of U-239 (1.410 secs) and Np-239 (2×10^5 secs). This component varies with fuel burn-up because of the variation of the number of U-238 captures per fission. Alpha decay of Cm-242 (1.41×10^7 secs) makes a significant contribution to the decay heat at longer decay times. This arises from neutron capture in Am-241 produced by the decay of Pu-241 (14.6 year). The fraction of Am-241 in the fuel depends on the length of time for which it was stored between the abstraction of plutonium from irradiated fuel and the loading of the plutonium into the reactor, and also the reactor residence time.

Structural material decay heat. Heat is generated in the steels of the fuel pin cladding and the subassembly wrapper of a fast reactor fuel subassembly by the decay of radioactive products. This component of the decay heat does not exceed 10% of the total decay heat at any time. Integral measurements have been made of the activity induced in structural materials and these enable this component to be predicted to an accuracy of about $\pm 10\%$

Energy yields and energy deposition. We distinguish point energy yield, which is the kinetic energy of fission product nuclei produced in fission, nuclear recoil following neutron scattering and the energies of α and β emissions, and distributed energy yield, the energy of neutrons and gamma rays which distribute their energies over a wide range. The gamma energy yield arises from inelastic scattering, (n,γ) reactions, other capture reactions (in association with other emissions such as α -particles) and from fission. The main sources of energy are fission and capture in the fuel isotopes. The energy produced by capture in the fissile isotopes is about 1% of the energy produced in fission. The energy produced by capture in the principal fertile isotope (U-238) is about 2% of the total energy. Thus capture reactions contribute only about 6 MeV in a total of about 200 MeV per fission. A high accuracy is therefore not required for this capture component when calculating the total heat generation.

The gamma energy is of more importance in calculations of energy deposition in structural materials, for example, for calculating the temperatures of samples in an experimental rig in a reactor. Such a rig might contain samples of structural materials which are undergoing irradiation endurance testing. Irradiation effects are dependent on material temperatures. The main source of heating in many of these cases is the prompt and delayed γ -rays from fission (the two components being of about equal importance). To calculate this heating the gamma spectra must be known because this determines both the gamma migration distance and the energy deposition.

Only about 3% of the energy is deposited outside the fuel and about a half of this is deposited in the fuel cladding.

Measurements of spatial distributions of gamma energy deposition. These are made in experimental critical assemblies using thermoluminescent dosimeters. These are also sensitive to β -particles and to the neutron flux. The assumption that β -particle energy is deposited at the point of production cannot be made in the interpretation of these measurements. The migration of β -particles is usually calculated using a Monte-Carlo tracking method. The interaction cross-sections of gamma rays with matter are more accurately known than the gamma energy sources and spectra. Consequently these measurements provide a check on the gamma source data and the methods used for calculating the gamma flux from the source. Gamma interactions are strongly anisotropic and Monte-Carlo tracking calculations are made when accurate predictions are required. More approximate methods, including equivalent diffusion theory methods, which involve the derivation of effective gamma diffusion coefficients, are used in simplified design methods.

4.2.2. The radioactivity of irradiated fuel

Kuesters [4.29] has reviewed the status and requirements for nuclear data relating to the radioactivity of irradiated fuel. He focuses attention on routes for the production of Pu-238, Cm-242 and Cm-244 because of their strong activity and the neutron sources from spontaneous fission and (γ, n) reactions. In the fast reactors studied by Kusters α -decay of Cm-242 and the route U-238 $(n, 2n)$ Np-237 (n, g) Pu-238 are the primary sources of Pu-238. For the production of Cm-242 the capture cross-sections of Am-241 leading to the ground and isomeric states of Am-242 are required and the Pu-242 (n, γ) and Am-243 (n, γ) cross-sections are required for the calculation of the production of Cm-244. The $(n, 2n)$ cross-sections of both U-238 and Pu-239 are required for fast reactor irradiated fuel inventory calculations. Measurements of the compositions of irradiated fuel elements provide a check on the nuclear data and can also be analysed to provide spectrum averaged data suitable for fuel inventory calculations. Irradiations of samples of isotopes provide the most accurate data, the PROFIL irradiations in the PHENIX reactor being an example of this [4.30]. Spent fuel analysis is also of high importance in nuclear safeguards investigations. A method called the isotopic correlation technique, which correlates measured isotopic ratios with fuel burn-up and plutonium content is being evaluated as a potential way of monitoring plutonium production.

One requirement is to predict the neutron source in a shut-down reactor so that flux measurements can be used to monitor reactivity changes. Another requirement is for the design of shielding for spent fuel transport and reprocessing. The main neutron sources are Cm-242 decay at shorter times and Cm-244 decay at longer times. For predictions at shorter times accurate data are needed for Am-241 (n, γ) Am-242g Cm-242 and the spontaneous fission branching ratio. Since the fission cross section of Cm-242 cannot be measured (because of the high background activity) improved nuclear theory methods are required. To improve the accuracy of predictions at longer times more accurate values of the Pu-242 (n, γ) and Am-243 (n, γ) Cm-244 cross-sections are needed.

4.2.3. Activation of structural and coolant materials

The build-up of strong gamma emitters within the coolant circuit and on reactor components causes maintenance problems. One source of gamma activity in the coolant arises from the decay of Co-58 and Co-60. These are reaction products which result from trace quantities of cobalt and nickel which are dissolved into the coolant from components in the primary coolant circuit, activated in the core and then plated out in various parts of the circuit,

such as the pumps and heat exchangers. Integral measurements of reactions which lead to such strongly radioactive products can be readily made in low power facilities, as well as in experiments made in power reactors (or samples taken from the reactors). Integral measurements made in zero power critical facilities have an accuracy, typically, of $\pm 5\%$ and they can be used to predict the reaction rates in power reactors to a satisfactory accuracy of $\pm 10\%$. However, measurements should also be made in power reactors to check on the importance of competing reactions and the transmutation of the radioactive products themselves. Two-stage reactions, and reactions less easily measured in zero power facilities (such as $(n,n'p)$ which only occurs at high neutron energies) can also be found in this way.

The activity induced in the sodium coolant of a fast reactor is also of importance. The reactions $\text{Na-23 } (n,\gamma) \text{ Na-24 } (15 \text{ hr})$ and $\text{Na-23 } (n,2n) \text{ Na-22 } (2.6 \text{ years})$ are important, as is the activity induced in trace contaminants in the coolant, such as $\text{K-41 } (n,p) \text{ Ar-41 } (1.8 \text{ hr})$.

4.2.4. Irradiation damage effects and dosimetry

Atomic displacement damage in structural materials is a function of the nuclear recoil energy, E_r , the temperature, and the presence in the material of nucleation sites for void formation, such as helium (resulting from (n,α) reactions). The recoil energy must exceed a threshold energy, E_T , for the atom to be displaced. For recoil energies higher than E_T the number of displacements is approximately equal to E_r/E_T but is less than this number by a factor which increases with increasing recoil energy. This is because there is a greater probability of a recoiling nucleus being displaced into an existing vacancy rather than an interstitial position. There are different models for calculating the number of displacements, one such model being the NRT Model (Norgett, Robinson and Torrens [4.31]). This has been adopted for international reference use. Having chosen a model the displacement cross-section can be calculated. It is equal to the sum of the cross-sections for each reaction multiplied by the number of displacements for the corresponding recoil energy.

The number of atomic displacements depends on the element, I , and also on the particular alloy. However, this dependence on the alloy is usually neglected and a displacement cross-section for iron is calculated which is used for iron in all different types of steel. The variation of E_T with alloy is not so great as to be significant compared with other sources of variability in the effects of atomic displacements (e.g. temperature, manufacturing method). The (n,γ) reaction contributes to the atomic displacement cross-section because of the nuclear recoil which occurs when the γ rays are emitted. Other reactions also contribute. In particular, inelastic scattering, (n,p) and (n,α) reactions. Atomic displacement cross-sections have been calculated for a number of structural material elements by Doran and Graves [4.32] and the data are available in a fine energy group form (the SAND II 640 group structure).

Helium embrittlement is another structural material damage mechanism. Helium is produced in (n,α) reactions. Trace quantities of boron and nitrogen in structural materials can make a significant contribution to the helium production. Consideration must also be given to (n,α) reactions in isotopes which are formed as a consequence of irradiation; for example: $\text{Ni-58 } (n,\gamma) \text{ Ni-59 } (n,\alpha)$

Integral measurements of (n,α) reactions in structural materials have been made by irradiating samples in power reactors and measuring the helium produced. Uncertainties in the amounts of trace quantities of elements such as boron and nitrogen can introduce large

uncertainties into the results. Uncertainties in the shapes of reactor neutron spectra at high energies can also result in uncertainties in the derived data. It is usual to derive equivalent U-235 fission spectrum averaged values from these measurements by applying a calculated factor. These are the results quoted, for example, by Gryntakis [4.33]. For Fe the values differ by ± 30 from the mean value and this uncertainty is larger than the required accuracy of $\sim \pm 15\%$.

Dosimetry. Irradiation exposure is monitored by means of foils or detectors. These are removed following the irradiation and the induced activity is measured. This induced activity depends on the cross-section for the reaction, the time history of the flux, the rate of decay of the activity and the rate of burnup of the primary isotope and of the activation product. The activity must be sufficiently strong to be accurately measurable, sufficiently long lived to measure the dose over the time period of interest and the absorption cross-sections of the isotope and the activation product must be sufficiently small for burnup to be negligible or to be a correction which can be accurately made. Dosimetry reactions suitable for different applications have been reviewed and the chosen dosimetry reactions have been compiled in an IAEA recommended International Dosimetry File, IRDF [4.34]. Standardisation is important because the measured information on irradiated damage effects is often correlated with dosimetry reaction dose measurements. The derived damage cross-sections are less accurate than the correlated data because of uncertainties in the dosimetry cross-sections used to deduce the flux and flux spectrum of the irradiation. By standardising the dosimetry cross sections and measuring doses using the same dosimetry reactions the materials damage can be predicted more accurately. Integral measurements of the dosimetry reactions in standard neutron spectra (or benchmark fields) are used to evaluate the differential cross-sections and, when appropriate, to adjust them, (and also to adjust the characteristics of the reference benchmark fields). These benchmark fields include the Cf-252 spontaneous fission neutron spectrum, the thermal neutron induced U-235 fission neutron spectrum and a number of well characterised spectra. The RB1 Research Reactor at Mol provides one such reference benchmark field facility.

The types of dosimetry reaction can be divided into fission and non-fission, threshold and non-threshold. The choice of the set of reactions to be used for a particular application depends on the intensity of the flux, the duration of the irradiation, the type of reactor spectrum (thermal reactor, fast reactor, core, shielding, vessel) and the neutron energy range of importance in the effect being monitored.

4.3. NEUTRONICS CALCULATION METHODS

The methods used for reactor calculations can be considered in three categories, the accurate reference calculation methods, the routine methods used for operating reactors, such as SUPER-PHENIX, and those used for exploratory design studies.

Deterministic methods, as distinct from Monte-Carlo methods, are the primary methods used, although continuous-energy Monte-Carlo methods are used to treat complex shielding configurations and to calculate the criticality of fuel storage facilities, transport flasks and the fuel dissolvers used in reprocessing plant. Monte-Carlo methods are also used to validate the approximations made in the deterministic methods and are now being used increasingly to calculate some core physics effects, such as gamma energy deposition, and the neutronics of complex geometries, such as control rods (the Siemens code MOCA being used in this way). However, Monte-Carlo methods still require too much computing time to be

used routinely for core neutronics calculations because of the high accuracy required in calculations of the effects of changes in reactor parameters, such as burn-up reactivity changes, and the effects of temperature changes.

Calculations of the neutronics characteristics of reactor cores made using deterministic methods involve two stages. Firstly heterogeneous medium calculations must be made for regions of the reactor to obtain equivalent homogenised cross-sections. These are then used in whole reactor calculations. A third stage can be required when it is desired to calculate detailed reaction rate distributions, rather than only whole reactor characteristics. This third stage involves the combination of the detailed flux distributions for the regions, calculated in the first stage, with the whole reactor flux solution calculated in the second stage. For some calculations the heterogeneous medium stage can be avoided because heterogeneity effects are small in fast reactors. Typically, the effects are of the order of 1% in the reactor effective multiplication, and 5% to 10% in Doppler effects and coolant voiding effects. However, for control rods a simple homogenisation of the material composition (over the lattice area occupied by a rod) results in a significant overestimation of the rod antireactivity, by 10% to 20%. Nevertheless, for some studies such approximations are acceptable and whole reactor calculations made using a standard broad group cross-section set, having about 35 energy groups, are used for general studies on a wide range of UPu oxide fuelled, sodium cooled, fast reactors.

4.3.1. Forms of heterogeneity

The types of heterogeneity to be treated in the first stage of calculation are:

- (i) the core subassembly, which consists of a bundle of fuel pins enclosed in a hexagonal wrapper. In SUPER-PHENIX there are 271 fuel pins in a subassembly. The diameter of the UPu oxide pellets is 0.74 cm. The hexagonal wrappers are 0.5 cm thick and the lattice spacing is $L = 17.9$ cm "across flats" of the hexagonal cell (an area of $2\sqrt{3} \cdot (L/2)^2 = 277.5 \text{ cm}^2$);
- (ii) the control rods. In SUPER-PHENIX these are of two types, the principal control system, SCP, and the complementary (or safety) system, SAC. The arrangement of the absorber material (highly enriched B,C) is different in the two axial sections of the SAC rods. These have an articulation at the join between the lower section, or link (with its ring of 8 absorber bars) and the middle/upper section (with its 4 absorber bars). The SCP rods have a close-packed assembly of 31 bars of B,C;
- (iii) the treatment of interface regions, such as those between core and blanket zones, and blanket and shield regions, poses particular problems because of the rapid variations of the neutron spectrum and the strong anisotropy of the flux. Broad group cross-sections which vary with position are required to treat these effects accurately;
- (iv) the heterogeneity of experimental critical assemblies such as MASURCA, FCA and BFS is different from that of a power reactor and an accurate treatment of this heterogeneity is needed to extrapolate critical assembly measurements to power reactor conditions. In most critical facilities the materials are in plate form, typically 5 cm square and several mm thick. In some facilities fuel in the form of pins has been used (for part of the core only). In the French facility MASURCA the primary materials are in rodlet form, but the larger MASURCA assemblies include regions composed of materials in plate form.

4.3.2. Methods for treating heterogeneity

Collision probability methods are most usually used to calculate the flux fine structure in a heterogeneous medium (a subregion of the reactor). It is assumed that this cell or macrocell is part of a repeating pattern of the cells, but with a net leakage into or out of the cell. It is divided into a number of regions within each of which the source of neutrons (resulting from fission or scattering reactions) is treated as uniform and isotropic (although it can be noted that methods have been developed for treating non-uniform sources and P_1 scattering sources). The problem of the treatment of heterogeneity is in two parts: how to calculate the cell flux and how to produce equivalent homogeneous cross-sections. The second part depends on the whole reactor calculation method to be used. For diffusion theory calculations a diffusion coefficient is required. This can be direction dependent, for example D_r and D_z . However, the transport theory codes currently available do not permit the use of direction dependent cross-sections. This is a problem because, when there are low-density channels, such as those present when a control rod is withdrawn from the core, or in the sodium plates of a critical assembly, there is preferential neutron streaming along the direction of the sodium filled space. Two-dimensional void channels present a particular problem because the diffusion coefficient becomes infinite unless account is taken of the finite extension of the void region or the curvature of the flux. Two-dimensional void channels can exist between regular arrays of pins, in particular in a square array of pins or a widely spaced array on a triangular grid, or in plate geometry assemblies simulating sodium voided regions. In practice, the subassembly wrapper box, or the containment box in the case of plates, limits the extension of the void channel. Special methods must be used to treat such neutron streaming problems.

The simplest form of flux calculation is the infinite homogeneous medium calculation. However, even in this case, when leakage is present (represented by a buckling) an approximation must be made. The approximations are of two types, P_n and B_n . In the P_n approximation the flux is expanded in spherical harmonics and the expansion is terminated at order N whereas, in the B_n approximation it is the source of scattered neutrons, or the scattering kernel, which is terminated at order N , the flux expansion being continued to higher orders. In the case of a homogeneous medium the higher order components of the flux are related by a simple formula to the lower order components. They can then be substituted back into the lower order P_n equations to give B_n -modified P_n equations, the modifications appearing in the form of a correction factor applied to the total cross-section. One then speaks of B_n -modified total, or transport cross-sections, or diffusion coefficients. However, these P_n -modified cross-sections should only be used in P_n equations in which the higher order P_n fluxes are not treated. For example, a B_1 correction can be applied to the diffusion coefficient used in a diffusion theory calculation, or a P_n calculation, but such corrected cross-sections should not be used in an S_n calculation or a higher order P_n calculation. However, a B_n calculation provides the better flux to be used for condensing the cross-sections in energy to produce the broad group cross-sections to be used in a whole reactor S_n or P_n calculation.

Another related question is the definition of the transport cross-section, which is an approximate way of allowing for P_1 scattering by treating the angular anisotropy of P_1 scattering but not the associated energy change. When hydrogenous material is present the P_1 scattering should be treated explicitly or the transport cross-section defined appropriately.

4.3.3. Control rod homogenisation

In the case of reactor subassemblies, or the cells of a critical assembly, one can make the approximation that the cell is a component in an infinite array of identical cells and with leakage represented by a buckling. In the case of a control rod, the problem is different because the rod is surrounded by fuelled subassemblies. The calculation of the flux must now be made for macrocell consisting of the control rod and a surrounding region of core material [4.35]. The homogenisation of the control rod region is also different. A simple flux x volume averaging of the cross-sections for the control rod region results in an overestimation of the rod antireactivity when the macrocell calculation is repeated using the cross-sections homogenised in this way. The approach adopted is to apply scaling factors to the control rod region cross-sections, homogenised in the above way (flux x volume averaging), to obtain an equivalence between the calculation made for the detailed representation of the structure of the control rod in a core

environment and one made using the modified homogenised cross-sections. This involves an iterative procedure, with the scaling factors being progressively refined.

Two criteria for equivalence have been used. The simplest method involves scaling the group absorption cross-sections until an equivalence is obtained in the absorption rate for each energy group [4.36]. The second method involves scaling the absorption plus moderation cross-sections and the transport cross-sections separately to give reactivity equivalence for each energy group and separately for leakage and absorption plus moderation [4.35]. The number of iterations required to get a satisfactory convergence is about 4. The treatment of leakage effects is also important for the low density channel which is present in the core when a control rod is withdrawn (the control rod follower region).

A method has also been developed which corrects for mesh size effects and for the difference between diffusion and transport theory calculations, for use in broad-mesh whole reactor diffusion theory calculations (the MONSTRE code [4.37]).

4.3.4. Derivation of broad group cross-sections

Broad group cross-sections can be derived from fine group data by integrating the P_n equations over energy, reaction cross-sections being weighted with the scalar flux and the P_n order transport cross-sections weighted with the P_n order net current. A compromise solution is then adopted, usually by defining the total cross-section suitably to treat the migration of neutrons and by calculating a corresponding "self-scattering correction". For core region calculations a P_1 or B_1 flux solution is found to be adequate but for blanket and shield calculations higher order components of the flux, and the associated scattering sources, must be calculated.

4.3.5. Whole reactor calculation methods

There are three broad categories of deterministic whole reactor calculation methods currently in use: (a) diffusion theory; (b) spherical harmonics approximations, or P_n methods, and (c) discrete ordinates or S_n methods. Diffusion theory is widely used for reactor core calculations although the faster P_n and S_n methods developed in recent years are now replacing them.

Finite difference methods, with a regular geometry grid in XYZ, HEX.Z or RZ geometry, with each mesh interval having constant cross-sections, are still in use although progressively being displaced by the nodal methods. The finite difference methods calculate a single value of the average flux in each mesh interval, or on each surface of the mesh interval. There is an error due to the finite size of the mesh. In diffusion theory, the error in k_{eff} is approximately proportional to the square of the mesh size, (tending to this value in the limit of small mesh sizes). The sign of the error is different for mesh centre flux and mesh edge flux methods. The mesh error is smaller in S_n calculations. In these methods the angular flux is represented by a set of directions and associated weights. The set of directions can be chosen to suit the particular problem although there are standard sets for reactor core calculations. For treating special classes of problem, such as plate geometry cells, or pin geometry cells, a different choice is more efficient.

In recent years, the first order finite difference methods have been superseded by nodal methods. In these the flux in each mesh element, or node, is represented by a set of orthogonal functions, such as Legendre polynomials for each direction, or other types of expansion. Using such flux representations, a more accurate solution can be obtained using a coarser mesh. The matrix equations relating the various components of the flux become more complicated, involving a relationship between components of the flux inside the node and on the surfaces.

The same general strategy of solution is followed as for the finite difference methods, consisting of an inner iteration and an outer fission source iteration. Starting from an assumed fission source distribution, the flux is calculated progressively in each energy group, and spatial node, from the source of fission neutrons plus scattered neutrons entering the group and the fluxes in neighbouring nodes. The flux is calculated by an iterative method, rather than by matrix inversion, and there are different strategies for doing this -line by line, with changes in direction between iterations-plane by plane-chequer board, etc. An alternative method is to calculate the flux in all energy groups for a node (or set of nodes) using the fluxes for neighbouring nodes from a previous iteration. Having calculated the fluxes in all nodes and energy groups corresponding to the assumed fission source a new fission source is calculated and so the procedure is repeated. There are ways to accelerate this procedure, and these have an important effect on running times.

In addition to the methods which use regular geometrical mesh arrays there are the finite element methods in which more general geometrical shapes can be represented. These are particularly useful in treating shielding configurations [4.38]. Potentially, such methods would also be useful for treating the internal structure of control rods within a whole reactor calculation

4.3.6. The sub-group treatment of resonance shielding

Because it is impractical to represent all the detail of the structure of cross-sections in reactor calculations approximate representations are required. It is particularly important to represent resonance structure and its variation with temperature. One way to represent the data is to have a library of broad group cross-sections which are a function of the background cross-section, σ_{σ} , and the temperature, $\sigma_{xg}(\sigma_0, T)$, or $\sigma_{xg}(\infty) \cdot f_{xg}(\sigma_0, T)$, where $\sigma_{xg}(\infty)$ is the cross-section at infinite dilution and $f_{xg}(\sigma_0, T)$ - the shielding factor for reaction x in group g . The shielding factor can be calculated using the narrow resonance approximation or obtained by means of a flux spectrum calculation made for a homogeneous medium containing the resonant material plus a diluent material having cross-sections σ^l and density

N^1 , σ_0 , being defined as the product of σ^1 and N^1 . Indeed, using the NJOY code system the shielding factors can be calculated for more general two region cells and more than one diluent material.

In a practical calculation an equivalence must then be found between the admixture of materials (with the associated heterogeneity) and a homogeneous background cross-section. Fortunately, in fast reactors heterogeneity effects are generally small and can be treated approximately. Also the resonances of uranium and plutonium isotopes at the energies of interest in fast reactor calculations are narrow compared with the energy change in scattering and so the narrow resonance approximation applies. This approximation cannot be made for the important resonances in structural materials (such as iron, chromium and nickel) nor for sodium and oxygen. For this reason calculations are made for reactor regions using a fine energy group structure, that is, in about 2000 energy groups having lethargy widths smaller than, or comparable with, the mean lethargy gain in scattering ($\Delta u \sim 1/120$ for uranium and plutonium). The assumption can be made that the scattering source is constant through the energy range of the fine group and any cross-section structure within the group can be treated using the narrow resonance approximation.

An alternative to the shielding factor method is the sub-group or probability table method. In this method the cross-section is assumed to have a simplified structure which, when used in flux calculations (for any geometry and heterogeneity), reproduces the correct reaction rates. Thus the problem of calculating an equivalent background cross-section is avoided. Within a fine group the cross-section is represented by a set of sub-group values and associated weights. The cross-section has a histogram from within a fine group and the widths of the histograms can be different for each histogram element. This does not present a problem because the scattering source is assumed to be the same in all the sub-groups within a fine group. There are different ways to calculate the sub-group data. One way is to calculate values which reproduce the shielding factors for a set of background cross-sections, a_0 . However, this method might not cover the effects of small cross-sections (cross-section minima) important in calculating the transmission through shields. Another method is to fit the transmission through blocks of material of different thicknesses, and the associated reaction rates in a foil exposed to the transmitted beams. A further method is to reproduce the variation of the shape of the total cross-section when it is reordered to be monotonic in energy. The advantage of this method is that the same ordering and fitting ranges can be used at all temperatures and thus a variation in temperature through a region can be treated because the sub-group data at different temperatures are correlated. However, this method results in a lot of sub-groups per fine group. A more efficient fit is obtained by calculating a set of positive and negative moments ($n = -10$ to $+10$) of the total cross-section and the associated reaction rates. Using this approach a good representation is obtained with about 10 sub-groups per fine group, and both the peaks and minima in the cross-sections are represented. This is the method used in the ECCO code, the data being derived using the CALENDF code [4.6]. The disadvantage of the sub-group approach, compared with the ultra-fine group representation which represents explicitly all the resonance structure, is that, in principle, the flux for all combinations of the sub-groups of one material with those of all the other constituent resonant materials must be calculated. This can involve a number of flux calculations comparable with that of the ultra-fine group treatment (of the order of 50,000 groups). Such ultra-fine group methods can treat temperature variations across a region and are required as reference solutions to test the accuracy of the sub-group methods.

In unresolved resonance regions a ladder of resonances is obtained by sampling from the probability distributions of the parameters, the resonance spacing distributions (Dyson-Mehta) and resonance width distributions. A set of point-energy cross-sections are then generated and treated in the same way as the resolved resonance region cross-sections. In the Monte-Carlo code MCNP [4.39], a probability table method is used to reduce the amount of data in both the resolved and unresolved resonance regions.

4.3.7. Perturbation theory methods

Perturbation theory methods are used to calculate reactivity coefficients, such as Doppler effects and the effects of coolant density changes. They are also used to calculate the sensitivities of parameters to cross-section changes for use, for example, in cross-section adjustment studies. Perturbation theory requires the solution of an adjoint equation, a transposition of the normal transport theory equation, the transposition being in energy and direction. A distinction is made between reactivity perturbation theory and generalised perturbation theory. In reactivity perturbation theory, it is the change in reactivity resulting from changes in the macroscopic cross-sections (or geometry) which is calculated. We distinguish two systems, the unperturbed system having cross sections Σ_u , and the perturbed system having cross-sections Σ_p . The flux is calculated for one of these systems (say ϕ_u) and the adjoint flux, ϕ^*_p , for the other. The adjoint flux, or neutron importance, $\phi^*(x',E')$ is the probability of a neutron (at position x' and of energy E') contributing to the production of a fission neutron in the asymptotic fission distribution.

In first order perturbation theory, ϕ^*_p is replaced by the adjoint flux calculated for the unperturbed system, ϕ^*_u . This results in an ambiguity for the leakage term in diffusion theory term because one has the option of replacing either the flux gradient or the current by the unperturbed value. The question must be considered when calculating coolant density reactivity coefficients. For whole reactor effects, the flux distribution shape remains approximately unperturbed and the approximation of $\text{grad } \phi_p$ by $\text{grad } \phi_u$ is acceptable. For small regions the current is approximately unperturbed and it is better to replace J_p by J_u .

Generalised perturbation theory permits the changes in properties other than reactivity to be calculated. To calculate these an appropriate adjoint equation must be solved which uses a source corresponding to the property for which the sensitivities are to be calculated. For example, to calculate the sensitivities for a central fission rate ratio the adjoint source is the fission ratio itself. Generalised perturbation theory can also be used to calculate the sensitivities of reactivity changes to changes in cross-sections. For a review of these methods reference can be made to [4.40].

4.3.8. Methods of adjustment of cross-sections to fit integral measurements

The objective of cross-section adjustment is to reduce the fractional discrepancy between the measured value, E_k , and calculated value, C_k , of integral property k taking into account the uncertainties in the cross-section data and the integral measurements. For a review of recent work in the subject see [4.41]. The assumption is made that the difference between C'_k , the value calculated using the adjusted cross-sections, and C_k can be approximated as linearly dependent on the fractional adjustments to the nuclear data parameters, X_i . The values of X_i are found by a least squares fit to the integral and differential cross-section measurements, relative to the uncertainties. The procedure produces the covariance matrix of the adjusted cross-sections from which the fractional accuracy of reactor

parameters, p , calculated using adjusted cross-sections can be obtained when the cross-section sensitivities of p have been calculated.

A typical procedure for adjusting cross-sections is to calculate the sensitivities for changes of cross-sections in about 15 energy groups and set up the covariance matrices for this group structure. Adjustment factors for the cross-sections averaged in these 15 energy groups are then calculated but the adjustments are then applied to the differential cross-sections by calculating a smooth fit to the group factors (such as a cubic spline fit). Having derived the adjusted differential cross-sections in this way the integral properties are recalculated to test the assumptions. These are that adjustments can be made in 15 energy groups and the assumptions of a linear dependence of the calculated values on the cross-section changes. It might be necessary to repeat the adjustment exercise to allow for non-linearities. An alternative to making adjustments in a few energy groups is to adjust the parameters of nuclear models used to fit the differential cross-section measurements. This approach has been used for fission product capture cross-sections and cross-sections of higher transactinium isotopes.

Instead of carrying out an adjustment of cross sections to obtain a simultaneous best fit to both the integral and differential cross-sections, the integral measurements can be used to guide the choice of differential cross-section measurements to be included in an evaluation. This approach is valuable when there are sets of discrepant measurements and it is evident that one or the other set contains an error larger than the estimated uncertainties. This approach has been adopted, for example, in evaluations for Am-241 and Am-243 to choose between different measurements of the fission cross-sections. Benchmark testing has also been applied in the development of Evaluated Nuclear Data Libraries.

4.3.9. Kinetics calculations

Kinetics calculations are required to study the response of a reactor to a fast acting change, in particular for the assessment of reactor safety. For the small fast reactors which were built before about 1970 point kinetics calculations were found to be adequate. That is, the flux shape could be assumed to remain constant in time, through the transient. For large fast reactors of the size of SUPER-PHENIX this is no longer the case, in particular for localised effects such as the rapid withdrawal of a control rod. The local changes in flux, power and temperatures can be much greater than the average changes and so a point kinetics model would underestimate the severity of the change. However, it is possible to calculate the time dependent flux as the product of slowly varying normalised flux distribution and a time dependent coefficient, $c(t)$, and to represent the source of delayed neutrons by a similar product, $d(t)$. The normalised flux distribution is calculated from the delayed neutron source distribution by a static source calculation. The variation of the cross-sections with time is calculated using separate modules which solve the heat transfer equations and hence calculate the region temperatures and cross-sections allowing for thermal expansion and Doppler effects. In the usual treatment axial sections of representative fuel pins are modelled, with several annular regions representing the fuel pin cell. The heat transfer coefficients can be temperature dependent, the values being determined in separate studies. In a typical calculation the values of $c(t)$ and $d(t)$ are calculated at time intervals of 10^{-4} secs. After n steps, the temperatures are recalculated and after m temperature step calculations the spatial flux distributions are recalculated. An example of a three dimensional kinetics code is the SPARK code which solves the flux equation using Pn methods. For a general introduction to reactor kinetics reference can be made to [4.42].

4.4. COMPUTER CODES USED IN FAST REACTOR NEUTRONICS

4.4.1. Codes based on diffusion theory

Diffusion theory still remains the main tool for fast reactor numerical analysis. Two reasons are mainly responsible for this: (1) in the central part of the reactor, the reactor core, the application of the diffusion approximation is satisfactory for most purposes, (2) the diffusion equation is relatively simple, its properties and the appropriate methods to solve it have long been well known. Although the diffusion equation was applied previously in the other field of theoretical physics, the numerical methods used to solve efficiently the neutron diffusion problems encountered in reactor physics had to be tailored to the properties of the parameters appearing in the equation and to the neutron distribution as a function of space, energy and time.

Applicability of the diffusion approximation requires that the condition of a nearly isotropic distribution of angular neutron fluxes is sufficiently well satisfied. This means that the application of the diffusion approximation becomes questionable in the immediate neighbourhood of local neutron sources, external boundaries and internal interfaces between material regions with different nuclear properties. Depending on the neutron energy and geometrical arrangement of materials inside a reactor, the allowed range of application may also be restricted within strongly absorbing media (control rods) and within components surrounding the reactor (blankets, reflectors, plena) where one could expect that the neutrons exhibit a pronounced preference for the outward flight direction which is not in accordance with the assumption of nearly uniform angular distributions of neutrons.

The methods and codes applied to solve the 2D and 3D multigroup diffusion equation are well established. Most of the codes used for fast reactor analysis are based on the finite difference equation, although very efficient diffusion codes also exist using other kinds of solutions, such as finite element [4.43], coarse mesh [4.44] and nodal methods [4.45]. One of the main advantages of

the last approach is that the methods of both diffusion and transport theory can be combined within the one calculational scheme.

2D diffusion codes are now used mainly for general evaluations of reactor concepts and to collapse fine group cross section data. 2D diffusion codes were developed in the 60 - 70's in most reactor research centres and many of these are still in use. However, it is interesting to note the new very efficient multigrid method [4.46] for solving the 2D diffusion equation is a relatively recently proposal for use in the diffusion synthetic acceleration scheme [4.47] implemented in the 2D finite-difference Sn-transport code TWODANT [4.48], which now seems to be the most efficient 2D Sn-code for fast reactor core calculations.

3D diffusion codes are not so numerous as 2D diffusion codes. Most frequently cited 3D diffusion codes are TRIGEX [4.49], DEGEN [4.50] (coarse-mesh finite difference), CITATION [4.51], 3DB, the D3D and D3E code system [4.52] (finite-difference), DIF3D [4.53] (finite-difference and nodal options) and HEXNOD [4.54] (nodal code).

Improved coarse-mesh and nodal methods are now two main directions of the development of 3D diffusion codes. The nodal diffusion method is usually considered as more efficient and exact than coarse-mesh finite-difference and provides solutions with very small

truncation errors. Another advantage of the nodal approach is that the transport theory methods can be implemented and work reasonably well within the nodal scheme.

4.4.2. Transport theory and codes

In some applications diffusion theory may be too approximate, especially if a pronounced angular dependence of the neutron flux exists in a reactor region. This situation becomes almost usual when analysing some new concepts, such as the axially heterogeneous design [4.55] with an axial uranium layer inside the core and a sodium plenum above the core.

Whole core multidimensional deterministic transport theory calculations, especially 3D calculations, were very slow and almost impractical in the 70's. But the progress in computers and calculational methods has changed the situation.

Efficient methods for 2D and 3D neutron transport calculations have been developed and applied in computer codes during the last 10 years, such as the traditional spherical harmonics method - MARC/PN [4.56], the Sn-method - BISTRO [4.57], TWODANT, TWOHEX [4.58] and TRITAC, the method of characteristics - MCCG [4.59], and the nodal transport methods - DIF3D, HEXNOD, HEXTR [4.15].

Finite-difference discrete ordinate codes provide the most rigorous solution of the transport equation. However, truly 3D finite-difference Sn methods are still too inefficient to be used as routine tools for fast reactor analysis. Therefore, nodal transport methods have been developed intensively in recent years, because these methods, although approximate, provide the

larger part of the transport correction to diffusion theory at a very low cost (sometimes only 50% to 100% more) than the nodal diffusion method.

There are two approaches to the nodal transport method, the first, almost conventional, being based on the transversal integration procedure [4.45], the second being the variational nodal transport method [4.60, 4.61].

The conventional method is to transversely integrate the diffusion equation to reduce it to a one-dimensional equation containing a transverse leakage term as an extra source term. Nodal balance equations are then derived from the set of coupled one dimensional diffusion equations, each of which is obtained via transverse integration along a different orthogonal direction. This method was originally developed for rectangular nodes. When applied to a hexagonal node, however, the transverse leakage becomes very complicated and contains non-physical singular terms of step function and delta-function types, which destroy the nice features appearing in the nodal equations for rectangular nodes [4.61]. In the HEXNOD code the approach was simply to ignore these singular terms. For compensation the transversely averaged flux was artificially modified to retain the neutron balance equation in a hexagonal node. The advantage of this technique is that the nodal equations remain essentially identical with those for rectangular nodes (except, of course, for having three instead of two sets of nodal equations on a radial plane). This method works reasonably well for fast reactor core calculations like control rod worth calculations [4.54]. Another approach in handling the singular terms in the transverse leakage was achieved in the HEXTR code [4.15] by splitting this term into two parts, each of which is not singular by itself. An interesting technique to accurately eliminate these singular terms was proposed in [4.62], where the conformal mapping procedure was suggested to transform the hexagonal node into the rectangular one.

However, this technique has not yet been incorporated in routinely used codes.

The second class of nodal transport methods more recently developed is based on the variational nodal transport method (VNM). VNM was incorporated in the code DIF3D, and then in the European system of codes ERANOS [4.63].

The last direction in transport theory methods development to be mentioned here is the collision probability method. This method starts from the integral transport equation, unlike the Sn-method, which starts from the differential form of the transport equation. To use the collision probability method we must calculate the probabilities, P_{ii} and P_{ij} respectively, that a neutron born or travelling in region i of a cell will have its next collision either in the same region i or in some other region j . Using some reciprocity and addition relationships we may facilitate the numerical integrations. For simple geometries (one-dimensional plane, cylindrical and spherical geometries, in particular) the calculation of the probabilities P_{ii} and P_{ij} is straightforward (involving exponential integrals, Bickley functions and associated functions). It is more complicated to calculate P_{ij} for a sophisticated system, such as an array of pins (or more complex geometries).

Some compromise has to be taken regarding the starting distribution of neutrons. We have two alternatives: 1) use a flat source distribution within a fairly small volume element, which leads to simple expressions for the collision probabilities but may demand a fine subdivision; 2) use of fairly coarse subdivision into few, fairly large volume elements but requiring improved approximations for a source distribution (i.e. linear or quadratic shapes). The optimum choice must be found between these two possibilities.

An interesting approach was suggested in [4.64] of calculating collision probabilities in complex geometry systems using Monte Carlo codes. This way takes off the geometric

limitations of the method. The collision probability method is usually used for cell problems, but has also been applied to reactor and shielding calculations [4.65].

4.4.3. Codes based on the Monte Carlo method

Several codes are available for carrying out a direct Monte Carlo simulation of a reactor problem using detailed geometrical models and continuous energy (or very fine group) representation of nuclear data. These can be used to provide reference values and investigate the effects of approximations in deterministic methods. Some widely used Monte Carlo codes are MCNP [4.39], MORSE [4.66] and KENO [4.67], amongst others.

Monte Carlo codes are relatively rarely used in fast reactor design, partly because they are usually time consuming. This also must be a reflection of the success of the standard deterministic methods, which involve a hierarchy of approximations, usually beginning from a simple cell or fundamental mode treatment of fine energy, followed by calculations in a more complex geometry in a coarser energy mesh and finally a whole reactor 3D calculation with few energy groups and a coarser spatial mesh.

The best of these deterministic methods, correctly applied, gives a perfectly adequate treatment of most reactor problems. However there are some important benefits from a more direct model of the physical problem. The current deterministic methods involve so many specialised approximations, the subject of many years of specialists effort during their development, that their range of validity is sometimes well understood only by their

originators. It's difficult to conceive of a way in which the next generation of users of these codes or even a group maintaining them, could become fully conversant with them. Under these circumstances there is always a danger that they will be applied to some new problem, apparently not too dissimilar from the standard one, and give incorrect results.

If problems of this kind are to be avoided, potential users will have to be trained to an exceptionally high level in the modelling technique used in the old methods and the overhead in doing this will be high. The Monte Carlo method could be the remedy. Due to its inherent slowness relative to the deterministic methods it cannot be used at present for all routine calculations. However, it can provide reference values which are transparent to physicists and engineers.

Monte Carlo codes are more flexible than the currently available deterministic code schemes for treating reactor geometries and cross section data. They can be used to treat any reactor type (provided that the cross section preparation scheme is sufficiently accurate). However the validity of the cross section data must be checked. Not all of the available Monte Carlo codes have data libraries which are suitable for fast reactor applications, the reason being that they are not able to treat self-shielding effects in the unresolved energy region. This can be done for example by applying the subgroup approach (as in MMCFK [4.11], which uses group cross section data) or by using continuous energy probability tables (as is done in VIM [4.68], which uses continuous energy data).

The probability table method, implemented in VIM, may be seen as a particular case of the subgroup approach suitable for a "continuous" cross section representation. The main steps to calculate probability tables for VIM are the following: (1) for each spin series of resonances the resonance spacing and width distributions are sampled to obtain a ladder of resonances; (2) pointwise cross sections are reconstructed from the resonance parameters with Doppler broadening to the desired temperature; (3) the average values of the partial cross sections between energy points on the grid are then binned by total cross section value, with weight equal to energy interval; (4) the above steps are repeated until some test parameter is exceeded and the average cross section in each bin is then calculated, and (5) the comprehensive probability distributions thus formed are condensed into library of tables with a small number of bands.

The VIM code was probably the first Monte Carlo code specially tailored to treat continuous energy neutron data in a manner suitable for general fast reactor problems. Mention can also be made of the MOCA Monte Carlo code which has been used for fast reactor control rod calculations and is included in the ERANOS scheme.

One of the most promising directions of development is the combinatorial approach. In this approach, hybrid schemes (Monte Carlo codes coupled with deterministic methods) are used, the Monte Carlo method being applied only for treating sub-regions having complex geometry. Outside, these complex domains simpler and quicker deterministic methods are used. A detailed review of these combined methods is presented in [4.69].

There are many successful ways to increase the efficiency of the Monte Carlo method, in particular by decreasing the dispersion, and these are described in several textbooks. Numerous variance reduction techniques, such as splitting/Russian roulette, weight windows, and the exponential transformation method have been proposed to improve the efficiency of Monte Carlo transport calculations.

Recently the "local exponential transformation method" [4.70] has been developed to approximate the zero-variance solution in source-detector problems. A numerical/deterministic solution to the adjoint diffusion equation is used along with an exponential representation of the adjoint flux in each cell to determine "local" biasing parameters. These parameters are then used to bias the forward Monte Carlo transport calculation in a manner similar to the conventional exponential transform, so that the transformed parameters are local in the space and energy variables. It has been shown that, for source-detector problems, the "local exponential transformation method" usually offers a significant improvement over the conventional geometry splitting/Russian roulette technique with weight windows.

4.4.4. Application of code systems to fast reactor calculations

The traditional way to calculate the physical characteristics of a fast reactor is to carry out the following steps: (1) preparation of the effective cross sections for regions of the reactor; (2) a three-dimensional calculation to obtain k -eff, and real and adjoint fluxes; (3) edit the results of the previous steps to estimate the power and reaction rate distributions, neutron kinetics parameters, control rod effectiveness, etc., and (4) a burnup analysis, calculating the variation of the isotopic composition with time, and then recalculating the results obtained in the previous steps for particular burnup states. This scheme has been implemented, for example, in the TRIGEX code [4.49]. This code calculates k -eff, few group real and adjoint fluxes, power spatial distribution, dose factor and reaction rates distributions, breeding parameters, burnup effects, and kinetics parameters (effective delayed neutron fraction, etc.).

Few group (usually 4 or 6) effective cross sections are prepared using the following scheme: (1) ARAMACO [4.16] calculations of 26-group effective cross sections, using subassembly averaged nuclear densities (for the new version of the cross section preparation system, designated CONSYST, the FFCP [4.18] cell code is also available); (2) condensation of the 26-group effective cross sections to 1-group, 26-group fundamental mode fluxes being used as weighting spectra; (3) 3D diffusion theory one-group calculations to obtain the fission source spatial distribution, one mesh point per hexagonal cell per plane being used; (4) 3D diffusion theory 26-group calculations using the fission source spatial distribution obtained in the previous step (only a few inner iterations); (5) correction of the 26-group removal cross sections (the slowing-down part) using the 26-group spectra, and condensation to few groups; (6) 3D few group coarse mesh calculations of real and adjoint fluxes, one point per hexagon (inner and outer iterations). During this step additional parameters are involved to reduce errors due to the rather coarse mesh used. These parameters are from time to time corrected during the power (outer) iterations; (7) computation of the spatial distribution of power, reaction rates, etc., and (8) evaluation of changes in the isotope composition during the burnup steps, using the CARE code [4.71]. The previous calculations can then be repeated for particular burnup steps. This scheme has proved to be very efficient for calculations of many reactor parameters, using 4 or 6 groups. However, the accuracy of such calculations of reactivity effects must be thoroughly tested. More detailed fast reactor analyses are usually carried out using a group of reactor codes, because the set of parameters to be calculated is in general too large to be provided by a single code. For the accurate treatment of burnup effects and for fuel cycle analyses special post-processing tools have been developed. Codes corresponding to ORIGEN-2 [4.22] use their own data libraries to accurately simulate the production and transformation of a large number of different nuclei. The related fuel cycle and fuel management problems can be handled by means of the REBUS [4.72] and FUMBLE [4.73] codes. The nodal methods require special techniques for 3D perturbation theory

calculations, an example being the recently developed method for reactivity worth calculations [4.50]. Generalised perturbation theory requires the special flux and special adjoint flux distributions to be obtained by solving equations with appropriately defined sources. Transport and Monte Carlo codes are usually used, in addition to diffusion codes, to accurately estimate transport and heterogeneity effects. To carry out diffusion theory, transport theory and

Monte Carlo calculations on a unified cross section data base, so as to have an opportunity to work with different codes in a unified way, several modular code schemes have been developed.

In the 1970s and 80s the following modular code schemes were developed in Western Europe: the French scheme CRR, the German schemes IANUS (Interatom) and KAPROS (Karlsruhe), and the UK scheme COSMOS. As part of the Western European Fast Reactor Project a new reactor physics code scheme has been developed, called ERANOS (European Reactor Analysis Optimised System). The main aim was to provide a very general and modular system of codes for performing standard neutronic design calculations as well as for analysis of experiments in critical facilities. Particular care was devoted to its generality and flexibility. The ERANOS system of codes involves: (1) cross section set generation; (2) solving the diffusion and transport equations in various geometries; (3) perturbation theory modules; (4) burnup calculations in all geometries; (5) shielding calculations, and (6) interpretation of results (Flux maps, traverses, reactivity coefficients, reactions rates, doses). Diffusion theory modules include coarse-mesh and nodal methods (DEGEN, HEXNOD and TGV). Transport theory modules include: the Sn-method (BISTRO); the nodal interface current method, based on a variational formulation of the even-parity transport equation (TGV), and the nodal method based on the approximation of one-dimensional transport equations derived by transverse integration over the spatial and angular variables (HEXNOD).

The development of computer technology has made it possible to create more powerful visualisation systems for input/output data, and new computer architectures can have an influence on the development of algorithms. The efficiency of calculations can be improved if special computers are used with:

- vector processing capability for arithmetic operations,
- special pipelines for fast vector processing,
- enhanced load/store pipelines for indirectly addressed vector elements,
- parallel processing capability for spatially and phenomenologically independent calculational paths.

An example of the implementation of new computer architectures is given in [4.74] and [4.75], where the general purpose Monte Carlo code MCNP-4 has been implemented on the Fujitsu distributed memory highly parallel computer. A dynamic load balancing technique using a control processor assignment technique was adopted. For the problem investigated a high efficiency of calculation was obtained using a system with 512 processor units, the speed attained being 48.7 times faster than a large scale scalar main frame computer.

An example of a fast reactor calculation, made for a reactor with a sodium plenum above the core instead of a breeding blanket, is the international intercomparison Sodium Void Benchmark, [4.20]. The list of cross section data sets and reactor codes, used in the benchmark calculations is given in Table 4.2 (taken from [4.20]).

4.2. CROSS SECTION DATA AND CODES USED IN THE SODIUM VOID BENCHMARK

Participant	Cross section basis	Codes
Germany	26 groups ENDF/B-4 and -5	3D coarse-mesh diffusion DEGEN Monte Carlo MOCA
India	25 groups, IGCAR	2D R-Z diffusion ALCIALMI 3D diffusion 3DB
Japan 1	18 and 7 groups JENDL-2	Tri-z diffusion CITATION 3d transport TRITAC
Japan 2	16 groups	3D coarse-mesh diffusion ICOM 3D Hex-Z transport HEXTR
Russia	26 and 4 groups ABBN	R-Z diffusion codes HEX-Z TRIGEX R-Z nodal transport 3D Monte Carlo MMCCK
United Kingdom	13 group FD-5	3D diffusion and transport MARC/PIN
United States	21 group ENDF/B-5.2	3D nodal and finite difference DIF3D HEX-Z nodal transport VARIANT, continuous Monte Carlo VIM

The main objective of the benchmark was to compare the ability of different codes to compute the sodium void effect in the complicated reactor model that was specially designed to reduce this effect. Concerning the sodium void effect, the main results of the seven contributions are as follows:

- the application of transport theory is necessary when voiding of zones above the core or the control rod follower positions is considered. Diffusion theory fails to predict this effect accurately because of an over-estimation of neutron leakage effects. The negative reactivity effect is overestimated by 0.33% dk/k' or about 1\$.

For the correction for the heterogeneity of the wrapper steel and interstitial sodium three solutions give a negative value of -0.2% to -0.3% dk/k' whereas one solution gives a positive effect of +0.2% dk/k' .

For operational parameters there is very good agreement. The ranges in values, with the exception of the k_{eff} , are smaller than the uncertainties in the prediction of these parameters.

4.5. VALIDATION OF METHODS AND DATA

The measurements available for validation studies comprise simple integral measurements, which can be used to adjust, or select, nuclear data, and mock-up type experiments, more appropriate for assessing the accuracy of methods, and possibly also for deriving bias factors.

The main sources of fast reactor core integral data have been: the Argonne National Laboratory facilities, ZPR-III, VI and IX, and ZPPR, in the USA; ZEBRA (Winfrith) and VERA (Aldermaston) in the UK; MASURCA (Cadache) in France; SNEAK (Karlsruhe) Germany; FCA in JAERI, Japan; and BFS-1 and 2 (Obninsk) in Russia. Of these only MASURCA, FCA and the BFS facilities are currently in use for fast reactor studies. In addition to these, studies on small fast reactor core zones have been made in coupled fast-thermal systems, such as MINERVE (Cadache) in France, PROTEUS at the PSI Institute in Switzerland, SEG/RRR (Dresden) in Germany and STEK (Petten) in the Netherlands. The latter two have been used for small sample reactivity worth measurements on fission product isotopes. The small Los Alamos criticals, such as Godiva and Jezebel, also provide a valuable check on higher energy data for fast reactors. A good range of integral data is to be found in the CSEWG Benchmark Book (ENDF-202) but this is far from complete. Also, in recent years many integral measurements have not been published in sufficient detail to permit their use outside the country (or collaborative project) which carried out the measurements. In addition to the measurements made in critical facilities, irradiations of samples in power reactors provide valuable data on spectrum averaged cross-sections.

The simple integral data are of the following types: (i) values of k_{eff} measured on simple geometry cores; (ii) critical bucklings in the central regions of cores; (iii) central reaction rate ratios (fission ratios and ratios of U-238 capture to U-235 or Pu-239 fission); (iv) central reactivity worth measurements for small samples; (v) k_{eff} values for zones having k_{eff} close to unity, and (vi) neutron spectra measured using different techniques. These are all used in nuclear data adjustment studies.

The more complex mock-up assemblies represent two-zone cores with control rods, or "rod-follower regions" in the core. Fission rate distributions are measured for different configurations of rods. Particularly large cores have been studied in ZPPR, corresponding to commercial sized fast reactors. Studies have also been made of different configurations of sodium voiding and possible fuel melt-down accident configurations.

Shielding studies have been made on a number of facilities such as the ORNL Tower Shielding Facility in the USA, NESTOR in the UK and HARMONIE in France (none of which are currently in use for shielding studies). Again the measurements are of two types, transmission through blocks of single materials (such as iron) and simple combinations (iron and sodium), or mock-up configurations. Again the simple geometry measurements are used for the adjustment of nuclear data. Measurements are made not only of neutron transmission but also gamma ray transmission. Measurements have also been made of gamma energy deposition in core regions.

Intercomparison exercises have been carried out, in particular of reaction rate ratio measurement techniques, a recent example being the IRMA intercomparisons carried out in MASURCA [4.76].

The overall scope of the measurement programmes can be seen by referring to conference proceedings, such as the Physor Conference (1990). In particular this includes a summary of the comprehensive programme of measurements carried out at the start-up of SUPER-PHENIX [4.77]. Also the measurements carried out on the large critical assemblies ZPPR-18/19 at ANL are summarised [4.78]. This includes measurements of the reactivity worths of different configurations of control rods and the associated fission rate distributions. Measurements carried out in the JANUS programme of shielding benchmark experiments are described. This is a step-by-step sequence of measurements on stainless steel, sodium and boron carbide (including different combinations) [4.79]. Reaction rate distribution measurements have also been made through the core and shields of SUPER-PHENIX [4.80]. Gamma energy deposition measurements made in MASURCA are also described [4.81] in the proceedings.

4.5.1. Effective multiplication of a core at start-up

At the initial start-up of a reactor none of the fuel has been irradiated and the reactor fuel loading programme must be planned to move progressively to the equilibrium cycle in which a fraction, N , of the core is replaced at each reloading. At the end of a stage of an equilibrium cycle $1/N$ of the core will be at the maximum average end-of-cycle burn-up, b , $1/N$ at $((N-1)/N).b$ and the average burn-up of the core as a whole at the end of an equilibrium cycle is $((N+1)/2N).b$. At the beginning of the new step in the cycle, when fresh fuel has been loaded into $1/N$ of the core the average burn-up is $((N-1)/2N).b$. The control rod requirements are designed to compensate for the change in reactivity with burn-up, b/N , in each cycle, together with the safety requirements and the control required to take the reactor from the normal shut-down condition to operating power level. The safety requirements include a provision for the failure of some rods to enter the core at shut-down. The method usually adopted to progress from the initial start-up condition to the equilibrium condition is to insert steel diluent assemblies in place of some of the core assemblies, to compensate for the reactivity change associated with the burn-up, $((N-1)/2N).b$. This initial core is therefore more complicated to calculate than the equilibrium core because of the added complexity of these diluent assemblies. The equilibrium core is difficult enough to calculate because it is the fuel enrichment required to provide a critical state at the end of an equilibrium cycle and at normal operating power (and temperatures) which must be predicted. Consequently, the variation of reactivity with burn-up and with power must also be accurately predicted to determine the required fuel enrichment.

Measurements have been made on operating power reactors, such as PHENIX, SUPER-PHENIX and PFR of the variation of reactivity with burn-up and with power level.

Measurements have also been made of the reactivity of the core loadings at initial start-up. In the SUPER-PHENIX start-up configuration measurements good consistency has been found with the results of analyses of measurements made on critical facilities, to within the expected accuracy of predictions of $\pm 0.5\%$ (or 500 pcm). These measurements also provide an accurate reference point for future predictions [4.82]. Measurements have also been made of the effect of replacing fuel subassemblies with steel diluent sub-assemblies. Agreement with calculation is good excepting for substitution experiments in outer regions of the core [4.83].

4.5.2. Variation of reactivity with burn-up

There are two main effects. One is the reduction of the proportion of fissile isotopes in the fuel and the second is the build-up of fission products which capture neutrons. There is also the effect of the breeding of fissile material in blanket regions. Measurements have been made of the spectrum averaged fission and capture cross-sections of actinide isotopes (e.g. the PROFIL irradiations in PHENIX) and also of the reactivity worth of samples having differing plutonium isotopic compositions (and also core zones having plutonium of different isotopic compositions, the PLUTO programme). Capture cross-sections for Pu-240, 241 and 242 are over-estimated by 13%, 24% and 17% respectively, in the calculations based on the JEF-2.2 library, whereas fission cross-sections are better predicted ($\pm 3\%$). The measurements used to validate the fission product nuclear data include small sample reactivity worth measurements made in STEK, and activation measurements made in CFRMF, ERMINE (the ZONA 1 and ZONA 3 programmes) and PHENIX [4.84]. The measurements have been made for 40 fission products which contribute about 80% of the total reactivity effect. Measurements made on PHENIX fuel pins have been used to develop a model for the time dependent release of gaseous and volatile fission products. This reduces the fission product reactivity effect typically by about 5% and the accuracy of the calculation of this reduction is estimated to be $\pm 20\%$ (1s).

Concerning the nuclear data in the JEF-2.2 library, a general conclusion was that the inelastic scattering cross-sections for many even mass nuclides were about a factor of 2 low because of the neglect of direct interaction effects in the nuclear models used to calculate these cross-sections. The contribution of inelastic scattering is of the order of 15% of the total fission product reactivity effect. The most important even mass nuclei are Mo-98, - 100, Ru-102, - 104, - 106, Pd-106, - 108, Xe-132, - 134, Nd-146, - 148 and Sm-152. Improved theoretical models have now been developed and validated by direct measurements of the differential cross-sections of Pd isotopes. As a consequence of the analyses of the integral measurements, it has been concluded that the contribution of fission products to the variation of reactivity with burn-up can be predicted to within $\pm 5\%$ (1s) for a conventional fast reactor.

4.5.3. Incineration of fission products

Feasibility studies on the incineration of actinide isotopes and fission products are being made in several countries. In the case of fission products attention has been focused on the incineration of Tc-99 and I-129. Following neutron capture both nuclides decay rapidly to the stable isotopes, Ru-100 and Xe-130. One method being considered is the use of special moderating assemblies located in the breeder regions of fast reactors. (This technique has been used successfully in PHENIX for the production of Co-60 from Co-59). An irradiation test has been carried out in the Fast Flux Test Facility. The percentage of transmutations in a 10.5 equivalent full power days irradiation were about 0.7% for Tc-99 and 0.4% for I-129. The

agreement between the measured and calculated values is about 15%. One can foresee transmutation rates of about 10% per year being achieved in this way.

4.5.4. Power distributions

The predominant source of power in a reactor is the fission reaction. Most of the energy of fission (which is about 200 MeV in total) is the kinetic energy of recoil of the fission fragments which appears as heat within the fuel. Some of the energy is in the form of kinetic energy of the emitted neutrons, the mean energy of each prompt fission neutron being about 2 MeV, making a total of about 6 MeV for Pu-239. This is deposited as nuclear recoil energy in scattering interactions and in reactions over a wide volume of the reactor. There is also the emission of γ -rays in fission, both prompt emission and the delayed emission in the β -decay of fission product nuclei, about 15 MeV in total. The gamma ray energy is also deposited over a wide region. The heat generation in structural materials is primarily by γ -energy deposition, with neutron scattering also making a contribution. For the prediction of energy distributions the most important requirement is the accurate prediction of fission rate distributions. These are usually well predicted in uniform cores, the problems arise when there are control rods either partly or fully inserted into the core. There can also be discrepancies in the interface regions between different zones, such as core-blanket interfaces, particularly when diffusion theory is used. As an illustration of the types of measurement which have been made and the results obtained, we summarise the measurements made in the ZEBRA core BZB and in ZPPR.

The Pu-239 fission rate distribution was measured for eight different control rod configurations using the multi-chamber scanning system in ZEBRA Assembly BZB [4.85]. The control rod positions were: the centre of the core, an inner ring of six and an outer ring of 12 near to the inner core-outer core boundary. Each control rod array studied had a combined reactivity worth of about 4% dk. All the arrays were symmetrical apart from Array 5, which had one rod fully inserted in the outer ring, the remaining outer ring rods being $\frac{1}{4}$ inserted. The other arrays included two with symmetrical patterns of rods fully inserted, Array 3 with the inner ring of six inserted and Array 8 with 9 of the outer ring of 12 inserted. In the other arrays there were different degrees of insertion in the inner and outer rings and the central position. There were changes in both the axial and radial fission rate distributions of up to about 30%. The fission rate distributions were analysed using XYZ geometry diffusion theory. For the values averaged over radial and axial regions it is found that, relative to Array 1, the mean deviations for each region are less than $\pm 0.5\%$ and the variations about the mean are less than $\pm 1\%$.

An extensive series of reaction rate distribution measurements has been made in the ZPPR Assemblies. They include Pu-239, U-235 and U-238 fission together with U-238 capture. Detailed analyses have been made for the 600 litre assemblies 10D (rods withdrawn) and 10D/2 (rods inserted) [4.86]. These cores have an approximate diameter of 2.8 m. The analyses were made using XYZ geometry diffusion theory with S_4 transport theory corrections. As was also found for the ZPPR-9 cores the calculations consistently over predict the Pu-239 and U-235 fission rates and U-238 capture rates in the outer core relative to the core centre by 2 to 3%. The overall effects of the control rods on reaction rate distributions were well predicted. However, the mispredictions of the reactivity worths of sodium filled control rod channels by diffusion theory have a significant effect on the power distributions in these large cores. Exploratory calculations made using axial buckling adjustment factors to account for axial transport effects in the sodium filled channels gave reaction rate corrections

of up to 2% in ZPPR-10D. Diffusion theory calculations also gave discrepant results within breeder regions close to the core-breeder boundary. It can be concluded from these analyses that a refined treatment of control rods and control rod follower regions (CRFs) is required for the calculation of reactor core reaction rate distributions. Diffusion theory calculations can then reproduce reaction rate distributions for the reactor core to accuracies of about $\pm 1\%$ relative to a reference configuration (for example a core with rods withdrawn). However, there can be discrepancies in the ratio of the average outer core to inner core reaction rates. These might be associated with nuclear data deficiencies or with the use of diffusion theory. Close to control rods diffusion theory overestimates Pu-239 and U-235 fission rates by about 1% (which is about a 10% error in the local flux dip into the rod).

4.5.5. Control rod reactivity worths

In the critical balance method, criticality (or reactor power) is maintained when the rod or group of rods is inserted by making one of the following changes:

- (1) moving calibrated or reference control rods. This method is usually only used to measure reactivity worths of single rods or small movements of a group of rods. The reference rods can be calibrated in terms of the delayed neutron fraction or the calculated effect of a compensating fissile material addition to the core;
- (2) increasing the radius of the core by adding extra fuel elements at the core edge. The reactivity worth is then related to the calculated effect of edge element addition. Consistency is checked by interchanging the added edge elements and comparing measurement and calculation for the different arrangements;
- (3) changing the fissile material content of a region of the core. The reactivity scale is then the calculated effect of the fissile material addition. This is an appropriate reactivity scale because one of the functions of the regulating rods is to compensate for the loss of fissile material in fuel burn-up, and
- (4) comparing the reactivity worths of different arrays which are calculated to have about the same reactivity worth, with a balance of type (1), (2) or (3).

The different reactivity scales can be interrelated in separate experiments (for example by measuring edge element worths in terms of calibrated rods, or distributed fissile material). It is necessary to recalibrate rods when the size of the core is changed or experimental rods are added.

The principal method used to measure subcriticality is the source multiplication technique. The ratio of the total flux to the source is approximately inversely proportional to the subcritical reactivity. Flux calculations must be made to obtain the flux at the counter positions because of the changes in the flux shape caused by insertion of the rods and the effect of the position of the source on the flux distribution. Normalisation of the reactivity scale involves a reference subcritical condition, such as that produced by inserting a calibrated control rod.

Measurements of subcriticality relative to the effective delayed neutron fraction can be made by calibrating a reference fine control rod by means of asymptotic period measurements following rod withdrawal, or by inverse kinetics analysis of the reactor power response following rod drop or rod withdrawal (fitting the response using the delayed neutron kinetics equations). There are uncertainties in total delayed neutron yields and in the time dependence of delayed neutron emission, the accuracy of this reactivity scale being estimated to be $\pm 5\%$.

There are a number of techniques for measuring subcritical reactivity relative to a calibrated reference control rod, in addition to source multiplication. These include rod drop, rod jerk, source jerk, pulsed source and reactor power noise. Account must be taken of spatial flux transients (either by calculating them or measuring them with arrays of counters) and of the spatial distribution of natural neutron sources due to spontaneous fission and (a,n) reactions and any fixed sources introduced to increase the subcritical flux level. The different methods have been reviewed and intercompared, for example, at the 1976 Specialists Meeting [4.87].

The units used to denote reactivity include the following:

- (1) the effective multiplication k -effective or k (sometimes in units of 10^{-2} dk (or mils) or 10^5 dk (or milliniles which is also denoted by mN, and by pcm, percent mille);
- (2) reactivity $\rho = 1 - 1/k$, and reactivity change, $\delta\rho = -\delta k/k^2$;
- (3) reactivity in units of the effective delayed neutron fraction, β_{eff} , also called the dollar, \$: 1% of this is called the cent, and
- (4) the inhour. This is the period of the asymptotic exponential time dependence of reactor power (resulting from the reactivity addition when the reactor is at delayed critical). It is related to the effective delayed neutron fraction. The equivalence is usually obtained experimentally with a reactivity addition which results in an asymptotic period of about 100 sec.

Results of control rod reactivity worth measurements. Extensive programmes of measurements have been carried out in all the fast critical facilities and also in SUPER-PHENIX during the start-up experimental programme. As an illustration of the accuracy of current methods and data we can refer to the results of the SUPER-PHENIX experimental analyses. (These were made by 4 different groups, France/Italy, Germany (KfK and Interatom) and the UK using different methods and data). The calculations were made for 4 experimental configurations and the largest deviation in C/E values was 11%. Interatom used a Monte-Carlo code, MOCA, and obtained a particularly good agreement. In the analyses of the measurements made for the large ZPPR assemblies 18A and 19B (using ENDF/B-V data and nodal transport methods), the values of (C/E) for the 5 different configurations studied in each core were within $\pm 6\%$ of unity.

4.6 REACTIVITY COEFFICIENTS

A knowledge of temperature and power coefficients of reactivity is required to determine the control rod reactivity required to raise a reactor to power and to study the response of the reactor to malfunctions. The coefficients are of two types, those due to thermal expansion effects and those arising from Doppler broadening of resonances. A uniform expansion of a reactor core results in an increase in the leakage fraction and a reduction in reactivity. However, different materials have different coefficients of expansion and so account must be taken of the relative changes in material densities, for example, the changes in the atomic fractions of coolant and structural materials relative to the atomic fraction of fuel. The expansion of the fuel can be affected by the expansion of the fuel cladding, with radial expansion of the fuel changing only the fuel-clad gas gap and the axial expansion being linked to the clad temperature. Axial expansion of the core, and expansion of control rod structures can result in movements of control rod absorber sections relative to the core and consequently an increased control rod insertion.

The temperature gradients across subassemblies result in bowing of the assemblies. The way they bow depends on the points in contact between them. In some arrangements an increase in temperature results in an increased inward bow and hence an increase in reactivity, a condition to be avoided. The subassembly lower support structure is at the temperature of the coolant inlet flow, whereas the temperatures vary axially through the core depending on the power and the flow rate. Bowing can result from radial variations of temperature. Bowing of subassemblies also results from irradiation induced swelling, the flux on one side of a subassembly being higher than on the other. However, this is a slowly varying effect. It can result in changes to the way subassemblies are in contact and hence to the way they bow in a temperature transient, however.

Coolant voiding is another effect which must be investigated. A subassembly might become voided as a consequence of a blockage and the vaporisation of the coolant above the blockage. In a severe accident, the temperature could rise to a point at which the coolant throughout the reactor is vaporised. Sodium voiding studies have been made in many critical facilities, for different axial sections of single sub-assemblies or groups of sub-assemblies at different radial positions and also for whole cores. Accident configurations which could result from the partial meltdown of a region of a core have also been simulated in critical facilities. The

calculation of the effects of voids in the core presented a problem in the past but now, with 3D transport theory codes being available, it is less of a problem.

4.6.1. Doppler effects

The Doppler effect provides a fast-acting negative reactivity feedback to fission power increases and other effects which increase fuel temperatures. The effect arises predominantly from the increase in capture in U-238 resonances. Smaller contributions arise from the resonances in plutonium isotopes and also from the narrow p-wave resonances in the cross-sections of the structural material elements (e.g. the 1.15 keV resonance in Fe-56). Because the effect arise mainly from low energy resonances (below about 10 keV) the magnitude depends on the fraction of the neutron reactions occurring at these energies. The effect is only about half as large in a reactor core from which the sodium has been voided. Local effects depend on the local neutron spectrum. A number of approximations are made in the usual calculation methods: (a) the large variation in temperature across a fuel pin is usually replaced by the average temperature across the pin; (b) the heterogeneity of the fuel pin and subassembly structure is often treated as homogeneous, and (c) the Doppler effects in different axial and radial regions of a reactor are treated as dependent only on the local average fuel temperature. Uncertainties in predictions of Doppler effects can be separated into two components: the uncertainty in prediction of fuel temperatures and the uncertainty in the change of Doppler reactivity with temperature. The uncertainty in the fuel temperature, arising from uncertainties in the clad-fuel gas gap conductivity and the fuel conductivity must therefore be considered. Separation of the uranium and plutonium in granular fuel could also have an effect as could the radial migration of plutonium within the fuel caused by the high temperature gradient (although studies show this latter effect to be negligibly small). Although the uncertainty in prediction of Doppler effects could be assessed in terms of uncertainties in knowledge of resonance structure and the fraction of the reactions occurring in the resonance region it is more usual to base the assessment on a comparison of calculations of Doppler reactivity feedback with measured values. However, because it is necessary to extrapolate to much higher temperatures than those for which measurements have been made some consideration must be given to the accuracy of the basic data and calculation methods.

The approximation is sometimes made that the Doppler coefficient has a $1/T$ dependence on temperature. The actual variation with temperature depends on the shape of the neutron spectrum through the resonance region and on the balance between the contributions from fertile and fissile isotopes. At low temperatures chemical binding effects can become important. These are usually taken into account by using an equivalent temperature (instead of the actual temperature) in the gas model Maxwellian velocity distribution. The equivalent temperature is usually expressed in terms of a Debye temperature which characterises the lattice vibrational motion of the U, Pu isotopes in the solid. This can be different from the Debye temperature for the solid as a whole. Values of the Debye temperature for UO_2 used in the analysis of experiments range from about 250°K to 650°K and this difference affects the conclusions drawn from Doppler coefficient measurements made from ambient temperature to a temperature a few hundred degrees higher. The accuracy of Doppler effect predictions has been assessed by analysing the SEFOR Doppler experiments [4.88]. In addition an analysis can be made of structural material Doppler effect measurements made in the Japanese critical facility, FCA [4.89]. Small sample reactivity worth measurements as a function of sample temperature have now been made for U-238 to about 2000 K [4.90]. Measurements of neutron spectra and the use of spectral index measurements made with detectors sensitive to resonances in the Doppler effect energy range are also valuable. As well as the uncertainties in Doppler effect predictions, account must be taken of the variation of the effect through the fuel cycle, firstly as the reactor is brought to the equilibrium cycle condition and then from fuel loading to discharge, as control rod absorption is replaced by fission product absorption and the reduction in fissile material worth. The build-up of fissile material in breeder regions and the consequent increase in temperature has an effect. Changes in the isotopic composition of the fuel, both of the feed fuel (when different sources are used) and the variation with burn-up, must also be allowed for.

In U-238 the Doppler effect arises mainly from the s-wave resonances. Uncertainties in the subdivision of the capture cross-section into s-wave and p-wave resonances (or between large and small resonances) are carried over almost directly into uncertainties in the Doppler effect. Less than 10% of the U-238 Doppler effect comes from energies above 10 keV, resolved resonance parameter data now being available up to this energy. It makes very little difference to the Doppler effect calculated for a power reactor whether the Debye temperature is 250°K or 650°K. At temperatures above the Debye temperature, q_D , the equivalent temperature T^* is close to the actual temperature, being less than about 5% different. However, for the analysis of experiments in the range 300°K to 1000°K this difference is significant. Analyses of cross-section shapes are more consistent with the lower value but some analyses of reactor Doppler effect experiments are more consistent with the higher value.

The temperature distribution radially across a fuel pin is approximately linear in terms of the volume of annular regions. It departs from a linear variation because of the dependence of thermal conductivity on temperature and when there is a central hole in the pin. For a fast reactor spectrum the effective temperature is estimated to be close to the average [4.91].

In a transient the temperature of the fuel depends on the specific heat, which is temperature dependent. Fuel melting at the centre of the pin can change the temperature distribution and these effects must be taken into account in calculations of Doppler reactivity feedback. Gas gap conductivity is another source of uncertainty in the calculation of effective fuel temperature. The temperature change across the fuel-clad gas gap is about 25% of the

difference between the mean fuel temperature and the inner clad surface temperature, a 10% uncertainty in gas gap conductivity resulting in a 1.3% uncertainty in mean fuel temperature.

A study of the effect of heterogeneity is described in ref. [4.92] which presents a general review. The effect can be separated into two components, the fuel pin heterogeneity effect and the subassembly wrapper effect. Compared with the homogenised model both effects are found to increase the Doppler constant by 2.5% giving a total increase of 5%.

Experimental Validation. The following types of measurement have been used to evaluate the accuracy of Doppler effect calculations: (a) the South-west Experimental Fast Oxide Reactor (SEFOR) was built and operated specifically to measure Doppler effects (or fast-acting fuel reactivity feedback effects with expansion effects minimised); (b) the dependence of reactivity on temperature in operating power reactors, such as PHENIX and SUPER-PHENIX (from the non-linearity of the temperature coefficient, for example); (c) the ZEBRA 5 Doppler Loop experiments, in which a test zone was heated. Experiments were performed with and without sodium present; (d) the temperature dependence of the reactivity worths of small samples oscillated at the centre of critical assemblies; (e) the differences in reaction rates in samples irradiated at different temperatures; and (f) temperature dependent thick sample transmission and self-indication measurements, which are usually analysed together with the differential nuclear data to provide average resonance parameter data. The uncertainties in extrapolating from these comparisons to the conditions in an operating power reactor must also be taken into account.

SEFOR Doppler effect measurements. Two versions of the SEFOR core were built, SEFOR-1 and SEFOR-2. Both were sodium cooled and used 20% enriched PuO_2/UO_2 fuel but SEFOR-1 contained a number of beryllium oxide rods to soften the spectrum, whereas, in SEFOR-2 these were replaced by stainless steel rods. The fuel pins were of large diameter so that a high mean fuel temperature could be achieved at low power. The experiments were of two types, static and transient. The first analyses were made by General Electric and by Karlsruhe. An improved analysis was later made by HEDL and this included a correction for chemical binding effects (assuming a high Debye temperature). The correction is small, however, about 1.5% in the case of the SEFOR measurements. The choice of delayed neutron data affects the results. The agreement between measurement and calculation is within the uncertainties (1s) for all of the analyses, including a recent one using JEF-2.2 data. Extrapolating these results to the spectra and fuel compositions of a conventional power fast reactor results in an increase in the uncertainties to $\pm 15\%$. The additional uncertainties associated with burnup effects, for the target burnup considered (10% maximum), do not increase this uncertainty estimate, but for extrapolations to low and high temperatures the uncertainties are increased to $\pm 18\%$.

Small sample Doppler Experiments and the steel Doppler effect. Small sample Doppler measurements have been made in several critical facilities, including the ANL ZPR and ZPPR facilities, SNEAK and FCA [93]. Measurements made for U-238 samples in ZPPR have been analysed using ENDF/B-IV data giving C/E values in the range 0.85 to 0.90. Measurements made in SNEAK and analysed using KFKINR data give C/E values of about 0.89. These two data sets give similar values for the Doppler constants in the SEFOR cores. Measurements of the Doppler effect of iron samples have been made in FCA Assemblies V-2 (a mock-up of JOYO) and VI-2 (a mock-up of MONJU). The samples were heated from room temperature to 823°K and 1073°K.

Measurements on operating power reactors. Measurements have been made on operating power reactors of the reactivity response to changes in temperature, power and flow. There are problems in deriving the Doppler effect, which is only one component of the reactivity change. However, for some purposes it is unnecessary to separate out the Doppler component. The reactivity change on going from the normal shut-down temperature to full power operation can be measured directly (in terms of the compensating control rod movements) and the response to transient reactivity, power or inlet coolant temperature changes can be measured. A separation of the components is required to enable deductions to be made about the response in transients for which measurements cannot be made, or to extrapolate to different fuel types and reactor designs. However, this separation need not necessarily be made into Doppler effect and expansion effects. Separation into a fuel power coefficient (together with its temperature dependence) and other coefficients could be sufficient, and possibly even more useful because of uncertainties in temperature response and fuel plus cladding expansion effects and their interactions. It would be valuable if a reassessment could be made of the parameters which are required for the different applications, together with the component break-down required to extrapolate to different designs of fuel and reactor core.

Doppler effect measurements have been made in PHENIX [4.94] and SUPER-PHENIX [4.95]. The measurements were of the isothermal temperature changes at very low power. The Doppler effect is identified with the non-linear component of the temperature coefficient assuming a dependence of the form b/T for the Doppler effect. The uncertainties in the analysis of the measurements arise from uncertainties in control rod reactivity worth and rod worth profile and from the statistical analysis of the data. It is concluded that the maximum uncertainty is $\pm 15\%$ and the probable error $\pm 10\%$. A more recent analysis is presented in [4.96].

4.6.2 Sodium Voiding and Sodium Density Coefficients

The reactivity effects of voiding the sodium coolant from regions of a reactor core, and the effects of sodium density changes resulting from changes in temperature can be considered in terms of two components, the central term (moderation plus capture) and the leakage term (capture being a small effect). A reduction in sodium density results in an increase in leakage, a negative reactivity effect. The reduction in moderation which results from the density reduction has an effect which depends on the energy dependence of the neutron importance. In a conventional plutonium/uranium fuelled fast reactor the reduction results in an increase in reactivity. The effect is a balance between high energy and low energy effects. The reduction in the inelastic scattering contributed by sodium results in an increase in U-238 fission (at MeV energies) - a positive reactivity effect. At intermediate energies (above about 10 keV), the effect is also positive because of the increase in Pu-239 alpha and the ratio of U-238 capture to Pu-239 fission as one goes towards lower energies. However, below about 10 keV Pu-239 alpha is approximately constant and the fission cross-section increases more rapidly than the resonance shielded U-238 capture cross-section. The effect of the reduction in moderation is negative at these lower energies. The net moderation effect depends on the plutonium enrichment of the fuel but is normally positive. For U-235 fuelled systems the net effect is normally negative, however. The balance of the moderation (or central) and leakage terms depends on the region of the core voided (or having the density reduced). In central regions the effect is predominantly due to the moderation term and even for the core as a whole, for a reactor of the size of SUPER-PHENIX, the net effect is positive. The largest

positive void effect can be of the order of 10 \$, when a large central region of the core is voided. Because of this many studies have been made of heterogeneous core designs with a reduced voiding reactivity effect.

Many experimental programmes have been carried out in critical assemblies to validate the methods and data used to calculate sodium voiding effects. The usual method of analysis is to derive bias factors and the associated uncertainties to be applied to the central term and the leakage term. Typical accuracies obtained are $\pm 5\%$ for each term [4.97].

The method of calculation is complicated by the need to treat heterogeneity effects and, in particular, the streaming in voided regions. In the experiments performed in plate geometry the voiding is achieved by replacing the sodium filled plates by empty cans. The streaming effects in these are significant. Experiments have also been performed in pin geometry assemblies (or mini-calandria) but even in this case the streaming effect must be treated.

4.7 SHIELDING STUDIES

As an illustration of the studies we consider the Iron Benchmark experiment performed in the ASPIS facility on the NESTOR reactor at Winfrith [4.98] (a water cooled, graphite moderated MTR reactor operating at power levels up to 30 kW). Now shut down, the reactor provided a source of neutrons in a central channel and also in the graphite reflector surrounding the reactor tank. Adjacent to the reflector were the four experimental caves, in one of which was the ASPIS shielding facility. A fission plate, containing 93% enriched uranium in the form of a uranium-aluminium alloy, provided the source of fission neutrons. This source could be modified by a suitable choice of moderating materials. The thermal neutrons from the graphite reflector cause fissions in the fission plate. The shielding configuration being studied was placed adjacent to the fission plate source configuration and the reaction rate distributions through the shielding configuration were measured. The usual reaction rates chosen for this purpose were $S\text{-}32(n,p)P\text{-}32$; $I\text{-}115(n,n')In\text{-}115m$; $Rh\text{-}103(n,n')Rh\text{-}103m$ and $Au\text{-}197(n,\gamma)Au\text{-}198$ (with and without a cadmium cover), the resulting activation being measured.

The experiments were analysed using the MCBEND Monte Carlo code with its 8220 energy group library. Analyses have also been made using MCNP. The MCBEND code has associated with it the DUCKPOND module which can be used to calculate the sensitivities of the measured quantities to cross-sections changes. These methods of calculation are reference methods. For more routine use multigroup methods are used. Coupled neutron-gamma group data sets are used in S_n computer codes to calculate the properties of interest. A widely used set has the neutron cross-section data in the VITAMIN-J group structure [4.99].

REFERENCES

- [4.1] Rose, P.F and Dunford, C.L. (Eds) ENDF 102 Data Formats and Procedures for the Evaluated Nuclear Data File ENDF-6 - BNL-NCS-44945 (1990).
- [4.2] MacFarlane, R.E., Boicourt, R.M., Njoy: A Neutron and Photon Cross Section Processing System, Trans. Amer. Nucl. Soc. (1975) v.22, p.720.
- [4.3] Sinitsa, V.V., Rineiskij, A.A., Grucon - A Package of Applied Computer Programs. System Input and Operating Procedures of Functional Modules., translated by A. Lorenz for the IAEA, INDC (CCP)-334, Vienna, Austria (1993).
- [4.4] Trubey, D.K., Hendrickson, H.R., "A Review of Multigroup Nuclear Cross -section Processing", Proc. Seminar-Workshop, Oak Ridge, TN, (14-16 March, 1978).
- [4.5] Henrison, II, H., Toppel, B.J., Sternberg, C.G., ETOE-2/MC -2/SDX, Multigroup Neutron Cross Section Processing System. -In Proc. Seminar on Nuclear Data Processing Codes, Ispra, Italy (1973).
- [4.6] Ribon, P., Maillard, J.M., Probability Tables and Gauss Quadrature: Application to Neutron Cross Sections in the Unresolved Energy Range. ANS Top. Mtg on Advances in Reactor Physics and Safety, SARATOGA SPRINGS, September, 1986.
- [4.7] Abagian et al. Group Constants for Reactor and Shielding Calculations, Energizdat, Moscow, Russia (1981).
- [4.8] Bazazyanz, N.O., et al. The ARAMACO-F system for neutronic data processing for Reactor and Shield Calculations, Moscow, IAM, (1976).
- [4.9] Gromov, B.F., et al. Heavy Coolant Fast Neutron Reactor BRUS-150 for Minor Actinides Burning and U-233 Build-up, Proc. Int. Conf. on Reactor Physics and Reactor Computations, Tel-Aviv, Israel (1994).
- [4.10] Bezborodov, A., The FFPC code, IPPE, Obninsk, Russia (1989).
- [4.11] Kazakova, L.V., et al. Proceeding of the All-Union Meeting on Monte Carlo Methods, Novosibirsk (1985).
- [4.12] Bednyakov, S. et al. Investigation of Neutron Characteristics of Minor Actinides in Experiments at the BFS Facility and Fast Reactors. Proc. of Int. Conf. on Reactor Physics and Reactor Computations, Tel-Aviv, Israel (1994).
- [4.13] JAERI Fast Reactor Group Constants System, JAERI-1995-70.
- [4.14] Ono, S., Wachi, E., Takeda, I., Sekita, T., Casup: Cell Calculation Code for Fast Reactor Analysis, Technology Reports of Osaka University, Vol.33, No.17088, p.207-209, 1983.
- [4.15] Tacite, T., Kitada, T., Ikeda, H., High-Precision Computational Methods for Fast Reactor Cores. Proc. of the Joint International Conf. on Mathematical Methods and Supercomputing in Nuclear Applications, April 1993, Karlsruhe, Vol.1, p.730.
- [4.16] Chaudat, J.P., et al. Data Adjustment for Fast Reactor Design, Trans. Am. Nucl. Soc. 27 (1977), p.877.
- [4.17] Kiefhaber, E., (Comp.) The KFKINR - Set of Group Constants, Nuclear Data Basis and First Results of its Application to the Recalculation of Fast Zero-Power Reactors, Karlsruhe, 1972.
- [4.18] Rowlands, J.L. et al., Production and Performance of the Adjusted Cross-Section Set FLG5, Proc. Int. Symp. on Fast Reactor Physics - p. 1133 - Tokyo (1973).
- [4.19] Grimstone, M.J., Tullet, J.D., Rimpault, G., Accurate Treatment of Fast Reactor Fuel Assembly Heterogeneity with the ECCO Cell Code. International Conference on the Physics of Reactors: Operation Design and Computation, PHYSOR 90, April 23-27, 1990.
- [4.20] Evolution of Benchmark Calculations on Fast Reactor Core With Near Zero Sodium Void Effect, IAEA-TECDOC-731, January, 1994.

- [4.21] Manturov, et al. Requirements on the Accuracies of Calculation of Neutron Physics Reactor Characteristics in Fast Breeder Reactors and Ways to Meet Them, *Sov. Atom. Energ.*, Vol.67(3), p. 181 (1989).
- [4.22] Groff, A.G. ORIGEN2 - A Revised and Updated Version of the Oak Ridge Isotope Generation and Depletion Code, ORNL-5624, 1980.
- [4.23] Katakura J. and Iijima S., Analysis of Uncertainties in Summation Calculations of Decay Heat Using JNDC FP, *Nuclear Data Library. Jour. Nucl. Sci + Tech.* 29, p. 11 (1992). Also: Rebah J. et al., Sensitivity and Uncertainty Analysis for Fission Product Decay Heat Calculations, *Proc. Int. Conf. on Radiation Shielding* p. 63, Arlington, USA (1994).
- [4.24] Tachibana, T. et al., *Prog. Theor. Phys.*, 84 p. 641 (1990).
- [4.25] Klapdor, H.V. and Metzinger, J., Predictions of the Decay Heat of Nuclear Reactors by Microscopic Beta Decay Calculations., *Proc. Int. Conf. on Nuclear Data for Science and Technology - Mito, Japan* (1988).
- [4.26] Tobias, A., Decay Heat, *Prog. Nucl. Energy* 5, p. 1 (1980).
- [4.27] Tasaka, K. et al., Recommendation on Decay Heat Power in Nuclear Reactors. *Jour. Nucl. Sc. + Tech.* 28, p. 1134 (1991).
- [4.28] American Nuclear Society Standards Committee. American National Standard for Decay Heat Power in Light Water Reactors, *ANS - 5-1* (1994).
- [4.29] Kuesters, H., *KfK 2917* (1980).
- [4.30] D'angelo, A. et al., Calculation and Experiment Comparison for Sample and Fuel Pin Irradiation Experiments in PHENIX, *Proc. Topical Mtg. on Reactor Physics and Safety, Saratoga Springs, USA* (1986).
- [4.31] Norgett, M.J. et al., *IAEA Meeting on Radiation Damage Units - Seattle, USA* (1972).
- [4.32] Doran, D.G. and Graves, N.J., *HEDL-TME 76-70 (UC-79 b,d)* (1976).
- [4.33] Gryntakis, E., *Jour. Radioanalytical Chem.* - 52, 219 (1979).
- [4.34] Szondi, E.J. et al., The cross-section library IRDF-90/NMF-G and its User-friendly Processing for Practical Applications. *Proc. Int. Conf. on Nuclear Data for Science and Technology, Gatlinburg, USA* (1994).
- [4.35] Rowlands, J.L., Physics of Fast Reactor Control Rods. *Prog. Nucl. Energy* 16, 3, p. 287 (1985).
- [4.36] Takeda, T, Sato, H and Ono, S, *Ann. Nucl, Energy*, 9, 509, (1982).
- [4.37] Palmiotti, G., A Method to obtain New Cross-Sections Transport-equivalent *Proc. Int. Mtg. on the Methods for Reactor Physics Calculations for Control Rods in Fast Reactors, Winfrith* (1988).
- [4.38] Finite Element Methods - Special issue of *Prog. Nucl. Energy*, Vol. 18 - No. 1/2 (1986).
- [4.39] Briesmeister, J.F. (Ed.), A General Monte Carlo Code for Neutron and Photon Transport, Los Alamos Report LA-7396-M - Rev. 2 (1986).
- [4.40] Gandini, A. (A series of reports on Perturbation Theory, issued by CNEN, Casaccia, Rome, Italy) *RT/FI(75)* (1975).
- [4.41] *Proc. NEACRP Specialists Mtg. on Application of Critical Experiments and Operating Data to Core Design via Formal Methods of Cross-Sections Data Adjustment, JACKSON-HOLE* (1988) - NEACRP-L-307.
- [4.42] Stacey, W.M.Jr, *Space-time Nuclear Reactor Kinetics*, ACADEMIC PRESS, Inc. New York (1969).
- [4.43] Frolich, R., A theoretical foundation for coarse mesh variational techniques, *Proc. Int. Conf. on Utilization of Research Reactors and Reactor Mathematics and Computation (Mexico, 1967)*, CMN-R-2 (1967) 219-237.

- [4.44] Dorning, J., Modern coarse mesh methods - a development of the 70's. Computational Methods of Nuclear Engineering, Proc. Conf., Williamsburg, 1979, American Nuclear Society, CONF-790402 (1979).
- [4.45] Lawrence, R.D., Dorning, J.J., A Nodal Green's Function Method for Multidimensional Neutron Calculations, Nucl. Sci. Eng. 76 (1980) 218.
- [4.46] Alcouffe, R.E., The Multigrid Method for Solving the Two-Dimensional Diffusion Equation, "Proc. Top. Meeting on Advances in Reactor Computations, Amer. Nucl. Soc., Salt Lake City, March 28-31, 1983.
- [4.47] Alcouffe, R.E., "Diffusion Synthetic Acceleration Methods for the Diamond-differenced Discrete-ordinates Equations", Nucl. Sci. Eng., 64, 344 (1977).
- [4.48] Alcouffe, R.E., et al. User's guide for TWODANT: A code package for two-dimensional, diffusion-accelerated, neutron-particle, transport, LA-10049-M, LANL.
- [4.49] Seregin, A.S., Annotation of the TRIGEX code for few group neutron physics reactor calculations in three-dimensional geometry, VANT, Series "Physics and Technology of Nuclear Reactors", Issue 4 (33), 1983, P.59.
- [4.50] Lucas et al. User's Manual for DEGEN. LANL, 1988.
- [4.51] Fowler, T.B., Vondy, D.R., and Cunningham, G.W., Nuclear Reactor Core Analysis Code: CITATION. Rep. ORNL/TM - 2496, ORNL, 1969.
- [4.52] Stehle, B., D3D und D3E Zweige eines FORTRAN-Programms zur Lösung der stationären dreidimensionalen Multigruppendiffusionsgleichungen in Rechteck-, Zylinder- und Dreieckgeometrie KfK, 1991.
- [4.53] Derstine, K.L., "DIF3D: A Code to Solve One-Two- and -Three-dimensional Finite Difference Diffusion Theory Problems" ANL-82-64 Argonne National Laboratory, April, 1984.
- [4.54] Wagner, M.R., Three-dimensional Nodal Diffusion and Transport Theory Methods for Hexagonal - Z Geometry, Proc. Conf. Jackson Hole, Wyoming, USA 28-30 Sept., 1988.
- [4.55] Wehmann, U.K., Chebeskov, A.N., Evaluation of Benchmark Calculations on a Fast Reactor Core with Near-zero Sodium Void Effect, Proc. of Int. Top. Mtg. Obninsk, Russia, October 3-7, 1994, Vol.1, p.35.
- [4.56] Fletcher, I.K., Users Guide to the MARC and PN, Computer Codes, UKAEA Report 1976.
- [4.57] Palmiotti, G., "Optimized Two-dimension Sn-transport (BISTRO)", Proc. Int. Top. Mtg. Advances in Reactor Physics. Mathematics and Computation, Paris, France, April 27-30, 1987.
- [4.58] Bando, M., et al. Three-dimensional Transport Calculation Method for Eigenvalue Problems Using Diffusion Synthetic Acceleration, Nucl. Sci. Tech., 22, 10 (1985), p.814-850.
- [4.59] Sooslov, I.R., Method of Characteristics in Fast Reactor Control Rod Calculations., Proc. IAEA Specialists Meeting, Winfrith, United Kingdom 6-8 December, 1988, IWGFR/69.
- [4.60] Miller, W.S., Lewis, E.E., Computational Methods of Neutron Transport Theory, Wiley, New York, USA (1984).
- [4.61] Dilbert, I., Lewis, E.E., Variational Nodal Methods for Neutron Transport, Nucl. Sci. Eng. 91. 132, 1985.
- [4.62] Chao, Y.A., Tsoulfanidis, N., Application of Conformal Mapping to Nodal Methods for Hexagonal Nodes, Proc. Joint Int. Conf. on Mathematical Methods and Supercomputing in Nuclear Applications, April 19-23, 1993, Karlsruhe, Germany, Vol. 1, p.605.

- [4.63] Doriath, J.Y. et al., Reactor Analysis using a Variational Nodal Method Implemented in the ERANOS system. Proc. Mtg. Reactor Physics Faces the 21st Century, KNOXVILLE (1994). Also: Ruggeri, J.M. et al., Mixed Transport-Diffusion Method, Int. Topical Mtg. Portland (1995).
- [4.64] Majorov, L.V., Gomin, E.A., Collision Probability Calculations in a System With Complex Geometry Structure, VANT, Ser. "Physics and Techniques of Nuclear Reactors", Issue 8 (21), 1981, p.62.
- [4.65] Grabejnoi, V.A., Usanov, V.I., A Collision Probability Method Applied to Neutron Shielding Calculations, Preprint-2270, IPPE, Obninsk, 1992.
- [4.66] Straker, E.A., et al. The MORSE Code - A Multigroup Neutron and Gamma-ray Monte Carlo Transport Code, Oak Ridge Natl. Lab. Rep. ORNL-4585 (1970).
- [4.67] Whitesides, G.E., Cross, N.F., Keno - A Multigroup Monte Carlo Criticality Program. CTC-5 (1988).
- [4.68] Levitt, L.B., Lewis, R.C., VIM1 - A Non-multigroup Monte Carlo Code for Analysis of Fast Critical Assemblies, AI-ABC-12951 (1970).
- [4.69] Korobejnikov, V.V., Usanov, V.I., Combined Methods in Transport Irradiation Problems. Energoatomizdat, Moscow, Russia (1994).
- [4.70] Baker, R.S., Larsen, E.W., "A Local Exponential Transform Method for Global Variance Reduction in Monte Carlo Transport Problem", Karlsruhe, 1993, Vol.2, p.725.
- [4.71] Kochetkov, A.L., Tsykunov, A.G., Scientific Research Program on Actinide Transmutation by Use of Fast Reactors, in: Proc. IAEA Spec. Meeting, Obninsk, 1992, IAEA-TECDOC-693, 1993.
- [4.72] Toppel, B.J., The Fuel Cycle Analysis Capability, REBUS-3, ANL-83-2, 1983.
- [4.73] Cowan, C.L., Rurssel, C.S., FUMBLE-II: A Fast Reactor Fuel Management and Burnup Code with an Influence Function Option for Predicting the Three-dimensional Effects of Control Rod Movements, Sunnyvale, CA, GEAP-1438 (1976).
- [4.74] Asai, K., Higuchi, K., et al. the JAERI Monte Carlo Machine, Proc. Joint Int. Conf., Karlsruhe, 1993, Vol.2, p.734.
- [4.75] Amnesiac, T., et al. A Parallelization Study of the General Purpose Monte Carlo Code MCNP 4 on a Distributed Memory Highly Parallel Computer, Karlsruhe, 1993, Vol.2, p.374.
- [4.76] Schltyse, W. et al., Proc. ANS Int. Symp. on Reactor Physics, Jackson Hole, USA (1988).
- [4.77] Cabrilat, J-C et al., Common Lessons Drawn from Different Laboratories Analyses of SUPER-PHENIX Startup Experiments, Proc. Int. Conf. on the Physics of Reactors, Vol. 1, p. VII.10 - Marseille, France (1990).
- [4.78] Brumbach, S.B. et al., Experiments and Analyses for Large Conventional Fast Reactors in ZPPR -18/19, Ibid, Vol. 1, p. V-63.
- [4.79] Calamand, D. and CURL, I.J., A Review of Progress with the JANUS Programme of Fast Reactor Shielding Benchmark Experiments. Ibid., Vol. I, p. V1.
- [4.80] Robinson, P.J. et al., Comparison of Calculation and Measurements of Reaction Rates in the Outer Regions of SUPER-PHENIX. Ibid., Vol. 1, p. VII-29.
- [4.81] De Wouters, R. et al., Measurements and Analyses of Gamma-ray Energy Deposition in a Critical Assembly Containing a Central Simulated Diluent. Ibid., Vol.1, p. V-12.
- [4.82] Newton, T. et al., The Evaluation of SUPER-PHENIX Core Reactivity Levels. Ibid. Supplementary Volume.
- [4.83] Bergeonneau, Ph. et al., Analysis and Interpretation of the Neutronic Experimental Results at the SUPER-PHENIX Restart-up in 1989, Ibid., Vol. 1, p. VII-1.

- [4.84] Rowlands, J.L and Salvatores, M., Fission Product Data Needs for Reactor Applications, Proc. Specialists Meeting on Fission Product Nuclear Data, Tokai, Japan (1992).
- [4.85] Rowlands, J.L. et al., Development and Validation of Control Rod Calculation Methods, Proc. Int. Symp. on Fast Reactor Physics (p. 83), Aix-en-Provence (1979).
- [4.86] Carpenter, S.G. et al., Experimental Studies of 6000 litre LMFBR Cores at ZPPR. Proc. Conf. Advances in Reactor Physics and Shielding (p. 521) Sun Valley (1980).
- [4.87] Specialists' Mtg. on Control Rod Measurement Techniques: Reactivity Worth and Power Distributions, Cadarache (1976) - NEACRP-L 162.
- [4.88] Caldarola, L. et al., SEFOR Experimental Results and Applications to LMFBR's, Proc. Int. Conf. on Engineering of Fast Reactors, Vol. 3, p. 1312 - Karlsruhe (1972).
- [4.89] Ishiguro, Y. et al., Measurements and Analysis of the Doppler Effect of Structural Materials, Proc. Int. Symp. on Physics of Fast Reactors, Vol. 2, p. 964 - Tokyo (1973).
- [4.90] Okajima, S. et al, Doppler Effect Measurements up to 2000°C at FCA, Proc. Int. Conf. on Nuclear Data for Science and Technology, Vol. 2, p. 1009.
- [4.91] De Kruijf, W.J.M and Janssen, A.J., The Effective Fuel Temperature, Nucl. Sci. and Eng. (1995).
- [4.92] Butland, A.T.D. et al., An Assssment of Methods for Calculating Doppler Effects in Plutonium Fuelled Sodium-Cooled Fast Reactors, Proc. Int. Symp. on Fast Reactor Physics, Vol. 1, p. 257, Aix-en-Provence (1979).
- [4.93] Lesage, L.G et al., Current Status of Fast Reactor Physics Reactivity Coefficients, Proc. Nucl. Energy, 16, p. 231 (1985).
- [4.94] Gauthier, J.C. et al., Comparaison calcul-expérience pour la mesure de l'effet Doppler sur PHENIX, Proc. Int. Symp. Fast Breeder Reactors, Lyon (1985).
- [4.95] Vanier, M. et al., SUPER-PHENIX Reactivity and Feedback Coefficients, Nucl. Sci and Eng. 106, p. 30 (1990).
- [4.96] Rimpault, G. et al., SEFOR and SUPER-PHENIX Start-up Doppler Experiments Analysis with the European Code Scheme JEF2/ECCO/ERANOS, Int. Conf. on Mathematical Methods and Super-computing in Nuclear Computations, Arlington (1994).
- [4.97] Butland, A.T.D. et al., An Assessment of Methods of Calculating Sodium-voiding Reactivity in Plutonium Fuelled Fast Reactors, Proc. Int. Symp. on Fast Reactor Physics, Vol. 1, p. 281, Aix-en-Provence (1979).
- [4.98] Calamand, D. and Curl, I.J, A Review of Progress with the JANUS Programme of Fast Reactor Shielding Experiments, Proc. Int. Conf. on the Physics of Reactors, Vol. 1, p. V-1, Marseille (1990).
- [4.99] Sartori, E., VITAMIN-J, ECCO-33, ECCO-2000 and XMAS, Standard Group Cross-section Libraries, OECD/NEA JEF/DOC-315 (1990).

BIBLIOGRAPHY
SOME TEXTBOOKS AND OTHER BASIC REFERENCES TO NEUTRONICS

(a) *General Reactor Physics*

WEINBERG. A.M and WIGNER E.P.
The Physical Theory of Neutron Chain Reactors,
Univ. of CHICAGO Press, (1958).

GLASSTONE S. and EDLUND M.C.
The Elements of Nuclear Reactor Theory
VAN NOSTRAND, NEW YORK (1965).

(b) *Theory*

BELL G.I. and GLASSONE S.
Nuclear Reactor Theory
VAN NOSTRAND, NEW YORK (1970).

BUSSAC J. and REUSS P.
Traité de Neutronique
HERMANN 2nd Edition (1985).

BARJON R.
Physique des Réacteurs Nucléaires
Université Joseph Fourier,
GRENOBLE I (1993).

BECKURTZ K.H. and WIRTZ K.
Neutron Physics
SPRINGER-VERLAG (1964).

DAVISON B.
Neutron Transport Theory
OXFORD Univ. Press (1957).

HENRY A.
Nuclear Reactor Analysis
MIT PRESS (1975).

MARCHUK G.I.
Numerical Methods for Nuclear Reactor Calculations,
Consultants Bureau
NEW YORK (1959).

WILLIAMS M.M.R.
The Slowing Down and Thermalisation of Neutrons,
NORTH HOLLAND (1966).

(c) *Kinetics*

KEEPIN G.R.
Physics of Nuclear Kinetics,
ADDISON-WESLEY (1965).

(d) *Fast Reactors*

JUDD. A.M.
Fast Breeder Reactors: an Engineering Introduction
PERGAMON PRESS (1981).

WALTAR A.E. and REYNOLDS A.B.
Fast Breeder Reactors
PERGAMON PRESS (1981).

(e) *Nuclear Data*

MUGHABGHAB S.F. - DIVADEENAM M. and HOLDEN N.E.
Neutron Cross-sections, Vol. 1, ACADEMIC PRESS (1981)

MC LANE V. - DUNFORD C.L. and ROSE P.F.
Neutron Cross-sections, Vol. 2, ACADEMIC PRESS (1988).

MICHAUDON A. (Ed)

Nuclear Fission and Neutron - Induced Fission Cross-sections
PERGAMON PRESS (1981).

(f) *International Conferences*

Note the International Conferences on Nuclear Data:

- GATLINBURG (1994),
- JULICH (1991),
- MITO (1988),
- SANTA FE (1985)
- etc...and the series of KIEV Conferences.

Reference should also be made to the series of International Conferences on the Physics of Reactors and on Mathematics and Physics sponsored by the American Nuclear Society, in

association with the European Nuclear Society, the Japanese Nuclear Society and the Canadian Nuclear Society:

- PORTLAND, OREGON (1995) (Mathematics + Physics),
- KNOXVILLE (1994) (Reactor Physics),
- KARLSRUHE (1992),
- MARSEILLE (1990).

Conferences on Radiation Shielding include:

- ARLINGTON (1994),
- BOURNEMOUTH (1988),
- TOKYO (1983),
- etc.

(g) *Special issues of Progress in Nuclear Energy*

Fast Reactor Physics Vol. 16 - N° 3 (1985)

Finite Elements Methods Vol. 18 - N° 1/2 (1986)

Monte Carlo Methods Vol. 24 - N° 1/3 (1990).

BASIC NUCLEAR DATA LIBRARIES

Measured nuclear data and libraries of evaluated nuclear data are available from the Nuclear Data Centres:

- NNDC Brookhaven National Laboratory, USA
- CDJ. FEI OBNINSK, RUSSIA
- IAEA Nuclear Data Section, Vienna, AUSTRIA
- OECD NEA Data Bank, Paris, FRANCE.

A bibliographic index, CINDA, is also produced.

Measured data are compiled in the EXFOR exchange format; current libraries of evaluated nuclear data are compiled in ENDF format.

Some libraries are now available in interactive packages for PCs.

EVALUATED DATA LIBRARIES

BROND	The Russian Evaluated Nuclear Data Libraries, compiled at Obninsk, and and FOND, Russia.
CENDL	The Chinese Nuclear Data Library, compiled in BEIJING, CHINA.
EFF	The European Fusion File, coordinated by the European Commission and compiled at ECN PETTEN, THE NETHERLANDS.
ENDF/B	The North American Evaluated Nuclear Data File, coordinated by the Cross-section Evaluation Working Group and compiled at the NNCD, BROOKHAVEN, USA.
ENDL	The Lawrence Livermore Laboratory Evaluated Nuclear Data Library, USA.
JEF	The Western European Joint Evaluated File, coordinated by a Committee of the OECD NEA and compiled at the NEA Data Bank.

JENDL	The Japanese Evaluated Nuclear Data Library, coordinated by the Japan Nuclear Data Committee and compiled at the JAERI Nuclear Data Center.
FENDL	The Fusion Technology Evaluated Nuclear Data Library, coordinated by the IAEA Nuclear Data Section.
IRDF	The International Reactor Dosimetry File, coordinated by the IAEA Nuclear Data Section.

Coordination committees, such as the NEA International Evaluation Cooperation and IAEA Coordinated Research Programmes, CRPs, bring together evaluators working on the different projects, to resolve discrepancies

**NEXT PAGE(S)
left BLANK**

Chapter 5

LMFR SAFETY: NEW TRENDS AND FINDINGS

5.1. NEW TRENDS IN SAFETY PRINCIPLES AND GOALS

5.1.1. LMFRs and main recent nuclear safety trends

New safety trends are taking shape in the field of nuclear safety:

- Improvement of understanding of the technical bases of safety;
- Maturation of long intensive programmes of research into engineering of safety;
- Feedback of experience in nuclear plant operating including the major lessons learned from the severe accidents to nuclear plants at Three Mile Island and Chernobyl;
- Steadily mounting desire of the public for improved safety in every sphere of life.

In this context the question of severe accidents involving core-melting is again a major concern and is, to some extent, new for thermal nuclear reactors (since core melting was not considered ten years ago). On the contrary licensing and safety analysis, for LMFRs, have been considerably influenced by the question of core melting since the beginning. Core disruptive accidents have a very low probability of occurrence and are usually termed hypothetical core disruptive accidents (HCDAs). Strictly speaking, HCDAs were not considered design basis accidents, but the design of some LMFRs (FFTF, SNR 300) was strongly influenced by them. In these cases, reactor design was very much determined by hypothetical events and it became questionable whether the safety-related design was really well-balanced with respect to the entire spectrum of possible incidents and accidents, and also with respect to the construction cost of the plant.

In the course of time, the safety approach has been improved and defined accurately by the drawing up of a full set of consistent criteria and safety options as well as design and construction rules. Since 1983 [5.7] a large consensus has formed among representatives of various nations according to which HCDAs ought to be removed into residual risk. Today this objective has been reached. However there still remains a concern about a possible "cliff edge" effect. Such a cliff edge effect must be excluded by means of appropriate measures.

5.1.2. Safety fundamentals

General safety objective: The overall safety objective for any type of nuclear plant is to protect individuals, the public and the environment by establishing and maintaining an effective defence against radiological hazards.

The fundamental safety principles applied to a typical LMFR in order to achieve the overall safety objective are:

- to compensate for potential human and mechanical failures by a defence in depth approach, all reasonable practical steps being taken to prevent accidents and to minimize the radiological consequences of accidents;
- to minimize the dose to operators and public during normal operation by respecting appropriate dose limits, dose below the prescribed limits being as low as reasonably practicable (ALARP principle).

Criteria and requirements

General criteria. The overall safety level should be equivalent to that of a future thermal reactor in the country concerned. In accordance with IAEA recommendations [5.5, 5.6] for future nuclear plants, the safety objectives can be specified. A limit for acceptable releases in term of isotope activities will be based on the following principles:

- a) Dose limit at the site boundary not requiring short-term off-site response;
- b) Unlikely severe accident management and mitigation measures reducing the probability or consequences of large off site releases requiring a short-term off-site response at least by a factor of ten

For the "a" type condition, a probabilistic target is set such as the frequency of exceeding the limit must be less than 10^{-6} /plant year.

Design targets. In order to meet this global target a number of design targets have to be set up:

- frequency of core melt less than 10^{-6} /year;
- frequency of loss of shut-down function 10^{-7} /year;
- frequency of loss of decay-heat removal function less than 10^{-7} /year.

Complementary targets. The containment must be such as to provide sufficient mitigation for postulated Beyond Design Basis plant states. This requires effective primary and secondary containments with no weak points and the avoidance of any "cliff edge" effect. Besides, off-site measures must be available, going beyond the level of protection provided in most human endeavours, to compensate for the extremely remote possibility that safety measures at the plant might fail. In such a case the level and delay of releases must be sufficient to allow for efficient countermeasures such as sheltering or evacuation of the public for a short period of time. As regards the definition of tolerable radioactive releases, discussions are still underway. But the trend is that possible radioactive material transport to food chains, or other pathways requiring permanent off-site evacuation for long periods, should not be considered as acceptable. Under these conditions the former "S3" limit should be reduced by at least a factor of ten.

5.1.3. Risk minimization and accident analysis approaches consequences for LMFRs

Risk concept: The central objective of safety is to minimize the global risk [5.2] defined by:

$$R = \sum_i p(i)C(i)$$

- S = Sum over all possible events
P(i) = probability of event number (i)
C(i) = consequences of event number (i)

A purely probabilistic approach to (1) is nearly impossible and would not be reliable for many reasons:

- it is impossible to demonstrate the completeness of the above list of events and consequently to be rigorous in approaching the global risk;

- theoretically, equation (1) requires taking into account very low probabilities with practically no lower limit since the upper value of C (total inventory of core fission products) is extremely high (this last point is important for severe accidents involving core melt);
- an accurate assessment of probabilities is extremely difficult and in certain cases practically impossible.

In spite of all these problems, the development of PSA analyses is currently leading to considerable insight in safety and is of great help in guiding safety designs and practices [5.3, 5.4]. However, defence in depth, which is a deterministic approach, is currently used for PWRs with undeniable success. Moreover, IAEA [5.5, 5.6] considers defence in depth as being the fundamental means of ensuring the safety of nuclear plants. That is why, for LMFRs, the safety approach commonly agreed upon in Europe is based on defence in depth [5.5]. However, to cope with requirements related to very low probabilities, we use, together with the defence in depth, the "line of defence" method which is between a purely deterministic and a purely probabilistic approach. Thanks to this method it is in practice possible to determine the limit between Design Basis Events and Beyond Design Basis Events; and among the BDBAs the limit between events taken into account (limiting events) and events not taken into account (residual risk).

We shall see how under certain conditions involving strengthening of the containment and certain complementary provisions it is possible to reject HCDAs into the residual risk.

Plant operating conditions and event rationale: The demonstration of the adequate safety of the plant is based on the general principle that the more severe the consequences of fault sequences, the lower their frequency. A practical application of such a principle (which is in agreement with the risk concept) leads to the grouping of faults on the basis of frequency into different categories and to the definition of acceptable consequences for each category. Practically, demonstration of the adequacy of the design has to be made by analysis of a very limited number of faults in each category. To be valid this demonstration must rely on the choice of faults as being representative of a family of events. As a result these faults must be chosen as a full envelope not only of the consequences but also the probability (i.e. the sum of the probabilities of the expected elementary events of the considered family).

Design basis initiating faults and operating conditions: Design Basis initiating faults are postulated faults which are assumed to occur, and may arise, due to component failure, operator errors or external hazards. Initiating faults to be considered within the Design Basis cover the whole range of faults from those which are likely to occur several times during the life of the plant to those whose occurrence is highly unlikely, but for which the consequences must be evaluated and, if necessary, design measures taken to restrict them. The Design Basis initiating faults studied are selected as the worst conditions representative of a family of events. The initiating faults to be considered in the Design Basis are assigned to three categories (in addition to Category 1 which covers normal operating conditions). The frequency of occurrence of the initiating faults is used as a guideline for their classification. Starting from critical conditions, the operating conditions are the changing plant conditions which arise as a result of an initiating fault combined with a conventional aggravating situation (cf. aggravating failure).

Category 1. Normal operating conditions including special conditions such as start-up, part load, shut-down states, maintenance

Category 2. Operating conditions not planned but expected to occur more than once during the life of the plant. Occurrence frequency: $f > 10^{-2}$ /year.

Category 3. Operating conditions not expected to occur during the life of the plant, but after which the plant restart is required following plant inspection, remedial action and requalification. Occurrence frequency: 10^{-4} /year $< f < 10^{-2}$ /year.

Category 4. Operating conditions highly hypothetical after which plant restart is not required. Occurrence frequency: 10^{-7} /year $< f < 10^{-4}$ /year. The lower value (10^{-7} /year) must be coherent with the figure of 10^{-6} /year (chosen as a probabilistic target for unacceptable consequences) and a very low number N of families of events in the fourth category ($N < 10$).

Beyond design basis events: Events having a frequency lower than 10^{-7} /year but with consequences likely to exceed Category 4 limits are termed Beyond Design Basis events and generally do not require design measures. However the completeness of the analysis performed within the Design Basis is difficult to demonstrate. Moreover the main objective of the safety strategy is to minimize the risk and to avoid any cliff-edge effect. Two types of events are distinguished in the Beyond Design basis regime:

- limiting events;
- residual risk events.

Limiting events. Limiting events are boundary cases of particular fault types for which it is anticipated that they may require evaluation for licensing purposes. The consequences of limiting events are investigated in order to show that widespread core melting is prevented.

Residual risk. Residual risk events are accident conditions which are not considered. The classification of an event into the residual risk requires demonstration by adequate preventive measures (see LOD approach).

Line of defence (LOD) approach: The major difficulty comes from the fact that it is nearly impossible to determine in a purely probabilistic way the limits between: Design Basis events and Beyond Design Basis events and, within the Beyond Design Basis regime, the limit beyond which events are rejected into residual risk. The line of defence (LOD) concept is a simple and conservative method which can be used to fix the limits between Design Basis and Beyond Design Basis events, and especially between the Beyond Design Basis events taken into account and Residual risk. This method can be used to show the adequacy of protective measures to demonstrate that core disruptive accident belongs to the residual risk and to classify operating conditions.

Classification of LODs: Taking into account their expected reliability, LODs are classified into two kinds:

- *type a load:* strong line of defence with an expected failure rate of about 10^{-3} to 10^{-4} per demand;
- *type b load:* medium line of defence with an expected failure rate of about 10^{-1} to 10^{-2} per demand.

The line of defence approach has to some extent a probabilistic nature but cannot be reduced to this sole aspect. The line of defence approach involves technical judgment, good sense, and phenomenological appreciation. Moreover, the experience gained with this approach allows different systems, barriers or provisions to be classified as an LOD. Examples:

Strong line:

- high quality active systems with internal redundancy (e.g. safety grade active systems complying with the single failure criterion;
- high quality passive components;
- inherent behaviour allowing a long delay for fault selection.

Medium line:

- classic active systems without internal redundancy;
- operator actions for which at least 30 minutes is allowed.

Practical application of LODs: The combination of LODs must be done carefully according to basic probabilistic rules. For instance, in case of addition of LODs, common modes have to be excluded. The frequency of considered initiators has to be considered in the final balance which is probabilistic. Safety strategy specifies a general requirement for LODs for the various fault frequencies as outlined in the following table:

TABLE 5.1. CLASSIFICATION OF AN UNPROTECTED FAULT AS RESIDUAL RISK

Initiator	LODs required to allow classification of an unprotected fault as residue risk
Cat. 2 event	$2a + b$
Cat. 3 event	$2a$
Cat. 4 event	$a + b$
Limiting event	b

Generally speaking, an event which may be at the origin of severe consequences requires $2a + b$ LODs to be rejected into residual risk. Limiting events should be emphasised because they are Beyond Design Basis events with a bounding character which have not been chosen for purely probabilistic considerations. It is usually considered that a medium line is required to reject limiting events into residual risk.

Rules for safety analysis: The rules for safety analysis result from probabilistic considerations, but most of the time these rules can be set up in a deterministic way which in many cases may be quite conservative. In the Design Basis faults are analysed with very stringent rules:

- worst conditions;
- analysis including both random and systematic uncertainties.

Random uncertainties are taken into account in such a way that the plant behaviour analysis results are evaluated at a high confidence level which may vary with the considered design basis conditions. Usually, a confidence level of 95% is adopted.

In order to avoid taking into account a large number of events, conservative rules are applied (such as aggravating failures) together with events representative of a family of accidents. In the Beyond Design Basis, in view of the very low probability of events, analysis should be performed without aggravating failures, with the use of best estimate values for in certain parameters and taking into account internal plant emergency plans.

Risk minimization by additional prevention: As has been pointed out before, in spite of the above efforts, complementary provisions must be taken in order to minimize residual risk.

Limiting events: Limiting events are Bounding cases which, it is anticipated, may require evaluation for licensing purposes. A typical list of events can be identified. According to EFR experience, this list may be as follows:

- leakage of main and safety vessels;
- fuel subassembly meltdown;
- large Na-water reactions in a steam generator;
- large Na leak outside the secondary containment up to guillotine failure of a main sodium pipe.

The analysis of the above limiting events aims to improve (or check the adequacy of) prevention.

Enhanced prevention: A complementary medium LOD should be introduced (as far as practicable) within the residual risk category to interrupt sequences which would have the potential to cause serious core damage. This is coherent with the criteria and requirements related to off-site releases. For instance, such an LOD may be obtained by means of a third shutdown level consisting of passive and active measures capable of bringing the reactor to a safe condition in case of postulated failure of the two basic shutdown systems (which comply with the (2a + b) LODs requirements).

Different passive or active complementary systems may be devised in different ways according to the project considered. Particular attention should be devoted to decay heat removal in order to provide reasonable assurance of failure prevention.

Mitigation: According to the defence in depth approach, mitigation is, after prevention, one of the two pillars of nuclear safety. In order to avoid any weak point in the primary containment (Fig. 5.1), the design must present homogeneous resistance to energy release in the short term, and resist thermal effects of HCDA in the long term. This last point requires a debris tray able to ensure retention and coolability of the whole core inventory via the DHR system.

Conclusion: It can be claimed that the risk minimization strategy has eliminated the risk of severe accidents and especially the risk of HCDA by minimizing its frequency. Furthermore analyses have demonstrated that the most likely outcome of a core accident would be a tolerably small energy release.

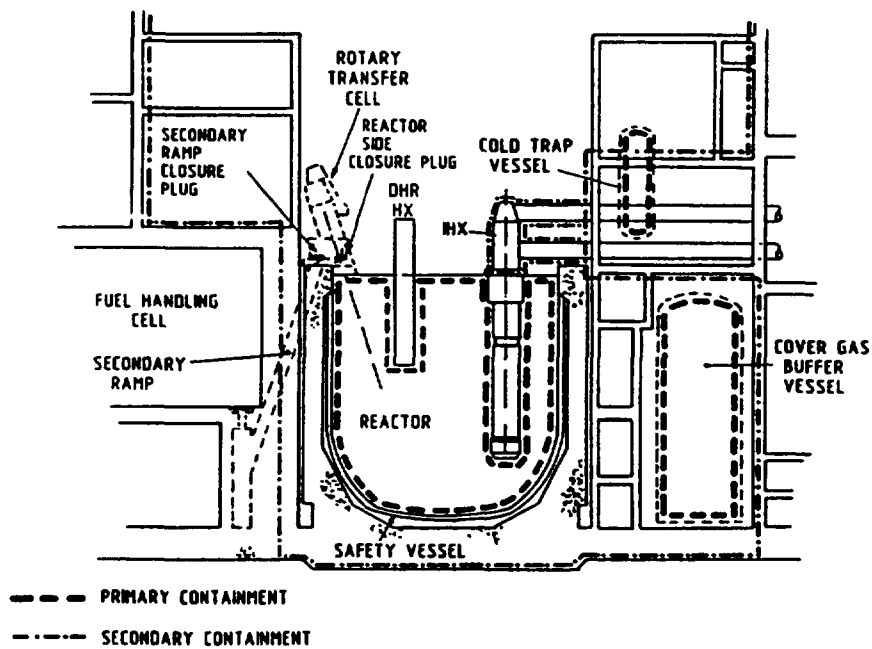


FIG. 5.1. Reactor containment boundaries (EFR)

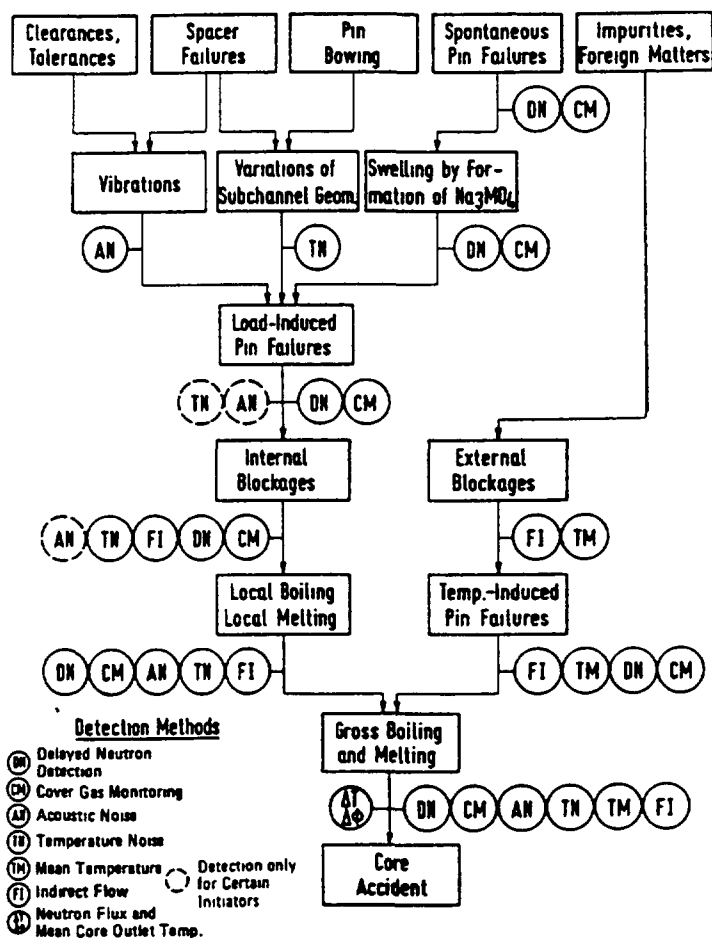


FIG. 5.2. Local fault propagation and related detection possibilities (source KFK)

TABLE 5.1a. TYPICAL RELATED PROJECT DESIGN TARGETS (e.g. EFR)

Frequency: /reactor yr (guidelines) (1)	Category	Dose target to public (effective dose equivalent)	Plant criteria
1	Normal operation	50 mSv/year	
10 ⁻²	2	50 mSv/event	Plant shall be able to return to full power in short term after fault rectifications
10	3	1 mSv/event	Plant shall be able to full power after inspection, rectification and requalification
	4	50 mSv/event	Plant restart is not required

- (1) Frequencies related to events representing a family of events and having as a result a frequency which is the sum of the individual frequencies of the considered events.

TABLE 5.1b. TYPICAL MAJOR DESIGN BASIS INITIATING FAULTS

<p>Spurious reactor trip Pin failure leading to DND signa Inadvertent withdrawal of an absorber rod Internal and external flooding Extreme weather conditions Large leak (IXH secondary circuits or DRC circuits) Multiple faults in fuel transfer and storage systems Conventional fire (1) Subassembly drop Local subassembly cooling disturbances Primary and secondary pump faults Leakage or rupture of primary pump diagrid connection of internal structures including the diagrid Primary sodium vessel leak Loading error Large leak of cover gas Abnormal passage of gas through the core Large steam generator leak Primary sodium circuit leakage in the secondary containment Dropped loads Earthquake</p>

- (1) The approach for these hazards has a deterministic character. Their categorization in Category 3 does not mean that their frequency is greater than 10⁻⁴/year, but that the plant is able to return to full power after inspection, rectification and requalification.

TABLE 5.1c. TYPICAL LIMITING EVENTS

Leakage of main and safety vessels
Fuel subassembly meltdown
Sodium-water-air reaction in a steam generator building
Large sodium-water-reaction in a steam generator (larger than Design Basis event)
Large sodium leak on the reactor roof
Large sodium leak outside the secondary containment up to guillotine failure of a main sodium pipe

TABLE 5.1d. EVENTS NEEDING THE DEMONSTRATION OF CLASSIFICATION AS RESIDUAL RISK

Large reactivity insertion (HCDAs) due to:
- core support failure;
- core compaction;
- voiding;
- large loading errors;
- ejection of control rod.
Design Basis initiating faults combined with failure to trip
Loss of decay heat removal systems
Dropped large load causing failure of primary coolant system
Primary pump flywheel failures
Primary vessel buckling due to external overpressure
Ingress of water into primary circuit
Large aircraft crash (could be classified in limiting events according to some national requirements)
Large gas cloud explosion (could be classified in limiting events according to some national requirements)

The containment systems would be effective in minimizing releases following a core accident making the net risk to the environment immeasurably small. That is why HCDAs are classified as residual risk.

Typical classification of events: The final result of the above approach is the classification of events. Such a list is a combination of probabilistic considerations and conservative choices. However, the extensive experience gained for many years in the study of LMFRs and especially in the study of EFR allows a typical list to be drawn up. The main results are presented in the following tables:

- Typical related project design targets, 5.1a
- Typical major design basis initiating faults, 5.1b
- Typical limiting events, 5.1c
- Events needing the demonstration of classification in residual risk, 5.1d

Design limits: the consequences of an operating condition, representative of a family of events must not exceed category 4 limits with a frequency $> 10^{-7}$ /year. Beyond Design upper limit: 10^{-7} /year or events protected by 2a LODs. Limiting events may be considered as bounding cases. Residual risk upper limit events protected by $(2a + b)$ LODs.

5.1.4. Local subassembly faults

Technical background: The worst consequences of Local Subassembly Faults (LSAFs) may be extensive fuel and clad melting. This situation is considered as a potential whole core accident initiator. The expectations are that melting should be precluded in the Design Basis and considered as a Beyond Design Basis event. The evaluation of the relevant initiators, the event sequences which follow them, and their detection are the essence of the safety case. The credibility of the arguments that are required depends heavily on R&D programmes which provide experimental observation, and also on analytical tools to interpret data and to extrapolate experimental results to the reactor case.

Design basis events: First of all, the consequences of clad failures, which cover a wide range of damage conditions, must be minimized according to the ALARP approach. This can be easily achieved by a combination of the natural behaviour of failed pins under normal conditions and the reactor protection systems, mainly DND systems which must be linked to the two reactor trip systems and possibly to cover gas monitoring system allowing for operator actions following an alarm. Many initiators can lead to different types of faults. Among the large number of possible local fault initiators and mechanisms investigated during last years, only a few have been identified to have the potential for local fault propagation (Fig. 5.2).

Local Blockages are of particular importance for several reasons : the tight package of the fuel bundle, the high power density and the possibility of particulate matter being swept into the assembly either from randomly defected fuel rods or from the primary system. An experimental test programme (ABACUS) [5.8 and Fig. 5.3] on particle transport within the SA has shown that the formation of internal blockages due to particles in the Na is unlikely because of the filter effect of the lower part of the SA. Thermal effects of inert internal blockages were studied in the Scarlet Test [5.9] (electrically heated). Finally, the consequences of many local disturbances (Design Basis faults) caused by blockages (porous or tight, extended or plate-type, internal or external) are predictable with good confidence by means of a number of codes, such as Bacchus and Sabre [5.10, 5.11].

It has to be noted that control rod withdrawal, combined with clad failure and possible ejection of molten fuel, is a very important LSAF initiator which does not belong to the family of blockages. Such a scenario must be precluded in the design by means of adequate performance of detection systems. However, the detection performance required to exclude any melting in Category 4 with a high degree of confidence is very stringent, so there is a strong incentive to define a modest melting limit (5 to 10% by volume) to preclude unacceptable consequences in case of adventitious clad rupture in Category 4. This very important question deserves further R&D efforts.

Conclusion related to design basis local faults: It is possible to claim that, within the Design Basis, prevention of local faults giving rise to unacceptable consequences is within the capability of competent engineering and protection measures. However, escalation of Design Basis Faults cannot be completely ruled out and has to be considered to ensure that there is no "cliff edge" effect and to provide possible insight into mitigation measures.

Beyond design basis events: The TIB (Total Instantaneous Blockage) has been chosen in Europe as a limiting event. The TIB is defined as an instantaneous blockage at the inlet of fuel SA at nominal operating conditions. It is a boundary case of any protected large internal or external BDB blockage sequence. The primary objective is to demonstrate that the

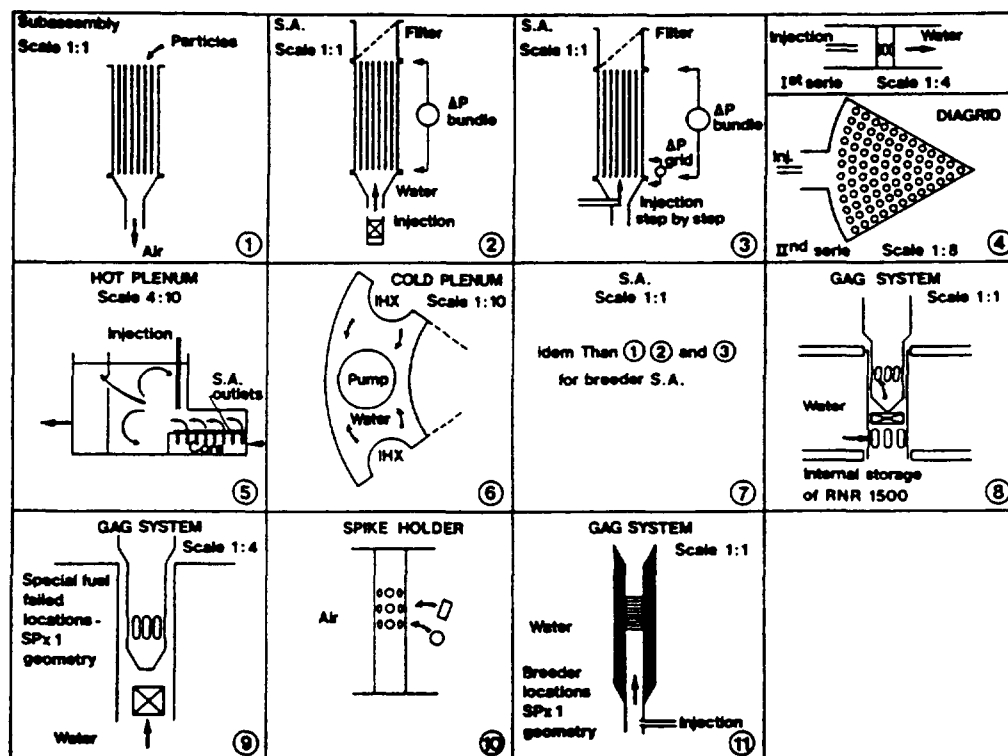


FIG. 5.3. ABACUS mock-ups (source CEA)

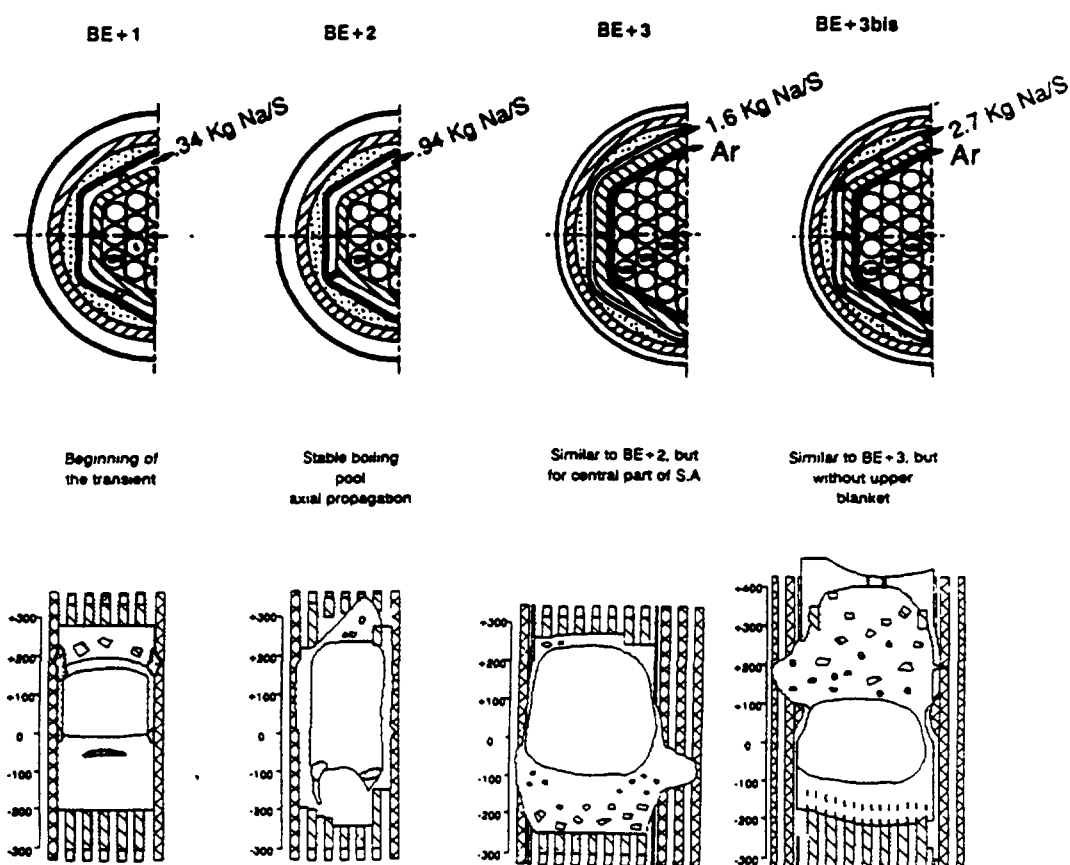


FIG. 5.4. Scarabee experiments - BE+ series - schematic views after tests, interpretations based on post-mortem examination

consequences of the TIB, taking account detection capabilities, are not such as to induce any large core accident. It was decided to adopt a very stringent condition: no propagation beyond seven SAs (faulted SA included).

Lessons from the Scarabee experiments: Two major programmes are devoted to the study of BDB subassembly melting accidents: the Scarabee programme to study the consequences of TIB; and the MOC 7C programme to investigate the consequences and the detectability of severe internal blockages. The Scarabee programme is mainly related to the Beyond Design Basis reference accident (i.e. the total instantaneous blockage of a fuel subassembly at nominal power, Fig. 5.4).

Analysis of the Scarabee tests (for fresh fuel) is close to completion [5.12,5.13]. Globally, the tests give clear answers in the main:

- no significant fuel ejection from the fissile zone and, consequently, no systematic DND signal before hexcan rupture;
- high heat transfer from the boiling pool;
- rapid melt-through of the hexcan and symmetrical propagation;
- no energetic MFCIs (point of major importance because, ten years ago, very energetic MFCIs were expected with a potential for rapid escalation into a whole core accident);
- no systematic DND signals from the blocked subassembly.

Modelling of the damage progression inside the faulted subassembly has reached a satisfactory state. For the subsequent events such as wrapper melt-through, material discharge into the subassembly gap and propagation of melt into the neighbouring subassemblies, models have been derived. Significant uncertainties still exist with respect to some points such as the heat transfer coefficients from a boiling pool and the very high heat fluxes at the location of wrapper melt-through. There is no other way of progressing than to improve the models in the codes. The extensive melting and pin damage induced in the Scarabee tests have proved particularly useful in validating the SIMMER code [18]. The most advanced state of the various models developed and qualified with the Scarabee experiments is to be found in the PHYSURA-GRAPPE code [14], and in the SURFASS code [15] which aims at calculating the whole scenario of the TIB in the reactor case.

Internal blockage experiments: The main objective of the last MOC 7C series was to investigate both the consequences and the detectability of severe internal blockages (Fig. 5.5) and [5.16, 5.17]. Thus, the information which can be drawn from these experiments is complementary to that drawn from the Scarabee experiments. The main lessons are:

- no energetic MFCI;
- no propagation to the whole bundle;
- clad failure before clad melting;
- large early DND signals.

It must be underlined that high DND signals were systematically generated after the first fuel pin failure, which would provide a reliable automatic trip under reactor conditions. The question of detection will be addressed further in order to demonstrate the bounding character of the TIB in the reactor case.

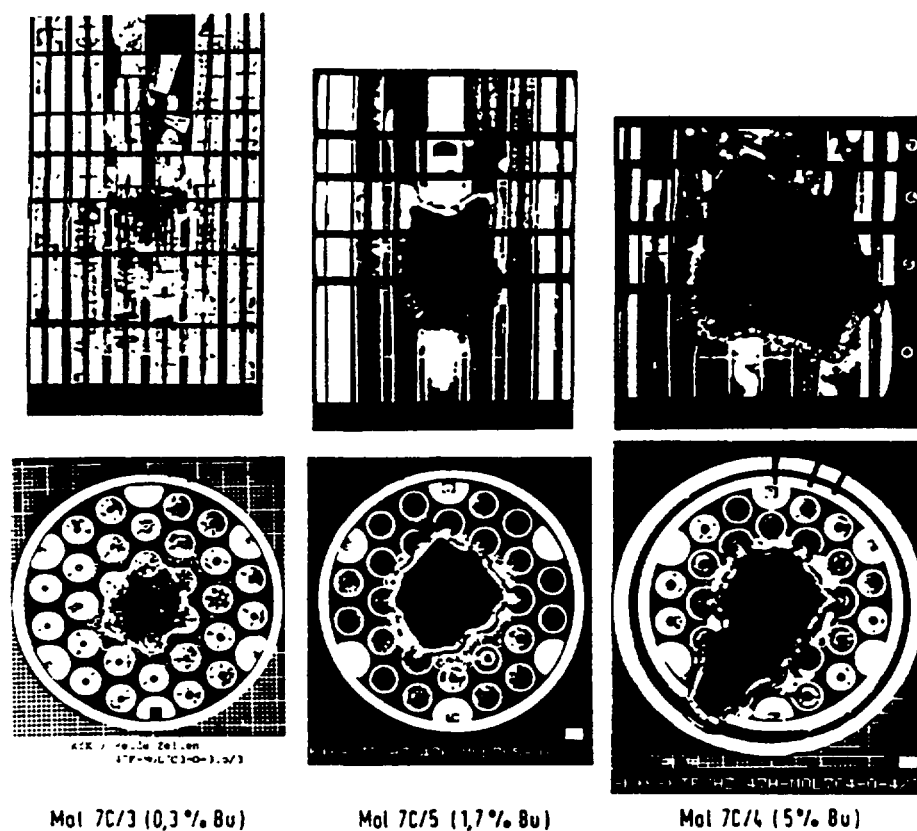


FIG.5.5. MOL 7C/3, 4,5: Longitudinal cross-cuts of the bundle in the region of the blockage

Reasonable agreement has been reached between experimental results and calculations with the SIMMER II code [5.18]. In particular, the formation of a closed cavity and the thermal equilibrium reached about 22 sec after the initiation of the transient correspond to the experimental observation in the case of MOL 7 C/5. Similar calculations are planned with the code SURFASS [5.15].

Extrapolation to the reactor case and detection performance: Important conclusions have already been drawn from experiments:

- large severe local melting of the MO7C type is detected early;
- thermal propagation initiated by a TIB is not self-limited.

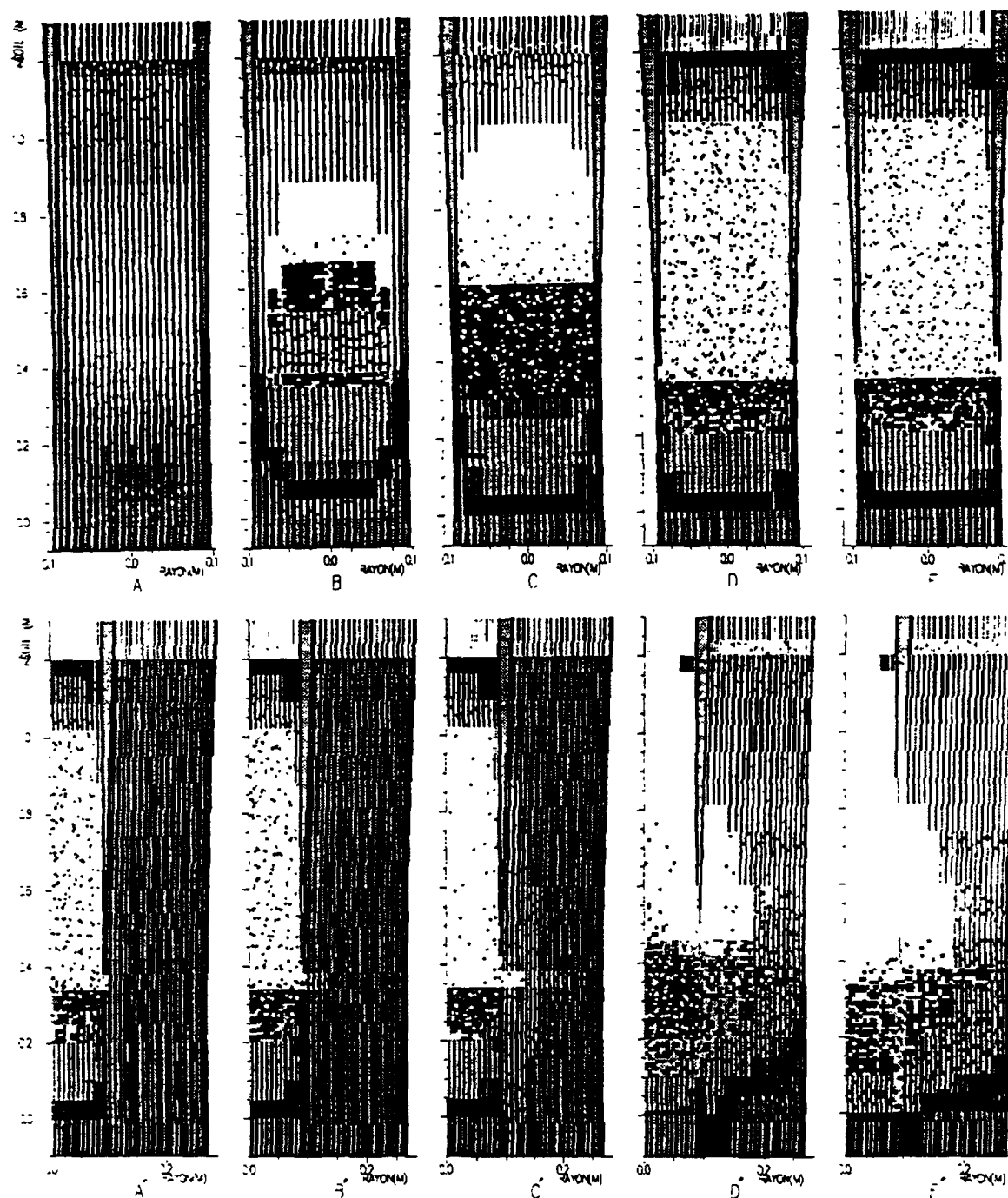
In order to go beyond such findings it is necessary to be able to describe the development of the fault up to cooling after the scram. This study must take into account the actual characteristics of the reactor plant, including systems for accident detection and shutdown. The Project code SURFASS [5.15] mentioned above provides for such a study and the demonstration of the enveloping character of the T.I.B. The parameters in such calculations are adjusted according to available test data and in particular to the Scarabee tests (not only the BE+ series but also the APL Tests [5.19]).

Many important points have been clarified by these calculations: the possible formation of a cavity, the temperature and pressure of the boiling pool, the time of occurrence of wrapper met-through, the role of the interassembly gap, and the number of subassemblies involved, taking performance of the detection system into account. Many studies have been devoted to the various reactor cases [5.20] and Fig. 5.6.

In the case of fresh fuel DND detection of the TIB must occur before 12 seconds to avoid propagation beyond 7SAs (of the EFR type). In practice in the real reactor case irradiated fuel will be present. Fission gases are expected to be the means of early detection with DND systems. For this reason a future test with irradiated fuel, planned for Scarabee, is very important.

Additional remarks about the question of detection of the TIB are required. The TIB was chosen to study local melting phenomenology, and basic answers have been provided. The question of the detection of the TIB has to be considered with a critical eye, however, because it is physically impossible. That is to say that in the worst reactor conditions (with subassemblies equipped with devices for feeding coolant radially), even if a total blockage were to occur inside the bundle, it cannot be instantaneous. An early DND signal would be emitted as soon as the first clad rupture occurs, at a time when the residual Na flow is sufficient to prevent the DND emitters from being trapped inside the faulted subassembly. In this respect, the lessons that can be drawn from MOL7/C tests are very clear.

In any case a major task of the designers still remains, to improve the performance and reliability of detection systems. The combination of a conventional hard-wired analogue system with additional digital systems may prove to be very efficient. The chief advantage of the digital system is the possibility of on-line testing of the measuring chains, including the sensors. It is expected that common mode problems can be solved in an acceptable manner. Reliability calculations show that system unavailability and the probability of undetected system failures can be brought down to very low values, especially for DND systems.



Faulted subassembly						Six neighbours (propagation)				
Ref	A	B	C	D	E	A'	B'	C'	D'	E'
time sec	8.5	13.5	18.5	22.4	23	22.5	23	23.5	34	60
events	clad melt down	pellets collapse	steel boiling	wrapper melt-through, upper blockage	wrapper 2 melt-through				SCRAM	PAH

FIG.5.6. Calculation of a TIB with SURFASS in a typical reactor case with melting, melt-through, propagation to the six neighbouring subassemblies, scram (fresh fuel)

General conclusion: The subassembly local fault prevention system is such as to preclude any local melting in the Design Basis regime. Should local melting occur in the Beyond Design Basis regime, in spite of prevention efforts, a very early detection would be ensured for any type of severe but realistic blockage. In the unrealistic case of TIB with fresh fuel, propagation would be limited at most to 7 SAs under the condition to have a DND detection within 12 s (in the typical case of EFR). In the case of irradiated fuel it is expected that fission products provide early detection. Finally, it is possible to claim that a local fault cannot be at the origin of a large core melting. The special event of control rod withdrawal, which is a potential whole core melting initiator, has to be addressed carefully and requires both prevention and substantiation by R&D related to very low melt fractions (5 to 10%) which may prove to be acceptable in category 4.

5.1.5. Sodium fires

According to experience from existing fast reactors and Na test facilities, leakage from Na-containing systems and components cannot be excluded.

Definition of events and associated risks: In the event of a leak, sodium will escape. Many sequences have to be considered. The Na may be forced out or merely exposed. Typically a leak may start in the first mode and develop to the latter if the environment is such that chemical reactions cause plugging of the breach by reaction products. Corrosion by these products may subsequently enlarge the leak area thus reopening the leak after a time interval. The Na escaping from the leak may impose loads on other structures by the jet force. If oxygen is available, sodium will react leading to a fire, which may increase the thermal loadings and raise the gas pressure by aerosol generation. The burning rate varies. The highest rate will be achieved when a sodium jet bounces against other structures and is dissipated into small droplets, thus increasing the Na surface in contact with air (spray fire). A low rate can be assumed when sodium only runs down the structures and collects in a catch pan (pool fire). Usually a combination of both extreme cases (spray fire and pool fire) has to be assumed. This situation is termed a combined fire.

The relation between leak rate and leak size depends on the system geometry, the location of the leak, and system characteristics such as the cover gas volume and pressure. Risks associated with a Na leak depend on the type of leak considered. In the case of the primary circuit heat removal from the core must be ensured, so loss of Na must be limited to allow decay heat removal via the DRC system. Primary Na being radioactive, leakages must be contained and possible releases controlled. Secondary leaks are of less importance, but they must be collected and guided out of the building without affecting any installation inside. Large and long-lasting sodium concrete reactions having potentially severe consequences must be excluded. In the beyond Design Basis range, potential risks associated with severe Na leaks and fire include:

- loss of the system function in which the leak occurs;
- radiation release;
- loads resulting from jet force;
- corrosion;
- sodium fire and associated phenomena;
- sodium-concrete reactions;
- sodium-water reactions if water circuits are involved.

Prevention, detection and mitigation: Sodium fires can be largely prevented by surrounding the sodium pipes and components with an inert gas, a Na-tight leak jacket, and steel-lined confinement cells. Outlets equipped with valves allow the build-up of pressure in the case of spray fire to be limited. Such design measures are to be found in FFTF or Super Phenix. In Super Phenix the four large areas (1000 m³) of the secondary loops were modified by the installation of partitions creating 100 m³ zones to limit the build-up of pressure on outbreak of a fire, the venting of the boundary via outlets equipped with valves set to open at 10 mbar to evacuate the hot gases outside the reactor building, and the cladding of the concrete walls with stainless steel sheeting to contain the secondary sodium in the event of a leak and to avoid Na-concrete reactions.

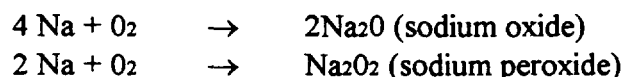
Other Design measures against pool-type Sodium Fires are so called catch pan systems Fig. 5.7. These collect leaking hot Na in such a way that it can run through holes into a leak recovery tank where it is isolated from the oxygen component of the air.

Various sodium fire-extinguishing powders have been developed and especially good experience has been obtained with graphite powders for quick and effective extinction of Na fires.

Leak detection plays an important role. Wire detection has been developed in many countries. Recently Super Phenix has been equipped with "Sandwich detectors" to cover welds on the piping exceeding 200 mm in diameter, on which insulating material may react with Na and prevent it from getting into contact with the classical wire detection system. Other detection systems such as flame spectrometers and smoke detectors are commonly used. The objectives pursued are the following:

- in all cases to prevent large leaks, corrosion, and fires by early detection;
- to exclude large leaks from the design by extensive application of the Leak Before Break (L.B.B.) criterion;
- to minimize large pressurized gas volumes which could act as driving forces for combined sodium fires in the event of leaks;
- to limit the duration of fires (15 minutes may be considered as an order of magnitude of an acceptable fire duration) to avoid serious damage to heavy structures by heating above acceptable limits;
- to preclude pressurization by relief openings; and
- to limit the drop height of any spray fire by arranging catch pans every 5 meters vertically (again this figure has to be considered as an order of magnitude).

Combined sodium fires develop according to the well known exothermic reactions:



The first reaction is the predominant mode. The evolution of a fire is very sensitive to the conditions of contact between oxygen and Na. That is why the extreme cases are pool and spray fires, the real case of a combined fire being a combination of the two.

Pool fires: A sodium pool fire will not normally ignite below about 250°C (if the pool is at rest). Since the fire occurs only at the pool surface it is appropriate to characterize the reaction rate on an area basis. A standard rate for a pool fire is 25 kg/m²h.

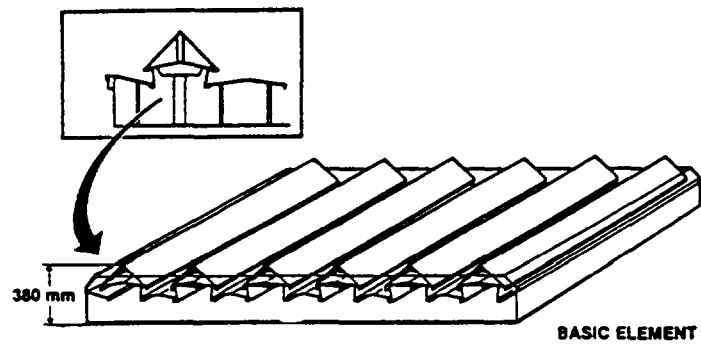


FIG.5.7. SUPER PHENIX smothering catch pan system (Source Novatome)

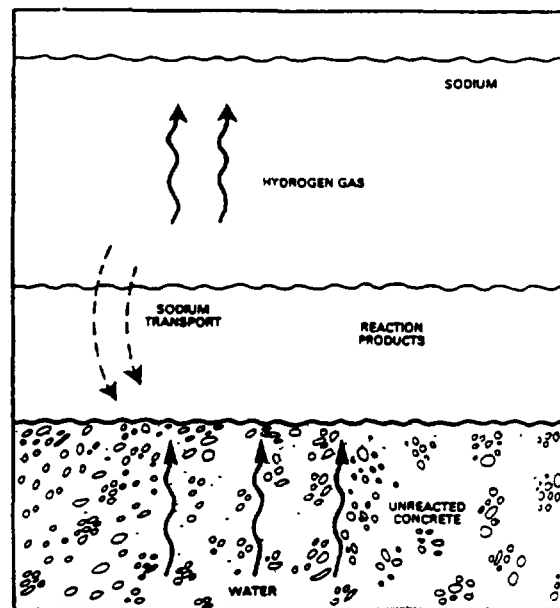


FIG.5.8. Diagram of the Na-concrete reaction model

The evolution of the fire depends on many parameters linked to the volume of the call and the heat transfer conditions. In reality the phenomena are more complex due to the fact that the pool is not really at rest and contact between Na and air is modified. The various phenomena have to be modelled in codes (see below).

Sodium spray fires: The ignition temperature for Na spray fires is lower than for pool fires and can be as low as 120°C depending on the Na droplet size. The sodium oxide aerosol production rates are much higher than for a pool fire (a factor of 5 or even more). Again the various phenomena involved have to be modelled in the codes.

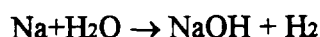
Models and codes: A common experimental programme concerning sodium combined fires was developed in France and in Germany [5.21]. It mainly focussed on prediction of the thermodynamic consequences due to upward vertical jets with a Reynolds number of about 106 and a nozzle diameter of 10 to 26 mm. Due to the lack of direct measurements of the spray parameters during the fire and the difficulty of predicting those parameters accurately in the case of a real fire, a simplified approach has been developed: in the new NABRAND code [5.22] an appropriate data set of droplet parameters was derived from realistic sodium fires, and in the FEUMIX Code [5.23] a global interfacial area between oxygen (air) and sodium droplets was found correlated with the jet Reynolds number. For both NABRAND and FEUMIX the comparison between calculation and experiment indicates that a simplified approach is valid for modeling the complex phenomena resulting from Na combined fires in the case of jet break up or impact.

Release of sodium fire aerosols to the environment: Experimental and analytical programmes were conducted in France and in the UK. At Cadarache realistic release tests were carried out in Esmeralda Facility [5.24]. At Dounray tests were conducted in the SOFA programme. All these experimental and analytical studies into the behaviour of sodium fire aerosols released into the environment demonstrate that there are problems arising from the characteristics of the source and the behaviour of the aerosols within the plume. These problems are being solved and the programmes have given a lot of useful information allowing the evolution of parameters of interest to be predicted under a large range of weather conditions. However, the effect of the building is important and has to be studied carefully.

Filters: Special filters have been developed to separate sodium oxide and fission product aerosols from air. The design criteria for these filters reflect the physical and chemical properties of sodium oxide and sodium hydroxide as well as the temperatures of these aerosols. Special Sanahed filters have been developed which attain a separation efficiency of 99,7 to 99,9%. They can be combined with wet scrubbers which can remove 70% of the sodium aerosols in a first step.

Sodium-concrete reactions: Sodium-concrete reactions have been studied thoroughly [5.23]. American workers [5.24] have suggested a generalized sodium-concrete reaction model shown schematically in Fig. 5.8.

In essence hot sodium, placed on top of ambient temperature concrete, heats the concrete, driving water to the hot surface where it reacts with Na to form hydrogen and NaOH according to the exothermic reaction:



Chemical energy from the reaction adds to heat from the Na to heat the concrete further and continue to drive off more water. When the concrete surface has been heated to about 500°C sodium and NaOH both react with concrete solids to produce more chemical energy. The extent of water release is determined by heat transfer in the concrete rather than sodium penetration of the concrete. The resulting NaOH phase at the concrete interface will generally form a barrier layer of reaction products, limiting the penetration into the concrete to a few cm of hard, rock-like consistency. In some cases, mechanical effects may cause disruption of the protective layer, resulting in rapid penetration of the dehydrated concrete by liquid sodium. The penetration rate is strongly dependant on Na temperature and varies from less than 0,5 mm/h at 200°C to 20 cm/h above 550°C. The reaction products associated with deep rapid penetration of Na in dehydrated concrete are characterized by a loose, friable, cinder-like consistency. Sodium penetration of concrete is of indirect concern due to possible effects on the structural integrity of the concrete.

Models and codes: A sodium-concrete ablation model SCAM [5.25] has been developed by Sandia. Very simple models related to evapourable and non-evapourable water release rates are to be found in [5.26]. More recently the RESSORT and SORBET Codes [5.27] have been developed and tested. Modelling covers chemical decomposition, thermodynamic equilibrium, and mass transfer of water, air, H₂ and CO₂. Heat transfer remains very important and may be strongly influenced by bubbling at the interface. Further developments are necessary.

Choice of concrete for minimizing interactions: The behaviour of concrete presented above varies considerably according to its composition. Various types of concrete have been investigated (Portland cement, Granite concrete similar in composition to basalt, Hydrous alumina cement, etc.). Some differences appear above 500°C. The most promising way to minimize interaction is to use refractory concrete which can be obtained by a combination of the following: - aggregate of Al₂O₃, MgO, high alumina cement, and firing of the concrete. The use of refractory concrete may be limited to a protective layer on conventional concrete. CEA have tested Corindon, Secar concrete (EdF) and PHLOX 188 (Lafarge Cement Co). The main conclusions were that the behaviour in contact with hot sodium at 350°C is satisfactory. It is difficult to apply refractory concrete to industrial buildings, and in consequence a new aluminous concrete was successfully tested and qualified: the INTRACAST AS 701 (produced by the Lafarge Refractaire Monolithique Co). The EFR anchored safety vessel option was tested with this concrete. The results were very satisfactory, but the cost is high so that the use of such concrete should be strictly limited to zones where the possible consequences of Na-concrete interaction would be unacceptable.

Liner systems: Long-lasting and large Na-concrete reactions are not acceptable, so liners are used extensively. Rapid heating to very high temperatures with large compressive stresses in the liners raises many problems which require careful design. In addition a considerable amount of heat can be transferred to the concrete, resulting in release of water vapor and other gases, with the potential to produce pressures behind the liner if the concrete is not adequately insulated and vented.

5.2. EMERGENCY HEAT REMOVAL BY NATURAL AND FORCED CONVECTION

5.2.1. Safety objectives of emergency heat removal systems (EHRS)

Decay heat removal (DHR) after shutdown of a nuclear reactor is one of the most important safety functions and must be accomplished with very high reliability. This, of course, depends on the overall target for infrequent occurrence of 10^{-6} /year of severe core damage set, for instance, by the IAEA. All technical means of attaining this ambitious goal have to be included into the design considerations and thoroughly evaluated. However, not only technical means such as, for example, good design and quality supported by code development and validation, adequate material, reliable components and redundancy, but also aspects like diversity, degree of independence from energy supply (passivity), simplicity have to be taken into account. And last not least, another indispensable factor is the overall demonstration of functional reliability under all essential operating conditions during commissioning. It has been demonstrated on several occasions on running reactors (e.g. PFR, FFTF) that there is an inherent capability to dissipate the decay heat in a "passive" way. This experience is the incentive to strive for this goal and the assurance that it can be attained. For the different LMFR concepts in general two different DHR systems are foreseen:

- Under nominal operating conditions, e.g., for a scheduled reactor shutdown, the decay heat is removed by the intermediate heat exchangers (IHXs) and cooling circuits via steam generators, water/steam systems, and condensers. The main components used for normal operation modes are sketched in Fig.5.9. This solution assumes that at least one heat removal circuit out of three or four remains undamaged and that the heat can be transported by forced or natural convection from the core to the condenser.
- In unlikely cases of unavailability of the water/steam system e.g. due to:
 - loss of station service power (LOSSP)
 - failure of the water/steam system in the DHR equipment
 - safe shutdown earthquake (SSE)
 - ISI&R on the water/steam side

the decay heat is removed by emergency heat removal systems.

5.2.2. Main design concepts

Various EHRS design concepts have been proposed and experimental and analytical studies have been carried out in a number of countries.

For different LMFR types and sizes the following main concepts can be defined:

1. Decay heat removal (DHR) via immersed decay heat exchangers (DHXs) in the hot or cold pool, intermediate sodium loop, sodium-air-cooler,
2. DHR via the vessel wall,
3. Combined versions,
4. DHR via the secondary loops.

In the following for each of these four main concepts typical systems will be described in more detail.

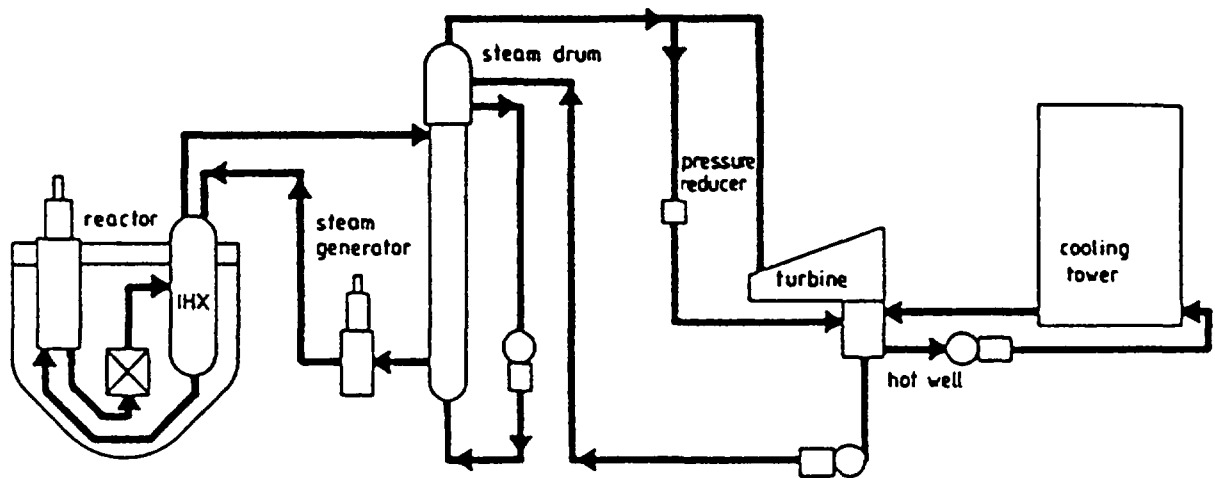


FIG.5.9. Normal: utilizes plant components used during normal operations and rejects heat to main condenser

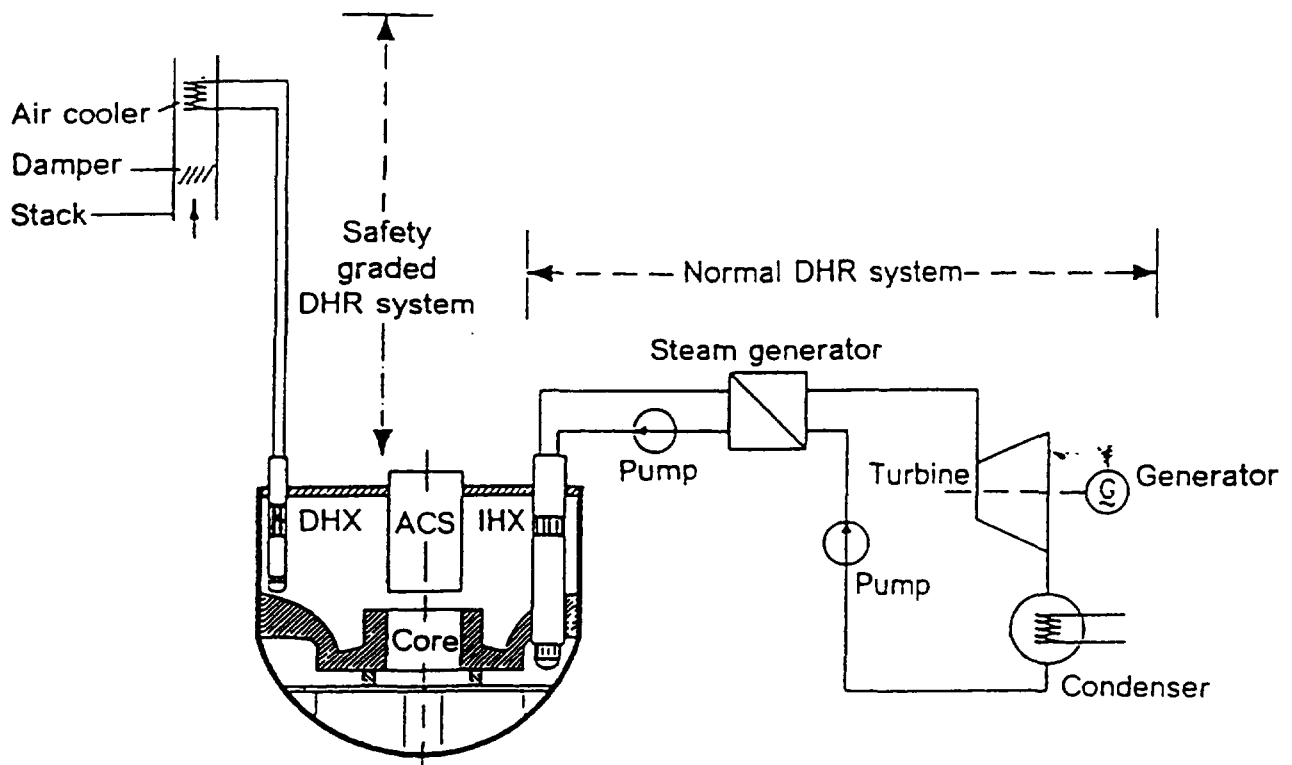


FIG.5.10. Normal and safety graded heat removal systems of EFR

Concept 1 (DHR via immersed decay heat exchangers in the hot or cold pool, intermediate sodium loop, sodium-air-cooler)

In the EUROPEAN FAST REACTOR (EFR) the decay heat is rejected from the primary sodium via a safety graded Direct Reactor Cooling (DRC) System [5.28-5.30] in the case of failure of the normal steam plant (Figs.5.10, 5.11).

There are two Direct Reactor Cooling Systems (DRC 1 and 2) of three loops each. All loops extract heat from the hot pool of the primary sodium by immersed sodium/sodium heat exchangers (DHX) and reject the heat to the environment by sodium/air heat exchangers (AHX) arranged above the DHXs [5.31].

DRC 1 relies exclusively on natural convection heat transfer, i.e. natural circulation on the loop side and natural draught on the air side.

DRC 2 is normally operated in forced flow conditions, i.e. each loop is equipped with a flow-supporting EM pump and with two fans in parallel on the air side. These active loops also have a high passive heat removal potential in case pump and fans are off, amounting to about 2/3 that of the active flow mode.

The DRC system must be able to remove the decay heat with only two out of six DRC loops available with their full heat removal capability respecting the criteria of the fourth category and without any support for the onset of natural circulation in the primary system by the circulation of sodium in the main secondary loops. The overall frequency target has been set at a level of 10^{-7} /year for the loss of the decay heat removal function.

The six DRC loops are segregated and separated and functionally independent of each other. They are provided with strictly loop-specific I&C equipment for operation and protection from freezing. The segregation and separation protects against adverse consequences from external and internal failures by means of barriers or distance.

To demonstrate the functioning of the system an extensive experimental and theoretical programme has been carried out with out-of-pile and in-pile tests in water and sodium in differently-scaled models [5.32-5.35], e.g. for the primary system:

RAMONA (3D, 1:20)

NEPTUN (3D, 1:5)

GODOM (3D, 1:5)

and for the direct reactor cooling chain:

KIWA (3D, 1:10)

ILONA (3D, 1:1).

For the interpretation of the experiments the following codes were used: TRIO-DYN, ATTICA-DYANA, FLUTAN, ASTEC. Accompanying in-pile tests have been performed in PHENIX and SUPERPHENIX [5.36,5.37].

A similar system is foreseen for the Japanese Demonstration FBR (top-entry loop type) [5.38-5.41]. In case of some types of failure such as loss of off-site power, decay heat is removed by forced convection of the decay heat removal system with emergency power supplies from diesel generators.

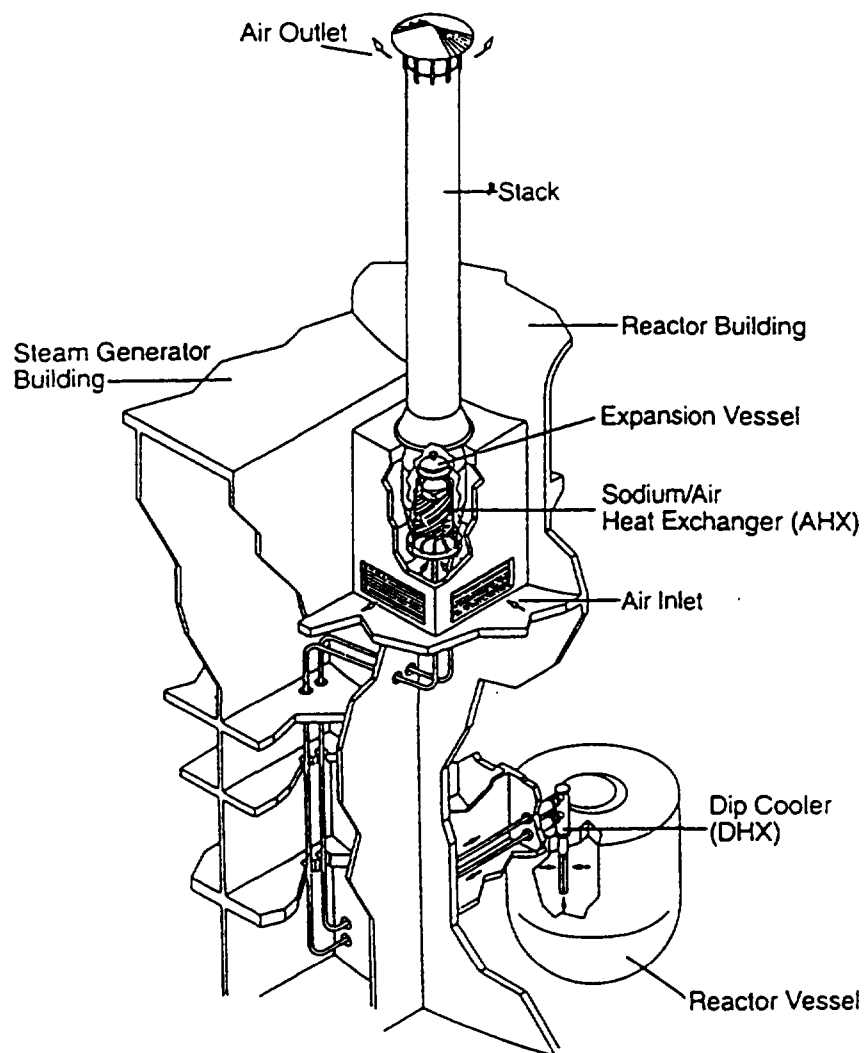


FIG.5.11. Direct Reactor Cooling (DRC-)System of EFR

The decay heat removal system is diversified by combining forced and natural circulation (see Figs. 5.12, 5.13). The concept is of an immersion-type direct reactor auxiliary cooling system (DRACS), based on the fact that when the external loop of the primary system cannot be used decay heat removal is possible only from the reactor vessel even. The shift to decay heat removal operation can be done very smoothly. The system consists of four 50% capacity loops each with a heat removal capacity of 14 MW/unit. This capacity was determined by analysis assuming loss of off-site power and start-up failure of one diesel generator unit. These are judged to be the worst conditions with respect to safety.

The design studies for the DFBR are accompanied by the following R&D activities related to natural circulation DHR:

- Natural circulation DHR experiments using the experimental fast reactor Joyo [5.42]. The tests are intended to demonstrate the natural convection DHR capability of Joyo and serve as a basis for the confirmation of similar but larger loop-type reactors.
- The feasibility of decay heat removal in the demonstration FBR was evaluated and confirmed with a 1/8th scaled model of the reactor system using water as a working fluid [5.43,5.44].
- Two types of multi-assembly sodium experiments, CCTL-CFR tests and PLANDTL-DHX tests, are being carried out in order to investigate the thermohydraulics in the core during natural circulation DHR condition for future large-scale FBRs [5.45-5.46].

Besides the reactor types described above (EFR, DFBR), the following FBR plants belong to the category of the DHR concept 1:

PFR (UK) [5.47], BN 1600 (Russia) [5.48-5.50], FFR (China) [5.51], PFBR (India) [5.52-5.54].

Concept 2 (DHR via the vessel wall)

The ADVANCED LIQUID METAL REACTOR (ALMR) plant has three redundant methods for shut-down heat removal [5.55, 5.56]:

Besides the normal water-steam heat transport system, it has

1. an auxiliary cooling system (ACS) which transports heat from the core by natural convection in the primary and intermediate systems, and rejects it from the outside surface of the steam generator by natural convection of air, and
2. a safety-related Reactor Vessel Auxiliary Cooling System (RVACS) which removes heat passively from the reactor containment vessel. The combination of one active and two passive systems provides highly reliable shutdown heat removal (Figs. 5.14,5.15).

The RVACS can dissipate all of the reactor decay heat through the reactor and containment vessel walls to the ambient air heat sink by the inherent processes of natural convection in fluids, heat conduction in solids, and thermal radiation. Heat is removed from the core and transported to the reactor vessel wall by natural convection of primary sodium. Two alternate sodium flow paths exist in the vessel during most of the decay heat removal period. Initially, the sodium flow path is the same as that during normal reactor power operation, i.e. from the core upwards to the hot pool, then down through the Intermediate Heat Exchangers

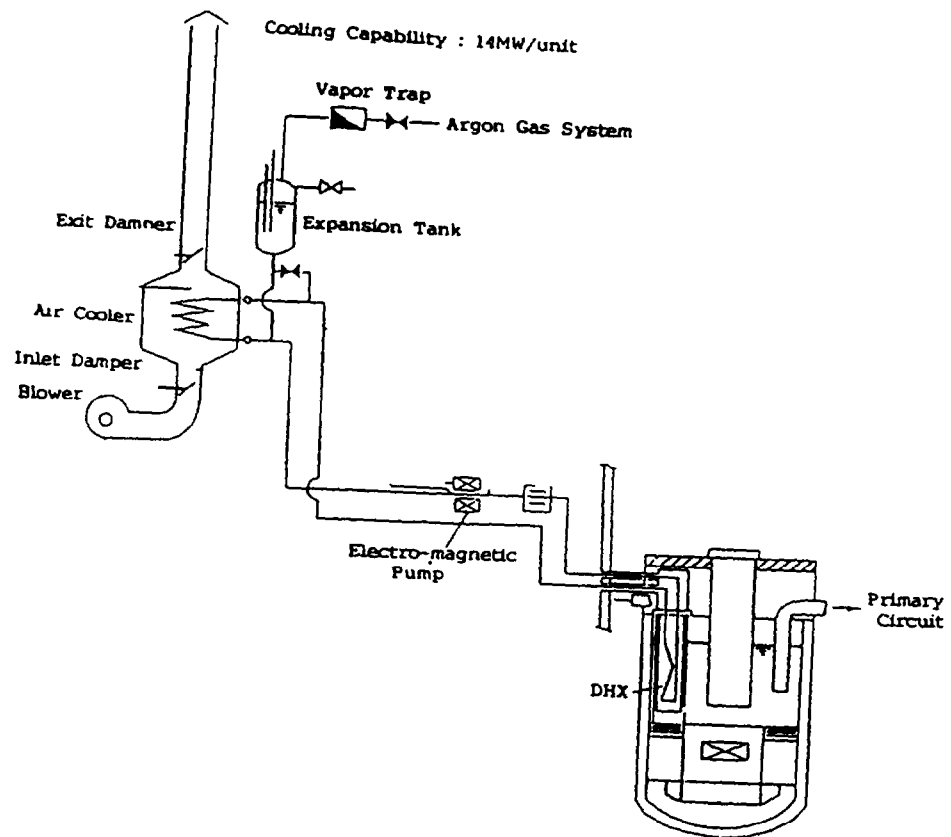


FIG.5.12. Decay heat removal system of DFBR

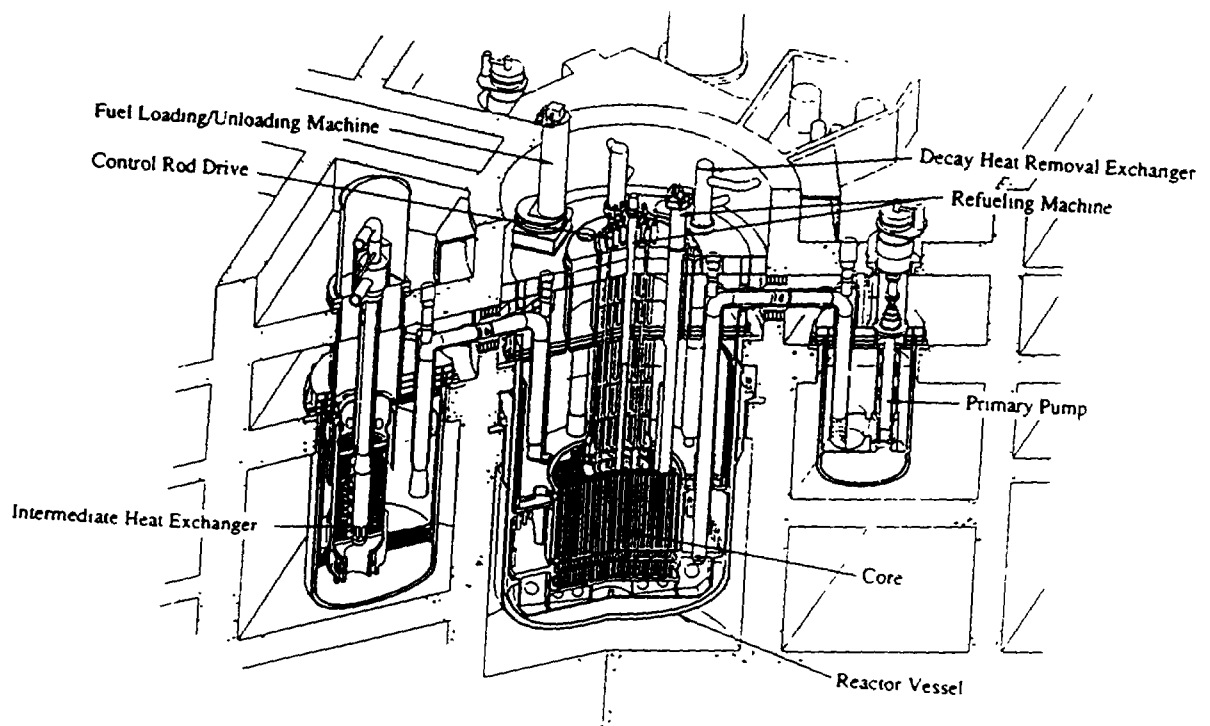


FIG.5.13. Bird's eye view of the primary system and IHX of DFBR

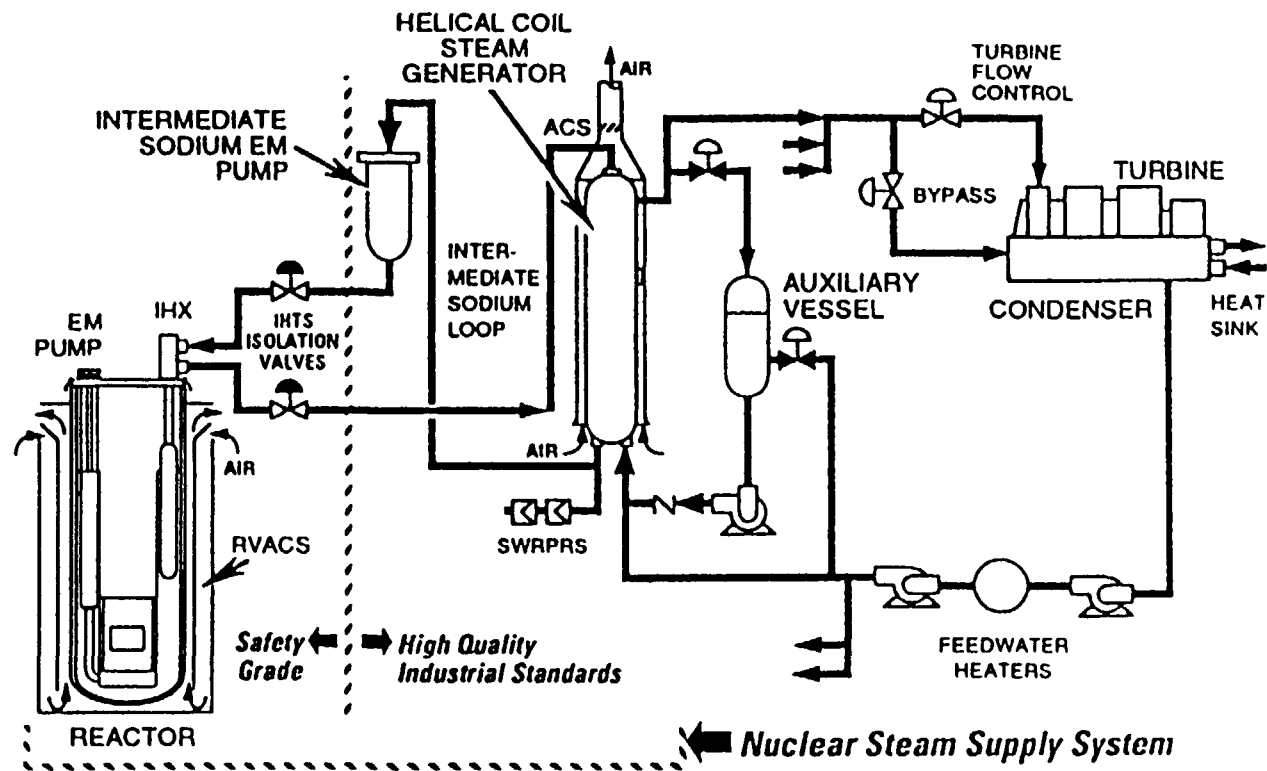


FIG.5.14. ALMR main power system

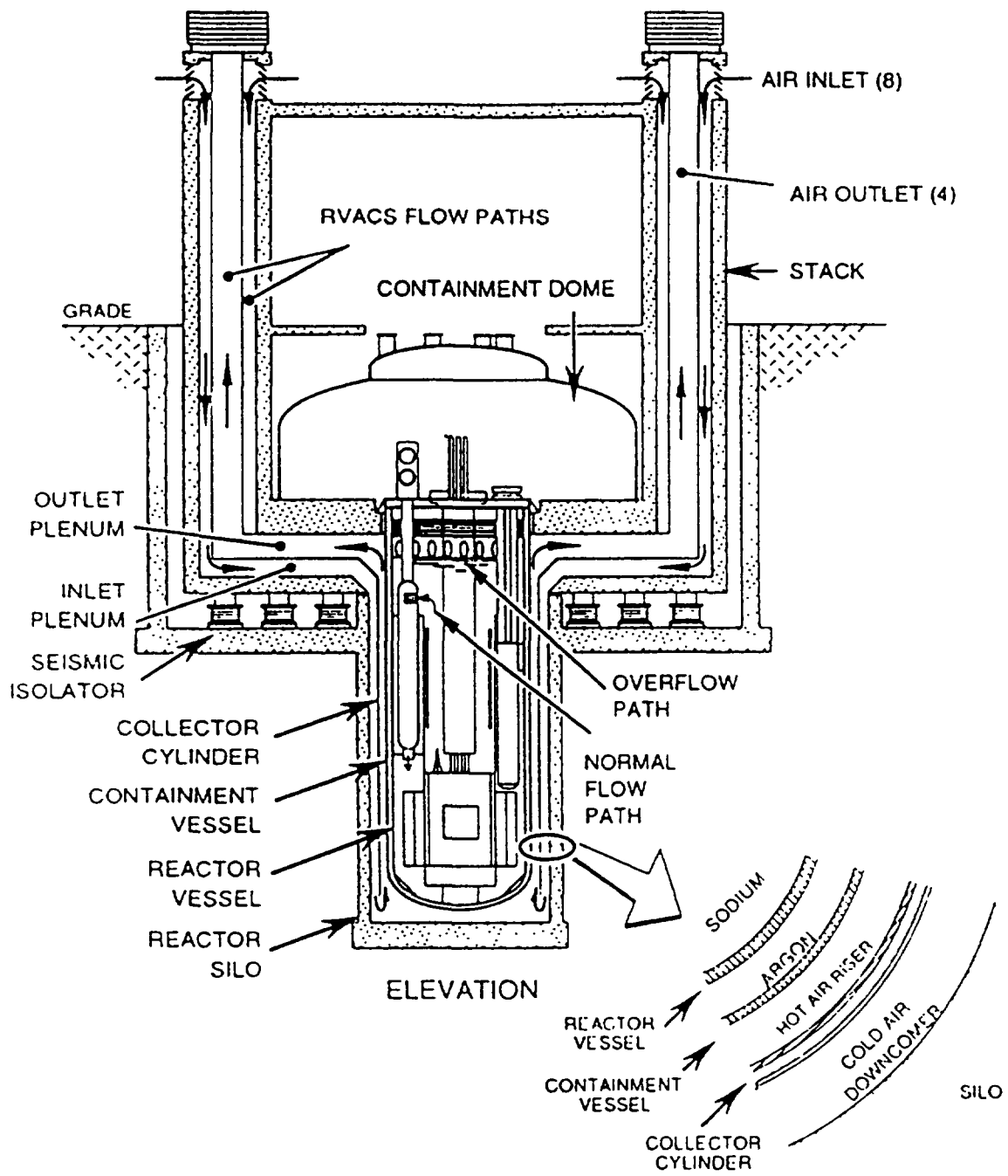


FIG.5.15. Reactor vessel auxiliary cooling system of ALMR

(IHXs) to the bottom of the vessel and then upward into the pump duct. The sodium then enters eight inlet pipes which lead to the high pressure core inlet plenum [5.57-5.59].

Second, a parallel sodium flow path becomes available after sodium temperatures have increased and the corresponding sodium volume expansion has resulted in overflow through slots provided in the reactor vessel liner, and downward through an annular gap between the reactor vessel and its liner. This path allows the sodium to give up some of its heat directly to the reactor vessel wall prior to exiting at an elevation near the IHX outlets. The remainder of the flow path is the same as during normal operation.

The practicality and economic viability of the use of RVACS for decay heat removal decreases with increase in reactor module rating. It is currently believed that the use of RVACS has advantages up to a reactor module rating of 500 MWe based on current technology. For larger module ratings, the size of the reactor vessel needed to reject the heat starts to increase faster than that required to accommodate the in-vessel components. Proposed air-side heat transfer enhancement methods may eventually allow the economic and practical use of RVACS for somewhat large reactor modules. However, for all the large monolithic plant concepts in the 1200 to 1500 MWe rating range being studied in several nations today, the use of RVACS is not practical. Instead, the use of multiple, naturally circulating heat removal loops, referred to as the Direct Reactor Auxiliary Cooling System (DRACS), has emerged as the preferred safety-related shutdown heat removal system concept.

The design of RVACS decay heat removal systems is supported by the following experimental and theoretical investigations:

- ANL Water Simulation Test (1:5.24 scale model of ALMR)
- ETEC Sodium Model Test (scale model of configuration similar to ALMR)
- FFTF IDS Air Natural Convection Test (air-side heat transfer test in the interim decay storage [IDS] at FFTF)
- ANL Air-Side Test (prototype RVACS configuration simulated).

For interpretation of the tests and application of the results the COMMIX code has been applied.

In contrast with the ALMR, decay heat is removed from the PHENIX reactor by the following two systems [5.60]:

1. The secondary cooling system: Under normal operating conditions three secondary coolant loops transfer decay heat to the steam generators by forced convection, which are cooled by natural convection of air within their compartments. Just one of the three loops is sufficient for the decay heat removal function.
2. The emergency cooling system: Under faulted conditions the decay heat is removed from the double wall reactor tank to a third, so-called safety tank, which has a water-filled tube coil system on its outer surface (Fig. 5.16). To improve the heat transport between the double tank and the safety tank it is foreseen to replace the nitrogen by helium totally or partly. The emergency cooling system comprises two independent circuits, each supplying water to half the tubes and coils, three pumps, and two heat exchangers. The two circuits are isolated from one another by a single valve. Of the three pumps two are normally operating, with the third on standby. In the event of loss

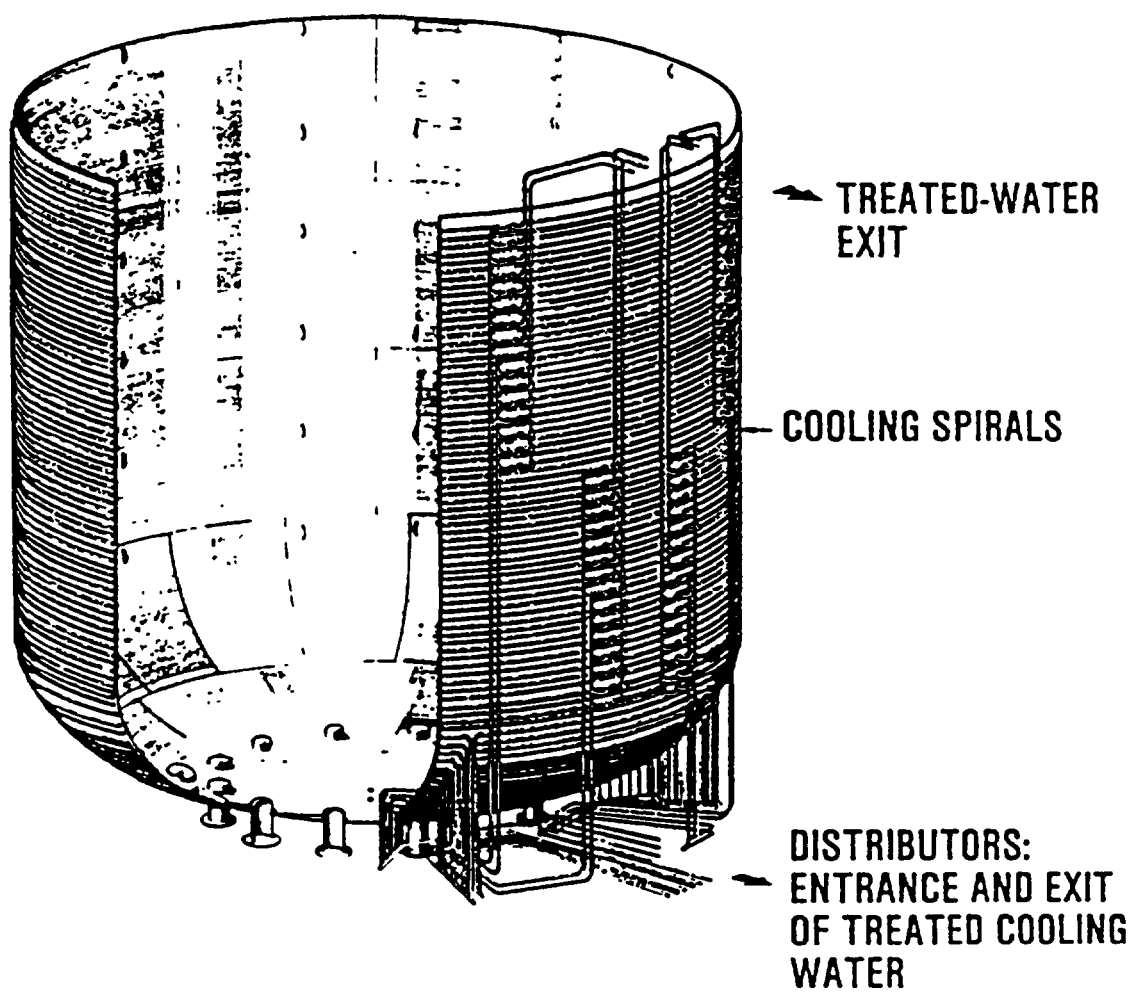


FIG.5.16. *PHENIX safety tank - emergency cooling system*

of off-site power, the pumps are powered by the diesel generators after 3 seconds. Heat removed by the coolant is transferred to raw water circulating in heat exchangers.

To improve the emergency cooling in case of failure of the secondary circuits, circulation of secondary sodium from the IHXs through an air cooler in an outer loop has been considered.

The emergency cooling circuits have a secondary permanent function: during normal operation, treated water is circulated through them to remove heat from the cylindrical part of the safety vessel and its lower head, the roof slab including penetrations, the primary containment concrete penetrations for auxiliary system pipes, and the upper part of the vessel.

Concept 3 (Combined DHR versions)

For SUPERPHENIX [5.61, 5.62] the decay heat removal systems are designed to attain two objectives:

- operating objective: after shutdown, to cool the reactor rapidly and keep it at a temperature compatible with handling and maintenance operations
- safety objective: to ensure core cooling, and keep structure temperatures at a level compatible with containment integrity under all nuclear steam supply systems (NSSS) design basis operating conditions (Figs. 5.17, 5.18).

The NSSS Decay Heat Removal Systems are:

- the secondary sodium-air exchangers (BPR system),
- the emergency sodium cooling circuits (RUR system),
- the vessel cavity cooling circuit (RUS system).

In the case of unavailability of the normal water/steam system at SUPERPHENIX, decay heat is removed by 4 sodium-air-exchangers, each located on a secondary loop by-pass line and designed to operate even in the event of an air-supply failure. Sodium circulates by forced convection (BPR system).

The cooling air flow is normally supplied by a motor-driven fan. However, in the event of unavailability of the fan, natural air circulation can be obtained by means of the draft created in a stack placed over the exchanger.

Should this system be unavailable, decay heat is removed by four emergency cooling loops (RUR system), each comprising a sodium-sodium heat exchanger immersed in the main vessel, an electromagnetic pump and a sodium-air heat exchanger. This system is permanently in service, the decay heat being removed, when necessary, by opening air-inlet shutters on the sodium-air heat exchangers. The loops are normally working with forced sodium circulation, but in case of natural sodium circulation the heat removal is reduced.

In addition the safety tank around the double-walled tank is cooled by water pipes as in PHENIX (RUS system).

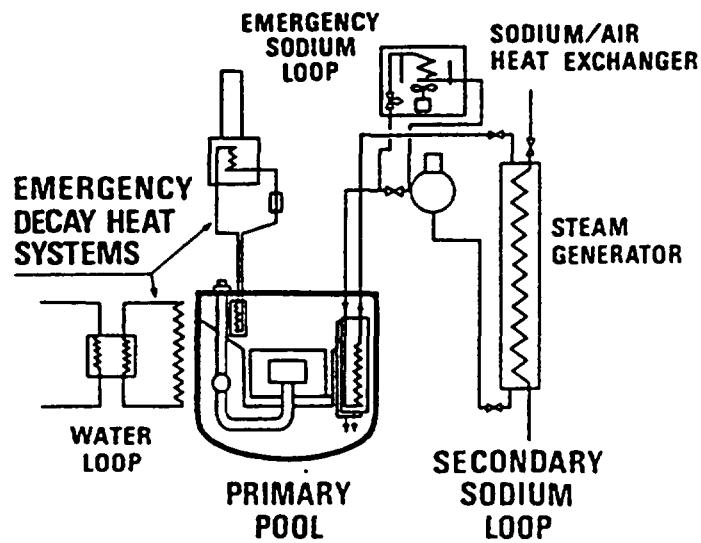


FIG 5 17. *SUPER-PHENIX decay heat removal system*

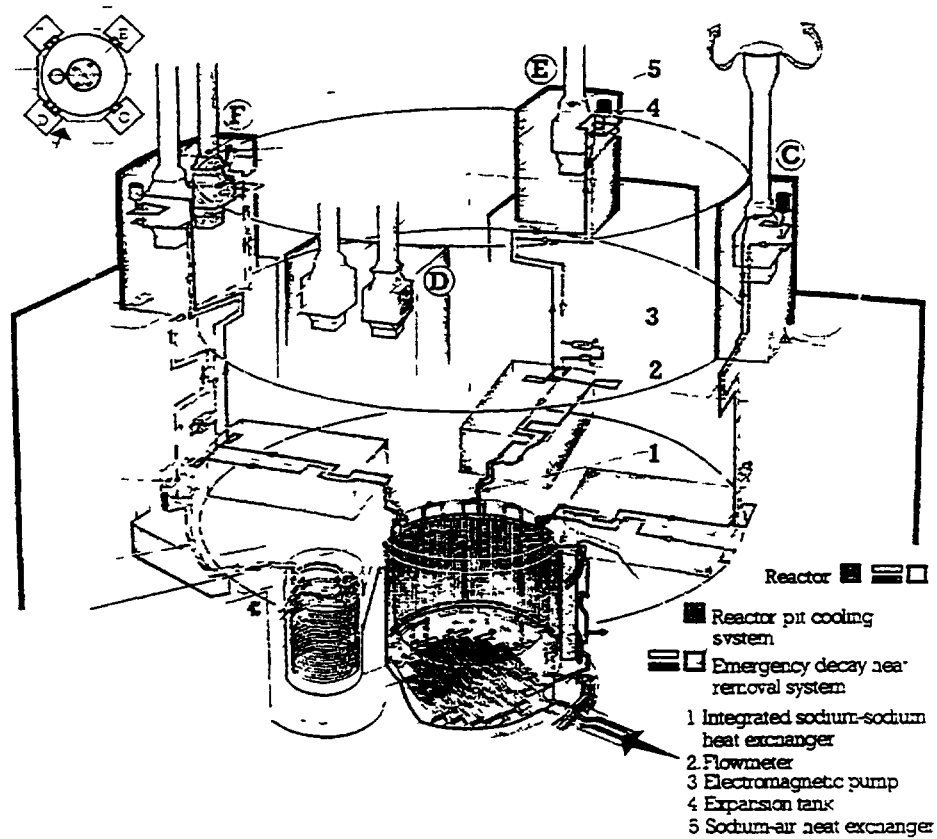


FIG 5 18 *Reactor decay heat removal of SPX*

Concept 4 (DHR from the secondary loops)

The rated thermal output of MONJU [5.63, 5.64] is transported through the primary heat transport system (PHTS) and intermediate heat transport system (IHTS) loops to the steam generators. Shutdown heat removal is normally by forced circulation (FC) provided by pony motors associated with each of the loop pumps. Heat is rejected to air at the air blast heat exchanger of the intermediate reactor auxiliary cooling system (ACS) which branches off from each IHTS loop. Thus the auxiliary cooling system (ACS) of the Monju reactor is coupled with the secondary system which also has the role as decay heat removal system.

The relative elevations of the core, IHX, an air cooler (AC) of the ACS and steam generator (SG) are appropriately arranged to assure natural circulation of the sodium in each primary and secondary loop.

The three independent ACSs are also designed as an engineered safety system and provide decay heat removal not only for maintenance and refuelling, but also for emergency conditions such as a loss of power or a piping failure.

The ACS is shown schematically in Fig. 5.19. At normal operating conditions the ACS is in stand-by and only a small amount of sodium flows through a bypass line around the AC outlet valve. This sodium flow keeps the sodium temperature at the AC outlet the same as that of the SG outlet.

In order to start up the ACS for decay heat removal, the secondary sodium flow path changes from the SG to the ACS by closing the SG inlet valve and by opening the AC outlet valve, following a change from the main motor to the pony motor for coolant circulation. It is also necessary to start a blower on the AC. While the ACS is operating for decay heat removal, the sodium temperature at AC outlet is controlled with an air dump and an inlet vane of the AC to reduce thermal shock and sodium over-cooling.

Although pony motors on the pumps of the primary and secondary loops are required to operate after normal or accidental shutdown of the reactor, natural convection DHR capability is preserved under extreme conditions, e.g. in case of both off-site power supplies and diesel generators being unavailable.

A maintenance cooling system (MCS) is provided (see Fig. 5.20) for the purpose of removing the decay heat during the maintenance period. Analysis has indicated that, after 20 hours following the reactor shutdown, the MCS can successfully remove generated decay heat.

To confirm the validity of the operation method mentioned above, a 1/5 scale model of ACS was installed in the 50 MWt SG test facility. Various tests were conducted to simulate the operation of the actual system. These results were reflected in the design of the ACS. The AC was also designed on the basis of research and development studies on the thermal and fluid dynamics characteristics of the system.

BN 600 is equipped with a similar ACS [5.65].

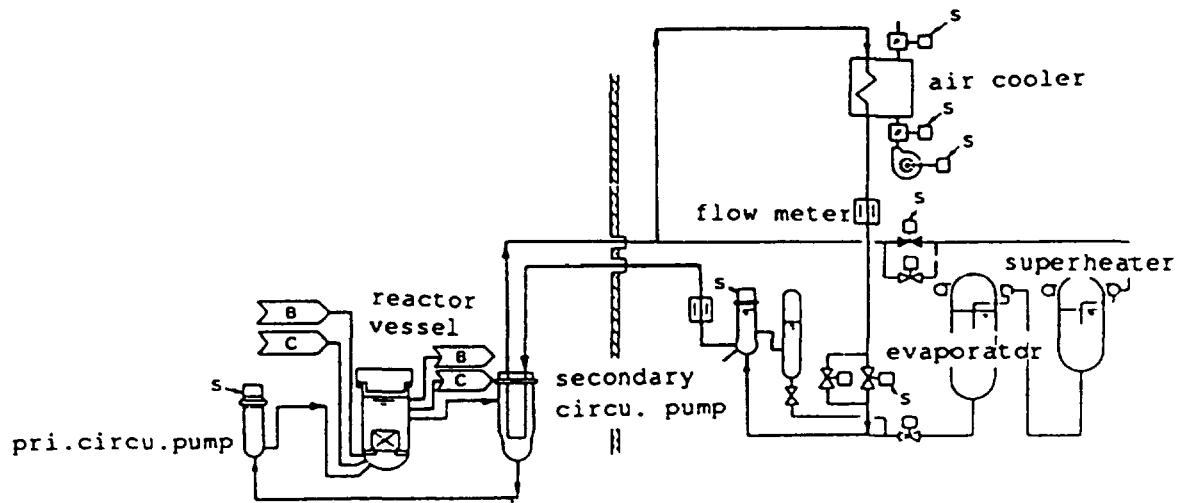


FIG.5.19. Schematic flow diagram if the auxiliary cooling system of Monju

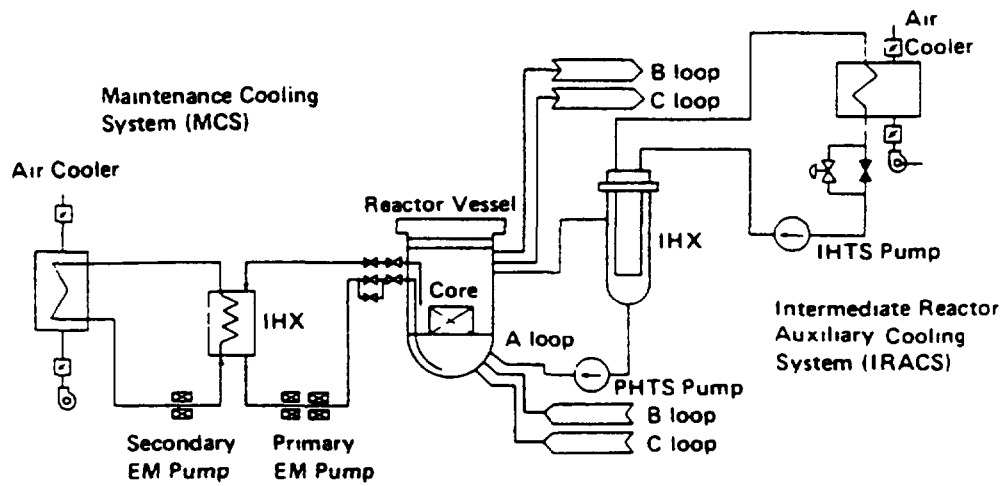


FIG.5.20. Flow diagram of decay heat removal system and maintenance cooling system of Monju

5.2.3. Status of international R&D activities and future needs

Experimental activities

Concerning the experiments, a very large number of tests has been performed up to now in various countries [5.64] to study decay heat removal phenomena under faulted conditions:

- (a) Different scaled models: 1:20 - 1:1
- (b) Different geometries: slab, sector and full model
- (c) Different fluids: water (many), sodium and air.

In most cases local temperature fields have been measured in free spaces (hot/cold plena, channels etc.). Measurements of local velocity fields have been carried out in a few cases, mainly related to simplified geometries.

On the basis of existing experimental results, it can be concluded that the thermohydraulics can be described globally mainly for natural convection conditions, but more emphasis has to be directed to the investigation of problems such as:

- Hot and cold jets, e.g. at the outlet of the core and the DHX,
- Scaling effects giving rise to different flow regimes,
- Penetration of flow under the above core structure and outer fuel elements, and backflow in fuel elements,
- Interwrapper flow,
- Creation of more detailed models.

Investigations of the complete DHR heat sink (DHX, stack and dampers) under steady state, natural convection and transient operation conditions, have shown that no problems occur.

Code development and validation

Extensive development and validation of multidimensional codes has been carried out. The comparison of computed and experimental results has provided a successful demonstration of the potential of 3D and 2D modelling. Qualitatively good results have been obtained. Quantitative results are reasonable depending on the modelling.

As a result of development and validation activities the following aspects of the codes have been identified as critical:

- Local mesh refinement,
- Body fitted coordinates,
- Robust solvers,
- Improved differencing schemes,
- Improved modelling of turbulent momentum transport (k-e models, large-scale eddy simulation),
- Improved modelling of turbulent heat transport,
- Modelling of heat conduction and capacity in structures,
- Radiation.

In particular the modelling of turbulent transport of momentum and heat has to be improved.

5.2.4. General conclusions

- (a) Two main DHR systems for advanced LMFR concepts are under consideration:
- Direct reactor auxiliary cooling system (DRACS) with immersed DHX in main vessel, intermediate sodium loop and Na-air heat exchangers.
 - Auxiliary cooling system which removes heat from the outside surface of the reactor vessel by natural convection of air (RVACS).

The practicability and economic viability of the use of RVACS is possible up to a modular type reactor or a middle size reactor based on current technology. For the large monolithic plant concepts DRACS is preferable.

- (b) The existing experimental results and the codes show encouraging results so that the decay heat removal by pure natural convection is feasible. DHR by pure natural convection is an essential feature of "passive safety".

REFERENCES

- [5.1] Waltar, A.E., Reynolds, A.B., Fast Breeder Reactors, Pergamon Press - New York, USA, (1981).
- [5.2] Farmer, F.R., Reactor Safety and Siting: a Proposed Risk Criterion. Nuclear Safety (1967).
- [5.3] Rasmussen, N. C., Reactor Safety Study: an Assessment of Accident Risks in US Commercial Nuclear Power Plants, Main report, Rep. WASH 1400 - MR (NUREG - 75/014), United States Nuclear Regulatory Commission -Washington, DC, USA, (1975).
- [5.4] Accident Risks: "an Assessment for Five US Nuclear Power Plants" - Rep. NUREG 6-1150, Washington DC., USA, (1989).
- [5.5] Basic Safety Principles for Nuclear Plants, IAEA Safety Series n° 75 - INSAG-3, 1988.
- [5.6] The Safety of Nuclear Power, INSAG-5, IAEA, 1992.
- [5.7] Status of Liquid Metal Cooled Fast Breeder Reactors, IAEA Technical Reports Series n° 246 (1985).
- [5.8] Fiorini, G.L., et.al., The ABACUS Programme: Experimental Study of Phenomenology Involving Subassembly Blockage; Computer Codes., - ENS Safety Lyon, France, 13-23 July, 1982, Proceedings - Vol. IV (1982).
- [5.9] Natural Circulation of Na in a 37-Electrically Heated Bundle: Results of the Scarlette., Experiments and Application. Decay Heat Removal in LMFB Subassemblies", ASME WINTER MEETING, Boston, USA, December 13-18, 1987.
- [5.10] BACCHUS: a Numerical Approach of two Phase Flow in a Rod Bundle. Nucl. Eng. - December, 1982.
- [5.11] Macdougall, J.D, Sabre 3B: a Version of the Sabre Computer Program for the Calculation of Flows in Rod Clusters, AEEW-M1850, June, 1981.
- [5.12] Livolant, M., et al., Scarabee: A Test Reactor and Programme to Study Fuel Melting and Proposition in Connection with Local Faults. Objections and Results, International Fast Reactor Meeting - Snowbird, USA, August 12-16, 1990.
- [5.13] Papin, J., et al., The Scarabee Total Blockage Series: Synthesis of the Interpretation, Nureth-4, 1, Karlsruhe, Germany, 0-13 October, 1989, FRS.
- [5.14] Papin, J., Stansfield, R., Thermal-Hydraulic Behaviour of a Fast Breeder Reactor Subassembly During an Undercooling Accident: the PHYSURA-GRAPPE Code and its Validations on Scarabee Experiments, NURETH-4, Karlsruhe, Germany, 10-13 October, 1989, FRG.
- [5.15] Anziev, J.M., et al., SURFASS-a Computer Code Describing the Consequences of total instantaneous blockade of a Subassembly on the RNR 1500, Proc. Int. Conf. on Science and Technology of Fast Reactor Safety. GUERNESEY 12 May, 1986, Vol. 1.
- [5.16] Borms, L., et al., Experiments MOL 7C/6 and MOL 7C/7: Results of Source Term Measurements, Proceedings of International Fast Reactor Safety Reactors - Snowbird-USA, August 12-16, 1990, Vol 1.
- [5.17] Weimar, P., Scheleisick, K., PIE Results of the in Pile Blockage Experiments MOL 7C/4 and 5. Discussion and Interpretation, - Ibid, Vol 1.
- [5.18] Analysis of the MOL 7C Experiments with the SIMMER II Code. Proceedings of the 14th Meeting of the Liquid Metal Boiling Working Group - Brasimone/Italy, 16-18 April, 1991.
- [5.19] Moxon, D., et al., An Interpretation of the Pump Trip and Inlet Blockage Series, Conf. on Science and Technology of Fast Reactor Safety, GUERNESEY, 1986.

- [5.20] Moreau, J., et al., Assessment of Local Meeting in a Typical Breeder Reactor: Lessons from MOL 7C and Scarabee Experiment., Ibid, Vol. 1.
- [5.21] Chappene, J., et al., Combined Sodium Fires - Experiments and Code Development, Ibid, Vol. 1.
- [5.22] Malet, J.C., European Experimental and Analytical Studies Concerning Sodium Combined Fires, International Fast Reactor Safety Meeting, Snow-bird, USA, 1990.
- [5.23] Dufresne, J., et al., Sodium Concrete Interaction, LMFBR Topical Meeting - Lyon, France, 1982.
- [5.24] Muhlestein L.D, Application of Na Concrete Reaction data to Breeder, Reactor Safety Analysis. Nuclear Safety. Vol. 25, April, 1984.
- [5.25] Puo-Antilla, a Sodium Concrete Ablation Model, NUREG/CR-2099, SAND 81-0415, October, 1981.
- [5.26] Empirical Models for the Thermal Decomposition of Concrete. Powers Trans, Vol. 26 (1977)
- [5.27] Malet, J.C., et al., Sodium Concrete Interaction Experimental Studies and Modeling, Fourth International Conference (LIMET) 1988, Avignon, France.
- [5.28] del Beccaro, R., et al., The EFR Safety Approach", Proc. of the International Conference on Design and Safety of Advanced Nuclear Power Plants, Tokyo, Japan, October, 1992, Vol. 3.
- [5.29] Noel, H., et al., "EFR Programme, Design Progress and Main Achievements", Proc. of the Internat. Conference on Fast Reactors and Related Fuel Cycles, Kyoto, Japan, 1991, Vol. 2.
- [5.30] Gyr, W., et al., EFR Decay Heat Removal System, Design and Safety Studies, Proc. of the Intern. Fast Reactor Safety Meeting, Snow-bird, USA, 12-16 August, 1990.
- [5.31] Morgenstern, F.H., "Safety Characteristics of Decay Heat Removal Systems", Proc. of the IAEA Specialists' Meeting on Passive and Active Safety Features of LMFBRs, Oarai, Japan, 1991.
- [5.32] Düweke, M., et al., The Direct Reactor Cooling System of EFR, Overview and R&D Activities, Proc. of the Intern. Fast Reactor Safety Meeting, Snow-bird, USA, 12-16 August 1990.
- [5.33] Webster, R., Natural Convection Cooling of Liquid Metal Systems - A Review, DNR 16, AEA, Dounreay, United Kingdom, February, 1990.
- [5.34] Hoffmann, H., et al., The European R&D Programme on Natural Convection Decay Heat Removal for the EFR, Proc. of the Internat. Conference on Fast Reactors and Related Fuel Cycles, Kyoto, Japan, 1991, Vol. 2.
- [5.35] Hofmann, F., et al., Investigations on Natural Convection DHR for the EFR - Status of the Programme, Proc. of the IAEA Specialists' Meeting on Evaluation of Decay Heat Removal by Natural Convection, Oarai, Japan, 1993.
- [5.36] Valentin, B., et al., Natural Convection Tests in Phénix Experiments, Proc. of the Intern. Fast Reactor Safety Meeting, Snowbird, Utah, USA, 12-16 August, 1990, Vol. IV.
- [5.37] Fave, D., et al., Natural Circulation Tests on SPX 1, Proc. of the Intern. Fast Reactor Safety Meeting, Snowbird, USA, 12-16 August, 1990, Vol. IV.
- [5.38] Satoh, K., et al., Summary View on Demonstration Reactor Safety, Proc. of the IAEA Specialists' Meeting on Passive and Active Safety Features of LMFBRs, Oarai, Japan, 1991.
- [5.39] Kotake, S., et al., Application of the PSA Method to Decay Heat Removal Systems in Large Scale FBR Design, Proc. of the IAEA Specialists' Meeting on Evaluation of Decay Heat Removal by Natural Convection, Oarai, Japan, 1993.

- [5.40] Miura, M., et. al., Safety Design Consideration for Japanese DFBR, Proc. of the Internat. Conference on Fast Reactors and Related Fuel Cycles, Kyoto, Japan, 1991.
- [5.41] Miura, M., et al., Present Status of DFBR Design in Japan, Proc. of the Intl. Conference on Design and Safety of Advanced Nuclear Power Plants, Tokyo, Japan, 1992.
- [5.42] Sawada, M., et al., Experiment and Analysis on Natural Convection Characteristics in Experimental Fast Reactor Joyo, Nuclear Engineering and Design, 1994.
- [5.43] Sasaki, K., et al., Study on Decay Heat Removal Characteristics by Natural Circulation for Top Entry Loop-Type FBR, Proc. of the Internat. Conference on Fast Reactors and Related Fuel Cycles, Kyoto, Japan, 1991.
- [5.44] Koga, T., et al., Natural Circulation Water Tests for Top Entry Loop-Type LMFBFR, Proc. of the Sixth Internat. Topical Meeting on Nuclear Reactor Thermal Hydraulics, Grenoble, France, 1993.
- [5.45] Ieda, Y., et al., Strategy of Experimental Studies in PNC on Natural Convection Decay Heat Removal, Proc. of the IAEA Specialists' Meeting on Evaluation of Decay Heat Removal by Natural Convection, Oarai, Japan, 1993.
- [5.46] Kamide, H., et al., Multi-bundle Sodium Experiments for Thermohydraulics in Core Subassemblies during Natural Circulation Decay Heat Removal Operation, Proc. of the IAEA Specialists' Meeting on Evaluation of Decay Heat Removal by Natural Convection, Oarai, Japan, 1993.
- [5.47] Gregory, C.V., Passive and Engineered Safety Features of the PFR, Proc. of the IAEA Specialists' Meeting on Passive and Active Safety Features of LMFBFRs, Oarai, Japan, 1991.
- [5.48] Mitenkov, F.M., et al., "BN 1600 Reactor Plant Main Decisions and Characteristics, Proc. of the Internat. Conference on Fast Reactors and Related Fuel Cycles, Kyoto, Japan, 1991.
- [5.49] Buksha, Yu K., The Status of Work in the USSR on Using Self-protection Features of Fast Reactors, of Passive and Active Means of Shutdown and Decay Heat Removal Systems, Proc. of the IAEA Specialists' Meeting on Passive and Active Safety Features of LMFBFRs, Oarai, Japan, 1991.
- [5.50] Birbraer, P.N., et al., Comparison of Decay Heat Exchangers Placing in the Primary Circuit of Pool Type Fast Reactor, Proc. of the IAEA Specialists' Meeting on Evaluation of Decay Heat Removal by Natural Convection, Oarai, Japan, 1993.
- [5.51] Xu Mi, Chinese FBR Programme and its First FR Conceptual Design, Proc. of Internat. Conference on Fast Reactors and Related Fuel Cycles, Kyoto, Japan, 1991, Vol. 2.
- [5.52] Paranjpe, S.R., An Update on Indian Fast Breeder Programme, Proc. of Internat. Conference on Fast Reactors and Related Fuel Cycles, Kyoto, Japan, 1991.
- [5.53] Paranjpe, S.R., Overview of Indian Position - Passive and Active Safety Features of LMFBFRs, Proc. of the IAEA Specialists' Meeting on Passive and Active Safety Features of LMFBFRs, Oarai, Japan, 1991.
- [5.54] Kasinathan, N., et al., An Overview of DHR Studies for Indian FBR Program, Proc. of the IAEA Specialists' Meeting on Evaluation of Decay Heat Removal by Natural Convection, Oarai, Japan, 1993.
- [5.55] Herzog, J.W., et al., US ALMR Safety Approach and Licensing Status, Proc. of the Internat. Conference on Design and Safety of Advanced Nuclear Power Plants, Tokyo, Japan, 1992, Vol. 3.
- [5.56] Berglund, J.R.C., et al., Performance and Safety Design of the Advanced Liquid Metal Reactors, Proc. of the Internat. Conference on Fast Reactors and Related Fuel Cycles, Kyoto, Japan, 1991, Vol. 2.

- [5.57] Boardman, C.E., Hundsbedt, A., Performance of ALMR Passive Decay Heat Removal Systems, Proc. of the IAEA Specialists' Meeting on Passive and Active Safety Features of LMFBRs, Oarai, Japan, 1991.
- [5.58] Hundsbedt, A., Experiments and Analyses in Support of the US ALMR Thermal-Hydraulic Design, Proc. of the IAEA Specialists' Meeting on Evaluation of Decay Heat Removal by Natural Convection, Oarai, Japan, 1993.
- [5.59] Glueckler, E.L., et al., Advanced Liquid Metal Reactor (ALMR) R&D Program-Focus on Innovation, Proc. of the Internat. Conference on Fast Reactors and Related Fuel Cycles, Kyoto, Japan, 1991, Vol. 2.
- [5.60] Jubault, M., et. al., Fast Neutron Reactor Safety Reliability Analysis of PHENIX Decay Heat Removal Function, Proc. of ENS Conference on Fast Reactor Safety, Seattle, USA, 1979.
- [5.61] Delbergh, Ph., et al., Decay Heat Removal at SUPER-PHENIX. Experience Gained on Sodium-Air Heat Exchangers during Start-up Tests, Proc. of ENS Conference on Fast Breeder Systems, Richland, Washington, USA, 1987.
- [5.62] Lauret, L., et al., SUPER-PHENIX Decay Heat Removal Design and Operation Aspects, Proc. of LMFBR Safety Topical Meeting, Lyon, France, 1992, Vol. 2.
- [5.63] Ninokata, H., Izumi, A., Decay Heat Removal System of the Monju Reactor Plant and Studies Related to the Passive Actuation and Performances, Proc. of the Internat. Fast Reactor Safety Meeting, Snow-bird, USA, 1990.
- [5.64] Oda, T., et al., Design and Construction of Heat Transport Systems of the Prototype Fast Breeder Reactor Monju, Proc. of the Internat. Conference on Fast Reactors and Related Fuel Cycles, Kyoto, Japan, 1991.
- [5.65] Kotchetkov, L.A., Kiryushin, A.I., Fast Breeder Reactors in the USSR, Proc. of the Internat. Conference on Fast Reactors and Related Fuel Cycles, Kyoto, Japan, 1991, Vol. 1.

Chapter 6

SOME ASPECTS OF INSTRUMENTATION AND INSPECTION OF MAIN LMFR COMPONENTS

6.1. STEAM GENERATOR: DESIGNS, INSTRUMENTATION AND PROTECTION

A valuable comprehensive survey of the design of steam generators for LMRs (and other types of reactor) is given by Mitenkov et al [6.1]. They include summaries of the steam generator design parameters for many of the world's fast reactors and information on performance.

6.1.1. Configuration

Steam cycle. The design of the steam generators for an LMFR depends on the nature of the power plant. If the steam conditions are sub-critical, a choice has to be made between once-through steam generators or recirculating boilers with separate evaporators and superheaters. In the former dryout occurs in the heated part of the tubes, and there is a possibility of fluctuating thermal stresses and precipitation of corrosive impurities in this region. In the latter the evaporators generate a saturated mixture of steam and water and the tube walls are always wetted. The two phases are separated, either in steam dryers at the evaporator exit or in separate steam drums, and the water is recirculated while the steam passes to the superheaters. If the steam conditions are supercritical there is no sharply-defined dryout point and once-through steam generators are used. Once-through steam generators are less complex and therefore tend to be less expensive.

Another important choice is between sodium-heated or steam-heated reheaters. Sodium reheat gives slightly higher thermal efficiency in principle, but has the disadvantage of more extensive high-pressure pipe work. This is because it is undesirable to bring sodium into the vicinity of the steam turbine, so the partly-expanded steam has to be taken from the turbine to the steam generator area for reheat and back again. More compact and economical steam plant layout can be achieved with steam reheat or, with only a small additional loss of thermal efficiency, with no reheat at all. In this case moisture separators are installed between the turbine stages.

Figure 6.1. shows a steam cycle with recirculating boilers and steam drums, and with sodium reheat. It is based on the PFR design of the early 1970s [6.2]. Figure 6.2. shows a steam cycle with once-through boilers and no reheat, based on the EFR design of the 1990s [6.3].

Heat transfer area. The overall sizing of sodium-heated steam generators is determined by the limitation of heat transfer on the steam side of the tubes [6.4]. For reasonable steam flow-rates of around 1 kg/s per tube, and for tube diameters about 20 mm, overall heat transfer coefficients of the order of 7 kW/m²K are typical. If the logarithmic mean temperature difference across the tubes is limited to 40 K, the total heat transfer area needed for a 3600 MWth reactor is about 13000 m², which implies a total tube length of about 200 km. The maximum length at which tubes can currently be manufactured is about 20 m, so if under-sodium welds in the length of the tubes are to be avoided some 10000 tubes have to be accommodated in the steam generators.

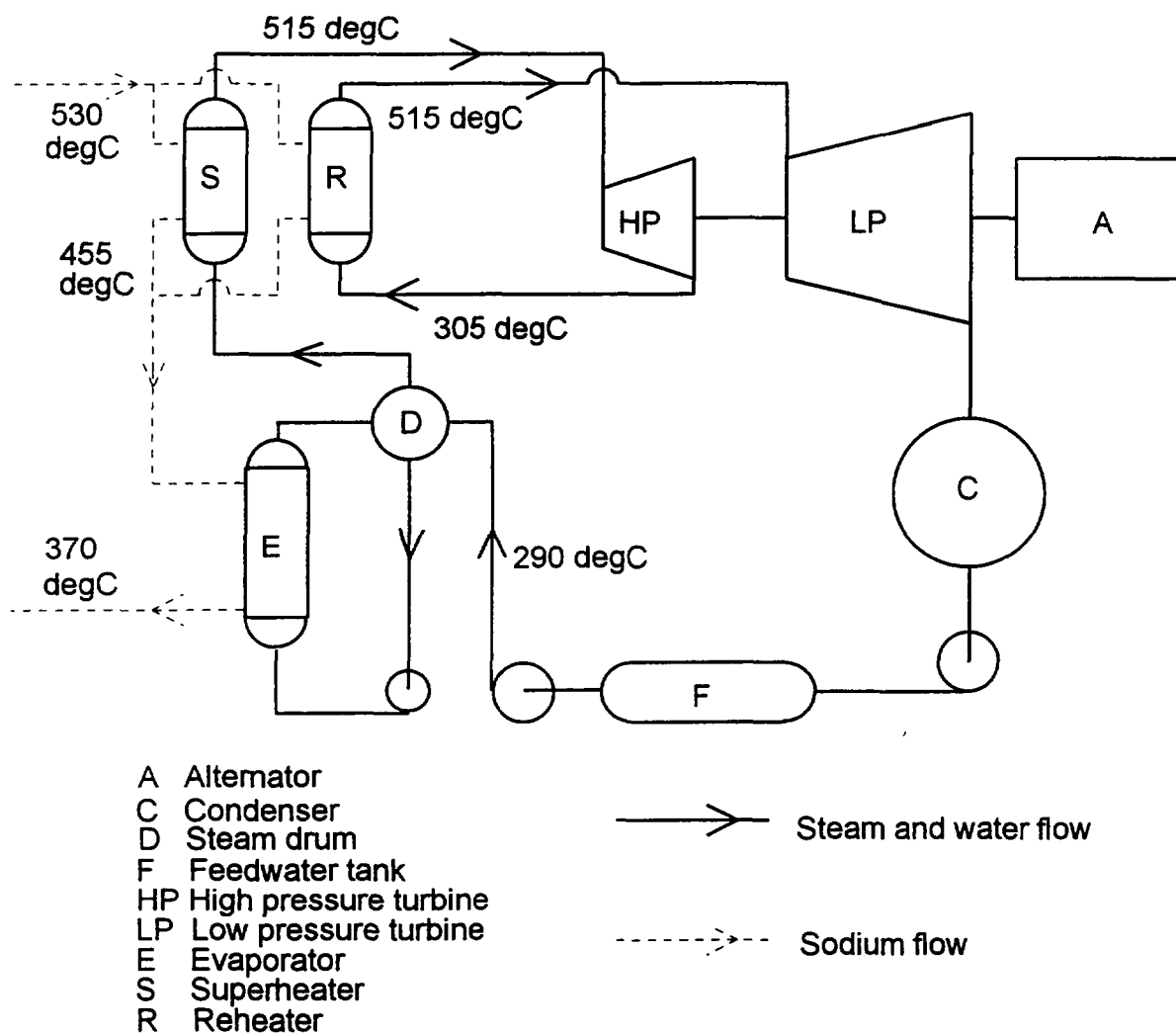


FIG. 6.1. Steam cycle for recirculating boiler with reheat
(Feed heating system not shown)

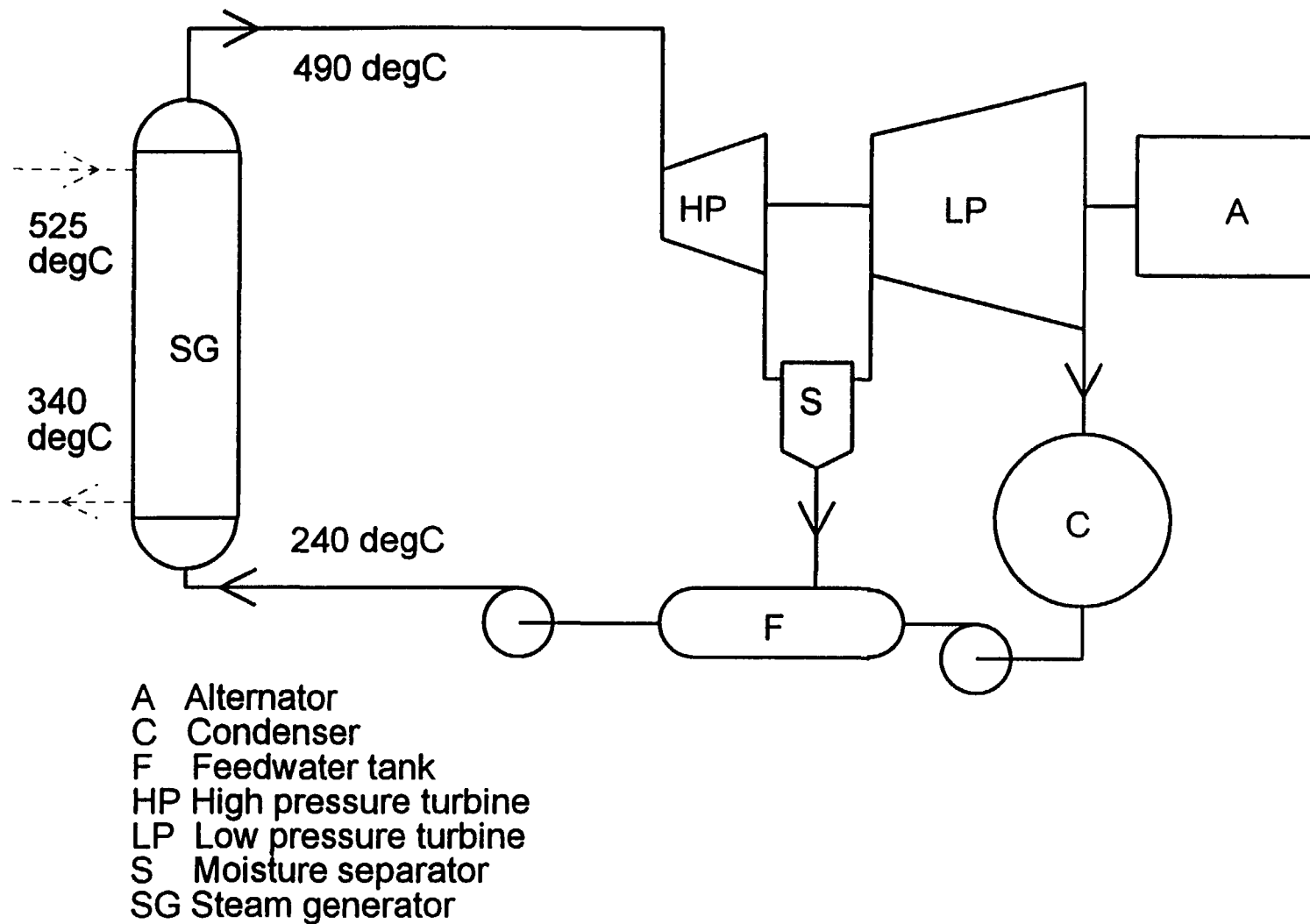


FIG. 6.2. Steam cycle for once-through boiler with no reheat
(Feed heating system not shown)

Number of units. The heat transfer tubes are normally arranged in shell-and-tube heat exchanger units, with the sodium on the shell side. There are two important factors in the determination of the number of separate units: cost, and availability. Considerations of capital cost suggest that the units should be few in number and as large as possible. This minimises the cost of connecting sodium and steam pipework to each of the units, of protective equipment such as bursting discs, effluent systems, and isolation valves, and of control and instrumentation systems. Most recently-designed reactors, especially where capital cost is an important consideration, have a small number of large steam generators. For example the Creys-Malville plant has 4 units [6.5], while the EFR design has 6, one for each secondary circuit [6.3]. The MONJU plant has 6, with a separate evaporator and superheater in each of the three secondary circuits [6.6].

However in the earlier years of the development of fast reactors there was a high incidence of leaks in the steam generators. Since leaks in sodium-heated steam generators are intolerable, however small they may be, whenever a leak occurs the unit in question has to be shut down and isolated for repair. This can be done without serious diminution of the power output only if there are a large number of separate units, any one of which can be isolated without reducing the total power significantly. The outstanding example of the advantages of the modular approach to steam generator design is afforded by the Russian BN-600 plant. This has three secondary sodium circuits, each with 8 separate steam generator modules, and each of these consists of separate evaporator, superheater and reheater sections, making a total of 72 separate heat exchangers. At least partly because of this the availability of BN-600 has been consistently high [6.7].

Arrangement of tubes. Differential expansion between the tubes and the shell, and between individual tubes, has to be taken into account. Because the heat transfer conditions and thermal inertia of tubes and shell are very different positive allowance for differential expansion between the tube bundle and the shell has to be provided. This can be done either by incorporating bends into the tubes, for example in a U-tube, J-tube or helical layout (Figure 6.3), or, if the tubes are straight, by incorporating a bellows into the shell. For example BN-600 and the proposed EFR utilise bellows, whereas Creys-Malville and MONJU have helical tubes.

Stresses due to differential expansion between different tubes have to be kept within acceptable limits. If the tubes have bends this presents little difficulty, but if they are straight it implies close limits on the tube temperatures, both during steady operation and in startup, shutdown, and operational transients. For ferritic tubes the length-averaged temperature differences between tubes have to be kept below about 10 K, corresponding to axial stresses of about 20 MPa. This means that the tube bundle has to be designed very carefully to ensure uniform flow patterns and heat transfer conditions, on both the shell and tube sides.

A Creys-Malville steam generator is shown in Figure 6.4. It has helical tubes. In contrast the proposed EFR steam generator, shown in Figure 6.5, has straight tubes. Both are once-through designs, producing superheated steam at outlet.

In most cases the tubes are welded to tube plates which form part of large, and therefore highly-stressed, entry and exit headers. The tube plates may be flat, or curved as in the EFR design (Figure 6.5). Alternatively the tubes may be joined together in a manifold outside the steam generator vessel, as at Creys-Malville (Figure 6.4). This has the advantage that none of the walls containing sodium, apart from the tubes themselves, and certainly none

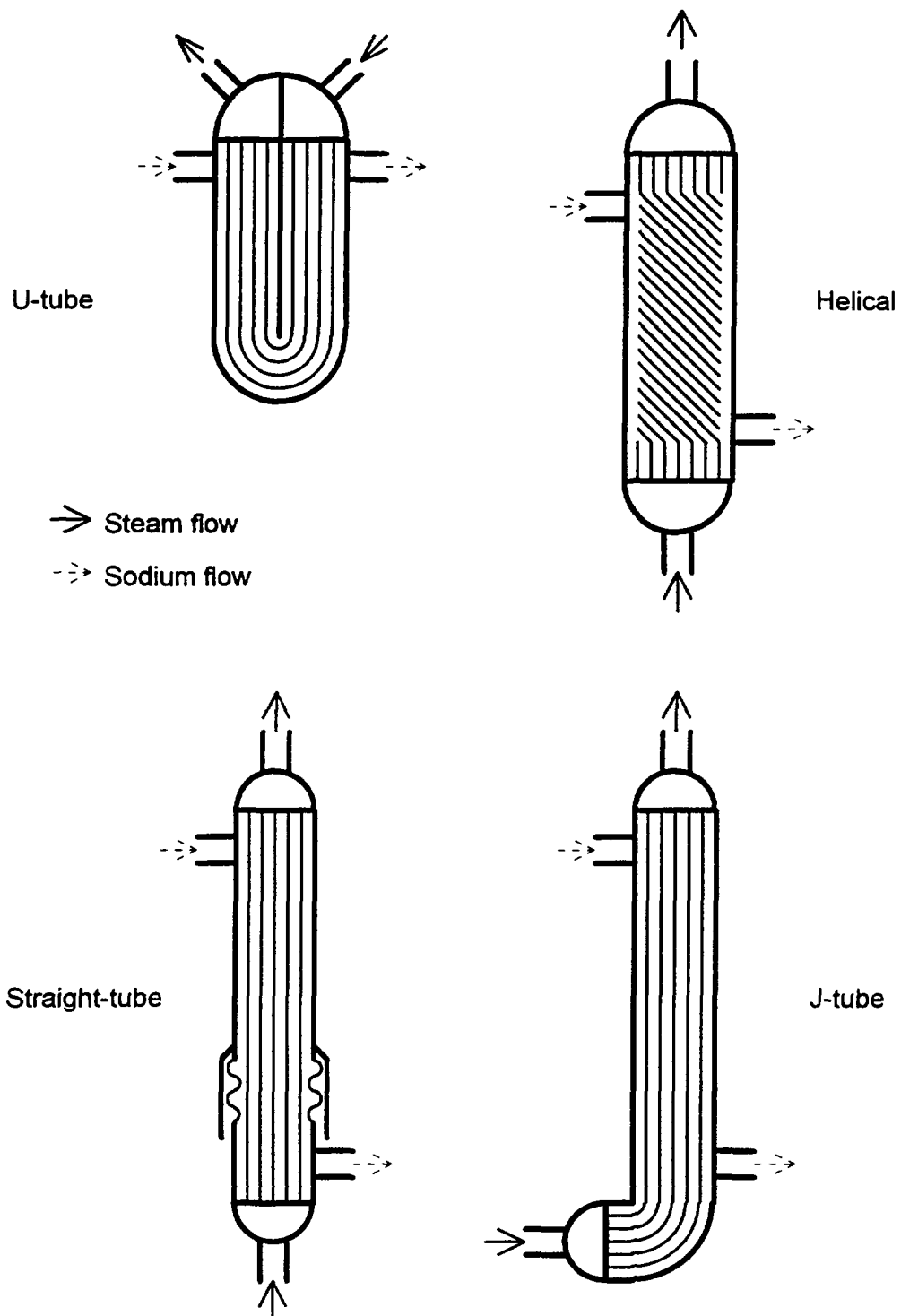


FIG. 6.3. Alternative arrangements of steam generator tubes

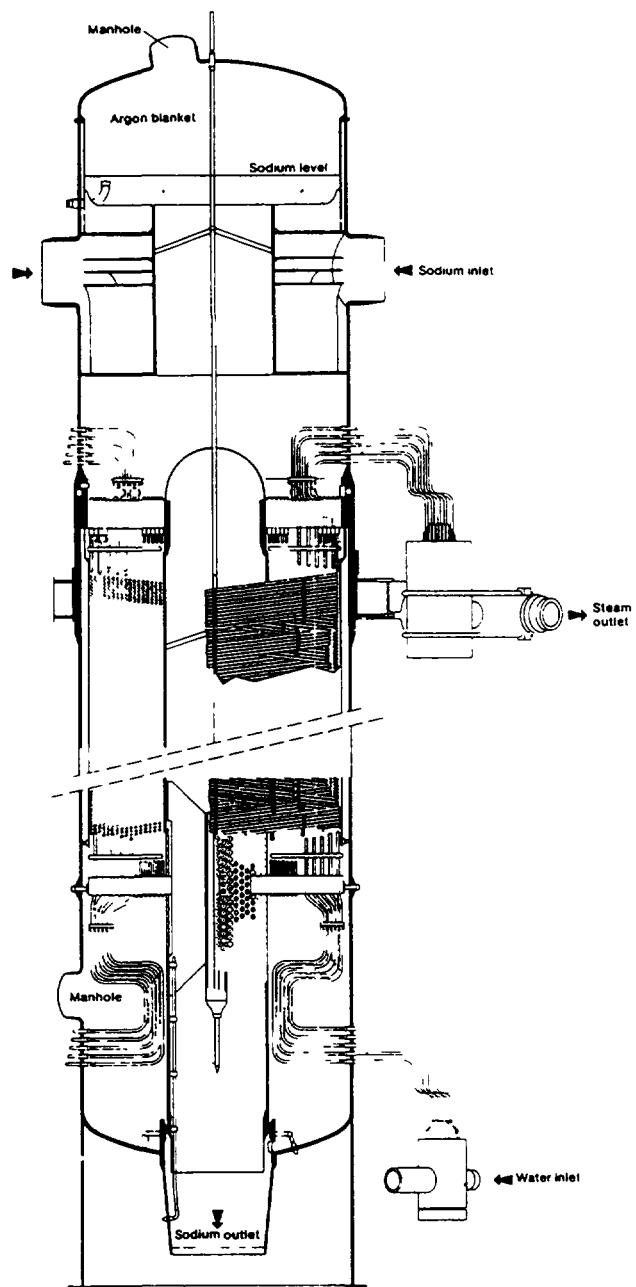


FIG. 6.4. A typical helical-tube steam generator (Creys-Malville)

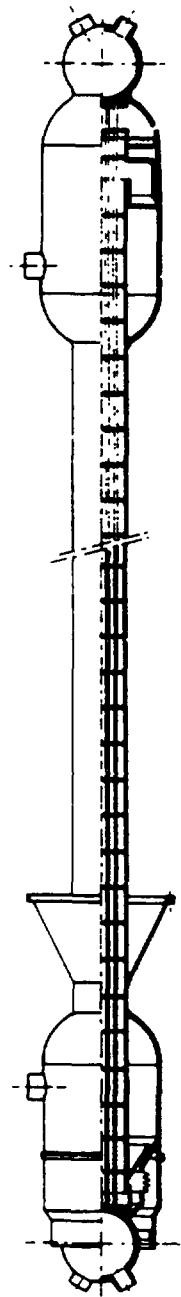


FIG. 6.5. A typical straight-tube steam generator (EFR)

of the sodium-containing welds, carries a high primary stress. The disadvantage is the great complexity, and therefore cost, of the manifolds to connect several hundred tubes, and the difficulty of gaining access to individual tubes for inspection or repair.

Double-walled tubes. So far all power-producing LMRs have had secondary sodium circuits between the radioactive primary sodium and the steam system, because the risk of leaks in the steam generators has been judged to be relatively high. An alternative approach is to use double-walled heat transfer tubes, so that the risk of a leak bringing steam into contact with sodium is reduced enough for the secondary circuits to be dispensed with [6.8]. The potential advantage is that the capital cost of the plant may be reduced significantly.

The principal feature of this approach is to monitor the interface between the two walls of the tube continuously for the presence of either steam or sodium. This would possibly be done by providing a system of small flow passages in the interface, into which any leaking steam or sodium would pass. The network of passages would then be connected to a sensitive monitoring system. It would be necessary to show that the passages would always be open, and to provide a fail-safe monitoring system.

6.1.2. Construction

Materials. To validate the design and ensure satisfactory performance over the entire lifetime of the plant there must be an adequate data base for the construction materials. This includes long-term data on creep, fatigue, and degradation of mechanical properties, reflecting typical plant design lifetimes of up to 40 years. As a result well-established and documented materials have to be used. It is a lengthy and expensive process to develop a new material to design standards.

In practice the choice for the steam generator tubes is between ferritic or austenitic steels, or high-nickel alloys. The material has to withstand the high operating stress due to the internal steam pressure and the differential expansion load. It also has to be compatible with both sodium and water or steam at high temperature. On the sodium side the main consideration is carbon transport [6.9]. The sodium can dissolve carbon from ferritic steels and transport it to cause carburisation, with associated embrittlement, of the austenitic steels which normally form the bulk of the secondary sodium pipework and the intermediate heat exchangers. It is possible to minimise or prevent this by incorporating stabilising additives such as niobium in the ferritic steel. Alternatively the heat exchanger tubes can be designed with sufficient margin to take account of the effects of carbon transport over the lifetime of the plant.

Austenitic steel is not suitable for the evaporator section of the steam generators because it is subject to chloride stress corrosion in the aqueous phase. Although the feed water purity can normally be controlled to keep chloride concentrations sufficiently low, there is always the possibility of an accidental increase due, for example, to failure of a condenser tube. This is of particular concern in a coastal plant where the condenser is cooled with sea water.

On the other hand austenitic steels have superior performance at high temperatures, and are therefore used for separate superheaters where these are fitted. Care has to be taken to avoid carry-over of droplets of water, which may contain corrosive materials in solution, into an austenitic superheater.

Once-through steam generators have to be made of high-nickel alloy (as at Creys-Malville) or ferritic steel (as EFR). To avoid exacerbation of problems of differential expansion the heat exchanger shells and the tubes are usually made of the same or similar material.

Ferritic steam generator tubes are subject to oxidation on the water side, where magnetite (Fe_3O_4) is formed. In the boilers of fossil-fueled plants there is a risk that the magnetite layer may become non-uniform or "rippled", which increases the water-side flow resistance. Also when the magnetite layer becomes thick temperature transients may cause spalling, when sections of the layer become detached leaving irregularities which act as nucleation sites. Evaporation takes place preferentially at these sites and impurities are precipitated giving rise to local corrosion or "pitting". For both reasons it is normal to clean the tubes to remove the magnetite from time to time. In sodium-heated steam generators, however, the higher heat fluxes lead to the formation of dense and uniform magnetite deposits which are rarely subject to rippling or spalling, and cleaning may be needed less frequently, if at all.

Welds. Welds are more subject to failure than the parent material because of the possibility of surface irregularities and fissures, because of residual stresses, and because of local variations in material composition. As steam generators are particularly sensitive to leaks close attention has to be paid to the design and manufacture of weldments.

Under-sodium leaks are usually reckoned to pose greater risks than leaks into the gas spaces, so there is an incentive to design the tubes so that the number of under-sodium welds is minimised. For example the BN350 and PFR steam generators were designed with U-tubes, having no welds in the tubes and with the tube-to-tube plate welds in the gas space above the sodium level.

The U-tube layout is not convenient for large steam generators, however, because the tubes are necessarily of different lengths, and because it is difficult to ensure uniform flow patterns. With other tube layouts (Fig. 6.3) the lower tube-to-tube plate welds are immersed in sodium. These are normally at the cool end of the tubes where material strengths are higher and rates of corrosion and crack growth are likely to be lower.

Welds have to be designed so that they can be inspected after manufacture, and throughout the life of the plant. X-ray inspection is normal during manufacture, but during the plant life ultrasonic or eddy-current methods are often easier to deploy. To reduce residual stresses it is normal to heat-treat the welds after manufacture. This is much simpler if the weldment can be heated locally, without imposing stresses on the rest of the tube bundle. The tubes are normally welded to pre-formed spigots machined from the tube plates, which allows both ready inspection and local stress relief during manufacture.

If straight tubes are employed, butt welds can be formed at one end but at the other there has to be an offset between the tube and the spigot so that, during assembly, the tube can be passed through the tube plate and the spigot and trimmed to length in situ. An advantage of this arrangement is that a damaged tube can be removed from the bundle through the larger spigot without removing the tube bundle from the shell. Figure 6.6 shows typical weld geometries.

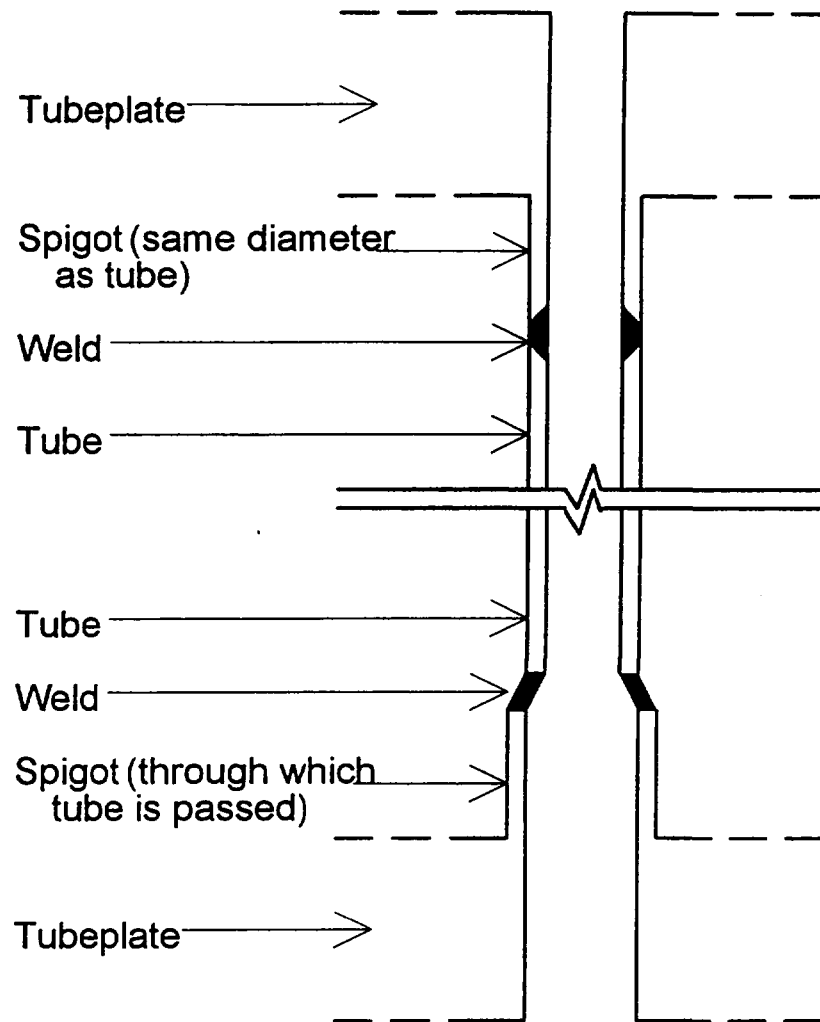


FIG. 6.6. Weldments for a straight-tube steam generator

In most cases it is possible to avoid welds in the length of the tubes, where inspection is particularly difficult, but with helical tubes such welds are unavoidable, and provision has to be made for inspection during operation.

6.1.3. Design details

Tube supports. The tubes are long and flexible, so they have to be supported to keep them in the correct position and to prevent vibration. Correct location is necessary in order to keep uniform flow and heat transfer conditions on the sodium side, which in turn is important to keep the tube temperatures uniform across the bundle. Vibration has to be minimised to prevent excessive noise which would make acoustic surveillance systems less effective, and, most important, to prevent abrasive damage of the tubes. A large under-sodium leak in PFR, which caused extensive damage to the affected tube bundle and significant loss of plant availability, was due to a tube which failed because it was vibrating and knocking against another part of the structure [6.10].

The tubes pass through holes in transverse grids which serve to locate them and prevent vibration. The clearances between the holes and the tubes are critically important. They must be large enough to allow the tube to slide through the hole without jamming to take up relative axial expansion, but they must not be so large as to allow significant rattling which would cause wear and generate noise.

Some rattling is inevitable, and has the potential to damage the tube. Damage can be minimised by correct choice of the grid material with which the tube comes into contact. Wear is usually severe when the contacting materials are similar, and can be reduced if the grid is made of a different material from the tube, or if the surface of the hole which contacts the tube is faced with a suitable bearing material such as a soft alloy (see Figure 6.7).

The axial spacing of the support grids has to be chosen to suppress tube vibration as far as possible. Vibration may be excited, for example, by eddy-shedding in the transverse flow of sodium across the tube bundle in the sodium entry region. This has a characteristic frequency, depending on the sodium flow rate. The grids should be spaced to suppress the tube vibration modes which have frequencies in the range of the eddy-shedding frequency.

The grids form part of the tube bundle. If provision is made for removing the bundle in the event of damage caused by a large leak the grids have to be supported from the tube plate by a structure in the gap between the periphery of the bundle and the vessel (Figure 6.7). Alternatively if the entire steam generator is to be replaced it may be possible to support the grids directly from the vessel.

Flow distribution. As the sodium enters the vessel it has to be directed by flow guides and baffles to give a uniform flow pattern at entry to the tube bundle.

The tube bundle is often surrounded by a shroud, which is a light steel barrier serving to confine the sodium flow to prevent overheating of the peripheral tubes by the excess flow in the gap between the bundle and the vessel. The shroud also provides some protection to the vessel in the event of a steam leak (Figure 6.7).

Within the shroud the tubes can be arranged in a triangular array, which makes the sodium-side flow channels uniform within the bundle, but it is more usual to place them in a

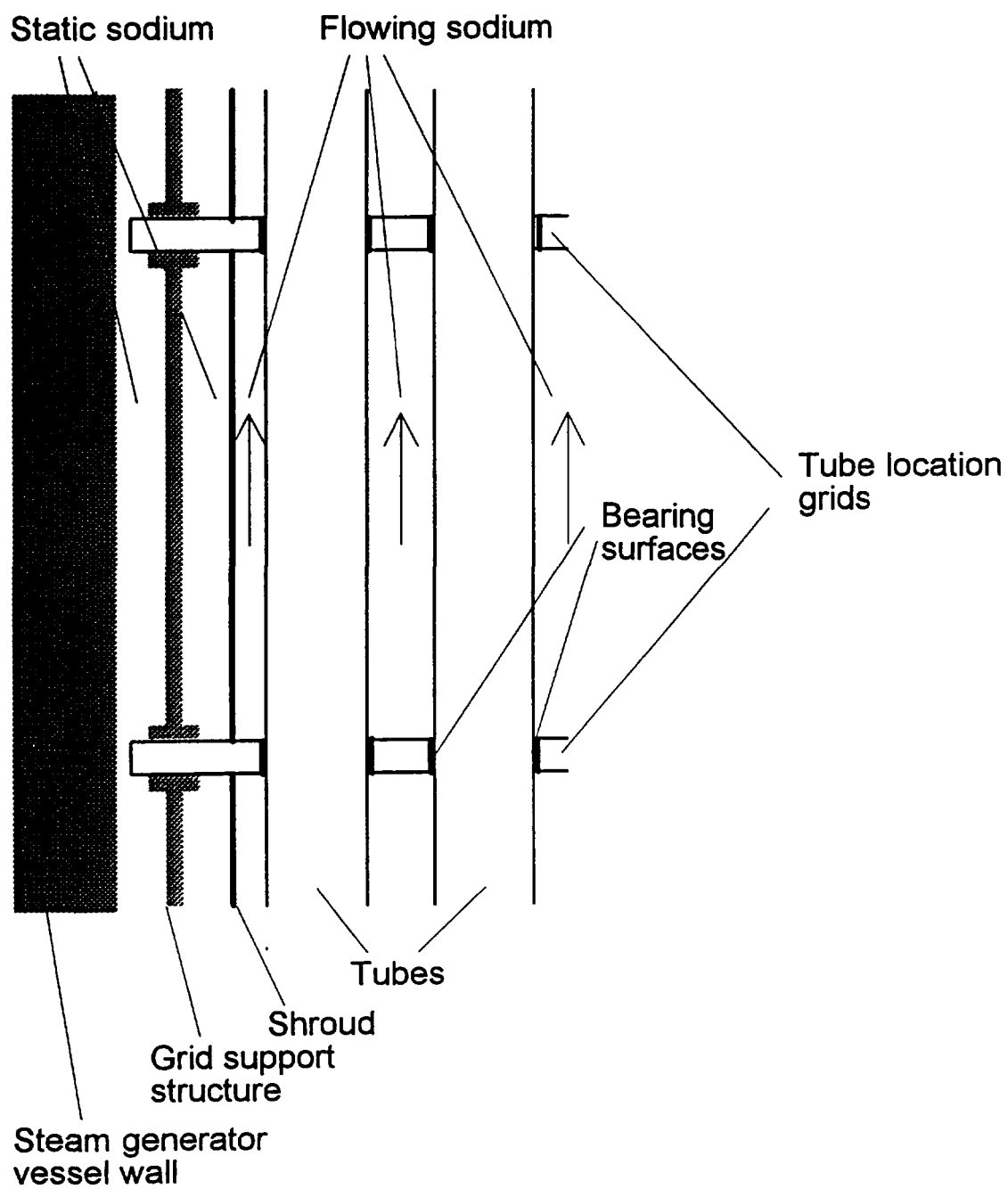


FIG. 6.7. Tube support grids and shrouds

circular array. This has the advantage that the sodium flow channels around the periphery of the bundle, between it and the shroud, are more uniform (see Figure 6.8).

Temperature differences on the sodium side can be minimised by careful design of the support grids. As the sodium flows through holes in the grids turbulence is generated which promotes interchange between the subchannels and tends to even out irregularities. Smaller holes generate more turbulence and give better mixing, but at the cost of a greater pressure drop in the sodium circuit.

6.1.4. Protection

Protection against small leaks. The main protection against small leaks is afforded by prompt detection. Once the leak has been detected the steam generator unit concerned has to be isolated and depressurised quickly, before the damage has time to propagate far.

Very small leaks can be detected reliably by means of the hydrogen generated provided the site of the leak is swept by flowing sodium, as is the case throughout most of the tube bundle. There may, however, be a stagnant region at the bottom of the tube bundle, below the exit of the main sodium flow, immediately above the bottom tube plate. Detection of leaks in this region can be enhanced by ensuring a small sodium flow through it.

The risk of microleaks in the tube-to-tubeplate welds in this region may be higher than elsewhere in the tube bundle. If such a leak goes undetected it might form a growing mass of corrosive sodium-water reaction products which in due course would attack an adjacent weld and allow the leak to propagate. This can be guarded against by inserting shields, in the form of a plate or a grid, between the tubes in the vicinity of the welds, so that any reaction products formed are prevented from attacking another weld.

Protection against large leaks. If there is a large leak it has to be accepted that there will be extensive damage to the tube bundle. The important thing is to isolate the affected steam generator unit quickly to prevent the spread of damage to other parts of the secondary sodium circuit, including the intermediate heat exchangers, and to depressurise it quickly and safely.

Isolation on the steam side is effected by fast-acting stop valves in the feed water and steam lines. In some cases stop valves have also been put in the sodium pipes, but this is not always desirable. The secondary circuits may form part of the reactor decay heat rejection system, which must be available at all times with a high degree of reliability. If the stop valves are under automatic control there may be a possibility of inadvertent closure, and if the risk of this is too high the reliability of the decay heat rejection route may be inadequate.

A large leak exposes the secondary sodium circuit to the operating steam pressure. It is essential to protect the intermediate heat exchangers, which are part of the reactor primary containment boundary, from damage by this pressure. This is normally done by a pressure relief system incorporating rupture discs set to burst at a pressure well below that which the rest of the circuit can tolerate.

When the discs rupture a large quantity of hydrogen, along with hot sodium and corrosive reaction products, is released. The hydrogen has to be separated and discharged safely, while the sodium and reaction products have to be trapped and retained for disposal.

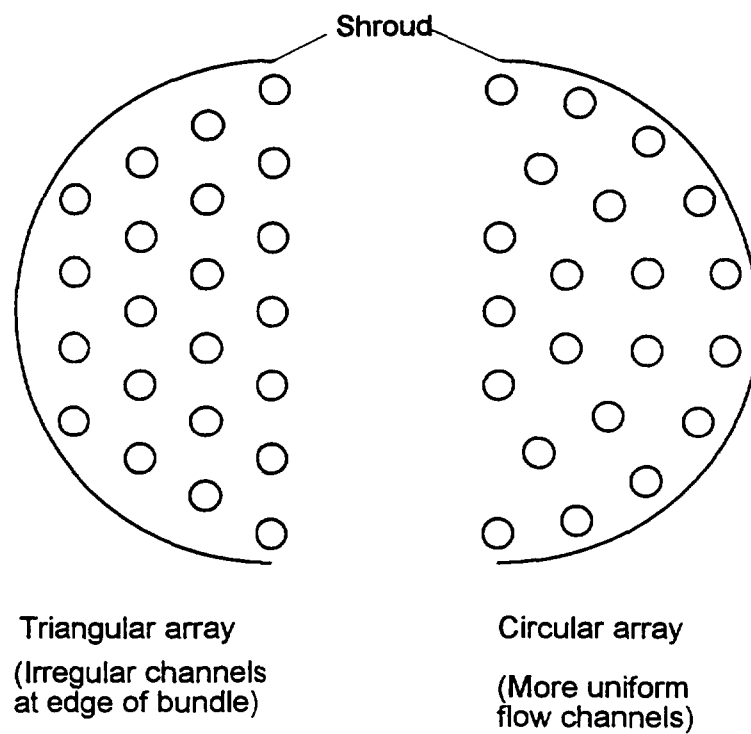


FIG. 6.8. Tube arrangement patterns

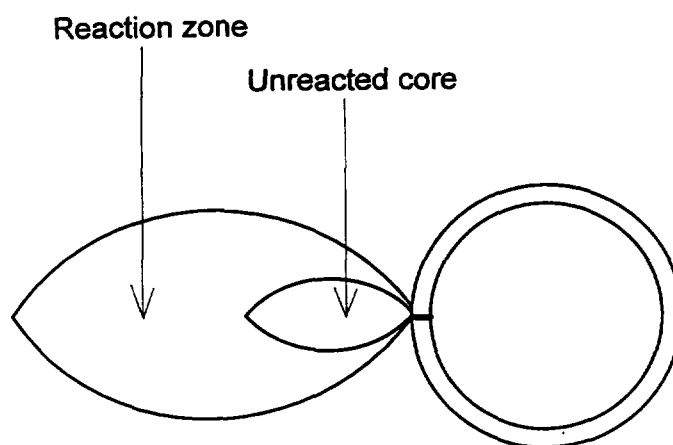


FIG. 6.9. Sodium-water reaction "flame"

This can be done, for example, by arranging the rupture discs to discharge into separators, from which the gaseous component flows to atmosphere. The separators have to be flooded with inert gas to prevent further combustion of the hot sodium.

6.1.5. Sodium-water reactions in steam generators

All highly-rated heat exchangers have a risk of failure, and the possibility of leaks has to be taken into account in the design. If the primary sodium of a sodium-cooled reactor were used to raise steam directly a leak in the steam generator would allow the possibility of radioactive ^{24}Na being released to the environment. Until now the likelihood of such an event has been assessed as being unacceptably high, so all sodium-cooled power reactors have had intermediate circuits of non-radioactive sodium which accept heat from the primary coolant via intermediate heat exchangers (IHXs) and deliver it to raise steam in steam generating units (SGUs). The IHXs are part of the primary containment barrier.

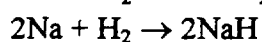
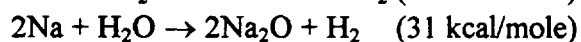
The secondary sodium circuits operate at low pressure so that the IHXs are normally subject only to thermal stresses. A leak in an SGU results in high-pressure steam or water being injected into the secondary circuit where it reacts chemically to form corrosive materials. The primary safety consideration in relation to SGU leaks is to ensure that neither the pressurisation of the secondary circuit nor the corrosive reaction products will jeopardise the integrity of the IHXs. The secondary consideration is to limit the damage caused by a leak, preferably so that it can be repaired, failing that so that at most only the affected tube bundle has to be replaced while the rest of the secondary circuit can be re-qualified for continued use.

Unless protective action is taken a leak in an SGU tube will both *grow* (i.e. the hole will enlarge so that the leak rate increases) and also *escalate* (i.e. leaks in other tubes will be caused, again increasing the overall leak rate). Safety against leaks is therefore ensured by appropriate means of detecting leaks quickly so as to prevent or minimise escalation, and a protective system to isolate and make safe the affected SGU.

Foerster et al. [6.11] review the current understanding of SGU leak behaviour and the design provisions necessary to protect against the consequences of leaks.

Leak behaviour

Sodium-water reactions. When sodium and water interact various chemical reactions compete: for example



The first of these reactions dominates under the conditions in an SGU, so that the main reaction products are sodium hydroxide and hydrogen, but depending on the initial conditions and quantities of the reactants and on the final pressure, some sodium oxide or hydride may be present. If the mixing ratio of sodium and water is not stoichiometric (i.e. equal numbers of moles), there will also be excess water or sodium, either of which may be present as liquid or vapour.

If the reaction is stoichiometric and adiabatic the temperature of the reaction products is a maximum which depends on pressure, rising from about 1250°C at 1 bar to 1450°C at 5 bars.

Classification of leaks. The behaviour of a leak and the opportunities for detection depend on its size. It is convenient to define four classes as follows.

- Microleak: < 0.1 g/s. This is a leak which is too small to be detected. It might be due for example to an inter-granular crack in an imperfect weld. Reaction products are formed so slowly that they do not damage other tubes.
- Small leak: 0.1 - 50 g/s. This is a leak which produces a reacting jet capable of impinging on adjacent tubes and damaging them. It might be due to a fatigue crack 1 cm or more long in a tube.
- Intermediate leak: 0.05 - 2 kg/s. This is a leak which engulfs many other tubes in reaction products and produces significant excess pressures in the secondary circuit. It might be caused by a complete failure of a single tube so that steam flows unimpeded from both the broken ends (this is sometimes known as a "Double-Ended Guillotine Fracture", DEGF). However, if water rather than steam flows from a DEGF, flowrates of 10 kg/s may be possible.
- Large leak: >2 kg/s. This is a leak which pressurises the whole secondary circuit and expels the majority of the sodium from the affected SGU. It might be caused by failure of several tubes.

Leak growth. Aqueous sodium hydroxide attacks steels notably by inter-granular corrosion. The corrosion rate is higher in ferritic than austenitic steels and higher still in Incolloy. The flow rate through a microleak is so small that the corrosion products are not swept away but remain in place. In some cases this has been observed to seal the leak so that the flow of water or reaction products to the sodium is stopped. However, the leak may still be active in the sense that water and sodium continue to diffuse through the corrosion-product plug, interact to form sodium hydroxide and then attack the metal, so that the plug of corrosion products grows. Eventually it is no longer able to support the pressure in the tube and blows out, leaving a hole up to 1 mm in diameter. The result may be a "small leak", with a flow rate of 10 g/s or more, appearing instantaneously with no detectable warning. The incubation period, from formation of microleak to the sudden appearance of a small leak, may last several days or weeks [6.12].

A small leak grows by a combination of corrosion and erosion. Although a high velocity jet of steam or water blows out of the leak, there is back-diffusion of sodium round the jet into the hole, where it reacts with water and corrodes the metal. Grains are loosened by inter-granular corrosion and swept away by the jet.

Small leaks grow at an accelerating rate. A leak of 1 g/s may grow over a period of minutes, while a leak of 50 g/s grows significantly in a few seconds.

Leak escalation. The jet issuing from a small leak forms a turbulent under-sodium "flame" [6.13] (Figure 6.9). The centre of the flame is a core of un-reacted steam at a temperature of 300-500°C. This is surrounded by a reaction zone in which the sodium concentration is low on the inside, high on the outside. In the centre of this reaction zone, where the molar concentrations of sodium are equal, temperatures of 1200-1400°C (depending

on pressure) are reached. Outside there is a sodium-rich zone where the temperature is around the sodium boiling point of 900-1000°C (again depending on pressure).

When the flame from a small leak impinges on another tube it causes wastage by corrosion and erosion. Currie et al. [6.14] give typical data on wastage rates in austenitic steels. A leak of order 1 g/s impinging directly on to an adjacent tube causes wastage at a rate of about 0.01 mm/s, so secondary tube failure in a period of a few minutes can be expected.

The flame from a large leak can cause significant overheating. At temperatures above 1000°C a steam tube subject to the normal operating internal pressure has a limited life. The higher the temperature the shorter the life. For example an austenitic tube at 130 bars might fail in 2 minutes at 1100°C, but fail instantaneously at 1300°C. At lower temperatures the failure is characterised by extensive plastic deformation and ductile flow leading to thinning of the tube wall and a knife-edged trans-granular fracture. At high temperature there is little deformation or thinning of the wall because inter-granular fracture occurs before significant plastic flow can take place.

The temperature reached by a tube depends not only on the temperature of the sodium-water flame outside it, but also on the temperature and flowrate of the water or steam inside it. For as long as the steam flows it acts to keep the tube cool, below the temperature at which it will fail rapidly. The cooling effect is more marked if the tube contains water.

When the leak rate rises into the intermediate range the reaction flame becomes large and affects many other tubes. The flame interacts with the flowing sodium and the result is a chaotic turbulent interaction region characterised by widely fluctuating temperatures.

Once the leak has escalated to become a large leak, with the equivalent of DEGF ruptures of 5 tubes or so, the steam flow rate is so large that the majority of the sodium is swept out of the SGU. In the main the sodium-water reaction is quenched by excess steam, temperatures fall and further tube failures are suppressed. Small sodium volumes may, however, remain trapped (for example in crevices in the tube support grids) giving rise to local hot spots.

Because of the complexity of these processes it is in general not possible to predict the evolution of an SGU leak event in a deterministic way. There is inevitably a substantial random component in the development due mainly to the highly turbulent nature of the flows. It may be possible, nevertheless, to place upper bounds on the rate and extent of leak escalation. Typically it may be possible to show that failure of more than a few tens of tubes (in an SGU containing say 1000 tubes) is very unlikely and that these failures cannot be simultaneous but will be spread over a period of a few seconds.

This understanding of leak behaviour was confirmed by observations of the consequences of a large leak in a PFR superheater in 1987 [6.10, 6.15]. It was initiated by failure of a single tube, and although a total of 40 tubes failed over the next 8 seconds, the pressures in the secondary circuit were mild, and no significant damage was done, apart from to the superheater tube bundle itself.

Pressures in the secondary circuit. The above conclusion is very important because it sets a limit on the pressures experienced by the secondary circuit components and in particular the IHXs. It implies that whatever pressure changes occur they take place relatively slowly so

that the effects of sodium compressibility are negligible. Thus the IHXs and the rest of the secondary circuit are subject to considerably less than the SGU steam-side pressure, typically 120-180 bars, because of the mitigating effect of the protective system (see below).

If the leak escalates much more rapidly, in a period of ms for example, compressibility effects may become important. Pressure waves may give rise to large impulsive forces, analogous to "water hammer" in water pipes, which could damage the IHXs.

Escalation as rapid as this cannot be caused by the corrosion-erosion or overheating mechanisms described above. An external mechanical cause either from a seismic event, impact of a foreign body, or sudden catastrophic failure of a tubeplate, would be needed. To predict the consequences of such an event in which the sodium side of an SGU is suddenly raised to the steam-side pressure, the flow and pressure in the secondary circuit and the protective systems have to be calculated taking account of the compressibility of the sodium.

Leak detection

A comprehensive survey of leak detection in steam generators is given by Hans and Dumm [6.16].

Hydrogen formation. A sodium-water reaction always generates hydrogen, which can be detected easily. This affords the most sensitive method of detecting a leak, in the sense that the hydrogen generated by very small quantities of water or steam in the sodium can be observed. A change of hydrogen concentration as small as 0.1 wpm in the secondary sodium, which may correspond to the leakage of a few hundred grams of water into a secondary circuit containing of order 100 tonnes of sodium, can be detected.

The major disadvantage of hydrogen detection is that it is not prompt. There is inevitably a transport delay of at least a few seconds while the sodium containing the hydrogen is convected to the detection device. This is often made longer because the detectors are situated in an auxiliary loop which takes a representative sample of the main sodium flow.

On the other hand hydrogen detection is an integral technique in that it measures the total quantity of steam or water entering the sodium over a period. It is therefore able to detect very small leaks. A leak of 1 mg/s of water, for example, is nearly 100 g per day, which gives a measurable change in hydrogen concentration over a few days.

Leaks are not the only source of hydrogen in the secondary sodium. If the steam generator tubes are made of ferritic steel they are continually undergoing oxidation on the water side, where a steadily-growing film of magnetite (Fe_3O_4) builds up. Some of the hydrogen generated by this reaction diffuses through the tube walls into the sodium. In normal operation the oxidation takes place steadily and the change in hydrogen concentration in the sodium can be predicted. A leak is then shown by a higher-than-normal rate of increase of hydrogen concentration.

The steady generation of hydrogen by formation of magnetite can be accelerated if the magnetite layer becomes cracked or spalled, by a rapid temperature change due to a plant trip for example. This can expose un-oxidised metal to the water, which begins to oxidise rapidly, generating hydrogen at an increased rate. This may give the appearance of a leak for a time.

Detection of hydrogen and oxygen. The simplest way to detect hydrogen in sodium is by means of a plugging meter [6.17] (Figure 6.10). This is a device in which a sample sodium flow is cooled and passed through an orifice. The cooling is increased until the pressure drop across the orifice increases, indicating that it has been "plugged" by precipitated impurities. The temperature of plugging is then an indication of the impurity concentration.

A plugging meter is sensitive to both oxide and hydride impurities. However, in the secondary sodium (unlike the primary) there is usually little oxide and its plugging temperature can usually be interpreted in terms of hydrogen concentration alone. Ambiguity can be removed, however, by measuring the "unplugging" temperature (the temperature to which a plugged orifice has to be heated to clear it). Hydride dissociates more readily than oxide dissolves, so the unplugging temperature is related more strongly to the oxide concentration and this can be used to correct the evaluation of the hydrogen concentration.

Diffusion affords a more selective means of detecting hydrogen alone. Hydrogen diffuses very readily through nickel at high temperature. A typical detection system takes a sample of the sodium flow, heats it, and passes it over a nickel membrane, through which the hydrogen diffuses into a carrier gas. The hydrogen concentration in the carrier gas can be measured either by a katharometer, which measures the thermal conductivity of the gas mixture (which is sensitive to small quantities of hydrogen) (Figure 6.11), or by other means such as a mass spectrometer [6.16].

Oxygen and hydrogen concentration can also be measured by electro-chemical methods [6.18-6.20]. An electro-chemical cell can be used in either an absolute mode, in which the electric potential of the contaminated sodium relative to a reference electrode is measured directly, or alternatively in a differential mode. In the latter case the relative potential of sample sodium streams from inlet and outlet of an SGU is measured directly. This enables the change in hydrogen or oxygen concentration as the sodium flows through the SGU and therefore the leak rate, to be measured directly. Figure 6.12 shows a typical design for an electrochemical oxygen meter.

Acoustic methods. The use of acoustic techniques for detecting steam generator leaks is given below. The great advantage is that they give a much more rapid response than hydrogen detection because they are not subject to the transport delay. It is possible to detect a 1 g/s leak within 1 s by acoustic means. Use of the two techniques together therefore gives a very wide coverage, with hydrogen detection giving warning of microleaks which may be growing over periods of hours or more, while acoustic detection of small leaks enabling protective action to be taken before significant escalation of the damage has time to take place.

Flow and pressure measurement. A leak detection system using hydrogen and acoustic methods, as outlined above, is still limited in that a response time of less than 1 s is not possible, so protection against sudden large leaks, caused by earthquakes for example, is imperfect. An alternative diverse means of protecting the IHX integrity may therefore be necessary. This function can be fulfilled by measuring the pressure in the secondary sodium circuit. Conventional pressure transducers located in expansion tanks can detect intermediate or large leaks in less than 1 s.

Alternatively sodium flowmeters can be used. The signals from flowmeters at inlet to and outlet from an SGU can be compared to give a rapid indication of changes in the fluid

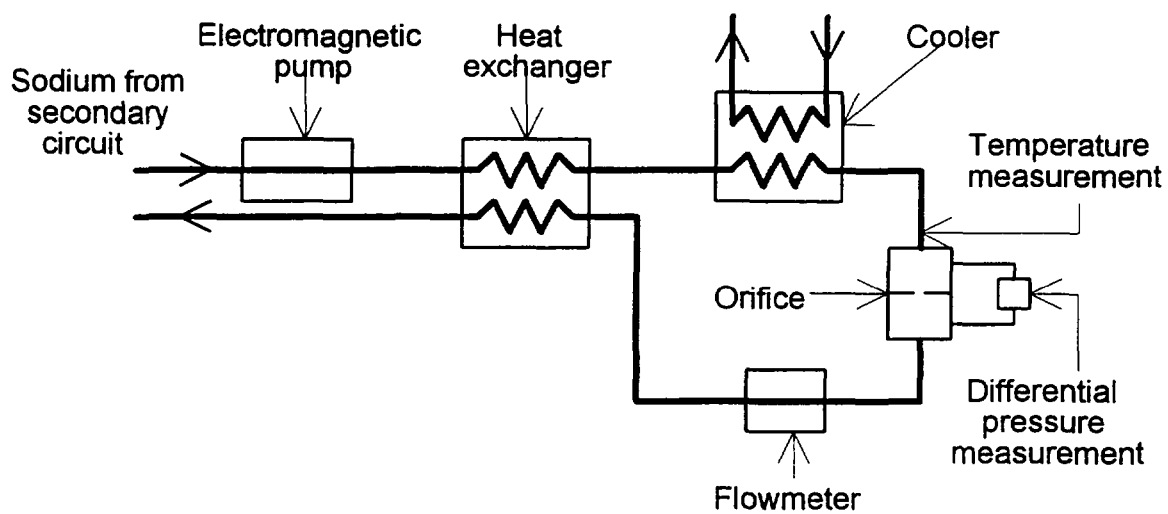


FIG. 6.10. Plugging meter for measuring impurity levels in sodium

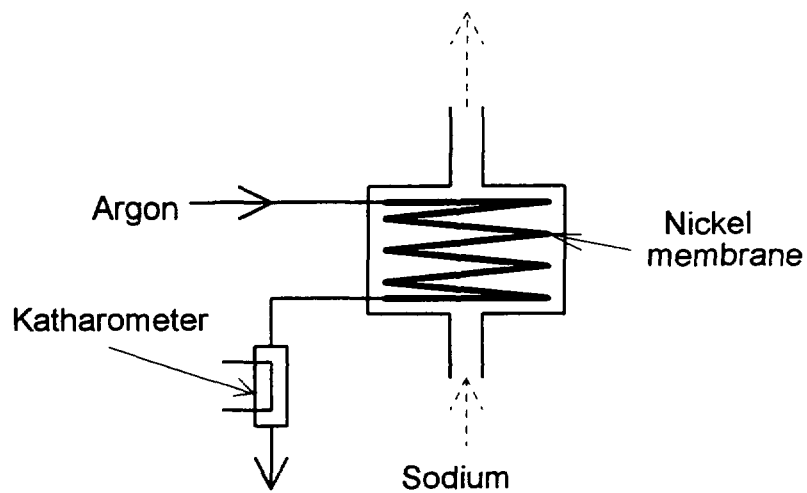


FIG. 6.11. Diffusion monitor to measure hydrogen concentration in sodium

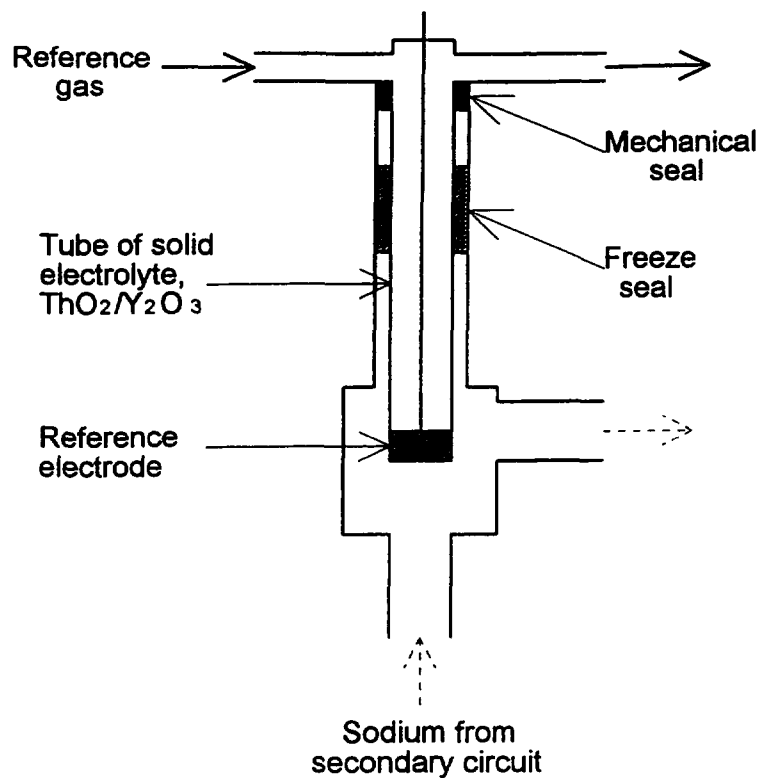


FIG. 6.12. Electrochemical meter for measuring oxygen concentration in sodium

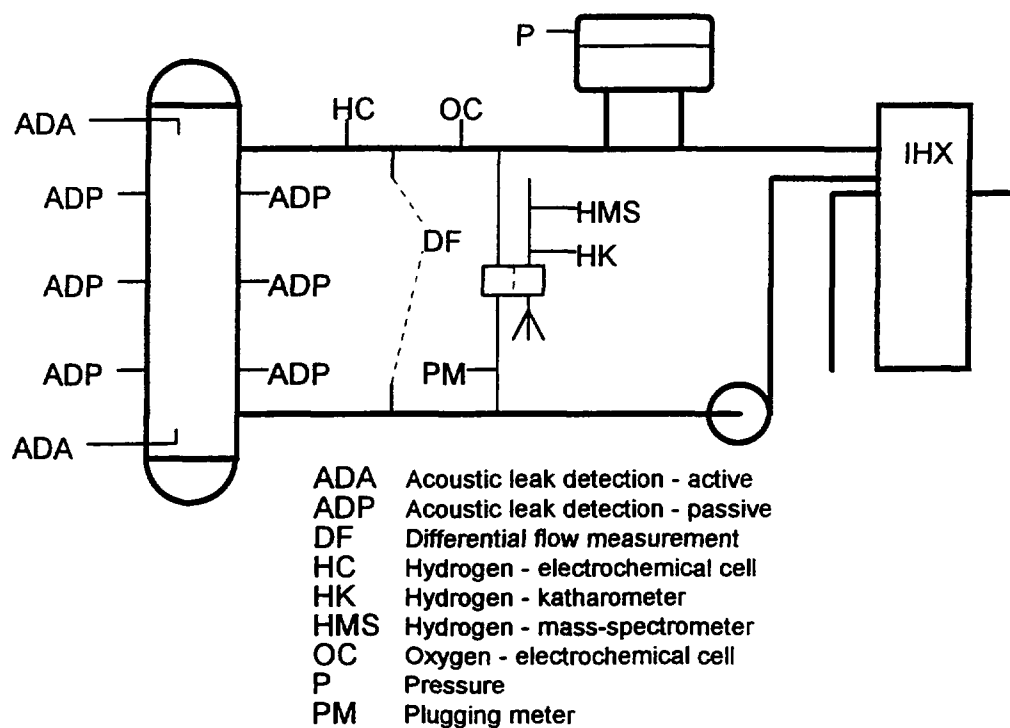


FIG. 6.13. Steam generator leak detection system

volume, and hence the presence of intermediate leaks. Conventional electromagnetic flowmeters can give a response time of the order of 1 ms.

Figure 6.13. shows a complete leak detection system for an SGU, incorporating various devices to respond to leaks of all sizes.

Leak location. If a leak is detected it has to be repaired. In the event of a small leak there is usually no difficulty in locating it, when the plant has been shut down, by pressurising individual tubes.

A microleak can be much more difficult to locate because it is likely to become blocked by reaction and corrosion products, either while the plant is running or during and after the shutdown process. It is hardly possible to examine all the tubes in an SGU (which might number 1000 or more, each 20 m long) visually.

Fortunately it has been found that, in spite of the pressure difference, sodium tends to diffuse back through a microleak to the steam side, and shows in the form of hydroxide impregnating the oxide layer. This can be detected chemically by swabbing individual tubes. A moist absorbent plug, or "mole", is driven through each tube in turn by compressed air and examined for the presence of hydroxide. The presence of the microleak can be confirmed visually, and the affected tube can then be plugged.

Plant protection

Pressure relief. The most important consideration is to prevent damage to the IHXs, which are part of the primary containment boundary. This can be done by providing bursting discs set to burst at a pressure below that which will overstress the IHXs, and with sufficient capacity to discharge the sodium, steam and reaction products from a large leak. The bursting discs should be of robust and reliable design and be entirely passive, in that venting should be independent of any signal from the leak detection system.

They should vent into a system which will receive the reaction products, including hydrogen, safely. There should be traps and filters to ensure that the release of sodium and other reaction products to the atmosphere is within acceptable limits.

Plant isolation. In the event of a major leak the affected SGU has to be isolated quickly in order to prevent the spread of corrosive reaction products.

The sodium can be dumped to a dump tank by opening fast-acting valves in a drain line. The drain line has to be permanently trace-heated to a temperature which will prevent solidification not only of pure sodium but of sodium which is highly contaminated with reaction products. The plugging temperature may be 300°C or more, and to ensure an unimpeded dump the drain line has to be kept above this temperature all the time.

In some systems the secondary sodium circuits are fitted with isolation valves, so that the affected SGU can be emptied of sodium while the rest of the circuit remains full. This may make the cleanup of the rest of the circuit easier, if sodium can be circulated in it. The disadvantages are that the isolation valves may pass, they may be difficult to maintain, and it may be hard to design them to withstand the pressure transients associated with a large leak. In addition if the secondary circuits have a role in the rejection of decay heat under emergency

conditions the presence of isolation valves, which might be closed inadvertently, may decrease their availability significantly.

The steam side of the affected SGU has to be depressurised to stop the flow of steam or water into the sodium. Fast-acting isolation valves disconnect it from the rest of the steam system, and relief valves open to vent the steam to the atmosphere.

The placing of the relief valves in the steam circuit is critical. It is desirable to avoid stagnation of the water or steam in the SGU tubes before the pressure has fallen. If the flow stops the tubes will no longer be cooled and they will be more likely to fail due to overheating by the sodium-water reaction flame. If the SGU is vented from one end only the pressure is relieved by the water or steam flowing through the tubes, the cooling does not stop until the pressure is low and the damage to tubes will be less extensive.

Particular care has to be given to the venting of sodium-heated reheaters, if these are fitted. When the SGU is isolated the entire steam plant is shut down and, among other things, the turbine stop valve closes. This exposes the whole of the turbine and the steam side of the reheaters to the condenser, so the pressure falls rapidly and may go below atmospheric. If there is a leak in the reheater this would allow sodium to pass into the steam pipework and even possibly the turbine, where it could do extensive damage.

In general it is important that during the isolation and dump sequence the steam side pressure does not fall below the sodium side pressure in any SGU, to avoid back-flow of sodium through any leaks which may be present.

After steam and sodium have been removed the SGU and secondary circuit must be filled with inert gas. Air must be excluded to avoid any moisture in it forming sodium hydroxide, which at low temperature may be aqueous and therefore particularly corrosive.

At higher temperatures sodium containing high oxygen concentrations is corrosive [6.21]. This is a particular problem with the secondary sodium left in the IHXs. In most cases this cannot be removed or circulated if the rest of the secondary sodium is dumped. It is therefore necessary to protect it from oxidation, especially if the reactor is to continue in operation. It is desirable to have a means of determining the impurity levels in the IHX secondary sodium.

Figure 6.14 shows the various components of the protective system for an SGU and secondary sodium circuit. Isolation and dumping would be initiated by operation of the rupture discs or by receipt of signals in excess of pre-determined limits from the leak-detection instrumentation shown in Figure 6.13.

Acoustic leak detection. The word "acoustic" is used to refer to sound in the audible range or a little above it, with frequencies up to around 100 kHz and wavelengths of a few cm or more in sodium.

Acoustic methods have a very important role in the detection of steam generator leaks. A leak of water or steam into sodium reacts chemically to form a mixture which is corrosive and hot. These reaction products may attack adjacent tubes, causing them to fail, and resulting in very rapid escalation of the accident. This can be prevented if the leak is detected quickly and the steam generator is isolated and depressurised. In the case of very small leaks, of the

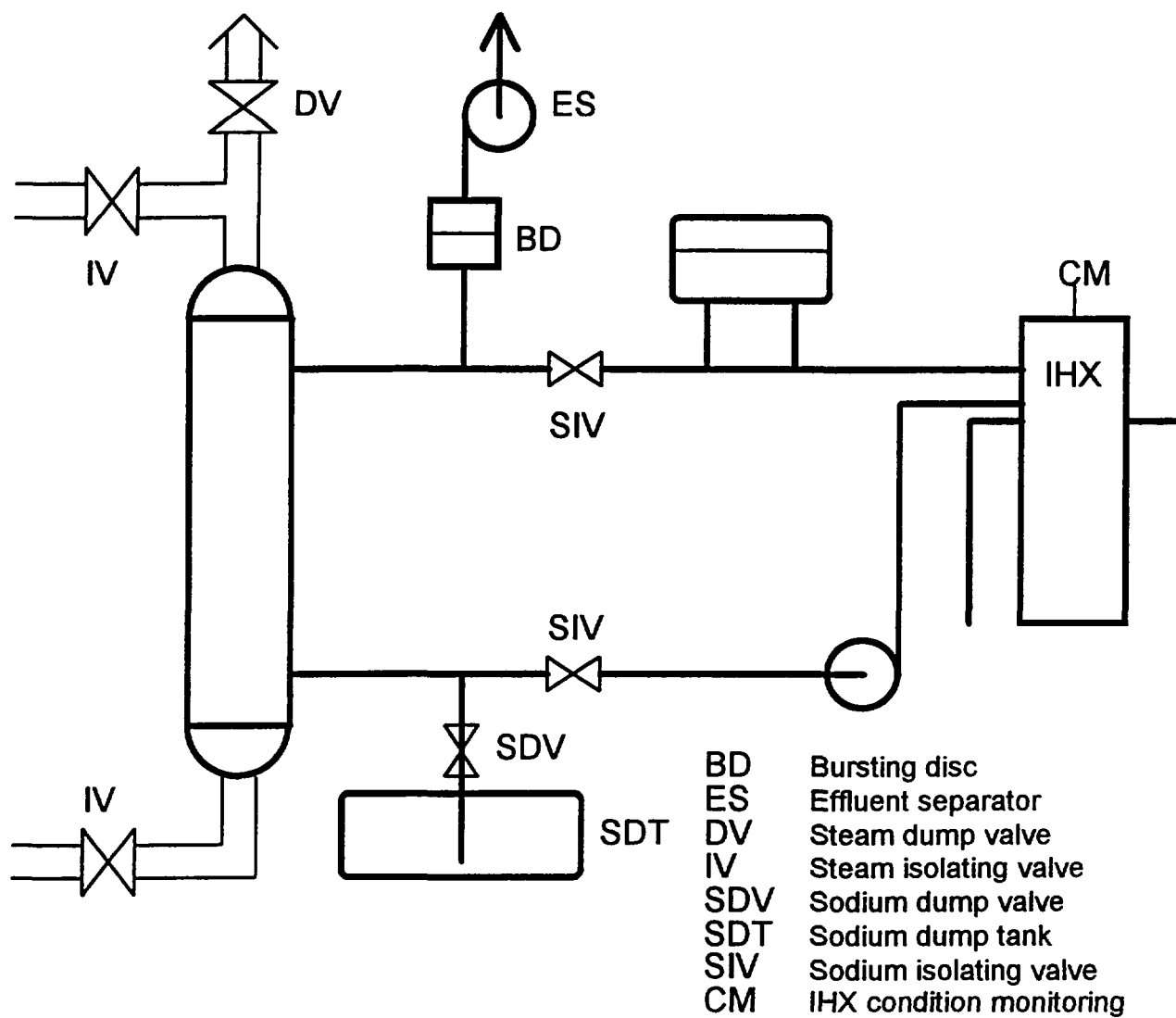


FIG. 6.14. Steam generator protective system

order of 1 mg/s or less, escalation is slow and detection by chemical means - usually of the hydrogen liberated - is quick enough. Larger leaks, of the order of 1 kg/s, can be detected readily by means of the pressure in the sodium system, but are so large that extensive damage to the steam generator is inevitable. A leak initially of the order of 1 g/s or so however might grow rapidly enough to damage other tubes within 10 s, too quickly for hydrogen detection systems to respond. Valuable protection is afforded therefore by a leak detection system capable of detecting such a leak within 1 s, so that action can be taken in time to protect the steam generator from extensive damage. This can be done by acoustic means. There are two distinct approaches: passive and active.

Passive detection relies on the fact that the effect of the leak is quite similar to boiling, in that it gives rise to rapidly-expanding bubbles. As a result the noise generated is similar to that generated by boiling and can be detected by similar, though not identical, means. Greene [6.22] describes different approaches to leak detection by passive means.

The IAEA Co-ordinated Research Programme on "Acoustic Signal Processing for Detection of Sodium Boiling or Sodium/Water Reaction in LMFR" covered acoustic leak detection as well as ABND. It made use of experimental recordings of leak noise from test rigs in Russia and elsewhere, and of background noise from operating steam generators, and showed that a 1 g/s leak can be detected within 1 s with high reliability and a false indication rate of the order of one in 25 years. A passive acoustic leak detection system can make use of the same detectors as a plant monitoring system to detect vibration, will be described below. Active acoustic leak detection makes use of the changes to the acoustic properties of the steam generator caused by the gas liberated. The cloud of bubbles formed increases the acoustic attenuation of the sodium. This can be detected by means of acoustic pulses transmitted along the length of the steam generator between the tubes. High frequency pulses of around 10 kHz are transmitted from one transducer, along the tube bundle to a receiving transducer, with a pulse repetition rate of around 1 Hz. If there is a significant fall in amplitude of the received pulses it is concluded that a leak is present. An advantage of this system is that it is fail-safe and self checking. Both passive and active acoustic leak detection methods are described in the report of an IAEA Specialists' Meeting[6.23].

6.2. REACTOR CORE WITH OTHER COMPONENTS: ACOUSTIC INSTRUMENTATION

6.2.1. Detection of boiling

Acoustic detection of boiling can play an important part in the plant protective system, because it affords a means of detecting local overheating and allows protective action to be taken before damage spreads to otherwise unaffected parts of the structure.

Local faults. As an example of the type of local fault against which acoustic boiling noise detection ("ABND") provides protection it is common to consider a complete instantaneous blockage of the coolant flow at inlet to a core subassembly while the reactor is operating at full power. Of course, subassembly coolant inlets are designed to make such a blockage very unlikely if not impossible, but a hypothetical accident of this type is important for the purposes of assessment because it is the severest of a class of accidental local coolant flow perturbations. A system which will protect against it will be effective against other accidents involving flow blockages of or within a single subassembly.

In the event of a complete instantaneous subassembly inlet blockage the temperature of the coolant in the core region will rise rapidly and reach the boiling point, typically in less than 0.5 s. When it boils the vapour will eject the bulk of the coolant from the subassembly, leaving the fuel pins essentially uncooled. The cladding temperature will rise very rapidly and reach the melting point in less than a further 1.0 s. Then, or earlier if the cladding is extensively disrupted by internal pressure, the fuel will be free to move. In a further 2 s or so, if it remains uncooled, it will melt. The molten fuel may contact the subassembly wrapper and melt it, and may then melt the wrapper of adjacent subassemblies so that the damage is no longer confined to the initially-affected subassembly. Alternatively violent mechanical interaction between molten fuel and coolant re-entering the subassembly by gravity may cause the propagation of damage to adjacent subassemblies. Reference [6.24] gives a general description of this type of accident.

The objective of the protective system is to intervene by shutting down the reactor, preferably soon enough to prevent fuel melting, certainly soon enough to prevent the propagation of damage beyond the affected subassembly. ABND has an important role in providing a signal, indicating that something is amiss, to initiate the protective action. Its importance lies in the fact that it may afford the only way of knowing promptly that the coolant is boiling.

Other potential detection systems have limitations as follows.

- Coolant outlet thermocouples will detect no abnormal temperature if the blockage is complete or, in the event of a partial blockage in the core region, unless it occupies almost the whole flow area. They may also fail to respond to the very rapid ejection of hot liquid coolant when boiling starts.
- There may be only a very small reactivity change when boiling starts (depending on the location of the affected subassembly in the core), so a reactivity meter may not respond until significant fuel movement takes place.
- Although cladding failure and break-up of the fuel can be detected very readily by delayed neutron monitors and fission product monitors, there is an inevitable transport delay of at least a few seconds, which may be long enough for damage to propagate.
- Outlet flowmeters on individual subassemblies are very difficult and expensive to engineer.

Detection of local faults. It has been shown that rapid cladding failure is very unlikely if the cladding temperature does not rise above the coolant boiling point. ABND offers the possibility of detecting a necessary precursor to extensive fuel failure or damage propagation, making use of a limited number of monitors to survey the whole core.

When sodium boils vapour bubbles grow and then collapse as they are carried to cooler regions. The collapse is very rapid and produces an acoustic impulse at the instant when the bubble vanishes. Boiling noise is made up of a series of these impulses, each being of only a few microseconds duration. Spectral analysis shows acoustic energy to be concentrated at high frequencies, above 10 - 20 kHz. Pulse repetition rates of 100 per second or more are observed by detectors close to the boiling source, but much lower repetition rates may be observed by remote detectors (1 m or more away from the source) because of attenuation by the vapour.

If boiling is to be detectable it has to be audible above the background noise. There are two main sources of background noise which can interfere with ABND: rattling of loose components, and cavitation.

The coolant flow may excite vibration of various components of the reactor primary coolant such as fuel pins or heat exchanger tubes. If the amplitude of vibration is sufficient the vibrating components may hit each other or the fixed structure. These impacts will generate noise, which may interfere with an ABND system. They are also likely to cause mechanical damage, and for this reason there is a strong incentive to prevent rattling by design.

Thus fuel subassemblies are designed with pin support systems (wires wrapped round the pins, or grids) which locate the pins positively to prevent movement, allowing for deformation due to temperature changes or irradiation. Similarly the heat exchanger tubes have to be supported by grids to limit vibration amplitude and prevent impact of tubes with each other or the support grids themselves. A more difficult design problem is to prevent vibration and rattling of components such as control rods which have to be free to move at all times.

Whatever design measures are taken to prevent it there is inevitably a certain amount of rattling noise present in the reactor as it operates. It is likely to be predominantly impulsive in nature, and may be characterised by well-defined periodicity. Either of these characteristics may allow an ABND system to discriminate against it.

It is much more difficult to discriminate against cavitation noise because cavitation is essentially the same phenomenon as boiling, though caused by falling pressure rather than increasing temperature. It is therefore particularly important that cavitation should be avoided by design. In practice this means avoiding coolant leakage paths between the high-pressure and low-pressure parts of the primary circuit. Such leakage paths may be present in expansion joints in the high-pressure pipes from the pumps to the diagrid or at the seals where the subassemblies are mounted in the diagrid.

It is particularly important to avoid sodium leakage past the subassembly seals because the associated cavitation may damage the feet of the subassemblies or the seating faces of the diagrid, as well as causing noise.

Other potentially serious sources of cavitation noise are the gags which adjust the flow of coolant through each subassembly to match the power generated in it. It is important that the gags should produce the required drop in pressure by viscous drag at relatively low velocities in narrow passages, rather than by the generation of turbulence by flow through orifices.

Fault detection systems. An ABND system usually involves acoustic sensors situated above the core. These may be either high-temperature transducers immersed in the coolant, or wave guides in the form of steel rods, arranged to conduct the sound from above the core to a cool region, usually in the reactor shield, where it can be detected by low-temperature transducers.

Acoustic transducers for LMFR applications are usually based on piezoelectric materials. The material used depends on the temperature at which it is to operate, because the piezoelectric properties are lost above the Curie temperature. At low temperatures, up to about 250°C, lead zirconate titanate ("PZT"), which has a Curie point of 350°C, is acceptable. At higher temperatures lithium niobate, with a Curie point of 1200°C, is used.

A typical transducer is shown in Figure 6.15. The piezoelectric element is in the form of a thin disc which is pressed against the diaphragm by a spring. For passive applications, when monitoring signals up to the high tens of kHz, firm pressure is adequate to maintain contact between the piezoelectric element and the diaphragm. For active applications, in which the transducer is also used to transmit pulses, the element has to be bonded to the diaphragm.

The efficiency of the system is strongly dependent on the attenuation of the sound between the source in the core and the detectors above the core. Attenuation in liquid sodium is low in principle, but is increased very rapidly by small quantities of gas in the form of bubbles. Gas bubbles can act either to absorb or to scatter sound, depending on their size, their natural frequencies for oscillations about a spherical shape, and the frequency of the sound.

Gas can be entrained into the coolant at the free surface by vortexes or falling streams and these should be avoided. It can also be dissolved at hot parts of the surface and then precipitated in the form of small bubbles in the cold pool. To avoid significant acoustic attenuation in the frequency ranges important for ABND, the volume fraction of gas in the form of bubbles of diameters of 1 mm or less should be kept below 10^{-6} .

The performance of ABND systems was the subject of an IAEA Co-ordinated Research Programme [6.25], aimed at determining whether boiling could be detected reliably, in the presence of background noise, with an acceptably low spurious detection rate. Background noise from the dummy cores of PFR and Creys-Malville, and from the operating cores of PFR and KNK2, was recorded. (The dummy core of PFR was much more noisy than the actual core because the subassembly gags in the former were found to generate significant cavitation noise. Partly as a result of these observations the gags were redesigned for the actual core subassemblies). In addition boiling noise from artificial boiling sources in PFR and KNK2, and from various out-of-pile test rigs, was recorded.

Various software methods for detecting boiling noise in the presence of background have been investigated [6.26]. The use of filtration, pattern recognition techniques, or a combination of both, allows boiling to be detected in the presence of a background which is noisier than the boiling source. The IAEA programme showed that with a signal-to-noise ration of -12dB (i.e. with the r.m.s. boiling signal power about a factor of 16 lower than the r.m.s. background signal power), boiling can be detected with a reliability of less than one error in 10^6 , and with less than one spurious indication in 10^6 years. Figure 6.16 compares boiling signal amplitudes and reactor background noise from various sources. Figure 6.17 shows in outline an ABND system prepared for EFR. An ABND system for EFR is described in Reference [6.27].

6.2.2. Plant monitoring

Rotating machinery. Acoustic techniques are important for monitoring the performance of rotating machinery, particularly the major components such as the primary and secondary sodium pumps and the boiler feed pumps. These components play an important role in the heat rejection system and it is necessary to ensure their reliability. This can be done by continuous in-service acoustic monitoring to detect the onset of mechanical abnormalities, such as damage to impellers or bearings, at an early stage. Repairs can then be undertaken before the damage becomes severe enough to endanger performance. As a result it can be demonstrated that the reliability of the system is high.

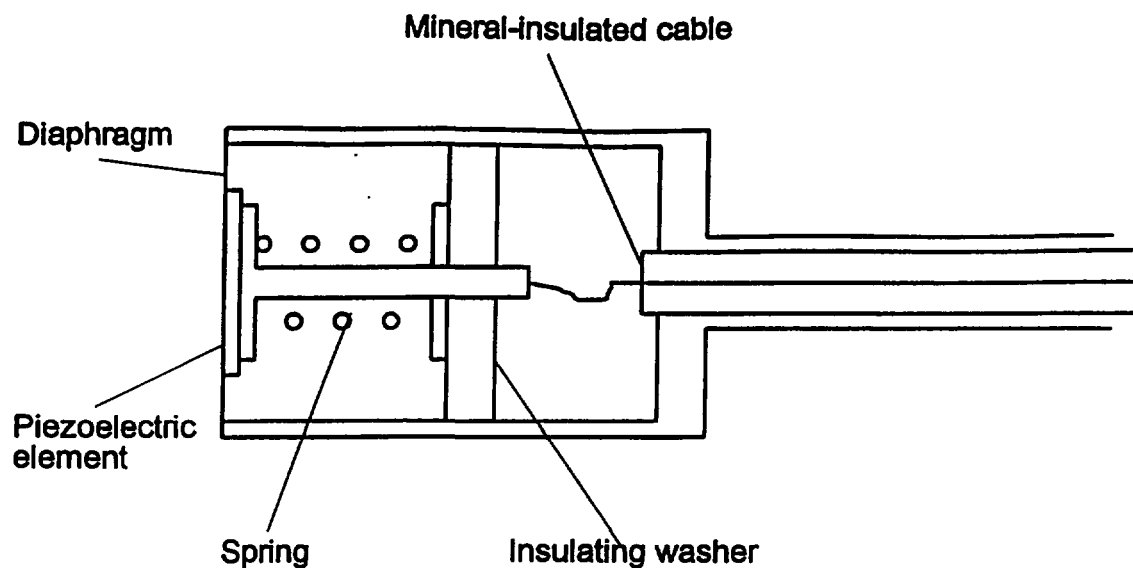


FIG. 6.15. Piezoelectric transducer for use under sodium

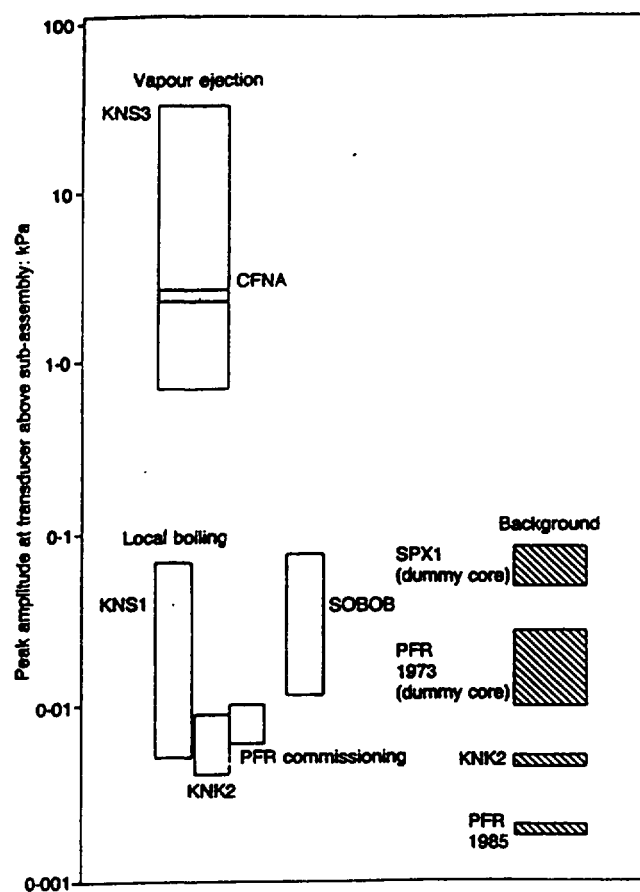


FIG.6.16. Comparison of sodium boiling signal amplitudes with reactor background noise

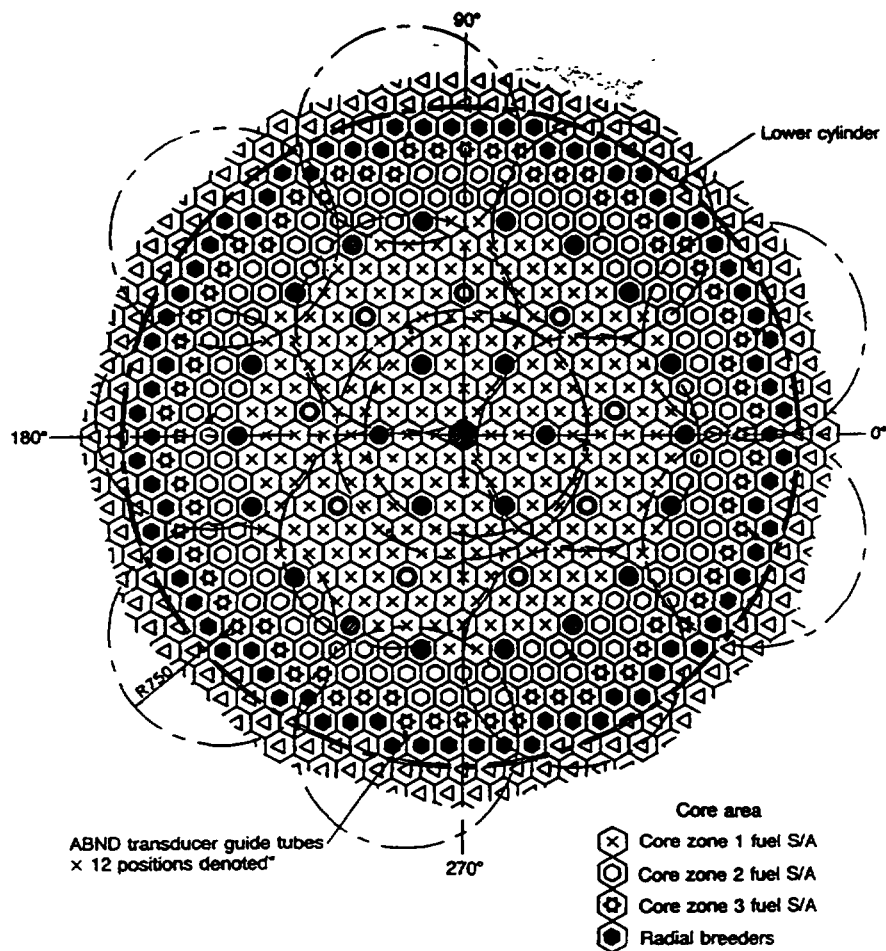


FIG. 6.17. ABND locations for the EFR core

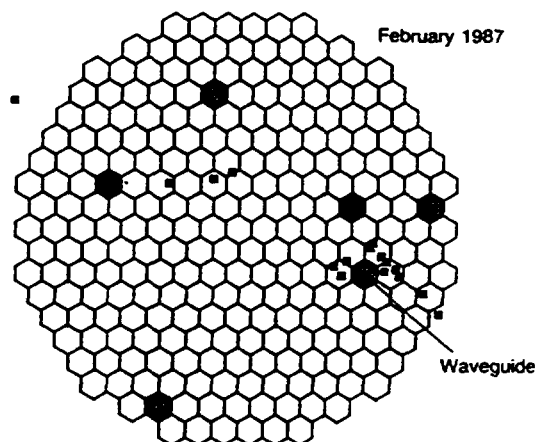


FIG. 6.18. Location of acoustic sources in the PFR core by a time-of-flight technique

Techniques for monitoring rotating machinery are conventional and not specific to liquid metal systems or nuclear applications. No further detail is given here therefore.

Loose part monitoring. The use of acoustic methods for identifying loose parts in complex structures also has a wide range of applications, but it is particularly important in liquid metal systems where visual inspection is impossible. In an LMFR the components most at risk from damage by vibration are the steam generators and, to a lesser extent, the intermediate heat exchangers and the core.

If the noise impulses from a source of vibration can be detected by an array of transducers, measurements of the pulse arrival times can be used to determine the distance of the source from each detector, and the location of the source can be deduced. PFR was equipped with six above-core wave guides with low-temperature transducers in the rotating shield. These were used to locate a number of apparent sources in the core, as shown in Figure 6.18. The application of this method to locate sources of noise in the PFR core is described in Reference [6.27]

The operating conditions of steam generators are complex because they are affected both by the coolant and water flow-rate, which are variable, and by the temperatures which are different in different states of plant operation, and may be affected by the formation of deposits or the presence of damaged tubes which have been plugged. For this reason it is desirable to monitor steam generators during operation to detect the onset of vibration and to estimate the severity of any impacts between tubes and structure so that wear-rates can be predicted.

This can be done by means of an array of acoustic sensors attached to the outside of the steam generator vessel. It is usually most convenient to mount the transducers on short wave guides in the form of steel rods welded to the vessel and projecting through the insulation. The transducers can then operate at close to ambient temperature.

A "fingerprint" of the steam generator is then taken by recording the output of all the transducers during normal operation under a range of conditions covering all likely variations of pump speeds, power, and temperature. Future operation can then be monitored by comparing the output of the transducers with the "fingerprint". Any new features of the output can be investigated. Of particular interest are periodic signals with frequencies in the range of the characteristic frequencies of the tubes, pulses with very short rise times such as are produced by impact, and pulses followed by "ringing", a decaying high-frequency oscillation.

If anomalous signals of this type are observed from several of the transducers it may be possible to localise the source by time-of-flight methods. This is likely to indicate the location of the source with a precision of the order of 10 cm, provided it is close to the outside of the tube bundle so that the transmission path from source to detector is mainly in the metal of the vessel itself. Noise sources deeper in the bundle are difficult to locate because there are multiple transmission paths to the detector.

6.3. ULTRASONIC INSTRUMENTATION

The term "ultrasonic" refers to the use of sound waves with frequencies in the MHz range. The advantage in LMFR applications is that the wavelength in sodium is of the order of 1 mm, so that measurements of high precision are possible in principle.

6.3.1. Ultrasonic imaging

An ultrasonic transducer can be made to produce a pulse which will propagate in a straight line into the sodium. If it encounters an interface with a region in which the speed of sound is different - a solid object, for example - it will be reflected. If the interface is flat and smooth and normal to the direction of propagation it will be reflected back to the transducer, which can be arranged to detect it. The time interval between transmission and reception can be measured and, if the speed of sound in sodium is known, the distance from the transducer to the object can be deduced.

If the transducer is scanned in a plane normal to the direction of propagation, a three-dimensional image of the objects in the line of view can be built up. This is the principle of under-sodium viewing, which has been demonstrated for example in PFR [6.28]. Figure 6.19 shows how a small array of downward-facing transducers was scanned over part of the reactor core. Two motions contributed to the scanning process: the head of the mast on which the transducers were mounted rotated about its axis and the reactor shield in which the mast was mounted rotated as well. In this way a ring-shaped area of the top of the core was scanned. By inserting the mast in three different penetrations in the rotating shield three concentric rings, covering about 70% of the core and breeder, were scanned.

The resulting image is shown in Figure 6.20. Considerable detail of the tops of the subassemblies and other core and breeder components can be seen. A precision of about 2 mm laterally and less than 0.5 mm vertically was achieved. The results of this scan were of considerable value in checking predictions of the distortion of the core components due to neutron-induced swelling, which resulted in displacements of subassembly tops from their nominal positions of up to 20 mm laterally and 5 mm vertically.

A difficulty with under-sodium imaging is that the response is affected very strongly by the orientation of the surface. Curved surfaces, or plane surfaces at an oblique angle to the ultrasonic beam, give a weak response. Internal rectangular corners between two plane surfaces, however, give a strong response whatever the orientation. Ultrasonic images of complex structures have to be interpreted with care, bearing in mind that large and important components may give weak images, and unimportant details may acquire prominence. Components with curved surfaces may be detectable by means of the "shadows" they cast by rendering features behind them invisible.

6.3.2. Ultrasonic monitoring

A simpler application of under-sodium ultrasonics in which these difficulties can be avoided is the identification of components, particularly fuel subassemblies. A final check that the fuel has been loaded in the correct pattern can be made by identifying each subassembly positively as it is loaded. Such a system makes use of a series of marks machined into the top of each subassembly to form a code which identifies its type and, in particular, its enrichment. This code is read by an ultrasonic scanner as the subassembly is loaded, so that the correct assignment to core enrichment zones can be assured.

Ultrasonic devices can also be used to measure displacements under sodium as a means of checking structural integrity. The distance between two reflectors can be determined to within less than 1 mm by measuring the time of flight of ultrasonic pulses between them and

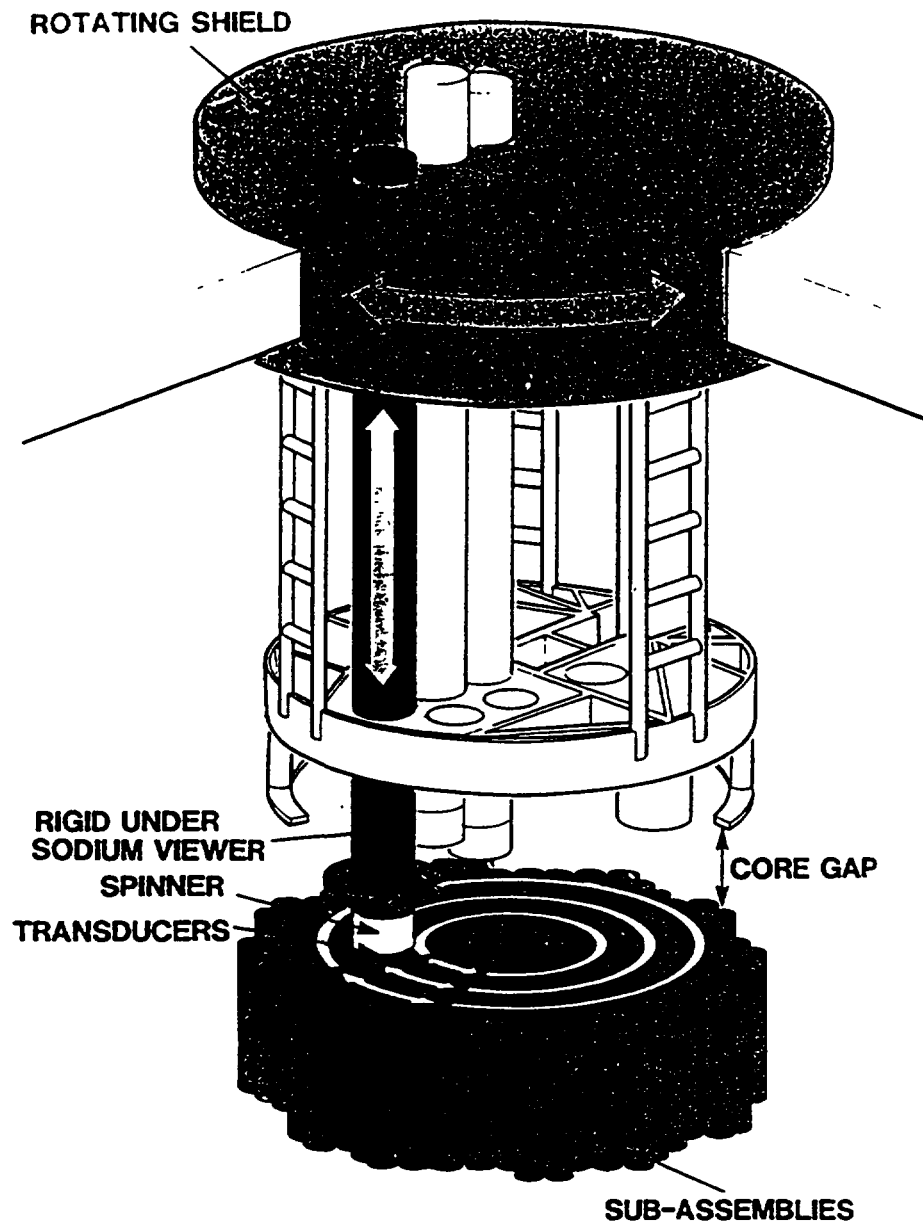


FIG. 6.19a. Arrangement for ultrasonic viewing of the PFR core

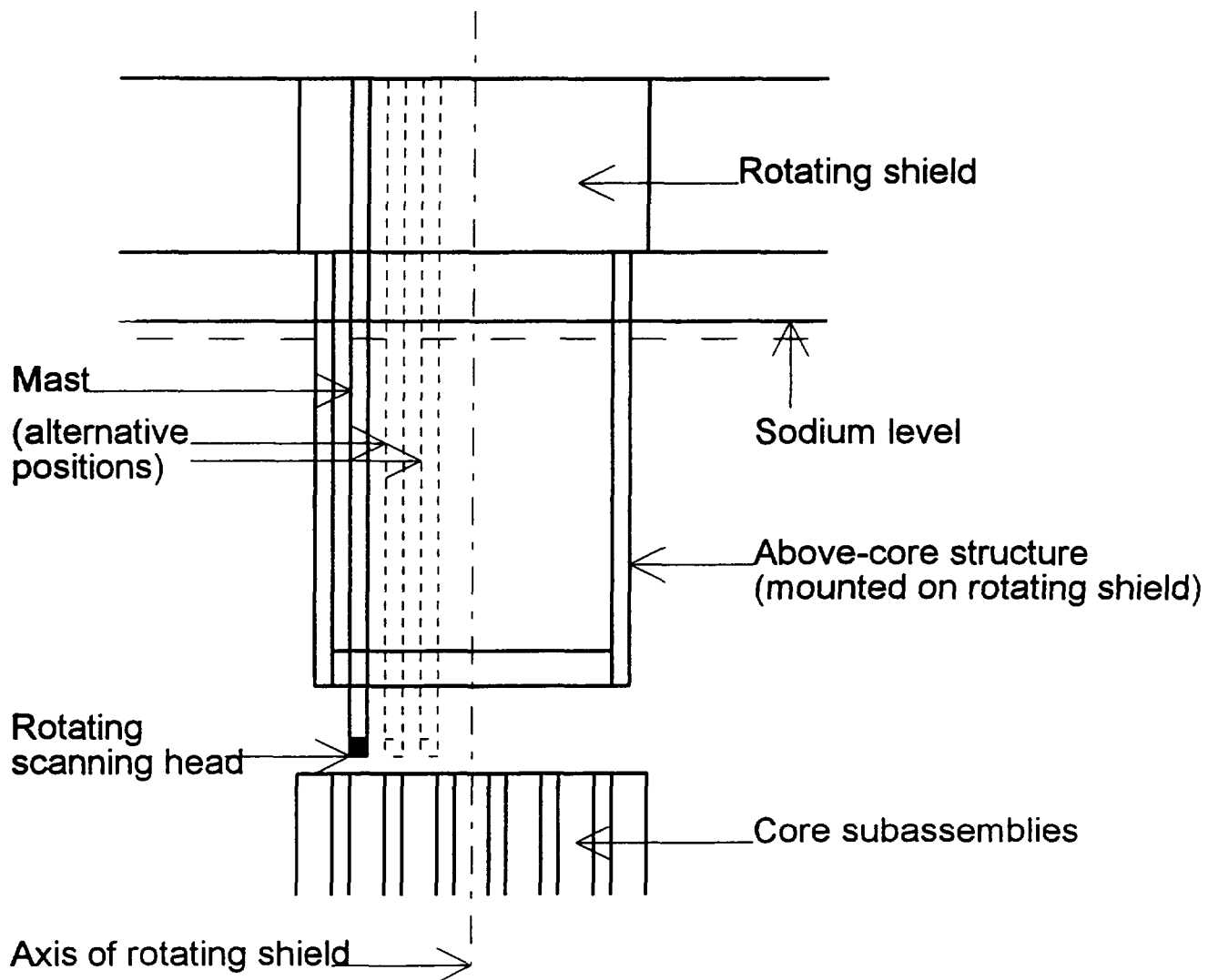


FIG 6 19b Arrangement for ultrasonic viewing of the PFR core

this can be used to give assurance that there has been no change in the structure, due to the growth of a crack, for example.

6.3.3. Ultrasonic measurement of temperature

In any of the above applications attention has to be given to the influence of sodium temperature on the speed of sound and corrections made where necessary. This effect can be put to positive advantage, however, by using ultrasonics as a means of measuring temperature. If the distance between two reflectors is known, the time of flight of a pulse between them can be used to determine the speed of sound, and hence the mean sodium temperature, in the region in between. The advantage of this method is that there is no need for a measuring device such as a thermocouple, nor for the structure to support it, in the region to be monitored.

This advantage may be very valuable in regions such as the outlets from breeder subassemblies. It is difficult to place thermocouple there because the support structure would be subject to damage by thermal striping. Figure 6.21 shows the arrangement of a scanner which measures the return time of ultrasonic echoes from each of a row of subassembly outlets. From these times the mean sodium temperature from each subassembly can be deduced. By averaging the times for several pulses the effects of turbulence and temperature noise can be allowed for. In-sodium tests have shown [6.29] that temperature can be measured in this way to within ± 7 K over the range 200 - 420°C.

6.3.4. Ultrasonic systems

For imaging and inspection purposes the ultrasonic beam has to be deployed suitably to scan the desired object. For example, in the PFR core imaging application described above downward-facing transducers were scanned above the core. However, for more complicated purposes a more flexible scanning system, capable of manipulating the transducers freely in the sodium volume, has to be used. Various manipulators have been designed for this application. One such is a "link arm", a semi-rigid chain which can be extended and rotated to give three degrees of freedom in locating a transducer and presenting it to the object to be examined [6.30].

An alternative is to steer the beam by entirely electronic means. A linear array of transducers each of which produces a pulse will form a wave front which propagates through the sodium. If the transducers fire simultaneously the wave front is a plane parallel to the array and propagates normal to it. If they fire in a linear sequence the front will form at an angle and will propagate away from the normal. By varying the time delays between the firing of individual transducers a curved wave front can be formed and made to focus at a pre-determined location. This is known as the Synthetic Aperture Focusing Technique (SAFT). The formation of wave fronts can be visualised by using Schlieren techniques to observe the behaviour in water, as shown in Figure 6.22.

The advantage of this approach is that a stationary array of transducers can be made to scan a range of objects without the use of moving parts under sodium.

6.4. IN-SERVICE INSPECTION AND REPAIR

The main objective of ISI&R (In-Service Inspection and Repair) is to provide fast-neutron reactors with effective inspection and repair capabilities in order to: (1) assist in

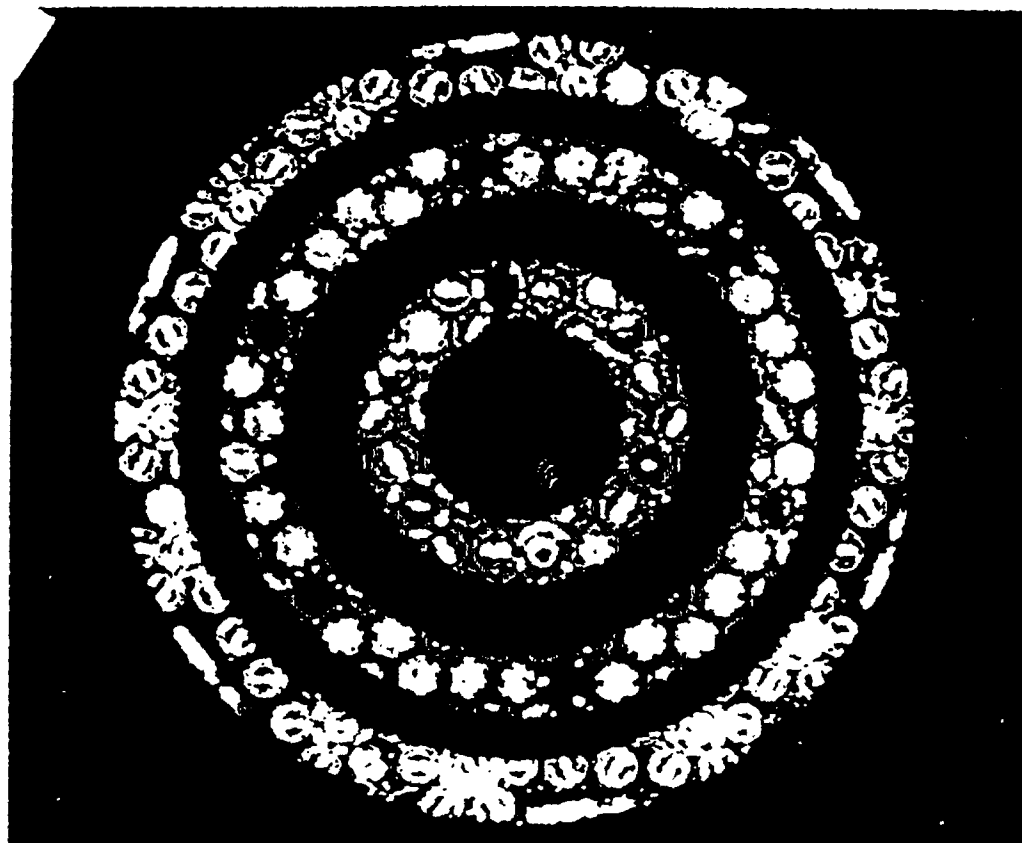


FIG. 6.20. Ultrasonic image of part of the PFR core seen from above

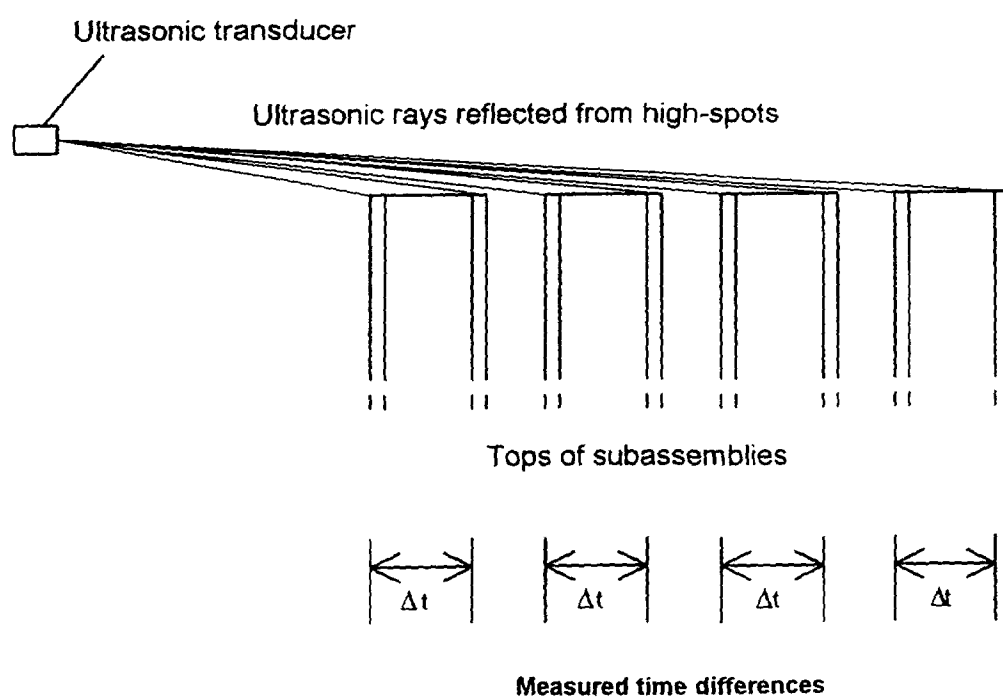


FIG. 6.21. The principle of ultrasonic measurement of temperature

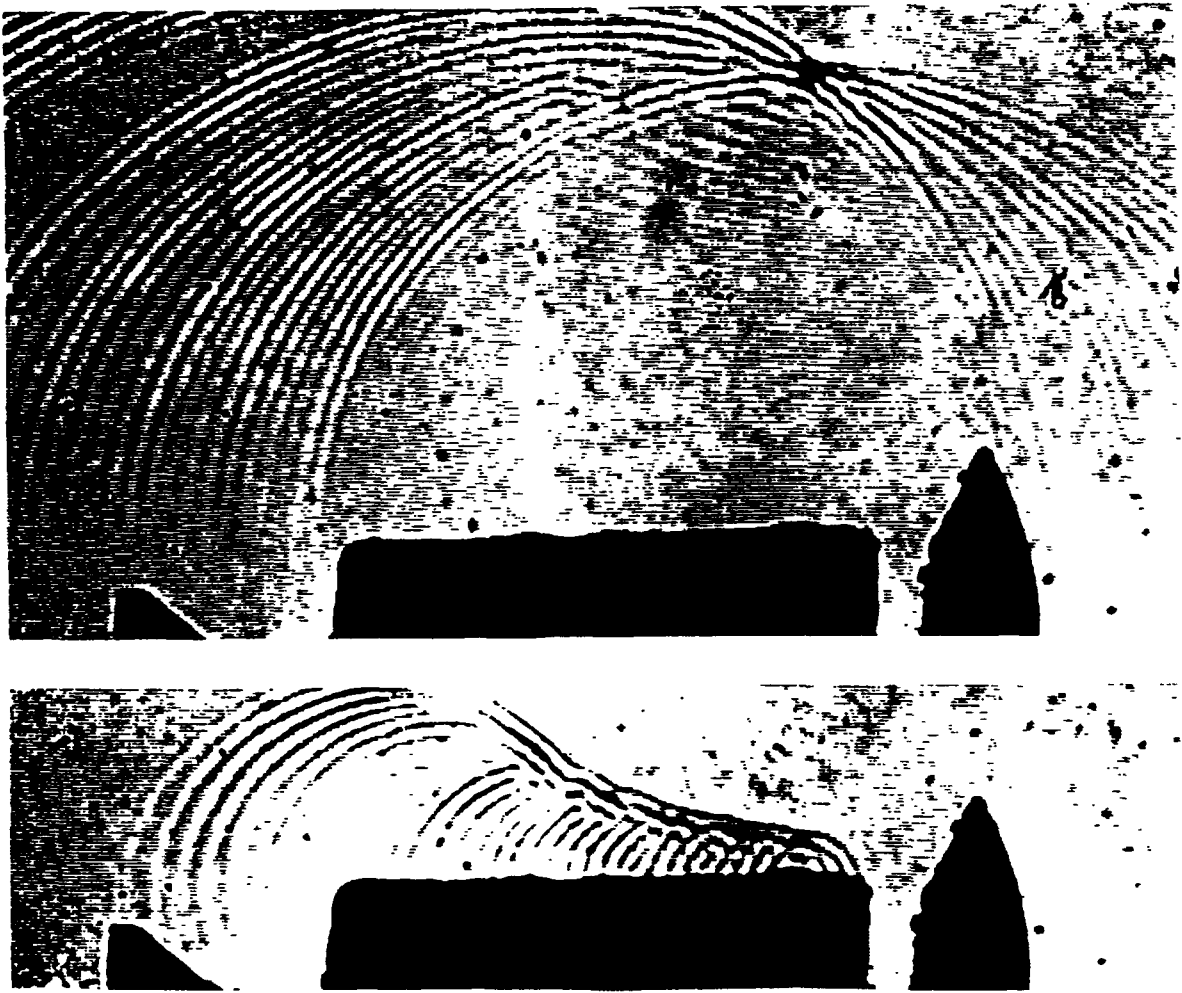


FIG. 6.22. Visualisation of ultrasonic wavefronts formed by an array of 32 transducers in water

avoiding situations leading to major accidents, (2) minimise reactor outage, (3) reduce repair costs. For that purpose, it is necessary: (1) to detect anomalies or flaws as early and as quickly as possible, (2) to locate and measure flaws so as to diagnose the problem and make appropriate decisions, (3) to carry out repair, if any, in conditions adapted to the reactor environment, and to minimise repair time.

6.4.1. Background

In-service inspection of PWRs is current practice and there is a general agreement that it is necessary to improve the inspection and repair capability of LMRs. Sodium as LMR coolant makes in-service inspection difficult because it is always at temperatures between 180-580°C, and poses physico-chemical problems: it must always be maintained in inert atmosphere: and it is opaque, which makes direct observation impossible. For LMRs, particular attention is devoted to the reactor block (but also to sodium pipings and steam generator tubes where problems due to the presence of sodium may arise). The main points in which a defect may put the safety of the reactor at risk are: (a) the main vessel, (b) the core cover plug, (c) the strong back support skirt, and (d) the LIPOSOs. On the other hand, components such as intermediate exchangers, pumps, etc... are removable, so that efforts in the ISI&R programme have been centered on unremovable structures.

Research and development work in different European countries was presented at two IAEA-IWGFR specialists' meetings at Bensberg, Federal Republic of Germany, in 1976 and in 1980. Since then, a common approach for EFR allowed ISI&R requirements and constraints to be taken into account at the design stage of the reactor block. Because of the demand from Safety Authorities for an ISI&R programme for PHENIX and SUPERPHENIX, France is currently conducting, with considerable financial commitment, research and development into in-service inspection and repair. It is the only European country still involved in such a programme. Consequently this review covers only: (1) the operational ISI&R components on PHENIX and SUPERPHENIX, and (2) the long-term research and development programme undertaken in France by the CEA in co-operation with EDF and Framatome.

6.4.2. Operational in-service inspection components

In-service inspection of the tank. In-service inspection of the LMFBR tank system will be necessary in all future commercial size LMFBRs. By way of example one design solution is described here: the MIR system for SUPERPHENIX. In SUPERPHENIX, in-service inspection of the reactor tank will take place during planned outages. The temperature condition will then be 180°C at the main pool tank and 130°C at the outer safety tank; The space between the tanks is filled with nitrogen. The tanks hang from the slab which has 12 man-holes of oval shape (0.7 X 0.44 m) through which the in-service inspection vehicle MIR (Machine d' Inspections pour Réacteurs rapides) can be inserted. The distance between the tanks will be some 600 mm at hot temperature conditions. The MIR system (Fig. 6.23) includes:

- the vehicle carrying the ultrasonic and visual testing equipment,
- a winch and drive assembly preventing damage to the thermal barrier,
- a computer assisted control system.

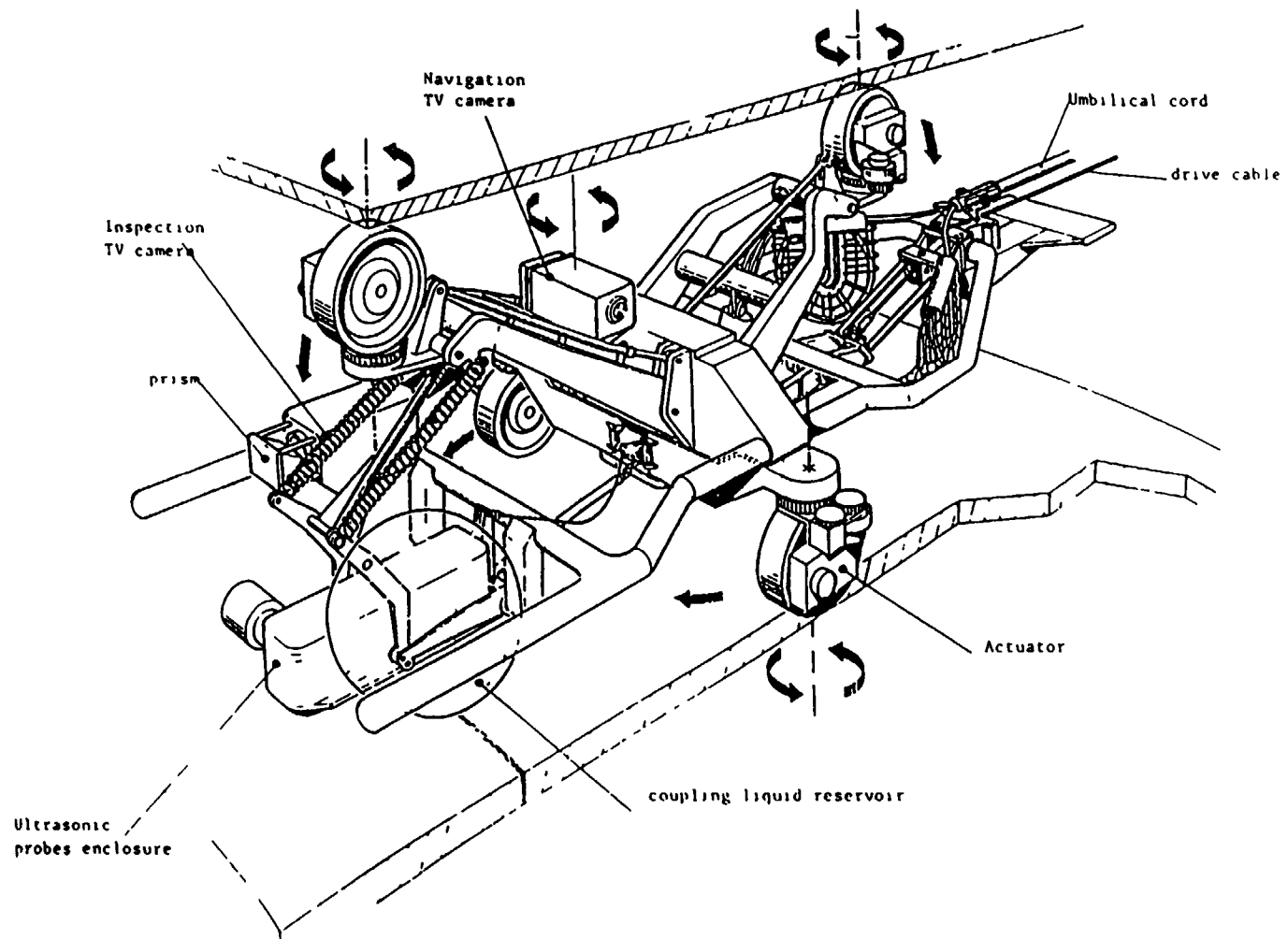


FIG 6 23 MIR Vehicle

The MIR vehicle consists of two steering traction wheels resting on the tank wall by means of a spring mechanism. The overall dimensions of the vehicle are: 1.8 m length, 0.56 m width, its weight is about 250 kg.

The inspection devices on board the vehicle are:

- TV cameras for weld examination, guidance of the vehicle in the space between the tanks and for general viewing of the environment,
- an ultrasonic testing device using focused probes adapted to the material plate thickness and welds to be examined.

The winch continuously controls and minimizes the traction force and torque exerted on the vehicle by the cable. It is located about 6 m above the upper part of the slab. In the event of emergency it can extract the vehicle from the space between the tanks. Control of the MIR system is achieved by a hierarchical computer system. A microprocessor carries out elementary orders and checks.

Under-sodium systems for visualization and telemetry. Under-sodium viewing and ranging systems have been developed to produce pictures of objects immersed in 5 m of liquid sodium in the reactor tank. The system operates in two modes: viewing and ranging. Scanning is accomplished by rotating a scanner arm that is positioned above the object to generate ultrasonic beams that are directed vertically downward. Typical viewing distances up to 5 m by operating the system in the ranging mode. The following capabilities have been demonstrated:

- core component identification, location and orientation can be determined by forming pictures of coded notches,
- adjustments in the position of in-vessel mechanisms can be monitored
- the relative elevation of adjacent subassemblies can be determined to within 0.05 m,
- objects up to 5 m from the scanner can be located to within $\pm 0.5\%$ of the actual scanner to object distance,
- the combination of ranging and imaging capabilities can assist in the location and retrieval of foreign objects or out of position components in the reactor tank.

Under-sodium viewing systems have been developed mainly in the USA (FFTF), in France (PHENIX, SUPERPHENIX) and in the UK (as described above in section 6.3).

In-argon television and periscope inspection methods. Remotely operated TV camera systems have been developed for continuous TV viewing and with the ability to provide high resolution photographs. They were applied to inspect the core of PFR. Miniature cameras have also been developed to inspect the superheater tubes in PFR from the outside and evaporator tubes from the inside. Periscopes and boroscopes were extensively used in RAPSODIE, PHENIX and SUPERPHENIX. Good image resolutions were obtained at temperatures up to 150°C during inspection of different components.

6.4.3. Research and development in France

Guidelines. The main objective is to define processes allowing inspection, diagnosis and intervention to be carried out in the reactor block. Any intervention is considered to take place during reactor shutdown, that is, with sodium at a temperature of about 180°C. For routine inspections, the level of sodium will not be lowered. Therefore, under-sodium

inspection methods have to be developed. Complete or partial draining would be reserved for exceptional interventions. In all cases, technological difficulties are considerable:

- in sodium, there are problems of opacity, temperature and compatibility of different materials.
- in argon, work must be performed at high temperature. Sodium films, aerosol deposits, mesos or may be found on the surfaces.

For the inspection of the reactor block, accessibility to the main unremovable components and structures is indispensable for allowing a diagnosis and an intervention, if needed. Accesses should be provided and tools should be developed but these are typical engineering design tasks. In the case of intervention in the lower part of the main tank, which would require draining the sodium, study reduction of the time for complete unloading of the core is also on of the engineering design tasks. The medium-term objective (5 years), rather than to develop materials and procedures, is to develop processes or, at least, to ensure that they could be developed. The programme then mainly includes research and development on basic techniques; it takes into account the needs defined by engineering.

Programme

Basic techniques

A. IN-ARGON INSPECTION

Telemetry. Telemetry is used for detecting displacements of structures or components. The methods chosen are optical measurement devices using light beams, preferably laser, which are reflected by targets or by the surfaces themselves. These techniques are subject to the difficulties specific to light transmission, in particular:

- to diffusion in case of aerosols,
- to refraction in case of thermal gradients.

The research and development already performed has shown that the uncertainties about the refraction factor are compatible with the accuracy sought. The characteristics of the targets or reflecting surfaces as well as their evolution over time (deposits), and the incidence of the diffusion factor, have still to be defined. The most adequate methods will have to be selected, taking account of the accuracy needed and the reactor constraints. These points are to be studied initially by means of models and a number of tests on a simplified mock-up. The process will then be validated on a mock-up representative of the cover gas.

Volumetric controls. They consist in detecting possible "health flaws" (cracks). The problem is rather similar to the control of the main tank but it is more difficult due to sodium aerosols and/or mesos that may have deposited over the surfaces to be inspected. The use of ultrasound is already known and research and development will allow specific difficulties to be assessed and solved:

- shape of the parts to be inspected,
- condition of the surfaces,
- coupling between transducers and surfaces to be inspected.

Multi-element sensors will also be evaluated in terms of their behaviour at high temperature and of their performance in order to solve, in particular, the problem of disturbances.

B. UNDER-SODIUM INSPECTION

Telemetry. In order to optimise known means, a study and a series of in-water tests have been performed. A measurement accuracy of 2 mm at a distance of 5 m was achieved. This accuracy will have to be confirmed by in-sodium tests on some particular points and by an overall qualification at full-scale 1 probe. New work is in progress in the CEA in order to develop a technique using ultrasonic reflection:

- either from targets fixed to the structures;
- or from the surfaces of the structures themselves.

The type of targets and surfaces best adapted to reflection have to be characterised; the accuracy of such measurements and the telemetry errors that may result have to be determined. This development involves model studies as well as in-water and in-sodium tests.

Visualization. Several techniques have already been developed to produce, by using ultrasound, 2 or 3 dimensional images of structures immersed in sodium (visus for Phenix and Superphenix, perch for PFR). Technological developments have also been carried out by NNC and AEA to visualise the EFR core and spacer grid using the link-arm system (see 6.3.4 above). The research and development programme involves actions on:

- the use of ultra-sound retro-diffusion by the asperities on the surfaces,
- the use of natural acoustic sources,
- the use of inherent acoustic sources,
- the use of the SAFT (see 6.3.4).

The first stage is a feasibility assessment; further steps will include model tests, a number of tests for developing transducers and last, in-sodium tests.

Volumetric controls. Volumetric inspection methods are indispensable to be able to diagnose a problem on an immersed structure. The points to be considered are:

- the development of appropriate ultrasonic transducers,
- the determination of operational characteristics so as to meet specifications,
- the approach and the positioning of the sensors.

Again, a modelling approach is planned, followed by some validation tests, some of which will be carried out in sodium.

C. DEVELOPMENT OF ULTRASONIC TRANSDUCERS

For all volumetric control and for under-sodium telemetry, ultrasonic techniques are used. Particular difficulties are the temperature and the presence of sodium. Research and development therefore involves developing transducers whose characteristics can vary according to their application; for instance, for volumetric control, a good damping is necessary. In order to develop in a short time versatile and reliable transducers, sensors for

temperatures not exceeding 200°C have been chosen. The routes selected for optimising transducers are:

- to search for diaphragms easing wetting at low temperature;
- to reduce the diameter and thereby the size of the probe;
- to use multi-element transducers allowing scanning and focusing to be adjusted. Mechanical motions can thus be reduced and the same control head can be used for different situations.

Experience acquired by the AEA as well as by SIEMENS on these themes is taken into account. For volumetric controls, complementing the use of transducers, EMAT sensors are being developed. Compared to transducers, they have the advantage of operating without a coupling liquid and can therefore be used in gas as well as under sodium.

Repair. As mentioned before in-sodium inspection is indispensable but of course, repair, if needed, will be carried out in gas. The exceptional character of such an operation justifies draining the sodium, at least partially. It is therefore indispensable to master the following processes:

- cleaning of the surfaces in order to confirm the diagnosis or prepare for the repair,
- cutting of the identified damaged part of a structure,
- welding of a replacement part,
- final control and requalification.

Priority has been given to this programme and a specific experimental facility has been set up (MIRSA). For each process, different techniques have been selected and will be evaluated, tested and qualified:

- mechanical cleaning, laser cleaning,
- mechanical cutting (classical) and laser cutting,
- TIG and laser welding,
- final controls are performed using the technologies developed for inspection.

Accessibility. There is no research and development on accessibility. For a new LMFR reactor project, accesses should be provided for inspecting as many areas zones as possible, or at least, identified sensitive zones. This implies taking into account the architecture of the reactor and the characteristics of the inspection and repair processes. This task is part of the engineering design. In case of an intervention in the lower part of the reactor requiring sodium-draining, unloading of the core would be a major preliminary operation. It should therefore be easy and fast.

Special applications

Primary tank controls. There is no reason to search for an alternative to the MIR system which has proved quite efficient. According to the needs (evolution of specifications) or to the new possibilities offered by technological progress on ultrasonic transducers (and in particular on multi-elements) improvement and optimization will be possible within the limits of basic techniques and processes.

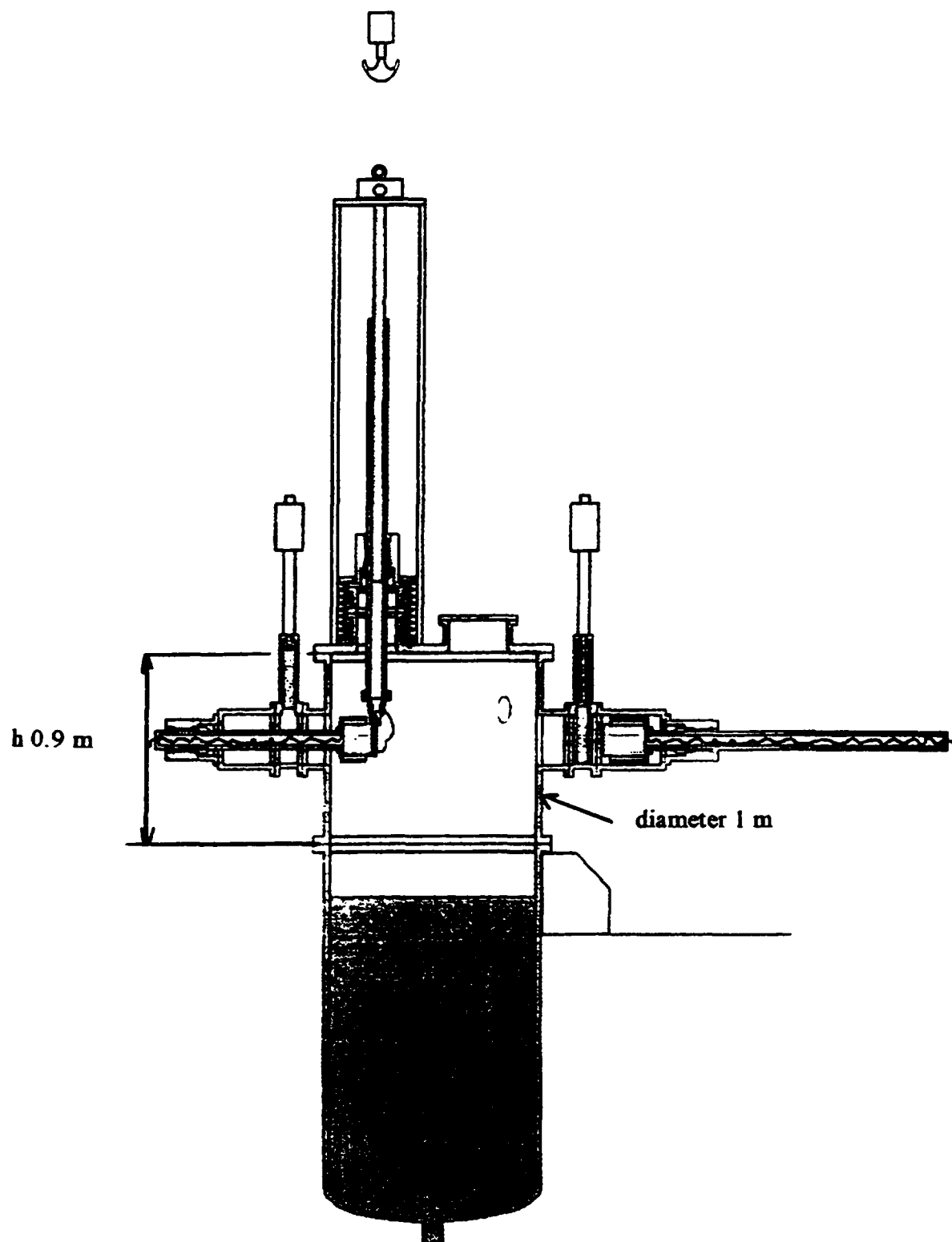


FIG. 6.24. MIRSA test facility processes validation

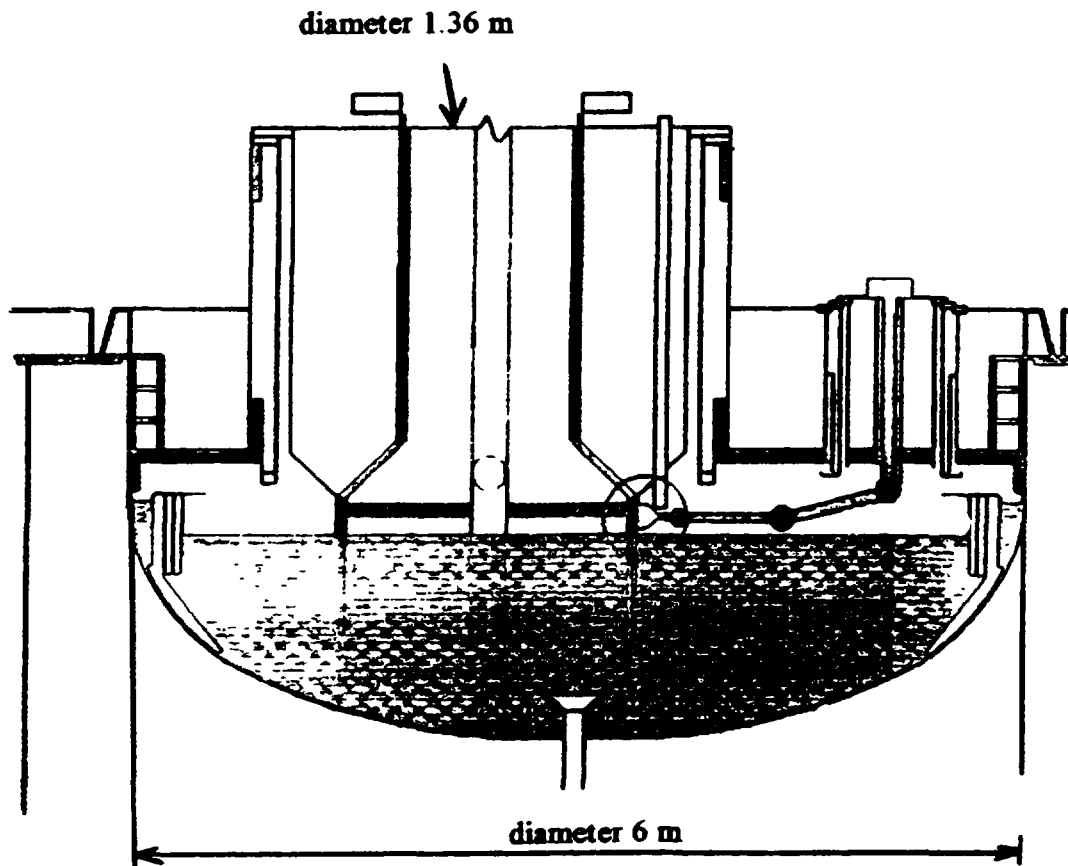


FIG.6.25. Gulliver mock-up processes qualification

Unloading of the core. Studies and tests on the thermal behaviour of fuel during unloading are in progress (LEDA programme). The tests consist of putting a subassembly into the different thermal conditions it will go through if transferred from the cover gas to the decay pool. The chosen configuration is a sequence of operations carried out one after another with no interruption in the process.

Timetable. The R&D programme as currently planned, should allow qualification of processes to be achieved by 2000. However, as this is a long-term programme, it may be subject to changes due to new requirements or needs and also to the budgets assigned

Experimental means. Beside the laboratory work and small-scale test devices required for the evaluation phase of the processes involved, large-scale facilities are also available:

- the MIRSA containment (Fig. 6.24) which is set up on a sodium pool, will be operational at the beginning of 1995 and will initially allow the validation of the TIG programme. All the repair processes will be validated on this test facility.
- the Gulliver mock-up which is representative of the reactor cover-gas (SPX1) will be used to qualify all processes (Fig.6.25).

REFERENCES

- [6.1] Mitenkov, F.M., Golovko, V.F., Ushakov, P.A., and Yuryev, Yu.S., The Design of Heat Exchange Equipment for Nuclear Power Plants, Energoatomizdat, Moscow, Russia, 1988.
- [6.2] Hayden, O., Design and Construction of Past and Present Steam Generators for the UK Fast Reactors, *J. Br. Nucl. Energy Soc.*, 15, 2, (1976), 129.
- [6.3] Mauget, C., and Gilroy, J. Advanced Steam Generators for EFR. Proceedings of the International Conference on Fast Reactors and Related Fuel Cycles, Kyoto, Japan, October 1991, 1, 9.8.
- [6.4] Judd, A.M., Fast Breeder Reactors - an Engineering Introduction, Oxford, Pergamon, UK, 1981.
- [6.5] Robin, M. G., Careful Attention to Detail was Necessary in Developing the SUPER-PHENIX Steam Generators. *Nuclear Engineering International*, 22 May, 1977, 46.
- [6.6] Sakai, S., et al. Design and Construction of the Steam Generator and Water Systems of the Prototype Fast Breeder Reactor MONJU. Proceedings of the International Conference on Fast Reactors and Related Fuel Cycles, Kyoto, Japan, October 1991, 1, 8.5.
- [6.7] Suraev, O.M., Oshkanov, N.N. and Vylomov, V.V., 14-year Operating Experience from BN600 Power Plant. Proceedings of the International Topical Meeting on Sodium-Cooled Fast Reactor Safety, Obninsk, Russia, October 1994, 4, 5-30.
- [6.8] Kishihara, N., et al. Feasibility Study on Double-wall-type Primary Steam Generator. Proceedings of the International Conference on Fast Reactors and related Fuel Cycles, Kyoto, Japan, October 1991, 3, P2.7.
- [6.9] Roy, P., and Licina, G.J., Carbon Activity Determinations in a Bimetallic Sodium Loop Mock-up of the Intermediate Heat Transport System of a Liquid Metal Fast Breeder Reactor. Proceedings of the Third International Conference on Liquid Metal Engineering and Technology in Energy Production, Oxford, USA, April 1984, 3, 207.
- [6.10] Judd, A.M., Currie, R., Linekar, G.A.B., and Henderson, J.D.C., The Under-sodium Leak in the PFR Superheater 2, February 1987. *Nuclear Energy*, 31, 3 (1992), 221.
- [6.11] Foerster, K., et al., LMFBR Steam Generators-realistic Investigations on Leakage Accidents. Proceedings of the Fourth International Conference on Liquid Metal Engineering and Technology, Avignon, France, October 1988, 1, 307.
- [6.12] Desmas, T. and Lemoine, P. A., Study of Small Leaks of Water in Sodium-heated Steam Generators: Self-evolution and Wastage. Proceedings of the Third International Conference on Liquid Metal Engineering and Technology in Energy Production, Oxford, UK, April 1984, 1, 1.
- [6.13] Greene, D.A., Sodium-water Reaction Phenomena Associated with Small Leaks Ion LMFBR Steam Generators. Proceedings of the Third International Conference on Liquid Metal Engineering and Technology in Energy Production, Oxford, UK, April 1984, 1, 13.
- [6.14] Currie, R., et al. Sodium-water Reactions: Production of Data for the European Steam Generator Accident Common Code System: Small Leak Wastage and Steam-sodium Surface Corrosion Investigations. *Ibid.* 1, 308.
- [6.15] Robertson, C., and Walford, J.D., The Leak in Superheater 2 - PFR February 1987. Proceedings of the Fourth International Conference on Liquid Metal Engineering and Technology, Avignon, France, October 1988, 3, 712.
- [6.16] Hans, R., and Dumm, K., Leak Detection of Steam or Water in Steam Generators of Liquid-metal Fast Breeder Reactors. *Atomic Energy Review*, 15, 4, (1977), 611.

- [6.17] Bouchacourt, M. et al. EdF Experience on Analysis of Non-metallic Impurities in Sodium. Proceedings of the Third International Conference on Liquid Metal Engineering and Technology in Energy Production, Oxford, UK, April 1984, 1, 45.
- [6.18] Smith, C.A. and Simm, P.A., Calibration and Performance of Galvanic Cell Hydrogen and Oxygen Meters in Sodium. Proceedings of the Third International Conference on Liquid Metal Engineering and Technology in Energy Production, Oxford, UK, April 1984, 3, 103.
- [6.19] Asher, R.C. et al., Recent Developments in the Design, Performance, and Application of Harwell Oxygen Sensors and Harwell Carbon Meters. Proceedings of the Fourth International Conference on Liquid Metal Engineering and Technology, Avignon, France, October 1988, 3, 602.
- [6.20] Gnanasekaran, T. et al., Experience with on-line Meters for Measuring Hydrogen in Sodium Coolant. Proceedings of the Fourth International Conference on Liquid Metal Engineering and Technology, Avignon, France, October 1988, 3, 604.
- [6.21] Thorley, A.W., Blundell, A., Bardsely, J.A. and Lloyd, R., Mass Transfer Behaviour of Stainless Steels in Flowing Sodium Environments at Different Oxygen Levels. Ibid, 3, 532.
- [6.22] Greene, D. A. et al., Acoustic Leak detection Development in the USA. Proceedings of the Third International Conference on Liquid Metal Engineering and Technology in Energy Production, Oxford, UK, April 1984, 1, 129.
- [6.23] Girard, J-Ph. (ed) Proceedings of the Specialists Meeting on Acoustic/Ultrasonic Detection of in-sodium Water Leaks on Steam Generators, Aix-en-Provence, France, 1-3 October, 1990. IAEA IWGFR/79, 1991.
- [6.24] Gregory, C.V., and Lord, D.J. The study of Local Blockages in FBR Subassemblies. J. Br. Nucl. Energy Soc., 16, 3 (1977), 251.
- [6.25] Acoustic Signal Processing for the Detection of Boiling or Sodium/Water Reaction in LMBFRs. IAEA IWGFR, to be published (Final report and proceedings of a Coordinated Research Programme organised by the IAEA, 1989-1995).
- [6.26] Signal Processing Techniques for Boiling Noise Detection, IAEA IWGFR/68, 1989.
- [6.27] Lennox, T., McKnight, J.A., and Rowley, R., Application of Acoustic Instrumentation for Use in Liquid Metal Fast Breeder Reactor. Nucl. Energy, 32, 1 (1993), 29.
- [6.28] McKnight, J.A. et al., The use of Ultrasonics for Viewing Components of the Prototype Fast Reactor Whilst Immersed in Sodium. Proceedings of Ultrasonics International 83, Butterworths Scientific, Halifax, Canada, pp135-140.
- [6.29] Brown, C.J. and Hughes, G., Remote Measurement of LMFBR Subassembly Outlet Temperatures by Ultrasonics. Nucl. Energy, 31, 4 (1992), 261.
- [6.30] McKnight, J.A., Burton, E.J., and Fennemore, P. Recent Advances in the Technology of Under-sodium Inspection in LMFBRs. Proceedings of the Third International Conference on Liquid Metal Engineering and Technology in Energy Production, Oxford, UK, April 1984, 1, 423.

**NEXT PAGE(S)
left BLANK**

Chapter 7

CORE STRUCTURAL MATERIAL AND FUEL TECHNOLOGY FOR HIGH BURN-UP

7.1 INTRODUCTION

The former IAEA Fast Reactor Status Report (1985), [7.1], provided detailed information on the description and irradiation performance of materials, fuels and components for fast reactor cores. The purpose of the present up-date is to review the experience gained on the behaviour of these core assemblies at high burn-up, highlighting the phenomena which can be life limiting. This survey will focus on fuel and absorber elements which represent the greatest challenge for high burn-up reactor cores, and will ignore other core components such as blanket assemblies, shielding elements, etc.

7.2 BEHAVIOUR OF MATERIALS FOR FUEL PIN CLADDING AND SUBASSEMBLY DUCT (WRAPPER)

7.2.1. Pin cladding materials

Austenitic steels Extensive R & D work has been devoted to austenitic steels by all the countries developing fast reactors. The status of development in the main national groups can be summarized as follows:

Europe (Refs. 7.2-7.5) The national programmes in France and Germany led to the selection of titanium-stabilized (0.4-0.5%) cold worked (15-20%) steels as reference candidates, namely the French 15-15 Ti alloy (10 CR Ni Mo Ti B) and the German DIN 1 4970 alloy (10 CR Ni Mo Ti). For these cladding materials more than 10 000 pins with oxide fuel and peak cladding temperature up to 650°C have reached dose values of 100 dpa (NRT) and about 1000 pins have exceeded 125 dpa with a maximum value of 148 dpa for an experimental sub-assembly (217 pins), still in the core of the PHENIX reactor. No actual endurance failure occurred with the reference fuel design. These large numbers of irradiated pins have emphasized the beneficial effects of an adjustment of cold work level and the addition of some minor elements (Ti, C, Si, P), on the swelling and irradiation creep behaviour where the increase of incubation dose before swelling occurs is the most important factor. As an example, results of post irradiation measurements are given in Fig. 7.1 which shows the improvement of the swelling behaviour by changing from the SS 316 through to the improved versions of the 15-15 Ti/1 4970 type. The mechanical properties of these materials have also been accurately investigated through tensile tests performed both in the longitudinal and transverse directions using specimens machined from defuelled PHENIX fuel elements. The results showed that the mechanical behaviour depends not only on the test and irradiation conditions but also on the swelling resistance. The effect of irradiation varies with temperature: hardening at low temperatures and softening at high temperatures was observed, associated with dislocation re-arrangements, but no recrystallization occurred. It appears (Fig. 7.2) that, at least up to about 120 dpa, these alloys have sufficient high temperature strength and adequate ductility in the temperature range of fuel pin cladding.

The post-irradiation results have also confirmed the excellent resistance of these materials to external sodium corrosion (maximum depth of 30 mm measured on a PHENIX pin irradiated to 13.6 at % over 826 EFPD (Equivalent Full Power Days)). Recent development

work has been carried out, within the framework of the European Collaboration, leading to the specification of a reference cladding material, the so-called AIM1 (Austenitic Improved Material number one), designed to meet the ambitious EFR (European Fast Reactor project) target (170 dpa). The first batches of this alloy have been fabricated and will be irradiated in the PHENIX reactor in the near future. In parallel, an R & D programme is under way to develop advanced austenitic cladding materials (10.15 Cr/15.15 Ni type - Ti Nb stabilization - high P content...). A Ti stabilized material containing 12 Cr and 25 Ni has been used to fabricate fuel pins under industrial conditions and 3 subassemblies have been prepared for irradiation in PHENIX. A first subassembly has been irradiated up to 108 dpa and the clad profilometries have been performed. The behavior of this material is very encouraging since, as displayed in Figure 7.1, its swelling resistance is clearly higher than the best alloy 15.15 Ti, even Si modified.

The United States. [Refs. 7.6-7.9] Valuable experience has been gained on the 20% CW titanium stabilized stainless steel designated "D9", irradiated in the FFTF (Fast Flux Test Facility) with oxide fuel at peak cladding temperatures up to 675°C. General features of the irradiation exposure reached to date are illustrated in Figure 7.3, including all the tested cladding materials. On the basis of more than 2000 highly irradiated pins, a target exposure of 100 dpa was demonstrated and exceeded up to a maximum value of about 140 dpa on a test subassembly which has not been yet examined. Alloy D9 reached 37% volume increase at a peak fluence $24 \cdot 10^{22}$ n/cm² [7.8]. D9 exhibits a longer fluence incubation period at higher temperatures than 316 SS. The D9 alloy has not, however, fulfilled the early promise of optimistic swelling correlations. This extensive experience demonstrated that the performance of the D9 alloy at large exposure was quite good, but it was also observed that when swelling is large (e.g. greater than 10% diametral), this type of cladding material is prone to brittle failure, particularly at handling temperatures (when examined in hot cells), attributed to localized channel fracture. Therefore, a functional limit of about 110 dpa was used for designs with 5.84 mm diameter cladding for the FFTF.

Japan. (Refs. 7.10, 7.11) Through out-of-reactor testing and neutron irradiation in JOYO and foreign fast reactors (RAPSODIE, PHENIX, DFR, FFTF,...), fuel cladding materials were developed by optimization of standard type 316 stainless steel. The reference versions (20% cold-worked) are designated PNC 316 for MONJU fuel and PNC 1520 for DFBR (Demonstration Fast Breeder Reactor) fuel. The swelling behaviour as a function of dose is shown in figure 4 for the various steel compositions progressively developed by PNC. Whereas PNC 1520 is at an early stage of irradiation testing, the high exposure capability of PNC 316 has been confirmed by irradiation in JOYO (more than 27000 fuel pins over 50 dpa) and in FFTF (a subassembly up to 120 dpa and material specimens up to 185 dpa), over a large range of temperature (415°C to 670°C). The results showed the excellent dimensional stability of this material (maximum diameter increase of less than 1% for a JOYO pin at 50 dpa - axial elongation much lower than for the D9 alloy in FFTF at 105 dpa). Good mechanical properties were also seen in out-of-pile testing (for example more than 200 MPa strength at 650°C and 10 000 h rupture time); they have yet to be confirmed at high exposure rates.

Russia. Conventional austenitic stainless steels have been optimized by addition of B, Ti and Mg. Extensive experience involving more than 100 000 fuel pins, has been gained on the 20% CW TschS-68 steel irradiated in BN-600 with oxide and MOX fuels at peak temperatures up to 700°C [Refs. 7.12, 7.13]. More than 2500 fuel pins reached doses more than 80 dpa, with a maximum dose of 94 dpa. This steel has been used successfully as the standard cladding material since the beginning of 1991. Post-irradiation profilometry has

shown quite high volume increase of the TchS-68 steel: up to 12% at doses 85-90 dpa. Destructive post-irradiation examinations (PIE) resulted in brittle failures of this type steel at handling temperatures [7.14]. Development work has been carried out for the further improvement of austenitic steel in order to increase its strength and ductility and to decrease its swelling by optimising the additive composition and improving the metallurgical and technological processes. Samples made of improved austenitic steels have been irradiated in BN-600 up to 108 dpa. The PIE is under way now.

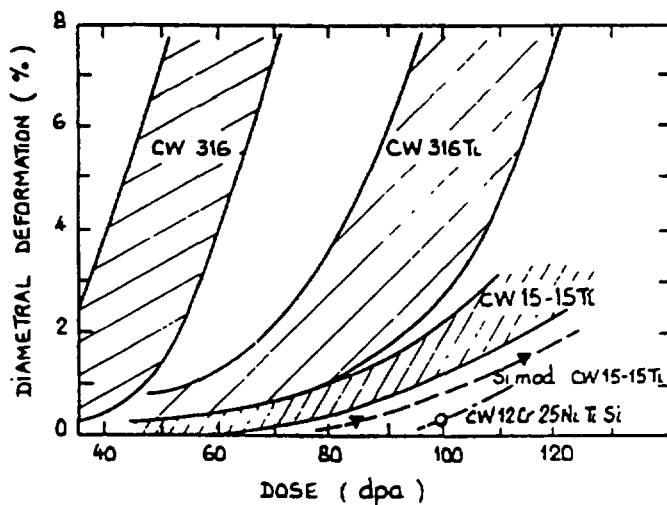


FIG. 7.1. Diametral deformation on various austenitic materials in the PHENIX reactor.

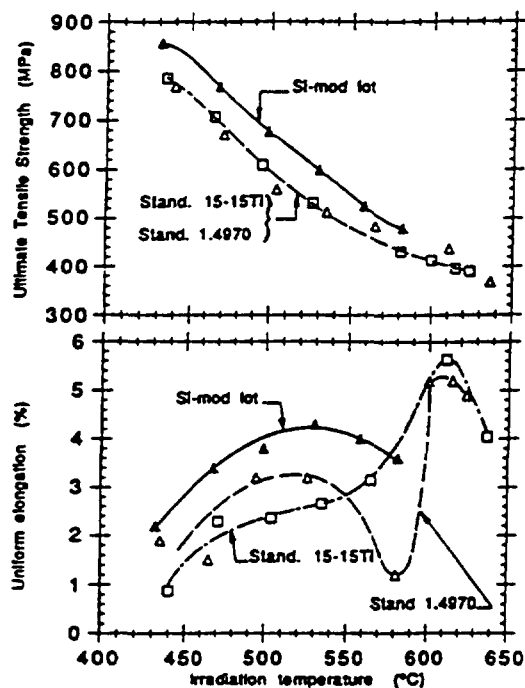


FIG. 7.2. Comparison of the tensile properties of the standard 15-15 Ti Phénix, 1.4970 standard and Si-modified 15-15 Ti irradiated to the same dose (115 dpa). Tests were performed at the irradiation temperature.

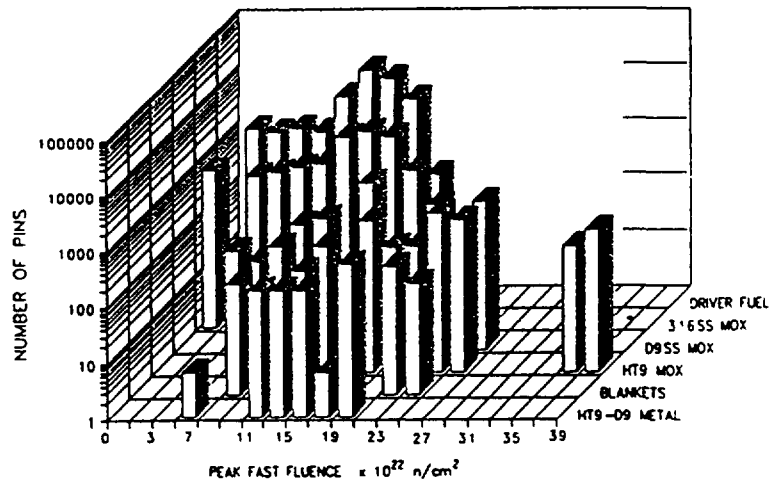


FIG 7 3 Status of accumulated fast fluence on driver and test pins in Fast Flux Test Facility

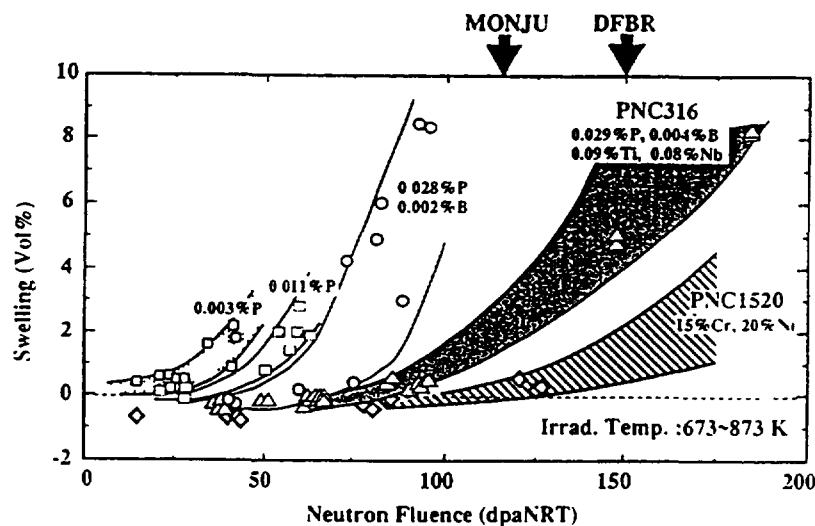


FIG.7.4 Progress of swelling resistance characteristics for PNC austenitic steels.

High nickel alloys A high Nickel alloy, designated STA Nimonic PE 16, was developed in the United Kingdom [7.2,7.5] as reference cladding material for PFR fuel and candidate for EFR fuel. This alloy was selected because of its high temperature strength and subsequent irradiations in both DFR and PFR showed an inherent resistance to void swelling. Much experience has been gained with PFR oxide fuel pins (5.84 mm and 6.6 mm OD).

Of a total 96,200 pins irradiated, approximately 3500 pins have exceeded a dose level of 100 dpa and 265 pins have reached a maximum exposure of 155 dpa, of the failure events which

have occurred only a very limited number have been associated with the high burn-up designs. The maximum diametral strain measured so far in any STA PE 16 clad pin in UK has been about 1% and there have been no indications of any rapid rise in swelling rate at high dose, so that diametral strains of around 2-3% are predicted at 200 dpa. The PFR pin irradiation programme which involved 30 different casts and over 100 different batches has shown no significant variation from the expected swelling behaviour of the pins examined to date, implying little sensitivity to composition variation within the specification given to the tube manufacturers. Post irradiation mechanical properties tests show considerable strength is retained at high doses with values similar to these measured at around 40 dpa (Figure 7.5). Ductility (Figure 7.6) does, however, appear to be decreasing with increasing irradiation temperature and at temperatures above 500°C falls below 1%. It would appear that this is related more to the structure developed during high temperature irradiation than to test temperature. In JAPAN [Ref. 7.15], a high nickel alloy with up to 40wt% of nickel has been designed and tests are being conducted. Two types of alloys have been designed by the d-electron concept focusing on phase stability; one is solution hardened and the other is precipitation (and phase) strengthened. Fabrication and out-of-pile mechanical tests are in progress for these alloys.

Ferritic/martensitic alloys. Ferritic/martensitic alloys are being developed as cladding materials, particularly in France, the former USSR and the United States.

The French candidate, designated EM 12 (9.6 Cr-0.12 Ni-1.91Mo-0.92Mn-0.37Si-0.41Nb-0.28V-0.086C-0.019P) has been tested in the PHENIX reactor where two subassemblies reached a maximum exposure of 120-130 dpa at a moderate peak cladding temperature (600-630°C max).

In the former USSR the EP 450 alloy (13%Cr-2Mo-Nb-P-B-V), also used as duct material, has been successfully irradiated in one BOR 60 demountable subassembly up to about 180 dpa (June 1996) at a peak cladding temperature of 680°C at the beginning of life. Subassemblies of standard design based on vibropac, polydispersive MOX fuel with metal uranium powder getter additions and EP-450 cladding, were tested in BOR-60 up to 26at.% burn-up (140 dpa). PIE revealed no corrosion damage of the internal surface of the cladding (Ref. 7.16).

A large amount of experience has been accumulated on the so called HT9 alloy considered as reference material for metallic driver fuel of EBR-II and FFTF (Refs. 7.6, 7.7, 7.17). The highest exposure doses were reached with FFTF oxide fuels at limited peak cladding temperature (600°C), with a record level of about 200 dpa, without cladding failure. Furthermore, some of the lead tests were performed at cladding temperatures in the range of 640°C-660°C. Post irradiation results confirmed the inherent characteristics of this type of material:

- very good resistance to void swelling: very small diameter changes (0,5% at 120-130 dpa) except, in some pins, a peak cladding deformation (up to 1,7% at 120-130 dpa) towards the top of the fuel column, associated with Caesium build-up and reduced creep strength at high temperatures in this upper part of the pins;
- limited high temperature strength which implies stringent design limits and raises some concern with regard to pin failure behaviour, especially in the context of current commercial reactor conditions (peak cladding temperature of about 650°C).

In JAPAN [7.18], the material designated PNC-FMS (0.12C-11Cr-0.5Mo-2W-0.4Ni-0.2V-0.05Nb-0.05N) is being tested in Joyo and EBR-II (present maximum exposure: 5.5 dpa). Some efforts have been made, particularly in Europe and in Japan to improve the high temperature strength of the ferritic alloys by optimizing their composition (out-of-pile development of a high Mo material in Japan [7.19]) and, significantly, by adding TiO₂ or YO₂ to develop a dispersion-strengthened type, designated "ODS" steels [Ref. 7.17-7.21]. A first generation of these ODS alloys (DT and DY MOL ODS), manufactured by mechanical alloying, was tested in reactor, up to a maximum dose of about 90 dpa and exhibited post irradiation embrittlement which led to numerous and severe cladding failures in PIE hot cells. Microstructure and tensile properties of these commercial alloys have been investigated as a function of their processing route [7.20-7.24]. Macro and microstructural evolution of the MA 957 type material has been determined as a function of time. Experimental observations have shown that, for the MOL ODS alloys, the main damage mechanism consists of microcracking of X phase precipitates on grain boundaries. Recrystallization phenomena have been seen in MA 956 and MA 957 alloys. Tensile properties of these materials are illustrated in Figure 7.7.

Out-of-pile development work is in progress in France and Japan [7.10,7.23,7.24], to manufacture and characterize new ODS alloys. The degradation of creep rupture strength in the bi-axial loading, as compared with the uni-axial loading, is mainly attributed to the elongated "bamboo" grain structure. The addition of Ti to 13Cr-3W ODS ferritic steel significantly increased the high temperature strength whereas introducing a transition to ODS martensitic steels improved the creep rupture strength. These encouraging results are illustrated in the Figure 7.8 for the PNC-ODS alloys, compared with other ferritic clad materials.

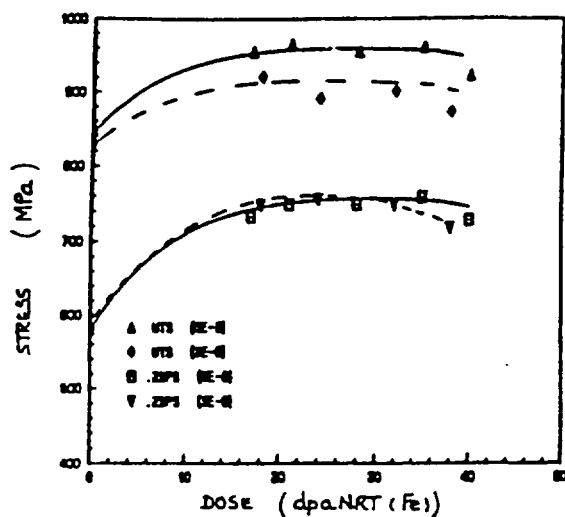


FIG. 7.5. Tensile properties of ST&A PE16.

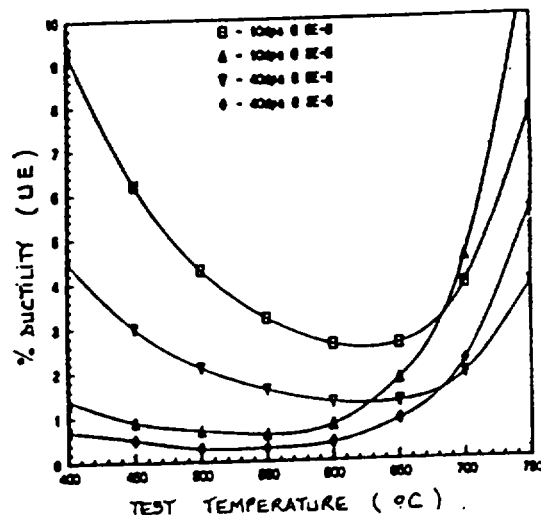


Fig.7.6. Ductility as a function of temperature for ST&A PE 16.

For a number of years there has been work on the technology and investigation of the properties of ODS alloys in Russia [Refs. 7.12,7.14]. A considerable amount of work has been carried out on development and investigation of a model ODS alloy based on steel 13Cr- 2Mo. The effect of alloying this steel with V, Ti, Al, W, Nb has been studied. Oxides of Y, Ti, Ca were used as hardening particles.

The transition of ODS steel with ferritic structure to a two-phase ferritic-martensitic structure is of great interest [Ref. 7.14]. Samples of newly-developed ODS alloys with a ferritic content of 40-60% have been made and irradiated in the BR-10 reactor at temperature 650°C to study their high-temperature strength. PIE is under way now.

Conclusions on cladding material development. World-wide research and development work on various cladding materials has reached a very high level of understanding of the basic phenomena involved as well as of the operational requirements to be met by a well-designed fuel element. Austenitic alloys (15.15 Ti, 1.4970, PNC 316, D9, PNC 1520) have proved their ability to reach exposure rates as high as 150 dpa and their advanced versions (AIM1, CEA 12.25,...) are very promising candidates for the current target doses (170 dpa) of the commercial Fast Breeder Reactors. Ferritic/Martensitic alloys (HT 9, EM 12, PNC-FMS, EP-450) are also able to fulfill these objectives, if a limitation on peak cladding temperature is acceptable. For more ambitious targets (over 200 dpa), a large amount of R&D is still required for qualification of the most promising candidates, namely the ODS steels.

7.2.2. Wrapper-tube (duct) Materials

The first generation of ducts were manufactured in austenitic steels which have since been progressively improved until they now satisfactorily reach neutron exposures as high as 140 dpa for the D9 alloy in FFTF [7.6] and approximately 125 dpa for the 15.15 Ti alloy in PHENIX [7.3]. In most of the countries developing fast reactors, attention is now currently focused on ferritic-martensitic steels. In Europe, [7.2], two candidates are under consideration, a plain 9 Cr 1 Mo martensitic steel (EM 10) and a 10.12 Cr Mo V Nb (FV 448/1 4914). The highest doses achieved at present are 155 dpa for a FV 448 wrapper in PFR, and 115 dpa for 1.4914 and 146 dpa for EM 10 wrappers in PHENIX. In the United States [7.6., 7.7], the HT 9 alloy has been successfully irradiated in FFTF to the record dose level of around 200 dpa. In Japan, the ferritic-martensitic alloy designated PNC-FMS is being tested in JOYO (present maximum exposure: 45 dpa). In the former USSR, [7.12], the most extensively studied alloy was a 13% Cr-Mo-Nb-P-B stabilized alloy (EP-450) irradiated in BOR 60 up to 140 dpa and in BN 600 up to 94 dpa. The principal results obtained for the majority of ferritic-martensitic duct materials studied in Europe have been reviewed, [7.5.,7.25]. The following points were notable:

- dimensional stability is very good, which correlates with a low swelling rate, especially for the fully martensitic alloys (less than 0.5% at all temperatures - Figure.7.9) with a maximum at the lowest temperatures (below 400°C).

Tensile, charpy and fracture toughness tests were performed either on samples irradiated in experimental rigs, or machined from wrapper tubes. The results indicate that irradiation hardening can only be observed at temperatures below 500°C, that this effect saturates at low doses and that the properties of the alloys investigated are quite similar. The post-irradiation UTS and uniform elongations of EM 10 and 1.4914 have been plotted in Figure 7.10 as functions of the irradiation temperature, which is equal to the test temperature; one can see that despite the wide range of doses investigated there is a single plot for both materials, and that the uniform elongation always remains above 1%.

Figure. 7.11 gives, as a function of the irradiation temperature, the post-irradiation DBTT (Ductile Brittle Transition Temperature) of various ferritic-martensitic alloys. The

measured values, which do not depend significantly on dose, differ only slightly from one ferritic martensitic alloy to another. The DBTT shifts are relatively small and clearly compatible with the use of these materials for wrapper applications.

Furthermore, test results at low dose rate on martensitic FV448 indicate that the post-irradiation fracture toughness above DBTT remains high as shown in figure 7.12.

A large amount of experience has accumulated in Russia on the irradiation behaviour of wrappers made of EP-450 steel: more than 400 subassemblies with EP-450 wrappers have been irradiated in BN-600 [7.26] to a maximum dose of 94 dpa. Valuable experience on EP-450 wrapper irradiation was gained also in the former USSR in BN-350, the peculiarity of this reactor being low inlet sodium temperature (280°C). These irradiations showed the high dimensional stability of EP-450 steel. Profilometry of a large number of wrappers in a water pool produced the following information [7.27, 7.28]:

- there is very smooth temperature dependence of EP-450 swelling with a maximum at 385-400°C,
- the dose dependence of EP-450 swelling is quite low: 0.004% / 1 dpa,
- the mean value of the irradiation creep modulus is equal to $0.25 \cdot 10^{-6} (\text{MPa} \cdot \text{dpa})^{-1}$ in the temperature range of $T < 480^\circ\text{C}$,
- there is a trend for the irradiation creep modulus to increase at temperatures 350-360°C.

Destructive PIE of samples machined from BN-350 and BN-600 wrapper tubes demonstrated the following [7.29, 7.30]:

- the maximum changes in tensile and impact (Charpy) toughness occur at the bottom of the core in the zone with the minimum irradiation temperatures: the minimum value of ductility (0.5% at $T=280^\circ\text{C}$) and the maximum value of DBTT (+ 175°C) were observed on samples machined from the bottom section of a wrapper with maximum dose 85 dpa.
- an irradiation hardening effect was observed at temperatures below 500°C. The dependence for a temperature of 350°C was as follows: in the dose range 20-25 dpa hardening increases; then an effect of saturation was observed; and for doses higher than 40 dpa there was a smooth decrease of the hardening.

In conclusion, on the basis of our present knowledge, the more promising martensitic duct alloys can be considered as able to meet the dose requirements (170 dpa) for commercial fast breeder reactors and even to reach more ambitious targets (over 200 dpa).

7.3. IRRADIATION PERFORMANCE OF OXIDE FUEL ELEMENTS

In the content of an intensive 30 years multinational development, a large amount of experience on highly irradiated UO_2 - PuO_2 fuel pins has been gained:

- in Europe, [7.2], more than 7000 pins have reached-up burn-up values of 15 at %. In addition, some experimental pins (with solid or annular pellets) have attained burn-up levels of 23.5 in % in PFR and 16.9 in % in PHENIX;

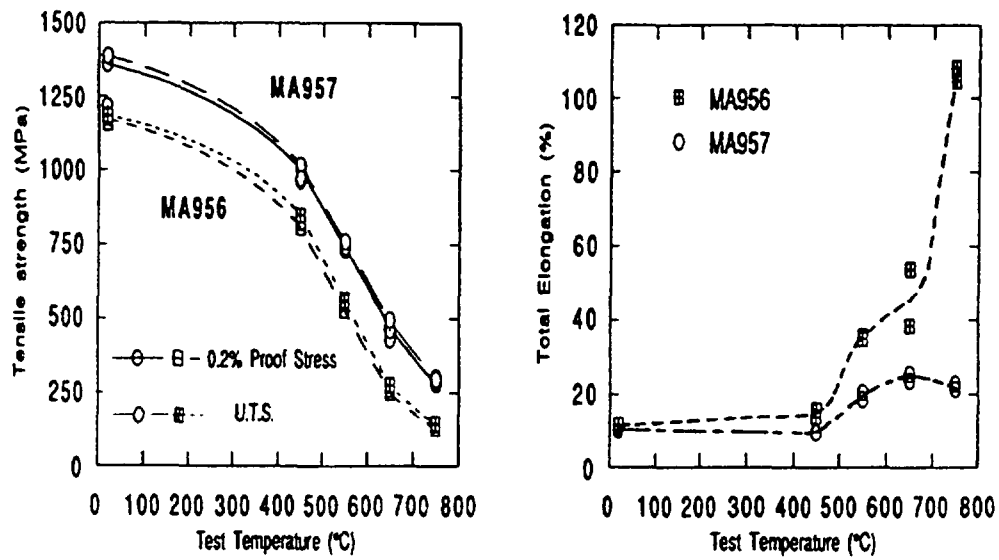


FIG. 7.7. Comparison of tensile properties of 25% cold-drawn specimens of MA 956 and MA 957 alloys.

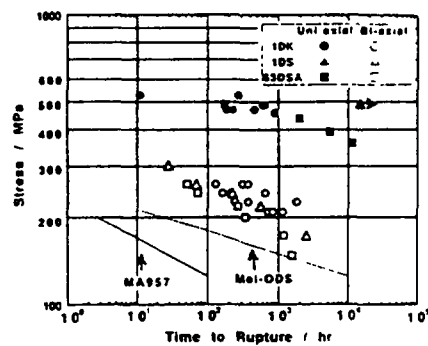


FIG. 7.8. Creep-rupture strength of the PNC manufactured ODS cladding alloys.

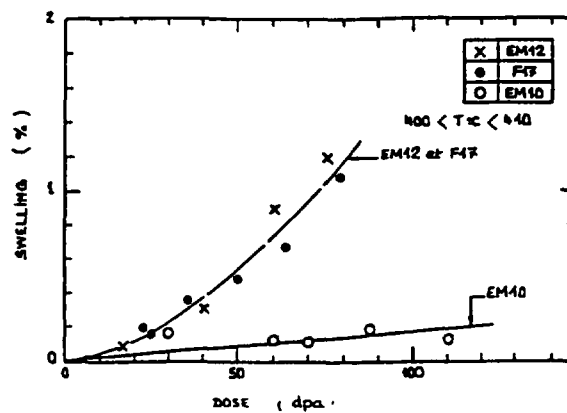


FIG. 7.9. Dose dependence of the swelling of EM 10, EM 12 and F17 steels.

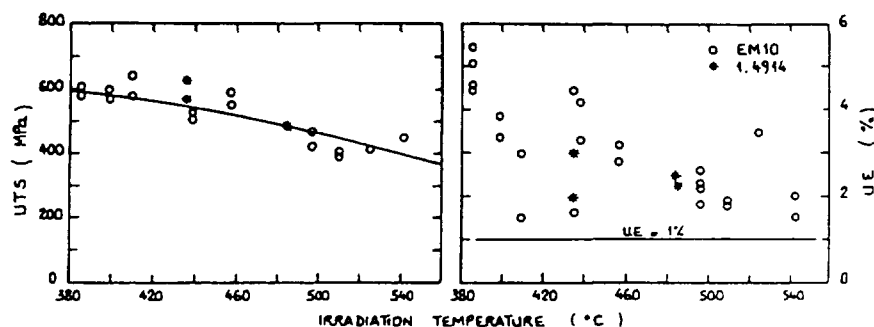


FIG. 7.10. Tensile properties of EM 10 and 1.4914 irradiated between 33 and 100 dpa.

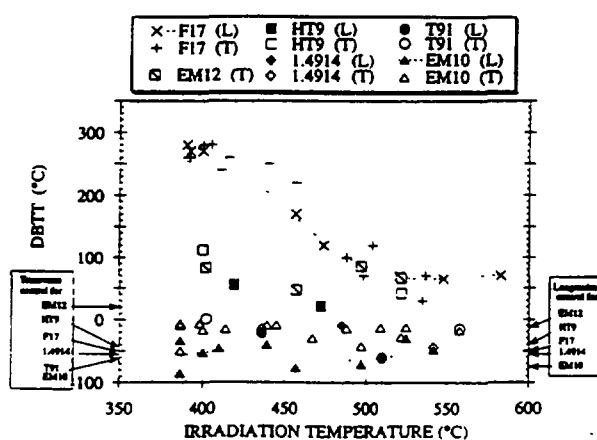


FIG. 7.11. Comparison of the DBTT observed after irradiation for various ferritic-martensitic steels.

- in the United States, [7.6,7.7], more than 63 500 pins (with solid pellets) have been irradiated in FFTF under prototypic conditions, with more than 3000 pins exceeding 15 at % and with maximum burn-ups of around 24.5 at %;
- in Japan: about 50 000 pins (with solid pellets) have been irradiated in JOYO and foreign fast reactors, with a maximum burn-up level of around 13 at % in JOYO and 15 at % in FFTF;
- in the former USSR, a large amount of experience was gained on vibro-compacted MOX fuel, [7.31]; a record burn-up level of about 33 at % has been successfully reached with an experimental subassembly in BOR 60 (6 fuel pins), and about 260 standard fuel pins have attained burn-up levels 24 - 29 at % (June 1996). More than 4000 fuel pins with pellet MOX fuel were irradiated in BN-350 and BN-600. The maximum burn-up in BN-600 is 11.8 at % (April 1996) [7.26].

Progress to reach high burn-up in the main countries is shown in figure 7.13. From this accumulated experience, a very good data base for understanding the phenomena predominant at high burn-up has been developed.

7.3.1. Fuel and fission product behaviour

In France, post-irradiation observations [7.26] on PHENIX pins (6.5 mm OD - solid pellets) irradiated at various burn-up levels (up to 14 at %) indicated a transition region between 7 and 9 at % characterized consistently by the following:

- increase of fission gas release, shown in figure 7.14,
- fission gas bubble precipitation inside the fuel pellets,
- decrease of intergranular caesium content,
- movement of fission product precipitates (Mo, Pd...) out of the fuel pellet,
- opening of a so-called JOG (Joint Oxide Gain, or fuel to clad join) filled with fission product compounds (mainly caesium molybdate) without uranium and plutonium; the evolution of the JOG width and its composition are illustrated in the figures 7.15 and 7.16,
- subsequent fuel shrinkage.

These observations have been confirmed by post-irradiation analysis of fuel pins (6.6 mm OD - annular pellets) highly irradiated (up to 21 at %) in PFR.

These events have been modelled [7.33], and a specific programme of in-pile experiments, so-called JOG 1 and JOG 2 tests, have been performed in the CABRI reactor [7.34] for further investigation of some parameters. The thermal conductivity of the JOG material is of particular interest since it is the main input parameter in any fuel-clad gap conductance calculation. Initial results tend to confirm the potential importance of this JOG layer in fuel behaviour at high burn-up; its presence may result in a stabilization or even lowering of fuel temperatures and provide a joint with beneficial plastic properties which could ease fuel-clad mechanical interaction effects.

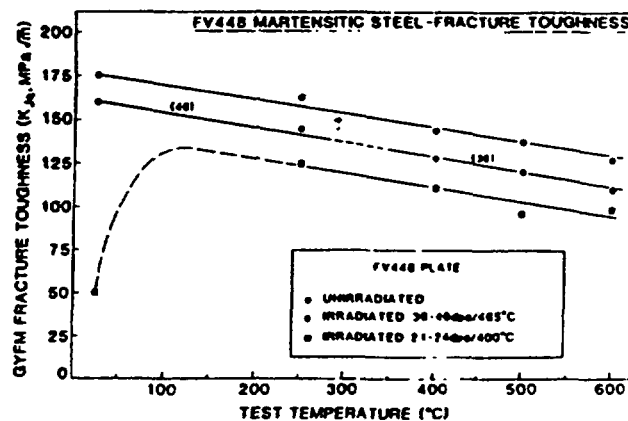


FIG. 7.12. Fracture toughness of FV448 irradiated between 21 and 46 dpa in PFR.

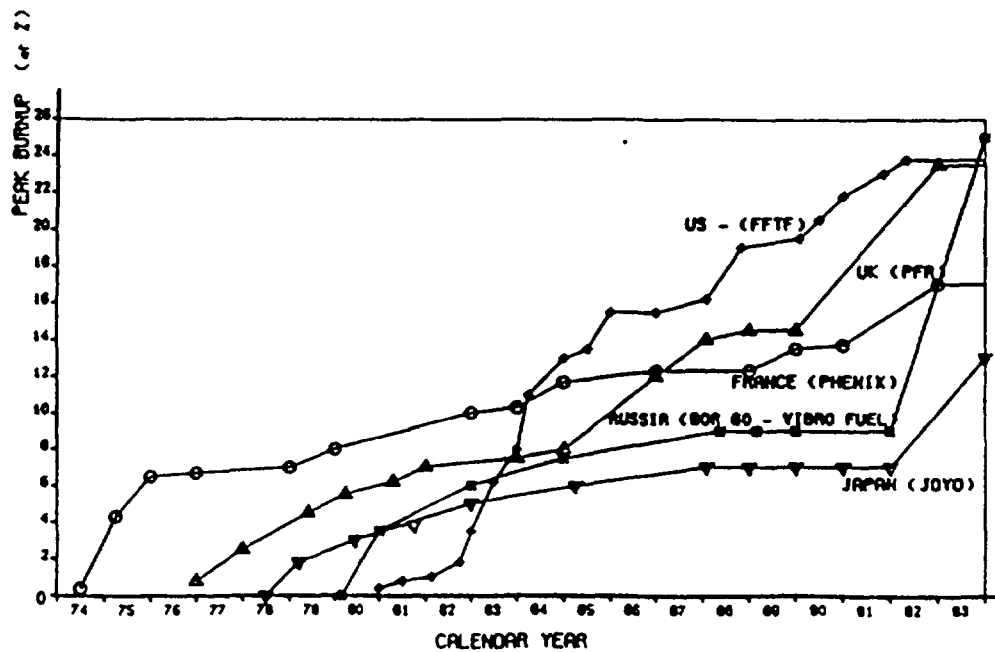


FIG. 7.13 Burnup achievements in mixed oxide fuel in liquid metal reactors

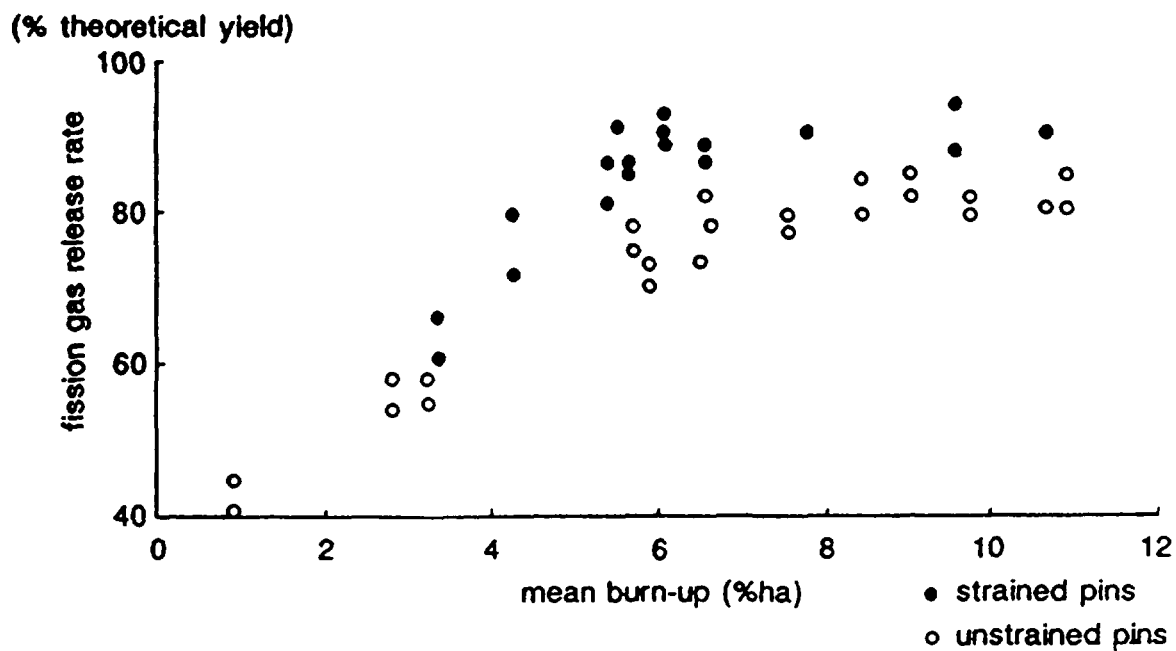


FIG 7 14 Fission gas release versus burn-up for PHENIX pins

JOG : diametral extension of the fuel to clad joint

- : 280-480 mm/bfc
- : 680-850 mm/bcf
- * : 0-180 mm/bfc

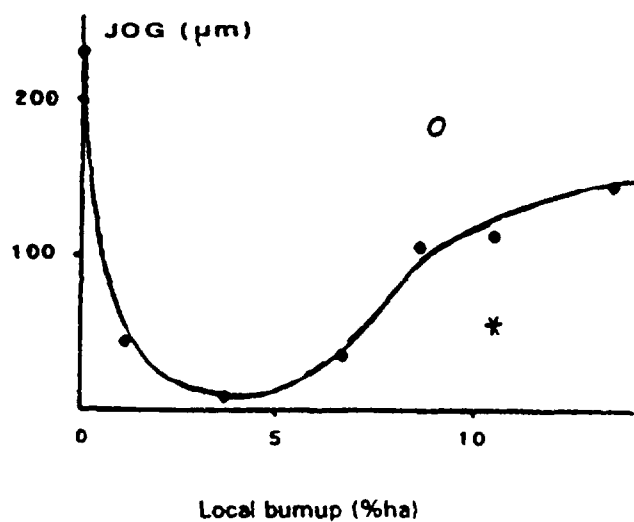


FIG. 7.15. Axial evolution of the JOG width in non unstrained PHENIX pins.



FIG. 7.16. X ray -mapping of the JOG compounds at Peak Power Node at high burn-up without polishing

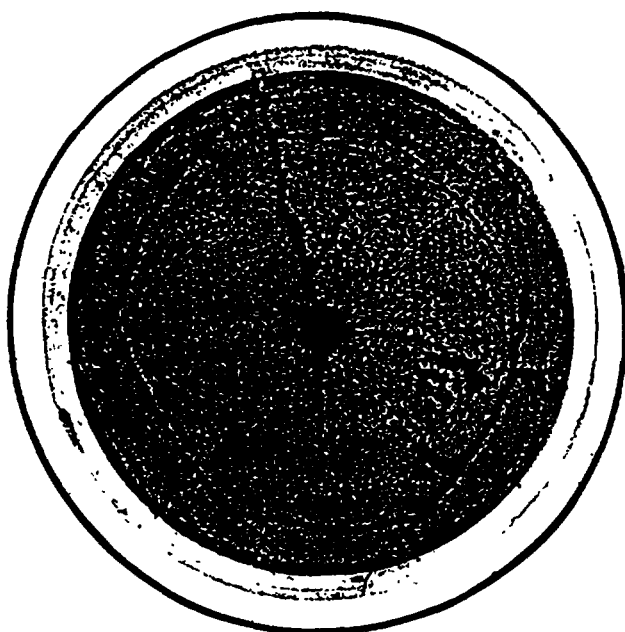


FIG. 7.17. ROG type FCCI on a PHENIX pin (peak burn-up 13.6 at %).

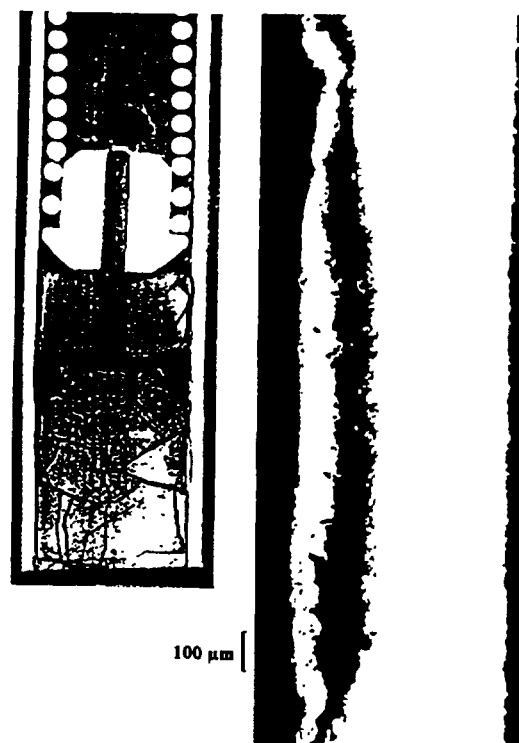


FIG. 7.18. RIFF type FCCI on a pin PHENIX (peak burn-up - 11.1 at %).

7.3.2. Mechanical interaction between fuel and cladding (FCMI)

Mechanical interaction between fuel and cladding (FCMI) during steady state and transient operation is a well-known phenomenon, generally taken into account in the fuel element design, has been confirmed by the operational experience of fast reactors (PHENIX, PFR, EBR-II, FFTF, BOR 60...) with high burn-up fuel, even in severe conditions (power changes...). A comprehensive data base has been developed and FCMI has been modelled [7.35]. A limit on the fuel element smear density (generally less than 0.85) has been suggested as a result.

7.3.3. Chemical interaction between fuel and cladding (FCCI)

A detailed analysis of FCCI measured on fuel pins highly irradiated in PHENIX [7.36] led to the main following conclusions:

- FCCI had developed significantly at burn-ups higher than 8-9 at % reaching thicknesses in the range of 120-290 nm at 13-16.9 at % with a maximum axial extent of about 80 mm,
- FCCI occurred at two levels along the fuel column: in the upper part of the fissile stack (FCCI known as ROG, for "Reaction Oxide Gain" or "Oxide Cladding Reaction") - (Figure.7.17) and at the top of fissile column, adjacent to the upper breeder pellet (FCCI known as RIFF, for "Reaction à l'Interface Fissile Fertile" or "Reaction at the Fissile-Fertile Interface") - (Figure. 7.18).

The ROG type FCCI was characterized as combined intergranular and matrix - type interaction, with the intergranular attack preceding the matrix interaction in the reaction zone. The RIFF type FCCI, of smaller axial extent, was usually characterized by a porous zone and some metallic (Cr, Ni, Fe...) ingots.

- a common explanation has been given to the two FCCI types, based on the role of caesium telluride (Cs_2Te) created by combination of Cs and Te fission products. Cs_2Te reacts with chromium in the cladding and/or with molybdenum in the fuel, releasing tellurium which dissolves cladding components (Iron, Nickel...) leading to a reduction of the sound wall thickness. These reactions are enhanced by O/M increase with burn-up and cladding deformation (leading to fuel and cladding temperature increase).

Most of these observations are consistent with analysis done in other countries, for example UK and United States, [7.37]. The influence of some parameters on FCCI extent was particularly investigated:

- cladding deformation (FCCI development was shown to be of small extent in unstrained highly irradiated PE 16 pins in PFR),
- cladding material (ferritic steels could be less susceptible),
- peak cladding temperature,
- O/M.

These extensive data from fuel pins irradiated in various reactors led to the development of correlation laws used by designers and reactor operators for predicting the extent of FCCI. Figure 7.19 gives an example of a correlation based on EBR-II and FFTF fuel pins with 316 SS and D9 cladding and irradiated to fuel burn-ups up to 17 at %.

In conclusion, even if the understanding of FCCI phenomena has been improved, it is still a potential life-limiting factor for high burn-up fuel elements and remedies are currently studied to limit its extent.

Lowering the O/M ratio to 1.97-1.98 by incorporating metallic getters inside the pin is a promising way to do this. Cr, Nb, V, Ti and U have been tested in the BOR 60 vibro-compacted fuel rods [7.31]; the best results were obtained with fine granular metallic Uranium. Figure 7.20 illustrates the reduction of corrosion layer (less than 20 mm for burn-up levels up to 15 at %).

Another potential remedy could be the use of the axially heterogeneous (AX-HET) fuel concept which is under development in Europe [7.38,7.39]; in this concept, a breeder slice is inserted into the central part of the fuel column.

In the ZEBRE programme, three full subassemblies containing pins clad with CW 316 Ti with 6.55 mm OD and solid pellets were successfully irradiated to peak burn-up between 11 at % and 14 at % and damage doses between 75 and 90 dpa. The pin design is shown in the figure 21 compared to a PHENIX standard pin.

An extensive programme of PIE has been carried out on these pins (more than 250 pins were examined non-destructively and 13 pins were submitted to detailed destructive examination). The results have shown:

- a lowering of the maximum cladding deformation due to a reduced dose for a given peak burn-up,
- an absence of deleterious effects in the internal breeder zone and at the fissile-fertile interfaces suggesting that the life limiting features for an AX-HET pin are no more severe than for an homogeneous pin,
- a substantial reduction in corrosion depth which is significantly less (about 3 times) than in comparable homogeneous pins; this may be due to the role of the internal breeder slice with regard to migration of oxygen and fission products from the lower part to the upper part of the pin.

A statistical verification programme is in progress in PHENIX to confirm the potential advantages of this AX-HET concept which has been selected as one of the two reference concepts for the EFR project.

7.3.4. Behaviour under off-normal conditions

Power and/or temperature transients may occur during reactor operations which could lead to excessive fuel pin loads, life limiting features or even fuel pin failures. Extensive R & D programmes to investigate oxide fuel pin behaviour during and after such transient conditions have been carried out on irradiated fuel pins:

- in Europe [7.2, 7.34, 7.41]: overpower, loss of flow and power-to-melt tests in the HFR reactor and ramp tests in the CABRI reactor (ramp overpower rate 1% of nominal power/second). Some of these experiments have been performed with fuel pins (6.5 mm OD - 15.15 Ti cladding) pre-irradiated in PHENIX (up to 10 at % -85 dpa);
- in the United States [7.6, 7.42, 7.43] transient testing in TREAT and operational transient tests (ORT) in EBR-II (joint PNC-US/DOE programme). In TREAT, full-length FFTF pins were subject to transient tests (overpower transient test ramp rates from 3 c/s to 3 \$/s). The exposure ranged from 0 to about 12.5 at % with doses up to about 60 dpa.

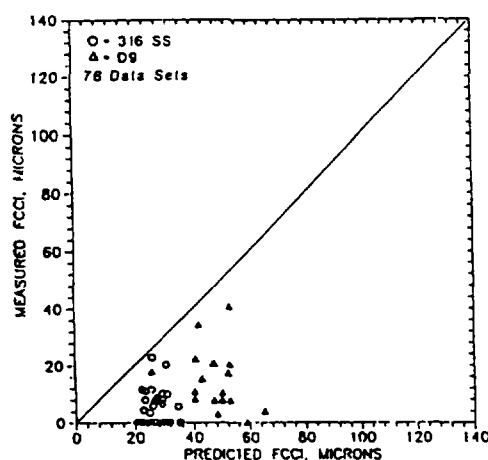


FIG. 7.19. Comparison of measured maximum FCCI depths in FFTF irradiated fuel pins with EBR-II based design correlation at the 95% confidence level.

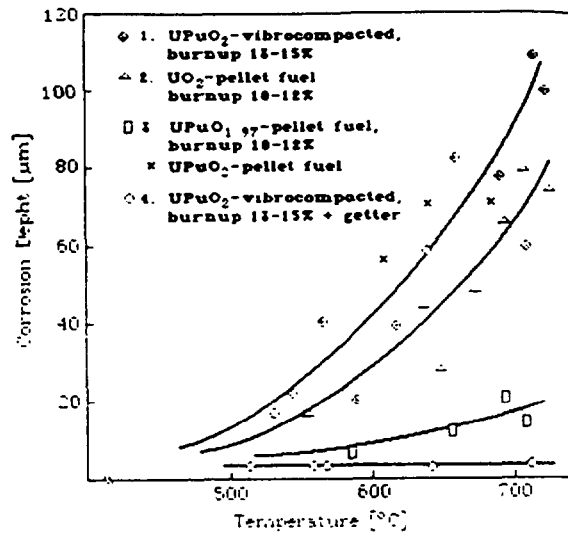


FIG. 7.20. Corrosion depth of the BOR 60 fuel rod cladding (Cr16Ni15Mo3) for various fuel types.

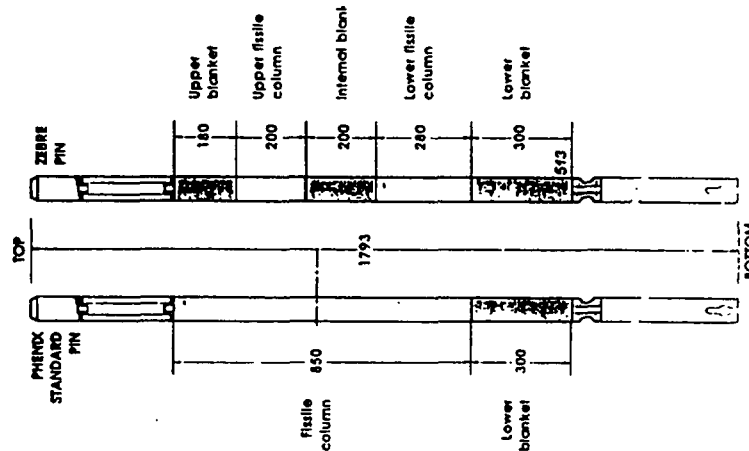


FIG. 7.21. PHENIX AX-HET and standard fuel design.

In the ORT programme, the irradiation tests combined steady-state irradiation with a range of operational (duty cycle) and overpower transients; various cladding materials were or will be tested (20% CW type 316, D9, PNC 316, PNC-FMS, PNC 1520, PNC-ODS). Some fuel pins were tested in transients at high exposure levels (up to 17 at % and 90 dpa for PNC 316 clad pins). These programmes provided an extensive data base and led to the demonstration of:

- the capability of mixed-oxide fuel to survive a wide range of duty cycle power histories and some off normal conditions inducing partial fuel melting;
- the excellent behaviour of some cladding materials (15-15 Ti, PNC 316..) at high exposure levels and aggressive conditions;

- the substantial margin of fuel pin overpower capability at low ramp rates, as illustrated in the figure 7.22, relative to the ORT programme performed in EBR-II.

7.3.5. Failed pin behaviour

The behaviour of subassemblies containing failed pins is of great interest with respect to reactor operation, element handling and intermediate storage. Hence a substantial programme of work in the field has been carried out, emphasising the behaviour of pins irradiated at high exposure level.

In Europe [7.2, 7.44, 7.45] more than 10 tests were carried out with artificially defective pins, in the thermal reactor SILOE, where the specific instrumentation allowed high flexibility in selecting the experimental parameters (burn-up rate, cladding material, size and location of the defect, operation conditions...). In addition, 60 natural fuel element failures have been recorded and extensively analysed in PFR, PHENIX and KNK 2, 41 with exposed fuel (delayed neutron signals) and 19 as gas leakers. The various failures occurred during all stages of pin lifetimes, up to about 20 at % and 135 dpa. A specific test was conducted at PFR to study the behaviour of a failed pin under lower power conditions (simulation of the intermediate in-pile storage).

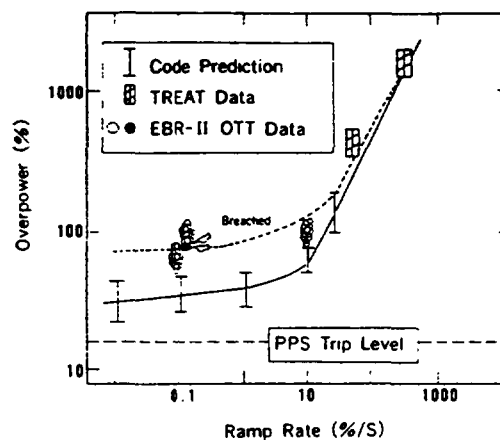


FIG. 7.22. Margins to failure demonstrated by transient tests.

In the United States [7.6, 7.7, 7.46, 7.47], a large amount of experience on oxide fuel breaches has been gained in FFTF and EBR-II. In FFTF, 11 cladding failures were experienced, 3 with exposed fuel and 8 as gas leakers. Most of them occurred at high burn-up (between 10 and 16 at %) and dose level (between 70 and 130 dpa) and in aggressive conditions (cladding temperature, fuel pin design...). In EBR-II a joint PNC-US/DOE Run - Beyond - Cladding - Breach (RBCB) programme has been carried out, coupled to the ORT programme reviewed in the previous sub-section. More than twenty tests have been performed including natural and artificial pin breaches and materials covering a broad range of parameters (316, D9 and PNC 1520 - 5.84 and 7.5 mm OD pins - peak burn-up up to 20.1 at % - type of

defects - steady state, transient and power-to-melt conditions...). All these extensive programmes led to the same encouraging conclusions which can be summarized as following:

- even large defects at the end of life resulted in limited fuel loss,
- no pin-to-pin failure propagation has been observed in usual operational conditions,
- the reaction products formed by the chemical reaction between sodium and mixed oxide, and the kinetics of the reaction, act beneficially and may protect open cracks,
- breached pins can be subjected to moderate overpower transients and power-to-melt conditions without severe degradation.

To sum-up, the accumulated experience has demonstrated conclusively that breaches are benign events and has provided the data base for reactor operators to define their own criteria for managing such events depending on their specific circumstances. However, these optimistic considerations have to be confirmed for the highest target burn-up and exposure levels, taking into account the potential embrittlement of cladding materials as dose increases.

7.3.6. Modelling of oxide fuel performances

Modelling codes have been developed, in the framework of national fast reactor programmes, to describe oxide fuel performance in steady state and transient operational conditions. These main reference codes are: TRAFIC in U.K [7.40] GERMINAL in France [7.33, 7.34] SATURN-TRANSIENT in GERMANY, LIFE [7.35] in the United States, CEDAR [7.10] in Japan, KONDOR in Russia [7.48]. For predicting fuel pin thermal and mechanical behaviour, all these modelling codes have been satisfactorily validated on experimental results for moderate burn-up levels (less than 12-15 at %). Their adaptation to higher burn-up targets, taking into account recent progress in understanding of some phenomena (FCCI, JOG layer, clad deformation) is underway. Some modelling codes are under development to describe the behaviour of fuel pins after failure: the ENPANNE code, [7.49] coupled to TRAFIC in UK, and the SAFFRON code in Japan [7.50].

7.3.7. Achievable burn-up

This review of the extensive worldwide experience provides valuable information on the capability of mixed oxide fuel elements to achieve high burn-ups. A limited number of experimental pins has successfully reached burn-up values ranging between 20 and 25 at %, but not generally under prototypic conditions. These highest achievements and the large statistical experience at burn-ups ranging between 10 and 20 at % tend to demonstrate that 20% BU (corresponding to 170-190 dpa) which is the current target for commercial fast reactors, can be safely reached with the currently proposed fuel designs and operational conditions (for example, for the EFR, annular pellets, with 95% density, smear density less than 85%, 52 kW/m linear rating at beginning of life, 650°C peak cladding temperature, austenitic or high nickel cladding...). Nevertheless some confirmatory evidence is necessary, particularly in respect of the cladding material behaviour (swelling and mechanical properties), at doses higher than 150 dpa, which appears to be one of the most likely life-limiting factors. Other additional issues also need complementary investigation at high burn-up, including the extent of FCCI, thermal behaviour in steady state and transient conditions, and fuel failure behaviour. No physical limitation to more ambitious targets greater than 20 at % has so far been identified.

7.4. IRRADIATION PERFORMANCE OF METALLIC FUEL ELEMENTS

Following successful irradiation of many EBR-II cores, interest in metallic fuels for fast reactors was revitalized, in the United States, when the Integral Fast Reactor (IFR) concept was introduced in 1984. Metallic fuel was selected mainly because of its fuel reprocessing scheme, which has economical and non-proliferation advantages, and its high breeding efficiency. From this date, a large amount of experience has been gained, [7.6, 7.51-7.53], to demonstrate the high burn-up and off-normal performance of the reference fuel element concept (U-Pu-10%Zr alloy, ferritic-martensitic HT9 cladding and duct). A number of subassemblies have been irradiated in EBR-II to meet various objectives, including tests to examine design options, experiments on prototype designs, and tests to validate the fuel specification. In addition, a series of tests was initiated to study the Run-Beyond-Cladding-Breach (RBCB) performance of metallic fuel. The highest burn-up achieved to date is about 20 at % on fuel elements still under irradiation. Table 7.1 shows the number of IFR fuel elements that have been irradiated to date.

Transient overpower tests on metal fuel pins also have been performed in the TREAT facility. Additional testing of long metal-fueled pins has been conducted in the FFTF: seven full size fuel assemblies containing U-10Zr fuel slugs loaded in non-swelling ferritic/martensitic HT9 cladding have been irradiated under aggressive conditions (high linear rate and cladding temperature respectively 54.8 kW/m and 640°C) without failure, to burn-up levels ranging

TABLE 7.1. NUMBER OF IFR METALLIC FUEL ELEMENTS IRRADIATED AS A FUNCTION OF BURN-UP

Subassembly type	All (10 at%)	Pu (10 at%)	All (10 at%)	Pu (10 at%)	Total
Experiment	1611	273	1014	329	2625
Standard core	NA	NA	11484	NA	11484
Total	1611	273	12498	329	14109

Note: The standard core has a very conservative design limit of less than 10 at% burn-up and does not contain plutonium bearing fuel.

from 4 to 15 at % (dose to 110 dpa). The duct and wire-wrap material in these test assemblies was also HT9. Post-irradiation results have characterized the behaviour and performances of metallic fuel including:

- fuel swelling, inducing axial fuel growth illustrated in the Figure 7.23;
- fission gas release, illustrated in the Figure 7.24;
- very benign behaviour of failed fuel elements even at high burn-up (12 at %);
- robust overpower capabilities with cladding failure threshold about 4 times nominal power;
- development and qualification of computer codes (LIFE - METAL and PPIN 2) to predict fuel behaviour in steady state and off-normal conditions.

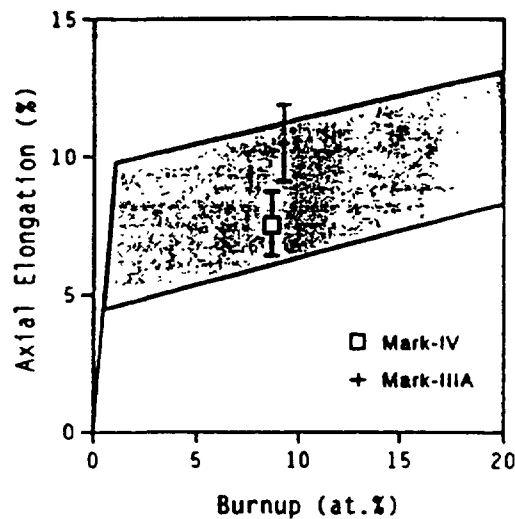


FIG. 7.23. Axial elongation for U-10Zr. Range of EBR 2 experiment data.

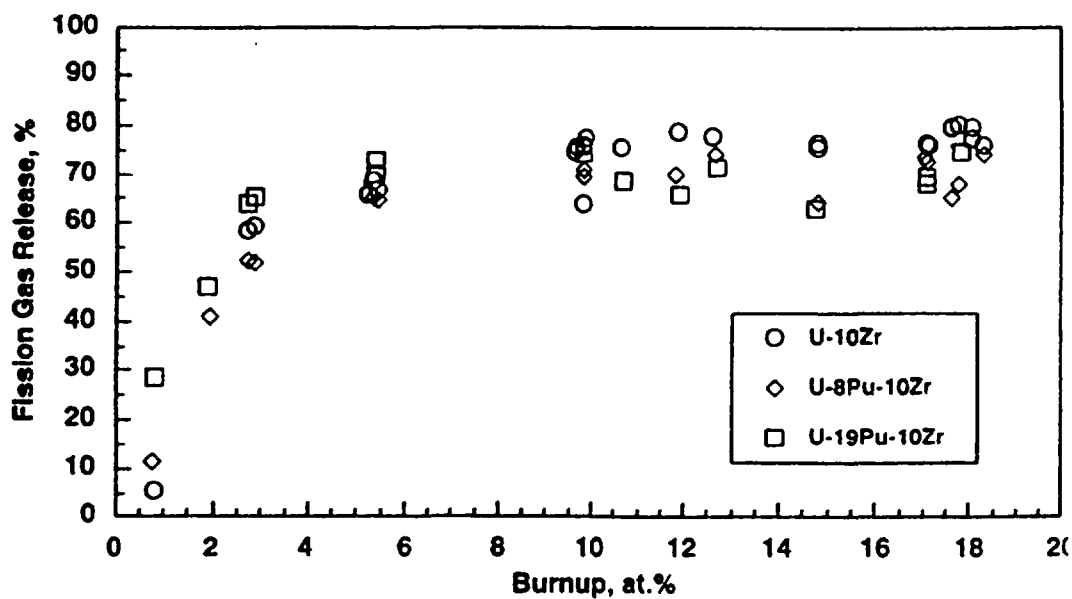


FIG. 7.24. Gas release from metallic fuel.

In Russia over the period 1960 - 1980 numerous investigations have been carried out at RIAR (Dimitrovgrad) and IPPE (Obninsk) concerning the physical and technological aspects of metallic fuel [7.14]. Unalloyed metallic fuel has been proposed, developed and investigated

as a fuel for absorbers and core fuel elements in RIAR. Table 7.2 shows the irradiation conditions of metallic fuel irradiation in BOR-60 and BN-350

TABLE 7.2. METALLIC FUEL IRRADIATION IN BOR-60 AND BN-350

Reactor	Fuel type	Max burn-up, at. %	Max clad temperature, °C
BOR-60	U in absorbers	1,65	670
BOR-60	U in radial blanket pins	1.4	670
BOR-60	U in axial blankets	0,45	630
BOR-60	U-Pu in core fuel pins	7.3	660
BN-350	U in absorbers	1.2	655
BN-350	U in axial blankets	2.6	

The investigations performed made it possible to recommend unalloyed metallic fuel to be used in absorbers and the fuel elements of radial blankets, and axial blankets (smeared density - 80%) and core fuel elements (smeared density - 70%) with gas bonded pins. As a certain protection against interaction between fuel and cladding a special oxide film is recommended to be applied to the fuel column. For core U-Pu fuel pins an additional protective coating on the cladding is recommended. Metallic uranium alloyed with zirconium and niobium was irradiated in BN-350 and BOR-60 as fuel material for absorbers and axial blankets. At present one subassembly with U-Pu-10%Zr is under irradiation in BOR-60, and one subassembly with U-10%Zr has been discharged from BOR-60 core with a maximum burn-up of about 10%.

In conclusion, all the irradiation results have demonstrated the reliable performance of metallic fuel and its potential to achieve high burn-up in prototypical elements. The key characteristics of behaviour have been shown clearly and no limitations to IFR applications have been identified.

7.5. IRRADIATION PERFORMANCE OF ADVANCED FUEL ELEMENTS

The history of "dense" FBR fuel development has been reviewed by H.Blank [7.54]. The following points were emphasized:

- At the beginning of the eighties the general energy scenario in the developed countries and the conditions for the introduction of commercial LMFBRs had changed profoundly with respect to the sixties. Consequently the requirements for the properties and performance of an FBR fuel are now quite different. The fuel cycle economy calls for cheap fuel element fabrication, and a burn-up as high as possible ($>150 \text{ GWd/t(U)}$) at moderate rating ($< 70 \text{ kW/m}$). During the long in-pile time of the fuel the loss of reactivity should be as low as possible in order to avoid the necessity of large reactivity corrections by the control rods. This requires high core breeding and hence a high density of the heavy metals in the fuel. Thus the question of a "dense" fuel and its competition with the oxide fuel has been posed again.
- Considerable progress has been made in the development of ceramic fuels. The swelling problems of the dense fuels (alloys, carbide and nitride) which prevented their application as LMFBR fuels in the early sixties have in principle been solved. The solution consists of two parts. The first is common to all three fuels and consists of

considerable reduction of the smeared densities. The second has to take account of the particular properties of each fuel in conjunction with the pin concept, the reactor operation conditions and the fuel specifications. In each case the corresponding parameters have to be optimized for use in the respective fuel cycle.

- In comparison with oxide, carbide and nitride show three advantages: higher heavy metal density, metallic thermal conductivity and compatibility between fuel and coolant. If full use of these advantages is made they can be transformed into a series of important improvements in the fuel cycle: i.e. cheaper fuel, simplified core design and easier reactor operation. Eventually, there remains the decision between carbide and nitride. Provided the general irradiation performance of both fuels turns out to be quite equivalent in the adopted pin design the carbide would have a slight advantage in-pile because of somewhat lower breeding in the nitride caused by the neutron capture in the ^{14}N (n,p) ^{14}C reaction. However, when judging the complete fuel cycle this is amply compensated (a) by a better chemical stability of the nitride against oxygen and moisture during fabrication and handling out-of-pile and (b) by easier dissolution in nitric acid at the head end of the PUREX process.
- The specification for an optimized pin design are practically the same for carbide and nitride fuels (Table 7.3).

TABLE 7.3. PIN DESIGN AND OPERATION CONDITIONS FOR OPTIMIZED DENSE CERAMIC FUELS [7.54]

Bonding	He
Clad	Low swelling, carburisation resistant, compatible with reprocessing technique
Pin outer diameter (mm)	8.5 - 9.5
Clad thickness (mm)	about 0.5
Smear density (%)	£ 80
Max. linear rating (kW/m)	£ 75
Max. burn-up (at%)	> 12

7.5.1. Carbide fuel elements

Carbide fuel development has been generally stopped everywhere except in India where only very little irradiation experience has been gained up to now from the (U,Pu)C driver fuel of the FBTR reactor. The main features of FBTR carbide fuel is high plutonium content: 70% in Mark I core and 55% in Mark II core. The out-of-pile thermophysical and thermomechanical properties of this fuel have been evaluated up to a maximum temperature of 1500°C and the effect of high Pu content on these properties has been studied. The fuel has seen a burn up of about 25 000 Mwd/t and its post-irradiation data are expected shortly [7.55].

At the Japan Atomic Energy Research Institute (JAERI) mixed carbide and nitride fuels have been investigated from the viewpoint of collection of basic data on advanced FR fuels and also fuels for transmutation of minor actinides [7.56, 7.61]. The research covers fabrication technology, property measurements [7.57, 7.58] and irradiation tests [7.59]. Nine fuel pins with uranium-plutonium carbide were irradiated in Japan Research Reactor-2 (JRR-2) and

Japan Materials Testing Reactor (JMTR). The main design parameters of fuel pins are as follows [7.56]:

- the bulk pellet density of about 85%;
- plutonium enrichment of 20%;
- cladding tubes of 20% CW SUS 316 of 9.4 mm in diameter;
- helium gas bonding;
- maximum burn-up - 4.7at.%;
- maximum linear rating - 42 - 73 kW/m.

The main results of post-irradiation examination are as follows:

- the carbide pellets fabricated by a conventional route showed fission gas release rates of 2 - 3% / at. % which is considered to be equivalent to those in the literature.
- thermally stable pellets of carbide fuel which were fabricated by the use of a pore former, showed very low fission gas release of less than 3% at 4 - 5at.%.

The programme of irradiation tests includes the irradiation of one fuel pin in JOYO over the period 1995 - 1999 by PNC.

In Russia the experimental study of carbide fuel was started in the BR-10 reactor [7.14]. A uranium monocarbide core was in operation from 1965 to 1971. The maximum burn-up was 6.2 at.%, and the burn-up at which unsealed fuel elements were detected was 1.6 at.%. This was the result of a very high carburization of the cladding from the fuel side, as a result of which the carbon content rose to 0.7%. The sodium used in the reactor at that time contained a lot of impurities: up to 0.017% of carbon and 0.003% of nitrogen, these might have caused carburization.

In the BOR-60 reactor 6 subassemblies with UC, UPuC, and UNC were tested [7.60]. The irradiation parameters of these subassemblies are shown in Table 7.4.

TABLE 7.4. IRRADIATION PARAMETERS OF CARBONITRIDE EXPERIMENTAL SUBASSEMBLIES IN BOR-60

Parameter	1	2	3	4	5	6
Burn-up, at. %	3.3	4.8	5.1	7.1	8.9	10.4
Fluence, 10^{22} cm ⁻²	1.7	2.2	2.8	4.1	4.3	6.1
Max. linear rating, kW/m	55	61	55	50	65	70
Max. fuel temperature °C						
-He bonded	1250	1450	1250	1500	1500	1550
-Na-K bonded	800	850	-	830	900	-
Max. clad temperature °C	600	720	650	650	720	680

Investigations of the carbonitride fuel gave important data on the effect of irradiation on the properties. The principal results are the following:

- fission gas release from the uranium carbide fuel does not exceed 13% and varies within 3-18% and 10-18% for uranium carbonitride and uranium-plutonium carbide fuels, respectively.
- swelling of carbide and carbonitride fuels varies within 1.2-2.5% per 1 at. % of burn-up.
- the maximum carbon content of the cladding was almost half the maximum mass carbon concentration (0.4%) permissible for this type of steel and was not a problem from the view point of the serviceability of the fuel pins. The interaction depth was not greater than 30 μm for mixed carbide and uranium carbide fuels. Significant carburization of the clad was observed in the Na-K-bonded fuel pins. The use of coated fuel reduced the clad carburization: the interaction depth was not more than 30 μm .

Successful tests confirmed the feasibility of achieving 10at.% in He-bonded carbide fuel pins, and also made it possible to determine the main fuel parameters to assure the satisfactory performance of the selected fuel design up to a burn-up of 10at.% (Table 7.5).

The principal results obtained for mixed carbide, nitride and carbonitride fuels in Europe have been reviewed by M.Coquerelle [7.62]. Fuels of the type $(\text{UPu})\text{C}_{1-x}\text{N}_x$ has been

TABLE 7.5. THE MAIN PARAMETERS OF CARBIDE FUEL PINS RECOMMENDED AFTER BOR-60 EXPERIMENTAL STUDY

Parameter	He - bonded	Na - K - bonded
Diameter/ wall thickness of pin clad, mm	6.9 / 0.4	6.9/ 0.4
Effective fuel porosity %	20	15
Carbon content in fuel, %	4.7 - 5.0	4.7 - 5.0
Max. linear rating, kW/m	65	80
Max. clad temperature, °C	700	700
Max. fuel temperature, °C	1500	1000

studied in the DN1 and DN2 irradiation experiments carried out in Rapsodie and Dounreay. The DN1 experiment was performed in DFR and investigated He-bonded $(\text{UPu})\text{N}$, $(\text{UPu})\text{C}$, $(\text{UPu})\text{C}_{1-x}\text{N}_x$ fuels ($x=0.2, 0.5, 0.8$). The maximum burn-ups achieved ranged from 1.3 to 7.8 at%. The DN2 experiment was carried out in Rapsodie and investigated He-bonded $(\text{UPu})\text{C}_{1-x}\text{N}_x$ fuel ($x=0.2, 0.5$). The maximum burn-ups attained ranged from 1 to 4 at%. The fuel pin specifications are summarized in Table 7.6.

The pins were irradiated at high linear power (135 kW/m maximum). This led to high central temperatures of 2300 K at the start of irradiation and 1900 K after gap closure. The investigation of fission gas release from fuels under conditions of high linear power has enabled the following conclusion to be drawn:

- at low burn-up (<1.5 at %) the xenon release from He-bonded advanced fuel is dependent on the chemical composition of the fuel. The release is greatest from UPuC (about 75%) and least from UPuN (35%).
- at medium burn-up, closer fuel-cladding contact in He-bonded pins leads to a decrease in the fraction of gas released from $(\text{UPu})\text{C}_{1-x}\text{N}_x$ fuel with $x<0.8$.
- the most important parameter determining fission gas release is the fuel structure. The fraction of xenon released from the outer unstructured region of the fuel is generally

lower than 15%, the mechanism controlling gas release appearing to be atomic diffusion. The fraction of xenon released from the central porous region is 50% or more, and is highly dependent on the composition of the fuel and on burn-up. In this region, the role of interconnected porosity is decisive. Besides diffusion, such supplementary mechanisms as bubble sweeping by grain boundary or pore migration as well as recoil and knock-on due to fission promote the transfer of xenon and krypton to the interconnected porosity.

In addition a study of clad carburization was carried out on different cladding materials after the irradiation of sodium-bonded pins in the Rapsodie and Dounreay fast reactors at burn-ups ranging from 2.6 to 12.5at.% and linear powers between 80 and 100kW/m. The following conclusion was drawn:

- cold-worked Type 316 stainless steel seems to provide the best resistance to carburization, but this observation is based on incomplete evidence.
- stabilized steels, which are presently considered because of their low irradiation swelling (DIN 1.4790, DIN 1.4988), display worse carburization properties at temperatures >900 K.

TABLE 7.6. FUEL PIN SPECIFICATIONS IN DN1 AND DN2 EXPERIMENTS.

Experiment		DN1			DN2	
	U/(U+Pu),w%	20	20	20	20	20
	U ²³⁵ /U,wt%	93	93	93	88	88
Fuel	Form	Pellet	Vibropac	Covibrated	Pellet	Covibratated
	Fuel density,%	85-89			86-89	
	Smeardensity,%	81-85	79-80	78	82-85	80-83
	Pellet diameter,mm	8.3			8.3,8.0	
	Fuel stack length,mm		475		320	320
Fue-to-cladding	Bonding gap,µm		He 200		Na 500	He 200
Cladding	Material			DIN1.49		
	o.d.,mm			19		
	i.d.,mm			9.5 8.5		
Fuel pin	Overall length,mm		790			726
	Gas plenum volume, mm		10			10

- ferritic alloys could offer substantial advantages with respect to austenitic steel: Their carbon content is an order of magnitude higher than that of Type 316 steel, and their mechanical properties are little influenced by carburization level. The experimental results obtained to date are very encouraging, showing a pronounced insensitivity of the carbon concentration in these ferritic alloys to variations of carbon activity in sodium.

More recently, valuable results have been obtained in FFTF from a joint US-DOE/Swiss-PSI irradiation test [7.63]. Fabrication of mixed carbide fuel by the dry powder-pellet route and by the wet gelation sphere-pac route demonstrated that both are capable of giving a stable homogeneous product meeting all requirements of stoichiometry, density and chemical composition. The successful irradiation of full-size fuel pins of both types in the prototypical FFTF conditions of burn-up and fluence showed trouble-free behaviour up to at least 8 at % with a large potential for higher burn-ups and ratings.

7.5.2. Nitride fuel elements

Interestingly, nitride fuel exhibits many of the same desirable characteristics as carbide, i.e., high heavy metal atom density, good thermal conductivity, and excellent compatibility with sodium. It has the added advantage of being compatible with existing fabrication and reprocessing methods established for oxide fuels. It has been reported from calculations that nitride fuel shows advantageous behavior in two accident conditions, transient overpower and loss of flow without scram, compared with oxide and metallic fuels [7.65]. As a result, a wide variety of R & D work is currently being conducted throughout the world and has been reviewed [7.64 - 7.67]. Most of the knowledge on irradiation performance has been gained:

The United States: Before 1988, approximately 100 helium and sodium bonded (U,Pu)N pins were tested in EBR-II. This programme investigated a variety of test parameters and pin geometries including pins with and without fuel shrouds (thin-walled, slotted stainless steel tubes surrounding the fuel pellets used to prevent the relocation of fuel fragments and reduce the possibility of mechanical interaction with the cladding). Pin parameters included theoretical smeared densities of 75-86%, 304 and 316 stainless steel cladding, peak linear powers of 67-107 kW/m, and peak burn-ups of 9 at %. The results of these tests indicated excellent performance by sodium-bonded fuel pins. The study also observed that the performance of unshrouded pins, while similar to that of the shrouded pins, could be greatly improved by increasing cladding strength and maintaining smeared densities of 80%. Low fission gas release rates and a lack of chemical interaction with the cladding and shrouds were also observed. Since 1984, current nitride fuel development activities have been supported by the SP-100 Space Nuclear Power Programme, for which UN utilizing refractory metal alloy cladding and operating at very high temperatures (cladding temperatures 1125°C) was selected as reference design. Testing of such UN fuel pins has been carried out in EBR 2 and FFTF and no pin failures have occurred in spite of the severe irradiation conditions. All these experimental results and some foreign ones have been analyzed using the SIEX computer code. It was observed that the gas release value is influenced both by stoichiometry and by impurities and structure of the fuel. Small stable pores and large grains decrease the swelling and, at the same time, decrease the gaseous fission product release [7.70].

Japan. Six mixed nitride fuel pins were fabricated for irradiation tests in JMTR and JOYO [7.56, 7.61]. The irradiation in JOYO started in August, 1994, for a target burn-up of about 4.5 at % (2 fuel pins). With regard to the fuel cycle, an innovative concept has been proposed, involving fused salt electrorefining and refabrication of sphere-pac fuel. At present the results of PIE of 4 pins are under analysis, but the features of fuel behavior observed in irradiation tests are briefly summarized as follows [7.56]:

- no significant reaction of fuel materials with the cladding was observed.
- the maximum diameter increase was smaller than that of carbide fuel pins.

- a very low fission gas release of a few percent at about 5 at. % burnup was confirmed. Further reduction of the gas release might be expected by proper optimisation of the pore former. This low gas release can be explained by both the low fuel temperature and the stability of the structure.

France. Two tests containing several helium-bonded (U,Pu)N are in progress in the PHENIX reactor. Parameters investigated in these tests include theoretical smeared densities of 75-78%; cold worked, titanium stabilized stainless steel cladding; peak linear powers of 40-70 kW/m, and target peak burn-up higher than 15 at. %. Interim examination of the pins from the initial test (at 7.5 at. %) indicate very good performance. Measured cladding diametral strains are below 30 mm (0.46%). No abnormalities were observed in the fuel microstructure and no trace of cladding corrosion was detected.

Russia. At present the BR-10 core is loaded with mononitride fuel. Up to now 667 fuel pins have been irradiated with the maximum burn-up being 9 at.%. All the fuel pins have remained intact. Currently another 590 fuel pins (the second loading) are under irradiation [7.14]. For the major part of the experimental work it has been assumed that dense fuels should operate at high linear ratings, and in this connection in most of the experiments the fuel temperatures are rather high. For fuel temperatures below 1200°C, limited data are available.

It should be noted in conclusion, that the irradiation results provide favourable expectations for the performance of nitride fuels. However they have to be confirmed at higher burn-up levels and to be extended to a larger statistic of scale. In addition, several other issues have to be addressed, including fabrication of ^{15}N -enriched fuels (to avoid production of radioactive ^{14}C), transient performance and high temperature dissociation, and reprocessing.

7.5.3. Fuel for high plutonium burning

The possible options for the fast reactor systems are very wide: in particular, they can work as breeders or burners. Extensive study of fast reactor cores which can efficiently burn excess plutonium and/or minor actinides, has been continued in France [7.71,7.72, 7.78], Russia [7.73, 7.75, 7.80, 7.84], Japan [7.74] in order to demonstrate the flexibility of the utilization of actinides in fast reactors. The studies are mainly focused around two types of fuels for burner reactors:

- mixed oxide fuel (MOX) with high plutonium content (maximum 40 - 45% Pu),
- "Pu without U" fuels, the so-called inert matrix fuel.

The study covers the technological aspects, irradiation behavior and reprocessing potential of new fuels.

MOX fuel with high Pu content. The plutonium content of the MOX fuel now in use in fast reactors is 20-25%. With a maximum of 45% Pu content, oxide appears to be compatible with the existing fuel cycle technology. Very limited experimental data on the irradiation behavior of MOX fuel with high Pu content are available in the literature:

- IFOP experiment in SILOE [7.72, 7.77]: one fuel pin with MOX fuel (45% Pu, O/M=2.) was irradiated for 70 days at a maximum linear power 46 kW/m. The fuel had an enlarged central pellet hole (the ratio of inner to outer pellet radius was 2.0). The aim was to evaluate the aspects of irradiation behavior at the beginning of life (BOL)

such as Pu redistribution and fissile column integrity. Preliminary PIE study showed no Pu redistribution. Similar evolution of the structure had already been observed in BOL experiments performed in Phenix and Rapsodie at the same power level.

- PROFI experiment in the Rapsodie reactor [7.71]: six fuel pins with solid pellets (76% density) were irradiated for 518 efpd to a burnup of 12.8 %. The main PIE results were that redistribution of the Pu (there was 85% Pu enrichment near the central hole), and that there were no defects in the cladding.
- The TRABANT experiment [7.72] is taking place in the HFR (Petten) in a three-pin TRIO vehicle: the fuel materials of the pins are $(UPu_{0.45})O_2$, $(UPu_{0.4}Np_{0.5})O_2$, and $(PuCe)O_2$. The maximum linear power of the first and second fuel pins is 50 - 52 kW/m, and of third is 38 - 44 kW/m.
- One experimental subassembly (19 pins) with 40% Pu was irradiated in BOR-60 to 4.7at.% [7.76]. The fuel pins were fabricated using vibropac technology. The main feature of the irradiation behavior of fuel pins was the increased concentration of Pu at the periphery of fuel at the middle plane, which caused corrosion damage to the inner cladding surface to a depth of 70 μ m. It should be noted that this vibropac fuel had a low value of the O/M ratio (1.94 - 1.95).
- Important experience of the irradiation behavior of high Pu content (~ 90%) MOX fuel was gained as result of the irradiation of two BR-10 core loadings of PuO_2 and subsequent PIE in a hot cell [7.79]. The principal design and operational parameters of the BR-10 fuel pins are shown in Table 7.7.

TABLE 7.7. PRINCIPAL DESIGN AND OPERATIONAL PARAMETERS OF BR-10 FUEL PINS WITH PLUTONIUM OXIDE FUEL

PARAMETER	I LOADING	II LOADING
Number of subassemblies	83	72
Number of fuel pins	1577	1368
Wrapper flat-to-flat size, mm	26.	26.
Wrapper wall thickness, mm	0.5	0.5
Cladding diameter, mm	5.	5.
Clad wall thickness, mm	0.4	0.4
Core height, mm	280.	320.
Gas plenum height, mm	-	105.
Wrapper- clad material	18Cr-9Ni-Ti	18Cr-10Ni-Ti-16Cr-15Ni-
Maximum burn-up, % at.	6.6	3Mo
Maximum clad temperature, C	580.	14.1
		585

In the pin design for the first core loading a fission gas plenum was not foreseen because of both limited design experience and inadequate knowledge of fuel behavior under irradiation. As a result, the gas pressure reached 30 MPa and caused fuel leakage. Ten SAs at the peak burn-up values from 2.2 to 6.7% at. were selected for PIE. Failed fuel pins were found in six of the SAs. Two of these 6 SAs at burn-ups of 4.9% at. contained pins with cracked cladding. Each of the other four SAs, at burn-ups of 5.6, 6.1, 6.6, 6.75% at.,

contained two or three pins which failed on withdrawal into two pieces with fuel fragments attached to them.

From the start of operation of the second core, because of manufacturing microcracks in the cladding of one or several pins, repeated fission gas releases were detected, but no changes in the delayed neutron activity in the coolant. At a burn-up of 10.8% at. the failed cladding detection system (FCDS) registered the first failed pin by means of delayed neutron signals. With further operation the FCDS registered four other delayed neutron signals. After the appearance of delayed neutrons in the coolant the fission product radioactivity in it increased by an order of magnitude but was not so high as to create obstacles to repair of the primary coolant circuit. An out-of-reactor FCDS was used and 13 SAs with failed fuel pins were found. Pin cladding defects of the "fuel-coolant" type were found in three of them.

For PIE seven SAs at maximum burn-up of 1.42, 3.18, 4.62, 5.81, 7.69, 9.21, 12.06 at % PuO₂ were selected. The following investigations were carried out:

- measurement of cladding diameter changes,
- examination of pin cladding integrity by means of gas composition analysis,
- gamma-scanning of fuel pins,
- fuel and cladding microstructure investigation,
- study of mechanical properties of cladding materials,
- analysis of fission gas release rate.

As a result 8 pins with gas leakage were found in the SAs with maximum burn-ups of 7.69, 9.21, 12.06% at. The following conclusions were derived from these PIEs:

- noticeable gas release was observed at burn-ups of 4% at. and more.
- solid fission products were distributed in fuel column according to the neutron fluence and had not evidently migrated along fuel column. No fuel mass transfer in the axial direction was observed either.
- radial cracks were observed in all fuel column cross-sections investigated. In many cross-sections the fuel had crumbled. For the midplane zones with three distinct types of fuel microstructure were observed: columnar grains, equiaxial grains and unrestructured. This microstructure is typical of oxide fuel irradiated in fast reactors.
- the cladding of all fuel pins at maximum burn-up levels of more than 4% at. suffered internal corrosion as a result of FCCI during irradiation. FCCI varied qualitatively and quantitatively for different parts of the cladding depending on the irradiation conditions. In the lower part of the fuel column no FCCI was observed with the exception of a 5 µm thick layer in which the grain boundaries were sensitive to etching. Near the core midplane the intergranular cladding penetration was 30-50 µm. In the upper part of the fuel column (at burnup of more than 8% at.) the intergranular penetration was 120 µm and followed by partial dissolution or loss of single grains. Perforating intergranular cracks in cladding of failed fuel pins were found near the core midplane and above. Besides the perforating cracks numerous microcracks on the inner surface of the cladding with various penetrations were observed at these cross-sections. For these fuel pins the FCCI penetration was 90-120 µm. On the outer surface of PuO₂ pellets which were taken from the core midplane with burn-up 12 at % a complex phase with Pu, Cs, Cr, Pd, Fe and Ni components was found.

The results of PIE on fuel pins irradiated in BR-10 to 12 % at. burn-up, and of traditional MOX fuel pins irradiated in the BN-350 and BN-600, allowed the following conclusion on irradiation behavior of high Pu oxide fuel to be reached:

- there is in principal no difference between PuO_2 or UO_2 or MOX fuel as regards swelling, gas release, fission products behavior, microstructural changes. The changes in these properties depend on fuel burn-up and temperature,
- fuel-cladding interaction increases with Pu content. Lowering of the initial O/M ratio in MOX fuel with high Pu content and utilization of improved cladding steel could probably decrease cladding corrosion damage to the level of UO_2 fuel pins.

In conclusion, there is hope, from available irradiation results, that there is in principal no difference in the irradiation behaviour of MOX fuel with high Pu content. However the performance has to be confirmed at high burn-up levels on larger statistical samples, mainly with respect to corrosion behavior. In addition some new aspects in fuel design (particularly the large pellet central hole) have to be confirmed.

Plutonium without uranium fuel (Pu with matrix). Use of Pu-without-U fuel allows higher Pu consumption rates to be reached. In fuel pin manufacturing, the use of such materials is still a highly innovative concept. Basic research is being conducted on this subject and consideration is being given to ways of identifying all potential and promising uses of the concept. Some experience on matrix fuel development has been gained in France [7.72, 7.82, 7.85, 7.86], Russia [7.80, 7.83, 7.84], Japan [7.74] and India [7.81]. To select potential candidates, several criteria regarding materials have to be taken into account, concerning both the fuel cycle (fabrication and reprocessing) and in-pile behavior [7.85]:

- fuel manufacturing; compatibility with the current processes would, of course, be an advantage;
- no generation of new active products under irradiation;
- fuel reprocessing: in a U-free fast reactor, since the reduction of the Pu inventory during fuel irradiation is of the order of 40%, multi-recycling of the Pu is necessary; this means that the fuel must be able to undergo reprocessing; compatibility with the current PUREX process would, of course, be an asset;
- thermal characteristics: two important parameters here are melting point and thermal conductivity;
- thermomechanics: the loading imposed by the fuel on the cladding during operation must remain allowable (the clad integrity should not be put into question), notably during power changes;
- chemical compatibility with sodium and cladding, as well as, to a less extent, air (fuel storage) or water (washing and storage prior to reprocessing);
- dimensional stability under irradiation.

There are two possibilities for inert matrices to support the fissile support [7.85]:

1. The combined material is single-phase and corresponds to a solid solution, such as $(\text{Pu},\text{X})\text{O}_2$ where X could be cerium or yttrium (or possibly another rare earth) or $(\text{PuZ})\text{N}$ where Z could be a rare earth, zirconium or titanium.
2. The combined material is two-phase and corresponds to a dispersion of fissile particles in an inert matrix. Two categories have to be distinguished.

- the cercers (dispersion of a fissile ceramic in an inert ceramic) of oxides such as $\text{PuO}_2\text{-MgO}$ or nitrides such as PuN-CrN ;
- the cermets (dispersion of a fissile ceramic in a metal) with a refractory metal (the candidates chosen to date are chromium and vanadium, pure or in the form of alloys with tungsten) or with a non-refractory metal (steel).

There are only a few data on irradiation tests of inert matrix fuel now:

in France:

irradiation of the MATINA1 experimental capsule started in December 1994 in Phenix [7.87]. The objective of the irradiation is to test a large number of candidate matrices. Nineteen pins in a capsule contain four different oxides, four metals and a nitride:

- MgAl_2O_4 , Al_2O_3 , MgO , $\text{Y}_3\text{Al}_5\text{O}_{12}$
- W, Nb, Cr, V
- TiN.

Some of the oxide matrices are mixed with 40 wt.% of UO_2 in order to test the effects of fission and to obtain representative temperature levels. After two irradiation cycles, an intermediate non-destructive examination of the pins will be carried out in order to obtain a first assessment of the in-pile behaviour. The irradiation will continue in the MATINA1bis capsule for two irradiation cycles. Three or five pins will be probably replaced by pins with new matrices: $(\text{UZr})\text{N}$, Y_2O_3 , and lanthanide compounds. The main operational parameters are estimated to be:

- max fluence: 17.10^{26} n/m^2 (for 4 cycles),
- maximum temperature of pellets with UO_2 : 1600-1700°C, temperature of pellets with inert matrices: 500°C.

More recently different types of fuel have been compared according to the following parameters : thermal properties, compatibility with sodium and potential for dissolution in nitric acid. This reached the following conclusions [7.88]:

- $(\text{PuCe})\text{O}_2$ and $(\text{PuRe})\text{O}_2$ have bad thermal properties and compatibility with Na.
- $(\text{PuRe})\text{N}$ and $(\text{PuZr})\text{N}$ have the interesting potential of solubility in nitric acid, but N^{15} enrichment is required.
- PuO_2/MgO or MgAl_2O_4 - there is no motivation for further investigation of this path
- PuN/AlN , TiN or XN - these are very attractive, but N^{15} enrichment required.

Metallic fuel is not under consideration at present: it is to be seen in the context of a fuel cycle based on electro-refining.

Two kinds of inert matrix fuel have been irradiated in the SILOE reactor [7.82]. They are made of UO_2 particles dispersed in molybdenum cermet or a MgAl_2O_4 cercer matrices. Both fuels contain 36 wt% of UO_2 . The irradiation conditions are:

- max burn-up: 55 400 Mwd/ t_u (cermet), 40 300 Mwd/ t_u (cercer),
- irradiation time: 104,5 EFPD (cermet), 80,6 EFPD (cercer),
- linear power: 30 kW/m,

- max fuel temperature: 520°C (cermet), 980°C (cercer).

The density, open porosity, redensification, pellet geometry and grain size of the sintered products are listed in Table 7.8.

The center line temperature of the fuel was measured by thermocouples during irradiation. The following facts were noted:

- the cercer has a thermal response very close to that of a conventional UO_2 ,
- the cermet is at much lower temperature regardless of the linear power; the difference between the two fuels increases continuously as power increases: a gain of factor 2 is obtained on centre line temperature at 30 kW/m.

TABLE 7.8. CHARACTERISTICS OF THE STUDIED INERT MATRIX FUEL BEFORE IRRADIATION IN THE SILOE REACTOR [7.82].

Parameter	Cermet full pellet	pellet/annular	Cercer full pellet
Geometrical density, g/cm^3	9.8/9.84		5.98
% of theoretical density	93.4/93.8		96.
Open porosity, vol. %	2.5/1.9		2.1
Redensification, %	1.54/-		0.58
Outer diameter, mm	4.917/4.916		4.917
Internal diameter, mm	-/1.3		1.3

- there is good agreement between measurements and calculations for the cermet; on the other hand for the cercer 20% better thermal conductivity is predicted compared with that observed under irradiation. The conductivity of the fuel was calculated, using the Maxwell-Eucken law of mixtures, from the conductivity of each component.

Thermal analysis confirmed the benefit of a metallic matrix for obtaining a significant increase in the thermal conductivity of fuel. The cermet remains relatively "cold" during irradiation whereas the cercer behaves like a conventional UO_2 fuel. The disagreement between measured and calculated data is perhaps a result of an imperfect composite structure which does not satisfy the conditions of the Maxwell-Eucken law of mixtures.

Post-irradiation examination showed the following:

- the cercer fuel came into contact with the cladding. Optical microscopy showed changes to the MgAl_2O_4 matrix state around the UO_2 particles at the pellet periphery. This transformation may have resulted a swelling and caused the pellet-cladding interaction. The cercer crack network was slightly different from that observed in UO_2 .
- the cermet pellets were not cracked and remained as they were before irradiation.
- the cermet fuel showed very low gas release rates on high-temperatures. The cercer gave higher release rates than UO_2 . These results validate the dual barrier concept with respect to fission gas release for UO_2 + matrix for the cermet but not for the cercer.

in Russia:

two synthesis processes for UC-ZrC and PuC+ZrC have been developed [7.83]:

- from metals,
- from oxides.

Using these processes the following fuel was fabricated:

- 56%UC +44%ZrC, 55% PuC+45%ZrC for the core region,
- 15%UC +85%ZrC for the blanket region

The solid solution obtained consisted of two phases. The nonuniformity of the Pu distribution was less than 5%. Fabrication techniques for synthesis of solid solutions of UN+ZrN from initial oxides, and fabrication of fuel columns with different density, shape and size, were also investigated. As mentioned above a method of synthesising PuC+ZrC solid solution from oxides was developed. Its properties are close to those of PuN+ZrN solid solution. This fact and existing experience of UN+ZrN fabrication proved the feasibility of carbothermal synthesis of PuN +ZrN from initial oxides. The feasibility of fabricating UN+ZrN and PuN+ZrN solid solutions from initial metals was also demonstrated. A subassembly with 19 fuel pins was irradiated in BOR-60. 7 of the fuel pins contained 55%PuC+45%ZrC fuel, and 12 contained 56%UC+44%ZrC. The irradiation parameters are shown in Table 7.9.

TABLE 7.9. IRRADIATION PARAMETERS OF INERT MATRIX FUEL IN BOR-60

Parameter	Value
Max.burn-up,% at.	8.
Max.fluence,cm ⁻² ,E>0.1Mev	4.43*10 ²²
Max. linear rating,kW/m	40.2
Max clad temperature, C	635±25

All the fuel pins were intact.

The principal PIE results of inert matrix fuel are the following:

- there was no deformation of cladding (measurement error ±0.01 mm),
- the gas release from the fuel was less than 2%,
- the fuel swelling was equal to 1% per 1% of fuel burn-up,
- the fine-grain structure and spheroidal voids were uniformly distributed over the fuel volume (as in the unirradiated fuel),
- instead of the initial two phases only one phase was observed, which seems to be a favourable factor for fuel performance;
- the distribution of the Pu was homogeneous,
- there was local carburization of the cladding only in the upper part of the pins.

One of the principal criteria for fuel with an inert matrix is its reprocessing ability. From this point of view solid solutions of plutonium carbides, plutonium nitrides and inert matrices ZrC and ZrN seem to be the best candidates.

In conclusion, even though there is little irradiation experience, it is hoped that the irradiation behaviour of some fuel types with inert matrices will be satisfactory. Extensive study will be needed to check this conclusion.

7.6. IRRADIATION PERFORMANCE OF ABSORBER ELEMENTS

Even although some attention is still given to alternative materials (Eu_2O_3 , EuB_6 , or Ta), Boron carbide, B_4C , is internationally accepted as the reference absorber material for fast reactors by virtue of its relatively high neutron absorption cross-section, its easy, economic availability and its good irradiation performance. Everywhere it is used in the form of pellets in absorber pins clad with the same range of stainless steels as are used for fuel pin cladding and subassembly ducts. The lifetime and burn-up targets for absorber elements are in the range of 800-1200 Equivalent Full Power Days (EFPD) and $200\text{-}300 \times 10^{20}$ captures/ cm^3 respectively, according to the reactor. Extensive irradiation experience has been gained particularly in Europe [7.89,7.95], the United States [7.90], the former USSR [Refs.7.91 - 7.94], and Japan[7.96], including various pin designs (sealed or vented; helium- or sodium-bonded; shrouded or unshrouded; with ranges of pin diameters and pellet - clad gaps) and B_4C characteristics (natural to 95% ^{10}B enrichment; 75% to 90% pellet density). High burn-ups have been successfully reached in FFTF (220×10^{20} capt/ cm^3 in sealed helium-bonded pins; 330×10^{20} capt/ cm^3 -n B_4C pellets), in PHENIX (220×10^{20} capt/ cm^3 in shrouded, sodium-bonded, vented pins), PFR (74.4×10^{20} capt/ cm^3 in sealed helium-bonded pins) and in BN-600 (183×10^{20} capt/ cm^3 in vented pins). This extensive irradiation testing has provided valuable information on the behaviour and performance of B_4C absorber rods.

Swelling and helium retention. Figure 7.25 shows collected European data on materials of various densities in the range of temperature-independent swelling.

PIE of BN-600 control rods with burn-up 183×10^{20} capt/ cm^3 led to the following conclusion [7.93]: to evaluate the lifetime of control rods with a criterion of absorber swelling it is possible to use the following values of its linear swelling rate: 0.6% per 1 at % B for enriched B_4C and 1.0% per 1 at% for natural B_4C .

Swelling is attributed to the retention of helium produced by the $^{10}\text{B}(\text{n},\alpha)^7\text{Li}$ reaction in lenticular bubbles. Figure 7.26 shows European measurements of the helium retained as a function of burn-up.

The helium release depends on the technological parameters (density, grain size, presence of impurities) and the irradiations conditions (temperature, burn-up). Russian investigations on BN-600 absorber materials showed [7.93] that with increasing burn-up to 15×10^{20} capt/ cm^3 , initially the helium release rate increases and then decreases, reaching a practically stationary value at a burn-up level of about 40×10^{20} capt/ cm^3 .

In the transient period of low swelling the helium release is substantial, then decreases to low values, and then increases again to 100×10^{20} capt/ cm^3 , which can become a life-limiting factor for sealed pins. Enhanced swelling has been observed at temperatures above 1500°C .

B_4C thermal conductivity and structural behaviour. The thermal conductivity of boron carbide reduces very rapidly with burn-up. In the unirradiated state, the conductivity decreases as T^{-1} with increasing temperature T , whereas for fast neutron irradiation at burn-ups higher than 4×10^{20} capt/ cm^3 conductivity is essentially independent of temperature. Figure 7.27 shows the fractional change in thermal resistance measured at 600°C . This change in conductivity is important as regards the critical temperature for swelling acceleration. The thermal expansion coefficient of boron carbide increases with burn-up, although it remains much less than that of potential cladding materials. The majority of boron carbide pellets exhibit thermal stress

fractures on first going to power, and the size of the fragments then decreases with burn-up, at least partly due to the reduction in thermal conductivity. Fragments of quite small size (1 mm) can be generated at high ratings and burn-ups particularly in sodium bonded pins (Figure 7.26). Indeed, it appears that the presence of sodium may accelerate this structural degradation and pellets irradiated in helium atmosphere up to 80×10^{22} captures/cm³ in FFTF have been recovered intact.

Pellet-cladding chemical interaction. Figure 7.28 illustrates carbon penetration into the cladding measured on an experimental vented, sodium-bonded pin called PRECURSAB A1, irradiated in PHENIX to a peak burn-up of about 180×10^{20} captures/cm³. The presence of boron and carbon in stainless steel produces severe embrittlement and for the long proposed lifetimes these penetration effects can be limiting factors.

During the investigation of the BN-600 control rods with cladding made of improved austenitic steel TcS-68 20%CW and irradiated to 500 efpd in the temperature range of 390 - 520°C no pellet-cladding chemical interaction was observed [7.93].

Pellet-cladding mechanical interaction. Pellet swelling is considerably faster than void swelling in cladding material, except for high burn-up levels when the swelling of the B₄C is reduced by burn-up of the ¹⁰B and the clad swelling rate is enhanced by high dose. Therefore, depending on its initial value, the pellet-cladding gap will tend to close at a certain burn-up, but eventually re-open. Gap closure and continued B₄C swelling results in mechanical pellet-cladding interaction inducing cladding strains and stresses which are potential causes of failure. From extensive experimental results covering a large range of pellet-cladding gaps, clad strain distribution was measured and compared with predictions. In some cases, cladding failures were observed. As an example, Figure 7.29 shows a mechanical interaction observed in a FFTF test control rod at the bottom of the absorber stack where the burn-up is greatest in normal FFTF control rod operation.

Local pellet-cladding mechanical interaction can occur even with conservatively designed pins (gap 10% of pellet diameter) because of B₄C fragments re-located into the gap. Figure 30 illustrates pellet fragmentation and relocation in the PHENIX PRECURSAB A1 which failed at about half the time predicted by design calculations.

- 1 - Clad failure
- 2 and 3 - B₄C fragments in gap

Failed absorber rod behaviour. Although limited, some experience with absorber pin failures has been gained particularly in PHENIX, PFR, EBR-II and BOR 60. Most of these defects were explained by pellet-clad mechanical interaction with clad-strains greater than 2% or local deformation due to B₄C fragment relocation. For all the observed failures, there was no evidence of material loss from any pin.

Design options. The B₄C absorber rod designs in various countries have been improved, in basically similar ways, in the field of pin diameter, cladding thickness, pellet density, B₄C enrichment (eventually 2 or 3 different values according to the axial position), operational conditions. In addition, in order to simultaneously overcome fragment relocation and pellet-cladding chemical interaction, a new French design is currently being tested. It consists of enclosing the pellet stack inside a confining shroud (for example, tubular sheath) made with similar material as the cladding; this kind of protection barrier against B₄C

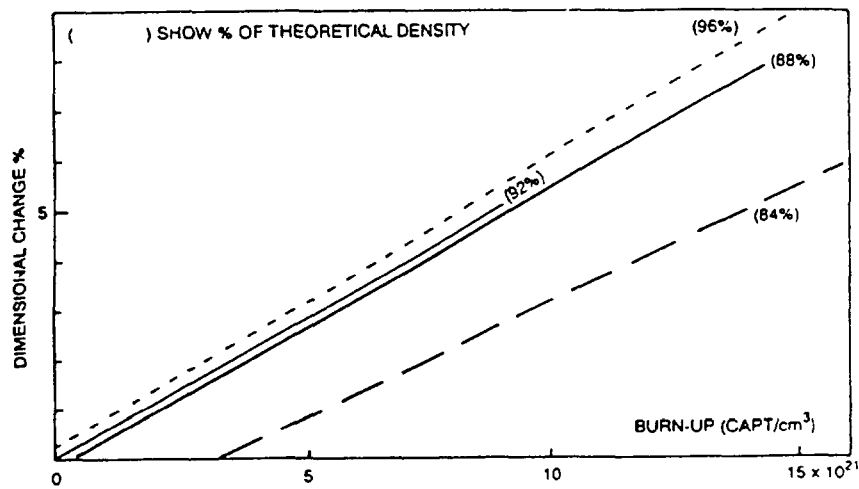


FIG. 7.25. Summary of European data on boron carbide swelling as a function of initial density

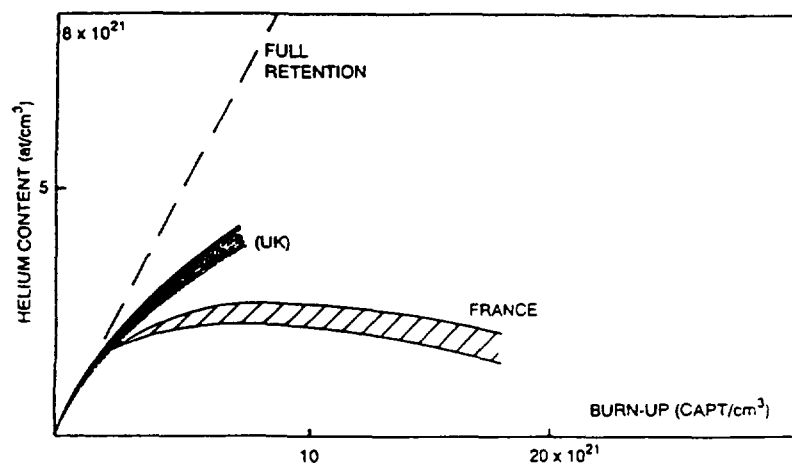


FIG. 7.26. European measurements of helium retention in B₄C.

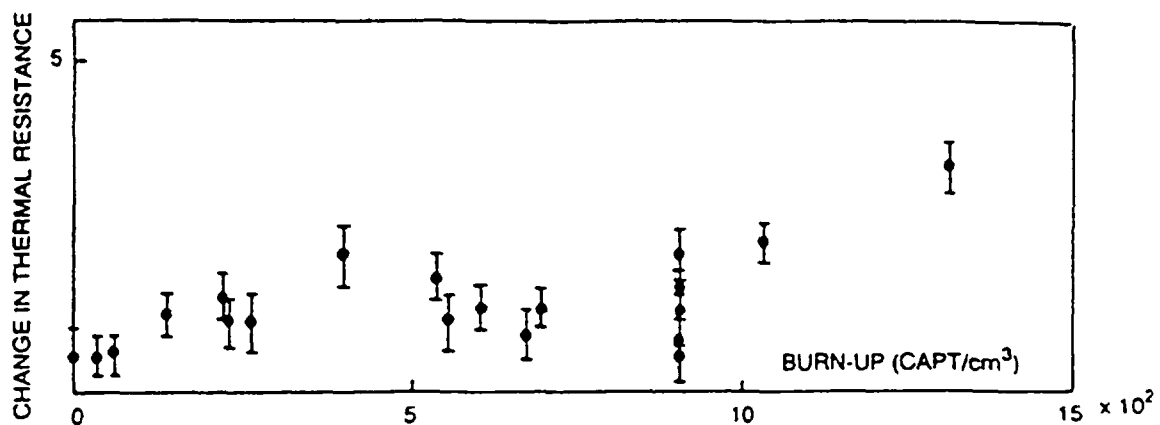


FIG. 7.27. Change in thermal resistance of boron carbide at 600°C.

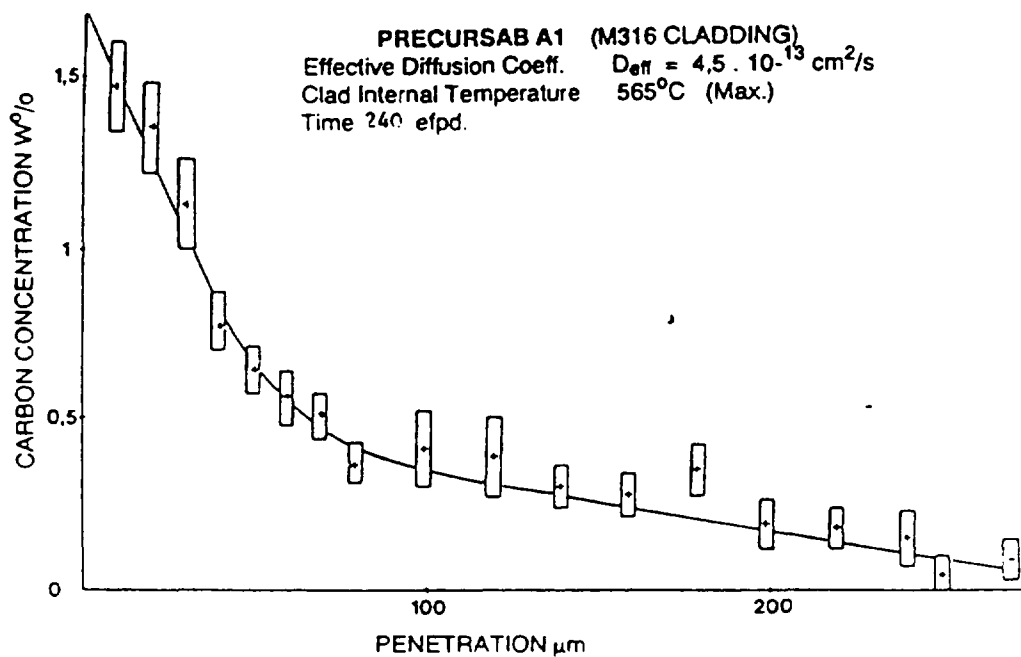


FIG. 7.28. Penetration of cladding by carbon diffusion - experiment PRECURSAB A1.

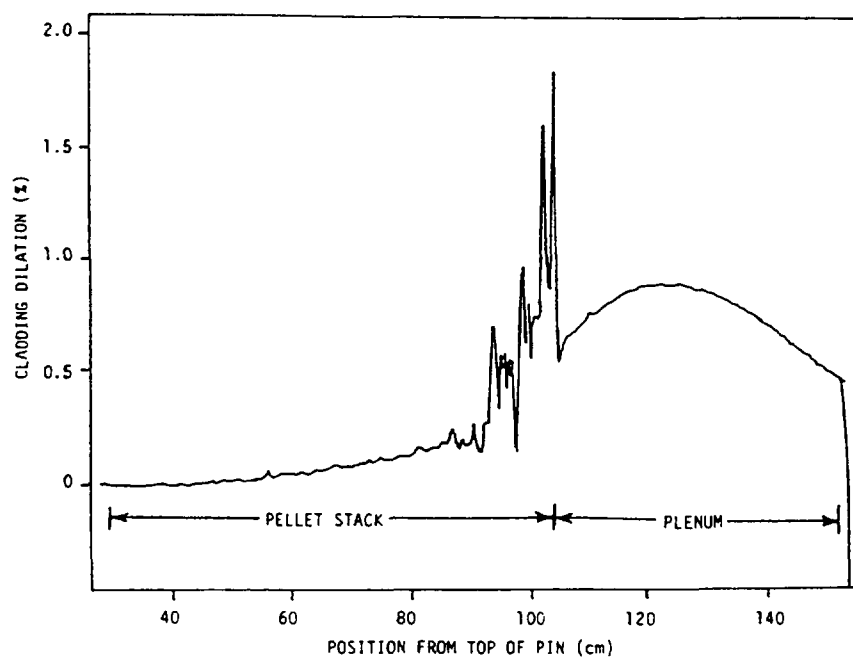


FIG. 7.29. Pellet cladding interaction in a FFTF test absorber pin.

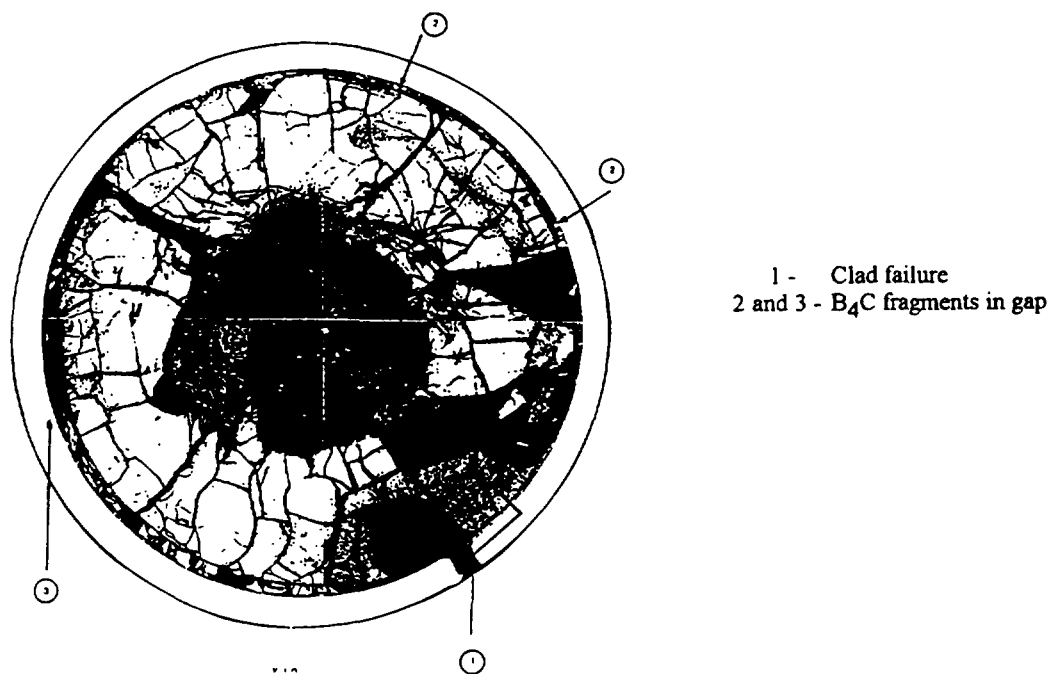


FIG. 7.30. PHENIX PRECURSAB A1 experimental absorber pin - Relocation of pellet fragments in pellet-clad gap and consequent clad failure.



FIG. 7.31. Illustration of the use of tubular shroud in the PHENIX experiment ANTIMAG-2.

fragments may also prevent Boron and Carbon dissolution and/or act as a getter. Figure 7.31 illustrates the beneficial effect of the shroud design for an experimental absorber pin irradiated in PHENIX up to 155×10^{20} captures/cm³ without failure. The shroud failed but could nevertheless prevent pellet-cladding interaction. Both sealed and vented absorber pins are still under development in various countries. Both designs have demonstrated their capacity to reach the current targets (150 to 220×10^{20} captures/cm³) for the fast reactors in operation (PHENIX, SUPER PHENIX, BOR 60, BN 600). In Russia work performed over thirty-years has resulted in practice in a complete solution of the problem of the control rod development for fast power reactors [7.91]. Up to the present time vented absorber pins with high efficiency, high reliability and extended specified life time of ~500 EFPD have been developed and tested in the BN-350 and BN-600 reactors. The pin design has some margin for an increase of lifetime up to 650 EFPD. It is a general consensus now that vented pins will be required for absorbers with extended lifetimes. Large pins with lifetimes of 1200 EFPD or greater are envisaged for future fast reactors. Additional test data with burn-ups to 300×10^{20} captures/cm³ are required to support these advanced designs. Sodium ingress at these high exposure levels is expected to be substantial even in vented pins that were originally helium-bonded; therefore it will be necessary to demonstrate the endurance potential of sodium-bonded or weeper-type vented absorber pins.

REFERENCES

- [7.1] IAEA Technical Reports Series No: 246, Status of Liquid Metal Cooled Fast Breeder Reactors, 1985.
- [7.2] Brown, C., Languille, A., Muehling, G., Journal of Nuclear Materials 204 (1993) 33
- [7.3] Maillard, A., Touron, M., Seran, J.L., Chalony, A., 16th Int. Symp. ASTM STP 1175 - Editors: ASTM Philadelphia, USA, 1993.
- [7.4] Fissolo, A., Levy, V., Seran, J.L., Maillard, A., Royer, J., Rabouille, O., 16th Int. Symp. ASTM STP 1175 - Editors: ASTM Philadelphia, USA, 1993.
- [7.5] Brown, C., Levy, V., Seran, J.L., Ehrlich, K., Roger, R.J.C., Bergmann, H., Int. Conf. on Fast Reactor and Related Fuel Cycles, 1991, Kyoto, Japan.
- [7.6] Legget, R.D., Walters, L.C., Journal of Nuclear Materials - 204 (1993) 23.
- [7.7] Baker, R.B., Bard, F.E., Legget, R.D., Pitner, A.L., Journal of Nuclear Materials - 204 (1993) 109.
- [7.8] Makenas, B.J., Chastain, S.A., Gneiting, B.C., Proc. LMR: a Decade of LMR Progress and Promise (ANS, Washington, DC, 1990).
- [7.9] Porter, D.L, Garner, F.A., Journal of Nuclear Materials - 159 (1988) 114.
- [7.10] Katsuragawa, M., Kashiara, H., Akebi, M., Journal of Nuclear Materials -204 (1993) 14.
- [7.11] Shibahara, I., Ukai, S., Onosse, S., Shikakura, S., Journal of Nuclear Materials - 204 (1993) 131.
- [7.12] Reshetnikov, F.G., Int. Conf. on Fast Reactor and Related Fuel Cycle, Kyoto, Japan, 1991.
- [7.13] Astaschov, S.A., et al, Russian Journal "Atomnaja Energiya", N75 (3), 1993, p.167.
- [7.14] Mourogov, V.M., at al, Proc. Advisory Group Meeting on Fuel Technology and Performance of Non-Water Reactors, Vienna, December 5-8, 1994, p.25.
- [7.15] Ukai, S., Harada, M., at al., Proc. Int. Symp. on Material Chemistry in Nuclear Environment, 1992.
- [7.16] Mayarshin, A.A., et al, Proc Int. Conf. on Evaluation of Emerging Nuclear Fuel Cycle Systems, Global 1995, France, p.1417.
- [7.17] Pahl, R.G., Lahm, C.E., Hayes, S.L., Journal of Nuclear Materials-204 (1993) 141.
- [7.18] Shikakura, S., and al., J.At.Energy Soc.Japan, Vol.33, no 12, p 1157 (1991), in Japanese.
- [7.19] Tokiwai, M., Horie, M., Kako, K., Fujiwara, M., Journal of Nuclear Materials - 204 (1993) 56.
- [7.20] Bodart, M., Baccino, R., Moret, F., EUROMAT 96-8, Paris, France.
- [7.21] Zakine, C., Prioul, C., Alamo, A., François, D., EUROMAT 93-8, Paris, France.
- [7.22] Alamo, A., Regle, H., Bechade, J.L., Novel Powder Processing - Advances in Powder Metallurgy and Particulate Materials 1992 - volume 7.
- [7.23] Ukai, S., Harada, M., et al, Journal of Nuclear Materials - 204 (1993) 65.
- [7.24] Ukai, S., Harada, M., et al, Journal of Nuclear Materials - 204 (1993) 74.
- [7.25] Seran, J.L., Levy, V., Maillard, A., Alamo, A., Dubuisson, P.H., IAEA Workshop - Ferritic martensitic steels - Tokyo, Japan, October 26-28, 1992.
- [7.26] Buksha, Y.K., Proc. 9th Annual Meeting of the IWGFR, Aktau, May 1996, p.181.
- [7.27] Zabudko, L.M., Korostin, O.S., Ogorodov, A.N., Proc. Int. Conf. Fast Reactor Core and Fuel Structural Behavior, Inverness, June 1990, p.263.
- [7.28] Zabudko, L.M., Trufanov, A.A., Korostin, O.S., Ogorodov, A.N., to be published in J.Nucl.Mat.,1996.

- [7.29] Khabarov, V.S., Dmitriev, V.D., Dvoriashin, A.M., Romaneev, V.V., Medvedeva, E.A., Proc. Int. Conf. Fast Reactor Core and Fuel Structural Behavior, Inverness, June 1990, p.263.
- [7.30] Khabarov, V.S., , A.M., POROLLO, S.I., Proc. 7-th Int. Conf. Fusion Reactor Materials, ICFRM-7, Obninsk, Russia, 1995, p.96.
- [7.31] Herbig, R., Rudolph, K., Lindau, B., Skiba, O.V., Maershin, A.A., Journal of Nuclear Materials - 204 (1993) 93.
- [7.32] Tourasse, M., BOoidron, M., Pasquet, B., Journal of Nuclear Materials-188 (1992) 49.
- [7.33] Melis, J.C., Piron, J.P., Roche, L., Journal of Nuclear Materials - 204 (1993) 188.
- [7.34] Melis, J.C., Plitz, H., Thetford, T.S., Journal of Nuclear Materials - 204 (1993) 212.
- [7.35] Boltax-ANS, A., Transactions - Vol. 62 - ANS Winter Meeting - Washington, DC, USA, November 1990.
- [7.36] Boidron, M., Boussard, F., Piron, J.P., Rarier, J.L., Tourasse, M., Proc. of 12th Scandinavian corrosion congress (Helsinki - 31 May - 4 June 1992).
- [7.37] Lawrence, L.A., Bard, F.E., Cannon, N.S., ANS Winter Meeting - Washington DC, USA, November 1990.
- [7.38] Pages, J.P., Brown, C., Steinmetz, B., Languille, A., Int. Conf. on Fast Reactor and Related Fuel Cycle, Kyoto, Japan, 1991.
- [7.39] Millet, P., Languille, A., Brown, C., Muehling, G., ANS Transactions 66 (1992) 214.
- [7.40] Mignanelli, M.A., Thetford, R., Journal of Nuclear Materials - 204 (1993) 173.
- [7.41] Plitz, H., Languille, A., Linekar, G., et al, Int. Conf. on Fast Reactor and Related Fuel Cycles, Kyoto, Japan, 1991.
- [7.42] Boltax, A., Neimark, L.A., Tsai, H., Katsuragawa, M., Shikakura, S., Int. Conf. on Fast Reactors and Related Fuel Cycles, Kyoto, Japan, 1991.
- [7.43] Tsai, H., Neimark, L.A., Asaga, T., Shikakura, S., Journal of Nuclear Materials - 204 (1993) 217.
- [7.44] Plitz, H., Crittenden, G.C., Languille, A., Journal of Nuclear Materials-204 (1993) 238.
- [7.45] Plitz, H., Kleykamp, K., Weimar, P., Hairion, J.P., Languille, A., Cecchi, P., Proc. Conf. on the Science and Technology of Fast reactor Safety, GUERNSEY, 1986, p. 393.
- [7.46] Strain, R.V., Bottcher, J.H., Ukai, S., Nomura S., at al, Proc. Int. Conf. on Fast Reactors and Related Fuel Cycles, Kyoto, Japan, 1991.
- [7.47] Strain, R.V., Bottcher, J.H., Ukai, S., Arii, Y., Journal of Nuclear Materials - 204 (1993) 252.
- [7.48] Struwe, D., Kuznetsov, I., Frizonnet, J.M., Holford, G., Proc. Int. Topical Meeting on Sodium Cooled Fast Reactor Safety, Obninsk, Russia, 1994, p.2-242.
- [7.49] Ford, I.J., Mignanelli, M.A., Journal of Nuclear Materials - 204 (1993) 180.
- [7.50] Ukai, S., Sano, Y., et al, to be published in J. Nucl. Sci. Tech. (1994).
- [7.51] Seidel, B.R., Batte, G.L., Dodds, N.E., Hofmann G.L., et al, ANS Winter Meeting, Washington, DC, USA, November 11-15, 1990.
- [7.52] Lahm, C.E., Koenig, J.F., Pahl, R.G., Porter, D.L., Crawford, D.,C., Journal of Nuclear Materials 204 (1993) 119.
- [7.53] Pitner, A.L., Baker, R.B., Journal of Nuclear Materials 204 (1993) 124.
- [7.54] Blank, H., Journal of Nuclear Materials 153 (1988) 171.
- [7.55] Sengupta, A.K., Jarvis, T., Kuty, T.R.G., et al, IAEA TCM Research of Fuel Aimed at Low Gas Release, Moscow, Russia, October 1-4, 1996.
- [7.56] Iwai, T., Nakajima, K., Arai, Y., Suzuki, Y., IAEA TCM Research of Fuel Aimed at Low Gas Release, Moscow, Russia, October 1-4, 1996.

- [7.57] Arai, Y., Suzuki, Y., Iwai, T., Ohmichi, T., Journal of Nuclear Materials - 195 (1992) 37.
- [7.58] Suzuki, Y., Maeda, A., Arai, Y., Ohmichi, T., Journal of Nuclear Materials - 188 (1992) 239.
- [7.59] Arai, Y., Suzuki, Y., Iwai, T., Maeda A., et al, Journal Nuclear Science and Technology 30 (1993) 624.
- [7.60] Arai, Y. Suzuki, Y., Handa, M., Proc Int. Conf. on Evaluation of Emerging Nuclear Fuel Cycle Systems, Global 1995, France, p.538.
- [7.62] Coquerelle, M., IAEA TCM Research of Fuel Aimed at Low Gas Release, Moscow, Russia, October 1-4, 1996.
- [7.63] Stratton, R.W., Ledergerber, G., Ingold, F., Latimer, T.W., Chidester, K.M., Journal of Nuclear Materials 204 (1993) 39.
- [7.64] Prunier, C., Bardelle, P., Pages, J.P., Richter, K., Stratton, R.W., Ledergerber, G., Proc. Int. Conf. on Fast Reactors and Related Fuel Cycles - Kyoto, Japan, 1991.
- [7.65] Lyon, W.F., Baker, R.B., Legget, R.D., Matthews, R.B., Proc. Int. Conf. on Fast Reactors and Related Fuel Cycles - Kyoto, Japan, 1991.
- [7.66] Lyon, W.F., Baker, R.B., Legget, R.D., ANS Winter Meeting, Washington, DC, USA, November 11-16, 1990.
- [7.67] A.D., Legget, R.D., Legget, ANS Winter Meeting, Washington, DC, USA, November 11-16, 1990.
- [7.68] Reshetnikov, F.G., et al. Proc Int. Conf. on Evaluation of Emerging Nuclear Fuel Cycle Systems, Global 1995, France, p.1359.
- [7.69] Rogozkin, B.D., et al, Proc IAEA TCM Unconventional Options for Plutonium Disposition, Obninsk, Russia, November 7-11 1994, p.229.
- [7.70] Matthews, R.B., Chidester, K.M., Hothalal, C.W., Journal of Nuclear Materials 33 (1988) 40.
- [7.71] Languille, A., et al, Proc Int. Conf. on Evaluation of Emerging Nuclear Fuel Cycle Systems, Global 1995, France, p.874.
- [7.72] Aletto, T.D., Languille, A., Proc Int. Conf. on Evaluation of Emerging Nuclear Fuel Cycle Systems, Global 1995, France, p.337.
- [7.73] Reshetnikov, G.G., et al. Proc Int. Conf. on Evaluation of Emerging Nuclear Fuel Cycle Systems, Global 1995, France, p.320.
- [7.74] Isikawa, M., Shono, A., Wakabayashi, T., Proc IAEA TCM Unconventional options for plutonium disposition, Obninsk, Russia, November 7-11, 1994, p.207.
- [7.75] Krivitski, Y.I., Matveev, V.I., "Mixed Oxide Fuel (MOX) Exploitation and Destruction in Power Reactors", NATO ASI Series.1.Disarmament Technologies - Vol.2,1995, p.151..
- [7.76] Mayorshin, A.A., Skiba, O.V., Tzykanov, V.A., "Mixed Oxide Fuel (MOX) Exploitation and Destruction in Power Reactors", NATO ASI Series. 1. Disarmament Technologies - Vol.2, 1995, P.241..
- [7.77] D'aleto, T., Proc. 3-rd CAPRA Seminar, November 7-8, 1995..
- [7.78] Carnier, J.C., Shono, A., Wakabayashi, T., Proc Int. Conf. on Evaluation of Emerging Nuclear Fuel Cycle Systems, Global 1995, France, p.882.
- [7.79] Zabudko, L., Moseev, L., Mamaev, L., Porollo, S., "Mixed Oxide Fuel (MOX) Exploitation and Destruction in Power Reactors", NATO ASI Series.1.Disarmament Technologies - vol.2,1995, p.157..
- [7.80] Poplavsky, V., Zabudko, L., Moseev, L., Rogozkin, B., Kurina, I., IAEA TCM on Advanced Fuels with Reduced Actinide Generation, Vienna, Austria, November, 1995.

- [7.81] Anantharman, K., Krishnani, P.D., Purandare, H.D., Purushotham, D.S.C., IAEA TCM on Advanced Fuels with Reduced Actinide Generation, Vienna, Austria, November, 1995.
- [7.82] Dehaut, P., et al. IAEA TCM Research of Fuel Aimed at Low Gas Release, Moscow Russia, October 1-4, 1996.
- [7.83] Rogozkin, B.D., et al. IAEA TCM Research of Fuel Aimed at Low Gas Release, Moscow, Russia, October 1-4, 1996.
- [7.84] Krivitski, I., et al. Proc IAEA TCM Unconventional Options for Plutonium Disposition, Obninsk, Russia, November 7-11, 1994, p.219.
- [7.85] Conti, A., et al. Proc Int. Conf. on Evaluation of Emerging Nuclear Fuel Cycle Systems, Global 1995, France, p.1316.
- [7.86] Cocuaud, N., et al. Proc Int. Conf. on Evaluation of Emerging Nuclear Fuel Cycle Systems, Global 1995, France, p.530.
- [7.87] Chauvin, N., Faugere, J.L., Morin, C., Babelot, J.F., Proc Int. Conf. on Evaluation of Emerging Nuclear Fuel Cycle Systems, Global 1995, France, p.1691.
- [7.88] Garnier, J.C., Lo Pinto, P., Languille, A., Rouault, J., Third CAPRA Seminar, Lancaster, UK , November 7 - 8, 1995..
- [7.89] Kelly, B.T., Kryger, B., Esclaine, J.M., Holler, P., Int. Conf. on Fast Reactor and Related Fuel Cycle, Kyoto, Japan, 1991.
- [7.90] Pitner, A.L., ANS Winter Meeting, Washington, DC, USA, November 11-16, 1990.
- [7.91] Matveev, V.I., Ivanov, A.P., Voznesenski, R.M., Evdokimov, V.P., Proc. IAEA TCM Absorber Materials, Control Rods and Design of Shutdown Systems for Advanced Liquid Metal Fast Reactors, Obninsk, Russia, July 3 - 7, 1995, p.11.
- [7.92] Maltsev, V.V., et al, Proc. IAEA TCM Absorber Materials, Control Rods and Design of Shutdown Systems for Advanced Liquid Metal Fast Reactors, Obninsk, Russia, July 3 - 7, 1995, p.141.
- [7.93] Tarasikov, V.P., Voznesenski, T.M., Rudenko, V.A., Proc. IAEA TCM Absorber Materials, Control Rods and Design of Shutdown Systems for Advanced Liquid Metal Fast Reactors, Obninsk, Russia, July 3 - 7, 1995, p.153.
- [7.94] Ponomarenko, V.B., et al., Proc. IAEA TCM Absorber Materials, Control Rods and Design of Shutdown Systems for Advanced Liquid Metal Fast Reactors, Obninsk, Russia, July 3 - 7, 1995, p.195.
- [7.95] Kryger, B., Gosset, D., Esclaine, J.M., Proc. IAEA TCM Absorber Materials, Control Rods and Design of Shutdown Systems for Advanced Liquid Metal Fast Reactors, Obninsk, Russia, July 3 - 7, 1995, p.127.
- [7.96] Kaito, T., Maruyama, T., Onose, S., Horiuchi, T., Proc. IAEA TCM Absorber Materials, Control Rods and Design of Shutdown Systems for Advanced Liquid Metal Fast Reactors, Obninsk, Russia, July 3 - 7, 1995, p.161.

Chapter 8

LMFR ENGINEERING

8.1. SODIUM PUMPS

8.1.1. Design basis

The design of sodium pumps must meet a complex of specific requirements. First of all the specified technico-economic characteristics have to be provided, the most important of which are delivery rate, dynamic head and efficiency. Meeting these requirements depends on the hydraulic perfection of the pump flow path including the impeller, guide duct or scroll, and the ducts for supplying sodium to the impeller and removing it. The pump design should provide for reliable performance, particularly for longevity and failure-free operation. The most important items of vane pumps responsible for meeting these requirements are the impeller (from viewpoint of cavitation-free operation) and the bearings. The bearings, in particular, must meet the following requirements:

- to have minimal wear of working surfaces during the specified lifetime, taking account of startups and shutdowns,
- to allow pump operation at any rotation frequency in the limits of the working range,
- to allow for reversing, and
- to consume a minimum amounts of cooling, lubricating or (for hydrostatic bearings) suspending liquids.

The chemical activity of sodium makes the requirement for sealing the pump inner cavities against ambient air very stringent. A mechanical face seal performs this function. The seal should eliminate the ingress of oil and oil vapors and cooling water into the sodium plenum. For safety reasons a gas blanket of inert gas (usually argon) under a pressure somewhat higher than atmospheric should be provided in the pump above the sodium surface. Structural materials for a sodium pump should be chemically resistant to sodium, to decontaminating alkali-acid solutions and to steam-water washing media. The materials of the flow path should be also resistant to erosion by sodium at high velocity. As a rule these are stainless steels with various kinds of thermal or chemico-thermal treatment, with facing in places where enhanced hardness is required. A vane pump can become a source of vibration because of unbalanced rotating masses, hydraulic forces, or misalignment of the pump and drive shafts. Therefore special design measures must be taken to ensure acceptable vibration levels. The pump drive has an important role. It should provide the capability to control the pump rotation frequency smoothly or stepwise over a wide range of rotation speed from 10 to 100% of nominal value. The design of a sodium pump is largely determined by its location. For example in the BN-600 reactor, where the primary coolant pumps are installed as integral parts of the primary circuit components in the reactor vessel, this dependence is manifest in the following way:

- the pump dimensions such as diameter, depth of submersion of the impeller and distance between the bearings are predetermined. For this reason the shaft dimensions, which were determined by mechanical design considerations, turned out to be such that the pump contribution to the total torque of the pump-coupling-electric motor

- assembly amounts to 30%. In contrast for the BN-600 secondary pump in the unrestricted conditions of the loop arrangement of the circuit this value is equal to 8%;
- the limited cover-gas pressure of the integral layout made the problem of cavitation-free operation more complex, and enforced the use of a double-suction impeller which complicated the flow path considerably and made the pump heavier;
 - the rigidity of the pump support (a shell 6.5 m in height on the reactor support belt) is less than that of a traditional ferroconcrete foundation, requiring additional restraint of the pump body in the region of the upper bearing;
 - the location of the pump in the immediate vicinity of the reactor core causes non-uniform heating of the pump body along its height and radius, especially at part power when cooling dependent on the pump delivery head becomes less effective. The resulting deformation of the pump body must be accounted for.

Placing the reactor coolant pump downstream of the heat exchanger (in the cold leg) is preferable for the following reasons:

- the pump circulates sodium at temperatures not higher than 400°C, which simplifies the choice of structural materials;
- relatively low heat fluxes along the shaft and pump body do not influence the operation of the upper bearing and shaft seals in practice;
- the pump is better protected against thermal shocks and transients.

All sodium vane pumps are vertical. This is dictated by the necessity to seal the shaft reliably where it penetrates the pump body. In early sodium pumps the lower radial bearing was placed above the sodium. This design was chosen because of the lack of experience of operating bearings in sodium, while the required characteristics allowed an acceptable shaft overhang. For this reason these were termed "cantilever" pumps. They turned out to be sufficiently compact, and they utilized bearings proved in other applications. It is important also that cantilever pumps can operate as gas blowers when the reactor is initially heated with gas. Despite high reliability cantilever pumps did not find wide application because:

- the small submergence of the impeller due to the limited shaft cantilever requires the cover gas pressure to be increased to ensure cavitation-free operation. This complicates the design;
- the use of oil-lubricated bearings requires additional measures to prevent the ingress of oil and oil vapors into sodium,
- for pumps of large capacity the allowable extent of the shaft cantilever cannot accommodate operational fluctuations of the sodium level.

An attempt to eliminate the disadvantages of cantilever pumps by the use of non-freezable seals found no wide application because of the low reliability of the seals.

The majority of sodium pumps in current fast nuclear reactor plants are submersible with lower radial hydrostatic bearings operating in sodium and fed from the delivery side of the impeller. With the introduction of hydrostatic bearings the structural scheme of sodium pumps has been finally determined: the pump shaft rotates in two bearings, the lower being a radial hydrostatic bearing and the upper usually a radial-axial roller bearing or a liquid- or grease-lubricated sliding bearing; the impeller is usually disposed below the hydrostatic bearing; there is an axial or radial guiding duct; a gas shaft seal is usually placed below the

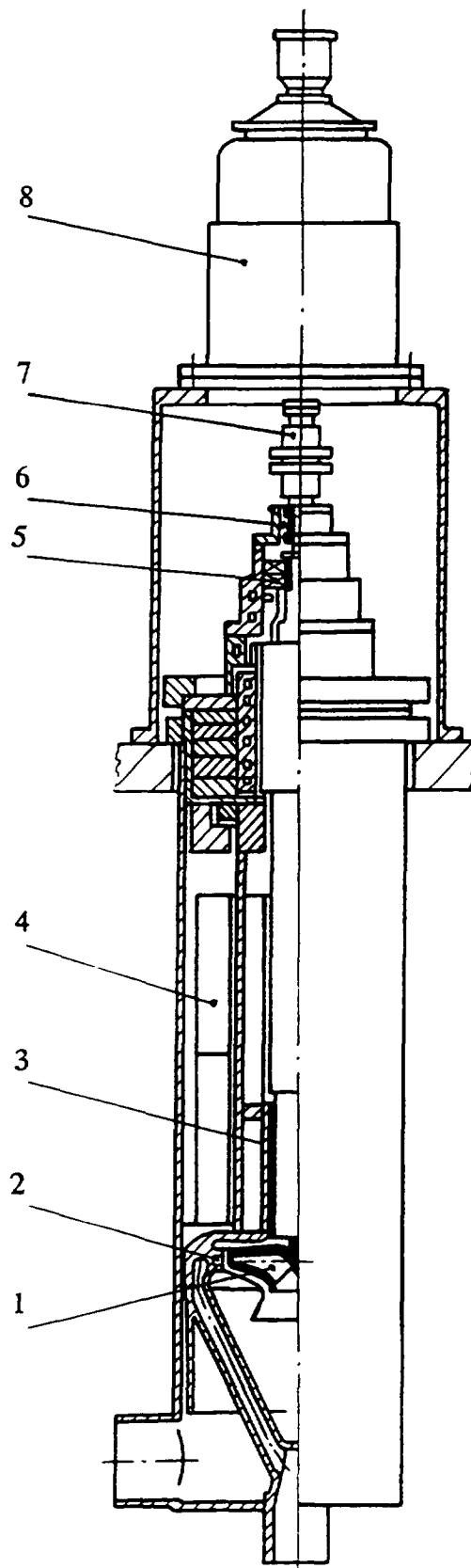
upper bearing; and a flexible coupling connects the shafts of the pump and its electric drive. In primary coolant pumps a biological shield is needed and (if necessary) there is a check valve in form of a shutter, float valve or obturator upstream or downstream of the guiding duct. For repairing the shaft seal without depressurizing the sodium circuit a repair seal is sometimes provided below the main seal.

Submersible pumps may be subdivided into deep- and shallow- submerged pumps. The axial dimension of a submersible pump is such that given any sodium level fluctuations (determined by the hydraulic resistance of the suction duct and thermal expansion of the circuit) a column of sodium sufficient to ensure cavitation-free operation remains above the impeller. This requires that the suction comes directly from the reactor tank (or expansion tank or pump tank) with no sealing devices between the tank and the pump assembly. For large capacity pumps meeting these requirements might require very cumbersome fabrication. For example the largest submersible sodium pumps for the Superphenix reactor weigh 120t and are 23m in length and 2.5m in diameter. If, because of the reactor layout, it is impossible to ensure that the level in the pump tank follows the hydraulic resistance of the suction path an artificial resistance has to be provided between the pump internals and the tank to retard or prevent the drop of sodium level. In emergency transients this helps to ensure the minimum allowable suction head at the impeller inlet and to prevent the entrapment of cover gas. In the BN-600 primary pumps, which fall into the category of shallow-submerged pumps, the resistance is provided by an annular slot 1 mm wide between the pump internals and the reactor support, and four throttling orifices of 50 mm diameter. If the removable internals of a shallow submerged pump are sealed completely from the tank the risk of loss suction head is eliminated. The level rises due to leakage of sodium from the delivery side of the impeller through the hydrostatic bearing, so provision to return the leakage to the circuit is needed. This function is usually fulfilled by an overflow tube which is connected to the suction portion of the flow path. Shallow-submerged pumps have better mass and size characteristics.

8.1.2. Sodium pump design features

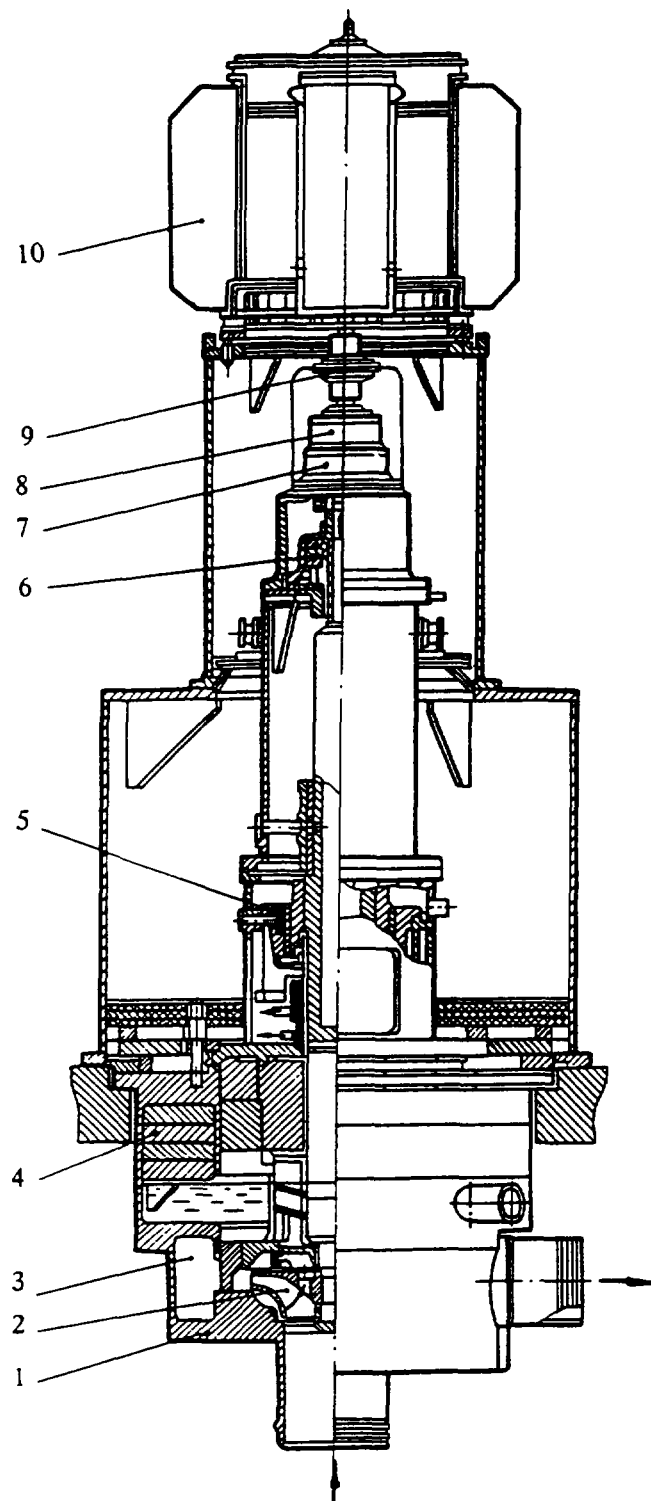
BOR-60, BN-350 and BN-600. These pumps are designed to circulate sodium coolant in the primary and secondary circuits. They are centrifugal, single-stage vertical pumps with protective gas blankets above the free sodium surface in the pump casing. The pumps are leak tight with respect to the environment. Tightness along the shaft is ensured by a mechanical face seal. The tightness of the joint between the removable internals and the pump tank is ensured by a repairable mitre weld seam. A repair seal is provided for keeping the loop leak tight during replacement of the shaft face seal when the pump is stopped. The structural scheme of primary sodium pumps is determined mainly by the reactor layout. For the loop-type reactors (BOR-60, BN-350) the pump consists of the removable internals and the tank; in the integral reactor (BN-600) the function of a pump tank is taken by load-carrying components of the reactor vessel. The BOR-60 primary and secondary coolant pumps (Fig.8.1) have similar removable internals and differ only in impellers and guide ducts. The impeller is submerged to a depth equivalent to the suction path resistance, taking account of the rise of sodium level in the tank due to temperature variations during operation. Sodium is taken immediately from the pump tank. The impeller, guide duct, sodium pressure header and delivery ducts form the removable internal assembly [8.1-10]. The BN-350 primary and secondary coolant pumps (Fig.8.2) differ only with respect to the impellers and guide ducts. Unlike the BOR-60 pumps the sodium pressure header is a part of the pump tank. The sodium leakage through the gaps between the removable internals, casing, tank and impeller are

Text cont. on p. 328.



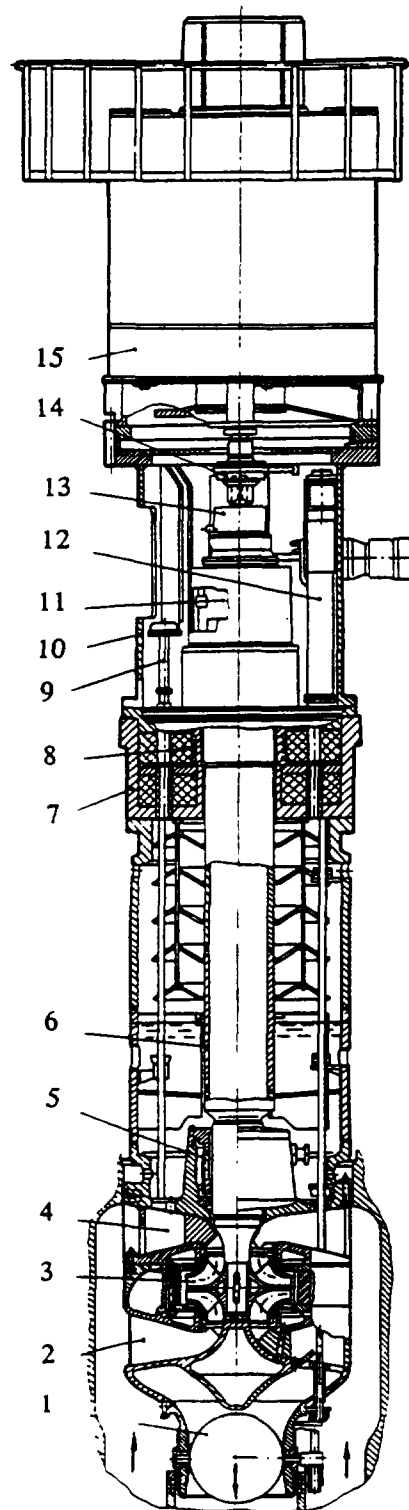
1 - impeller, 2 - guiding duct, 3 - radial bearing,
4 - displacer, 5 - radial-thrust bearing, 6 - shaft seal,
7 - coupling, 8 - motor.

Fig. 8.1. BOR-60 Reactor Coolant Pump CNN-1



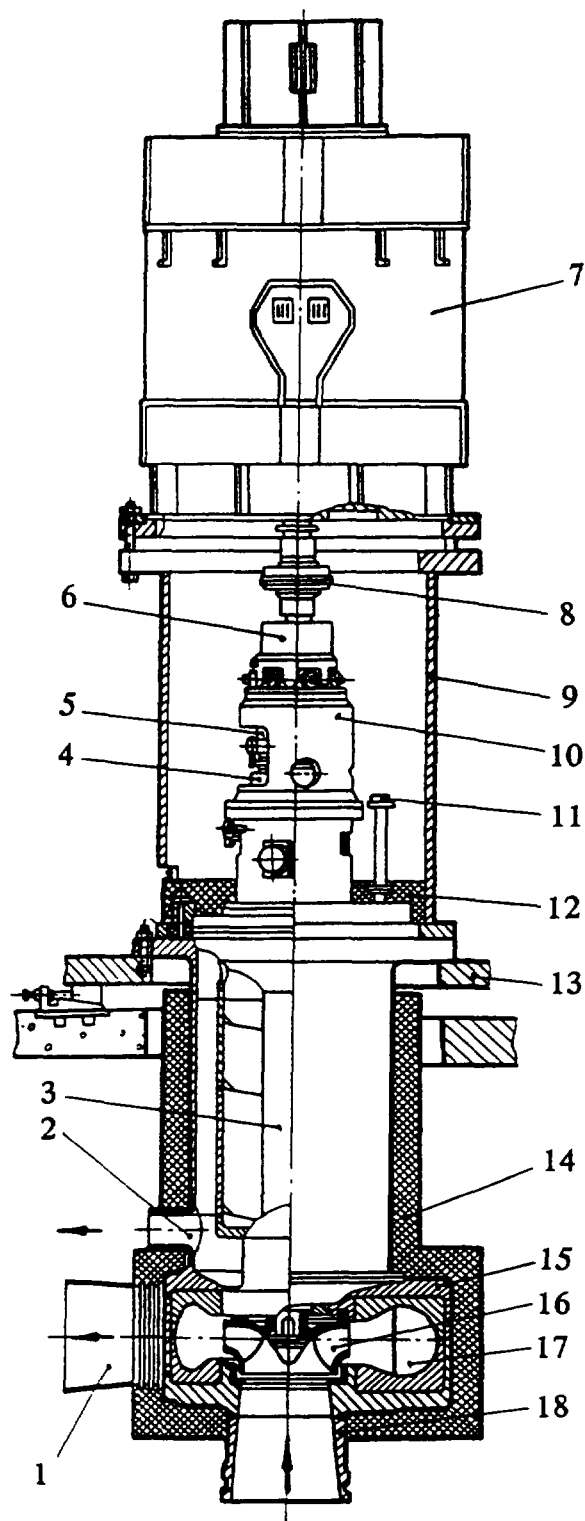
1 - casing, 2 - impeller, 3 - pressure header,
 4 - biological shield, 5 - radial bearing, 6 - radial-thrust bearing,
 7 - repair seal, 8 - face seal, 9 - coupling, 10 - motor.

Fig. 8.2. BN-350 Reactor Coolant Pump CNN-3



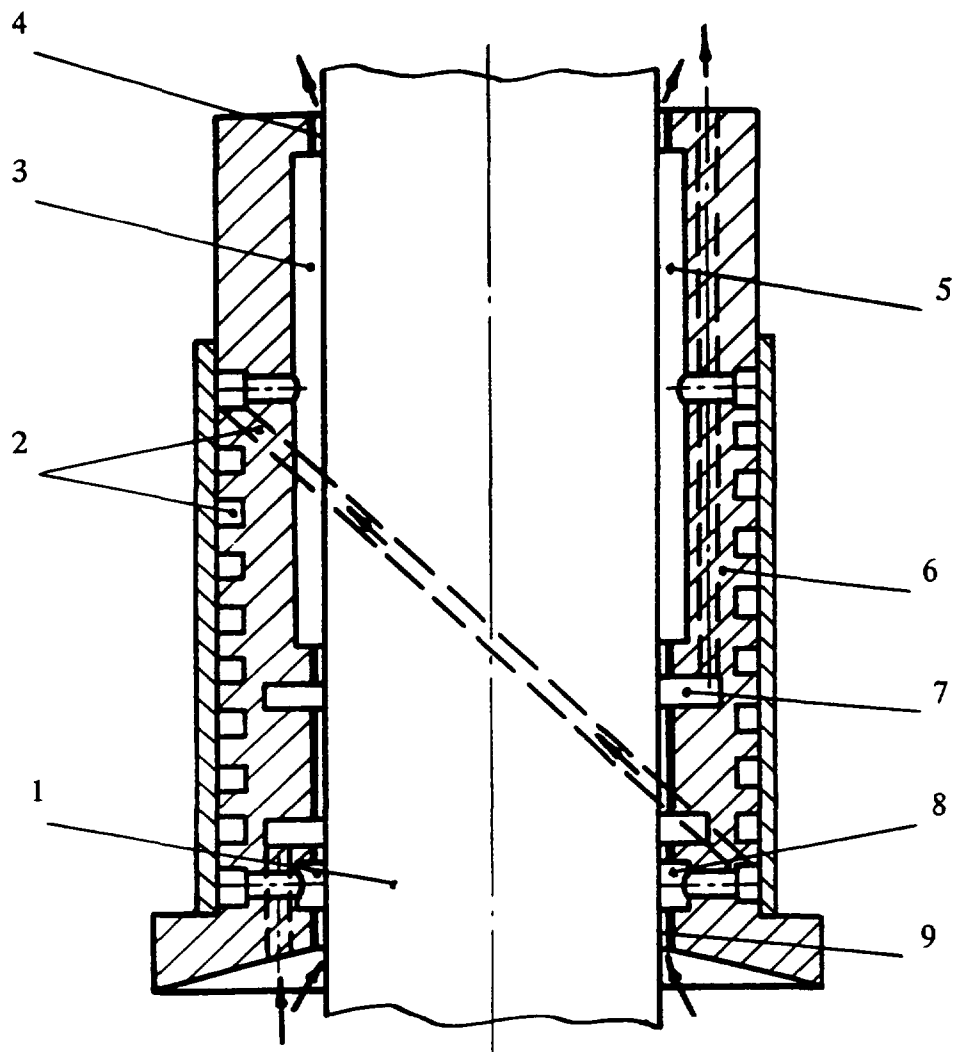
1- check valve, 2 - lower scroll, 3 - impeller, 4 - upper scroll,
 5 - hydrostatic bearing, 6 - shaft, 7 - cover, 8 - cooler, 9 - level
 gage, 10 - motor base, 11 - face seal, 12 - check valve drive,
 13 - radial-thrust bearing, 14 - coupling, 15 - motor

Fig. 8.3. BN-600 Reactor Coolant Pump CNN-9



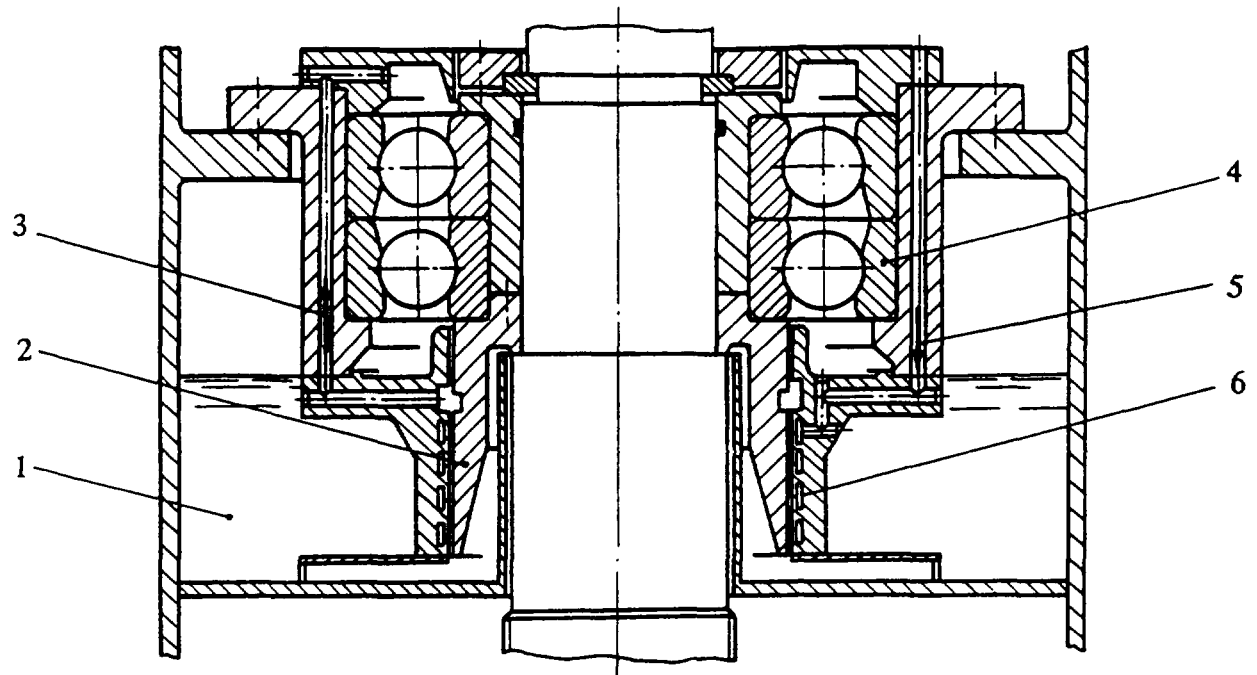
1 - pressure nozzle, 2 - discharge of leakages, 3 - shaft, 4 - repair seal, 5 - face seal, 6 - radial-thrust bearing, 7 - motor, 8 - coupling, 9 - base, 10 - removable part, 11 - level gage, 12 - thermal insulation, 13 - support plate, 14 - electric heater and thermal insulation, 15 - tank, 16 - impeller, 17 - scroll, 18 - suction nozzle.

Fig. 8.4. BN-600 Secondary Coolant Pump CNN-8



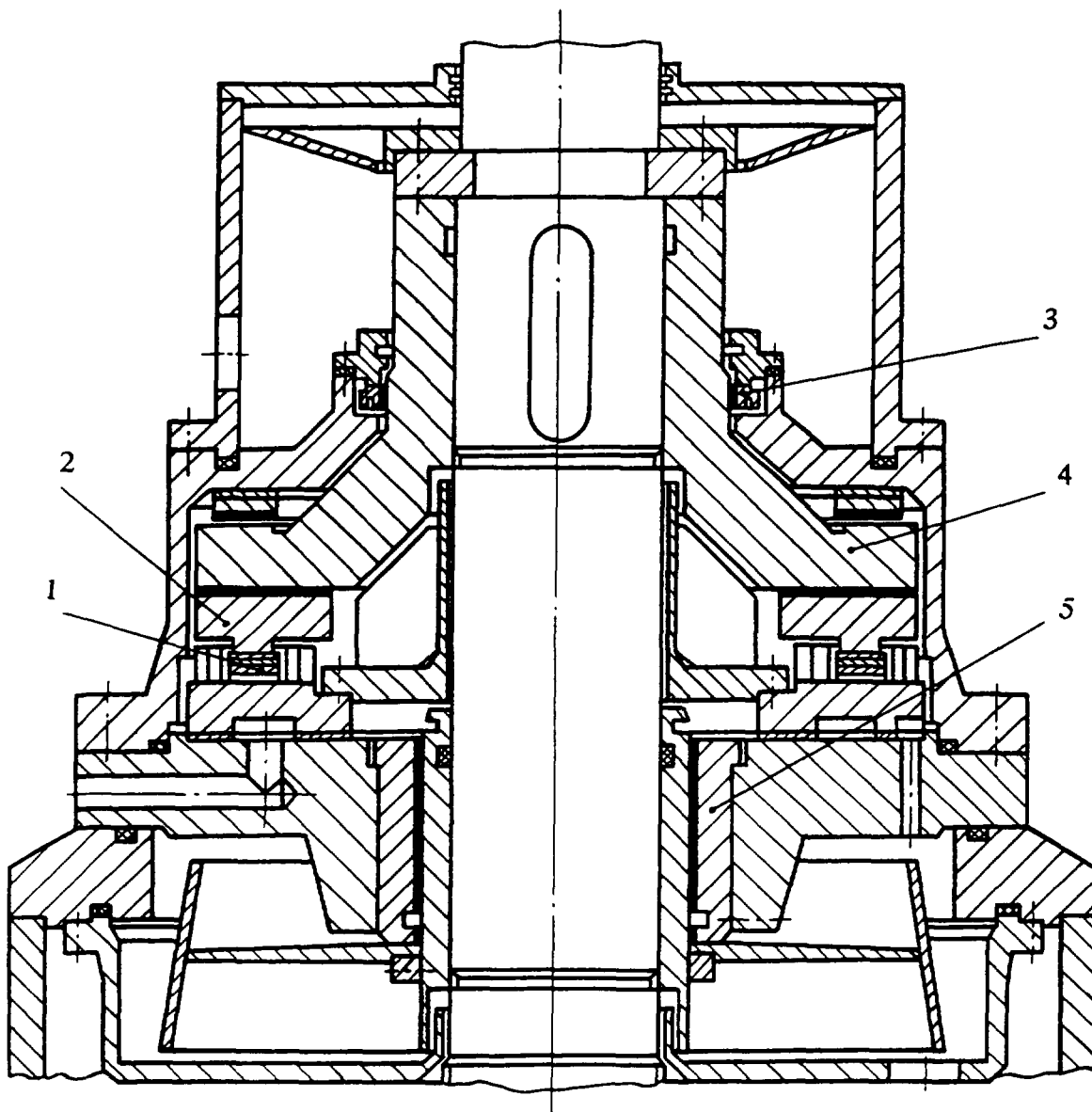
1 -shaft, 2 - spiral channel, 3,5 - working chambers, 4,9 - gaps, 6 - bearing body, 7 - discharge header, 8 - control chamber.

Fig.8.5. BOR, BN-600 Pump Hydrostatic Bearing



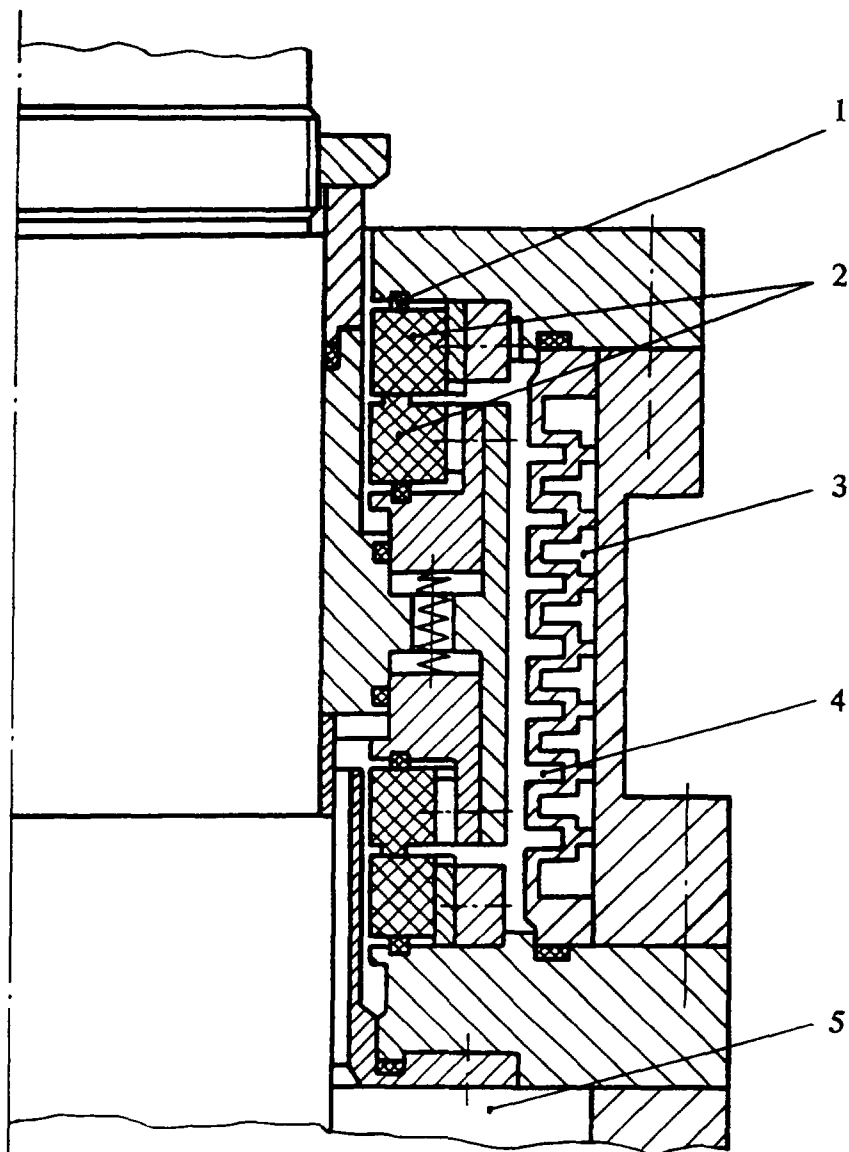
1 - oil bath, 2 - labyrinth pump, 3 - oil, 4 - ball bearing, 5 - cooling water, 6 - cooler.

Fig. 8.6. BOR-60 Pump Bearing Assembly



1 - spring, 2 - thrust pad, 3 - floating ring, 4 - thrust journal, 5 - radial bearing.

Fig. 8.7. BN-600 Pumps Bearing Assembly



1 - rubber gasket, 2 - graphite rings, 3 - water cooler, 4 - oil-sealed joint, 5 - gas cavity.

Fig. 8.8. BOR-60 and BN-600 Pumps Shaft Face Seal

drained from the pump tank to the suction duct through a bypass line in which there is a sodium leakage tank with an automatic float-type level regulator which maintains the sodium level in the pump tank constant under various operating conditions. This allowed the pumps to be placed in the uppermost point of the circuit and the lower bearing to be lubricated with oil [8.2-12].

In the BN-600 primary coolant pump (Fig.8.3), because of the layout of the primary components and the low positive suction head, there is a double-suction impeller with a guide duct. The sodium is led to each half impeller axially through channels in upper and lower volute ducts, and delivered from the impeller through the guide duct and vertical channels in the lower volute. This made it possible to reduce the pump size to a minimum. In the BN-600 secondary coolant pump (Fig.8.4) the suction pressure is higher than in the primary circuit, so an axial single-suction impeller is used. The flow is discharged through a two-entry spiral volute located in the pump tank [8.1, 8.2, 8.9, 8.10, 8.13, 8.14]. For all the pumps except BN-350 the lower radial bearing is of the hydrostatic type, submerged in sodium and fed from the impeller delivery side (Fig.8.5). The bearing is of double-split throttling, and the working surfaces of the bearing and the shaft neck are stellited. Throttling of sodium entering the bearing chambers takes place in the gap between the rotating shaft and the stationary bearing. In this design there is no need for special purification of the sodium. Along with this advantage the high load-carrying capability of the bearing must be highlighted together with its insensitivity to potential wear of the sealing rings. The bearings differ only in size and number of chambers. If the shaft 1 is displaced towards working chamber 3, the pressure of the sodium in it rises because gap 4 at the chamber outlet gets smaller and gap 9 at the sodium inlet to the flow control chamber 8 communicating with chamber 3 through spiral channel 2 gets larger. The pressure in the opposite chamber 5 is falling correspondingly. The restoring hydraulic force allows the shaft to rotate without contacting the bearing body 6. The upper bearing is located so that it is accessible for maintenance, and can be of various designs to form a single axial-radial bearing unit. In the BOR-60 pumps, for example, the unit consists of double ball bearings carrying axial and radial loads. The lubrication system is circulatory, enclosed in an oil bath. The oil is circulated by a threaded sleeve rotating with the pump shaft (Fig. 8.6). The BN-350 pumps have one axial and two radial sliding bearings whose working surfaces are babbitted. The radial bearings have non-split sleeves. The thrust bearing consists of self-aligning Mitchell-type pads. The lubrication system is of an external circulatory type, with cooled and filtered turbine oil supplied to the bearings under pressure. Unlike the BOR-60 pumps the flow of oil to the bearings does not depend on the speed of the main pump. The BN-600 pump upper radial bearings are identical to those of BN-350. The thrust bearings are provided with a device to ensure the uniform distribution of load between the thrust pads by the use of steel springs (Fig.8.7).

The upper bearing lubrication system is external and of a circulatory type. The main items of the system, pumps, filters, cooler, tank and valves, are mounted as a single "oil-block" assembly on a common plate. Turbine oil is used as a lubricant. For all the pumps the shaft seal is of mechanical face type (Fig.8.8). Two friction pairs together with the casing form a closed plenum filled with vacuum oil which functions as a hydraulic seal. The rotating rings of the friction pairs are freely movable axially as well as radially relative to the shaft, ensuring self-alignment to the stationary rings of the casing in operation. The seal is installed on and removed from the shaft as a single unit, which eliminates displacement of worked-in friction pairs and facilitates assembly. In the BN-600 pump in contrast to BOR-60 and BN-

350 the shaft gas seal is placed beneath the upper bearing. This prevents oil from entering the flow*path of the pump even in case of seal failure.

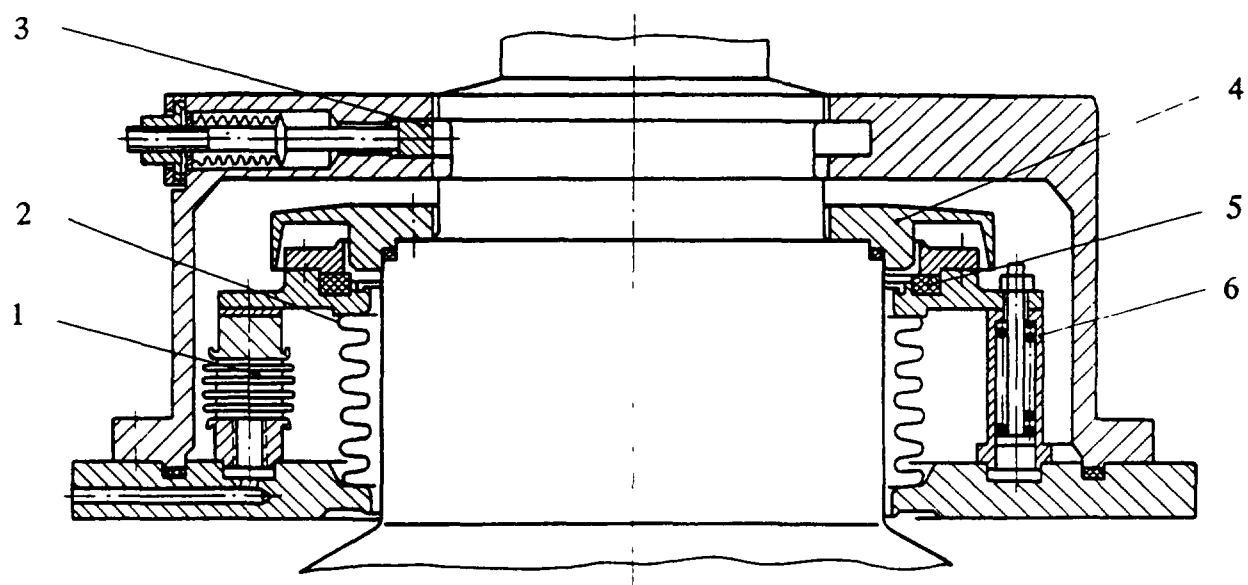
The sealing members of the standby (repair) seals (Fig.8.9) located below the shaft seals are rubber (BN-350) or fluoroplastic rings (BOR-60 and BN-600) fixed in a movable flange. The repair seal is tightened by pressing the sealing ring to the shaft by feeding gas into the working bellows.

The BOR-60 pumps are driven by standard motors with stepless speed control. For the BN-350 pumps special squirrel-cage induction motors with two speeds (250 and 1000 rpm) are used. For the BN-600 pumps controllable synchronous motors are used coupled to synchronous-rectifier drivers with phase rotors.

The BN-600 primary pump pressure nozzles incorporate flap-type check valves preventing backflow of sodium if one pump is deenergized. The check valve drive is hydraulic, responding to signals from the automatic control system.

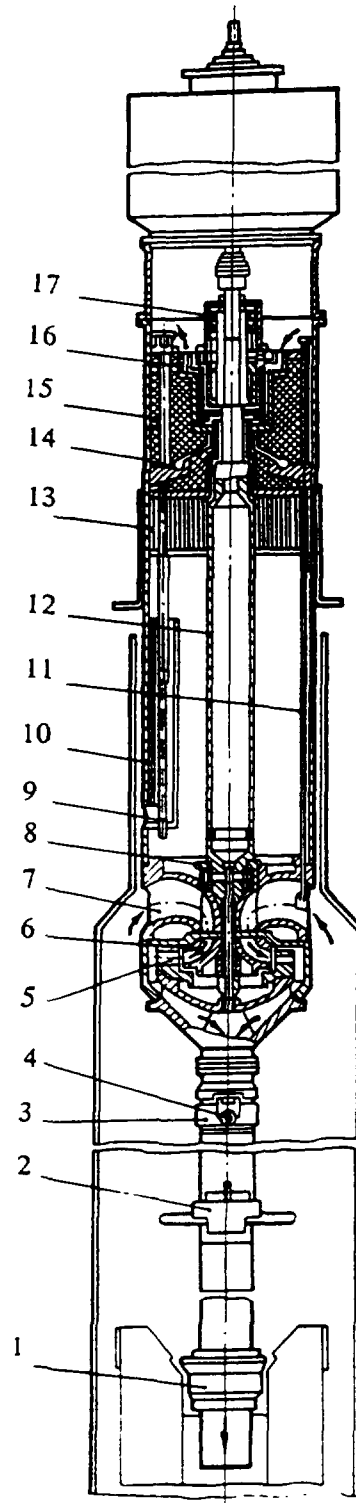
Rapsodie pumps. The primary coolant pumps are of the centrifugal single-stage submersible type (Fig.8.10). They are installed in the cold leg of the primary loop. The pump shaft rotates in two bearings: the lower is hydrostatic and the upper is a double radial-axial roller bearing. The drive is a synchronous canned motor. Sodium entry is from the top into an inverted impeller. Sodium from the impeller enters a guide duct and a delivery nozzle. A check valve consisting of a float with a locking disc is built into the pump. The hydrostatic bearing is fed through a hole in the shaft from the delivery side of the impeller via three holes of 12 mm diameter and a hole in the impeller fairing. A mesh filter is built into the fairing to avoid clogging of the 7 mm diameter throttling orifices. The bearing surface is hard-faced with colmonoy. The shaft is sealed by a double face seal with an oil lock. The seal oil is circulated in a closed system by a labyrinth pump on the pump shaft. The oil is cooled by water in a cooler which is placed outside the pump casing. The stationary ring of the friction pair is of stellited steel and the rotating ring is of graphite. Upper items can be repaired without depressurizing the circuit. The repair seal consists of a disc hermetically set onto the shaft and a rubber ring pressed onto the disc. When the nut fixing the upper roller bearing is unscrewed the rubber ring seats onto a shoulder in the pump casing. Design of the upper bearing unit allows the bearing and seal to be dismantled as a single unit. The secondary coolant pump has the same structure without the biological shield and check valve.

Phénix pumps. Each of the three primary coolant pumps is a vertical, centrifugal, submerged unit with a free sodium level (Fig.8.11). The Rapsodie reactor coolant pump was taken as a prototype. Coolant suction is taken from top. From the impeller the coolant enters the guide duct and then a delivery chamber with a built-in check valve. The entire length of the pump from the motor to delivery nozzle is 17 m, with two supports. The upper support is a double roller bearing and the lower is a throttle-type hydrostatic bearing fed from the impeller delivery. The diameter of the hydrostatic bearing is 320 mm and the radial gap is 0.5 mm. When tested with water the bearing rigidity was shown to be sufficient to limit shaft displacements in the range of 20% of the gap width. Testing the pump at approximately, 650 rpm frequency has shown good operating performance of the bearings. Leak-tightness of the pump with respect to the environment is ensured by a gas shaft seal consisting of a mechanical double face seal with an oil lock. A repair seal can be closed to allow upper items of the pump to be repaired without depressurizing the circuit.



1 - working bellow, 2 - sealing bellow, 3 - stop, 4 - shaft flange,
5 - sealing ring, 6 - return spring.

Fig. 8.9. BOR-60 and BN-600 Pumps Repair Seal



1,3 - lower and upper seals respectively, 2 - flow meter, 4 - hinge,
 5 - guiding duct, 6 - impeller, 7 - inlet scroll, 8 - hydrostatic bearing,
 9 - level gage, 10 - pump casing, 11 - thermocouple, 12 - shaft, 13 - thermal
 insulation, 14 - incidental oil leakage collector, 15 - biological shield,
 16 - air cooling shroud, 17 - bearing-shaft seal unit.

Fig. 8.11. Phenix Primary Coolant Pump

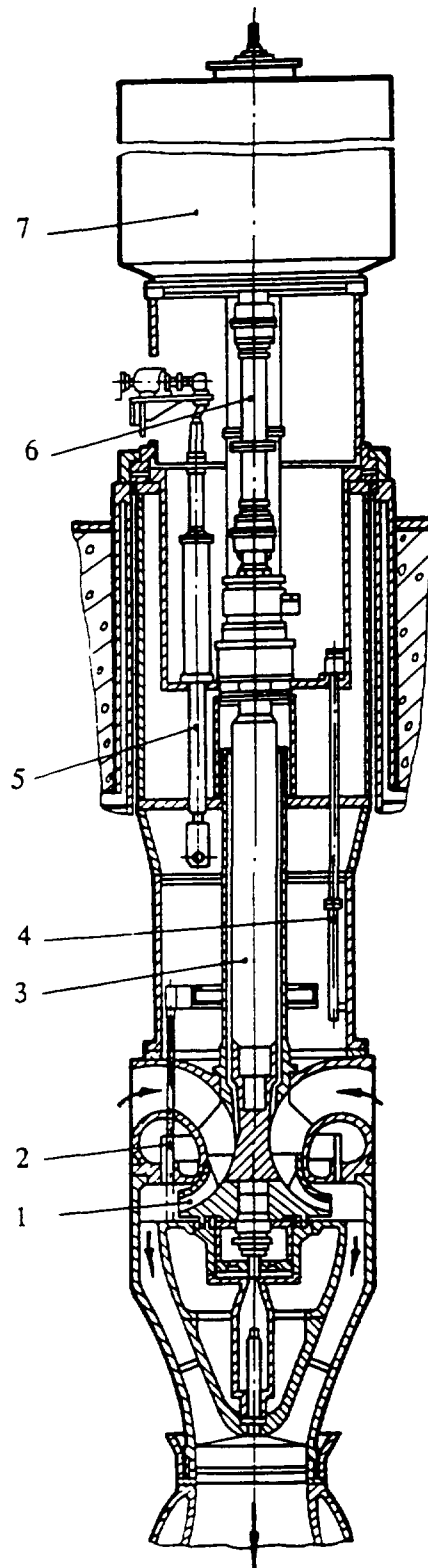
The biological shield is a plug filled with iron shot. On the upper flange of the shielding plug there is a double gasket which seals the radioactive gas in the pump cavity from the atmosphere. The gasket is made of thermoresistant rubber. Below the shielding plug there is a layer of thermal insulation which reduces the heat flux to the upper items of the pump. The pump is connected to the delivery pipeline by a hinge joint which eliminates misalignment and displacement of the pump relative to the delivery pipe. The design of the joint also provides for a high degree of leak-tightness. There is an inertial flywheel to sustain sodium flow for three minutes on loss of power supply to the reactor plant. In the event of more prolonged interruption the flywheel ensures smooth reduction of the pump speed down to 100 rpm, when the auxiliary motor is switched over to batteries. The main drive of the pump is a synchronous motor provided with a static frequency converter which regulates the pump speed smoothly in the range 250 to 975 rpm. The motor is cooled by a water-air heat exchanger operating in a closed cycle. An auxiliary drive motor is fed from batteries connected via a rectifier to a low voltage auxiliary power grid. In the event of complete failure of the grid the batteries can feed the auxiliary motor for one hour. There is a brake which acts on the flywheel rim, and prevents the pump operating in a turbine mode if the check valve should fail to close. The secondary coolant pumps are built into expansion tanks in each of the three loops. The design is identical to that of the primary pumps except for the biological shield, flywheel and check valve.

Superphénix pumps. The general design of the primary pumps (Fig.8.12) is similar to that of the Phénix primary pumps but its flow path is different:

- the sodium hydrostatic bearing is placed beneath the impeller,
- the diameter of the lower labyrinth (approx. 1000 mm) is chosen to reduce the axial force considerably without changing its downward direction,
- the check valve is in the form of a ring shell or obturator at the impeller outlet.

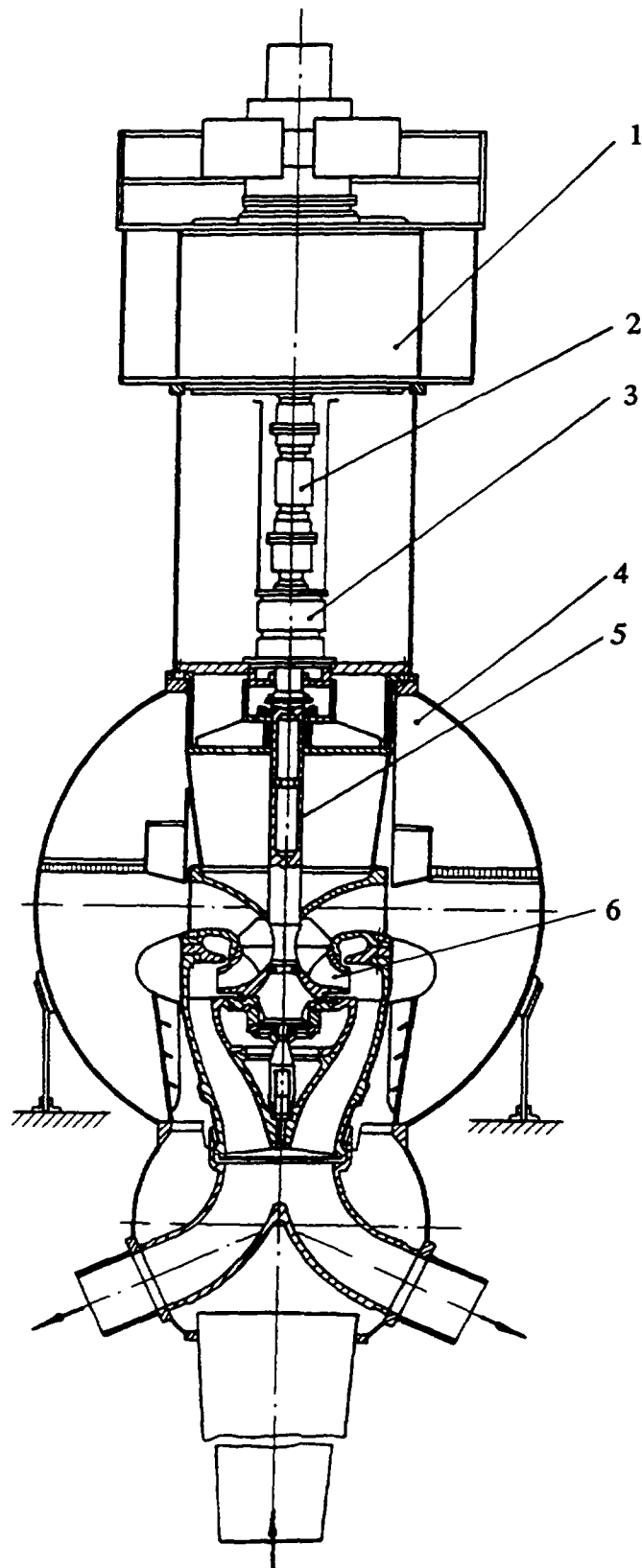
To reduce the mass of the rotating parts and the loads on the upper bearing the pump shaft is hollow with a wall thickness in the central region of up to 20 mm at 600 mm diameter. The distance between supports is 10 m. The hydrostatic bearing is of a chamber throttle design without discharge grooves between the chambers. This has the advantage that, at a lower load-bearing capacity than that of the Phénix bearing (because of the pressure equalization between the working chambers due to the leakages) the risk of the Superphénix shaft jamming on contact with the casing is reduced due to the higher hydrodynamic effect because of the absence of grooves. It is also better from the point of view of fabrication. The designs of the upper bearing and seal are similar to those of the Phénix primary pump. The diameters are increased but the linear velocities at the seal (approx. 10 m/s) are the same because of the lower rotation frequency. An interesting scheme is used to compensation for temperature elongation. The pump is suspended from an elastic ring and displacements are accommodated in the lower part of the pump on the support surface of the delivery nozzle. This design has the following advantages:

- compactness and simplicity,
- minimum surface for hard-facing,
- ease of dismantling,
- minimum leakage of sodium between the delivery and suction regions.



1 -impeller, 2 - check valve, 3 - pump shaft, 4 - level gage, 5 - check valve drive, 6 - connecting shaft, 7 - motor.

Fig. 8.12. Superphenix Primary Coolant Pump



1 - motor, 2 - connecting shaft, 3 - shaft seal, 4 - expansion tank, 5 - pump shaft, 6 - impeller.

Fig. 8.13. Superphenix Secondary Coolant Pump

Novel design choices overcame the problems caused by the large dimensions of the pump. The secondary coolant pump (Fig.8.13) is placed at the highest point of the loop in a sodium expansion tank, the upper flange of which serves to support it. The pump casing and rotating parts are the same as those of the primary coolant pump, but there is no biological shield and thermal insulation is used to protect the roller bearing and seal. Although the impeller and shaft are smaller the hydrostatic bearing is the same as in the primary pumps. The construction material for the primary and secondary pumps is stainless steel.

8.1.3. Pump testing techniques

The experimental development procedure for pumps includes the following kinds of tests: models test in water and air; tests of individual items on special rigs; pilot tests in water; and, finally, pilot tests in sodium.

From model tests (at scales from 1:2.2 for the BOR-60 pumps to 1:6.6 for BN-600) the following data were determined:

- optimum design of the flow paths,
- hydraulic, power and cavitation characteristics,
- pump efficiency components,
- hydraulic radial and axial forces acting on the impellers,
- efficiency of various types of liquid damping device for the pump tank and the associated power losses.

On the basis of the model tests corrections to the calculated data were made and recommendations concerning the development and modification of individual structural items were given. A range of seals were tested including various sealing ring friction pairs (bronze - carbon chromium steel, graphite - carbon chromium steel, graphite-stainless steel, graphite - nitrided carbon steel, graphite-graphite). The load applied to the sealing rings was varied during the tests and the seal performances were checked with increased pressure differences up to 2 MPa and with loss of oil and cooling water supply for extended periods of time. During oil bearing tests the temperatures were checked and the optimum oil and cooling water flowrate and pressure were determined. Bearings endurance tests under various loading conditions and at various rotation frequencies were also carried out.

In the hydrostatic bearing test rig two types of bearings were investigated: double split throttling; and chamberless with constant inlet throttling. The operability of the bearings was determined at various pressure drops, rotation frequencies, loads, eccentricities and shaft skewness. During tests of the check valve hydrodrive a hydraulic control system was developed.

The most important stage in pump development was the testing of prototype pumps in water and sodium. Hydraulic and cavitation characteristics of the pumps, mechanical and power parameters of the motors, hydraulic axial and radial forces, and vibration intensity were determined. Operability under start-up, transient and anticipated emergency conditions was tested.

In sodium rigs the thermal conditions for the main pump components were checked, and operational issues associated with the peculiarities of sodium as a coolant were studied. Accident tests were also carried out modelling loss of lubrication and cooling systems. It should be noted that in the BOR-60 and BN-600 sodium rig tests impellers with reduced flow capacity compared with design were used. This simplified the rigs and reduced the power consumption for the endurance tests. During the tests operability was checked for reversed rotation of the shaft, low speed operation, maximum sodium levels and temperatures (up to 500°C), and loss of the lubrication and cooling systems. The following features were investigated: gas entrainment at the suction, vibration of the pumps and rigs, and the influence of starts and stops on operation of the bearings. The number of starts for various pumps was in the range of 100-400. After completion of the sodium tests the pumps were removed after the sodium tanks were drained at a temperature of 100-150°C. The initial lifting force for removing the BN-600 primary coolant pumps was not less than 1000 kN (the weight of the internals was 86 t); for the BN-600 secondary coolant pump the initial removal force was less than 150 kN (the weight being 12 tons). The surfaces of the pumps which had been in contact with sodium were clean, and the pumps had drained satisfactorily.

8.1.4. Pump operating experience

Long-term operation of the reactors BOR-60, BN-350 and BN-600 has provided a sound basis for the design and technical decisions adopted for the sodium pumps. The pumps are working reliably and ensure all the specified modes of reactor operation. The BOR-60 pumps have been operated since 1969, and the maximum service age of the primary pumps exceeds 25 years without replacement of the internals. Similarly the BN-350 pumps have 24 years of operating experience. The BN-600 pumps, which are some of the biggest in the world, have the following performance indicators:

- the primary pump operating age is more than 60,000 h for one life cycle and more than 80,000 h for two cycles, with replacement of the impeller at the first removal of the pump from the reactor,
- the secondary coolant pump operating age is more than 15 years without replacement of the internals.

The pump operating factor (the ratio between the number of hours the pump was operative and the total number of hours in the period) is very high: by the tenth year of operation of the BN-600 it is in the range of 90-95%. Valuable experience has been obtained which is indispensable for the next generation of sodium pumps. The main technical parameters of the pumps being operated and developed are given in Tables 8.1 and 8.1a respectively. Bearings are the most important components of sodium pumps. The service ages given above were attained without replacement of the bearings. Wear in the bearings is virtually absent. This is true both for the hydrodynamic sliding bearings used in the BN-350 and BN-600 pumps and for the roller bearings used in BOR-60 (Fig. 8.6, 8.7). Turbine oil is used as lubricant in the bearings. The hydrostatic bearings in the BOR-60 and BN-600 pumps, in which pumped sodium serves as a working medium, showed themselves to be exceptionally reliable items (Fig. 8.5). The best results were obtained for the most highly loaded bearings of the BN-600 pumps, whose working surfaces kept their initial mirror finish without visible traces of running-in. This may be explained by the high purity of the sodium coolant in BN-600. The design load-bearing capacity of the hydrostatic bearings of the BN-

Tabl. 8.1. Operating Sodium Pumps Main Data

Parameter	BOR-60		BN-350		BN-600		Rapsodie		Phoenix		Superphenix		EBR-II		FFTF		PFR		SNR-300
	Prim.	Second.	Prim.	Second.	Prim.	Second.	Prim.	Second.	Prim.	Second.	Prim.	Second.	Prim.	Second.	Prim.	Second.	Prim.	Second.	Prim.
	circ.	circ.	circ.	circ.	circ.	circ.	circ.	circ.	circ.	circ.	circ.	circ.	circ.	circ.	circ.	circ.	circ.	circ.	circ.
	CNN-1	CNN-2	CNN-3	CNN-4	CNN-9	CNN-8													
1. Flow rate, m ³ /h	600	830	3200	3700	9700	8000	374	380	4000	3500	18000	13600	1250	1475	3000	3000	4920	4200	4970
2. Delivery head, m	85	60	110	68	95	52	32	18	76	65	62	30	61	44	152	79	80	32	85
3. Sodium temp.(max.), °C	500	500	400	400	400	400	250	420	390	360	395	348	372	371	500	390	354	370	560
4. Speed, rev/min	1500	1500	1000/250	1000/250	970	970	1100	875	1000	1000	470	550	1075	-	1110	700	980	925	910
5. Specific speed	80	120	100	157	138	268	-	120	100	157	138	268	293	171	312	350	132	350	138
6. Required power, kW	170	170	1300	850	3150	1350	55	55	880	560	4800	1500	260	370	1300	875	1300	600	1500
7. Gas pressure, MPa	0.01	0.05	0.09	0.2	0.04	0.2	-	-	-	-	0.007	0.16	-	-	0.11	-	-	-	0.05-0.15
8. Efficiency, %	71	71	70	73	72	76	70	70	-	85	80-85	81	70	40	-	-	72	82-85	83
9. Speed variation range, %	20-100	20-100	-	-	25-100	25-100	15-100	15-100	25-100	25-100	-	-	10-100	20-100	0-100	-	20-100	20-100	5-100
10. Weight of removable internals, t	12.2	0.82	18.5	12.0	73.0	11.4	-	-	-	-	-	-	-	-	-	-	-	-	-
11. Weight of pump, t	69.5	31.0	86.0	60.0	120.0	69.0	-	-	35.0	-	120.0	63.0	-	-	-	-	-	-	-

Table 8.1a. Prospective Sodium Pumps Main Design Data

Parameter	BN-800		BN-170		BN-600M			BN-1600		Superphenix 2	
	Prim.	Second.	Prim.	Second.	Prim.	Second.	Second.	Prim.	Second.	Prim.	Second.
	circ.	circ.	circ.	circ.	circ.	circ.	circ.	circ.	circ.	circ.	circ.
	CNN-11	CNN-10	CNN-2,3	CNN-7,3	CNN-16	CNN-14	CNN-7,2	CNN-18	CNN-18		
1. Flow rate, m ³ /h	12300	11500	2300	7260	17000	14600	7280	18200	17300	19500	17300
2. Delivery head, m	101	48	60	35	70	45	35	98	55	65	39.5
3. Sodium temp.(max.), °C	500	500	400	400	400	400	400	400	400	390	348
4. Speed, rev/min	980	980	980	980	740	740	980	740	740	500	500
5. Specific speed	147	355	132	350	171	312	350	138	293	147	355
6. Required power, kW	4000	1800	450	850	3500	1820	730	5600	3200	6200	2100
7. Gas pressure, MPa	0.055	0.025	0.04	0.15	0.055	0.37	0.25	0.04	0.2	-	0.16
8. Efficiency, %	72	77	75	75	80	80	80	75	80	-	-
9. Speed variation range, %	25-100	25-100	25-100	25-100	20-100	20-100	25-100	25-100	25-100	-	-
10. Weight of removable internals, t	67.5	14.5	20.0	15.0	46.0	14.0	10.0	77.0	42.0	-	-
11. Weight of pump, t	120.0	65.0	23.0	20.0	95.0	52.0	24.0	180.0	100.0	72.0	21.0

600 primary pumps exceeds 10^5 N, while for the hydrodynamic bearings it is more than $3 \cdot 10^5$ N.

Reliable sealing of the internal cavities of the pumps from the environment is provided by hydrodynamic shaft face seals with an oil-sealed joint (Fig. 8.8). The seal allows a pressure difference of up to 2 MPa and ensures a minimum steady oil leakage flow of less than $10 \text{ cm}^3/\text{h}$ independent of the mode of operation. There were no difficulties with the repair seals (Fig. 8.9) which performed the function of the main shaft seals during their replacement when the pump is shut down.

During the initial period of operation of each of the reactors certain technical problems were solved. These concerned adjustment of the systems and components, bringing the reactor to nominal (rated) power, and feedback of operating experience. Thus, in BN-350, there were disturbances in the pumps at start up after a long-term outage, caused by solidification of sodium in the gap between the pump shaft and its casing. There were also difficulties resulting from an increase in the sodium leakage flow from the impeller delivery due to temperature variations in transients, which prevented the sodium level rising or varying in the pump tank.

For BN-600 there was an acute problem of avoiding operating the primary coolant pumps in the resonance bands of shaft rotation frequencies. It was found that the frequency-controlled motor coupled to the synchronous-rectifier drive induced torsional pulsations of 6-8% of the nominal torque. When the torque pulsations coincided with a natural frequency of shaft vibration resonances arose resulting in adverse consequences, such as cracks in the shafts and failure of the couplings. During 1982-83 strain measurements were made to evaluate the pump shaft stresses and prohibited zones in the shaft rotation frequency range were determined. The problem was solved completely when the damaged shafts were replaced by modified ones of the same strength and when the pump control algorithm was changed. After the reactor attains a prescribed power level the pump frequency control is suspended (the synchronous-rectifier stage being switched off).

Long-term operating experience has allowed the factors which limit the lifetime of the pumps to be identified. Cavitation-erosion wear of the impeller blades is now the single factor requiring periodical removal of the primary coolant pump internals (both for BN-350 and BN-600) to replace the impellers. The operators were not satisfied with the design lifetime of the face shaft seals, which was limited by degradation of the rubber sealing collars (lose of elasticity and cracking). The seals were replaced with spares, as a rule, during planned maintenance outages. The design of the seals currently in use has been modified significantly compared with the original design (which is used now only in BN-350 pumps) and has the following advantages:

- the possibility of misalignment of the sealing surfaces is reduced by improvement of the items which transfer the torque to the rotating sealing rings,
- a wear-resistant "graphite-to-graphite" sealing pair is used instead of "graphite-to-steel",
- the oil-cooling surface in the seal is increased,
- rubber sealing rings are used instead of collars.

On the basis of operating experience and resulting from the improvements made in design the specified operating life for the pump internals has recently been increased significantly:

- up to $140 \cdot 10^3$ h for the BOR-60 primary pumps and to $80 \cdot 10^3$ h for the secondary pumps,
- up to $50 \cdot 10^3$ h for the BN-350 and BN-600 primary pumps and to $100 \cdot 10^3$ h for the secondary pumps.

The life-time of the BOR-60 and BN-600 pump shaft face seals is $50 \cdot 10^3$ h.

8.1.5. Cavitation in sodium pump impellers

Despite the fact that cavitation in blade hydraulic machines has been known for a long time and studied intensively, avoiding its manifestations remains an important issue. This particularly concerns sodium pumps where the high temperature of the sodium and its chemical activity do not allow the methods of detection of the initial stages of cavitation, which are widely used for water circulators, to be employed. Cavitation in the pump occurs when the available positive suction head (PSH) is less than the allowable cavitation margin, i.e. the net positive suction head (NPSH), of the pump. The PSH value, which is a hydraulic parameter of the plant loop independent of the pump rotation frequency, is determined by the cover gas pressure, the submergence of the impeller below the sodium level, and by the hydraulic resistance of the flow path from the reactor to the pump. As a rule the last two quantities are close so that the PSH is determined mainly by the cover gas pressure in the reactor vessel. The NPSH is the characteristic representing the minimum pressure at the pump suction in excess of the saturation vapor pressure of the pumped liquid, which is necessary to ensure cavitation-free operation. It depends on the pump speed and the design of the pump impeller and flow guide duct, and is expressed by the formula:

$$Dh = 10 \times K \times (n \times C^{-1} \times Q^{0.5})^{4/3},$$

where: Dh - NPSH of the pump;
 K - a factor accounting for pump operating conditions,
 n - pump speed,
 Q - flowrate of a single-flow impeller,
 C - cavitation specific speed factor, which allows different pumps to be compared with respect to their anti-cavitation properties.

Hence an increase in the pump rotation frequency requires a rise in the reactor pressure (to the NPSH value) or the development of a special flow path with low NPSH. Increasing the reactor cover gas pressure complicates the design and makes it more expensive, while creation of a special flow path with low cavitation margin complicates the pump design.

The allowable BN-600 reactor coolant pump speeds with respect to cavitation versus cover gas pressure (Pg) in the reactor are given below:

Pg, MPa	0.005	0.02	0.04	0.06	0.08
n, rpm	820	900	1020	1110	1230

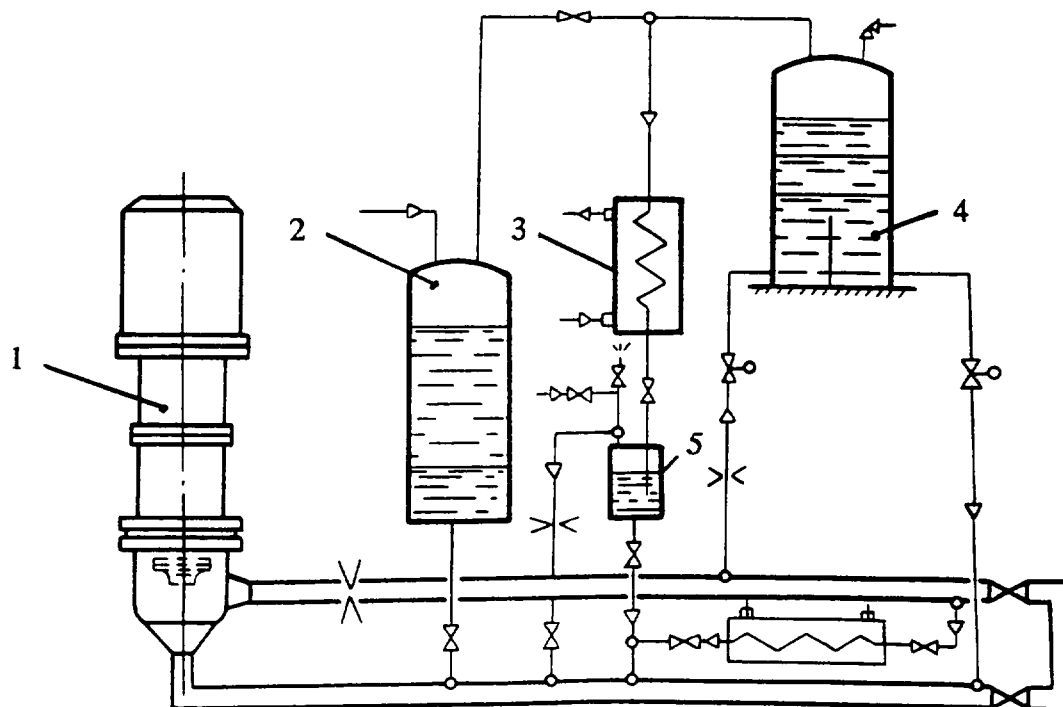
During design of BN-600 it turned out that in terms of the reactor vessel strength and mass the cover gas pressure should be in the range of 0.04... 0.05 MPa. Thus, according to the above data the pump speed should be not more than 1000 rpm. Sodium pump designers solve the problem of preventing cavitation by reducing the flow velocity, as a rule. The flow velocity is reduced either by decreasing the shaft rotation frequency or by adoption of a multistream flow scheme, or both. Methods for improving the anticavitation properties of the impeller, such as the mounting of flow inducers ($C=5000$) at the suction or increasing the impeller inlet cross-section, are not used in Russia because such impellers would necessarily operate under heavy cavitation conditions causing accelerated erosion wear and reduction of the operating life. In the development of large capacity sodium pumps the critical value of the cavitation specific speed factor is set equal to $C=1000... 1200$. This value has been proved by operating experience from water pumps having similar speeds and capacities and sufficiently long operating life. In spite of the fact that there are impellers with $C>2000$, limitation of the C value is justifiable because it permits an increase in the cavitation margin to accommodate anticipated deviations of operating conditions from design. The optimization of sodium flow path geometry is carried out using water models. The models are tested on special test rigs adapted for cavitation investigations. The basic flow diagram of a typical test rig is given in Fig.8.14. It is a closed loop with a cavitation tank, isolation and control valves. There are gas, vacuum and other auxiliary systems and related instrumentation. The models are designed to allow the dimensions and shape of the flow path to be changed during the test. The following parameters have been determined:

- minimum positive head at which there are no symptoms of cavitation;
- positive head at which an erosion effect is detected without affecting the delivery head;
- critical positive head at which cavitation affects the pump power characteristics;
- presence of cavitation-erosion areas and methods for their prevention by various design measures.

The characteristics obtained from the models are then recalculated for the real pump by the known laws of similarity. However, it is necessary that the model pump flow path is similar to the real one in all geometrical parameters including the gaps in the suction plenum labyrinth seals. If these requirements are not fulfilled the test results are not sufficiently representative. Based on model test results corrections are made to the detail drawings of the actual pumps. On the full-scale pumps operation in cavitation modes up to the limit of head reduction is studied. Such an approach is quite justifiable because when determining the cavitation characteristics of the full-sized pump it is necessary, accounting for its structural features, to maintain conditions that preclude failure of the pump under test. For example, if the pump being tested has a hydrostatic bearing fed from the impeller account should be taken of the fact that if cavitation becomes developed the delivery head may be reduced to such an extent that the hydrostatic bearing would become inoperable. Moreover, in the cavitation mode hydrodynamic radial forces might increase sufficiently to impair operation.

The BOR-60, BN-350, and BN-600 sodium pumps were designed with respect to these principles, particularly:

- critical cavitation specific speed factors in the range of $C=1000... 1200$ were adopted;



1 - pump, 2 - pressurizer, 3 - heat exchanger, 4 - cavitation tank, 5 - separation tank.

Fig. 8.14. Cavitation Test Rig Flow Diagram



Fig. 8.15. BN-600 Reactor Coolant Pump Impeller - Cavitation traces after five years of operation

- flow path geometries to provide the specified power parameters and to avoid erosion of varnish coatings under simulated conditions were developed and tested on water models.

Much attention has been paid to the full-scale pump tests. The BN-350 pumps were tested both in water and sodium. They showed identical power and cavitation characteristics in water and sodium. Therefore, the characteristics of the subsequent BOR-60 and BN-600 pumps were measured in water only, and recalculated for sodium. This allowed the test rigs to be simplified significantly. The pumps for BN-350 were subjected to long-term endurance tests in a full-scale test rig. The total operating age of the primary pump in the test rig reached approx. 3500 h. Inspection of the tested pump revealed no signs of erosion wear of the flow path components. However in sodium cooled fast reactors operating conditions in which cavitation in the flow path can not be eliminated completely are probable. The most unfavorable in this respect are operating modes in which due to some circumstances the pumps are operated beyond the limits of the specified parameters. In such cases local cavitation centres can arise in the pump. Cavitation can occur on vanes, in labyrinths and impeller discharge orifices, on the vanes of diffusers, and on various elevations and depressions in zones of high local flow velocities. Such operating conditions are usually not long-lasting and their consequences do not influence the pump life-time, but they should be accounted for. The operation of the BOR-60, BN-350 and BN-600 pumps confirms this. The complete absence of traces of cavitation on the BOR-60 pump impellers after 50...80 thousand hours of operation is explained by the relatively low sodium velocity on the impeller blades.

Traces of cavitation are also absent from the BN-600 secondary pump because it is possible to pressurize the gas in the circuit. The marked zones of cavitation-erosion wear on the impeller vanes of the BN-350 primary and secondary pumps and more significant zones in the BN-600 primary pumps are similar in principle since the form of the impellers is the same. Wear zones revealed after 35... 50.103 hours of operation were located on the rear concave side of the vanes near the inlet edge, sometimes involving the edge and the impeller disc. The cavities on the BN-600 impeller vanes reached up to 150 mm in length and 70 mm in breadth, and 18 mm in depth (Fig.8.15). Extensive wear of the BN-600 primary pump impeller vanes might be explained by the fact that it is not possible in an integral reactor to provide a cover gas pressure of more than 0.04 MPa, and by prolonged operation of the pumps in a non-optimal mode due to the necessity of stepless regulation of rotation frequency in the range of 250... 970 rpm. For these reasons it was not possible to provide the desirable 4 times overpressure at the impeller inlet in excess of saturation sodium vapor pressure. The actual ratio was 1.8. The wear of the vanes did not influence the operating parameters of the pumps. The resulting release of metal particles into the primary coolant was undesirable.

On the basis of the test rig operation the BN-350 and BN-600 impeller vane profile was optimised. Spare impellers with new vane profiles were fabricated for the BN-600 pumps. Replacement of the BN-350 primary coolant pump impellers is planned.

8.1.6. Structural improvements in new sodium pump designs

The positive experience of operating the BOR-60, BN-350 and BN-600 pumps was made use of when the sodium pumps for the prospective advanced fast reactors BN-800, BN-1600M, BMN-170, BN-600M were designed. Some items determining the life-time and reliability of the pumps were designed to be similar to the operating pumps, most importantly

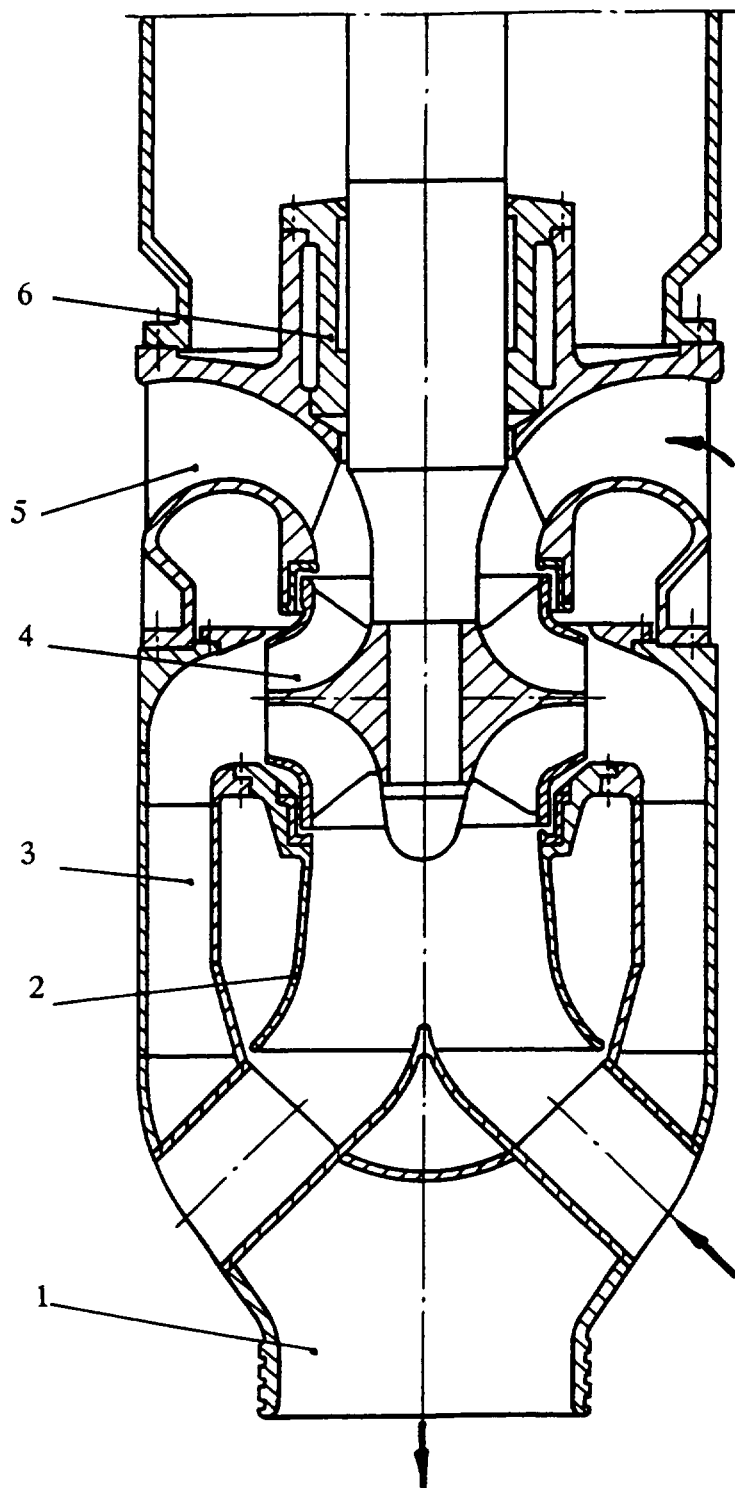
the bearings. In light-weight pumps for BMN-170 and the BN-600M secondary circuits oil-bath roller bearing of the BOR-60 type are used as the upper support for the shaft, but more effective cooling of the oil is provided by shifting the cooling zone to the labyrinth pump (Fig.8.6). For powerful pumps with heavy rotors for BN-800, BN-1600 and the BN-600M primary coolant the upper sliding bearings of BN-600 pumps are used where the problem of the uniform distribution of axial load on the tilting pads of the thrust bearing is solved by a set of steel springs and optimal arrangement of the pad tilting rib (Fig.8.7). A hydrostatic bearing as the lower radial shaft support is unavoidable for the integral reactor pumps because of the deep submergence of the impeller in sodium. The positive operational experience of the bearings in the BOR-60 and BN-600 pumps indicates use of these bearings in secondary coolant pumps as well. Throttling of the sodium entering the bearing chambers takes place in the gap between the rotating shaft and the bearing, so no special purification of the sodium is required (Fig.8.5). The design of the face and repair seals (Fig. 8.8, 8.9) is borrowed virtually entirely from the current pumps. Most attention in the development of prospective pumps is paid to the choice of an optimal flow path from the view point of cavitation and economic efficiency. The structural complexity and large mass of the BN-350 and BN-600 pump flow paths made the designers change the location of the guide duct in the BN-1600 and BN-600M primary pumps, from axial to radial. This allowed the diameter of the flow path of the BN-600M pump and the rotation frequency to be reduced to eliminate cavitation. At the same time the suction and delivery channels were greatly simplified (Fig.8.16). Cavitation is eliminated in the BMN-170 primary pump by a simple flow path consisting of a single-sided upper suction impeller in combination with an axial guide duct (Fig.8.17). It is easier to develop hydraulically effective flow paths for secondary pumps since no strict size or weight limitations are imposed by the layout. However, for these pumps the manufacturing technology issues can play a determining role. For this reason it was decided for the BN-800 secondary pumps to abandon the typical but expensive flow path used in the BN-600 pumps. A low suction impeller with an axial guide duct and flow delivery header located above it was used (Fig.8.18). It should be noted that simplification of the design did not result in a reduction of the efficiency. This flow scheme was also evaluated for the BN-600-M and BMN-170 pumps, but in these pumps as well as in the BN-1600 secondary pumps preference was given to a flow path promising (on the basis of rig tests) higher efficiency - not less than 85%. It became standard practice for the Designer (OKBM) to select a one-sided impeller with a radial guide duct and a spherical delivery header with one or several sodium delivery nozzles (Fig.8.19).

The Superphénix 2 (RNR 1500 project) pumps were designed on the basis of operation experience from Rapsodie, Phénix and Superphénix. In Fig. 8.20 and 8.21 the Superphenix and RNR 1500 primary and secondary coolant pumps are compared. The main concern was reduction of weight, dimensions and cost. For the primary pumps these goals are attained by decreasing the pump diameter by the use of a higher speed impeller, elimination of the check valve, and returning to a hinge joint between the pump and the diagrid with rigid restraint in the upper region (similar to the Phenix primary pump). There were more significant modifications of the secondary pump due to the arrangement of the removable internals in a small tank instead of in an expansion tank.

At present several problems still await solution. They are the following:

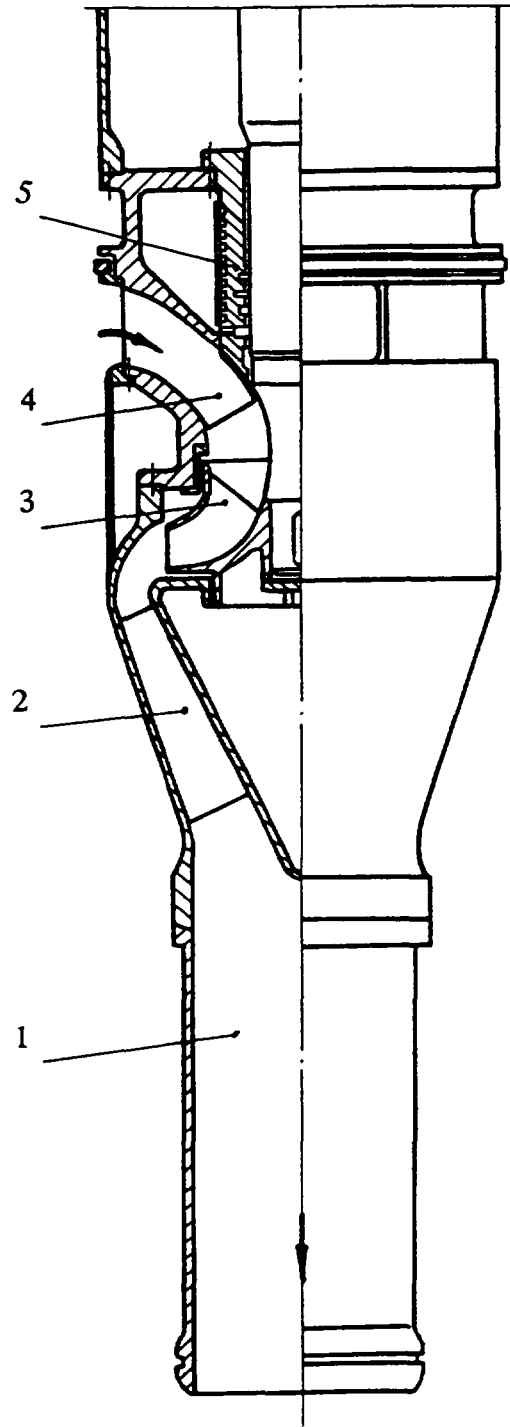
- substitution of oil lubricant in the roller bearings by grease; the short term operating experience of the BOR-60 pump bearings using "Litol" grease is promising,

Text cont. on p. 351.



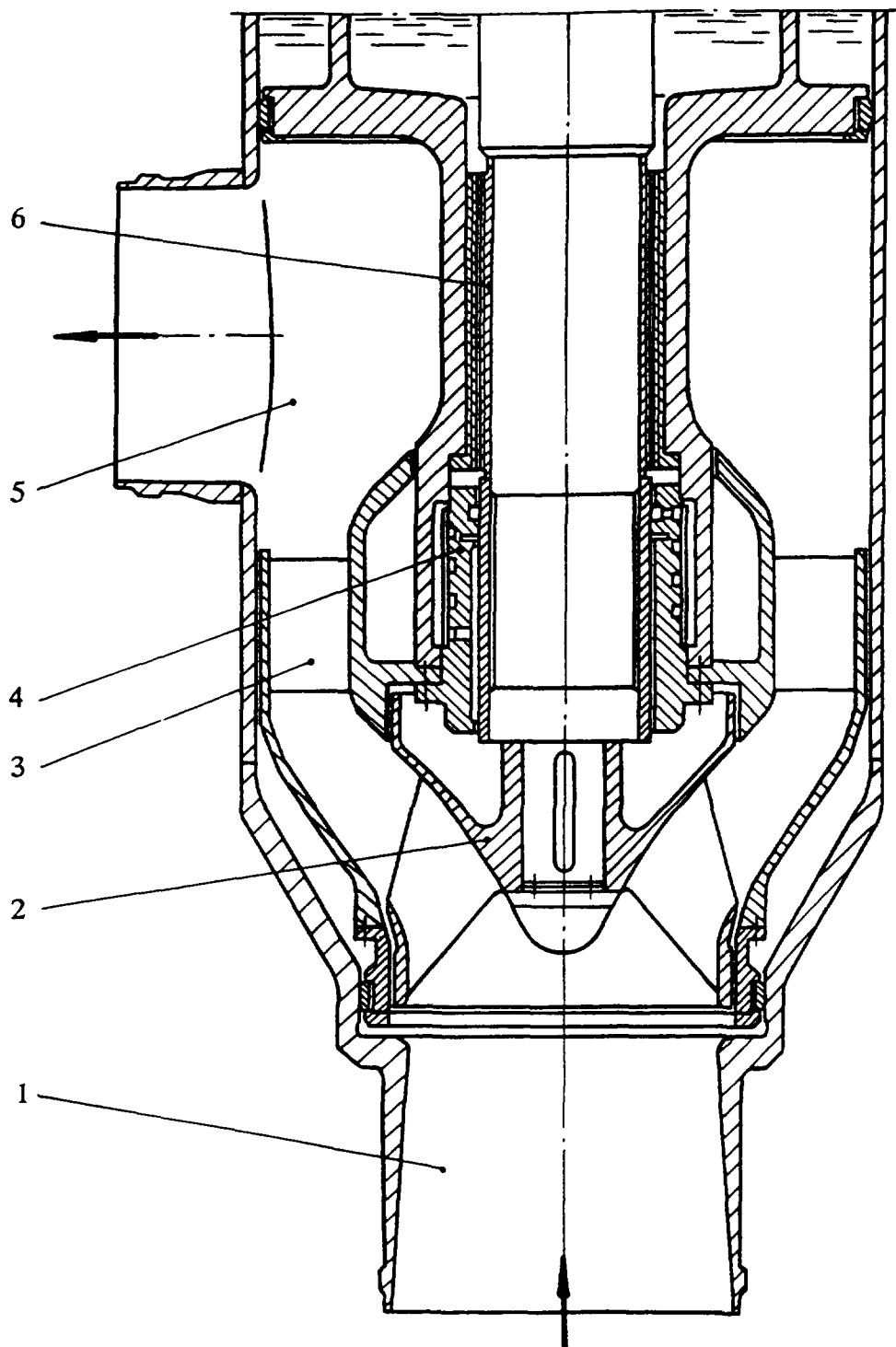
1 - delivery header, 2 - suction confuser, 3 - guiding duct, 4 - impeller,
5 - suction duct, 6 - hydrostatic bearing.

Fig. 8.16. BN-1600 and BN-600M Reactor Coolant Pumps
Flow Path



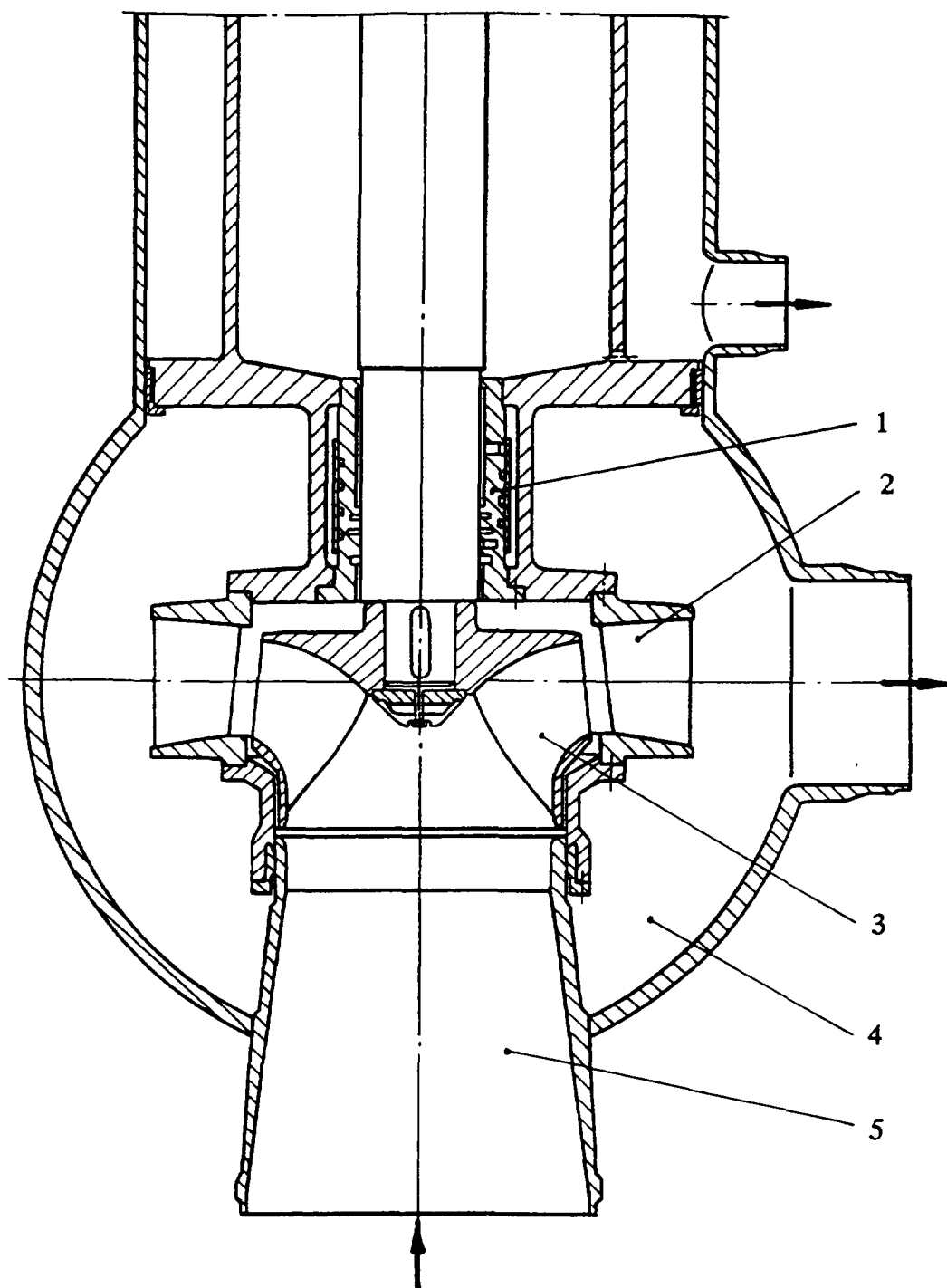
1 - delivery header, 2 - guiding duct, 3 - impeller, 4 - suction duct,
5 - hydrostatic bearing.

Fig. 8.17. BMN-170 Reactor Coolant Pump Flow Path



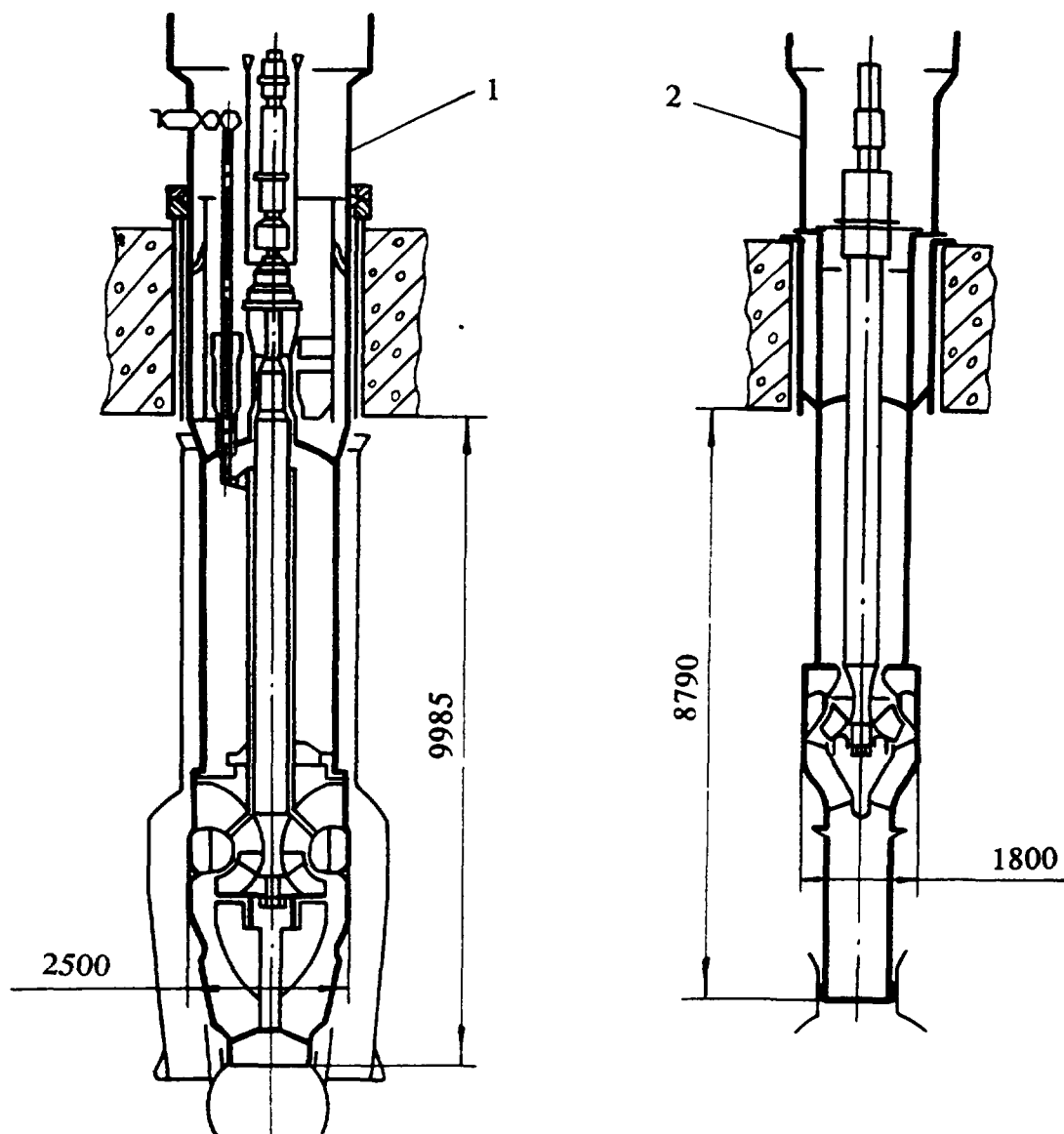
1 - suction confuser, 2 - impeller, 3 - guiding duct, 4 - hydrostatic bearing,
5 - delivery header, 6 - labyrinth pump.

Fig. 8.18. BN-800 Secondary Coolant Pump Flow Path



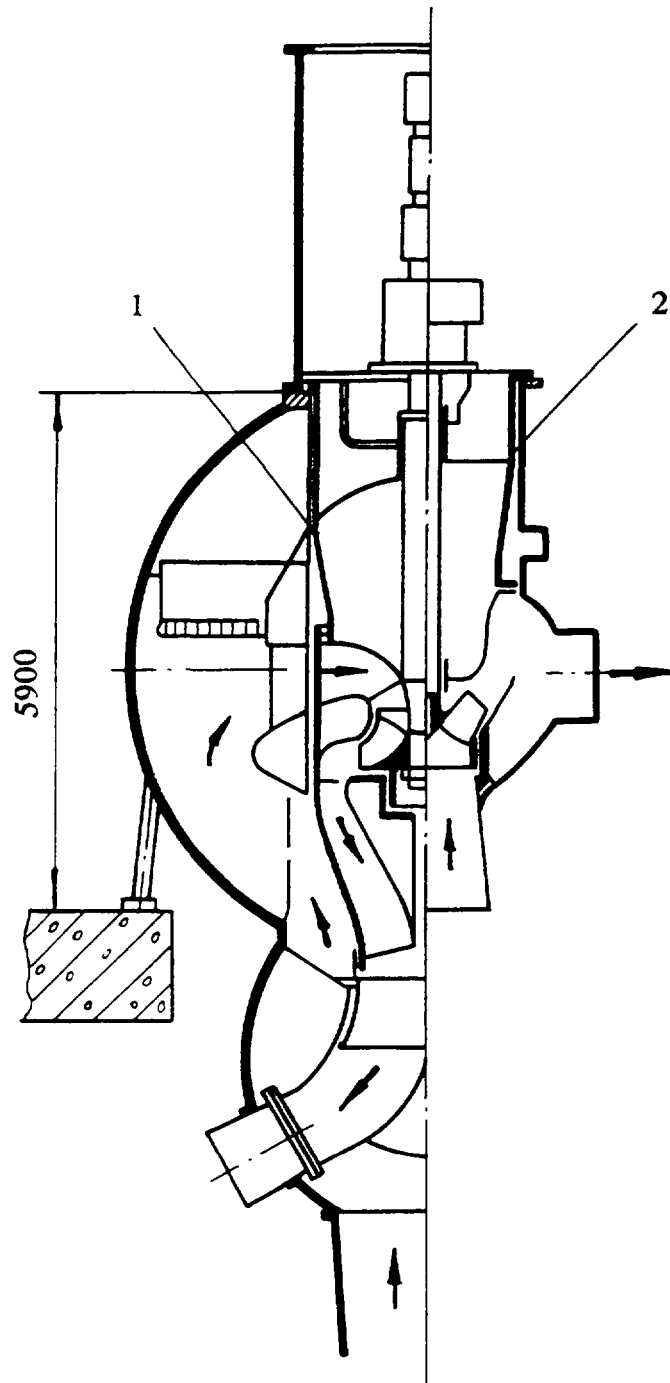
1 - hydrostatic bearing, 2 - guiding duct, 3 - impeller, 4 - delivery header,
5 - suction confuser.

Fig. 8.19. BMN-170, BN-1600 and BN-600M
Secondary Coolant Pumps Flow Path



1 -Superphenix pump, 2 - Superphenix 2 pump.

Fig. 8.20. Superphenix Reactor Coolant Pump Evolution



1 -Superphenix pump, 2 - Superphenix 2 pump.

Fig. 8.21. Superphenix Secondary Coolant Pump Evolution

- substitution of water cooling of pump items by air cooling; the problem has been solved unambiguously only for air cooling of the upper parts of future pump shafts,
- use of "dry" shaft seals instead of oil face seals,
- the need for check valves for primary circuit pumps; it might be possible to dispense with them for the BN-600M and BMN-170 pumps,
- expediency of steeples control of pump rotation speed,
- extension of the pump coastdown time on de-energization,
- etc.

8.2. THERMAL-HYDRAULICS OF THE PRIMARY CIRCUIT

8.2.1. Introduction

The use of sodium as a coolant fluid in fast reactors allows a high temperature thermodynamic cycle of high efficiency without having to pressurize the circuit. Under atmospheric pressure, sodium boils above 800°C. From this choice therefore follow two fundamental characteristics for the reactor vessel:

- low pressures that do not exceed 10 bars at the pump outlet;
- high temperatures with variations that, according to the steady state or transient operating conditions, can affect the velocity field.

As regards mechanical loads, these factors have several major consequences:

- fluid static pressure loads rarely influence the structural dimensions;
- high temperatures and temperature variations induce significant thermal stresses in the internal structures of the reactor block which make large contributions to the total structural damage.

8.2.2. Objectives of the thermal-hydraulic studies

One of the objectives of thermal-hydraulic studies is thus clear: to foresee the thermal loads the internal structures will be subject to during different reactor operating conditions. To obtain these thermal loads, we must know the detailed thermal-hydraulic behaviour of the reactor block, including both velocity and temperature fields. Generally speaking, assessment of thermal loads uses data from operating conditions as input and feeds into structural design studies. These three stages must of course be interactive; feedback to operating conditions can reduce excessive loads via, for example, changed thermal-hydraulic behaviour.

Thus, the different components of thermal-hydraulic studies are mainly:

- knowledge of velocity and temperature fields in the vicinity of the reactor block structure for nominal and part-load steady state or transient operating conditions,
- heat and mass transfer in the cover gas,
- gas entrainment at the free surface,
- thermal striping.

Additionally, particular systems that depend directly on thermal-hydraulics must not be forgotten:

- core outlet temperature measurements,
- measurements linked to the detection and localization of clad failure.

A general remark is that the various thermal-hydraulic problems which occur in the primary circuit are connected; it would therefore be unrealistic to attempt to treat them separately. Improvement in one respect can lead to deterioration in another. In the present state of project development the quest for a reduction of dimensions, and more generally of mass, for constant power, has led to a desire to reduce uncertainty margins. This can only be done at the cost of continuously improved knowledge, taking more and more parameters into account, leading to a better accuracy in the study of the thermal-hydraulic behaviour [8.26, 8.27, 8.46].

8.2.3. Steady state studies of the hot pools of pool-type reactors

In the hot plenum, thermal-hydraulic behaviour studies must lead to a knowledge of the thermal loads, in particular on the above core structure and the internal vessel. These studies must be carried out for various reactor operating conditions, for steady state operation at different power levels, and for transients.

Thermal-hydraulics of steady state operating conditions. The thermal-hydraulic behaviour of the hot plenum depends on the imposed boundary conditions:

- at the core outlet, the presence or absence of breeder assemblies and/or in-vessel storage will impose a temperature difference between the hot inner area (fissile) and the outer part of the core,
- in the lower part of the hot plenum, the presence of a cold flow due to leakage from the feet of the subassemblies,
- the difference of temperature between the hot plenum and the cold plenum induces a thermal flux through the inner structures.

There is no single method of approach to these problems and generally thermal-hydraulic calculation programmes coupled with representative mock-ups using simulant fluids are used. As a result, due to the distortion of the Prandtl number, the boundary layers on the walls through which heat is exchanged (such as the internal vessel, the primary pump pods, and the core support plate) have, according to classical fluid scaling models, a structure that is not representative of liquid metals. Thus, an experimental study using simulant fluid to determine the effect of the heat flux through the internal vessel, and to find its temperature, cannot be realistic. Calculations are therefore needed to estimate the heat flux and the temperature of the internal vessel. Classic fluid tests are used, on one hand, to ensure the validation of the modelling used in the calculation and, on the other, to study certain specific problems, concerning, for example, transient or three-dimensional effects.

Study of the influence of the core outlet temperature difference. In this case, [8.16, 8.38, 8.48], the thermal-hydraulic behaviour of the hot plenum can be characterized by a Richardson number (Ri), the relation between the buoyancy and inertia forces involved in the flow. This dimensionless parameter is constructed with the core outlet temperature difference (DT) between the fissile zone and the mean of the fertile and in-vessel storage zones. In the model, this condition is respected if $\hat{Ri}=1$ is imposed. For all thermal-hydraulics tests, in

order to ensure a fully turbulent flow, only a slight distortion of the Peclet number should be chosen ($\hat{P}e \gg 10$) and an acceptable distortion of Reynold's number ($\hat{Re} \approx \frac{1}{200}$).

In reference to nominal operating conditions the parameter Ri^* is defined by:

$$Ri^* = Ri \text{ state considered} / Ri \text{ nominal}$$

The different steady state operating conditions of the power plant enable a range for Ri variations to be defined. Studies show that there exists a critical Richardson number Ri_c^* , beyond which the form of the flow in the hot plenum is modified in comparison with the flow in nominal operating conditions. Figure 8.22 shows the configuration of the flow when $Ri^* < Ri_c^*$, which is not very different from the flow in isothermal conditions. On the other hand, when $Ri^* > Ri_c^*$, fig. 8.23, stratification sets up above the anti-convection device, fed by the cold outlet flow from the subassemblies stored around the periphery of the core and enhanced by the cold sources in the anti-convection device zone (heat flow through the internal vessel, leakage flow from the feet of the subassemblies). In this situation a large and fluctuating thermal gradient is experienced by the main part of the internal vessel, and consequently there is a risk of unacceptable thermal stresses.

The objectives of such studies are therefore to check that this stratification does not occur during normal operation of the reactor. In order to do so, a solution is sought whereby the subassembly outlet jets, which are the origin of the problem because they are at different temperatures, are well mixed. Accurate representation of the hydraulics of the core outlet zone between the upper end of the subassemblies and the above core structure must therefore be ensured.

This necessarily implies using experiments, which afford the only way of representing the geometry with sufficient accuracy.

A parametric study on a water mock-up of the core outlet jet formation was reported [8.16, 8.38], which shows the importance of geometric parameters:

- interior form of the subassembly tops,
- perforation of the above core structure skirt,
- presence of core surveillance system tubes (for localization of clad failure and measurement of temperatures) (fig. 8.24),
- thermocouple support grid,
- levels of core top and grid,
- distribution of core flow rate zones.

The conclusion of this study is that all these geometric and boundary condition parameters have an influence on the core outlet zone and therefore on the hot plenum zone generally. This gives rise to two ideas:

- the plenum mock-up for this type of study must be extremely representative of reactor behaviour and requires particular attention to geometry and boundary conditions,

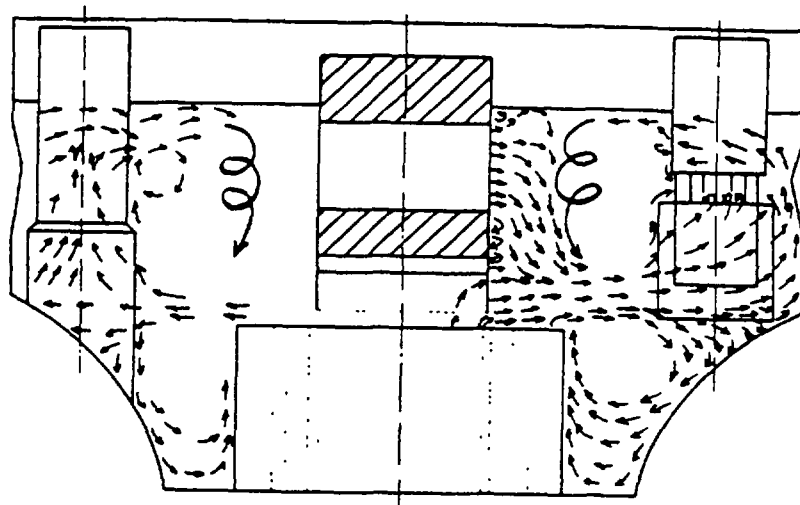


Fig. 8.22. Nominal flow in SPX2 hot plenum

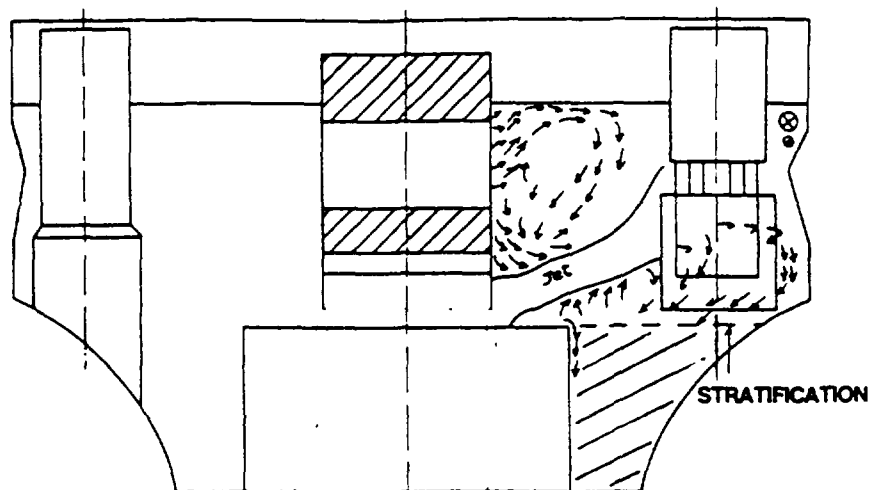


Fig. 8.23. SPX2 hot plenum flow with rising jet

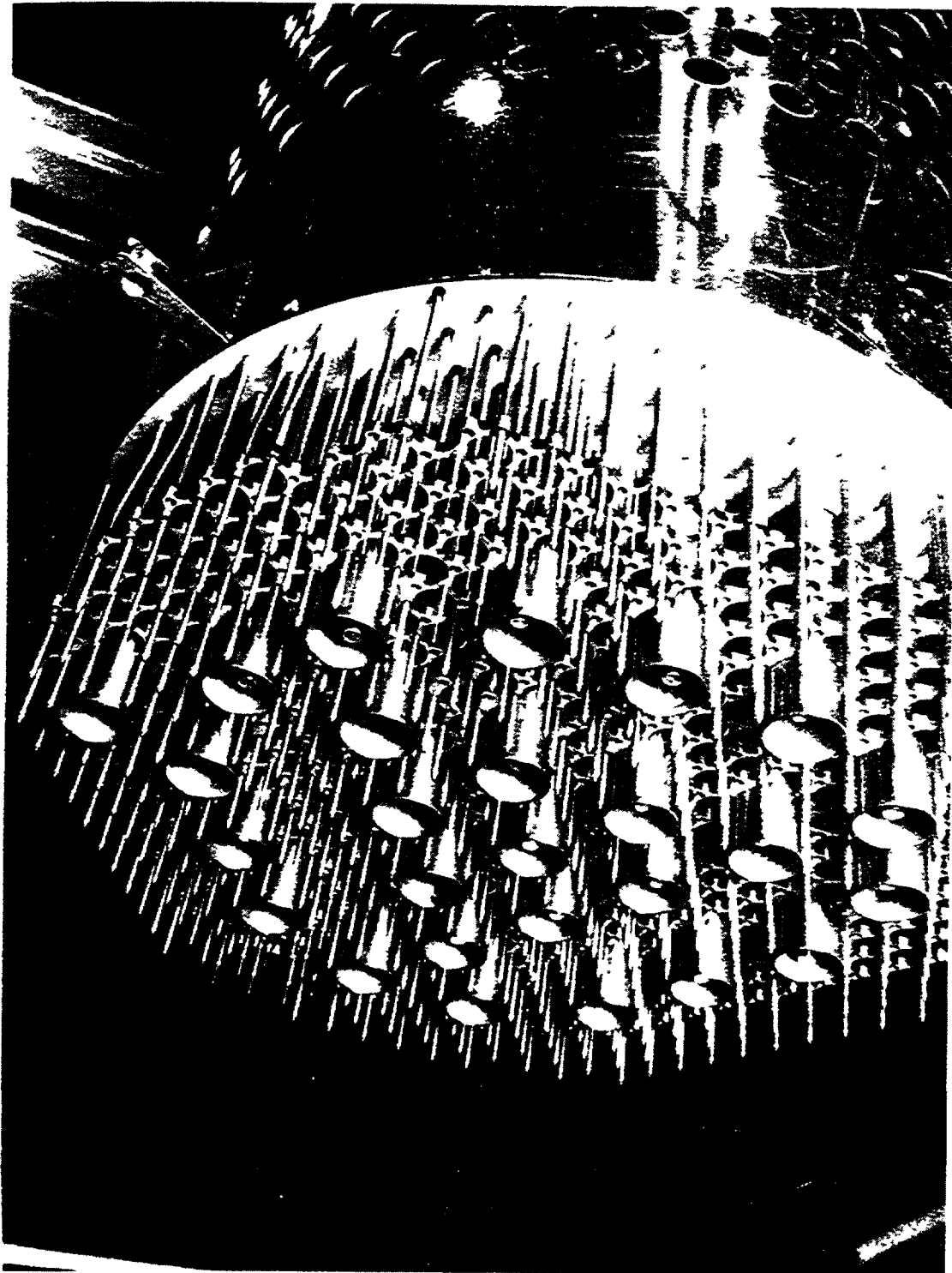


Fig. 8.24. SUPER DONALD mock-up - Above Core Structure

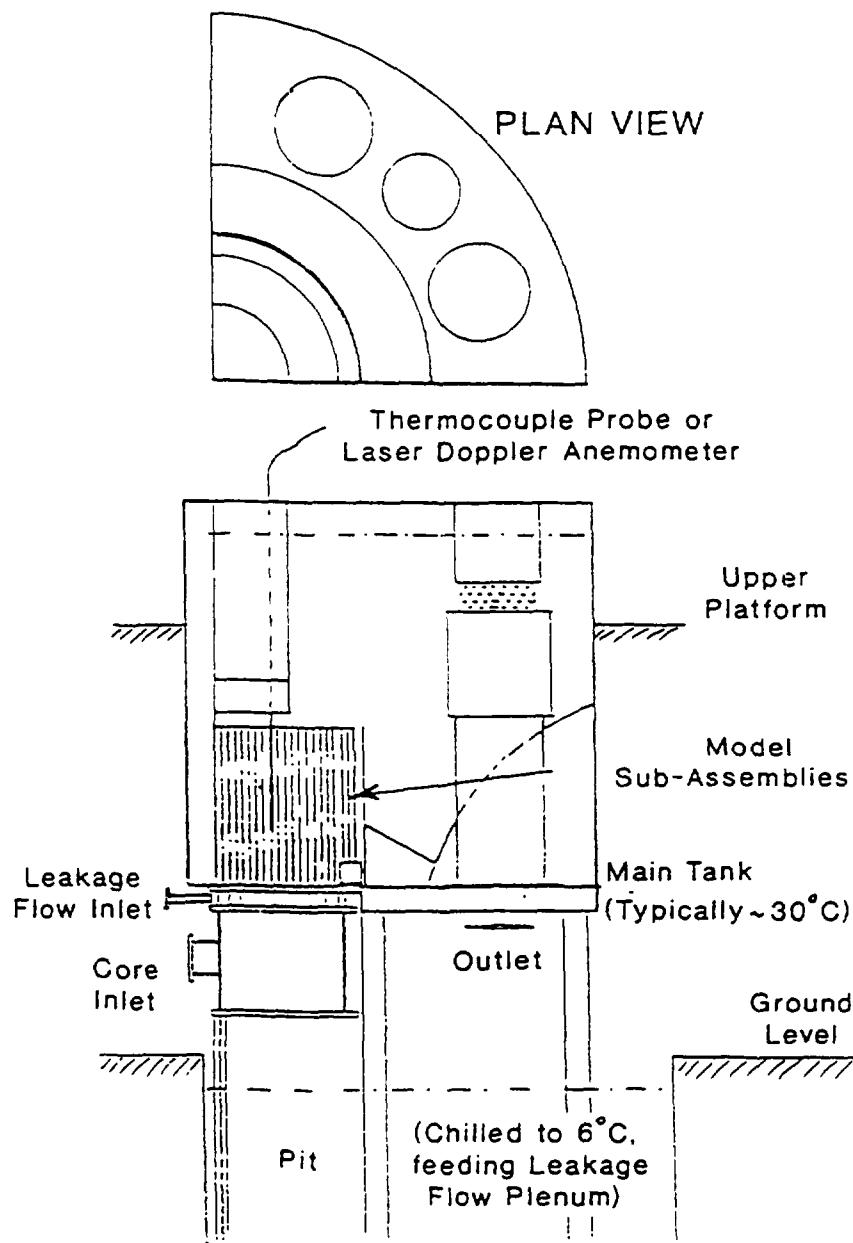


Fig. 8.25. HIPPO water model arrangement

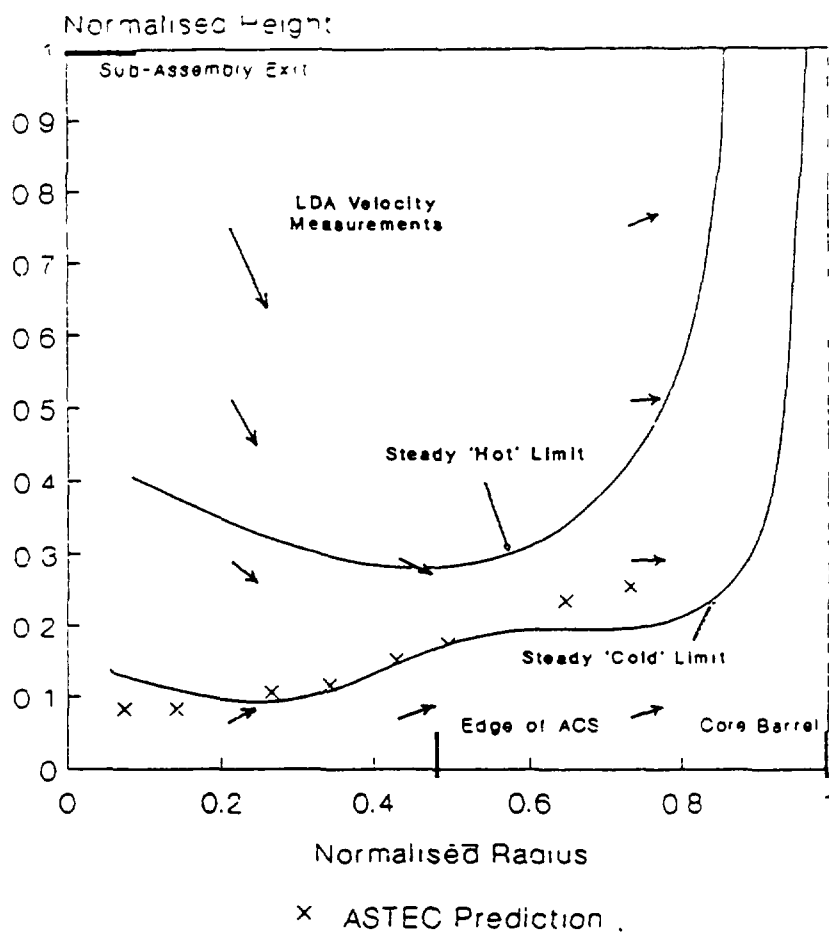


Fig. 8.26. Position at interwrapper hot-cold interface measured in HIPPO

- the sensitivity of the phenomenon or phenomena to be studied to these parameters must be known, so that even a slight change in the parameters in the reactor will not disturb the overall reactor behaviour.

Flux through the internal structures. The difference of temperature between the hot and cold plena induces a heat flux through the internal structures. The buoyancy forces produced can, in certain cases, modify the general behaviour of the plenum and must therefore be considered in this type of study. This can only be done by calculation, which is the only way of taking into account wall heat transfer correctly. The difficulty then lies in representing, flow in the plenum and in particular under the above core structure accurately in these calculations. In the present state of calculation programmes, it is not possible to represent all the geometric details listed in the paragraph above accurately; it therefore becomes necessary to modelise, that is to say to represent the realistic geometric and boundary conditions. The question is then to validate this modelling. There is no definite, systematized answer to this question today.

Nevertheless, various studies [8.33, 8.50, 8.20, 8.29, 8.39, 8.48] confirm the ability of a numerical approach to attain a minimum level of accuracy for such problems. In particular, reference 8.20 shows that the velocity profile in the hot pool is influenced by the wakes generated by the presence of the shroud tubes in the core outlet zone, and concludes that further progress in computer capability is needed to obtain predictive tools for such thermal-hydraulic problems.

Thermal-hydraulic of the inter-wrapper zone. The core of a Fast Reactor is formed from assemblies of fuel pins contained in hexagonal wrapper tubes. Gaps of a few millimetres between the adjacent faces of the triangular pitched wrapper tubes form a complex network of passages connecting with the hot pool. In many fast reactor designs, a radial pressure gradient is generated at the subassembly exit plane by interaction of the subassembly outlet flows with the Above Core Structure (ACS). The radial pressure-gradient causes a small fraction of the hot core exit flow to be forced downwards into the central inter-wrapper gaps. This flow rejoins the main hot pool flow at the core periphery after passing through the labyrinth of the inter-wrapper gaps. Additionally, cold flow, coming from leakage around the spikes of the subassemblies enters the inter-wrapper flow passages at diagrid level. The "hot" flow, initially at core outlet temperature, but with the possibility of losing heat to the subassemblies as it travels downwards, will meet the cold upward flow at a level determined by the geometry and the boundary conditions. The hot/cold interface may be unstable and turbulent, giving the potential for significant local temperature fluctuations. In [8.34], for an EFR design, a coupled experimental and numerical approach of such problem is shown. The use of the large scale model HIPPO of both velocity and temperature field allowed the computational approach to be validated (fig. 8.25, 8.26).

Thermal-hydraulics design of the clad failure detection system. This system is used to detect possible clad failures in the fuel subassemblies while the plant is operating. Clad failure causes a release of fission products emitting delayed neutrons, that are transported to the hot plenum and to the detectors. In SPX1 the detector itself is placed outside the hot plenum with a continuous popped sampling system for analysis of the primary sodium was set up; other systems in which neutron detectors are placed near the intermediate heat exchanger inlets and enabled activity to be measured directly, have been studied. In both cases thermal-hydraulics studies were necessary to measure the hydraulic transfer functions between the various core

assemblies and the detectors, thus enabling the performance of the detection system to be determined. From an overall point of view, transit time and signal attenuation, as well as sector partition performances for different measurement points had to be determined. These studies have to be carried out on a representative mock-up of the hot plenum ensuring that there is a sufficient similarity of flow patterns, which is obtained in practice by respecting the free surface Froude number (Fr), which ensures accurate representation of the flow in the mock-up. It is also advisable to represent the above core structure and in particular flow through the shroud tubes properly. For certain subassemblies in the vicinity of the control rods a large part of the flow does in fact travel through the above core structure. Not to take this bypass path into account would therefore lead to an overestimation of the ability to detect the emitted signal. The measurement of hydraulic transfer functions (transit time and attenuation) constitutes one of the difficulties in this type of problem, and requires particular attention.

Core outlet temperature measurements. Safety rules require the surveillance of the outlet temperatures of fuel and sometimes fertile assemblies. This function is ensured by thermocouples set above each subassembly and supported by the above core structure. Each thermocouple is supposed to be placed in the jet of sodium from the subassembly it monitors. Thermal-hydraulics studies are necessary in order to ensure that these measurements are properly representative, as they depend considerably on the geometry of the above core structure. They are very sensitive to geometry (support grid, control rod mechanism, shroud tubes, subassembly upper end shape, etc.) as well as to slight variations of the geometric parameters such as the distance from the top of the subassembly to the thermocouple, or the offset between subassembly and thermocouple. In view of the complexity of the geometry and the boundary conditions, tests at a large-scale with exact mock-ups, and with Reynolds similarity to allow the flow to be represented accurately, are needed. For the EFR project, the JESSICA (1/3 scale, water, fig.8.27) and FREYJA (1/6 scale, air) facilities have been used to investigate such problems [8.48]. Marking one particular subassembly by means of fluid at a different temperature enabled the quality of response of the monitoring thermocouple to be determined, taking into account the different parameters involved.

Fluctuations in the lower part of the hot pool. In a Liquid Metal Fast Reactor, the bottom part of the hot pool is a transition area between the hot and cold zones of the reactor. It is called the "corps mort" area. This region is annular and bounded laterally by the core barrel and the outer shell called which is called the redan. Its behaviour is linked to two conflicting phenomena:

- cold boundary layers, due to the heat flux across the redan shell and the core barrel, flow down and create a cold stable layer,
- the main hot plenum flow causes penetration of hot sodium into this area. This main flow is the consequence of the recirculation created by the core outlet flow.

The equilibrium between these two effects causes mixed convection and stratified flow. The stratification interface oscillates and may induce severe damage to the neighbouring structures. Furthermore, the support structures at the bottom of the hot pool have to be protected from hot sodium. The behaviour of such a region has been studied, namely for SPX1 [8.27] and EFR [8.19]. Studies were mainly conducted through scale model tests, because computations are not yet able to predict the fluctuation characteristics for such complex situations. As the main physical phenomenon of interest is the interaction between buoyancy forces (natural convection) and inertia forces (forced convection from the main pool

JESSICA

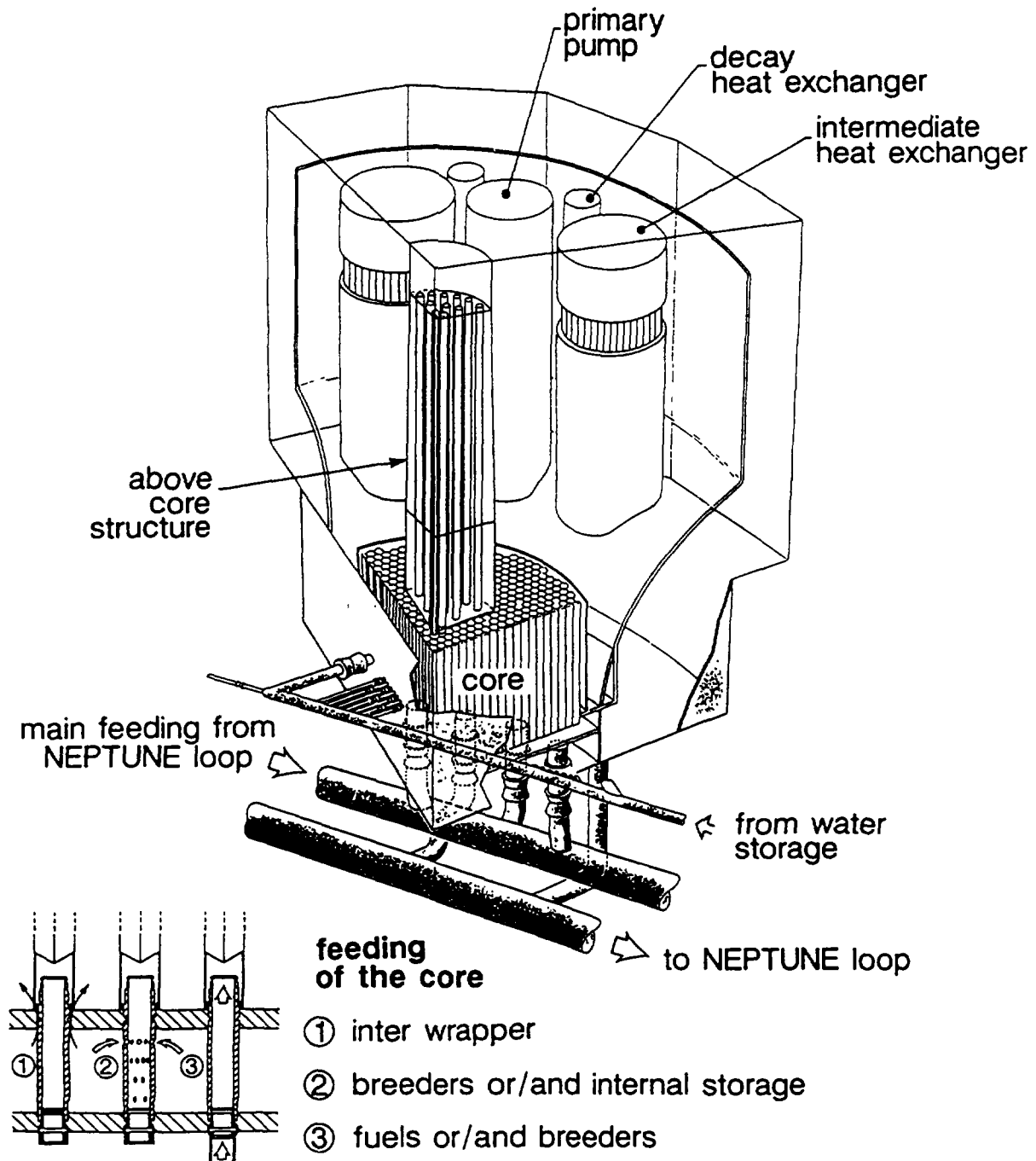


Fig. 8.27. JESSICA hot pool model

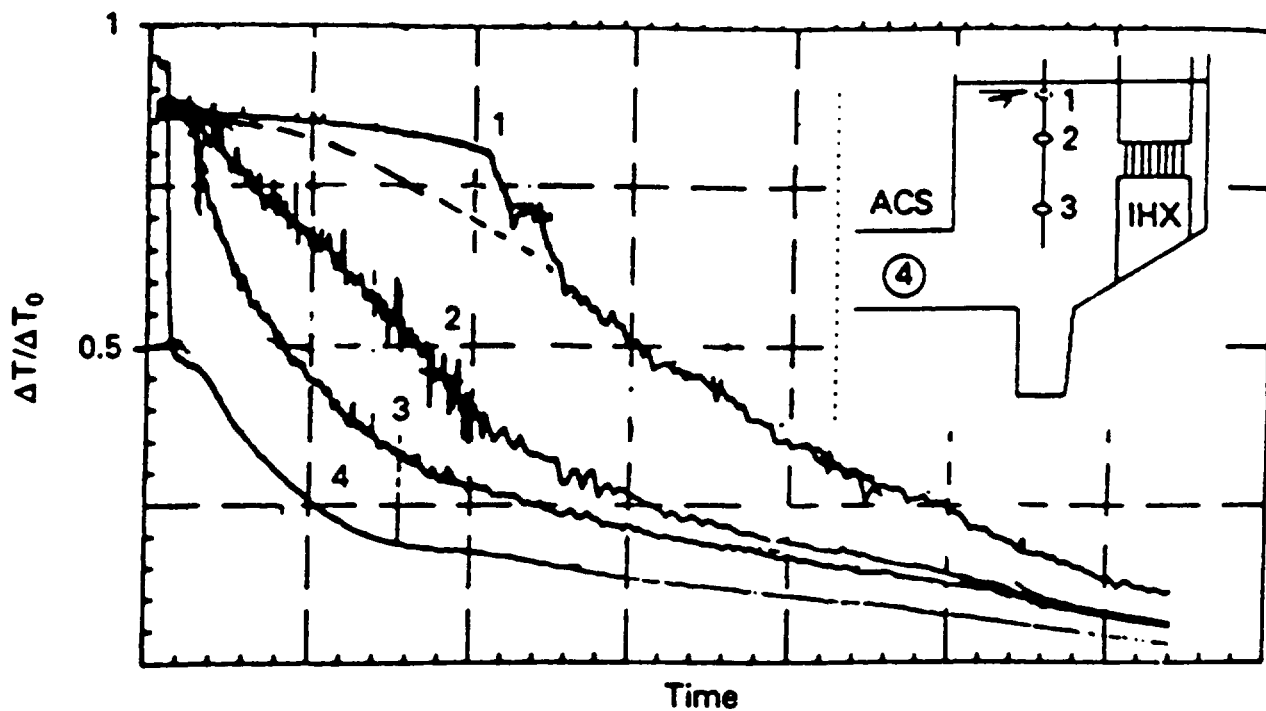


Fig. 8.28. Hot plenum stratification after a scram at 23 % nominal power in SUPER PHENIX

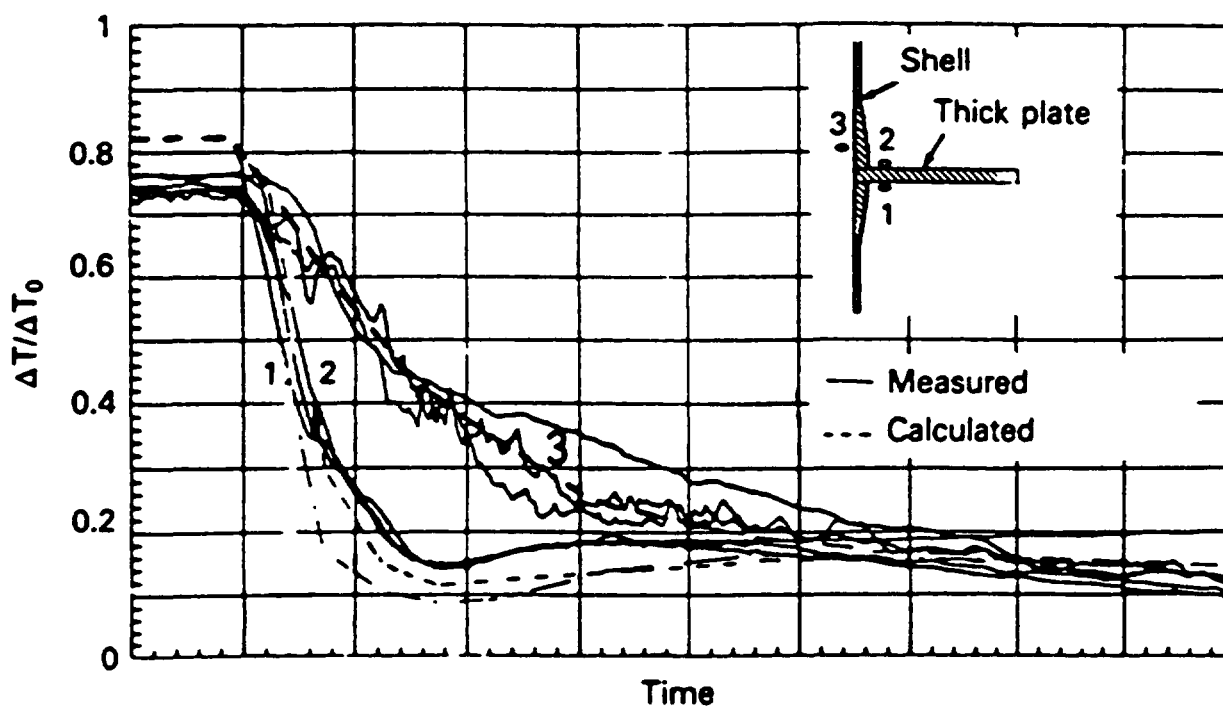


Fig. 8.29. Temperature evolution in the joint between the outer shell and the support plate of the ACS after a scram at 80 % nominal power in SUPER PHENIX

flow), Richardson similarity was used. For SUPER PHENIX, phenomena observed in mock-ups were also measured by the thermal instrumentation in the reactor [8.27]. However, the appearance of considerable fluctuations and a low gradient at the interface do not allow a definitive conclusion to be drawn, and complementary studies have still to be made. More fundamental studies [8.21,8.25] on thermal stratification show the capability of the computational approach to estimate the time average vertical temperature gradients and interface position correctly, making use of classical k-ε turbulent models. Additionally, three-dimensional large eddy simulation modelling calculations have been shown [8.21] to provide simulations of turbulent fluctuations and global instabilities. In this field, more work is necessary to assess to what extent time-averaged gradient characteristics are representative of instantaneous conditions, and to validate more precisely the prediction of the frequency and amplitude of temperature fluctuations.

8.2.4. Transient studies of hot pools

The limiting transient states are emergency shutdowns or rapid shutdowns. During these transient conditions, the sodium temperature at the core outlet falls rapidly ($DT = 130^{\circ}\text{C}$ at 20°C/s). Moreover, depending on operating choices, the primary flow rate can also vary. When these transients occur, two problems must be examined:

- the evaluation of the thermal shock on the structure (the above core structure in particular) induced by the rapid change in core outlet temperature,
- the evaluation of the flow changes generated by the influence of buoyancy forces (DT core, minimal flowrate); depending on the operating conditions these can, in fact, produce considerable flow changes in the hot plenum, and can even lead to the formation of a stratified hot layer above the inlet windows of the intermediate exchangers.

Influence of the core outlet temperature transient. The thermal-hydraulic behaviour of a plenum can be characterized by means of a Richardson number (Ri) constructed with the core outlet temperature difference DT during the transient. In the same way as for steady-state conditions, fully turbulent flow in the model must be ensured by imposing a low Reynolds distortion.

In SPX1 geometry [8.17, 8.48] comparisons (fig. 8.28) made between mock-up test measurements and reactor measurements showed that, by respecting Richardson similitude, analogous behaviour in the mock-up and the reactor, including within the above core structure, was observed.

Above core structures studies. The above core structure is another particular zone that must be carefully studied. Placed above the core, it plays an essential role in the thermal-hydraulics of the plenum, but must also be studied from the point of view of its own thermal loading, whether steady or transient. Considering the particularly complex geometry of this component (fig. 8.26), the use of tests remains essential. A large-scale mock-up, able to represent geometric detail very precisely, has to be used in this case. For SPX1 [8.17], the GODOM1 mock-up (90 deg sector, 1/5 scale) was used, and model and reactor measurements were shown to be very close (fig. 8.29).

8.2.5. Studies of the cold pool of a pool-type reactor

For the cold plenum, thermal-hydraulics studies should enable the thermal stresses in the structures (in particular the main vessel and the internal vessel) to be calculated, and the correct hydraulic supply to the primary pumps to be ensured. These studies should be carried out for the various operating states of the reactor; symmetrical and asymmetrical with a secondary circuit out of operation, and for steady state conditions as well as transients.

Hydraulic study of the cold plenum. For the cold plenum, hydraulic studies are particularly focused on the problems of supply to the primary pumps. For these to function correctly the supply should be homogeneous [8.18, 8.22]. Moreover, knowledge of the velocity field in the cold plenum is used to validate calculations. In hydraulic studies of this type, flow is similar if the Reynolds number is respected. In the reactor flows are fully turbulent, and flows obtained in scale models are accepted as being representative of reality as long as they are also fully turbulent. For practical reasons tests are carried out on scale models with Reynolds numbers $\geq 3.10^4$.

Steady-state thermal-hydraulics. In the cold plenum there are two main problems in steady-state thermal-hydraulics:

- the temperature profile (as well as the velocity profile) at the intermediate heat exchanger outlets is generally not uniform due to the behaviour of the IHX itself. The question is, therefore, to know the effect of this temperature difference in the vicinity of the structures (main vessel and internal vessel), both in terms of mean temperature and fluctuations,
- the difference of temperature between the hot plenum and the cold plenum induces a thermal flux through the internal structures that, according to the operating conditions or the design can have an influence on the cold plenum thermal-hydraulics.

In order to deal practically with these two problems it is essential to use a numerical approach [8.54, 8.22, 8.18]. In a water mock-up, neither the thermal flux through the structures, nor an exact distribution of the temperatures at the intermediate heat exchanger outlet can, in practice, be realistically represented. However, taking into account the complex geometries being considered calculations of the general hydraulics field must be validated by comparison with measurements on a representative mock-up.

Transient condition thermal-hydraulics. The transient operating conditions to be studied are characterized by:

- the variation of the temperature at the intermediate heat exchanger outlets with time (hot shock and cold shock),
- the temperature difference between the top and the bottom of the intermediate heat exchanger window which also varies, and can even be inverted,
- the variation of the primary flow, according to operating options.

As in the case of the hot plenum, two problems have therefore to be examined:

- the evaluation of the thermal shocks on the structures (main vessel or baffle, internal vessel) induced by the rapid temperature changes at the intermediate heat exchanger outlets,

- the evaluation of the flow changes brought about by the influence of buoyancy forces (DT at the intermediate heat exchanger outlets, minimal flowrate): these, in fact, can produce, depending on operating conditions, considerable changes of flow in the cold plenum, and may even lead to the formation of a hot stratified layer above the lower part of the pump supply shell at the bottom of the plenum.

In the two cases, the thermal-hydraulic behaviour of the plenum can be characterized by means of a Richardson number, constructed using the temperature difference at the exchanger outlets during the transient [8.27].

8.2.6. Strongback

The strongback is located in the bottom part of the reactor vessel, and is fed by the leakage flow from the bottom ends of the subassemblies in the diagrid, which is used to cool the primary vessel. In normal steady state operation at nominal power or part load, this region of the reactor is isothermal at low temperature. The problems that arise concern behaviour during transients (hot shocks or cold shocks), whether these are symmetrical or not. The difficulty lies in the fact that the flow supplying the core support plate is very small, which gives great importance to natural convection phenomena in the case of transient states, sometimes inducing considerable temperature differences between the inner and the outer edges of the plate. The essential problem consists in arranging the geometry so as to reduce the temperature asymmetry, which can penalize the mechanical strength of the core support plate during thermal transients, as far as possible.

Two types of information are required in this case:

- the overall behaviour of the plenum under the effect of buoyancy forces: in the case of a hot shock, the setting-up of stratification and thermal shocks; in the case of a cold shock, the mixture of the cold flow and thermosiphon effects between the various compartments, depending on the design details,
- localized behaviour: depending on the design details natural convection can possibly lead to considerable local temperature differences that must be determined.

The global thermal-hydraulic behaviour of the core support plate can be characterized by means of a Richardson number, constructed using the temperature difference DT of the leakage flow during the transient. Moreover, considering the low flow rate values involved, it is advisable to ensure that the nature of the flow is the same in the reactor as in the mock-up. In other words, that the Reynolds number characterizing the mock-up flows remains "sufficiently high". In practice, this can only be done by choosing a sufficiently large mock-up scale [8.48].

Local behaviour can be approached by means of three-dimensional numerical modelling, at the cost of much difficulty in establishing the boundary conditions [8.17].

8.2.7. Diagrid

For the diagrid, thermal-hydraulic studies are needed to predict the thermal stresses in the structures and ensure correct core cooling. These studies have to be carried out for the various operating states of the reactor, in symmetrical or asymmetrical steady-state operation

(with an intermediate circuit out of operation) as well as in transients. Moreover, it is generally considered that catastrophic failure of a pipe between a pump and the diagrid should be taken into account, as this is the severest accident for core undercooling.

Hydraulic study of the diagrid. The aim of hydraulic studies here is to ensure a proper knowledge of the velocity field and to evaluate friction losses in the diagrid for various operating conditions, including part load and incidents. The two objectives are distinct. As the flow in the diagrid is under forced convection with a high Reynolds number, the hydraulic study can be carried out in a mock-up with a "usual" Reynolds distortion ($\gg 1/50$). With regard to the evaluation of the friction losses, it must be checked that the operating range of the mock-up is above the critical Reynolds number, above which the pressure loss coefficients are independent of Reynolds number. This implies a parametric study over a sufficiently wide range. For unbalanced hydraulic conditions, in particular in the case of a pump-dia-grid pipe failure accident, where it is necessary to quantify the part of the flowrate that is passing through the break, it is advisable to represent core friction loss as well.

Thermal-hydraulic studies of the diagrid. For the diagrid, the thermal aspects must be studied for transient states corresponding to symmetrical or asymmetrical hot or cold shocks. For the latter, it has been found that there is thermal partitioning, each pump-dia-grid pipe supplying only a part of the diagrid, and the objective is to characterize the circumferential temperature variation. In the diagrid, heat transfer is dominated by turbulence, so temperature acts as a tracer to mark the flow, molecular diffusion being negligible. For a detailed thermal description the subassembly coolant supply tubes, which represent a considerable portion of the mass in the diagrid, and therefore a significant thermal inertia, must be taken into account. This justifies the use of a calculation programme.

8.2.8. Gas entrainment at the free surface

In the primary circuit of a fast reactor, gas from the blanket argon can be entrained by the sodium at various points of the free surface. Part of this argon is released rapidly, whereas some can be entrained through the pumps into the core. The most important consequences of argon entrainment involve the effects on reactivity. The passage of gas bubbles through the core can lead to a partial void inducing variations of reactivity. These can be detrimental to reactor operation and plant safety. The need to study the gas entrainment rate and its variation is therefore clear. Gas entrainment from the free surface of a plenum is a difficult problem to study and its obvious coupling with the general thermal-hydraulic behaviour of the plenum allows for little adjustment. Dimensional analysis shows that, for the phenomena concerned, each of the three dimensionless parameters: Reynolds (Re), Froude (Fr) and Weber (We), are important. For experimental study of the phenomena, numerous references exist [8.23, 8.28, 8.30, 8.30, 8.49]; the main conclusions to be drawn from these studies are the following:

- geometry is an essential element to be taken into account,
- similarity based on Froude number is necessary to avoid distortion of the flow, but only low intensity vortices are then correctly simulated,
- the Reynolds number of the model must exceed a threshold giving a representative modelling of the local flow,
- for vortices entraining gas one must, in addition, respect the Weber number. When this is not possible experiments must be done above a certain threshold which is ill-defined.

Studies have been generally conducted [8.31, 8.27] on small scale models (1/15 to 1/8) of pools, with respect to Froude similarity. Direct viewing of the free surface made during isothermal tests in SPX [8.17] confirmed the absence of vortices, as predicted on the basis of models. The EFR pool was made more compact to reduce costs, and this led to a more energetic flow being convected to the free surface, which promoted waves and vortices, created by eddy shedding from the structures and colliding surface currents. Such phenomena increase the potential for entrainment of the cover gas into the primary sodium. Fig. 8.30 [8.49] proposes a classification of free surface vortices, from an acceptable swirl to gas entrainment situations. Comparison between different models at increasing scales [8.17, 8.31, 8.32], operating with respect of Froude similarity and different Reynolds and Weber distortions, shows that reduced scale models underestimate the number and depth of the vortices: the severity of vortices increases with the scale of the model. Despite numerous studies, further work remains necessary to obtain a clear methodological approach for gas entrainment investigations. Key points seem to be the development and validation of measurement techniques for the characterization of local velocity and free surface shape to allow the relationship between those parameters and the severity of vortices to be defined. In [8.32, 8.48] it was shown that computational analysis can give a good prediction of local velocities which are useful to determine vortex occurrence.

8.2.9. Cover gas thermal-hydraulics

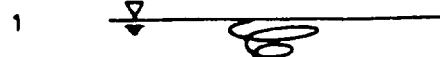
The primary circuit of a liquid metal reactor is closed above by a roof. This structure supports various components and the rotating plugs. Penetrations provide annular spaces between the roof and the components. These gaps are filled with argon which communicates with the argon cover gas above the free surface of sodium. These annular gaps may be subject to significant axial temperature differences which can induce convection. Therefore heat and mass transfer between the free surface and the roof structures must be known so as to be able to design cooling circuits correctly, to determine thermal stresses and to prevent sodium deposits [8.40, 8.56]. Sodium aerosols are formed in the cover gas space and can affect the total heat transfer through the cavity as well as the gas temperature. Mass transfer may result in sodium deposits, especially in the cooler regions, which may cause serious problems [8.36]. For SPX1 the problems were solved by means of the large mock-up GULLIVER [8.57], fig. 8.31 which represented the upper closure of the reactor. Agreement with the values predicted by Gulliver was shown to be good [8.17], for both the cover gas temperature and the axial temperature profile in the annular space. From a more fundamental point of view, it has been noted [8.37, 8.35, 8.53, 8.56] that aerosol formation depends mainly on sodium temperature, the temperature gradient between the sodium and the roof, the argon flow rate and temperature, the presence of cold spots and the characteristics of the vessel. Exact representative models [8.57, 8.41] of the thermal performance of the roof still require improvement to increase the level of confidence in design. Development of theoretical models and verification on specific experimental models remain necessary, particularly for:

- sodium aerosol mass concentration,
- particle size distribution,
- radiation in volumes filled with sodium vapor.

8.2.10. Thermal striping studies

In a liquid metal reactor primary circuit, some structures in mixing regions, such as the above core structure, the core outlet zone, the IHX outlets, and thermal stratifications zones,

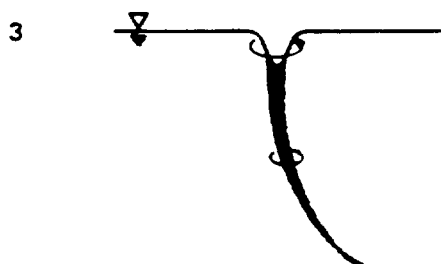
**VORTEX
TYPE**



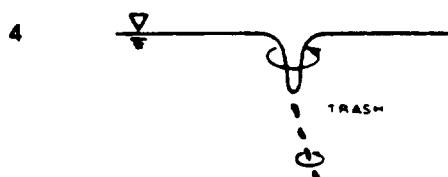
INCOHERENT SURFACE SWIRL



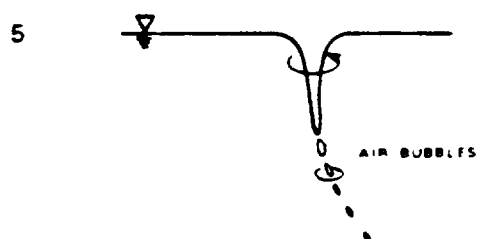
SURFACE DIMPLE,
COHERENT SWIRL AT SURFACE



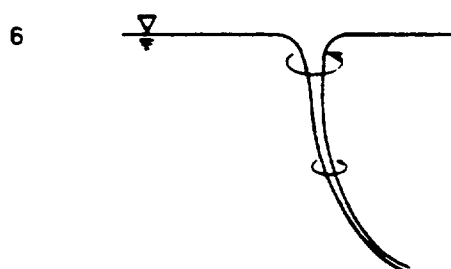
DYE CORE TO INTAKE,
COHERENT SWIRL THROUGHOUT
WATER COLUMN



VORTEX PULLING FLOATING
TRASH, BUT NOT AIR



VORTEX PULLING AIR
BUBBLES TO INTAKE



FULL AIR CORE
TO INTAKE

Fig. 8.30. Classification of free surface vortices

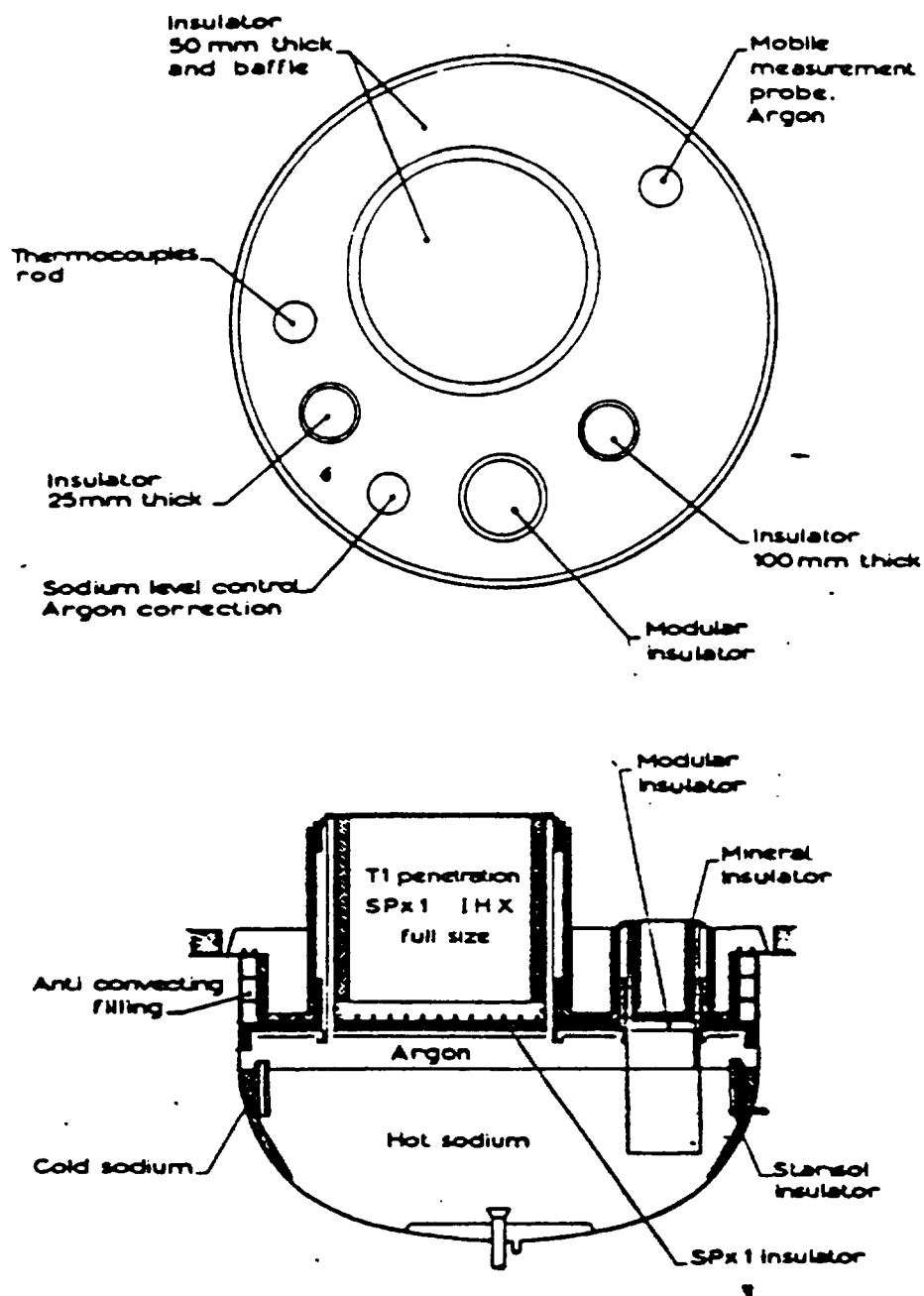


Fig. 8.31. GULLIVER mock-up

are submitted to random temperature fluctuations. These fluctuations, known as thermal striping, may, if transmitted to the surface of a structure, cause surface cracking and component failure. After a first step using global thermal-hydraulic models to identify the areas where thermal striping may occur, the characteristics of the fluctuation have generally been estimated from model tests using sodium as the working fluid [8.42, 8.44, 8.45]. Of course, this increases the cost and the time needed to perform the experiment. Additionally, in sodium experiments, technical difficulties are often encountered in obtaining an adequate amount and quality of data. As a result complementary approaches were considered. The first and the most widely used approach is to use stimulant fluid [8.24, 8.42, 8.43, 8.45].

The interpretation of simulation using a fluid with a high Prandtl number to give information on temperature fluctuations in a liquid metal is generally well known, at least in a forced convection situation. It has been shown that if the Reynolds and Peclet numbers are high enough, simulation is good. For a buoyancy-influenced flow, the Richardson number has to be taken into account, but no general rule yet exists. For thermal striping evaluations, it is necessary to know the wall temperature fluctuations, then to study the heat transfer between fluid and solid. There is no general answer to the question. In the specific geometry of parallel impinging jets, comparison tests show that there are significant differences exist between the behaviour of water and sodium. Computational approaches [8.55, 8.21] have been shown to be promising for evaluating the distributions of the intensity and frequency of temperature fluctuations in liquid metal reactor situations, by using high order accurate numerical schemes and advanced turbulence models (Large Eddy Simulation)

8.2.11. Conclusions

Knowledge of primary circuit thermal-hydraulic phenomena is necessary for the determination of structural loads. The methodology used to establish thermal stresses is generally based on close links between research on phenomena and an experimental approach using scaled models. Transposition to the reactor is made using similarity rules directly from experimental results, or using calculation codes, after validation on models or in-pile experiments.

The increased compactness of the next generation of liquid metal reactors is accompanied by greater complexity of the hydraulic and thermal problems, and a need to decrease uncertainties, particularly for gas entrainment phenomena, temperature fluctuations for thermal striping, and modelling of the core outlet area.

Nomenclature

Pr	Prandtl number, mC_p/λ ,
Pe	Peclet number, $= VL/a$
Re	Reynolds number, $= rVL/m$
Fr	Froude number, $= V/\sqrt{gD}$,
Ri	Richardson number, $= gbDTL/V^2$,
We	Weber number, $= rV^2L/s$,
s	surface tension,
m	dynamic viscosity,

V	velocity,
L	length,
C_p	specific heat,
a	thermal diffusivity,
g	acceleration due to gravity,
b	coefficient of thermal expansion,
t	time scale,
DT	temperature difference,
r	density,
X'	$X_{\text{model}}/X_{\text{reactor}}$.

8.3. DECOMMISSIONING OF THE EXPERIMENTAL LIQUID-METAL FAST REACTOR RAPSODIE

8.3.1. Introduction

The RAPSODIE experimental reactor, the first French fast neutron reactor constructed and operated by the CEA, went critical in 1967 and was definitively shut down in April 1983. RAPSODIE was designed, built and operated to obtain data on the physical behaviour of a fast neutron reactor under static and dynamic conditions, to offer information of direct use for the design of future LMRs, and to supply a fast neutron flux for irradiation tests of fuels and materials. During its 15 years of operation, more than 30,000 fuel pins of the driver core were irradiated, of which about 10,000 reached a burn-up beyond 10%, and 300 irradiation experiments and more than 1000 tests were performed. The decision to stop running the reactor was taken after two successive defects were detected in the primary system containment. The first defect, which appeared in 1978, consisted of a sodium micro-leak: radioactive sodium aerosols were found in the double wall of the reactor vessel. Investigations did not find any liquid sodium in the gap nor locate the defect. The reactor was subsequently operated at a reduced power level ($\sim 0,6 P_N$), which was high enough for irradiation needs but did not cause the leak to reappear. The second defect appeared in 1982 and consisted of a small leak from the nitrogen blanket surrounding the primary system. Before the final shut-down of the reactor a series of end-of-life tests were conducted in April 1983. These are reported in Reference 8.58. Pre-decommissioning operations were then conducted until 1986. They consisted essentially in unloading the fuel and fertile assemblies and in draining the sodium from the primary and secondary circuits. It was initially envisaged to launch an appraisal programme to evaluate the state of the primary system and components and, possibly, to find some explanations for the defects. This programme had to be abandoned in 1986 for budgetary reasons; the CEA, therefore, decided on partial dismantling which started in 1987.

8.3.2. Main features of the installation

The RAPSODIE installation consists of six main buildings (Fig. 8.32), access to three of which is restricted; these are :

- *The reactor building* or secondary containment including the reactor vessel and its upper closures, as well as the two primary loops, each equipped with a mechanical pump and an intermediate heat exchanger. All these components were enclosed in

concrete cells to provide radiation shielding (Fig.8.33). The secondary, non radioactive sodium, was piped to a conventional building containing the components of the two secondary loops including a sodium/air heat exchanger in each.

- *The active building* comprising interim storage facilities for both fresh and used fuel, and various other facilities such as the washing cell for decontaminating components polluted with primary sodium, and a dismantling hot cell used for conditioning used irradiated equipment for long term storage as waste.
- *The fuel assembly dismantling building* comprising hot cells for non-destructive examination of fuel pins, and the assembly of experimental sub-assemblies.

The reactor was initially operated at 24 MWth and then, a few years later, at 40 MW_{th} after the modifications of the FORTISSIMO project were completed. In operation, the primary sodium entered the core at 400°C and flowed out at a mean temperature of 550°C. All the circuits and components were made of austenitic stainless steel, the main pipes and vessels having a double wall. The reactor vessel is immediately surrounded by special high density concrete, containing rare earth oxides, and called Sercoter. This is protected externally

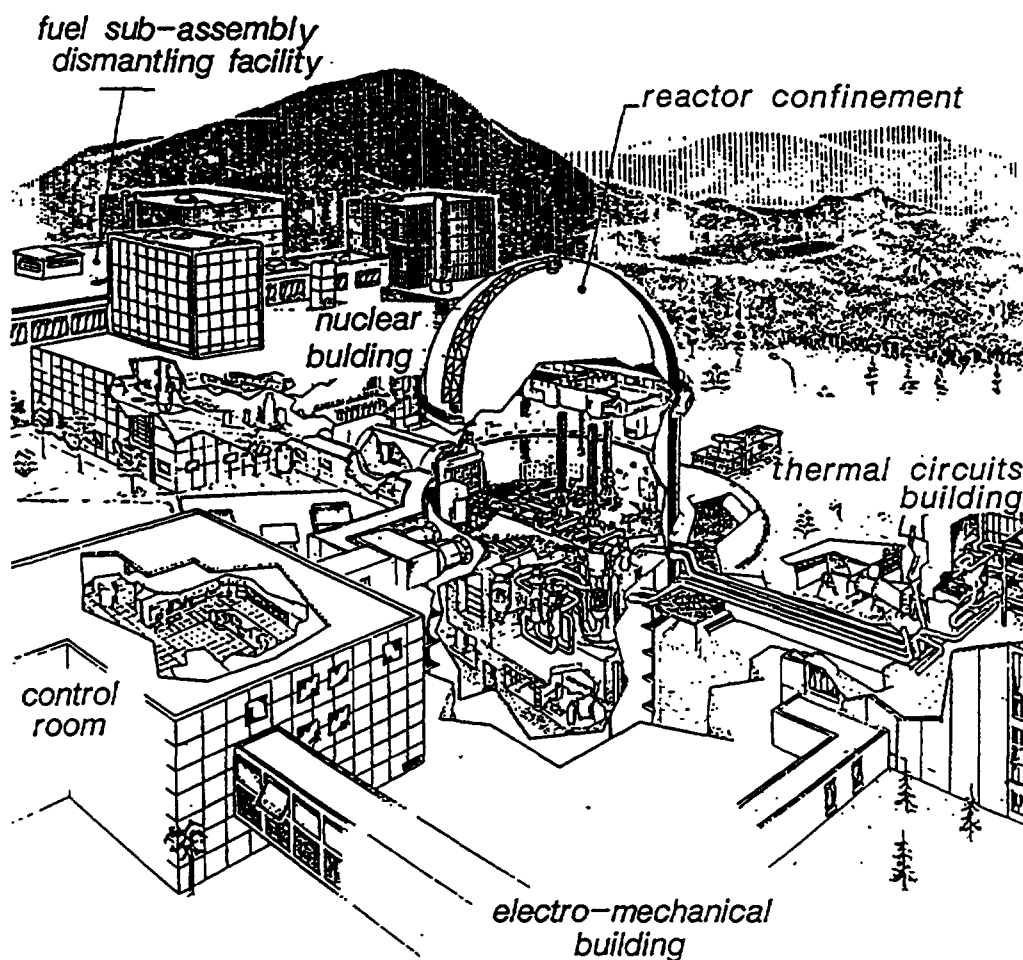


FIG. 8.32. The RAPSODIE facility.

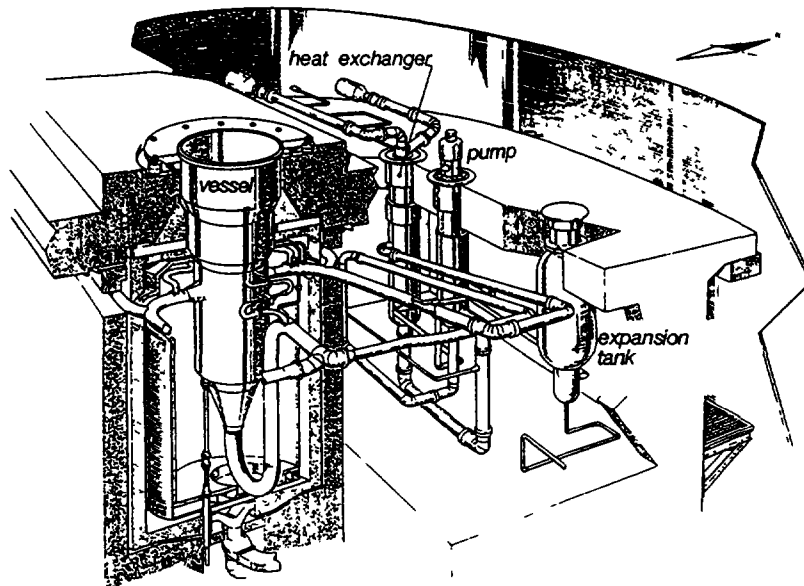


FIG.8.33 One RAPSODIE primary loop.

by a steel liner which was considered to constitute the 2nd barrier when the decision was taken for dismantling to level 2 (of the IAEA scale), leaving the reactor block in place. The following paragraphs explain in chronological order how this situation was reached.

8.3.3. Pre-decommissioning operations (1983 - 1985)

These include the preliminary actions previous to washing and rinsing the system (which might have caused corrosion damage). Initially cleaning all the circuits and components of sodium for examination and sampling purposes was contemplated. In any case, sodium removal is necessary as it reduces the chemical and radioactive risks of future work. First, all the standard and experimental fuel assemblies (120 in all) were unloaded from the reactor vessel, put into containers and stored in the cooling pond or in a dry well in the normal manner. The fertile assemblies (240) and the six control rods were also unloaded and dismantled in the hot cell normally used for the disposal of irradiated equipment.

Only the reflector assemblies (390 in total), made of stainless steel or nickel, were left in place in the reactor vessel as it was intended to wash them along with the vessel itself. At the same time, all the experimental devices were removed from the main vessel while certain components, pumps or IHXs were extracted from their vessels for decontamination. These operations, executed in accordance with current maintenance rules, were concluded with the blanking-off of all penetrations and vessels. The primary circuit was then drained of its sodium into the usual storage tank (RENa 300) situated in a cell in the lower part of the reactor building. Another storage tank, (RENa 302), located outside in a peripheral gallery and full of clean sodium for flooding the reactor in case a leak occurred, was also emptied. Finally, the primary system was tightly sealed and kept under an inert atmosphere of argon and, later, nitrogen. In addition the secondary circuits were also drained of their sodium and later isolated from the IHXs by cutting the main pipes. One of them has since been reactivated for experimental purposes.

Here, it is interesting to examine what the remaining radioactivity of the primary system was composed of. Table 8.2 below gives an inventory dated 1 January 1984. After the

removal of the fissile and fertile assemblies, the reflector assemblies and the reactor vessel were the main cause of the radioactivity with ^{60}Co as the predominant species. The Sercoter shielding concrete containing rare earth oxides was the second source, predominantly ^{152}Eu . The sodium source of ^{22}Na from activation and ^{137}Cs as the main contaminant was negligible numerically compared to the others, but active enough to necessitate preventive measures during the washing and decontamination operations, as explained below.

These values were obtained from calculations adjusted to a few measurements. For the reactor vessel, for instance, the ^{60}Co radioactivity was deduced from direct measurements in the reactor vessel and by gamma counting of a few samples extracted from the assembly support plate. These were made of stellite, a high nickel content alloy.

TABLE 8.2. RADIOACTIVITY INVENTORY OF THE RAPSODIE REACTOR BEFORE DISMANTLING AS OF 1.1.1984 (VALUES AS OF 1.1.1994 IN PARENTHESIS).

<i>Reflector assemblies</i>		
Steel	gamma (^{60}Co)	580 TBq
	beta (^{63}Ni)	11 TBq
Nickel	gamma (^{60}Co)	3800 TBq
	beta (^{63}Ni)	630 TBq
Total		5021 TBq
<i>Reactor vessel (and internals)</i>		
gamma (^{60}Co)	1160 TBq	(310 TBq)
<i>Sercoter concrete</i>		
beta-gamma (^{152}Eu)	160 TBq	(95 TBq)

8.3.4. Decommissioning operations (1986 - 1994)

The decommissioning operations involved in the partial dismantling programme which was finally adopted were designed to eliminate the radioactivity as much as possible without exposing the operators excessively (the ALARA concept applies here as everywhere), to confine the residual radioactivity and, as a result, to minimise monitoring and surveillance measures pending complete dismantling. In the RAPSODIE case, the successive operations were:

- Removal and disposal of the steel and nickel reflector assemblies as waste,
- Washing and decontamination of the primary circuit,
- Dismantling of the primary circuit, of one secondary circuit and of the auxiliary systems of the reactor,
- Completion of the primary and secondary containment of the nuclear island,
- Dismantling of the auxiliary equipment used for handling, washing and storing nuclear materials or contaminated components,

- Destruction of the primary sodium (37 tons) and cleaning of the active area.

Washing and decontamination of the primary system. After draining the primary sodium, washing and decontaminating of the circuits are essential before any further action is taken for important reasons:

- The removal of any sodium remaining in the system improves the safety of future operations, and
- The removal of a large part of the radioactive contamination of the circuit walls, due mainly to ^{137}Cs , allows the dose accumulated by the operators during dismantling work to be reduced.

At RAPSODIE or PHENIX methods for washing experimental devices such as large components using either water mist or vapour have been developed and used for years. The washing of a complex circuit comprising pipes of different diameters and capacities in which relatively large amounts of sodium may persist as oxide deposits adhering to the walls or as puddles trapped in undrainable areas, requires special attention. In the case of RAPSODIE, it was estimated that around 170 kg of sodium remained in the reactor vessel for instance. As a result, it was judged preferable to take a more straightforward way by using a "heavy" alcohol (EC: ethylcarbitol) instead of water for neutralizing the sodium. Neutralization is achieved by changing the sodium into a caustic-free alcoholate which is inert from the corrosion point of view. Of course hydrogen is produced and there is some risk of explosion, but several tests showed that it was easier to control sodium destruction in this manner [8.59]. As the alcoholate becomes viscous at high concentrations, an excess of alcohol has to be maintained at all times and the waste volume consequently increases. It is considered that one cubic meter of sodium results in 4 cubic meters of alcoholate + alcohol with the same content of radioactive contamination. Preliminary caesium decontamination of the RAPSODIE primary sodium was carried out just before, and during, its transfer from the normal dump tank to the "flooding" tank. About 2 to 4 TBq of radioactive caesium had to be removed from 37 tons of primary sodium (i.e. 100 MBq/kg maximum value). A special loop provided by Interatom comprising filters and an absorbent section containing reticulated vitreous carbon (RVC) was connected to the dump tank. This material, selected by Interatom among others, had also proved efficient during preliminary tests performed at RAPSODIE when the reactor was in operation. This was also the case this time, as measurements showed an overall purification factor in the 15-40 range [8.60]. The first washing operations took place in 1986. They began with the washing of the normal dump tank which was assumed to contain about 100 kg of sodium forming a large 3m² puddle. The process consisted in introducing small quantities of EC into the tank which was kept unheated and under an internal nitrogen atmosphere. The total destruction of the sodium took about two days without any noticeable difficulty [8.61].

A few weeks later, an attempt to wash some auxiliary circuits, including the purification system (without the cold traps which had been previously disconnected) and the filling-draining lines, by using the 2500 l of EC and alcoholate left in the dump tank failed. Plugs of solid or viscous alcoholate formed at some lower points. It was then decided to cut these circuits into pieces and to wash them by standard means. At the end of 1986, the reactor vessel evaluation programme having been dropped, there was no longer any need for its immediate washing and decontamination. The vessel was isolated from all the circuits and the main and auxiliary pipes were disconnected and blanked-off. The washing of the primary system was performed during the second quarter of 1988. It was done in several steps by

making up a series of loops, each including a portion of the system. EC was circulated in the pipes and sprayed into the cavities simultaneously. After that, rinsing with demineralized water and then flooding of the whole system completed the process. In all 4,200 l of alcohol and 11 m³ of water were used for the various rinsing procedures. In all the washing operations involved the destruction of 125 kg of sodium with a content of 0.4 TBq of ¹³⁷Cs, most of it removed from the system walls. This caesium was partially trapped on the ion exchanging resins during the subsequent regeneration of the alcohol. As a result, the dose rates in the concrete cells were generally reduced by a factor of 10, and even 100 locally. It was then decided to decontaminate the primary system, on the grounds that it would reduce the cost of dismantling by decreasing its duration, because it would be possible to use high-speed cutting devices such as a plasma torch. Briefly, this consisted of two operations, washing with caustic soda and decontamination using a sulfo-nitric mixture, each followed by rinsing with demineralized water, with a passivation solution being utilised at the end [8.62]. Again, to limit the volume of liquid effluent, the vessels and circuits were treated either by flooding and recirculation (the lower sections in particular) or by spraying (the upper sections of the vessels). In all, 46 m³ of effluent were generated and around 100 MBq of radioactivity (¹³⁷Cs mainly) were removed. The average erosion thickness of the internal decontaminated area (164 m²) was 12 m. The residual activity, measured first from samples taken just after the decontamination and then throughout dismantling was essentially due to ⁶⁰Co resulting from steel activation by thermal neutrons. Again the dose rates in the cells decreased significantly. Overall the values after decontamination compared to those before washing decreased by a factor of 50 to 200 for the hottest spots.

Dismantling of the primary and auxiliary systems. Partial dismantling involves the removal of all the equipment around the nuclear block which has to be kept under safe conditions for a certain cooling time. As ⁶⁰Co is mainly responsible for the residual radioactivity, a relatively short cooling time of 25 - 30 years allows a reduction factor of 30 to 60. Again it is expected that this would be sufficient to decrease costs in the future by using simple techniques and high speed tools during the last dismantling phase. One can also note that the nuclear block is not necessarily the only radioactive source remaining on the site. Some other sources resulting from the dismantling work, even wastes, can be stored on site pending further treatment if they are properly conditioned to avoid any dissemination into the environment. The plasma torch was used extensively except in some high-risk areas where the cutting was performed using saws or chain-saws. This was the case in particular with auxiliary systems such as the purification circuit or the filling-draining system which could not have been washed as described above. Naturally, usual protective measures were taken at all times. Vinyl tents were installed to isolate the working areas from the environment and small teams of 3-4 people worked on the same spot. More than 500 pieces were taken from the primary circuit, while the main components were dismantled under a special tent installed in the active building with its own ventilation system and its own filters. In all 650 m of plate and pipes from 3 to 12 mm thick, were cut with 51 man-days of effort. This represents a production rate of 12.75 m per man-day. A strict waste management organization had to be set up: at each dismantling station the steel pieces were separated and divided into washed and unwashed categories, the latter being treated in the decontamination area of the active building before being considered as waste and treated accordingly. In all, the primary circuit produced 13.5 tons of low activity stainless steel. In addition large quantities of non-contaminated materials were obtained from dismantling one secondary circuit out of two, the entire nitrogen system, and conventional equipment such as instrumentation, electric supply systems, control systems, etc.

Isolation and containment of the reactor block. The residual sodium remaining in the reactor vessel had a negligible radioactivity but steel corrosion might have been possible in the case of formation of caustic with the humidity of the air. It was therefore decided to maintain a nitrogen atmosphere in the vessel with a positive over pressure (10 - 250 mb). After separation from the primary and auxiliary circuits, the openings were closed with welded plates and an additional upper head cap was sealed onto the vessel. The first barrier was thus completed. The outer enclosure of the Sercoter concrete, the steel liner, with a series of steel housings covering the holes on the six sides of the reactor block, constitutes the second barrier. Its internal volume is linked to the building ventilation exhaust through high efficiency filters. Figure 8.34 shows the reactor block with its two leak-tight barriers and Figure 8.35 gives a diagram of the gas equipment.

At the beginning of 1994, the amount of radioactivity enclosed in the reactor block was estimated at around 400 TBq (310 TBq of ^{60}Co and 95 TBq of ^{152}Eu).

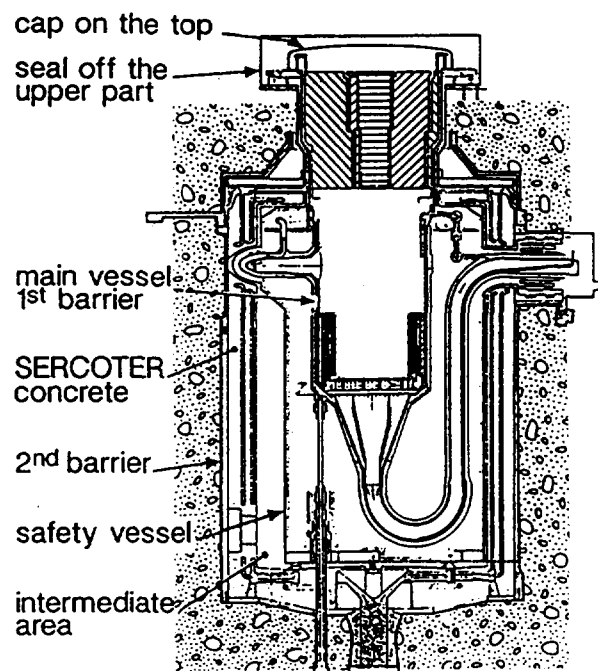


FIG 8.34. Reactor block with the leak-tight barriers.

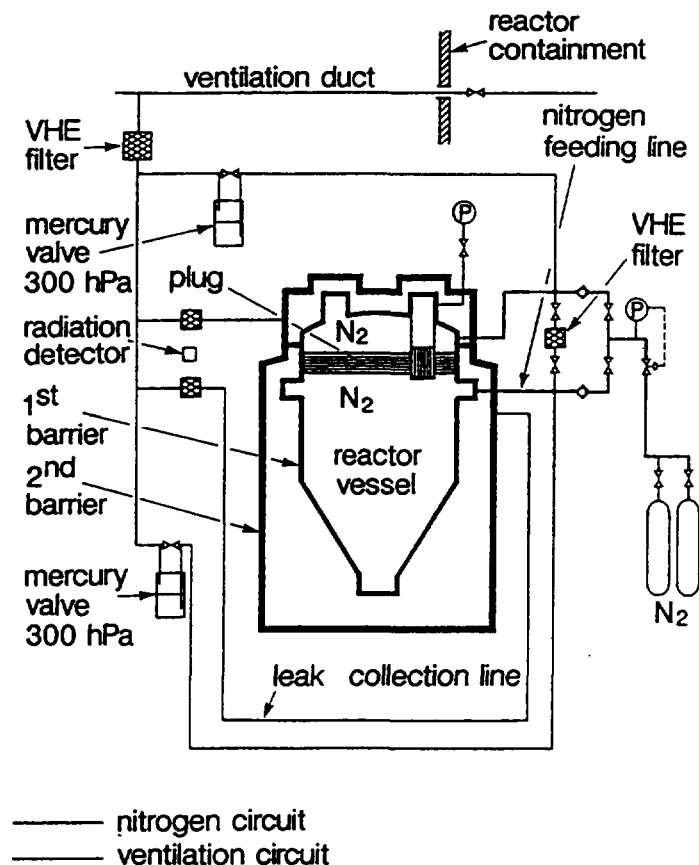


FIG.8.35. Gas equipment of the two vessel's barriers.

Waste production and disposal-primary sodium destruction. The amounts of waste produced from 1987 to 1993 by category are shown in Table 8.3 below.

TABLE 8.3. WASTE AND DOSE RATE BALANCE

<i>Solid waste volumes</i>		
Low activity	drums (100 l)	77 m ³
	cases (50 or 100 m ³)	170 m ³
Medium activity	waste-bins (50 l)	1 m ³
High activity	containers (45 l)	5 m ³
<i>Liquid waste volume</i>		240 m ³
<i>Integrated personal dose rate</i>		300 - 320 mSv
<i>Recovered materials</i>		
Steel		308 t
Lead		98 t
Copper		33 t

Low activity waste consisting of technological residues such as vinyl sheets, gloves, boots, cotton, etc ... or thermal insulating materials was incinerated or compacted before being

transferred to an ANDRA¹ storage centre. Low activity metallic waste, which represents the largest volume, was sent to a ground-level storage centre initially, and later was melted into ingots in a special furnace installed at Marcoule in the framework of the G2-G3 dismantling project [8.63].

Medium and high activity waste is stored at the Cadarache Center. High activity waste consists mainly of parts from the nickel and steel reflector assemblies or from control-rod mechanisms and irradiation devices. These account for the major part of the total radioactivity (4800 TBq) which has been removed from the reactor. The liquid effluent produced by washing and decontaminating operations was transferred to the Liquid Waste Treatment Facility at Cadarache where it has been neutralized, concentrated by evaporation and encapsulated in bitumen or cement. Furthermore, on completion of the partial dismantling work, about 300 tons of material (steel and lead in particular) will be returned to service. Much of this will be turned into biological radiation shielding.

In 1989, it was decided to remove the 37 tons of primary sodium by direct transformation into aqueous caustic soda, using the NOAH process. A specific facility named DESORA was designed and constructed in 1992 [8.64]; a diagram of this facility is given in Figure 8.36. It shows the sodium to be neutralized being stored near the reactor building in the former "flooding tank" (RENa 302), the destruction facility comprising the reaction vessel (01BA) where a thin sodium stream driven by a dosing pump reacts with a water jet. An intermediate sodium storage tank linked to the larger one and the liquid effluent collecting tank (RENa 300) situated inside the reactor containment can also be seen. The hydrogen gas produced is rejected into the ventilation exhaust duct of the building. Destruction operations lasted for 2-3 months at the beginning of 1994. They produced 160 m³ of aqueous caustic soda which were sent to a COGEMA plant and used for pH correction of chemical effluent. Soon afterwards it was decided to wash the sodium storage tank RENa 302 (located in a peripheral gallery beside the reactor building - see figure 8.36) using EC as was done 8 years earlier with the previous storage tank RENa 300. The amount of sodium left in the tank had been estimated, at that time, at ~ 100 kg. Several days after the beginning of this operation a violent explosion occurred causing casualties and heavy damage to the gallery. Only slight radioactive contamination was detected on the scene of the accident resulting from the caesium content of the vessel. Investigation of the circumstances and possible causes of this accident have not yet been completed.

8.3.5. Conclusions

The *partial dismantling* of RAPSODIE which began in 1987 is almost completed. It was the first experience of this type for a fast, sodium-cooled, experimental reactor. The reactor block including the main vessel, its internal structures and upper closures, and a layer of shielding concrete are contained within a two-barrier system. The remaining radioactivity enclosed in the system is estimated to be of the order of 400 TBq in 1994, mainly due to ⁶⁰Co. The dismantling should be completed after 25-30 years' cooling time. This option minimizes the risks due to normal radioactivity and no difficulty arose from this point of view. Of course this is an incomplete picture of the Rapsodie dismantling. The most interesting and delicate works will consist in the washing and cutting of the reactor tank (underwater cutting

¹ANDRA is the French company for storing radioactive wastes. Two ground level centers have been put into operation: La Hague and now the Centre de l'Aube.

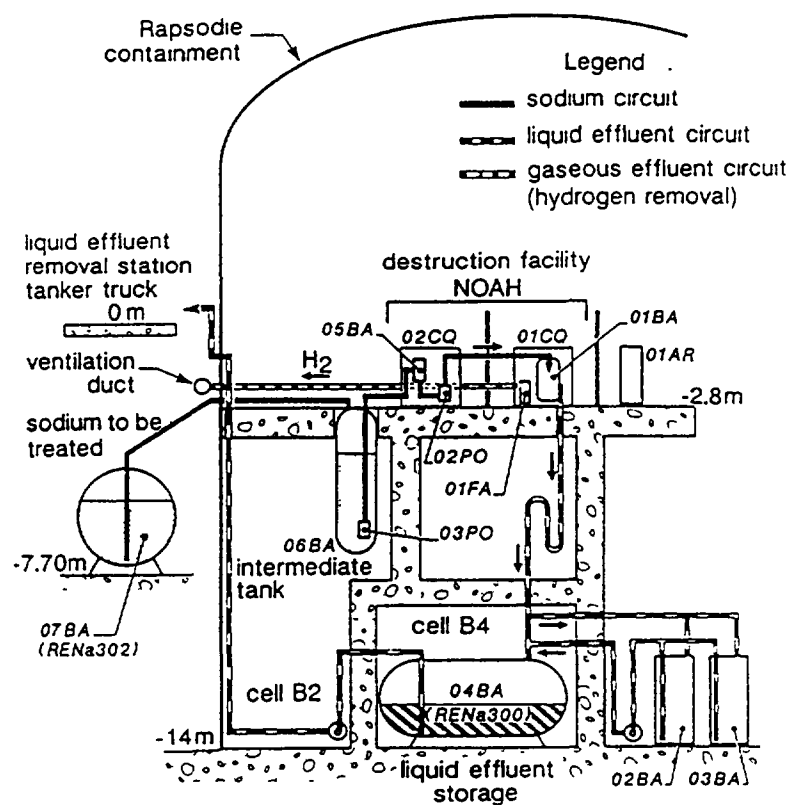


FIG 8.36 The DESORA facility for the destruction of the primary sodium

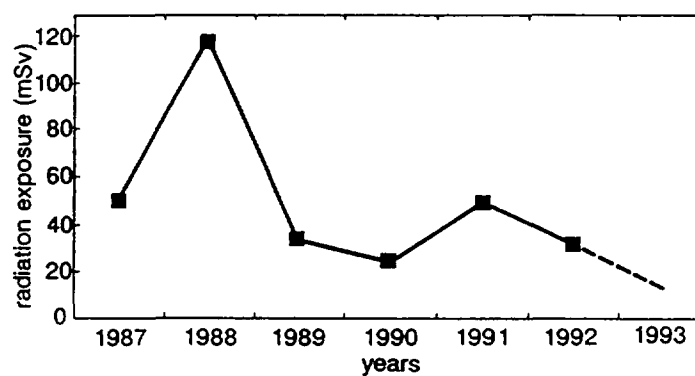


FIG. 8.37. Total radiations exposure during the Rapsodie dismantling.

possibly) with around 170 kg of primary sodium left inside, and in the treatment of the two primary cold traps each containing 400 l of sodium, sodium oxides and other impurities. At this time it is possible to give only partial figures for the overall costs of the dismantling from the point of view of both expense and radiation exposure. Dismantling costs over the last twelve years, from 1983 to 1994, were estimated at 144 MF (1989 money values) with a breakdown according to the OECD categories as follows:

- Preliminary operations	5%
- Management and studies	14%
- Equipment	11%
- Dismantling operations	25%
- Wastes	11%
- Operational expenses	32%
- R & D and others	3%

The overall radiation exposure of the workforce is shown in Figure 8.37. A total of 300 - 320 mSv was reached from 1987 to 1993 with a peak at 117 mSv during the year 1988 due essentially to the operation separating the reactor vessel from the primary system before the latter had been washed and decontaminated.

REFERENCES

- [8.1] Mitenkov, F.M., et al. Main Circulating Pumps for Nuclear Power Plants. Moscow, Atomenergoizdat, 1984.
- [8.2] Mitenkov, F.M., et al. Main Circulating Pumps for Nuclear Power Plants. 2nd ed. M., Atomenergoizdat, 1990.
- [8.3] Budov, V.M., et al. Development of BN-350 and BOR-60 Pumps. Report to Scientific-Technical Conference of CMEA countries "Nuclear Power, Fuel Cycle, Radiation Material Science". Obninsk, Russia, October 25-28, 1970.
- [8.4] Mitenkov, F.M., et al. Report to Seminar of CMEA Countries on Fast Reactors. Dimitrovgrad, NIAR, October 25-28, 1972.
- [8.5] Novinsky, E.G., et. al. Experience of Pump Development for Fast Reactor Power Plants. Moscow, ZNII Atominform, 1/2 ed., 1973.
- [8.6] Kostin, V.I., et.al. Pumps for BN-350 and BOR-60 Power Stations. Int. Conf. on Pumps for Nuclear Power Plants. Great Britain, Bath, Institution of Mechanical Engineers, Apr. 22-25. 1974.
- [8.7] Mitenkov, F.M., et al. Erfahrungen aus der Entwicklung der Pumpen für energetische Anlagen mit den Reaktoren BN-350 und BOR-60. Kernenergie, 1975, Bd. 18, no. 4, pp. 105-114.
- [8.8] Koshkin, Y.N., et al. Development and Testing of Sodium Pumps for BN-350 and BOR-60 Reactors. in: "Status and Prospectives of Works for Development of Fast Reactors, Obninsk, Russia, FEI, 1975, vol. 1, pp. 573-607.
- [8.9] Budov, V.M., et al. Sodium Pumps for BOR-60, BN-350, BN-600 Reactors. Nuclex-75, Basel, Switzerland, 1975.
- [8.10] Belov, S.A., et al. Design and Experimental Development of Sodium Pumps. Liquid Metal Engineering and Technology. Proc. 3rd Int. Conf., Oxford, Apr. 9-13, 1984, vol. 3, London, UK, 1985.
- [8.11] Leypunsky, A.I., et.al., Reactor Sodium Technology and Equipment. of BN-600 Atomnaya Energia, 1967, vol. 22, pp. 13-19.
- [8.12] Afrikantov, I.A., et al. BN-350 Sodium Circulation Pump. Symposium of CMEA countries 'Status and Prospectives of Works for Creation of Fast Reactor Power Plants. Obninsk, Russia, 1968, vol. 1, pp. 287-311.
- [8.13] Kostin, V.I., et.al. Main Circulating Pumps for Primary Circuit of Prospective Nuclear Plants with Sodium Coolant. Teploenergetika, No. 3, 1978.
- [8.14] Babin, V.A., et al. Prevention of Cavitation Erosion in Sodium Pump Flow Path. Report to IAEA Specialists Meeting on Cavitation, FRG, October, 1985.
- [8.15] Crette, J.P., Frealon, H., From Superphenix 1 to Superphenix 2. Nucl Energy, 1986, 25, no. 2, Apr., pp. 85-92.
- [8.16] Tenchine, D., et.al. Sodium Thermal-hydraulics in the Pool LMFBR Primary Vessel, Nuclear Engineering and Design 124 (1990).
- [8.17] Astegiano, J.-C., Assessment of Thermal-hydraulic Characteristics of Primary Circuit, Nuclear Science and Engineering 106 (1990).
- [8.18] Simonneau, J.P., Stratified, J.P., Flow in a Liquid Metal Gas Reactor Induced by a Gas Dam Insulation, Proceedings of the Sixth International Topical Meeting on Nuclear Reactor Thermal Hydraulics - Grenoble, France, 1993.
- [8.19] Fluctuation in the Bottom Stratified Area of a Liquid Metal Reactor Hot Pool. Ibid
- [8.20] Menant, et. al. Detailed Numerical Studies of the Thermal-hydraulics in the Hot Plenum of a Liquid Metal Fast Breeder Reactor. Ibid.

- [8.21] Surle, F., et. al. Comparison Between Sodium Stratification Tests on the CORMORAN Model and TRIO-VF Compuation. Ibid.
- [8.22] Marin, F., Thermal-hydraulic Transients in the Cold Collector of an EFR-type Reactor. Ibid.
- [8.23] Hagiwara, T., et. al. A Prediction of Bubble Entrainment by Submerging Flow Beneath a Free Surface, Proceedings of the International Conference on Fast Reactor and Related Fuel Cycles, Kyoto, Japan, 1991.
- [8.24] Moriya, S., et. al. Prediction of Thermal Striping in Reactor, Proceedings of the International Conference on Fast Reactor and Related Fuel Cycles, Kyoto, Japan, 1991.
- [8.25] Iritani, Y., et. al. Development of Advanced Numerical Simulation of Thermal Stratification by Highly-Accurate Numerical Method and Experiments, Proceedings of the International Conference on Fast Reactor and Related Fuel Cycles, Kyoto, Japan, 1991.
- [8.26] Nakagawa, H., et. al. Design Studies and R & D Activities for DBFR Evaluation, Proceedings of the International Conference on Fast Reactor and Related Fuel Cycles, Kyoto, Japan, 1991.
- [8.27] Ninomiya, S., et. al. Thermal-hydraulic Study Aiming Compact Reactor Assembly, Proceedings of the International Conference on Fast Reactor and Related Fuel Cycles, Kyoto, Japan, 1991.
- [8.28] Ueda, H., et. al. Experimental Investigation on Free Surface Movement on Pool-type FBR's, Proceedings of the International Conference on Fast Reactor and Related Fuel Cycles, Kyoto, Japan, 1991.
- [8.29] Velusami, K., et. al. Thermal-hydraulic Work in Support to PFBR, Proceedings of the International Conference on Fast Reactor and Related Fuel Cycles, Kyoto, Japan, 1991.
- [8.30] Guidez, J., Cognet, G., Simulation by Water-test of the Argon - Entrainment in the Sodium of a Breeder, Presented at 2nd International Symposium on gas transfer at water surface-Minneapolis, USA, 1990.
- [8.31] Eguchi, Y., Tanaka, N., Experimental Study on Scale Effect on gas Entrainment at Free Surface, Proceedings of the Fifth International Topical Meeting on Reactor thermal-hydraulics - Salt Lake City, USA, 1992.
- [8.32] Funada, T., et. al. Gas Entrainment in the IHX Vessel of Top-entry Loop-type LMFBR, Proceedings of the Fifth International Topical Meeting on Reactor thermal-hydraulics - Salt Lake City, USA, 1992.
- [8.33] Brown, G.A., Three-dimensional Computer Simulation of Flow in a Complex Fast Reactor Geometry, Proceedings of the Fifth International Topical Meeting on Reactor thermal-hydraulics - Salt Lake City, USA, 1992.
- [8.34] Betts, C., et. al. European Studies on Fast Reactor Core Inter-wrapper Flows, Proceedings of the International Conference on Fast Reactor and Released Fuel Cycles, Kyoto, Japan, 1991.
- [8.35] Schutz, W., Minges, J., Experiments on Heat Transfer and Sodium Aerosols in the Cover gas for Future Breeder Reactors, Proceedings of the Fourth International Conference on Liquid Metal Engineering and Technology - Avignon, France, 1988.
- [8.36] Klemme, B., et. al. The Importance of Sodium Aerosols to Fast Reactors Operation, Proceedings of the Fourth International Conference on Liquid Metal Engineering and Technology - Avignon, France, 1988.
- [8.37] Julien-Dolias, M., Sodium Aerosols Development in an Argon Cooler Gas M. JULIEN-DOLIAS, Proceedings of the Fourth International Conference on Liquid Metal Engineering and Technology - Avignon, France, 1988.

- [8.38] Roubin, P., et. al. Thermal-hydraulic Study of LMFBR Hot Pool with Internal Storage. An Experimental and Computational Approach, Proceedings of the Fourth International Conference on Liquid Metal Engineering and Technology - Avignon, France, 1988.
- [8.39] Velusamy, K., et. al. Thermal-hydraulic Analysis in the Design of PFBR Inner Vessel, Proceedings of the Fourth International Conference on Liquid Metal Engineering and Technology - Avignon, France, 1988.
- [8.40] Gajapathy, R., et. al. Thermal Design of Top Shield for PFBR, Proceedings of the Fourth International Conference on Liquid Metal Engineering and Technology - Avignon, France, 1988.
- [8.41] Roux, S., Elie, D., Comparison Between Measurement and Computational Analysis on Open Azimutal Thermosiphons in Annular Spaces of the LILLIPUT Model, Proceedings of the Fourth International Conference on Liquid Metal Engineering and Technology - Avignon, France, 1988.
- [8.42] Canyon, J.C., et. al. Comparison of Thermal Fluctuation Measurements Made on Two Loops of Similar Geometry in Water and Sodium CRABE, Proceedings of the Fourth International Conference on Liquid Metal Engineering and Technology - Avignon, France, 1988.
- [8.43] Betts, C., et. al. Air as an Analogue Fluid for Liquid Sodium in Thermal Striping Investigations, Proceedings of the Fourth International Conference on Liquid Metal Engineering and Technology - Avignon, France, 1988.
- [8.44] Sheriff, N., et. al. Thermal Striping Heat Transfer Measurements in Sodium AKB Experiments, Proceedings of the Fourth International Conference on Liquid Metal Engineering and Technology - Avignon, France, 1988.
- [8.45] Moriya, S., et. al. Thermal Striping in Coaxial Jets of Sodium, Water and Air, Proceedings of the Fourth International Conference on Liquid Metal Engineering and Technology - Avignon, France, 1988.
- [8.46] Judd, A.M., Sheriff, N., The Outstanding Problems of LMFBR Thermal-hydraulics, Proceedings of the Fourth International Conference on Liquid Metal Engineering and Technology - Avignon, France, 1988.
- [8.47] Grand, D., et. al. Three-dimensional Computation of Thermal-hydraulic Phenomena in Reactor Vessels, Proceedings of the International Topical Meeting Advances in Mathematics, Computations, and Reactor Physics - Pittsburgh, USA, 1991.
- [8.48] Astegiano, J.C., et. al. EFR Primary System Thermal-hydraulics - Status on R & D and Design Studies, Proceedings of the international Conference on Fast Reactor and Related Fuel Cycles, Kyoto, Japan, 1981.
- [8.49] Durgin, W.W., Hecker, G.E., The Modelling of Vortices and Intakes Structure, Proceedings of the ASCE/ASME/International Association for Hydraulic Research Joint Symposium on Design and Operation of Flux Machinery - Colorado State University - Fort Collins, USA, 1978.
- [8.50] François, G., Azakian, G., SUPER PHENIX Reactor Block Thermal-hydraulic behaviour - Comparison Between Calculations and Experimental Results, SMIRT - 1986.
- [8.51] Burns, J., et. al. Numerical Prediction of the Flow in a Sector of a Fast Reactor Hot Pool, Proceedings. Fourth International Topical Meeting on Nuclear Reactor Thermal-Hydraulics - Karlsruhe, Germany, 1989.
- [8.52] Smith, Williams, Experimental Studies of Similarity Criteria for Gas Entrainment Phenomena Using Water Models of a Fast Reactor Hot Plenum, Proceedings. Fourth International Topical Meeting on Nuclear Reactor Thermal-hydraulics - Karlsruhe, Germany, 1989.

- [8.53] Minges, Schutz, Experiment on Heat Transfer and Sodium Aerosols in a Cover Gas for Future Breeder Reactors, Proceedings. Fourth International Topical Meeting on Nuclear Reactor Thermal-hydraulics - Karlsruhe, Germany, 1989.
- [8.54] Villand, et. al. Thermal-hydraulic Computation of the Cold Plenum of the Liquid-Metal Fast Breeder Reactor, Proceedings. Fourth International Topical Meeting on Nuclear Reactor Thermal-hydraulics - Karlsruhe, Germany, 1989.
- [8.55] Muramatsu, T., Intensity and Frequency Evaluation of Sodium Temperature Fluctuation Related to Thermal Striping Phenomena Based on Numerical Methods, Proceeding of the 5th International Symposium on Refined Flow Modelling and Turbulence Measurements - Paris, France, 1993.
- [8.56] Specialist Meeting Heat and Mass Transfer in the Reactor Cover Gas IAEA - IWGFR - HARWELL - 1985.
- [8.57] Lemerrier, G., Experimental Studies on Fast Reactor Upper Closings, Second International Conference on Liquid Metal Technology in Energy Production Richland, USA, 1980.
- [8.58] Status of Liquid-Metal Cooled Fast-breeder Reactors, Technical Report series No: 246 - IAEA 1985.
- [8.59] Caramelle, M., et. al. Techniques de Nettoyages de Matériels Souillés de Sodium, Fourth International Conference on Liquid Metal Engineering and Technology. LIMET 88 - p. 302/1.
- [8.60] Hanebeck, N., et. al. Development of Caesium Traps for Commercial Sodium-Cooled Fast Breeder Reactors, Fourth International Conference on Liquid Metal Engineering and Technology, LIMET 88 - p. 631/1.
- [8.61] Olliver, J., et. al. Expériences de Nettoyage à L'éthylcarbitol de Réservoirs et de Circuits en Sodium, Fourth International Conference on Liquid Metal Engineering and Technology, LIMET 88 - p. 303/1.
- [8.62] Costes, J.R., et. al. Decontamination Before Dismantling a Fast Breeder Reactor Primary Cooling System, Proceedings of the 1989 Int. Conf. on the "Decommissioning of Nuclear Installations", p. 544.
- [8.63] Lafaille, C., Les projets de Démantèlement de l'UDIN, Proceedings of the 1992 Int. Conf. on the "Dismantling of Nuclear Facilities" - p. 276.
- [8.64] Latge, C., Roger, J., Contaminated Sodium Disposal - NOAH Process, N. de Seroux, Safewaste 93 "Safe Management and Disposal of Nuclear Waste". Vol. 3 - p. 146.
- [8.65] Antoine, P., Stage 2 Dismantling of the RAPSODIE Reactor, Conference at the Institute of Mechanical Engineering (UK) 1992, Paper C 436/054.
- [8.66] Roger, J., Stage 2 Dismantling of Reactor. Case of the Experimental FBR RAPSODIE, International Conference of Knoxville (USA) - 1994.

Chapter 9

ACTIVITIES IN PROGRESS ON LMFR PLANTS

9.1. EUROPEAN FAST REACTOR

9.1.1. Introduction

Utilization of breeding to secure the long term fuel supply for electricity generation with nuclear power has always been the main aim of fast reactor development, and this remains the ultimate goal. However, due to the lower growth rate of electricity consumption and the improved fuel utilization in modern nuclear power plants, the commercial introduction of fast reactors could be postponed. In the medium term, say during the first decades of the next century, it is intended to take benefit from their flexibility in fuel utilization to achieve an optimum balance between production and consumption of fissile materials including plutonium. Also under investigation is the use of fast reactors to control the minor actinide content of nuclear waste. It is well known that a fast neutron flux is one of the best means available for destroying certain high level radioactive waste. This could be realised by recycling the waste extracted from the spent fuel from thermal reactors in fast reactors. Thus, there is an immediate interest in developing a fast reactor fuel cycle from the perspective of facilitating the management of the back end fuel cycle of the current thermal reactors. In the long term, the unique breeding capability of fast reactors will be essential to secure energy supplies against the depletion of uranium resources.

It is against this evolving background that the European Fast Reactor (EFR) project was launched in 1988. It has now reached an important milestone with the completion of the Concept Validation phase. The twin goals set by the customer utilities at the outset for the design have been demonstrated to be achievable:

- economic performance, with the generating cost of a commercial series of EFR being competitive with its contemporary PWRs; and
- licensable in all participating countries, with a requirement for safety level which meets the ambitious targets for future nuclear plants.

The R&D support has been extensive and has provided comprehensive validation of the design features necessary to meet these goals.

9.1.2. Organizational structure of the European fast reactor cooperation

In 1984 the governments of France, Germany and the United Kingdom, together with Italy and Belgium, signed a Memorandum Of Understanding for the cooperation in the fast reactor field. Subsidiary agreements focused on pooling the resources and minimising duplication of efforts while expanding the technical knowledge base. Then a number of utilities formed the European Fast Reactor Utilities Group (EFRUG), which put forward in 1988 an outline technical specification for the European Fast Reactor (EFR). The membership of EFRUG initially comprised EDF (France), ENEL (Italy), Nuclear Electric (UK), Bayernwerk, Preussen Elektra and RWE (Germany). Later on, in 1993, BNFL (UK) and UNESA (Spain) joined EFRUG. The design and construction companies specialising in fast reactor engineering, Framatome/Novatome (France), NNC (UK) and Siemens-KWU (Germany), combined as "EFR Associates" to cooperate in design, construction and marketing.

SENER (Spain) joined as an associated partner in 1993. Finally, to ensure the necessary support in research and development for EFR the R&D organizations AEA Technology (UK), CEA (France), KfK and Siemens-KWU (Germany) agreed to pool their efforts in 1989. A clear sharing of responsibilities has been established between these entities as follows:

- the utilities decide on general policy matters; specify technical, safety and economical requirements; supervise Nuclear Island design work and monitor R&D substantiation, and carry out design studies of conventional Balance of Plant (BOP),
- the industry propose the nuclear island design to the utilities and assess the technical feasibility of its design features, compliance with safety requirements and the economic prospects of the concepts proposed, and
- the R&D organizations perform theoretical and experimental studies to establish fundamental knowledge in sodium cooled fast reactor technology and validate the design features and design tools, e.g., computer programmes, utilised by industry.

Each of the above groupings has established management teams for the coordination of the daily project work. For EFRUG, the "Secretariat" deals with executive functions, assisted by a "Project Management Group (PMG)" for technical matters; the Secretariat reports to the 'EFRUG Board' for general policy matters. On the design side, the 'Project Management Team' (PMT), which coordinates the work made within each partner company, corresponds to the EFRUG Secretariat and the PMG. The PMT reports to a "Supervisory Board". On the R&D side, the "Management Group for Research and Development (MGRD)", staffed with Liaison Agents and a Technical Secretariat, with the support of Working Groups of experts (AGTs), collects the R&D requests from the design companies, transmit them to the national R&D organizations and monitors progress. The MGRD reports to an 'R&D Steering Committee' and is in close contact with the PMT. All design and R&D works are executed in the various national centres ranging from Dounreay in the north of Scotland, via Risley in England, Bensberg and Karlsruhe in Germany, to Lyons and Cadarache in the south of France. The PMT staff is located in Lyon and the MGRD staff is shared between Karlsruhe and Cadarache.

9.1.3. EFR programme status

Following the Conceptual Design phase (March 1988 - March 1990), the Concept Validation phase (April 1990 - March 1993, Figure 9.1) has achieved its intended objectives of a technically and economically well-established Nuclear Island design and a preliminary non-site specific safety analysis report, accompanied by initial probabilistic risk assessment studies. In this three year period, the system engineering for EFR was completed and the R&D results were integrated into the design. Detailed studies concentrated on the analysis of crucial features in the Consistent Design, on comprehensive assessments of the safety approach and the economic prospects. In advance of any formal involvement of the national regulators, EFRUG decided to seek the advice from a representative panel of assessors composed of senior safety experts from various national organizations.

The economic assessment was a joint activity between EFRUG and EFR Associates. The assessment involved a number of qualified nuclear equipment manufacturers in Europe who provided quotations for the main components of EFR. Also, the major companies for fuel fabrication and reprocessing provided fuel service cost information enabling an assessment of the EFR fuel cycle costs to be carried out. The technical and economic achievements of the Concept Validation phase satisfy the objectives set by EFRUG. However, the preconstruction

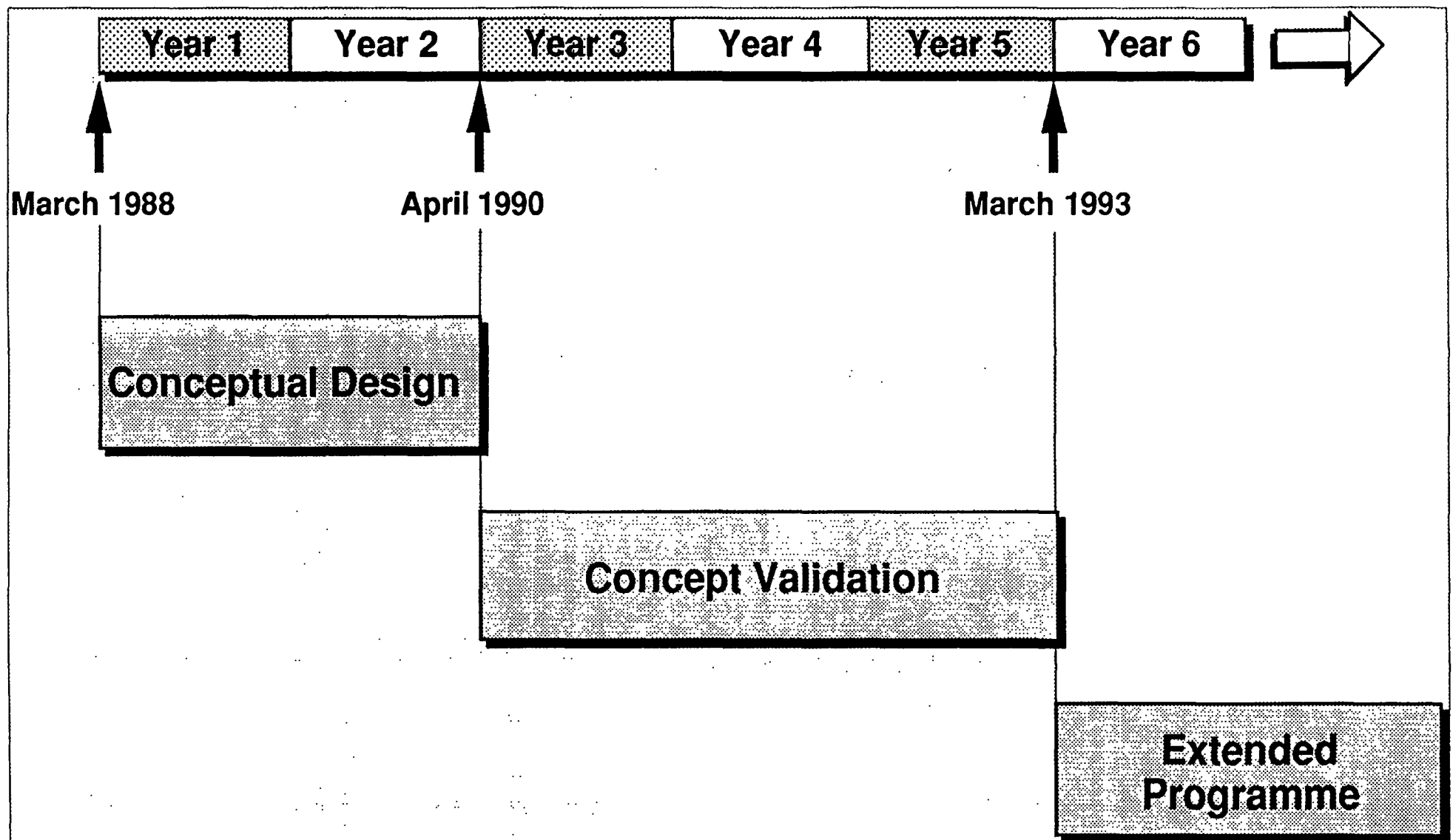


FIG. 9.1. EFR Programme

studies which were planned to follow have been postponed in the light of the following considerations:

- the uranium market does not give rise to any pressing need for commercial deployment of breeder reactors, and
- conversely, there is now an interest in assessing the potential for fast reactors to manage the plutonium stockpile.

Consequently, the period following on from the Concept Validation will be devoted to further investigation of design alternatives which bring technical, economic or safety benefit. The objective is also to establish the range of flexibility of fast reactors to respond to the prevailing needs of the fuel cycle in the medium term. In particular their potential to manage the plutonium stockpile arising from the thermal reactors and to transmute minor actinides in order to reduce the quantities of high level waste is to be assessed, whilst retaining the capability of breeding for the longer term when fissile material resources are no longer abundant. In this extended programme, the following main tasks will be performed:

- to establish the flexibility of the fast reactor for the new missions,
- to evaluate the potential for further technical and economic improvements which were identified at the end of the Concept Validation phase, and
- to assess the optimum size of a prototype from the point of view of demonstrating a large EFR plant and as an irradiation facility for the next century.

A large proportion of this forward programme will concentrate on "Generic studies", i.e., a number of topics which have the potential to improve the product and provide key information to face evolving requirements regarding the missions and performance of a future prototype. These studies address the areas of core physics, safety behaviour in case of severe accidents, in-service inspection and repairability, improvement in prevention and mitigation of sodium hazards, continued development of design and construction rules specific to fast reactors, and feedback of operating experience from existing reactors. Also development of the Consistent Design will be continued by integration of results from the generic studies so that there will be available an up-to-date yardstick for comparison with other design proposals with regard to technical performance and economics.

9.1.4. Main design features

The objective was to produce a design which would both ensure a high plant availability and meet the lifetime target of 40 years. This necessitated special attention to components and structures where failure would lead to prolonged outage for repair (of which the permanent reactor structures, the heat exchangers and the steam generators are particularly important), and the development of efficient in-service inspection and repair methods. The approach to meeting this objective was to use, as far as possible consistent with the other requirements, technology which was already verified or which could be expected to be fully endorsed by R&D. Consideration was also given to optimization of parameters to ensure high component endurance coupled with continued study to develop well founded and validated design rules.

Layout of plant and buildings

The general site plan (Fig. 9.2) is, as an example, based on a river site with a cooling tower. The centre of the Nuclear Island (NI) is formed by the cylindrical Reactor Building (RB) with three adjacent Steam Generator Buildings (SGB) (Figs. 9.3, 9.4). In addition the NI incorporates the

Switchgear Buildings which house the essential and non-essential electrics and the main control room, and the Auxiliary Building housing the fuel and component handling equipment, decontamination facilities and stores for new and spent fuel.

The Reactor Building (RB) is designed to accommodate the reactor and its associated protection and cooling systems based on a six-circuit sodium cooling system for heat transfer to the steam generators. Other major features for sizing the RB are the provision for flasking of reactor components via a polar crane and a transfer corridor, fuel handling by an A-frame and a handling cell, an electrical system with three safety divisions and two conventional sections, and provision for protection against aircraft crash. A cylindrical building has been adopted, concentric with the reactor vessel. The reactor building (RB) is constructed of unlined reinforced concrete and forms the secondary containment boundary. It is designed to prevent the release of radioactivity, to withstand the pressure resulting from a sodium fire and to provide radiological shielding. The RB together with the adjacent Steam Generator Buildings, Switchgear Buildings and Auxiliary Building are all on a common raft with bearing pads for effective isolation of horizontal earthquake-induced loads. The reactor vault is additionally separated from the raft by springs to reduce the vertical seismic loads. This design also allows adjustment of the reactor in case of abnormal horizontal or vertical displacements.

The three *Steam Generator Buildings (SGBs)* are arranged on the perimeter of the RB. The location of the SGBs is dictated by the component arrangement on the reactor roof. Each SGB is separated into two Steam Generator Compartments (SGCs). Each SGC comprises one secondary loop, one direct reactor cooling loop and parts of one feedwater/steam piping system, with their auxiliaries/ancillaries. All components of these systems are located outside the RB; the Sodium/Air Heat Exchangers (AHX) are located beside the upper part of each SGB. In each SGC the water/steam areas and the sodium area are strongly separated by concrete walls. The Steam Generator Unit (SGU) itself is vertically located in the sodium plant cell. The outer shell of the SGU is connected to the live steam and feedwater chamber by short steel cylinders to make the connection to the Main Steam System while respecting the separation of the two areas.

Sodium fire protection for the pipework within the RB is achieved by leak jackets connecting the heads of each IHX and DHX with their respective piping chambers. Sodium leak drainage from all floors of the SGB and from the RB piping chambers is routed towards leak collecting pans on the foundation raft in the SGB. Provisions are made for quick removal and replacement of the Steam Generator Unit (SGU) and the Secondary Pump. Access to the two SGCs of one SGB is by a common staircase including lifts.

The Switchgear Buildings are the buildings located in parts of the annulus around the RB, between the Steam Generator Buildings No 1 and 2 and Steam Generator Buildings Nos 3 and 1. They house the electric and control and instrumentation equipment for the essential and non-essential loads. Additionally, the Heating, Ventilation and Air Conditioning systems are arranged inside these buildings. On the roof of each Switchgear Building (as well as the

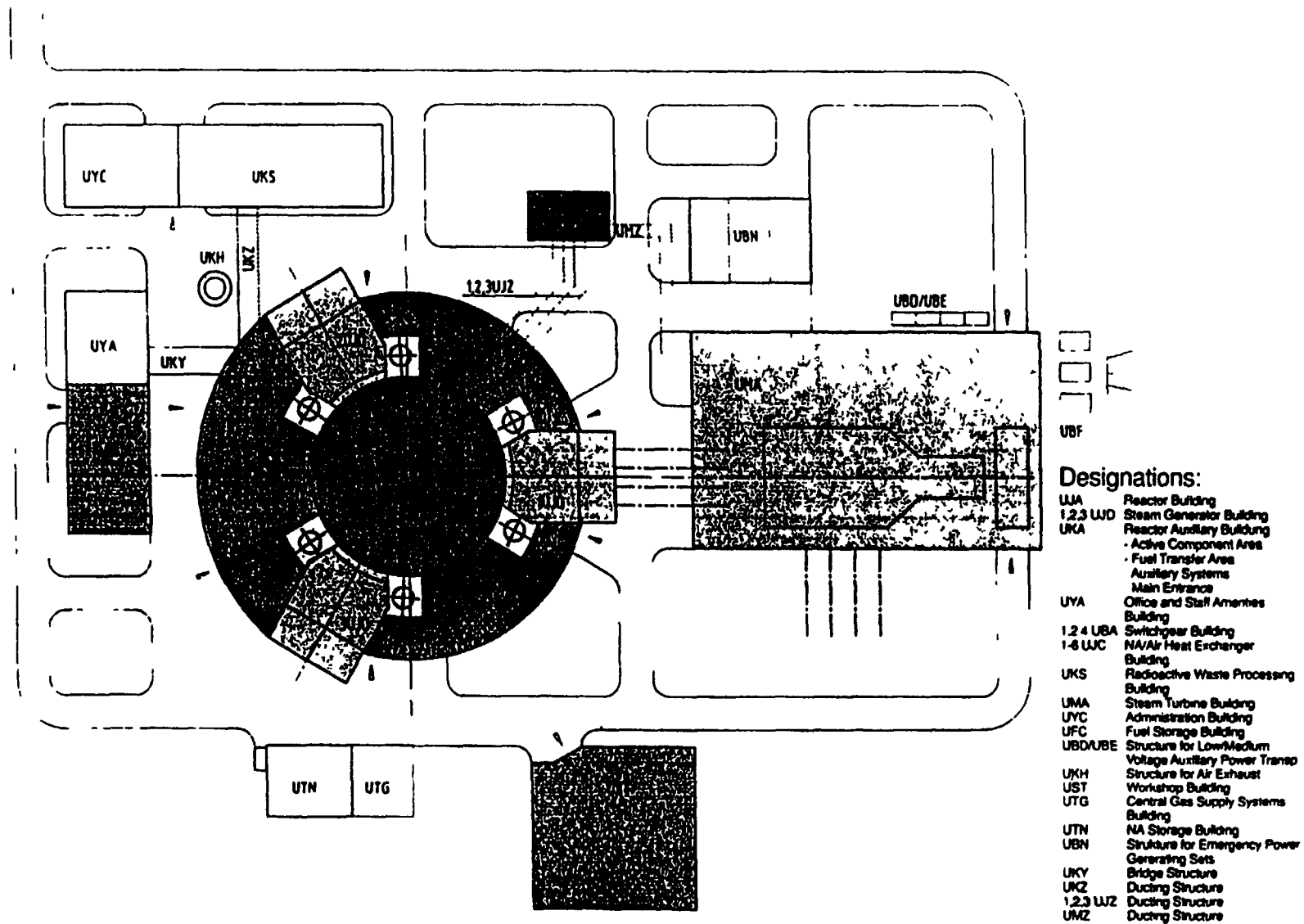


FIG 9 2 EFR Station plot plan

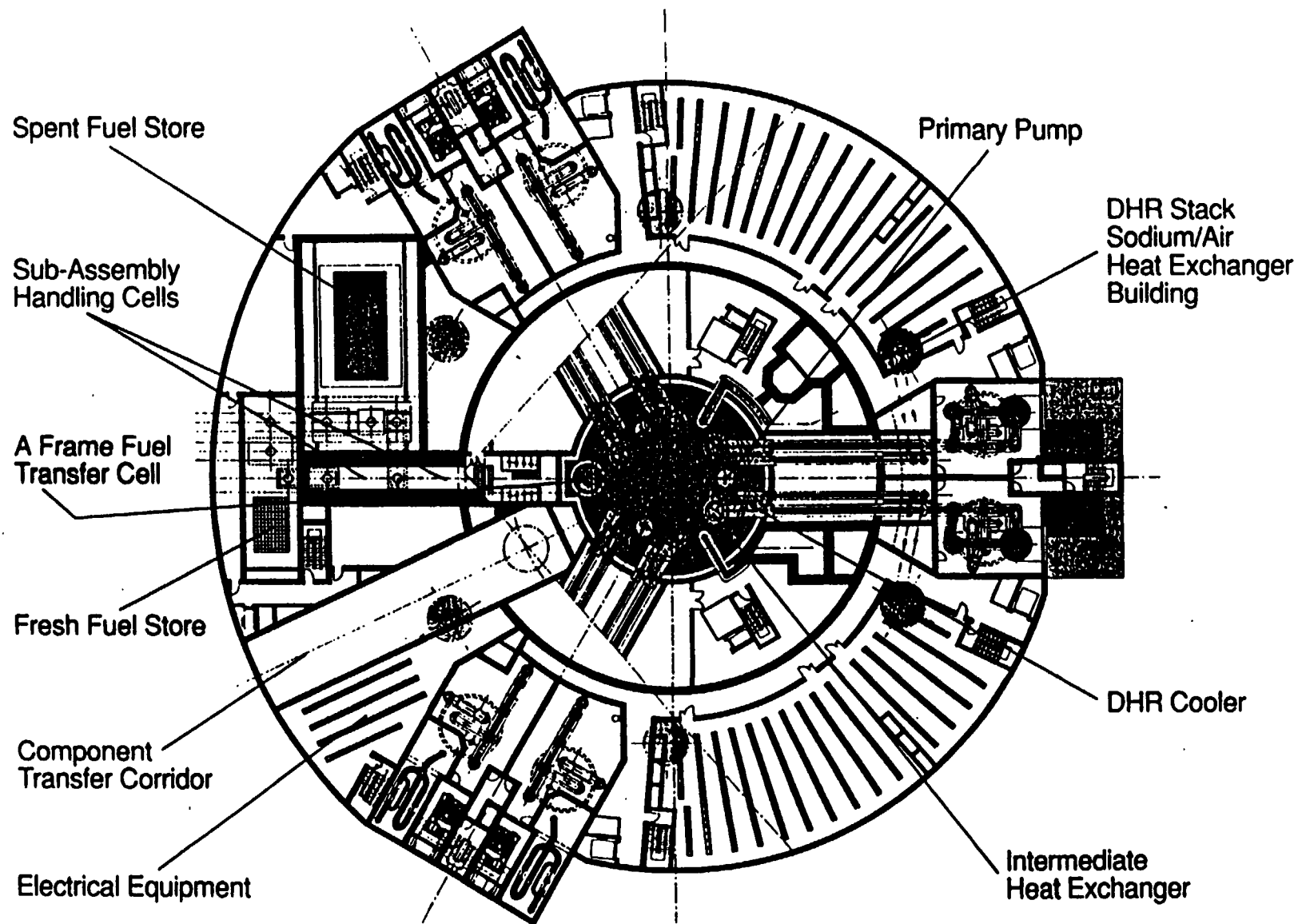


FIG. 9.3. EFR Nuclear island- plan view

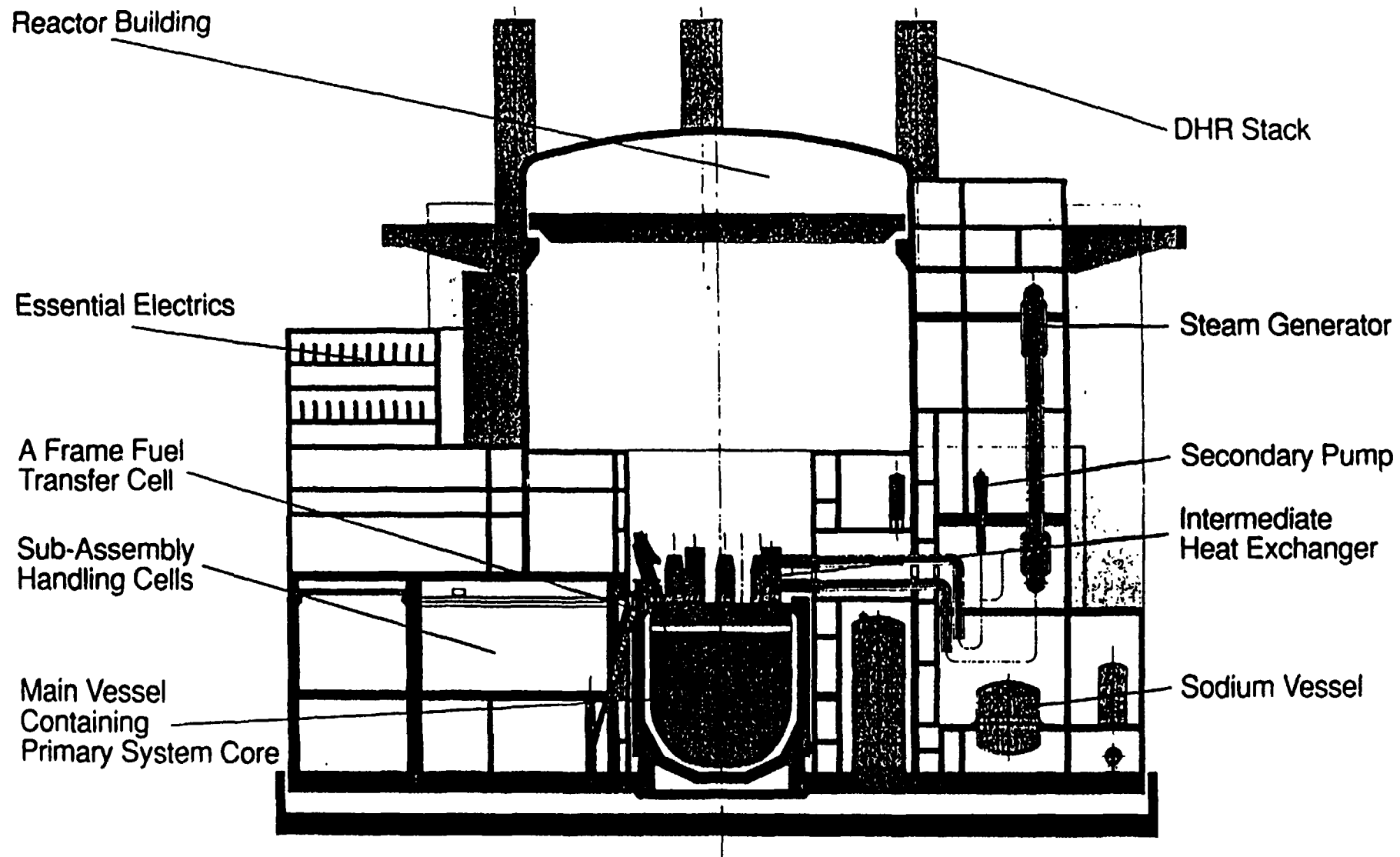


FIG.9.4. EFR Nuclear island - elevation

Reactor Auxiliary Building) there are 2 Sodium/Air Heat Exchangers, such that each SGB has an AHX on each side.

The Turbine Generator Building contains all components of the water and steam plant including the turbine generator. Large components are handled with a bridge crane through a central assembly opening. In general, the overall layout is similar to that of Turbine Generator Buildings in PWRs.

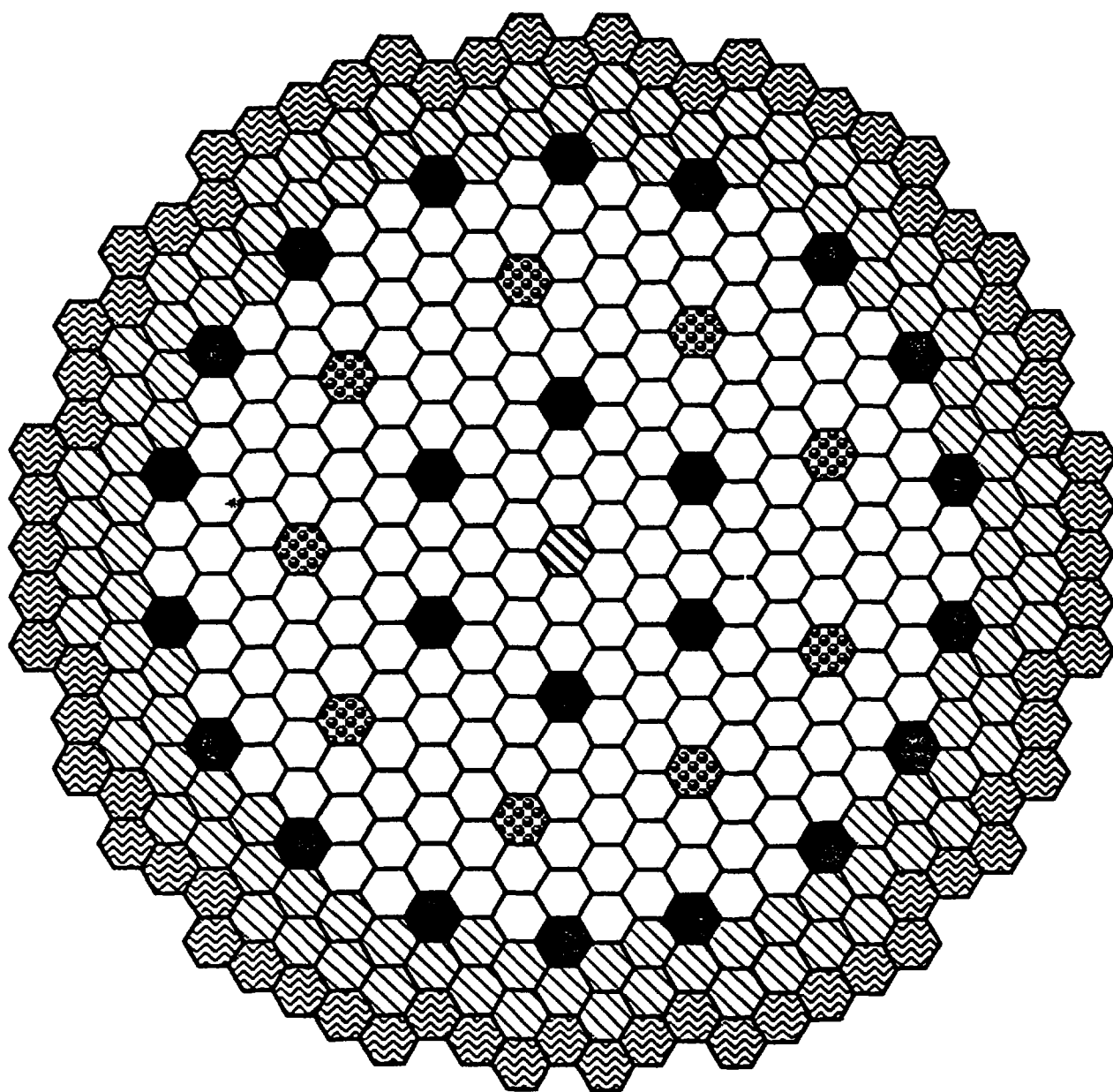
The Reactor Auxiliary Building is located adjacent to the Reactor Building between the Steam Generator Buildings No 2 and 3. It houses the components of the auxiliary systems based on a modular design.




Reactor core

Two options are considered for the reactor core: a conventional homogeneous core and an axially heterogeneous core with an internal fertile slice just below core midplane. Both concepts have three radial core zones with different plutonium contents, and are fully compatible with each other (Fig. 9.5). The inner zone contains 207 fuel subassemblies, while the intermediate and the outer zones are formed by 108 and 72 fuel subassemblies respectively. The core is surrounded by 78 breeder subassemblies in one row. The reactor core is 1 m high and, in the case of the axial heterogeneous concept, it comprises a 0.12 m high internal breeder zone. Axial breeder blankets having a thickness of 0.15 m and 0.25 m are located above and below the reactor core, respectively. As a feature of the design flexibility with regard to the breeding characteristics, either the suppression of the axial and radial blanket, or the addition of axial blanket (up to a total of 0.8 m) and of one additional radial breeder row are possible. This feature is also important in connection with potential new missions of fast reactors for plutonium management and transmutation of minor actinides.

Viewed from the core centre the radial core shielding consists of 2 rows of stainless steel reflector subassemblies, 1 row of B₄C pin subassemblies and 4 rows of B₄C block subassemblies. The core shielding is completed by the axial shielding integral with the subassemblies. In the bottom core regions, this is realised by steel inserts in the fuel and breeder subassemblies. The upper axial shielding is a bundle of 19 pins filled with steel and B₄C. The design criterion for the core shielding is consistent with permissible damage rate values at the in-vessel structures, limitation of secondary sodium activation to values which allow the Steam Generator Building to be classified as a radiologically uncontrolled area, as well as fulfillment of the core monitoring requirements with the detectors located in the above core structures. Finally, well separated from the core by the radial shielding, there is the in-vessel storage with a capacity of 234 fuel subassemblies.

For core control the EFR is equipped with two diverse fast acting shutdown systems. They are independent of each other from the sensors to the actuating trip systems. The latter are assigned to different electrical divisions where functional isolation of the different trip safety trains is provided. Each system on its own is capable of controlling all accidents requiring rapid shutdown of the reactor. An absorber rod group is associated with each shutdown system. In each of these groups, two types of absorbers are used: the control and shutdown rods and the diverse shutdown rods. The 24 control and shutdown rods provide sufficient anti-reactivity to shut the reactor down, in addition to their primary mission of power control and compensation of the various reactivity changes during reactor operation. The 9



	CORE 1	207
	CORE 2	108
	CORE 3	72




	CSD 24
	DSD 9
	DUMMY S/A 1

FIG. 9.5. Core layout

diverse shutdown rods have only the safety function of fast insertion. The two rod groups together guarantee subcriticality during handling operations.

Core subassemblies

Each *fuel subassembly* contains a bundle of 331 fuel pins with a diameter of 8.2 mm. The pin clad thickness is 0.52 mm. In addition to the fuel and the fertile material pellets of (U, Pu) O₂ and UO₂ respectively, the fuel pins contain a 1.2 m fission gas plenum and have a total length of 2.645 m. Above the fuel pin bundle, the upper neutron shield consists of a 19-B₄C-pin bundle of 0.85 m overall length. Including the approx. 0.6 m long spike, the fuel subassemblies have a total length of about 4.8 m. The hexagonal wrapper tubes are identical for all core subassemblies. The internal width across flats is 174.2 mm and the wrapper thickness 4.4 mm. With the 5 mm gap between the wrapper tubes, this results in a lattice pitch of 188 mm. The *breeder subassemblies* contain a bundle of 169 pins with a diameter of 11.5 mm and a clad wall thickness of 0.6 mm. The other main dimensions are the same as for the fuel subassemblies. The *control and shutdown rods* contain a hexagonal bundle of 37 absorber pins with a diameter of 22.8 mm, enclosed in a rigid hexagonal wrapper tube; the length of the B₄C stack is 1 m. The diverse shutdown rods contain a circular bundle of 55 absorber pins with a diameter of 16.4 mm, enclosed in a rigid circular wrapper tube. The bundles and their wrapper tubes are inserted into a hexagonal guide tube. B₄C with 90% B₁₀-content in the upper part of the absorber pins is used as absorber material. The B₁₀-content is reduced in the lower 0.3 m of the B₄C stack of the control and shutdown rods and in the lower 0.1 m of the diverse shutdown rods in order to limit the burnup of the B₁₀.

Reactor unit

A compact reactor unit has been achieved (Fig.9.6) with considerable simplification to the structures and components, and for surveillance. The large pool plant layout is an evolution from Superphénix taking full advantage of the national studies for CDFR, SNR 2 and Superphénix 2. The core, neutron shield and internal fuel store are supported by a diagrid which sits on a strongback to transfer the weight to the main vessel. Sodium is circulated through the core by 3 primary pumps and the heat transferred to the secondary sodium by 6 intermediate heat exchangers (IHXs). Hot sodium leaving the core is separated from the cold sodium feeding the core by a single shell called the "redan". Decay heat can be rejected from the hot pool by the 6 coolers which form part of the direct reactor cooling (DRC) system. A key to the compactness of the design is the reduction in the rotating plug diameter, made possible by the fuel handling arrangements which employ an intermediate 'put-down' for the fuel subassemblies in the central part of the core. The smaller number of large components compared with Superphénix (6 IHXs instead of 8 and 3 pumps instead of 4) then leads to a main vessel diameter of only 17.2 m. Simplification of the internal structures has been achieved by means of a redan formed by a single shell directly connected to the diagrid. The main vessel cooling feed has also been simplified. A solid steel reactor roof was adopted following design and manufacturing assessments which established the feasibility and advantage over the more conventional fabricated box structure used in large "pool" designs.

The *roof* is 0.85 m thick and is fabricated in sectors using narrow gap welding. It is lightly protected on its lower surface by metallic insulation and, because the component penetrations are machined, the tolerances are more controlled so smaller gaps are possible which give a further benefit of lower heat transfer from the cover gas. A directed air flow rejects the heat from the top surface of the roof to the reactor building and maintains the

EFR : REACTOR UNIT

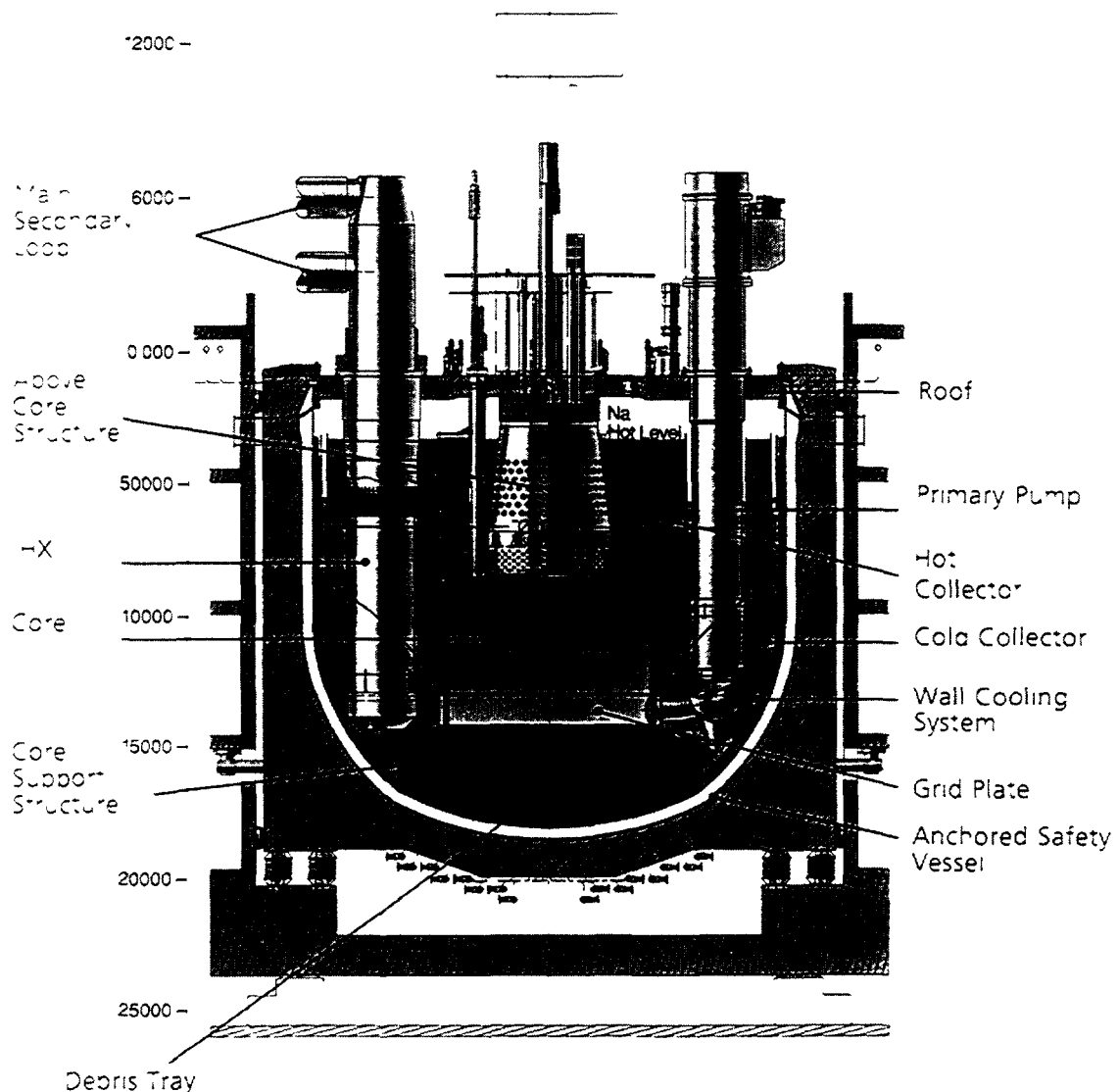


FIG 9 6 Cut view of reactor unit - elevation

temperature at 120°C. An important attractive feature is that on loss of electrical supplies natural cooling is adequate to maintain a stable roof temperature. The higher resistance to dynamic loading compared to the fabricated roof is an advantage when making the safety case for the reactor containment. Another feature which has been incorporated to improve the safety is self draining of the roof in the event of a sodium leak from the pipework above it.

The *rotating plugs* are also solid steel making a consistent upper closure design. A device has been provided which raises the plugs before rotation so that the thermocouples which monitor the core can be set close to the subassembly heads to provide a fully representative measurement.

The *main vessel* is fabricated in austenitic steel and has been the subject of a number of improvements which simplify and enhance its structural integrity. It is cooled in the cylindrical part by the sodium leakage flow from the support spikes of the core sub-assemblies. This

keeps the vessel at core inlet temperature. The triple point connection with the core support structure is by a forging which improves the integrity and inspectability both after manufacture and in service. In combination with the solid roof design, it has been possible to eliminate the tensile loaded transition weld to ferritic steel in the core support path. A sound demonstration of the leak-before-break behaviour of the main vessel has been made.

The *primary pumps* have a top entry, single mixed flow impeller and a flywheel to extend the run-down time on loss of power supply. A decision was taken to opt for a simple design without valves which implies all three pumps must be available for reactor operation. An innovative feature, recently introduced to the pump design, is a magnetic upper bearing with a ferro-fluid seal to eliminate oil and the potential hazard of its ingress into the sodium completely.

For the *intermediate heat exchangers (IHX)* a simple straight tube design is used with the primary sodium on the shell side. Because of the limited head to drive the primary flow, the lower flow resistance on the shell side gives the most compact unit. Extensive analysis has demonstrated that adequate flow and temperature distribution are achieved throughout the operating range. A new feature in the design is the use of piston rings to seal the IHX to the redan. Similar piston rings are used in PFR but the feasibility to accommodate thermal movements between the components and the redan requires a novel design. This feature replaces a gas seal and avoids any question of a large gas inventory being held below the sodium surface and offers some reduction in main vessel diameter. The IHX has a valve so that it can be isolated when necessary from equipment and components in the associated secondary circuit and steam plant. The reactor can be operated with one or two IHXs isolated.

Intermediate heat transfer system

This system transfers the heat from the intermediate heat exchangers to the steam generator units during power operation and during operational decay heat removal via the water/steam plant after reactor shutdown. Additionally, it represents a barrier between the radioactive primary system and the non-radioactive water/steam system. The intermediate system comprises *six parallel and independent secondary sodium loops*, each consisting of one mechanical pump, one steam generator unit, one dump vessel and the pipework connecting them to each other and to the intermediate heat exchanger located in the reactor vessel (Fig.9.7). The arrangement of the components is based on the 'Regain' concept. The economic incentive of this concept is the location of the secondary pump at a low level in the circuit allowing the function of an expansion vessel to be taken by the dump vessel. This design allows also a smaller, faster and more economic secondary pump to be used, because of the higher net pressure suction head available. Each secondary loop has a sodium purification loop. The purification pump acts also as level holding pump transporting the pump and steam generator sodium overflows from the dump vessel back to the main loop. The cover gas spaces of secondary pump, steam generator and dump vessel of each loop are interconnected. Thus only the dump vessel has to be connected with the cover gas system and the gaseous effluent system located in the steam generator building. Two secondary loops are housed in each Steam Generator Building. Each Steam Generator Building is divided by walls into two SG compartments to provide complete segregation between the loops. The loop design is monoplanar with vertical U-loops to compensate for thermal expansion. The design is for natural sodium circulation in the event of loss of electrical power. The straight main pipes inside the reactor building from the intermediate heat exchanger to the Steam Generator Building are enclosed by leak jackets which are part of the secondary containment boundary.

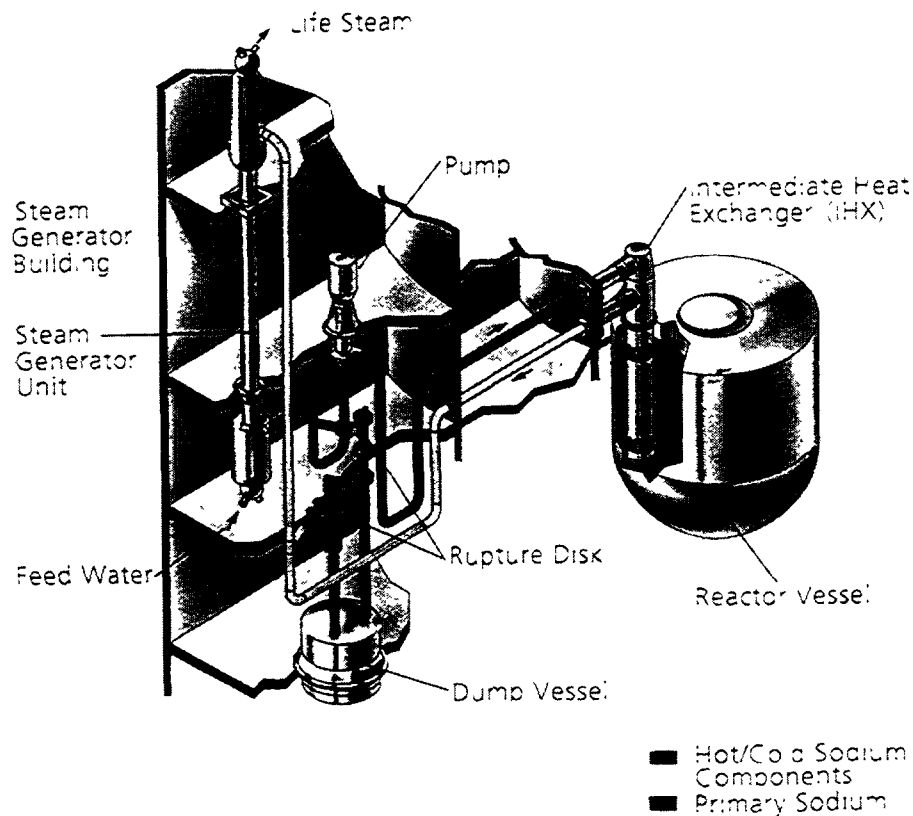


FIG. 9.7. Secondary sodium loop

The *mechanical secondary pump* is of single centrifugal type with cavitation-free impeller, bottom entry flow to the impeller, sodium lubricated hydrostatic lower bearing and a synchronous drive motor connected with the pump shaft by a cardan shaft with self-aligning couplings.

The *steam generator units* (Figs. 9.8., 9.9) are once-through straight tube units with a tube bundle arranged in a circular pitch between two ferritic steel tube-plates. Sodium flow is outside the tubes. There will be no welds in the tubes other than one at each end required to attach the tube to the tubeplates. Austenitic expansion bellows on the main shell above the

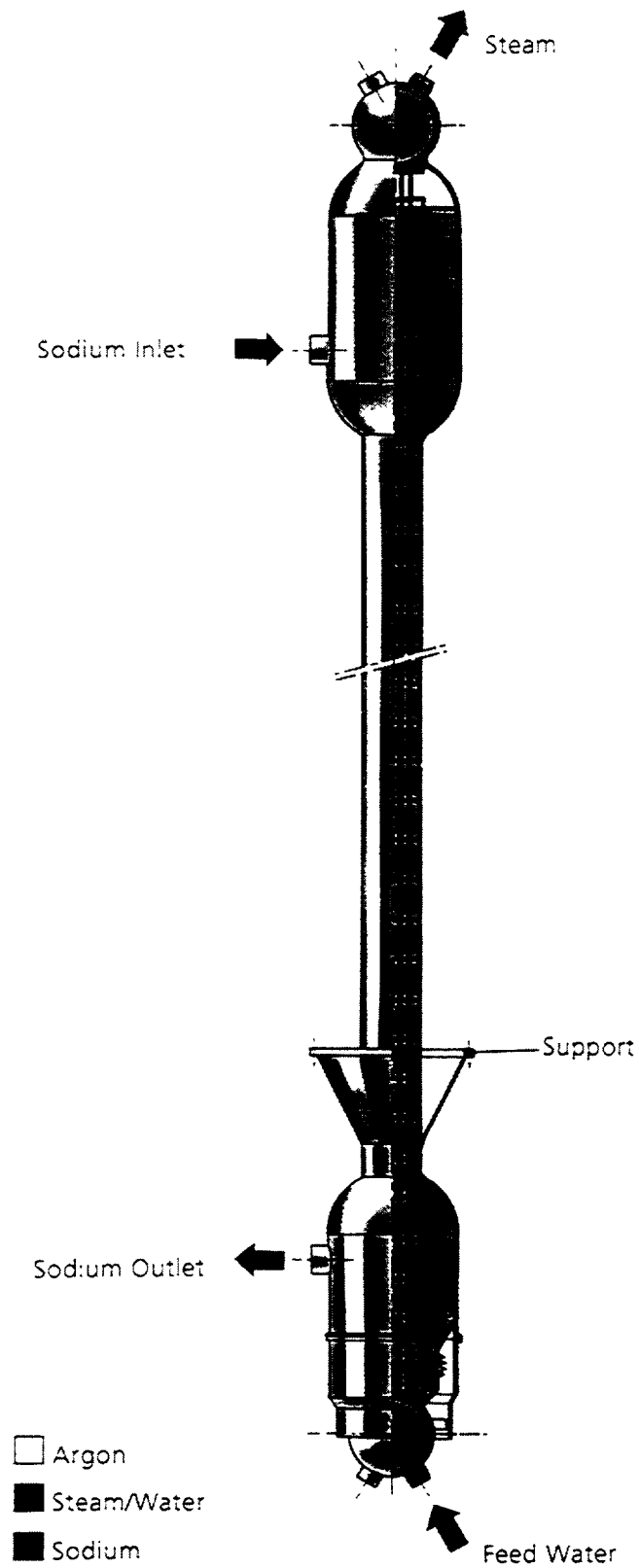


FIG. 9.8. *Steam generator unit - overall drawing*

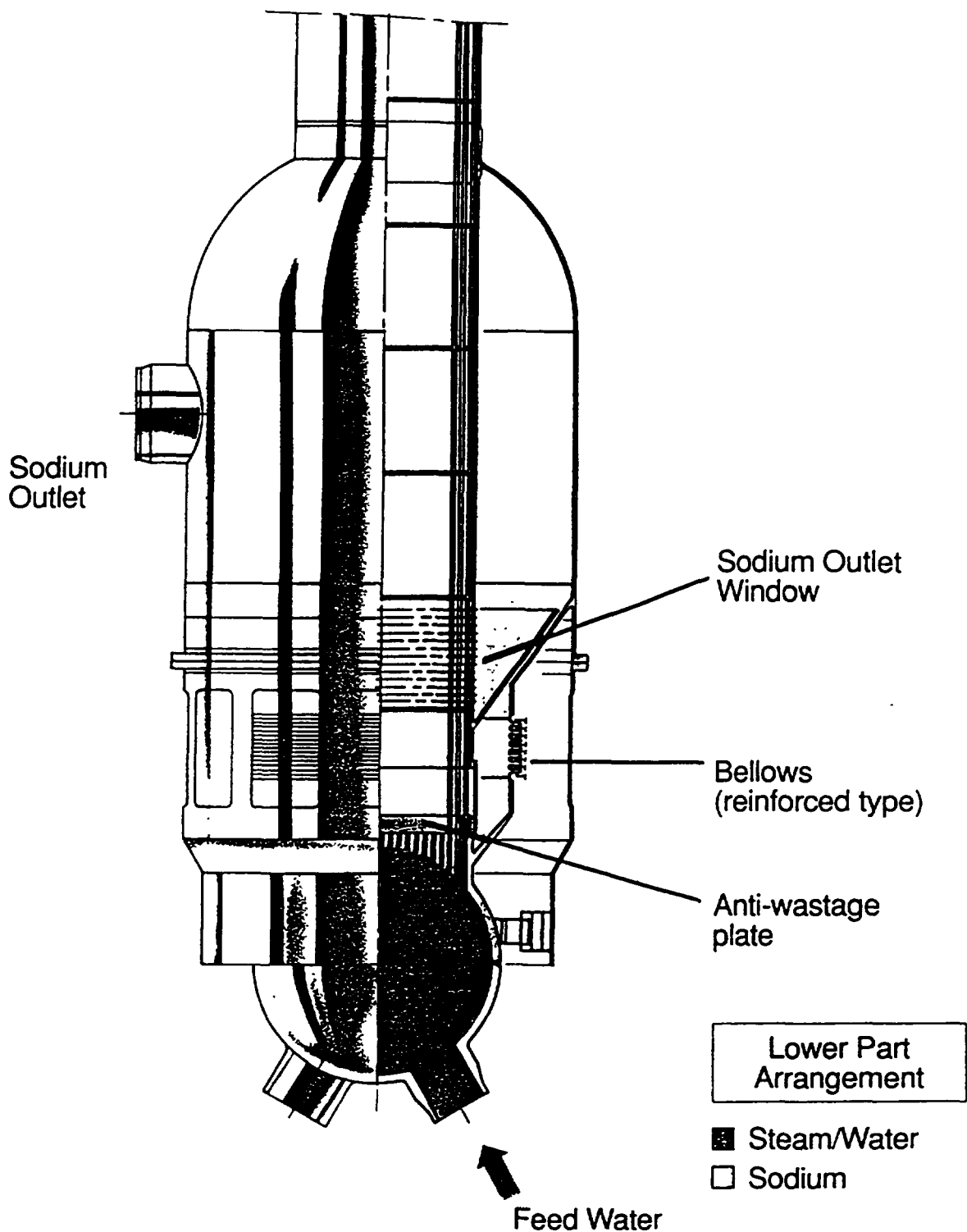


FIG. 9.9. Steam generator unit - Bottom end detail drawing

lower tubeplate provide a large flexibility to compensate for differential thermal expansion of tube bundle and shell. Specific attention has been paid to the protection against leaks in the upper and lower tube welds. Wastage due to sodium-water reactions and leak propagation is minimised by the adoption of a gas space at the top welds, and a thick antiwastage plate at the bottom welds. To detect tube leaks from the water to the sodium side of the steam generator rapidly and reliably, different leak detection methods are applied, such as detection of hydrogen under sodium and in argon, and active or passive acoustic leak detection.

Water/steam plant and turbine generator

The goal is to design the entire water/steam plant in compliance with guidelines and quality requirements applied in conventional (fossil fired) power plants. This presupposes that it need not perform any safety related tasks. For this reason the conventional water/steam plant can be designed according to utility/national practice. This minimises the special operator expertise and can be readily accommodated without real impact on the EFR NSSS.

As it is only used for operational decay heat removal, the measures that have to be implemented in the water/steam system in the event of a steam generator accident are the only function whose safety-related importance has to be evaluated in detail, in particular with regard to protection of the intermediate heat exchanger as a part of the primary containment. In addition, highly energetic failure of vessels must be taken into consideration for the water/steam plant. It must be demonstrated that the safety related protection goals (containment of radioactivity, shutdown and decay heat removal) are not at risk.

In the event of a leak in a steam generator it is necessary to limit the mass of water/steam available for a sodium/water reaction in order to restrict the pressure buildup in the secondary sodium system. Thus it is necessary to prevent additional flow of water or steam to the leak and to remove the water from the steam generator as quickly as possible. For this purpose, each steam generator can be isolated on the water and steam sides. This not only meets the requirements in case of a steam generator leak, but also permits isolation in case of steam generator repairs. At the same time as the faulty steam generator is isolated from the water/steam loop it is depressurised. For depressurization the feedwater side of each steam generator is connected to an atmospheric depressurization tank, specially provided for this accident. The steam side is directly connected to the atmosphere via a silencer. When the lower pressure limit has been reached the relief valves are closed to prevent sodium flow to the water side of the steam generator.

Direct reactor cooling systems (DRC)

The DRC systems provide highly reliable heat removal direct from the primary system in the event of the main heat transfer through the secondary system and the water/steam plant being unavailable. They comprise two direct reactor cooling systems (DRC1 and DRC2) each consisting of three sodium-filled loops. All loops extract heat from the hot pool of the primary sodium by immersed Na/Na heat exchangers and reject the heat to the environment by Na/air heat exchangers arranged some 34 m above the Na/Na heat exchangers (Fig. 9.10). All six loops are rated for a thermal power of 15 MW in nominal conditions (primary sodium temperature at 530°C, ambient air at +35°C). DRC 1 relies exclusively on natural convection heat transfer, i.e., natural circulation on the sodium side and natural draught on the air side. DRC 2 is normally operated in forced flow, and each loop is equipped with a flow supporting electro-magnetic pump (EM pump) and with two fans in parallel on the air side. These active loops possess passive heat removal potential when the pump and fans are off, amounting to about 2/3 of that in the active flow mode. For standby operation of the active loops (DRC 2) the air dampers are completely closed, the EM pumps are running and the fans are off. Operation of the DRC systems is initiated by an automatic signal from the reactor protection system or by the operator.

During maintenance and ISI&R campaigns on the water/ steam plant the DRC systems alone must remove the decay heat. ISI and refuelling is foreseen to take place at 220°C

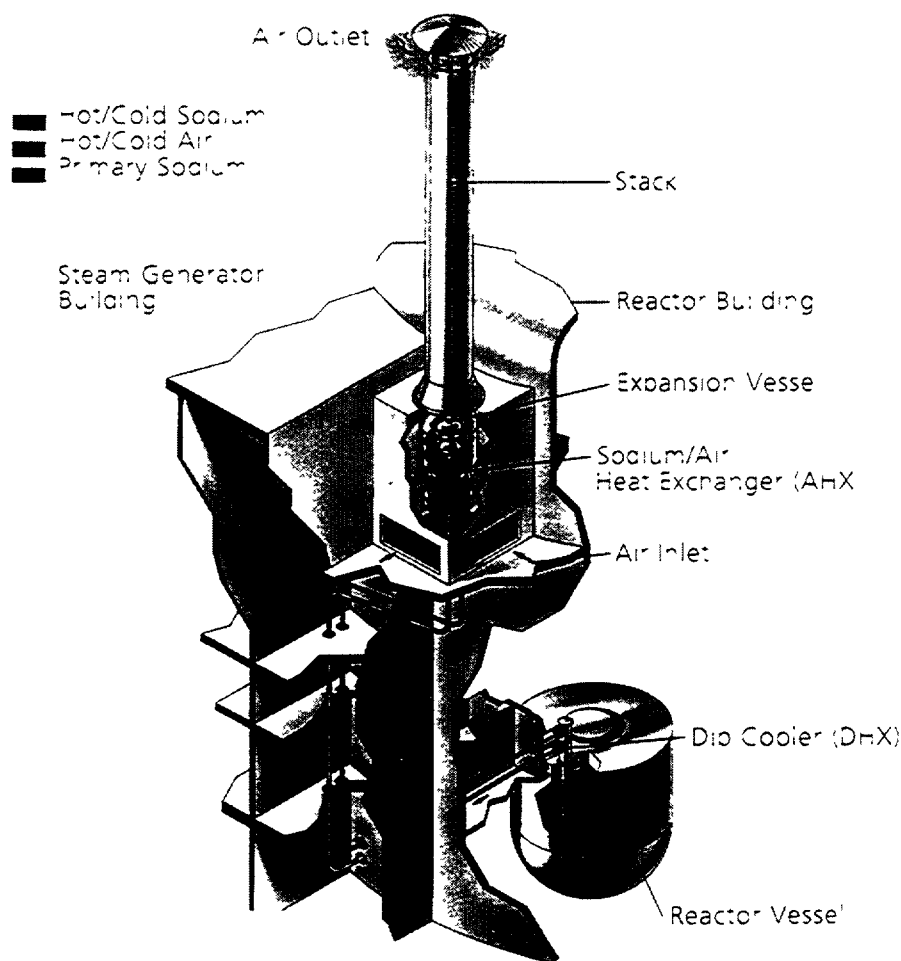


FIG. 9.10. Direct reactor cooling loop (DRC)

primary sodium temperature. To allow the DRC systems to take over the DHR duty as soon as a few days after reactor shutdown, the DRC cold leg temperature is allowed to fall to 160°C. This is controlled by throttling of the air dampers of the passive loops (DRC 1) and by reduced fan speed and damper throttling, if necessary, of the active loops (DRC 2). A special Na/air heat exchanger freezing protection is activated if the sodium outlet temperature in individual pipes falls below 140°C. The protection is based on multiple temperature measurements in selected areas of the heat exchanger with automatic damper closure for the affected loop. This action has priority over leg temperature control and DHR initiation.

The frequency target for the loss of DHR function is less than about 10^{-7} per year. Since the degree of redundancy of the DHR equipment in the water/steam system is determined only by operational and plant availability, and since the water/steam plant is not available after loss of station service power, the DHR reliability is essentially that of the DRC systems. Because of the high reliability target an appropriate degree of redundancy and diversity has been introduced into the DRC systems to exclude common mode failures from design basis considerations.

- There are significant differences in the design of the heat exchanging components between DRC 1 and DRC 2. This is also true for the active parts of the air side: the dampers, the damper drives and their power supplies.
- The combination of three passive loops with three active loops also leads to operational diversity between the two systems.

The use of sodium as coolant in the DRC loops meets the thermal-hydraulic requirements economically and enables the application of common sodium auxiliaries for DRC and secondary loops.

Auxiliary systems

The *primary sodium purification system* consists of an in-vessel EM pump and an ex-vessel cold trap, heat exchangers and plugging meter, arranged in a shielded concrete cell with steel liner and inert gas. The pipework outside the purification cell has double walls. In the case of sodium leakage the purification cell atmosphere (argon with sodium aerosols) is relieved into the buffer vessels of the reactor cover gas system.

The *primary sodium filling system* takes the sodium from the supply vessels into the reactor vessel via one low point vessel, an EM pump, a sodium filter and two ejectors. The low point sodium vessel enables the draining of the sodium volume of the filling system. After filling of the reactor vessel three of the supply vessels act as buffer vessels for the reactor vessel cover gas system.

Each *secondary sodium purification loop* is associated with one main secondary loop and one direct reactor cooling loop. All associated loops are arranged in the same Steam Generator Building compartment and are supplied from the same electrical division. Each of the six parallel and independent purification loops consists of a cold trap with recuperative heat exchanger, a plugging meter unit, an EM pump and the pipework with valves.

Between the steam generator and dump vessel, there are two *pressure relief lines with rupture discs*. A second pressure relief system connects the gas space in the dump vessel to the environmental atmosphere above the steam generator building.

The *reactor vessel cover gas system* protects the primary sodium against ingress of impurities, in particular those caused by air ingress, and establishes the gas pressure in the reactor vessel needed for the whole range of primary system operation. Three buffer vessels with a total volume of about 1,200 m³ to ensure constant cover gas mass during all operating conditions within a small bandwidth of the set pressure range. During normal operation the cover gas is circulated via a cover gas purification system (cryogenic absorber filled with activated charcoal) to hold the radioactivity level in the reactor vessel gas space as low as possible. Hydraulic safety valves are provided to protect the reactor vessel cover gas system from under or overpressure.

The *secondary cover gas system* protects the sodium of the secondary system and the direct reactor cooling systems against air ingress and keeps the different pressures in the cover gas subsystems in the predetermined range. The cover gas system is located in the three steam generator buildings and is divided into six identical subsystems corresponding to the six main secondary loops.

The *main vessel/safety vessel interspace gas system* inerts interspace between the reactor vessel and the safety vessel with nitrogen and maintains a constant pressure difference between the interspace gas and the reactor vessel cover gas.

Core subassembly handling systems

Refuelling takes place during scheduled reactor shutdowns, which occur at approximately annual intervals. Fuel subassemblies which are at the end of their life are removed from the core and placed in the in-vessel store. Fuel subassemblies which have been retained in the in-vessel store during the previous reactor operating period and, therefore, have a lower decay heat rating are transferred from the in-vessel store to the secondary fuel handling facilities. Other irradiated core components, such as breeder subassemblies and absorber rods, can be removed from the reactor vessel without using the internal store.

The in-vessel transfers of core elements are performed by two handling machines. The *direct lift charge machine* is located on the small rotating plug in the centre position of the above core structure. It is used for removal and insertion of subassemblies associated with the inner core zone. The *fixed arm machine* is also located on the small rotating plug, but outside the above core structure. It is used for removal and insertion of subassemblies associated with the outer handling zone. It also forms the link between the primary ramp and the transfer bucket of the A-frame system and the direct lift charge machine. Transfer positions are used as intermediate put down between the two handling zones.

Subassemblies are discharged from the reactor in a sodium filled bucket via the primary ramp of the A-frame system. The secondary ramp terminates in a transfer cell below the handling cell. The subassemblies are raised by a handling machine into the handling cell which is inerted with nitrogen and which accommodates a cleaning facility for sodium removal and an encapsulation facility for failed subassemblies. After sodium removal the subassemblies are transferred under water to a water storage system. In case of encapsulation, the subassembly in its canister is transferred to a dedicated storage position or to a special transport cask. Following 4 year storage, when decay heat has reduced to about 2 kW, the intact subassemblies are loaded bare into transport casks. These casks leave the fuel handling building through an air lock to an on-site or off-site dry store for long term interim storage. Alternatively, they can be shipped to the reprocessing plant.

The dry store is of modular design and, therefore, can be increased in capacity as storage requirements demand. Subassembly cooling is achieved by natural convection.

New subassemblies are transferred from the new fuel store into the reactor vessel on a one-to-one basis in exchange for irradiated subassemblies. They enter the fuel handling building via the transport cask air lock. They are then inspected and stored in the new fuel dry store which is cooled by natural convection. During the handling campaign, they are transferred from there to the reactor vessel via the handling cell.

Handling, decontamination and maintenance facilities for main components

Maintenance facilities for NSSS components are provided within the Reactor Building, within the transfer corridor and, if necessary, within a specially constructed off-island building. New or replacement reactor components can be delivered to the transfer corridor for movement to the reactor. Transfer of activated and contaminated components from the reactor building or transfer corridor to any off-island facility and vice versa will be within a transit flask, and in conjunction with a special purpose transport system.

Within the reactor building, components of the primary system are handled by shielded flasks. These flasks are transported by the polar crane in the reactor hall. A flask is raised to a fixed height, to engage a secondary retention feature which is directly attached to the crane grab. Adaptors and valves operate in conjunction with the flask valve to provide the connection between the flask and the reactor roof during handling operations.

Small and medium-sized components of the primary system are serviced and repaired inside the reactor building either by remote techniques in an inert gas atmosphere or by hands-on maintenance after washing and decontamination. Large components, like intermediate heat exchangers and primary pumps, can be repaired in a specially constructed off-island maintenance building. The basic facilities comprise the following:

- one large shielded flask for handling intermediate heat exchangers, primary pumps and the fixed arm charge machine, and
- one small shielded flask for handling absorber rod drive mechanisms, the direct lift charge machine, measuring probes and miscellaneous primary system equipment.

Sodium-wetted components or components with other types of surface contamination are cleaned and/or decontaminated in differently-sized washing and decontamination vessels inside the Reactor Building. The shielded flasks can be directly transferred to the washing and decontamination vessels.

Inspection, repair and maintenance work on activated components or handling flasks can be carried out in the maintenance cell inside the Reactor Building. The cell is within the operating range of the polar crane.

Electrical systems

The power supply concept is characterised by a twofold connection to the grid: the main grid and the standby grid. In normal operation power is fed from the generator to the main grid and the plant service system. In the event of loss of the main grid connection, the plant switches over automatically to house load operation, i.e., direct supply by the generator, the reactor being maintained at about 20% of nominal thermal power. If the main grid is not available and house load operation fails simultaneously, the power necessary for safe reactor shutdown and operational decay heat removal is drawn automatically from the standby grid.

The power supply system of the plant distinguishes 4 different levels according to the different tasks of the connected loads. It is arranged in so-called sections (supplying operational loads) and divisions (supplying safety equipment). For the Nuclear Island there are 3 sections and 3 divisions protected against external events. For the Conventional BOP two sections are provided.

The *normal power supply system* (level A) supplies all those components performing non-safety classified functions which are not needed after a loss of station service power (LOSSP).

The *spare power supply system* (level B) provides supply to components performing non-safety classified functions which are needed after LOSSP with regard to investment protection. It is backed by one diesel generator and 3 batteries.

The *standby power supply system* (level C) supplies those components indispensable for nuclear safety but only needed after a delay which allows corrective measures to be implemented. In case of a LOSSP 3 diesel generators, one for each division, ensure power supply after at most 32 h. The diesel generators can also feed into the spare power supply system.

The *emergency power supply system* (level D) supplies components performing functions indispensable to nuclear safety and needed immediately after LOSSP. Three emergency power supply batteries, one for each division, ensure an uninterruptable power supply for at least 32 h. The batteries are charged by the standby diesel generators.

9.1.5. R&D support of the design

The R&D organisations Atomic Energy Authority (AEA Technology) in the UK, Commissariat à l'Energie Atomique (CEA) in France, Kernforschungszentrum Karlsruhe (KfK) and Siemens-KWU in Germany are committed to support EFR by providing validation of its advanced design features. The research programmes in their nuclear centres have been realigned to meet the requirements set by the project team.

The entire R&D programme is structured into 11 experts working groups (AGTs), each with a precisely defined area of responsibility:

- AGT 1: Fuel elements and core materials,
- AGT 2A: Sodium chemistry,
- AGT 2B: Instrumentation,
- AGT 3: Core physics,
- AGT 4: Safety research,
- AGT 5: Core thermal-hydraulics and mechanics,
- AGT 6: Reactor system, handling systems and auxiliary systems,
- AGT 7: Heat transfer systems and components,
- AGT 8: Reactor operation,
- AGT 9A: Structural material characterization,
- AGT 9B: Structural integrity, design and construction rules.

The European R&D programme for EFR gave rise to more than one hundred "work packages" comprising more than a thousand individual tasks, some of which have involved considerable resources, e.g., reactor thermal-hydraulic experiments in large scale sodium and water mock-ups.

In the field of *AGT 1*, the main objective is to validate the final choice of clad and wrapper materials, based on the assessment of parameters such as neutron-induced swelling, high temperature creep and evolution of mechanical properties. Three classes of alloys are

under examination: austenitic steels, high nickel alloys and ferritic-martensitic steels. A large-scale irradiation programme of pin bundles to the target burnup of 20 at. % has been undertaken in Phénix, Superphénix and PFR. In parallel computing models are provided for the design of fuel and breeder pins and subassemblies, which are used to determine the operational limits for partial fuel melting in transients and clad failure.

The scope of *AGT 2A* covers the control of sodium quality and its purification, the behaviour of trapping devices and methods of decontamination and waste treatment. Extensive information on the interaction of metallic and non-metallic impurities in the coolant and the cover gas has been gathered in data sheets and designer's handbooks. Trapping devices for fission products such as cesium are being developed. The mechanism of hydrogen and tritium distribution is studied for the management of contaminated cold traps for sodium purification. Ways to improve cold trap performance are investigated. In the sodium hydrogen detection system for the steam generators has been improved by the use of multichannel devices. Provision of validated processes for cleaning, decontamination and requalification of NSSS components are of great operational and economic significance.

The scope of *AGT 2B* covers the development of instrumentation for continuous monitoring, especially of the core and steam generators, and for in-service inspection and repair interventions. The core instrumentation comprises individual subassembly temperature monitors, failed fuel detection systems based on cover gas activity monitoring and delayed neutron detection in the coolant, wide range neutron flux meters, sodium flow meters, sodium leak detection systems, etc. High performance acoustic detection methods have been developed to achieve very early detection of small leaks in the steam generator tube bundles and prevent degradation into severe sodium/water reaction accidents. Under-sodium viewing and telemetry methods using ultrasonic sensors has been developed for in-service inspection purposes and as an aid during fuel handling.

In the area of *AGT 3* the main task is the development of a common neutronics code system (ERANOS) comprising a complete set of modules for core physics and neutron shielding design calculations. This goes together with the establishment of a unified nuclear data base. These data and the computing models have been validated by experiments in the test reactors MASURCA (Cadarache) and NESTOR (Winfrith).

The *AGT 4* conducts safety studies, especially in connection with phenomena in the core. Assessments of sub-assembly faults, sodium fires, containment loadings, and, in particular, the core disruptive accident are of great importance for supporting the work of the designers' team.

The *AGT 5* is concerned with the thermal-hydraulics and mechanics of the core and core components. The contact forces between sub-assemblies distorted as a consequence of irradiation effects were investigated in the CHARDIS III rig (Risley). The dynamic behaviour of core arrays during earthquakes was examined in the RAPSODIE test facility (Saclay). Flow patterns at the core outlet and between sub-assembly hexagonal wrapper tubes were simulated in the HIPPO test rig (Risley).

The *AGT 6* was involved in thermal-hydraulic studies of the primary system and the decay heat removal system by means of facilities such as COLCHIX 4 and JESSICA (Cadarache), THOR (Risley), NEPTUN, RAMONA and KIWA (Karlsruhe) and ILONA (Bensberg). In addition, R&D was conducted on the thermal environment of the cover gas

and reactor top closure and the fuel handling systems. The inflatable elastomer seals of the rotating plugs were tested extensively with respect to friction wear and behaviour in temperature and under irradiation.

The scope of *AGT 7* is to study the main components of the heat transfer systems, such as the steam generator units (SGUs), the intermediate heat exchangers and mechanical sodium pumps. Assessment of sodium-water reactions in SGUs with tests at the SUPERNOAH rig (Dounreay), development of computer programmes for the thermal-hydraulic design of heat exchangers and the dynamic analysis of rotating pump shafts, and validation of design criteria for impellers with sufficient margins against cavitation hazards, constitute the main areas of work of this group.

The *AGT 8* is concerned with exchanging experience arising from the operation of European fast reactors, namely PHENIX, SUPERPHENIX, PFR and KNK II. Analysing and comparing the in-service behaviour of the equipment, and the lessons gained from maintenance or repair works of main components, are particularly valuable.

The *AGT 9A* has to provide verified data for the materials used in EFR. Materials of chief interest are the austenitic steel 316 L(N), which makes up the greater part of the reactor structures, and the ferritic steel 9 Cr1Mo (modified) employed in the SGUs. The need for data is particularly important in the upper temperature range (500-650°C) where creep phenomena become significant. In addition, methods of non-destructive testing and in-service inspection techniques are being developed, including in-gas and under-sodium telemetry and volumetric inspection using ultra-sonic sensors.

Finally, the *AGT 9B* has the duty to issue common design and construction rules in the field of structural mechanics so that the required standards of safety and reliability can be met. Among many other subjects, one of the most important is the validation of material descriptive equations involved in complex inelastic computing models and the setting up of component sizing criteria to protect against creep and creep-fatigue damage.

9.1.6. Concept validation phase achievements

The approach to competitive fast reactors

Continuation of fast reactor development, although it appears desirable in the light of the general arguments exposed in the introduction, must also be economically justifiable. This means that the electricity generating cost must be sufficiently close to that of PWRs. Demonstration of the economic potential was, therefore, an important objective of EFR design studies, leading to thorough investigation of all components of the kWh cost, i.e., investment, fuel cycle and operation. This investigation was conducted as a joint enterprise between EFR Associates and EFRUG, each being responsible for clearly identified areas of work as is outlined in Fig. 9.11. The design work on EFR has achieved substantial investment cost reductions for the NSSS, as is illustrated in Figure 9.12, which displays the specific weights of steel in te/kW(e) employed for the main systems of SUPERPHENIX and EFR.

In order to confirm the favourable trend deduced from this comparison of economic indicators, EFR Associates launched a comprehensive cost enquiry campaign which involved experienced component manufacturers in Europe. The manufacturers were asked to provide quotations against specific "Cost Enquiry Specifications" for a number of components typical

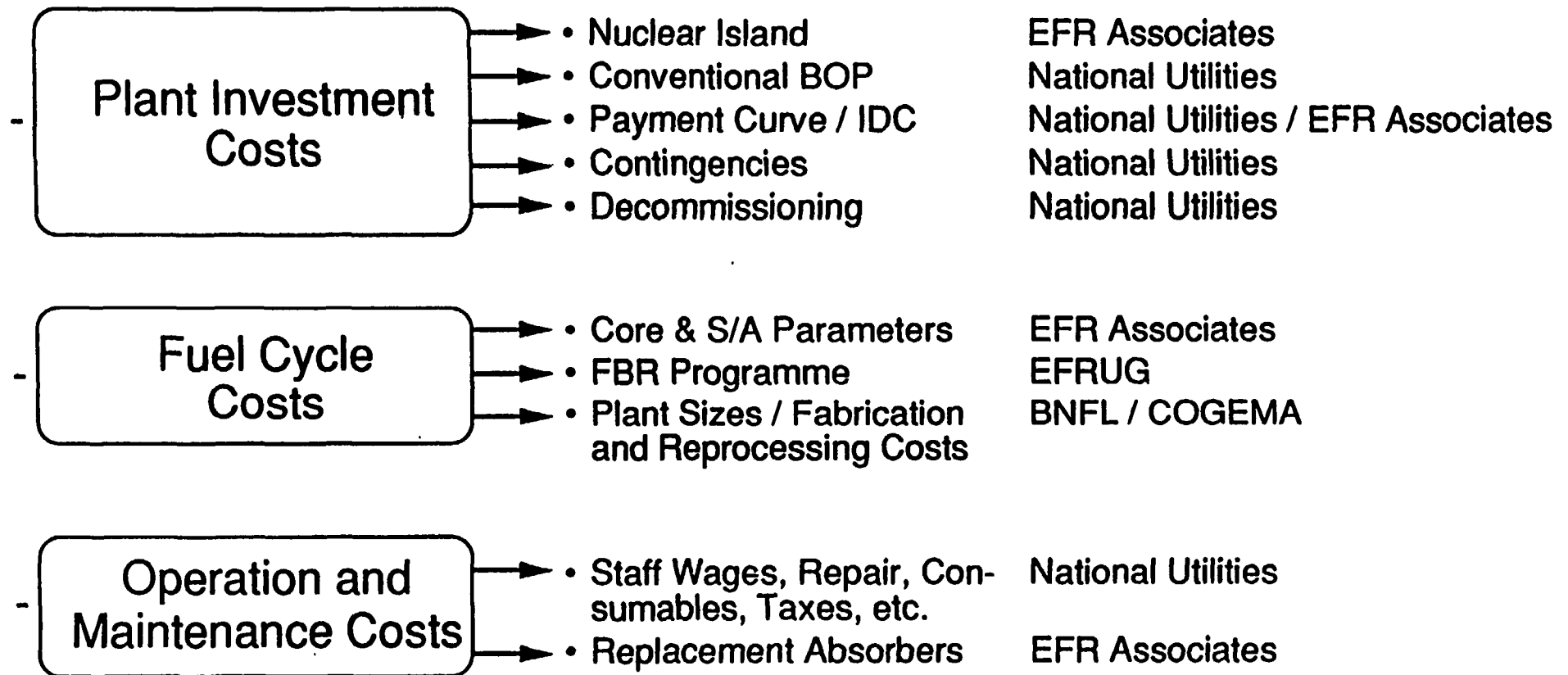


FIG. 9.11. Economic assessment of EFR ● Sharing of responsibilities

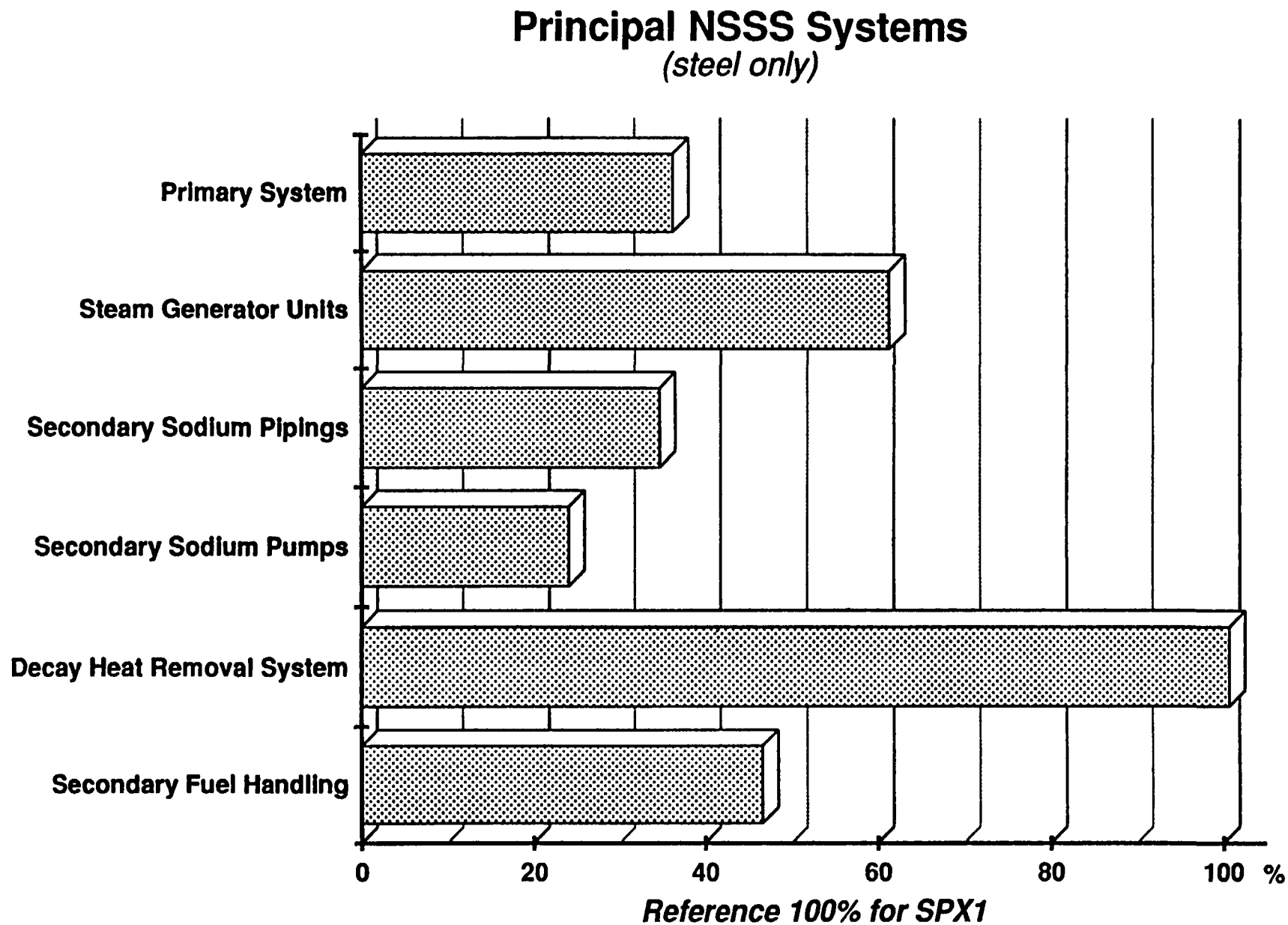


FIG. 9.12. Steel quantities comparison: EFR - SPX1

of fast reactors. These specifications were established on the basis that the manufacturers had only to comply with their national standards for the fabrication of nuclear components. This approach avoided cost distortions due to a need to accommodate foreign standards, and is consistent with the fact that a site for EFR has not been selected yet and could be located in any of the partner countries. Moreover, when the construction of EFR starts, much progress will have been made in establishing common European standards which will supersede national standards in line with the realization of the single European market.

Against that background, 21 key components were selected for quotation by manufacturers, and corresponding cost enquiries were addressed to 19 manufacturers in 4 countries: Austria, France, Germany and the UK, giving rise to 57 quotations. Component costs were obtained for the first-off EFR station and for a series unit in a programme of fast reactors so that cost reduction due to the learning effect and series construction could be fully exploited. The Nuclear Island cost assessment by the EFR Associates was combined with Conventional BOP cost estimates by the EFRUG utilities to establish the construction cost of the whole station under the conditions prevailing in each country. This provided the main input for computation of generating cost.

To secure an assessment of EFR fuel cycle costs, EFRUG requested the major companies specialising in nuclear fuel fabrication and reprocessing, BNFL and COGEMA, to provide up-to-date information on fuel service costs. As for plant construction the fuel service cost assessment was requested for the first-off station and for a series unit in a programme of fast reactors with an established fuel cycle operating under similar industrial conditions as for PWRs.

In the transition period preceding the launching of a series, fast reactor fuel services will be provided by existing PWR recycled fuel (MOX) fabrication and reprocessing plants, leading to a fast reactor fuel cycle not operating at its economic optimum. Successive replacement of thermal MOX fuel plant services by plants designed for fast reactor services on a commercial scale will continuously improve fuel cycle performance, leading finally to a minimum cost expected to be markedly lower than that of thermal reactors.

The assessment of operational costs was based on utilities' experience of nuclear power plant operation. A goal of EFR design is to avoid there being significant differences in operation and maintenance (O&M) costs compared with PWRs, this intention being supported by a comparison of the number and complexity of the nuclear related systems and auxiliary plant. It is an established fact that radiation doses to operators are substantially lower in a fast reactor station than a PWR; this has favourable consequences for O&M costs.

As far as possible, a common set of assumptions and economic parameters was used in the generating cost computations. However, some variation in generating costs arises due to differing national practices for conventional plant and evaluation of the operation and maintenance and fuel cycle costs.

The evaluated generating costs of EFR and PWRs in France, Germany and the U.K. are compared in Figure 9.13, which demonstrates that the goal of competitiveness for EFR can be considered achieved. This figure shows a larger range of kWh cost values for a PWR than for EFR. This is due to the PWR reference stations being of different designs in the three countries, whereas the major part of the EFR station, the Nuclear Island, is a common design and only the Conventional BOP is peculiar to each country.

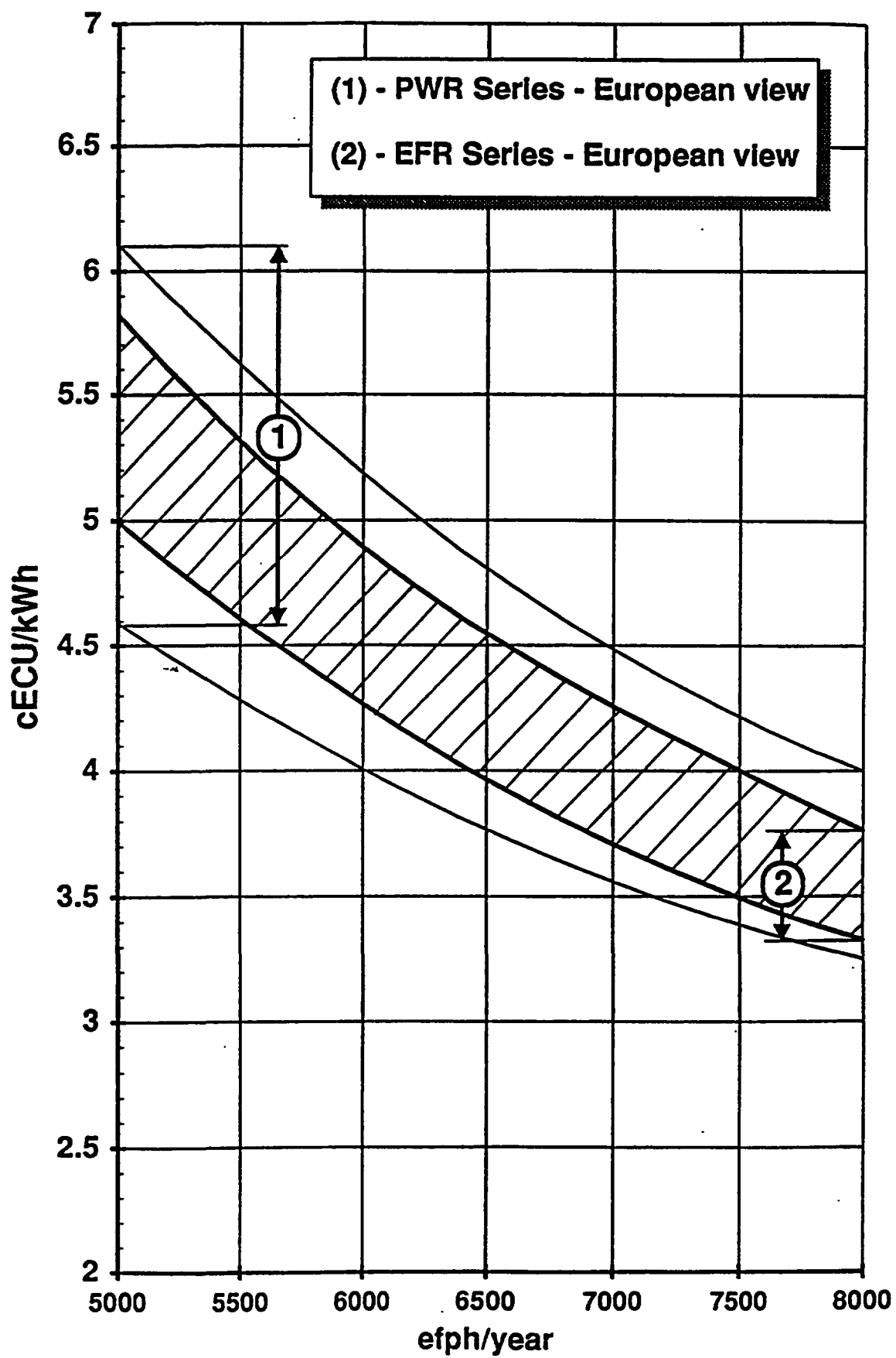


FIG. 9.13. Generating cost comparison: EFR - advanced PWR

The safety approach

A prime feature of the safety design of EFR is the extensive application of "defence in depth" concepts. The successive protection levels include:

- careful design, high effort in quality assurance, extensive R&D to ensure a good design and performance,
- systems to protect and control failures or deviations from normal operation,
- protective systems and engineered safety provisions,
- physical barriers to confine any radioactive release, and
- ultimate risk minimization measures to enhance further the reliability of shutdown and decay heat removal, and the retention capability of the containment.

Because the reactor is not pressurised and is located in a close-fitting pit, loss of coolant is precluded and core melt preventive measures are concentrated on enhanced shutdown and decay heat removal. Through these preventive measures the risk of core melt is extremely low (remote in the residual risk domain) and beyond the objectives set by INSAG for future reactors. As such, there is no need for special containment provisions to meet the requirements on accident release limits. Nevertheless, according to the ALARP principle, strong primary and secondary containment are included, which further mitigate against postulated loadings. The core design has been optimised for safety through:

- the fuel pin linear rating, chosen to prevent local fuel melting in the case of inadvertent absorber rod withdrawal,
- the core height chosen to minimise the positive reactivity effect of sodium voiding, and
- the Doppler coefficient to provide efficient reactivity feedback to rapid transients.

Reactor shutdown is assured by two independent and diverse basic shutdown systems which guarantee very high reliability so as to relegate shutdown failure into the domain of residual risk. In the domain of residual risk, however, the "Third Shutdown Level" becomes effective. It consists of a bundle of additional engineered safety features which are incorporated in the design as a result of extensive risk-minimization studies. The system consists of active and passive subsystems and is supported by beneficial natural core behaviour. For example, the following features of the absorber rod actuators are part of the "Third Shutdown Level":

- a device which uses thermal expansion of the drive mechanism to trigger rod drop,
- automatic interruption of the power supply to the electro-magnets by which the rods are suspended,
- mechanical stroke limitation restraints to mitigate inadvertent rod withdrawal, and
- motorised drive of the whole rod bank to follow up insertion.

The "Third Shutdown Level" is capable of maintaining core integrity in the case of a postulated failure of the two basic shutdown systems.

Decay heat removal (DHR) is normally achieved by means of the steam/water plant. This is backed up by two diverse DHR systems, both safety qualified. Also, the use of the steam generator shell surface for heat removal by air cooling is an effective risk-minimising measure. Provision of a close-fitting guard vessel and pit surrounding the reactor vessel is a simple and effective measure to mitigate the consequences of primary coolant leakage and

ensures long-term cooling of the core under such post-accident conditions. As a result loss of coolant leading to an inability to remove decay heat is not possible due to the low operating pressure of the primary sodium system, which ensures that primary sodium leaks do not involve any boiling.

The containment concept complies with the "defence-in-depth" principle, by providing a multiplicity of barriers between radioactive fission products and people. The high reliability of the first of these barriers, the fuel cladding, has been confirmed by the operating experience of prototype FRs. This enables radioactivity of the primary coolant and other sodium systems to be kept very low with corresponding benefits for the operators both in normal and abnormal situations. The fact that the primary containment (made up by the primary system boundaries-the second barrier) is at low pressure, gives a further essential advantage in that any leakage from it will not threaten the secondary containment (the third barrier) with large overpressure. Even with the high level of prevention of core disruptive accidents, the capability of the primary containment to resist dynamic loadings has been assessed and all weak points have been designed out. Similarly, the integrity of the secondary containment has been demonstrated for a range of plant states representing various stages of degradation of the primary containment.

The challenge for EFR is that it must satisfy the same level of safety as future LWRs and be capable of being licensed in each of the participating countries. An important achievement has been to demonstrate the potential licensability by means of an independent review of the essential elements of the safety case by a group of prominent safety experts from France, Germany and the UK. This review allowed in-depth discussions on the general approach, the main safety functions and the proposed risk minimization measures. The outcome was as follows:

- on core melt; adequately low levels of risk are achievable,
- on sodium fire hazards and in-service inspection; significant progress has been made with EFR compared to previous fast reactor designs, and
- on decay heat removal; the improvements incorporated in the design are judged satisfactory.

The review concluded, notably, that the approach adopted for EFR results in levels of safety comparable with those of future PWRs. It also provided useful advice on areas where work would substantiate the EFR safety case further, e.g., some additional studies were recommended concerning:

- the containment; additional demonstration of the validity of the chosen "plant states" as part of the ALARP principle implementation, and
- common cause failures; due to the concentration of safety equipment on the reactor roof, it is necessary to show that measures have been taken to make the risk acceptably low.

In conclusion, the final view expressed by the independent experts was that « they were favourably impressed by the progress that has been made with the current EFR design, and they consider that it provides a sound basis from which to proceed to licensing application in each of the participating countries ». There is no doubt that EFR can achieve levels of safety comparable with those expected for future PWRs.

9.1.7. The success of the EFR project

The EFR project was widely regarded as a success, matching the ambitious expectations of the customer utilities. This has been achieved as a result of the partnership between the design companies, the R&D organizations and the utilities. The success of the project was a shining example of European cooperation which demonstrates how an advanced technological development can be handled across nations, thereby sharing costs and taking benefit from each other's skills and expertise.

At the completion of the Concept Validation phase the economic assessment, involving the key manufacturers in the participating countries, confirmed the potential for the EFR design to be competitive with national PWRs. It was also confirmed that the EFR design and safety features can confidently be expected to be licensable in each of the participating countries. This statement can be made following the positive outcome of the independent safety review.

If the early closure of SPX leaves open a number of questions concerning the validation in industrial conditions of the FR technology, the basic sodium technology and Reference EFR design are not called into question from the design point of view regarding:

- its ability to respond to stringent operational and safety requirements,
- its potential for a better economic performance than SPX making possible a future competitiveness considering missions of uranium savings and transmutation of nuclear wastes.

Nevertheless, EDF and BNFL considering the evolving situation together with the good status of the EFR design work have decided to close down in a very structured manner the current EFR work programme by the end of 1998. EFRUG, which appears now no more suitable for the new conditions, has been dissolved with agreement of all partners in January 1998. Now interest of EDF, BNFL and other utilities will be mainly through association with the R&D programmes and corresponding R&D agreements.

9.2. BN-1600M

9.2.1. Stages of development and design concept evolution

Design of the large reactor BN-1600 is a logical step in the line of fast nuclear reactor development in the ex-USSR. In the early stages of design development (1970s), virtually all the principal design decisions of the preceding prototype (the BN-600 reactor) were retained, i.e. integral layout of the primary system equipment, bottom support of the reactor vessel, separate suction plena for the primary coolant pumps, a spent fuel storage drum filled with sodium, emergency residual heat removal system based on use of the steam generators (SGs), cold trap located outside the reactor vessel, modular SGs. Modifications were associated mainly with the increase in unit power and were related to the fuel assembly (FA) duct size, the number of the primary and secondary loops, the size of the reactor vessel, and the unit power of the main equipment items. The approach to safety was based on the current regulatory documents which did not cover the specific features of fast reactors entirely. The reactor design was aimed at providing increased fuel breeding gain and on this basis reducing

significantly the demands of nuclear power on natural uranium resources. A comprehensive programme of R&D efforts had been launched and equipment manufacturers were selected. Development of the design was accelerated. Facilities for testing the basic equipment items such as the reactor coolant pumps, rotating shield plugs, elevator, refuelling machine, SGs, etc. had been designed and constructed. Development of the BN-1600 Basic Design was completed in 1986.

However, by that time views on the rate of uranium consumption for nuclear power had been altered, stringent requirements for fuel breeding gain and doubling time were removed, and new approaches to the safety issues and to the deadline for the large-scale introduction of fast reactors into the nuclear power park were formulated, while the economic requirements became more rigorous. Additionally, the accident at the Chernobyl NPP adversely influenced nuclear power development in general. In 1986 a governmental resolution was adopted which shifted the commissioning of BN-1600 to the end of 1990.

At the same time, efforts to optimise the design were continued. A number of innovations were drafted whose realization in the design promised to reduce the capital cost, improve the technical and economic characteristics of the plant and to enhance its safety. Simultaneously, new regulatory documents with more stringent safety requirements appeared and a promising way to enhance the safety of nuclear reactors was identified, namely, the implementation of inherent self-protection and defence-in-depth principles. The approach to the economic target was also changed when sufficient information was provided to assess the competitiveness of fast reactors compared with LWRs, taking into account their fundamental physical and technical features, as well as the accumulated experience in development and commercial operation. This resulted in a decision on substantial reworking of the design with the emphasis on the safety issues and on improvement of technical and economic performance.

Conceptual design of the advanced reactor plant BN-1600M was completed in 1992 in a full compliance with the up-to-date requirements for safety and economic efficiency of the new generation NPPs. It is expected that this design can be realized in the Russian Federation not earlier than 2010, taking into account the fact that in the near future the fast reactor development programme in this country will be primarily focused on ensuring reliable operation of the BN-600 plant, construction of the pilot BN-800 reactors, and creation of the closed nuclear fuel cycle production plants. This phase will be of exceptional importance for the subsequent development of fast nuclear reactors and should precede their wide incorporation into the nuclear power park. Large fast nuclear reactors are considered to be rather promising due to their ability to provide the best economics and enhanced safety features. The BN-1600M has to be the pilot demonstration reactor in a prospective series of such reactor plants in Russia.

9.2.2. Basic parameters and design optimization

The following major objectives and goals were adopted for the BN-1600M advanced design.

- 1) Improvement of the economic efficiency of power production to a level comparable to PWRs in terms of generating cost, through the maximum feasible reduction in specific mass of major components and of the reactor unit in general, through simplification of the plant components and systems and increase of the steam cycle efficiency.

- 2) Enhancement of both nuclear and radiological safety through further development of positive safety properties inherent to fast nuclear reactors and through wide implementation of innovative passive devices and systems for safety functions.

The unit power of the reactor plant and main thermal-technical parameters were optimized against the following design criteria: (a) unit power increase is the most effective method for specific cost reduction, (b) unit power of the reactor plant must meet the restrictions imposed by the power grid, (c) standard equipment similar to that of fossil-fueled power plants should be used for the steam-water (tertiary) system, including the turbogenerator, and (d) the thermal efficiency (not less than 42.0%) should be maximised by optimization of the steam cycle parameters. As a result the following thermal parameters were adopted for the design:

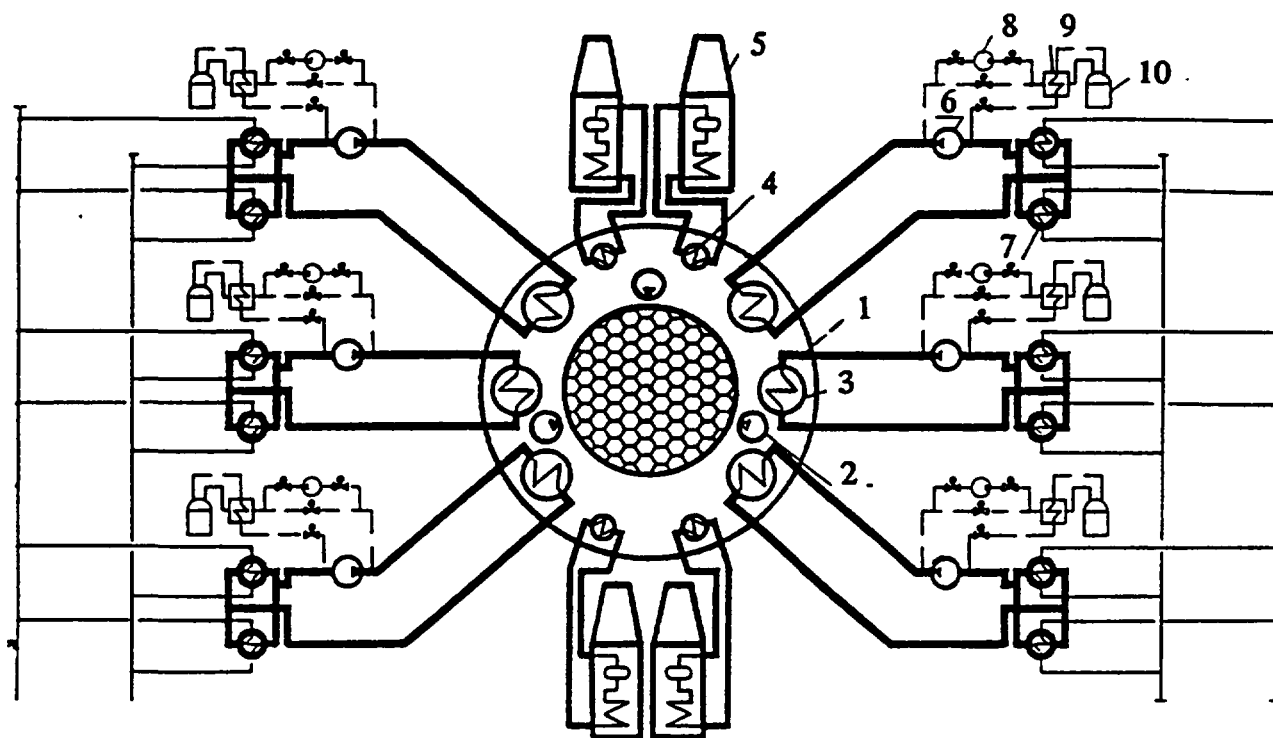
TABLE 9.1. BN-1600M MAIN THERMAL PARAMETERS

	Parameter	Value
1.	Reactor thermal output, MW	3850
2.	Electric output, MWe	1620
3.	Steam cycle efficiency (gross)	42.0
4.	Primary coolant parameters:	
	- core inlet temperature, °C	395
	- IHX inlet temperature, °C	550
5.	Secondary coolant parameters:	
	- SG inlet temperature, °C	515
	- SG outlet temperature, °C	345
6.	Tertiary system parameters:	
	- main steam temperature, °C	495
	- main steam pressure, MPa	13.7
	- feed water temperature, °C	240
	- steam reheating	by steam
7.	Auxiliary power, % nominal	5.5

The power unit includes: BN-1600M reactor plant, twelve steam generators, two standard turbine plants K-800 (Fig. 9.14).

To reduce the specific mass of the reactor plant large vessel-type steam generators are used with integrated secondary coolant expansion tanks. These have the least mass per kW compared with other types of steam generators. This design also minimizes the volume of the SG building. Bellows are provided to accommodate secondary piping thermal expansion, which additionally reduces the total mass of the secondary system and the volume of the building.

The same integral layout of the primary circuit components is adopted as for the previous BN-600 and BN-800 reactors. But in this design the reactor vessel is suspended from an upper roof slab (in contrast to the earlier bottom support scheme) which avoids the need for the heavy support belt for primary components in BN-600 and BN-800. The top-suspension design allows a simpler solution of the problem of the primary circuit penetrations through the reactor roof, which is complicated for large reactors. In particular, the large bellows which are needed in the bottom-support design for sealing the reactor interior and for accommodating the difference in thermal expansion of the reactor vessel and the primary component supports



1 - reactor, 2 - reactor coolant pump, 3 -intermediate heat exchanger, 4 -ERHR submerged heat exchanger, 5 -ERHR air cooler, 6 - secondary coolant pump, 7 -steam generator, 8 - secondary sodium purification system, 9 - recuperator, 10 - cold filter-trap.

FIG. 9.14. BN-1600M reactor plant flow diagram

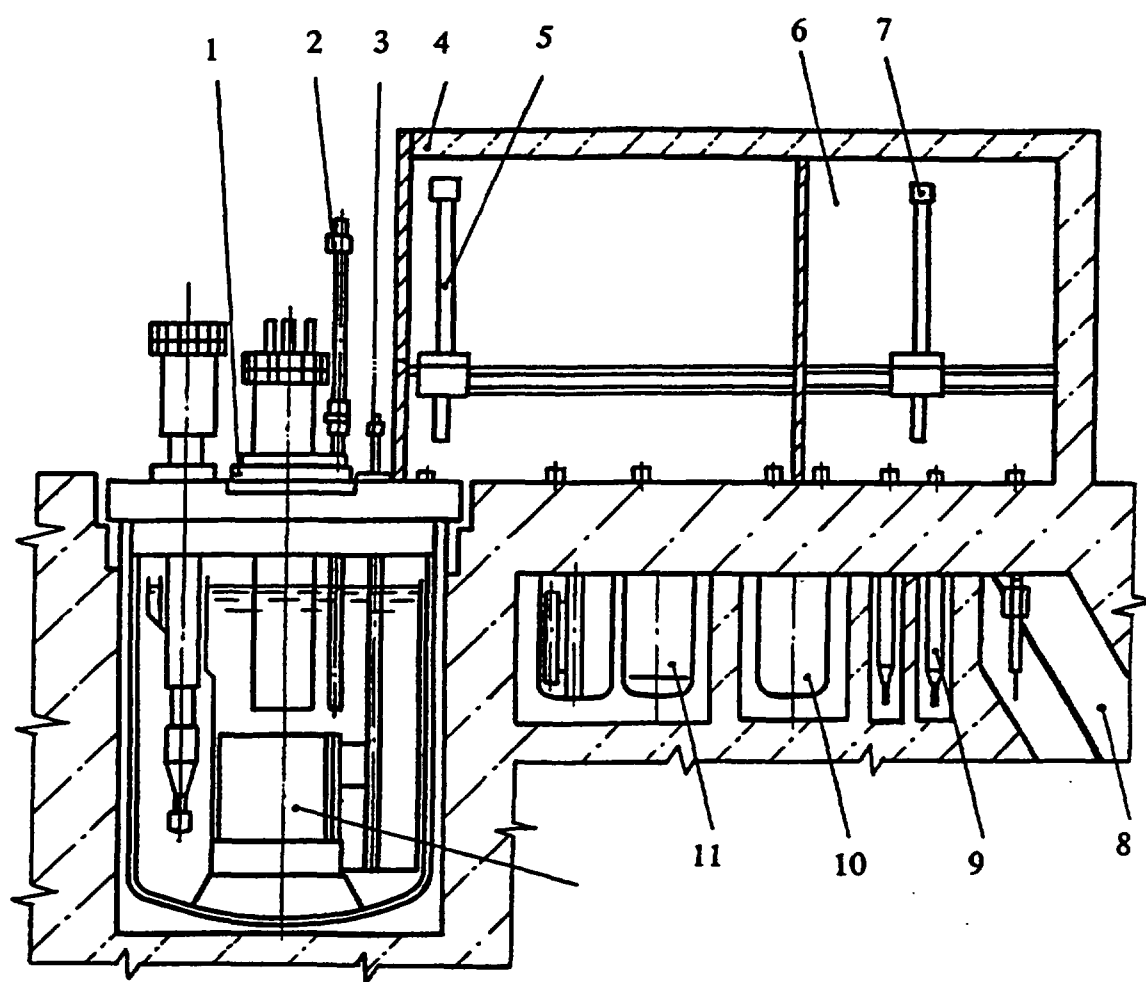
can be excluded in this design. Comparative mechanical analysis of bottom-support and top-suspension designs showed that they both meet the requirements for strength, but the top-suspension design gives the following advantages:

- better accessibility for in-service inspection of the outer surface of the reactor vessel thanks to the elimination of separating baffles between the main and guard vessels,
- more favourable operating conditions for the reactor vessel support in a gas environment (compared to sodium-immersed support),
- absence of a rigid link between the main and guard vessels giving the possibility of manufacturing the guard vessel from ferritic steel, and
- simpler solution of the problem of accommodating thermal expansion of the secondary system pipelines.

At the same time the top-suspended reactor has the complication of accommodating the thermal displacement of the primary coolant pressure pipes relative to the sodium pumps, taking into account the large temperature difference between the "cold" upper support slab (60°C) and the relatively "hot" (approx. 400°C) sodium pipes. To solve this it is necessary to use longer sodium pipes, or a greater number of small diameter pipes, or as a last resort to introduce movable items into the sodium pipes. Changing to the top-suspension design

allowed the optimization of the rotating shield plug structure (elimination of submersible steel sheets) and the intermediate heat exchangers (unit power increase and reduction of the heat-exchange tube wall thickness from 1.4 to 1.0 mm), and significant reduction of the reactor specific mass to approx. 2.5 t per MW(e) with a reactor vessel diameter of 17 m.

The refuelling system is only partially based on the choices proven by the operating experience of the BN-350 and BN-600 reactors. This is associated with the change to a new design of a fuel assembly and a desire to simplify the fuel transport route as much as possible. In particular, a sloping elevator has been substituted for a straight mechanism for transporting the FAs from the in-reactor store to the ex-vessel mechanism (Fig. 9.15). The ex-reactor portion of the refuelling system comprises a rectangular leaktight cell filled with noble gas and connected to the reactor through a refuelling penetration. The refuelling machine moves along the cell on rails. The fuel transfer air-lock through which spent FAs are transported to washing, and the new fuel drum, are both connected to the cell via penetrations equipped with gas gate valves. To reduce the mass of the reactor refuelling system it was decided to increase



1 - rotating shield plug, 2 - refuelling mechanism, 3 - elevator, 4 - refuelling cell, 5 - FA transfer mechanism, 6 - washing cell, 7 - FA transfer mechanism, 8 - duct for FA transfer to storage pool, 9 - washing seat, 10 - spent FAs drum, 11 - new FAs drum (2 pieces)

FIG. 9.15. Reactor refuelling complex scheme

the delay of spent FAs in the in-reactor store and to incorporate one or two rows of B_4C -filled assemblies between the reactor core and the store. Reduction in the residual power of unloaded FAs allows sodium-filled canisters and a spent fuel storage drum with its related auxiliary systems to be dispensed with. The overall result of all the design improvements in terms of specific metal mass of the reactor plant in general is 4.8 t/MWe.

The reactor unit is enclosed in a concrete well with a leak-tight steel liner. Above the reactor roof the liner is joined to a protective dome housing the Control Rod Drive Mechanisms (CRDMs), primary pump motors and in-reactor refuelling mechanisms. The secondary pipes are jacketed inside the dome. To replace a primary component the corresponding part of the dome has to be removed. A robust concrete containment building houses the reactor unit (Fig. 9.16). The DHR air coolers, secondary coolant pumps and steam generators are located in individual compartments outside the containment.

9.2.3. Reactor unit design

The integral reactor contains the core and the main primary system components arranged around the core in the sodium pool (Figs. 9.17, 9.18, 9.19). The core diagrid with the FAs and the in-vessel neutron shield is located in the lower section of the reactor vessel on the support structure which transmits the gravity loads to the bottom of the vessel. Below the diagrid there is a core catcher designed to confine and cool fuel debris in the event of a beyond-design-basis accident. The reactor pool is divided into "hot" and "cold" plena. The "cold" plenum serves as a common collector for the inlet nozzles of all three primary coolant pumps. There are no check-valves in the primary pumps, while the Intermediate Heat Exchangers (IHXs) can be isolated from the primary coolant flow by special movable devices (obturators).

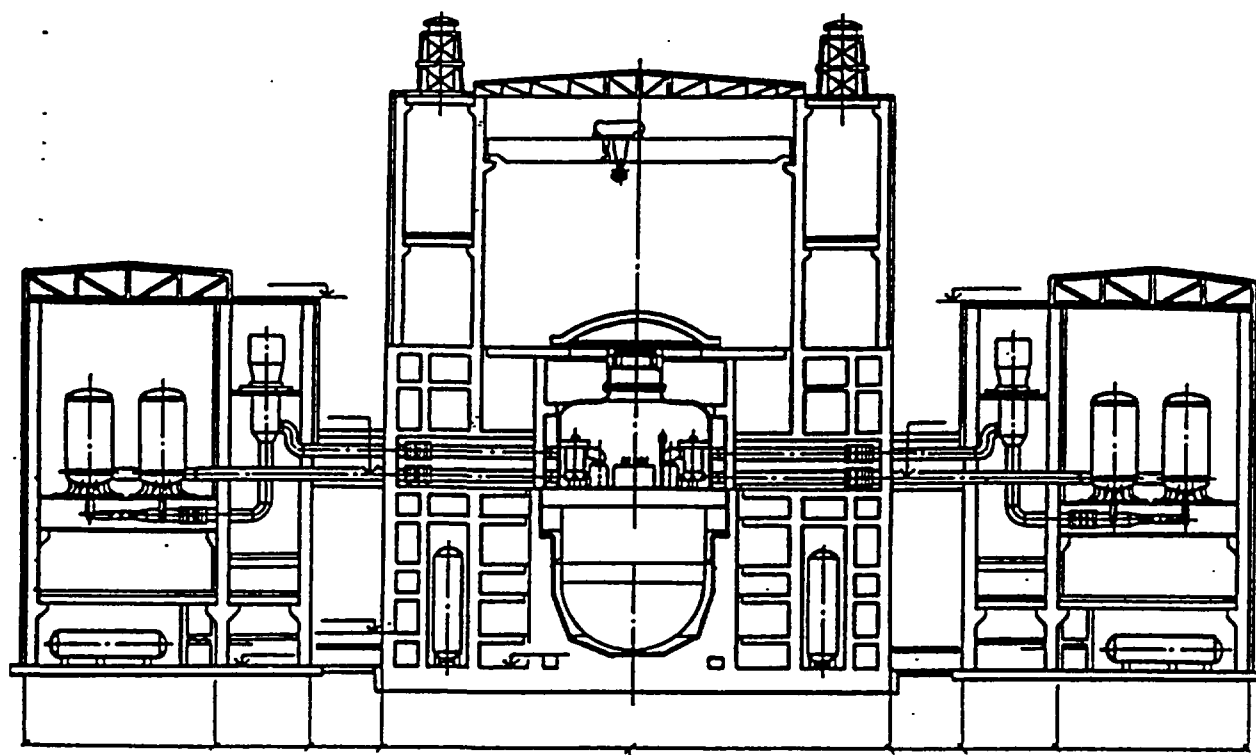
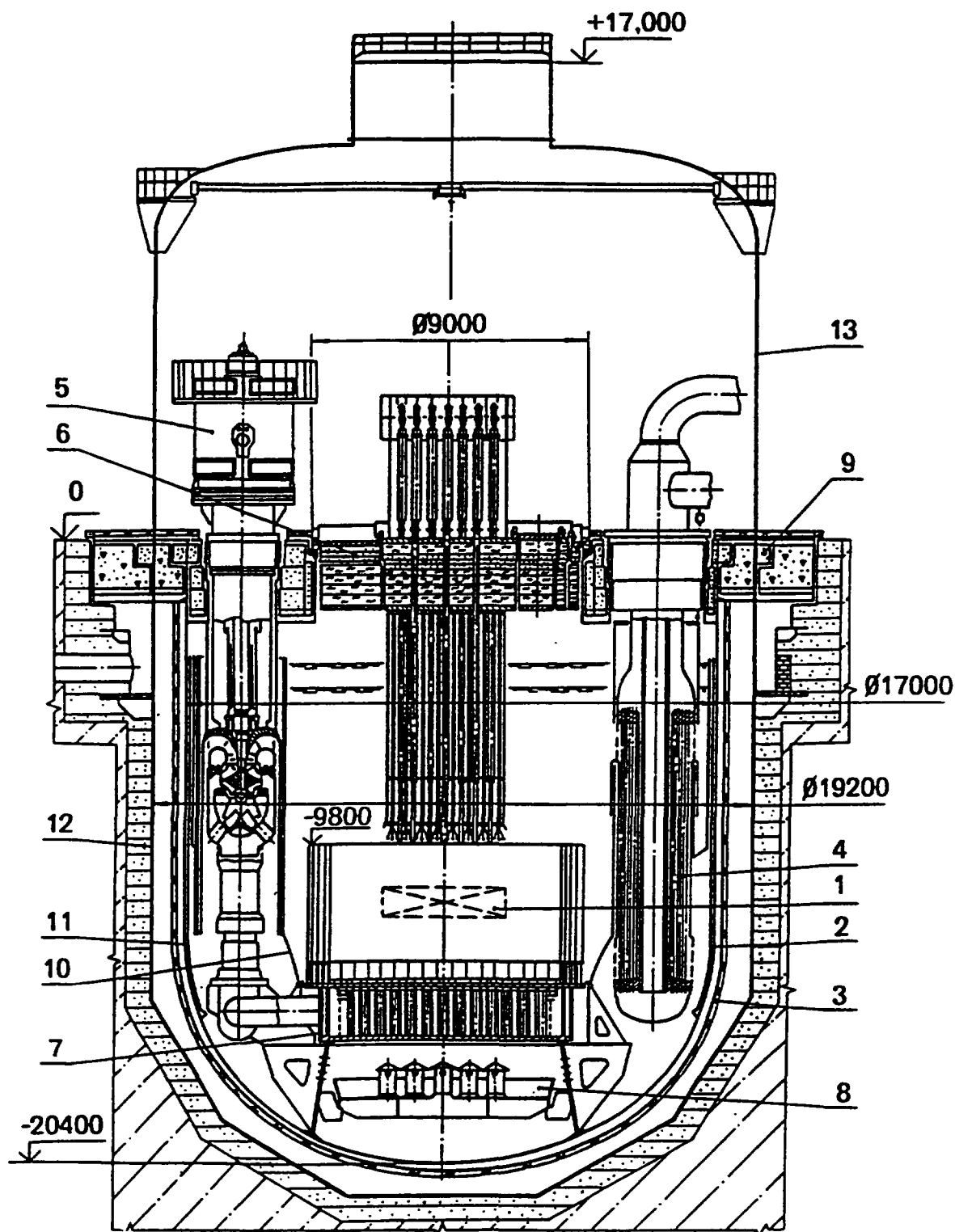
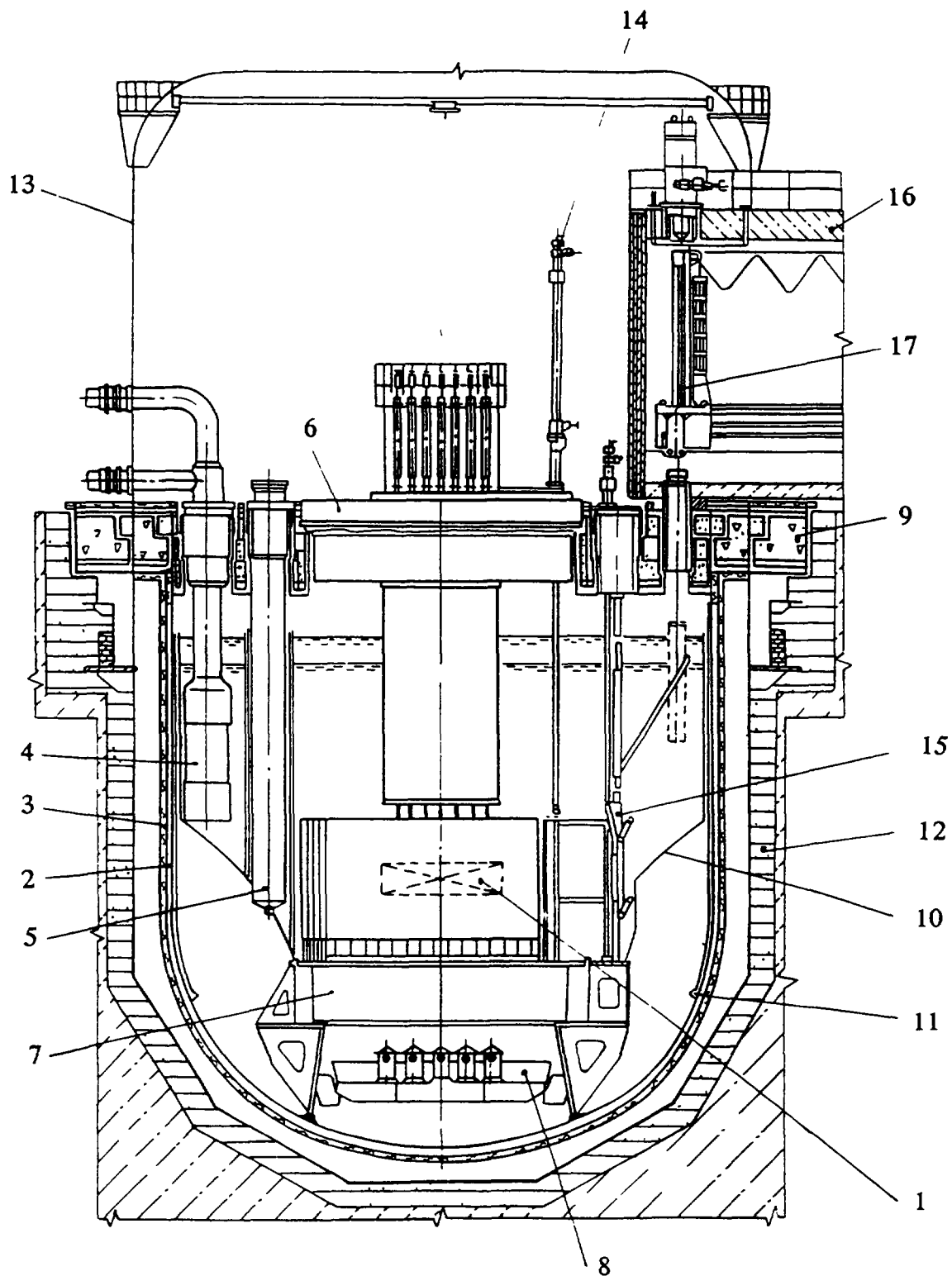


FIG. 9.16 BN-1600M power unit cut-away view (transvers)



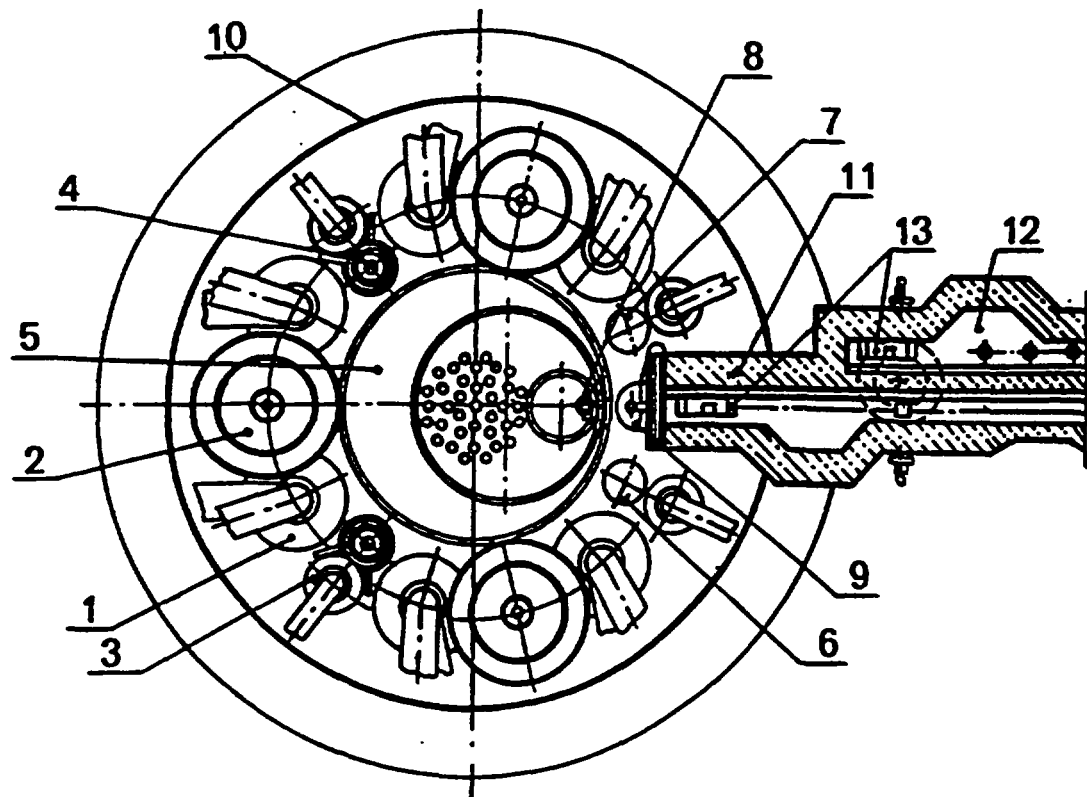
1 -reactor core, 2 - reactor vessel, 3 guard vessel, 4 - intermediate heat exchanger, 5 -reactor coolant pump, 6 - rotating shield, 7- core diagrid, 8 - core catcher, 9 - upper stationary shield slab, 10 - "hot" inner tank, 11 - baffle, 12 - well liner, 13 - protective dome.

FIG. 9.17. BN-1600M Reactor unit cut-away view
(through main primary system components)



1 - reactor core, 2 - main reactor vessel, 3 - guard vessel, 4 - ERHR submerged heat exchanger, 5 - cold filter-trap, 6 - rotating shield plug, 7 - core diagrid, 8 - core catcher, 9 - upper stationary shield, 10 - "hot" sodium collector, 11 - thermostabilizing baffle, 12 - well liner, 13 - containment, 14 - refuelling mechanism, 15 - elevator, 16 - refuelling cell, 17 - FAs transfer mechanism

FIG 9 18 BN-1600 Reactor unit cut-away view
(through refueling cell)



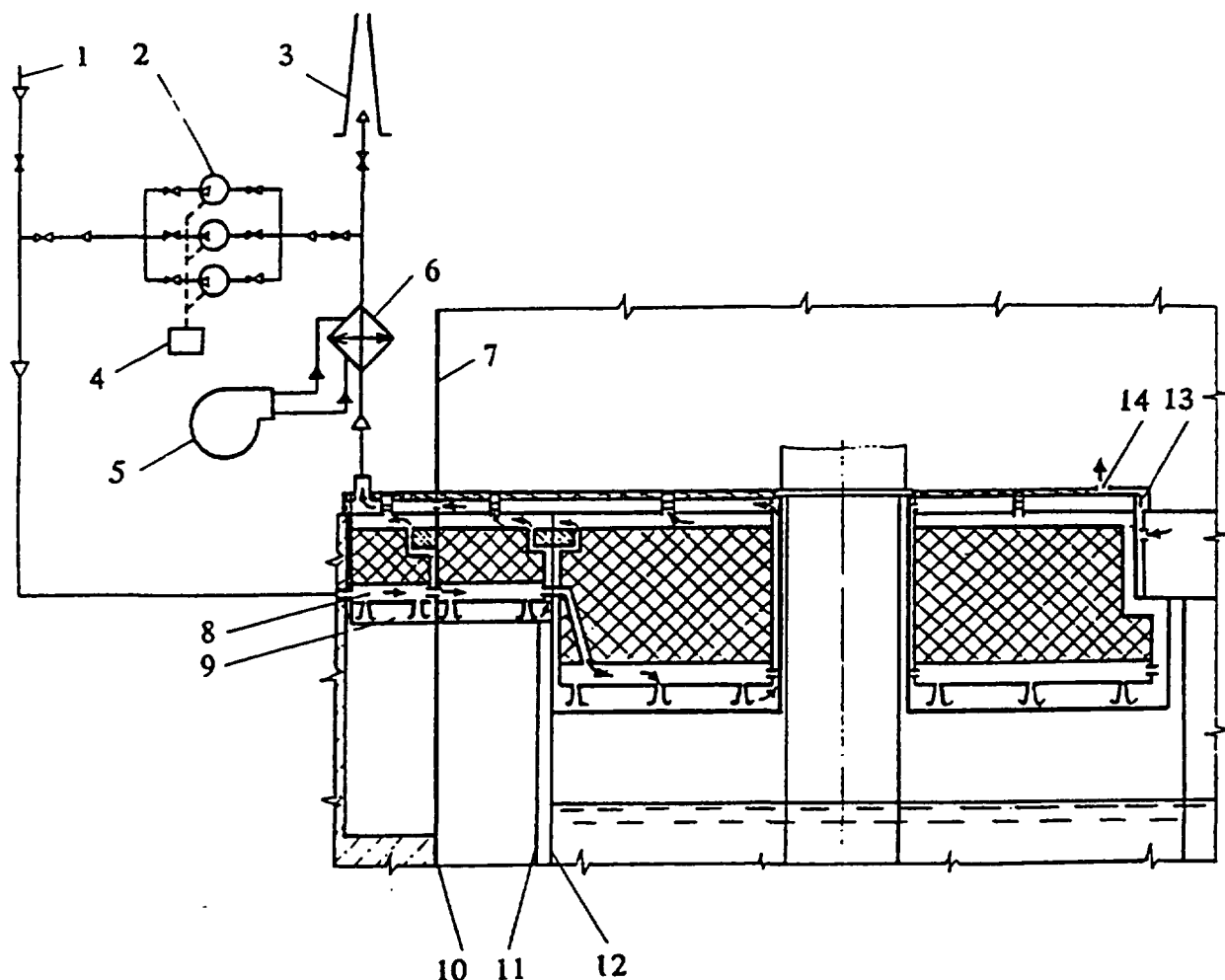
1- intermediate heat exchanger, 2 -reactor coolant pump, 3 - ERHR heat exchanger, 4 - cold filter-trap, 5 -rotating shield, 6 -penetration for caesium trap, 7 penetration for sodium quality control instrumentation, 8 -refuelling machine, 9 - elevator, 10 - protective dome (containment), 11 - fuel transfer cell, 12 - washing cell, 13 - fuel transfer mechanism.

FIG.9.19. BN-1600M Reactor unit (plan view)

The six IHXs and the primary coolant pumps are suspended from the reactor roof. The central penetration in the reactor roof accommodates a rotating plug that locates the refuelling machine and the control rods drive mechanisms in the appropriate positions relative to the core.

The reactor vessel is a vertical cylindrical tank 17 m in inner diameter and of total height 20.4 m with a toroidal-spherical bottom. The external guard vessel is identical in shape and encloses the reactor vessel. The annular gap between the vessels is chosen so as to ensure continuous circulation of the primary coolant through the heat exchangers if the integrity of the reactor vessel should be lost. The outer surface of the guard vessel is covered with steel foil thermal insulation.

The reactor vessel is cooled and thermally stabilized by "cold" sodium flow supplied from the core diagrid through the gap formed by the reactor vessel and a special baffle. A closed nitrogen cooling system is provided to assure the necessary temperature conditions in the upper-support roof items (Fig. 9.20). In case of a plant black-out it is possible to cool the reactor roof by air under natural convection.



1 - air forced ventilation, 2 - fan, 3 - vent stack, 4 -diesel generator, 5 - water circuit, 6 - air cooler, 7 - containment, 8 - gas collector, 9 - cooling plenum, 10 - reactor roof support, 11 - reactor guard vessel, 12 - reactor main vessel, 13 - rotating shield cooling gas outlet collector, 14 - rotating shield cooling gas outlet.

FIG. 9.20. BN-1600M Reactor roof cooling system

The goals of core development are to provide a negative sodium void reactivity effect, minimum reactivity margin for fuel burn up and sufficiently high fuel breeding gain. A flattened core with an upper sodium plenum, large diameter fuel rods and high volumetric fraction of fuel achieves these goals. For initial operation a core with oxide fuel and a breeding ratio of around 1.15 is being developed. A core with carbide and nitride fuels capable of providing a breeding ratio of approximately 1.4 and a reactivity margin for fuel burnup of the order of β_{eff} is proposed for the next period of operation. The core contains 474 fuel assemblies (FAs), forming two zones of different fuel enrichment, i.e. a low fuel enrichment zone comprising 258 FAs and a high enrichment zone comprising 216 FAs. The radial blanket consists of one row of 84 FAs, surrounded by four rows of radial shielding assemblies protecting the in-reactor store which accommodates spent FAs during a delay of two fuel cycles. The fuel assembly is a 184x3.5 mm hexagonal duct which contains a bundle of 331 fuel rods of 8.5 mm outer diameter if oxide fuel is used, or 271 fuel rods of 9.5 mm OD if carbide or nitride fuel is used. The maximum heat rating of the fuel rods is 50 kW/m and 60 kW/m

respectively. The active height of the fuel in the rod is 750-800 mm. In the lower section of fuel rod there is an axial blanket made of depleted UO_2 350 mm long, and above the top of the fuel there is a sodium-filled plenum and an upper shield made of boron carbide.

There are 37 control assemblies including 25 reactivity-compensating assemblies moved by individual electric drives and 12 absorber assemblies for reactor scram in emergencies. Some of them are dropped into the core by de-energization of the electromagnets which hold them, and the others are moved into the core by gravity. The control rod drive lines include fuses or magnets ensuring self-actuation of the rods when the primary sodium temperature at the core outlet rises to a trip level (100°C above the normal temperature for fuses, or the Curie point for the magnets). All the CRDMs (Fig. 9.21) have the same dimensions and are able, besides operating the related control assembly, to lift the gripper guide tube before reactor refuelling lower it after completion of refuelling.

Two nitrogen-cooled cold-traps for primary sodium purification are incorporated in the reactor vessel (Fig. 9.22). Sodium is fed to the filtertrap by an electromagnetic pump from the "cold" plenum of the reactor. It is possible to replace the filter-traps.

There are four independent DHR channels. Each is composed of the following items:

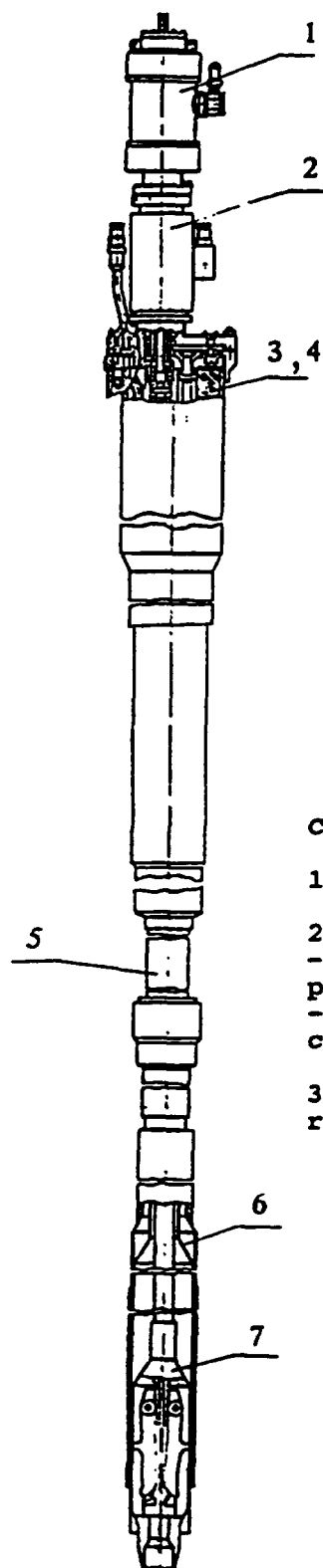
- an independent sodium/sodium heat exchanger (ISHX) immersed in the reactor coolant pool,
- a Na/air cooler with air dampers,
- a ventstack providing draught for air flowing through the cooler, and
- sodium piping.

There are no pumps or sodium valves in the system. There is only one active component in the DHR system, namely the air damper in the cooler. When the system is in a standby mode the dampers are partially closed to let air to pass through the cooler with a flow rate of approximately 10% of the nominal value. The DHR channel is activated for maximum capacity by complete opening of the air dampers. The DHR system is activated by the following initiating events associated with loss of capability to remove residual heat through the SGs:

- off-site power loss,
- loss of feed water supply to all SGs, and
- seismic impact.

In the event that the electric drives fail to actuate the dampers there is difficulty with manual opening, an emergency passive drive could be provided. It would be based on natural effects such as gravity and a "shape-memory" effect in special alloy structural materials manifesting itself as temperature changes. The passive drive could be installed in the reactor sodium pool or in the expansion tank of the air cooler. It would actuate as the primary sodium temperature approached 600°C.

The DHR design capacity is determined taking account of the heat capacity of the primary sodium and the reactor metalwork. The ultimate temperature of the reactor vessel is limited to 650°C, at which the vessel still retains its performance on a temporary basis. The resulting heat removal capacity of one DHR channel is 27.5 MW. Two design options for the DHR system are under consideration, distinguished by the ISHX arrangement in the reactor pool. In the first the ISHXs are disposed in the "hot" plenum and suspended from the upper

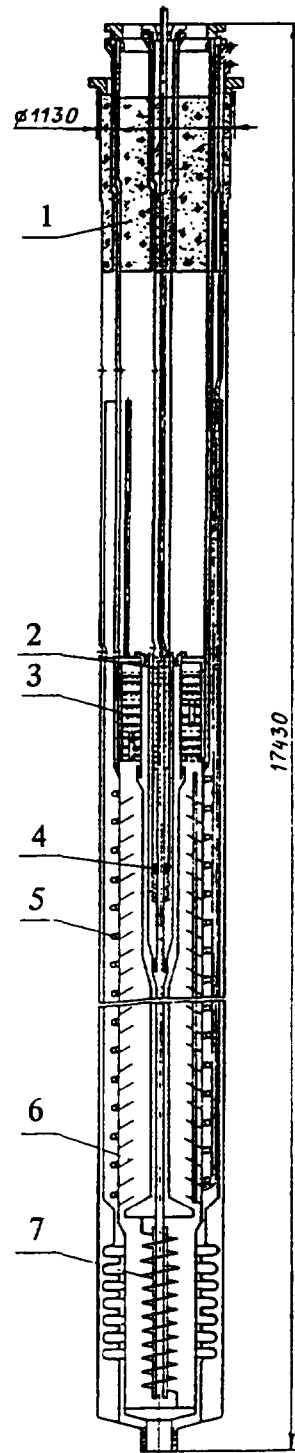


CRDM Characteristics:

1. Grip stroke	1000mm
2. Travelling speed:	
- for emergency protection mechanism	2mm/s
- for reactivity compensetion mechanism	5mm/s
3. Emergency protection rod insertion time	1 s

1 - motor, 2 - controlling couplings, 3,4 -grip moving and control drives.
5 - drive line tube, 6- grip guide tube, 7- grip.

FIG. 9.21. BN-1600M Control and protection system actuator

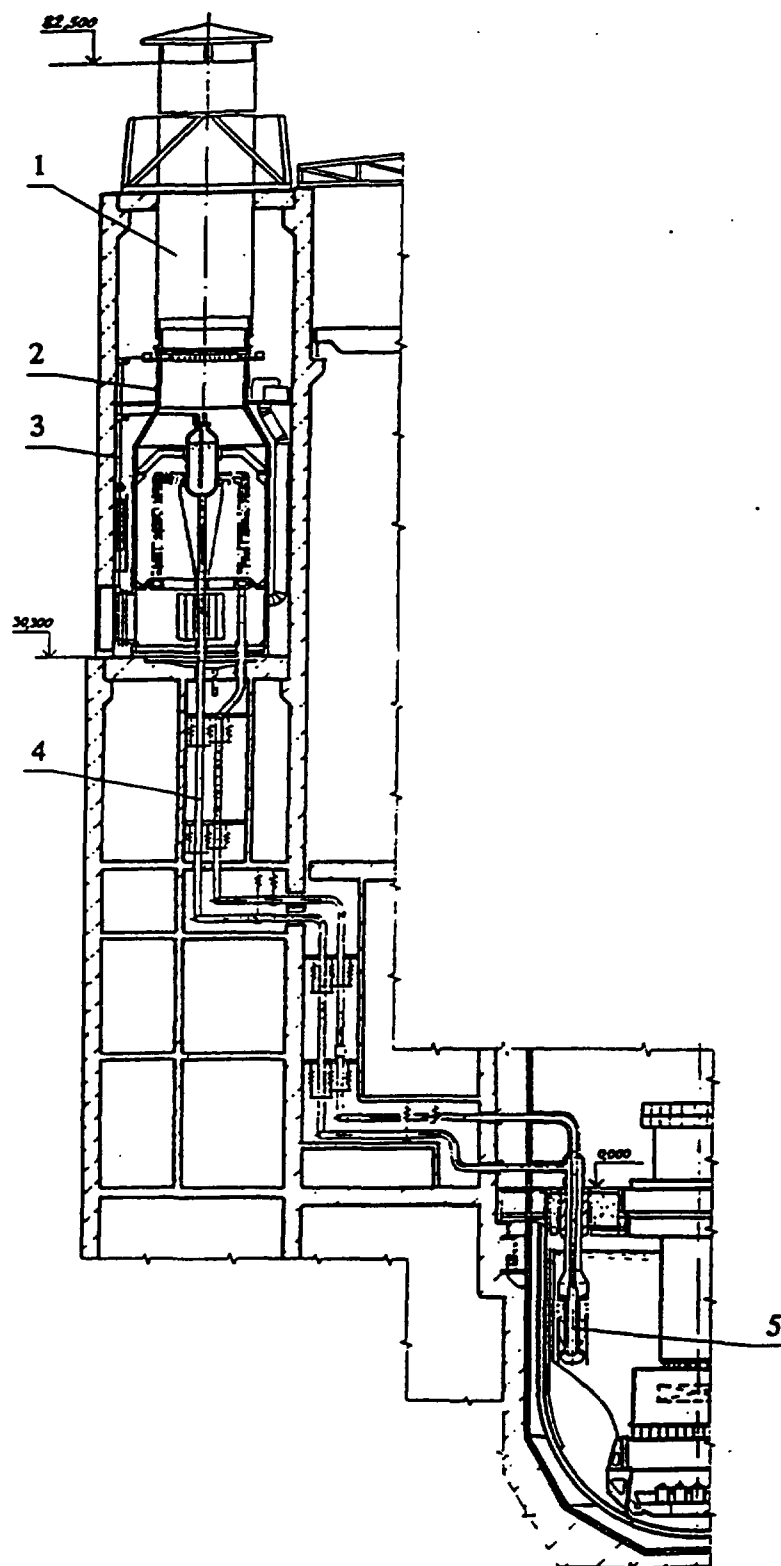


1 - biological shield, 2 - electromagnetic pump, 3 - metallic wool filter, 4 - flow meter, 5 - sodium/nitrogen heat exchanger, 6 - impurities accumulator, 7- recuperator.

FIG. 9.22. BN-1600M Cold filter-trap

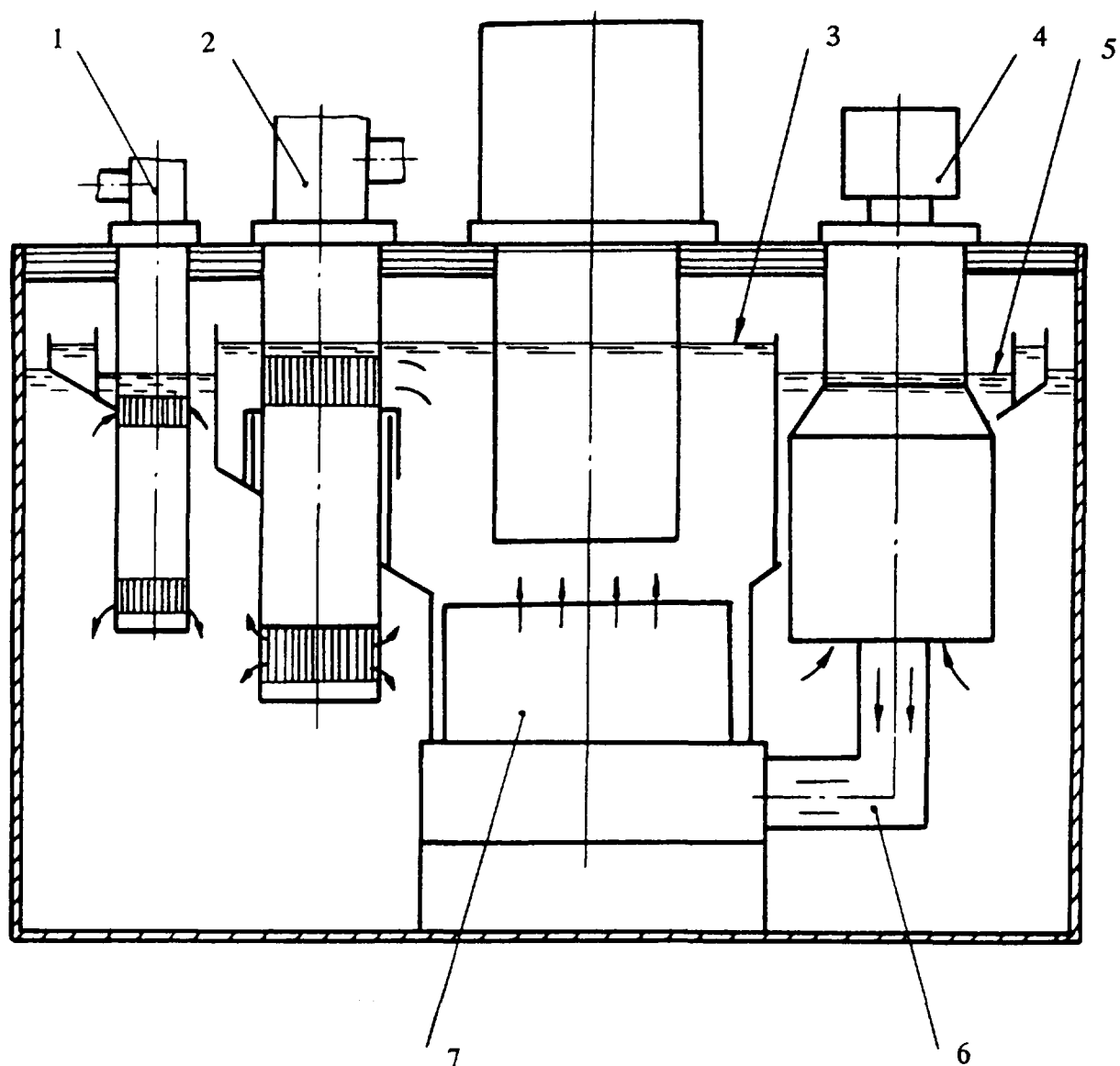
stationary shield slab (Fig. 9.23). The inlet openings are located below the reactor coolant level so that in a loss-of-coolant accident sodium circulation through the ISHXs would not be interrupted.

In the second design the ISHXs are located in a fenced-off plenum of the cold pool (similar to the reactor coolant pumps) and primary coolant enters them downstream of the intermediate heat exchanger (Fig. 9.24).



- 1 - stack, 2 - air cooler, 3 - passive drive, 4 - sodium pipelines,
5 - submerged heat exchanger

FIG. 9.23. BN-1600M ERHR system with HX in "Hot" plenum



1 - ERHX submerged heat exchanger, 2 - intermediate heat exchanger, 3 - "hot" coolant plenum, 4 - reactor coolant pump, 5 - "cold" coolant plenum, 6 - pressure sodium pipe, 7 - reactor core.

FIG. 9.24. BN-1600M ERHR system with HX in "Cold" plenum

9.2.4. Reactor plant safety

Enhanced safety of the reactor plant is ensured by realization of basic safety principles such as:

- defence-in-depth,
- self-protection,
- protection in case of accidents,
- tolerance to personnel errors,
- resistance to common cause failures,
- protection against external impacts, and
- accident management.

Self-protection means that the reactor plant is capable of preventing damage to physical protective barriers in emergency situations in the event of failure of active safety systems and non-intervention or errors by the plant personnel, by virtue of passive safety systems and inherent safety features based on the action of physical laws of nature which result in self-limitation of the reactor power and temperature.

The inherent safety of the reactor plant relies upon the following features:

- negative temperature and power reactivity coefficients over the entire range of the reactor plant parameters,
- large heat capacity of the primary circuit of the integral reactor,
- low pressure of the coolant with no pressure build-up in emergency situations due to the protective gas plenum in the upper part of the reactor vessel and the passive depressurization system connected to this plenum,
- high natural convection capability of the reactor plant loops provided by the thermal-physical properties of sodium and by the optimum layout of primary and secondary components,
- minimization of the core reactivity margin by virtue of high breeding in the core, and
- absence of positive reactivity excursions in emergencies including those with sodium loss from the core (negative sodium void reactivity effect).

The wide spectrum of self-protective properties inherent to fast reactors in general, together with passive means of reactor scram and decay heat removal which minimize probability of accident initiators, prevent the development of emergency situations into design basis accidents and further progress to beyond-design basis accidents. These properties and features allow even more stringent requirements for NPP safety than those established by the current regulations to be met:

- 1) radioactive discharges in normal operation at least one order of magnitude lower than the specified limits, and
- 2) equivalent radiation doses to an individual at the boundary of the safety restricted zone and beyond it do not exceed the following values: 0.02 mSv per year in normal operation and violations of normal operation conditions; 10 mSv in design accidents; and 50 mSv per year in beyond-design accidents.

The elimination or at least minimization of the positive coolant density component of the temperature reactivity effect is a favourable factor in limiting the consequences of ULOF and UTOP. The negative reactivity feedback caused by a thermal expansion of the control rod drive lines also plays an important role. Analysis of a ULOF accident shows that sodium boiling and fuel melt are excluded because the core outlet temperature does not exceed 800°C. Nevertheless a refractory sodium-cooled tray beneath the core is provided to prevent release of corium beyond the reactor vessel boundary and formation of a critical mass. Preliminary safety analysis for the BN-1600M reactor plant shows that:

- the frequency of severe core damage or melting does not exceed 1.E-6 per reactor-year, and
- the frequency of beyond-design accidents with radiological consequences corresponding to those given above does not exceed 1.E-7 per reactor-year.

9.3. BN-800 REACTOR PLANT

9.3.1. Design status

The BN-800 reactor is designed to be utilized in unified power units for the South-Ural and Belojarsk nuclear power stations in the Cheljabinsk and Sverdlovok regions of Russia respectively. The detailed design of the reactor plant was completed in the 1980s and fabrication of individual components was begun, as well as preliminary construction activity on both sites. But later the construction work was suspended due to financial shortages and protests by the local population. However, research and development activity was continued aimed at design features for further improvement and upgrades in compliance with regulatory development. The design of a nuclear power station with BN-800 reactors has been considered by the Commission for Ecological Safety Review of the State Department of Nature, by the independent group of the Academy of Science, and by other authorized safety review institutions including the State Regulatory Body (Gosatomnadzor), and has been acknowledged to be safe from the ecological and nuclear standpoints, while the reactor itself was recognized as corresponding to the present world level of nuclear science and technology. All the review reports contained the recommendation to resume construction.

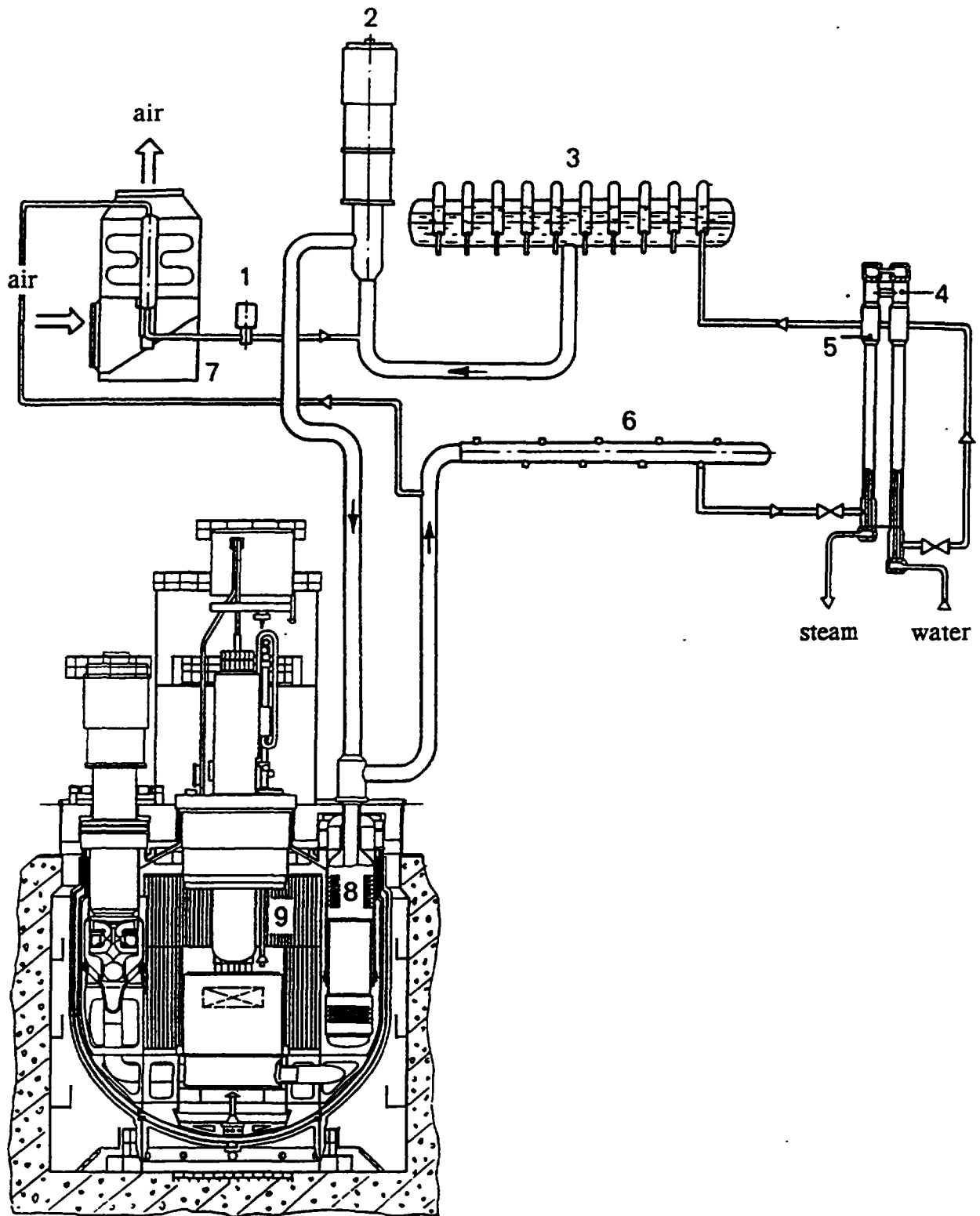
9.3.2. Reactor design basis

The BN-800 design has been developed by upgrading the reactor prototype BN-600, aiming at creation of a highly reliable and safe nuclear reactor relying to the maximum feasible extent on proven structural and technological choices and on equipment items verified by operating experience. In the development of the design particular attention was paid to enhancement of the reactor plant safety in compliance with up-to-date safety regulations, and also to reduction in capital and operational costs. With these objectives in mind the following main technical tasks were defined and design decisions were adopted. These are the distinctive features in comparison with the reactor-prototype BN-600.

- (1) The BN-800 power unit was designed to take account of such external impacts as earthquakes and other external natural phenomena (eg tornados), aircraft crashes and shock waves.
- (2) Independent safety systems have been provided in conformity with the "loop principle" ensuring that each loop is self-sufficient with respect to operating control, power supply and technological links.
- (3) The residual heat removal function is provided by a special emergency system through "sodium/air" coolers connected to each secondary loop, thus excluding the steam generators and tertiary circuits from the safety-grade systems.
- (4) The design of the main and auxiliary equipment and their technical features have been improved on the basis of the BN-600 construction and operating experience and of the latest R&D results.
- (5) Advanced fire-fighting systems have been incorporated.

9.3.3. Reactor design concept

Like the reactor-prototype BN-800 has a three-circuit flow scheme with sodium coolant in the primary and secondary systems and water-steam in the tertiary circuit (Fig. 9.25). The reactor plant comprises the fast nuclear reactor with three primary loops, three secondary loops and three steam generators of sectional-modular type. The reactor uses the



1 - ERHR electromagnetic pump, 2 - secondary coolant pump, 3 - secondary coolant expansion tank, 4 - evaporator module, 5 - superheater module, 6 - secondary sodium distributing header to SG, 7 - ERHR air cooler, 8 - intermediate heat exchanger, 9 - reactor.

FIG. 9.25. BN-800 principal flow diagram

same integrated layout as the reactor-prototype the reactor core, coolant pumps, main primary coolant pressure pipes, intermediate heat exchangers and radiation shield are enclosed in the main reactor vessel (Fig 9 26) The primary coolant flows through three parallel internally-arranged loops each comprising two heat exchangers, a submerged double-suction centrifugal circulating pump and pressure pipes The pumps are fitted with check valves The reactor core and radial blanket are built up of fuel assemblies having similar size hexagonal ducts (Figs 9 27, 9.28). The reactor vessel is a cylindrical tank with a toroidal-conical spherical bottom and a conical roof The conical and spherical parts of the vessel bottom are joined by the ring which supports the reactor vessel through a bearing unit on a circular shell welded to a foundation support in the reactor well (Fig. 9 29) The ring carries a box-shaped support belt that functions as the main load-bearing structure within the reactor vessel The support belt is designed to take gravitational loads from the core diagrid with the fuel assemblies and the primary neutron reflector, the lateral and lower primary shields, the thermal baffles, the six IHXs and the three primary pumps The pumps and heat exchangers (Fig 9 30) are mounted in cylindrical casings installed on the support belt.

Six nozzles are provided in the reactor roof to receive the heat exchangers and three for the pumps Bellows are provided to accommodate the thermal expansion differences between the flanges of the support casings and the nozzles The reactor vessel walls are cooled by sodium delivered from the core diagrid The radiation shield consists of steel cylindrical baffles, steel blanks and graphite-filled tubes The main reactor vessel is enclosed in the external guard vessel The difference in the temperature displacements between the two vessels is accommodated by a bellows mounted on the necks of the vessels and by the toroidal expansion joint in the conical roof of the reactor vessel The reactor vessel top serves to support the rotating plugs (large, medium and small) which allow the refuelling mechanism to be located above the fuel assemblies These plugs also serve as an upper radiation shield

The fuel assemblies are loaded and unloaded by an integrated mechanical system comprising the refuelling mechanism mounted on the small rotating plug, two loading/unloading elevators, a rotating refuelling machine housed within a leak-tight cell and two storage drums for new and spent fuel assemblies, respectively (Figs 9 31, 9 32)

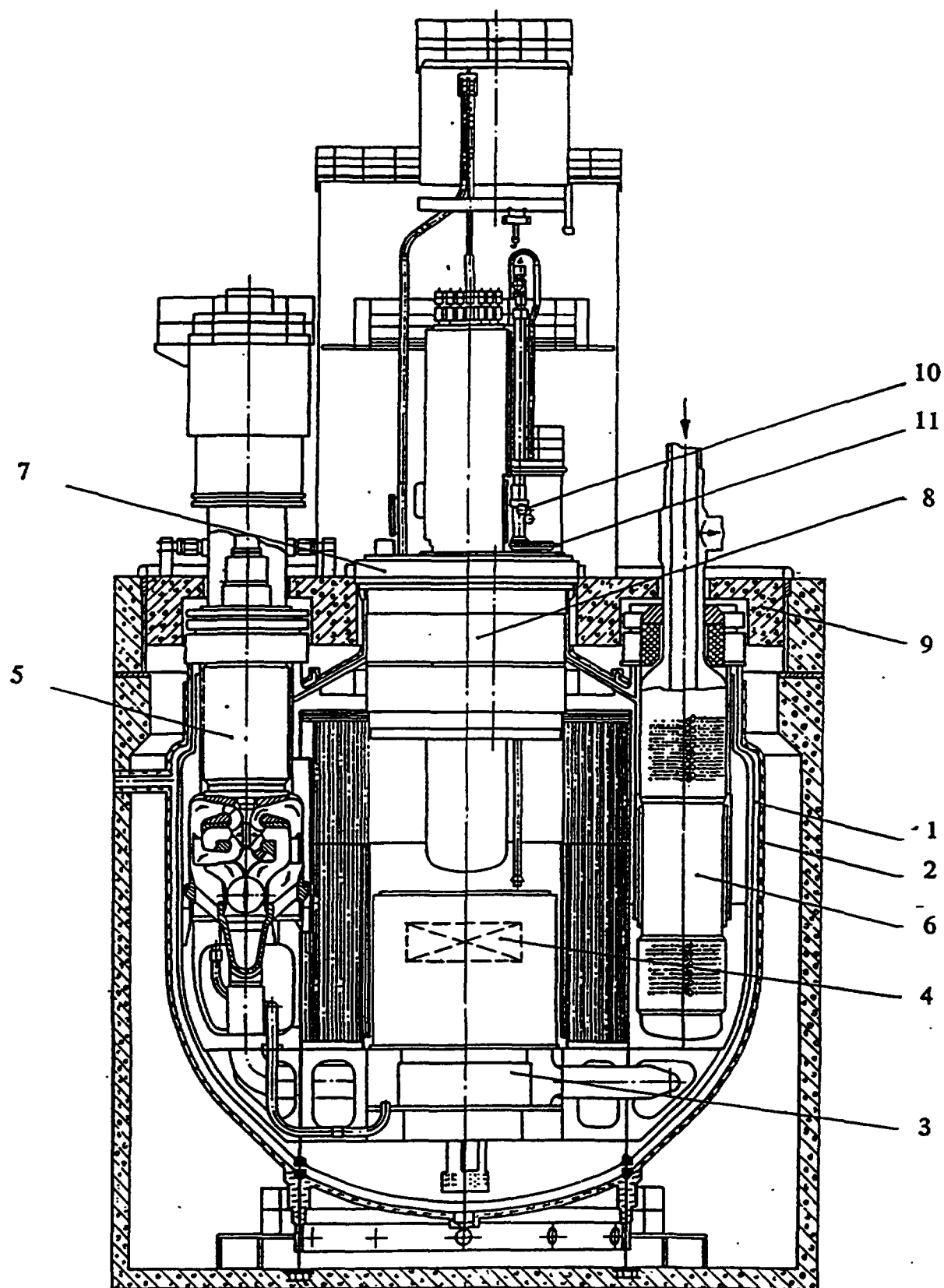
9.3.4. Main design improvements and reactor plant features

According to the main objectives and tasks adopted the following are the major development features of the BN-800 design.

Improved economic and operational performance This objective has been reached by means of a 47% increase in the reactor thermal power (compared to the reactor-prototype BN-600) due to larger core volume, utilization of MOX fuel, and changes in the operating parameters. While reduction of thermal parameters caused a certain deterioration of the plant thermal efficiency (down to 39.5% compared with 41.7% for BN-600), simplification and easier operating conditions for the tertiary system components have allowed the reliability of the plant to be enhanced and its operating performance indicators to be improved. A breeding ratio of around 1.0 is considered sufficient taking into account that in the present phase of nuclear power development in Russia there is no need for expanded production of plutonium. The breeding ratio could be increased if necessary.

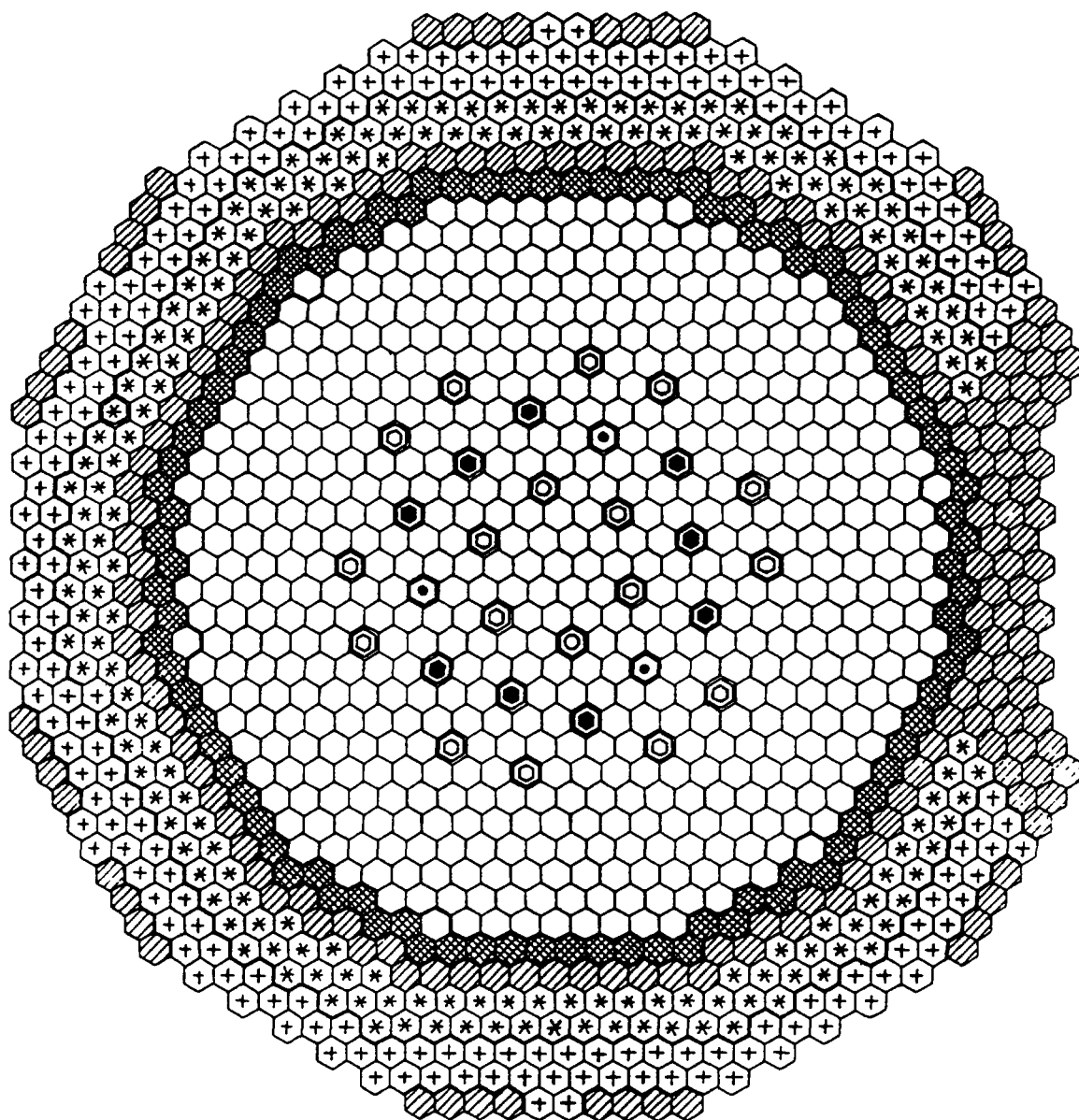
Enhanced reliability of components and extension of their operating life In the BN-800 design the reactor vessel supports (Fig.9.26) are nearer the reactor axis than in BN-600,

Text cont on p 440



1 - main reactor vessel, 2 - guard vessel, 3 - core diagrid, 4 - reactor core, 5 - reactor coolant pump, 6 - intermediate heat exchanger, 7 - large rotating plug, 8 - above core structure, 9 - upper stationary shield, 10 - refuelling mechanism, 11 - small rotating plug.

FIG. 9.26. BN-800 Reactor unit cut-away view
(through main equipment)












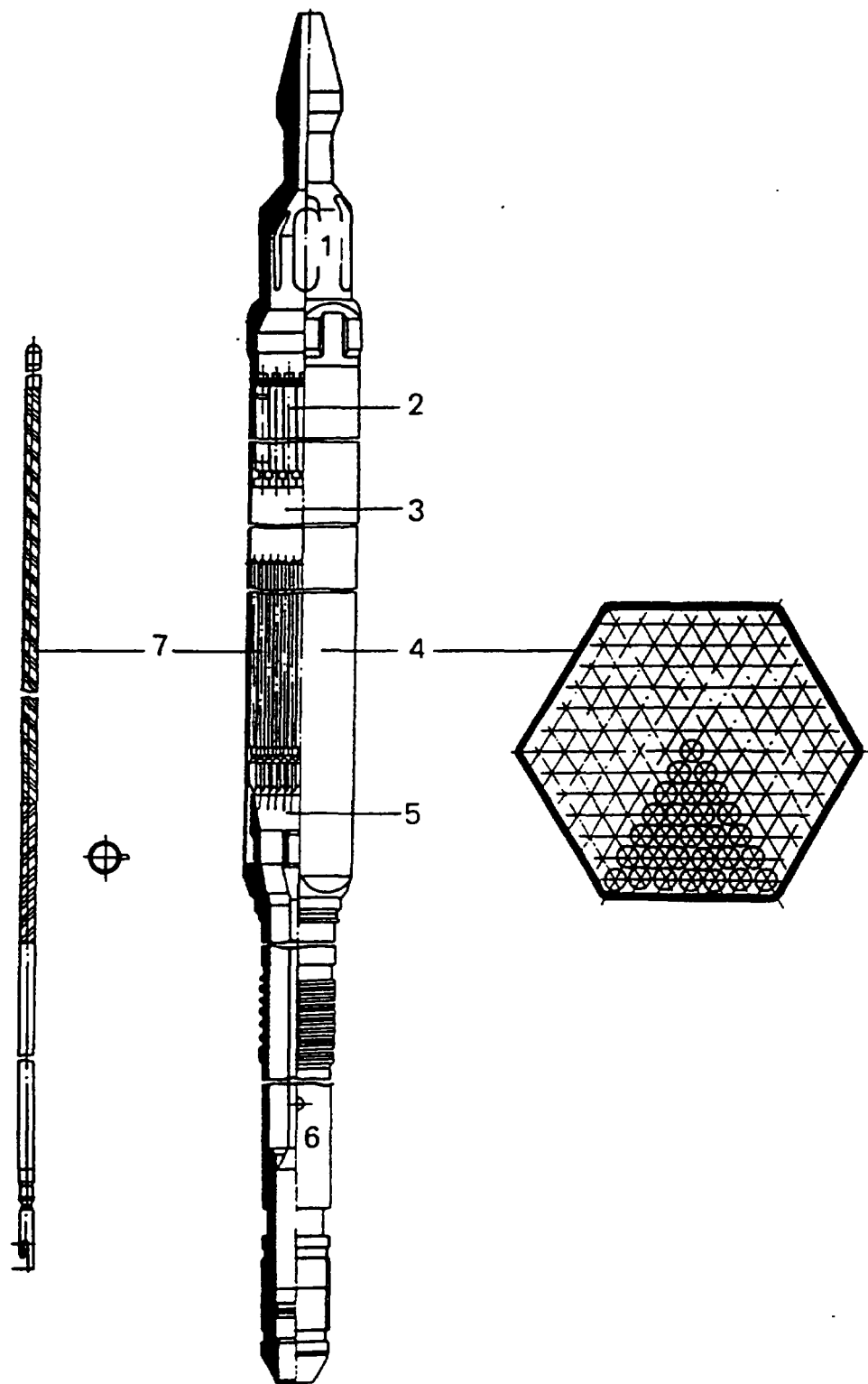
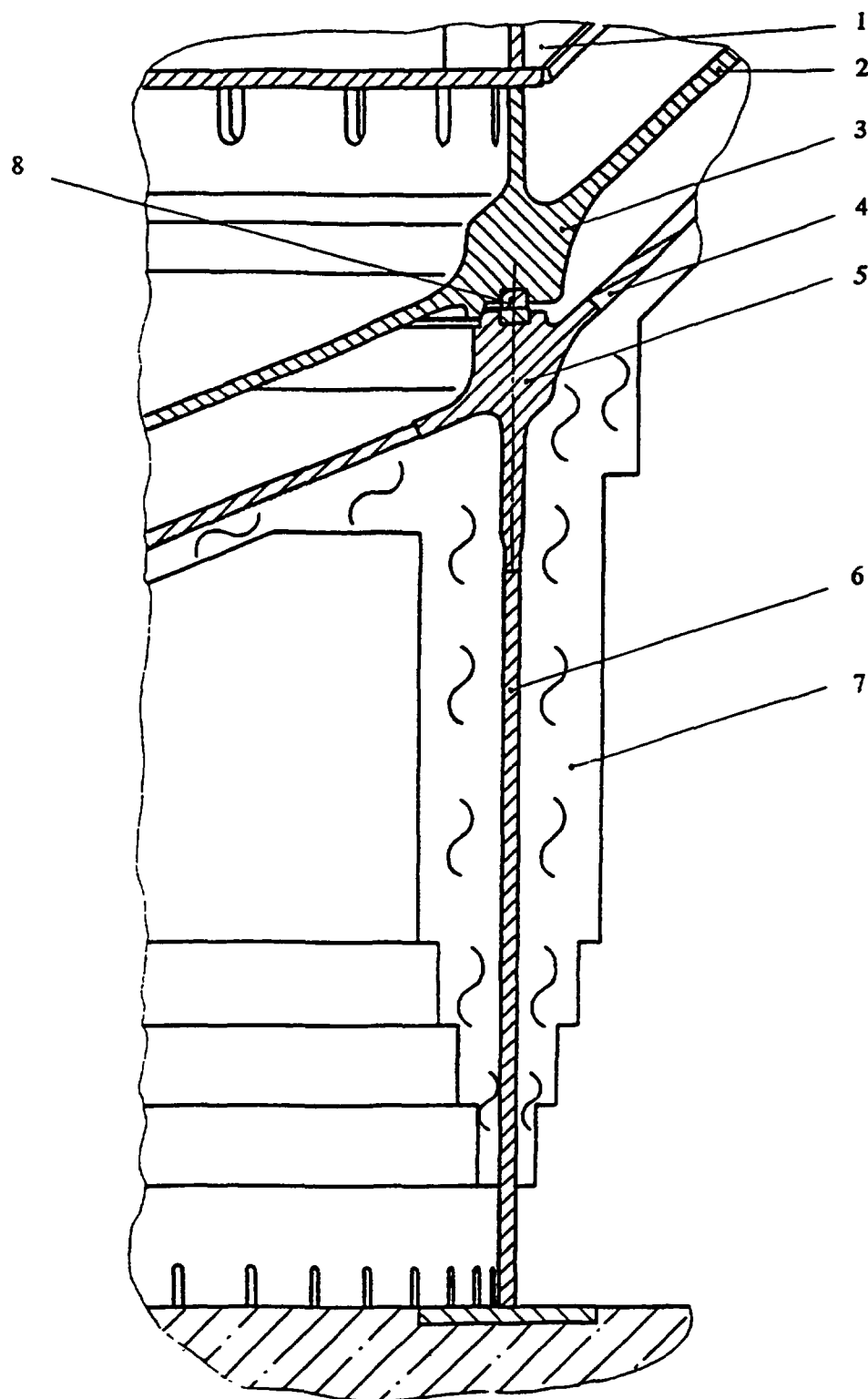
-  Core FAs
-  Radial blanket FAs
-  Steel shielding assembly
-  Boron shielding assembly
-  Passive emergency protection rod
-  Reactivity compensating rod
-  Control rod
-  Emergency protection rod
-  In-vessel store seats

FIG. 9.27. BN-800 core layout



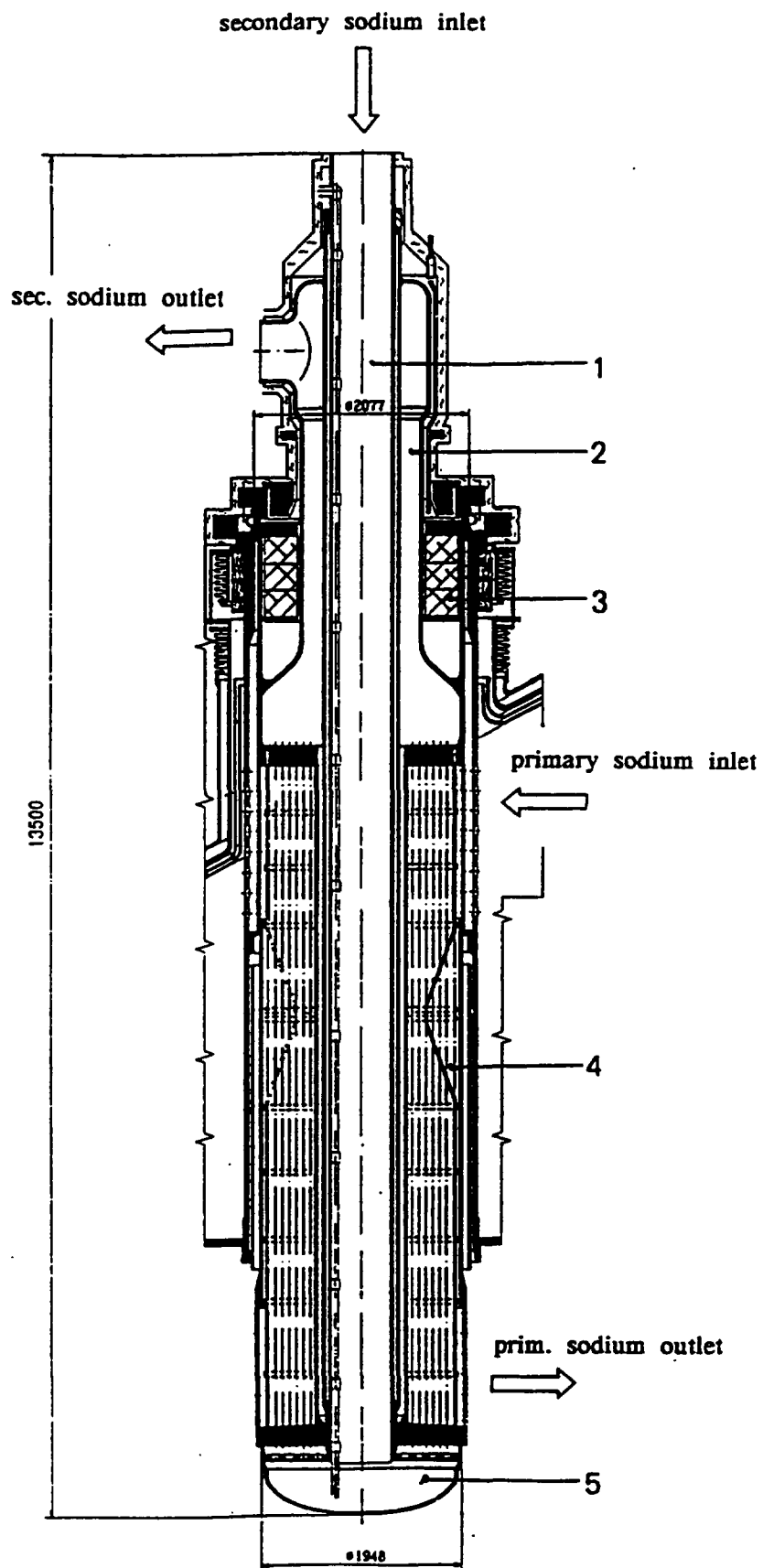
1 - upper end fitting, 2 - boron carbide rod, 3 - sodium interlayer, 4 - duct, 5 - grid, 6 - lower fitting, 7 -fuel rod.

FIG. 9.28. BN-800 fuel assembly



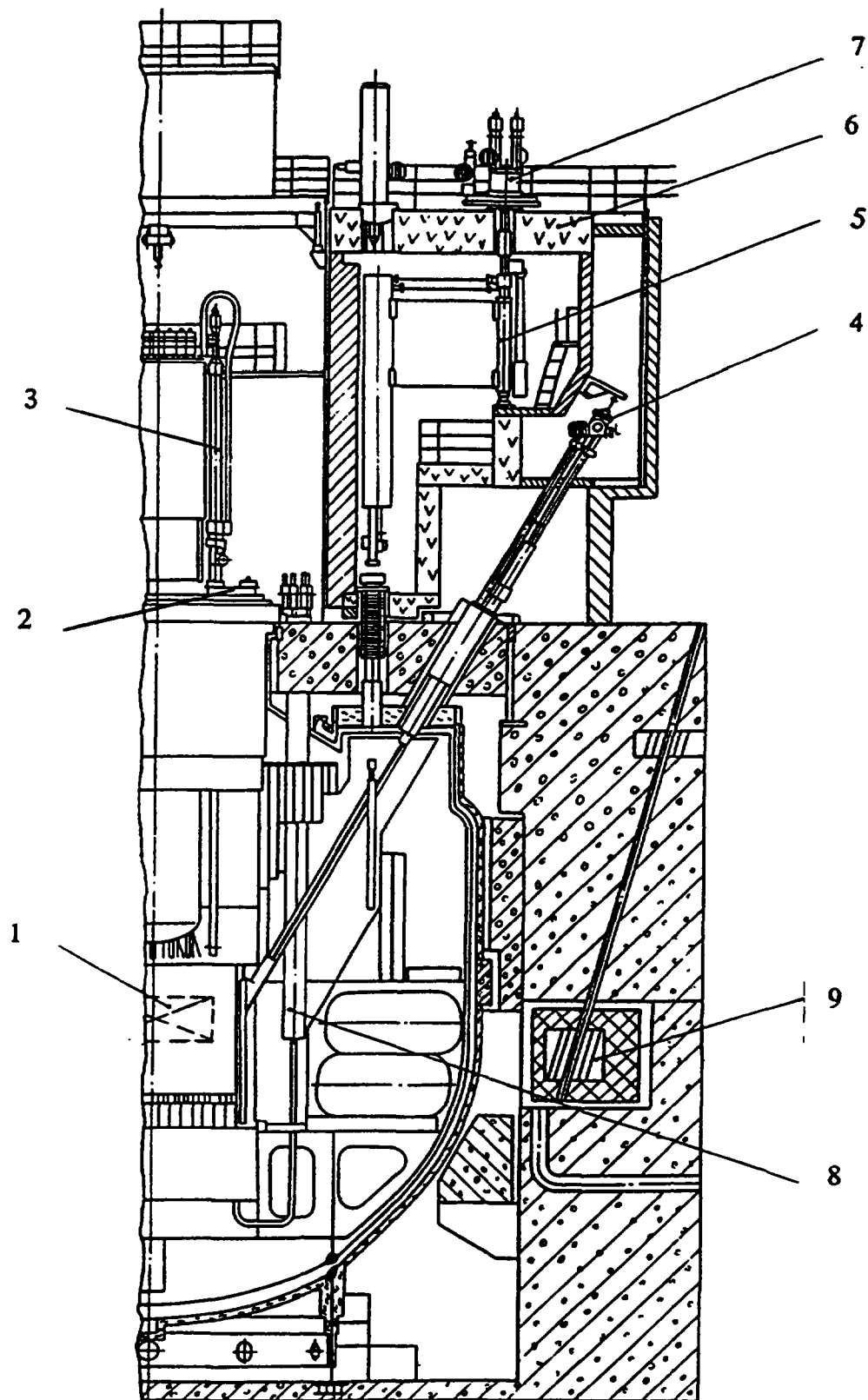
1 - support belt, 2 - reactor vessel, 3 - reactor vessel support ring,
 4 - guard vessel, 5 - guard vessel support ring, 6- support shell, 7 - thermal
 insulation, 8 - support inserts.

FIG. 9.29. BN-800 Reactor bottom support



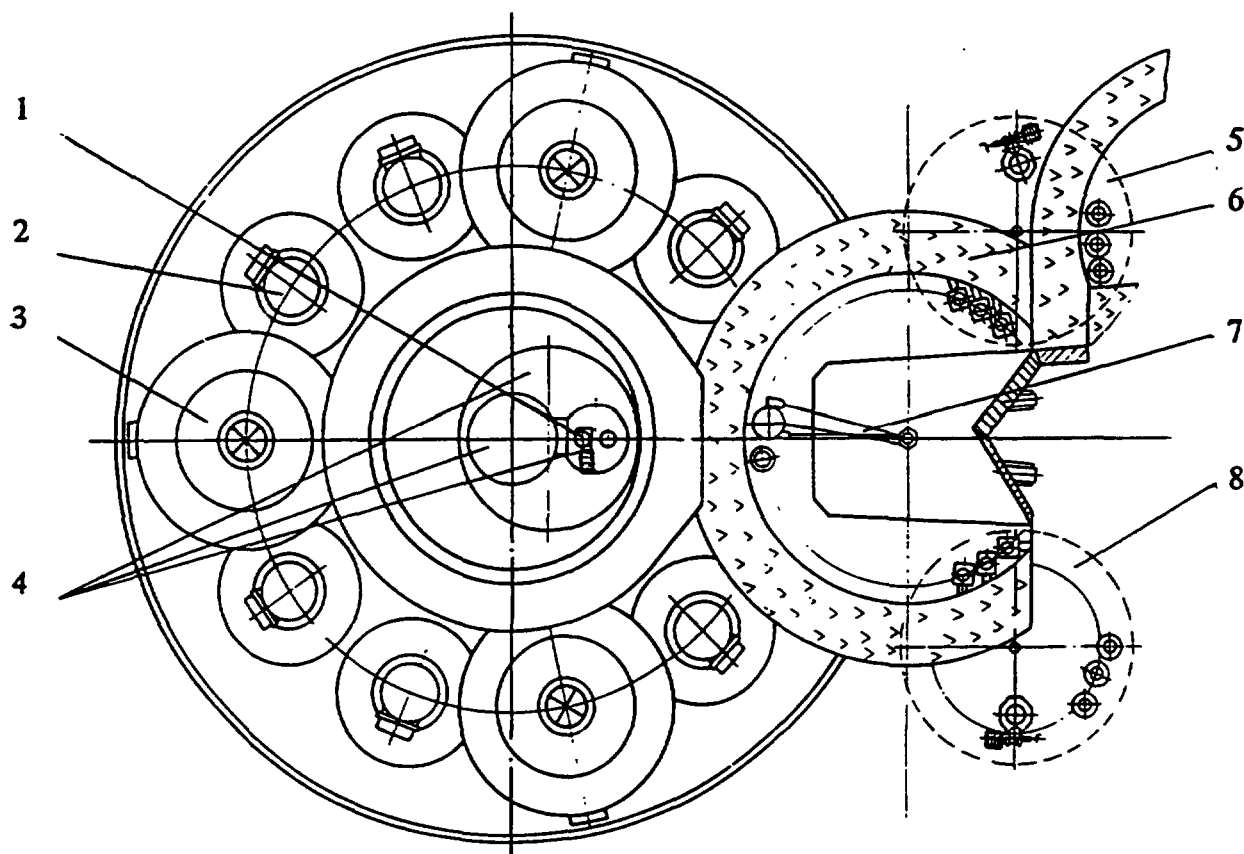
1- central downcomer tube, 2 - secondary sodium outlet chamber, 3 - shielding block, 4- heat exchange tube, 5 - bottom.

FIG. 9.30. BN-800 Intermediate heat exchanger



1 -reactor core, 2 -rotating plugs, 3 - refuelling machanism, 4 - elevator,
 5 - refuelling machine, 6 - refuelling box, 7 - refuelling machine drive,
 8 - in-vessel ionization chambers, 9 - beyond-vessel ionization chambers.

*FIG. 9.31. BN-800 Reactor cut-away view
 (through refueling cell)*



1 - in-reactor refuelling mechanism, 2 - intermediate heat exchanger, 3 - reactor coolant pump, 4 - rotating plugs, 5 - spent fuel drum, 6 - refuelling cell, 7 - refuelling machine, 8 - new fuel drum.

FIG. 9.32. BN-800 Reactor plan view

and the scheme of load transfer to the reactor vessel support has been changed to reduce welding stresses and the number of weld seams, and to enhance the reactor vessel strength and dynamic stability.

The configuration of the bottom of the reactor vessel has been changed and its thickness and that of the guard vessel have been increased, improving their strength and reliability. The monitoring systems for the reactor core and internal components have been improved, e.g. additional internal and external ionization chambers have been introduced to improve neutron flux control during both power operation and refueling. Introduction of the third (small) rotating plug in the refueling system gives the possibility of using a single refueling mechanism in stead of the two in BN-600. Clearances in the refueling mechanisms were increased to improve the reliability of handling bent and swollen fuel assemblies. Steam reheating by sodium has been excluded to simplify the heat-flow diagram and to enhance the reliability of the steam generators. As a result, the number of heat exchange modules in the SG has been cut from 72 to 6. The 20 % reduction in the heat-exchange surface, which is the boundary between sodium and water in the SG, enhances its reliability correspondingly. 10Cr2Mo ferritic steel is used for the superheater tubing (in stead of Cr18Ni9 steel in the BN-600 SG) which increases its resistance to moisture carryover from the evaporator and allows the start-up separators to be eliminated.

Reduction and simplification of systems. One of the major distinctions of the BN-800 design is the simplification of the entire power unit by utilization of a single steam turbine in stead of the three turbines in BN-600, and by the elimination of steam reheating by sodium in the SG.

Passive safety systems. To prevent overheating and destruction of the reactor core in unscrammed beyond-design accidents a passive emergency protection system is provided, comprising three flow-suspended absorber rods (Fig.9.33). The hydraulic characteristics of the system of rods and sleeves ensures that the rods float to the upper working position at startup and drop at a flowrate of less than 0.5 of the nominal value. To prevent the rods floating up during refuelling and consequent erroneous raising of all the coolant pumps to full speed, a minimal hydraulic resistance is provided when the rods are in the lower position by bypassing the working member. The passive emergency protection system ensures reactor shutdown without exceeding the temperature limits and with a 200°C margin to the sodium boiling point.

For collection and retention of fuel debris inside the reactor vessel, to prevent formation of a critical mass and contact between fuel and the reactor bottom in beyond design core-disruptive accidents, a special localizing device is provided (Fig.9.34). This is a tray shaped as truncated cone, with an outer conical shell and a tube with a cap under which there are orifices to allow coolant to flow from the plenum beneath the device. The inner surface of the device is lined with molybdenum alloy sheets. Decay heat from the device is removed by natural convection of primary sodium to the intermediate heat exchangers. This natural convection capability in all loops is increased by virtue of a more favourable layout of the components.

The use of a guard vessel for the reactor and guard jackets on certain sections of the primary system auxiliary pipes (in combination with a passive device for interrupting a siphon if a sodium leak should appear) ensures that the core will be kept covered with coolant in a reactor vessel loss-of-integrity accident. To protect the reactor main and guard vessels from overpressurization safety devices with hydraulic seals are provided, giving passive hydrostatic protection (Fig. 9.35). There is a protective dome above the reactor unit as an additional external barrier for controlling radioactive releases and protecting against external impacts.

Reactor self-protection. The self-protection, self-control and self-limitation properties of the reactor are ensured in BN-800 by the negative temperature and power reactivity coefficients and the zero sodium void reactivity over the entire range of reactor power.

Immunity to personnel errors and to common-cause failures. The design decision has been made that the reactor must be shut down and kept in a safe state independent of the operator's ability to assess the situation correctly and of his actions. The large heat capacity of the reactor and the slow development of transients and accident processes give the operator ample time to analyse an emergency situation and to organize, if necessary, accident management measures (large grace period).

Safety system redundancy and diversity. The electronic and electrical hardware of the emergency protection system consists of two equipment sets, each capable of controlling the operation of all absorber rods. The independence of the equipment sets is ensured by location in separate rooms, by communication lines lying in separate cable trays, and by energizing from various power sources. There are three independent channels in each set to form deviation signals for each parameter under control. There are two emergency residual heat removal

TABLE 9.2.BN-800 MAIN DESIGN DATA

	Parameter	Value
	<i>Overall Plan</i>	
1.	Reactor thermal power, MW	2100
2.	Operating power variation range, % nominal	17-100
3.	Equipment seismostability, MSK-64 units	6
4.	Operation life, year	30
5.	Breeding ratio	1.0
	<i>Primary System:</i>	
6.	Coolant temperature, °C	
	- core inlet	354
	- core outlet	547
7.	Protective gas pressure, MPa	0.054
8.	Gas plenum volume, m ³	132
9.	Reactor coolant volume, m ³	1000
10.	Coolant flowrate, kg/s	8500
11.	Pump delivery head, m	101
12.	Number of circulating pumps	3
	<i>Reactor Core:</i>	
13.	Equivalent core diameter, m	2.56
14.	Active core height, m	0.88
15.	Average core power density, MW/m ³	354
16.	Number of core fuel assemblies	565
17.	Fuel assembly duct width across flats, mm	94.5
18.	Fuel assembly pitch, mm	100
19.	Fuel	MOX sintered pellets
20.	Initial core fuel inventory, kg	12600
21.	Average Pu content in new fuel, %	22
22.	Fertile material inventory (initial), kg	11600
23.	Number of fuel rods per assembly	127
24.	Fuel cladding outer diameter, mm	6.6
25.	Fuel rod linear heat rating (max.), kW/m	49
26.	Average fuel burnup, MWday/kg	66
27.	Maximum fuel burnup, % ha	10
28.	Core lifetime, ed	420
29.	Core refuelling interval, ed	140
	<i>Reactor Main Vessel:</i>	
30.	Outer diameter, m	13.4
31.	Overall height, m	15.0
32.	Weight (empty), tons	33.60
33.	Material	stainless steel 09Cr18Ni9
	<i>Secondary Loop:</i>	
34.	Secondary coolant temperature, °C	
	- SG inlet	505
	- SG outlet	309
35.	Secondary sodium volume, m ³	375
36.	Gas plenum volume, m ³	18

37.	Gas plenum pressure, MPa	0.245
38.	Pump delivery head, m	53
39.	Coolant flowrate, kg/s	2800
40.	Number of SG sections	10
41.	Number of DHR air cooler sections	2
42.	Number of DHR electromagnetic pumps	2
43.	Number of main circulating pumps	1

Tertiary Circuit:

44.	Main steam pressure, MPa	13.7
45.	Steam mass flowrate, kg/s	876
46.	Feedwater temperature, °C	210
47.	Main steam temperature, °C	490

systems: - a DHR system involving the tertiary circuit with forced circulation of feed water by three emergency electric feed pumps (Fig. 9.36); - and a DHR system involving air coolers connected to the secondary loops in parallel with the SGs, which assure residual heat removal from the shutdown reactor even, in the event of loss of power supply by natural convection of coolant and air (Fig. 9.37).

All requirements of the regulations concerning nuclear, radiological and technical safety are met. The annual radiation dose to an individual of the local population at a distance of 3 km during normal operation of the plant away will not exceed 0.004 mSv, which is much lower than the limit set in Russia and is quite negligible compared with the natural radiation background (less than 0.2%). The assessed value of the frequency of severe core-disruptive accidents for BN-800 is less than $1 \times E-6$ per reactor-year. The probability of a radioactivity release corresponding to the limit for severe accidents is not more than $1.E-8$ per reactor-year.

Safety Analysis. Safety analysis of BN-800 is based on a combination of deterministic and probabilistic approaches, relying on operating experience and analogous data from the prototype reactors and consideration of a wide spectrum of emergency situations and accidents. Together with design basis accidents, accidents in which the number of failures exceeded the single failure principle were also considered, including beyond design accidents with failure of highly reliable redundant safety systems.

Economic potential of a BN-800 NPP. Comparative assessment of the economic performance and safety of a NPPs based on BN-800 and VVER-1000 (Russian PWR) reactor units deployed in the same region showed the advantages of the fast reactor. By virtue of the unique features of BN-800 the following functions can be fulfilled which are not possible for other types of nuclear reactors: (a) burner of highly radioactive plutonium formed by operation of other nuclear reactors, particularly naval reactors; (b) production of new "clean" nuclear fuel by burnup of highly radioactive plutonium, and various isotopic products needed for medicine and industry; (c) significant reduction in thermal pollution of the environment due to the high efficiency of the steam cycle; and (d) burnup of weapons-grade plutonium and actinides. All these applications of BN-800, along with power generation, are being scrutinized by the designers of this reactor.

Refuelling	Engagement	Release	Power operation	Actuation at plant black out, at reactor trip
	$G=0.2G_{nom}$	$N=0$ $G=0.7G_{nom}$	$N=N_{nom}$ $G=G_{nom}$	$G<0.5G_{nom}$

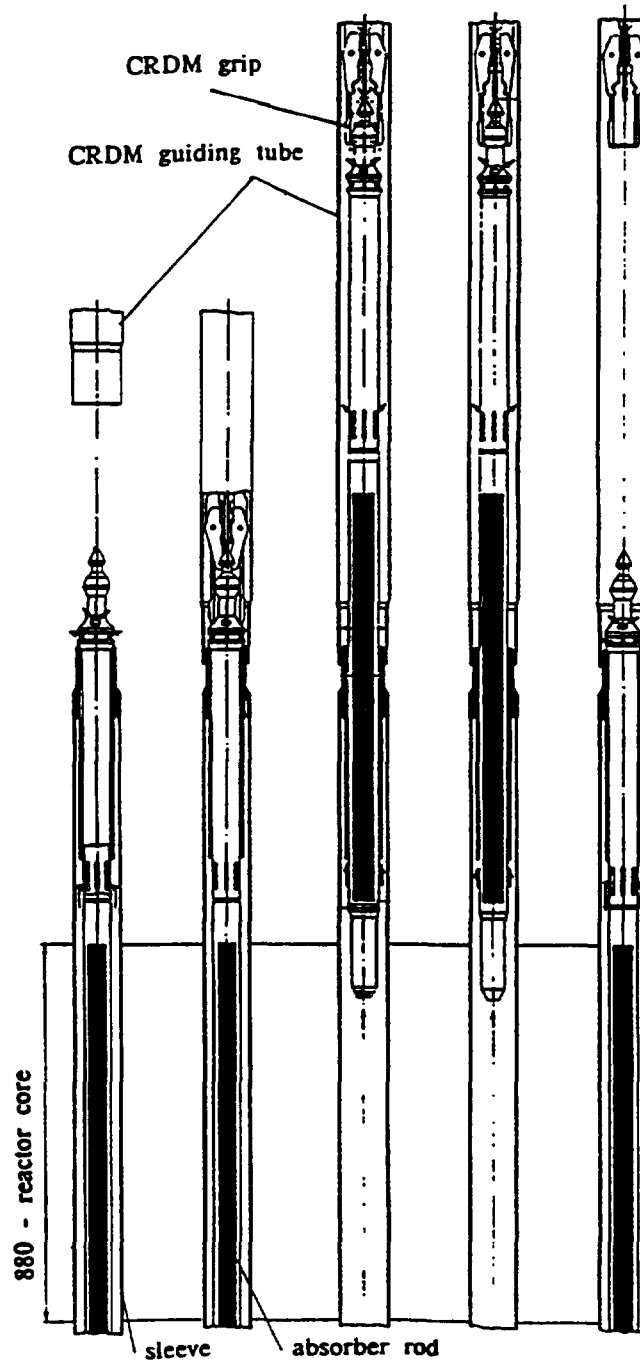


FIG. 9.33. BN-800 Passive secondary shutdown system with flow-suspended rods

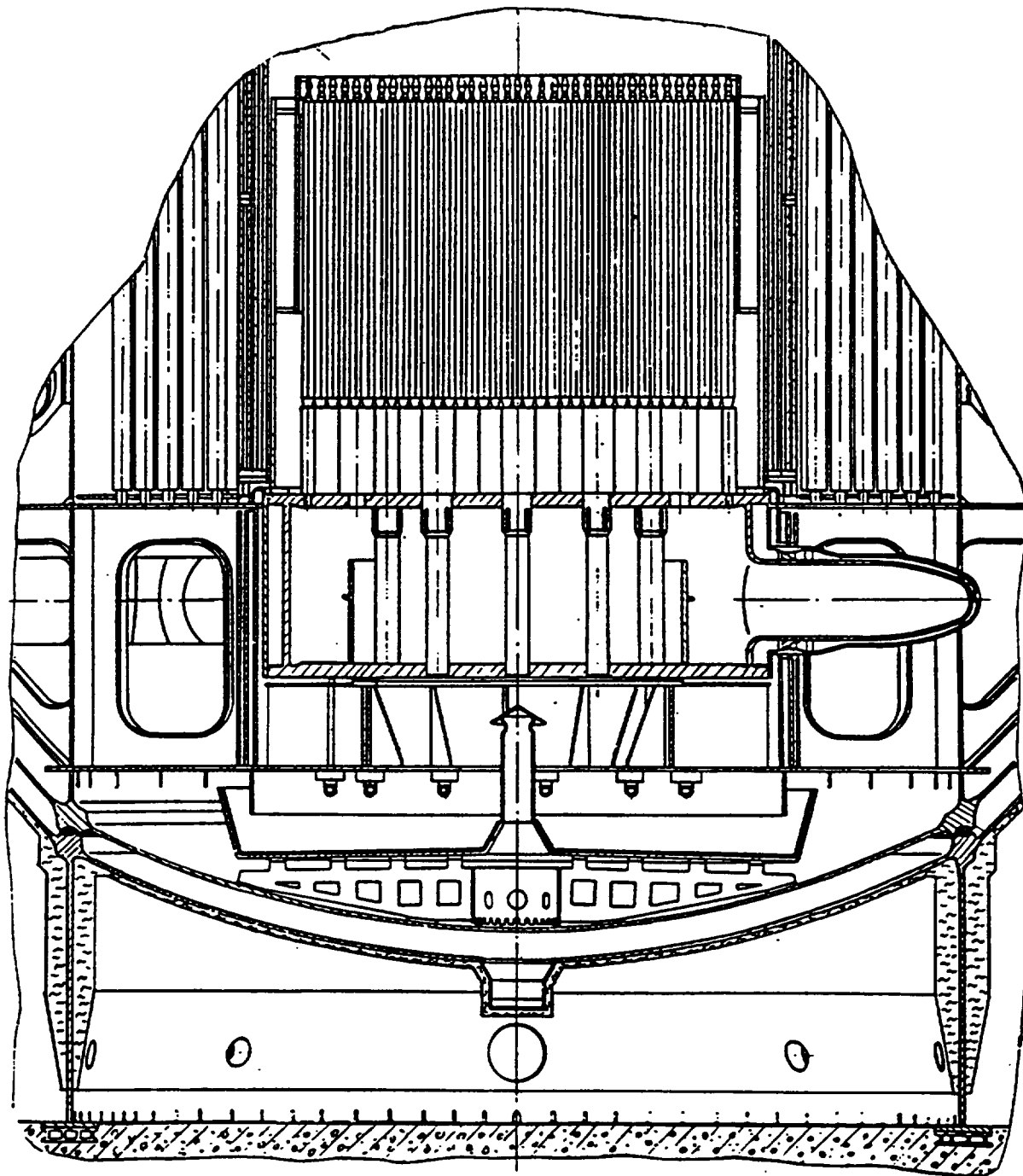


FIG. 9.34. BN-800 Core debris tray

9.4. BN-600M ADVANCED LMFR

9.4.1. Design status

The BN-600M reactor plant with a fast sodium-cooled nuclear reactor is being designed in accordance with the development of nuclear power in the Russian Federation towards a competitive fast breeder reactor of the BN type, aiming at closing the nuclear power fuel cycle (including the burning of weapons-grade plutonium) and conserving indigenous

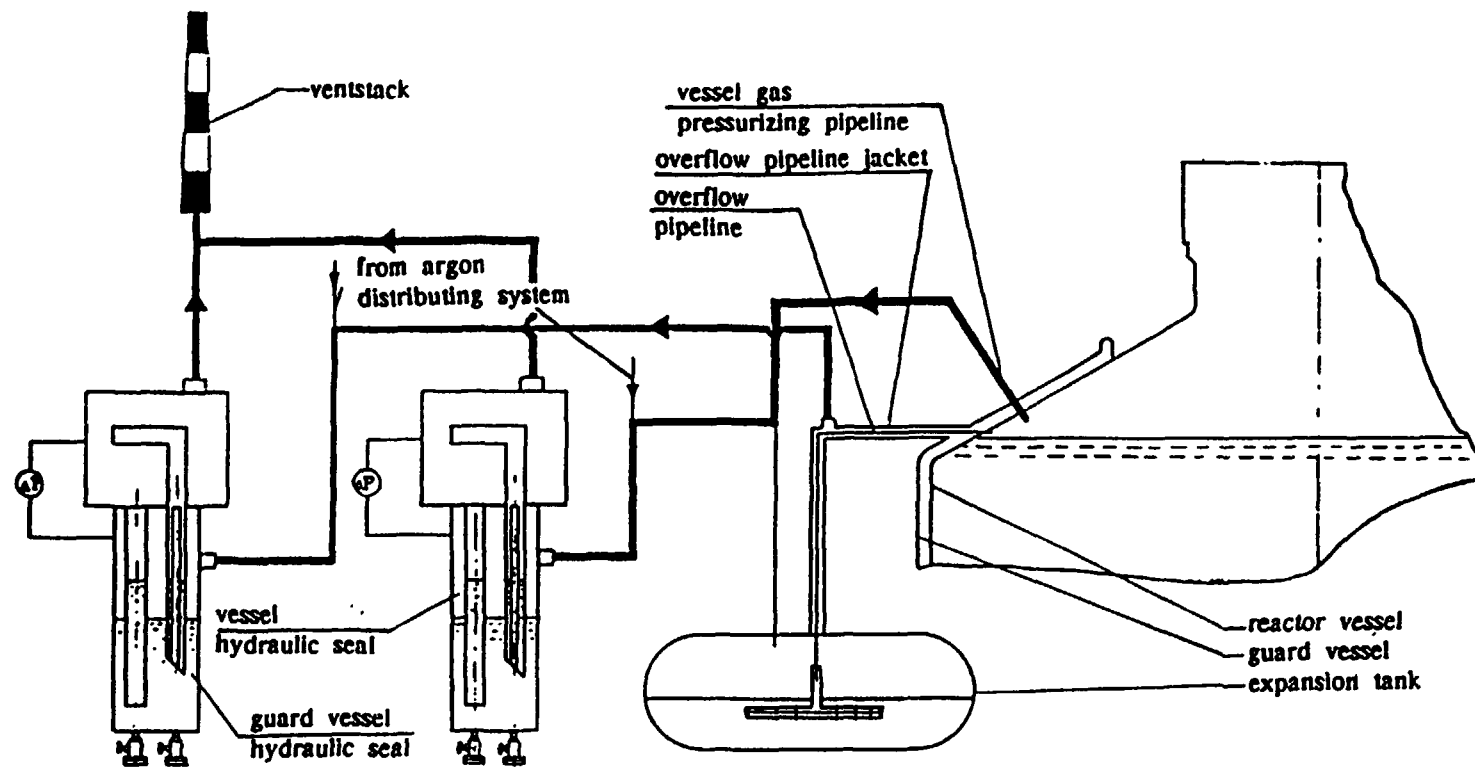


FIG. 9.35. BN-800 Reactor vessel overpressure protection system

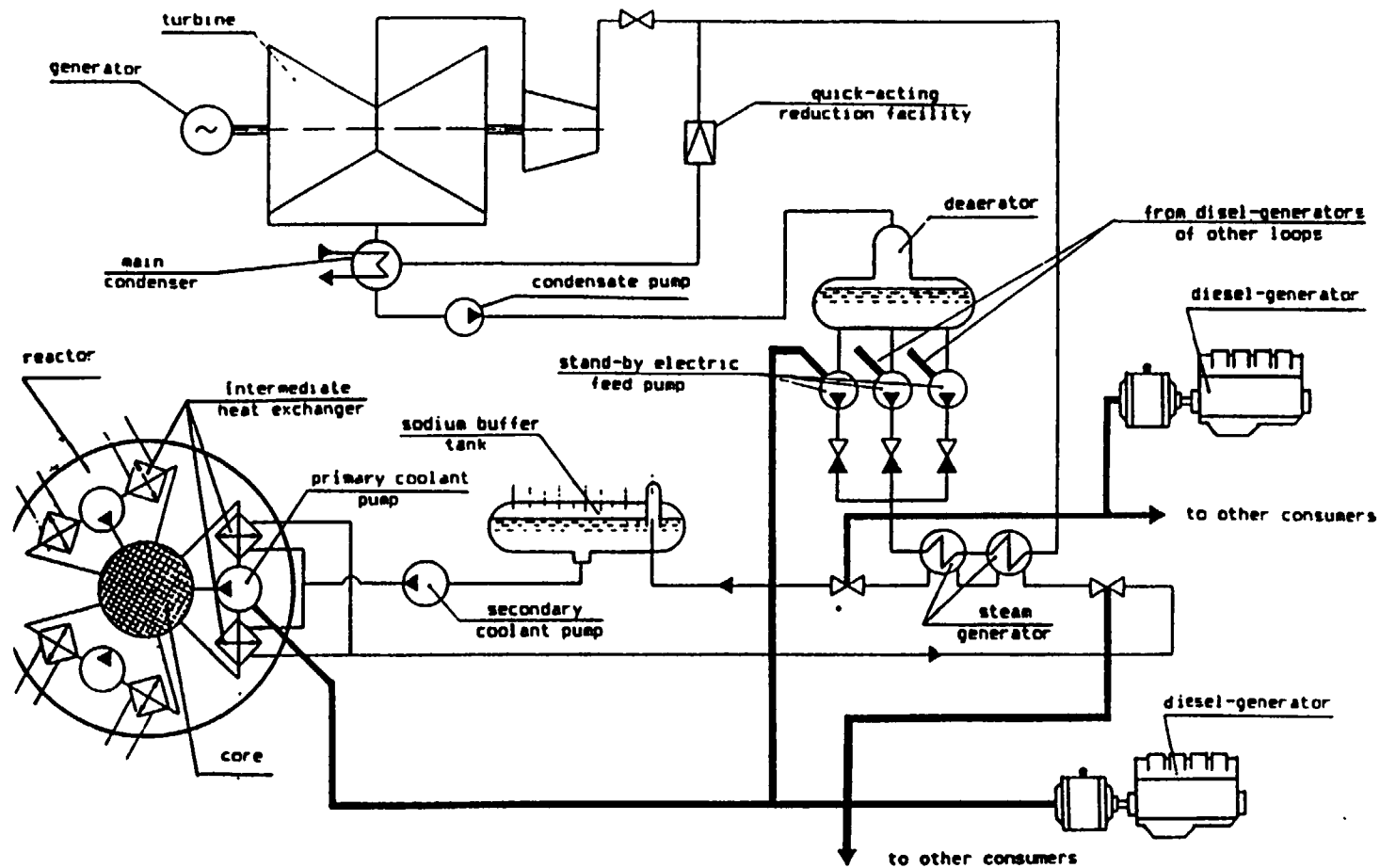


FIG. 9.36. BN-800 ERHR system involving tertiary circuit with reliable power supply

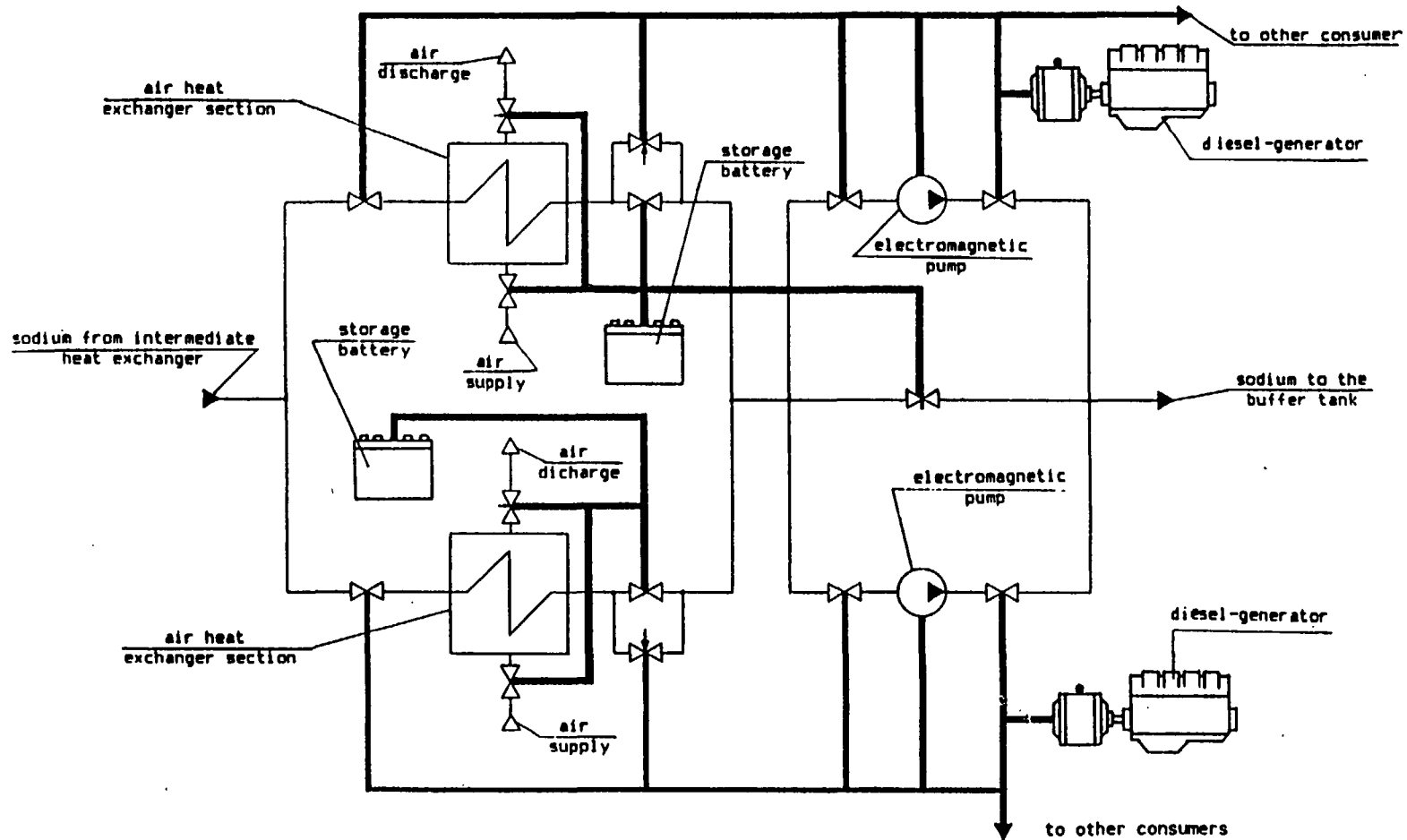


FIG. 9.37. BN-800 ERHR system involving air heat exchanger with reliable power supply

nuclear fuel for the distant future. These developments correspond to the general trend of world nuclear power development towards enhanced safety and intermediate-power reactors. The physical and technical features of sodium-cooled fast reactors allow them to compete successfully with PWRs today with respect to nuclear and ecological safety. The solution of the key problem of economical competitiveness for BN-type reactors compared with VVERs (Russian PWRs) will allow the share of fast nuclear reactors and their contribution to the national nuclear power park to be increased in the future. At present the basis of the concept for the BN-600M power unit has been developed. The current status of design development, building on the basic technology and technical decisions of the reliably-operating prototype BN-600 and the completed BN-800 design, give confidence that this design can be successfully licensed and realized in the next ten years. A preliminary feasibility study for a NPP with BN-600M power units was completed in 1993 as an option in a competition for construction of a 2000 MW(e) power station in central Russia.

9.4.2. Design basis

The extensive experience of building and operating the Beloyarsk-3 power unit with the BN-600 fast reactor have demonstrated since 1980 its high economic efficiency, reliability, and nuclear and ecological safety. This is the scientific and technical basis for the development of the advanced BN-600M design. The main objectives for development are the following: (a) creation of a medium power unit for a nuclear power station of the new generation; (b) provision of the maximum feasible level of reactor safety based on state-of-the-art engineering and proven for fast reactor technology; and (c) development of a nuclear power unit comparable with respect to economics with VVER-type reactors of the same unit power. The BN-600M reactor is being developed as an evolution in the sequence of BN-type reactors, relying on the proven features of the prototype BN-600 and the BN-800 design which has been licensed and is ready for construction. The main dimensions of the BN-600 reactor vessel structures have been retained, and the major portion of the thermal-mechanical equipment of BN-600 and BN-800 have been borrowed, as well as the refuelling mechanisms and the reactor control and protection systems. Considerable enhancement of safety has been achieved by elimination of the external systems containing radioactive sodium, which are present in BN-600 and BN-800, and by the use of DHR heat exchangers submerged in the reactor pool and passive features for reactor shutdown in emergency situations.

The arrangement of the additional equipment items (DHR heat exchangers and cold-traps) in a reactor vessel of the BN-600 and BN-800-type without changing its dimensions is possible only by changing to a two-loop primary system utilizing four IHXs of the BN-600-type and two reactor coolant pumps. The use of two heat transport loops in BN-600M is made possible by the decision to remove the residual heat in emergencies via special independent cooling systems relying to a realistic extent on the passive principles of operation. When the BN-600-type IHXs are used in the two-loop primary system instead of three, the reactor capacity can be increased above 600 MW(e). The transfer of heat through each IHX can be increased by 1.5 times compared with BN-600 by virtue of the margins available in the heat transfer surface, by increasing the logarithmic temperature difference and by increasing the heat transfer coefficient by reducing the IHX tube wall thickness from 1.4 to 1.0 mm.

9.4.3. Reactor design concept and main data

The BN-600M power unit is being developed as a "monoblock" i.e. an integrated power unit involving the reactor and a single turbine with a 647 MW(e) generator. The

reactor has an integral layout with all the primary components and systems arranged in the main reactor vessel (Fig. 9.38). Heat is transported from the reactor to the steam generators by two sodium coolant circuits.

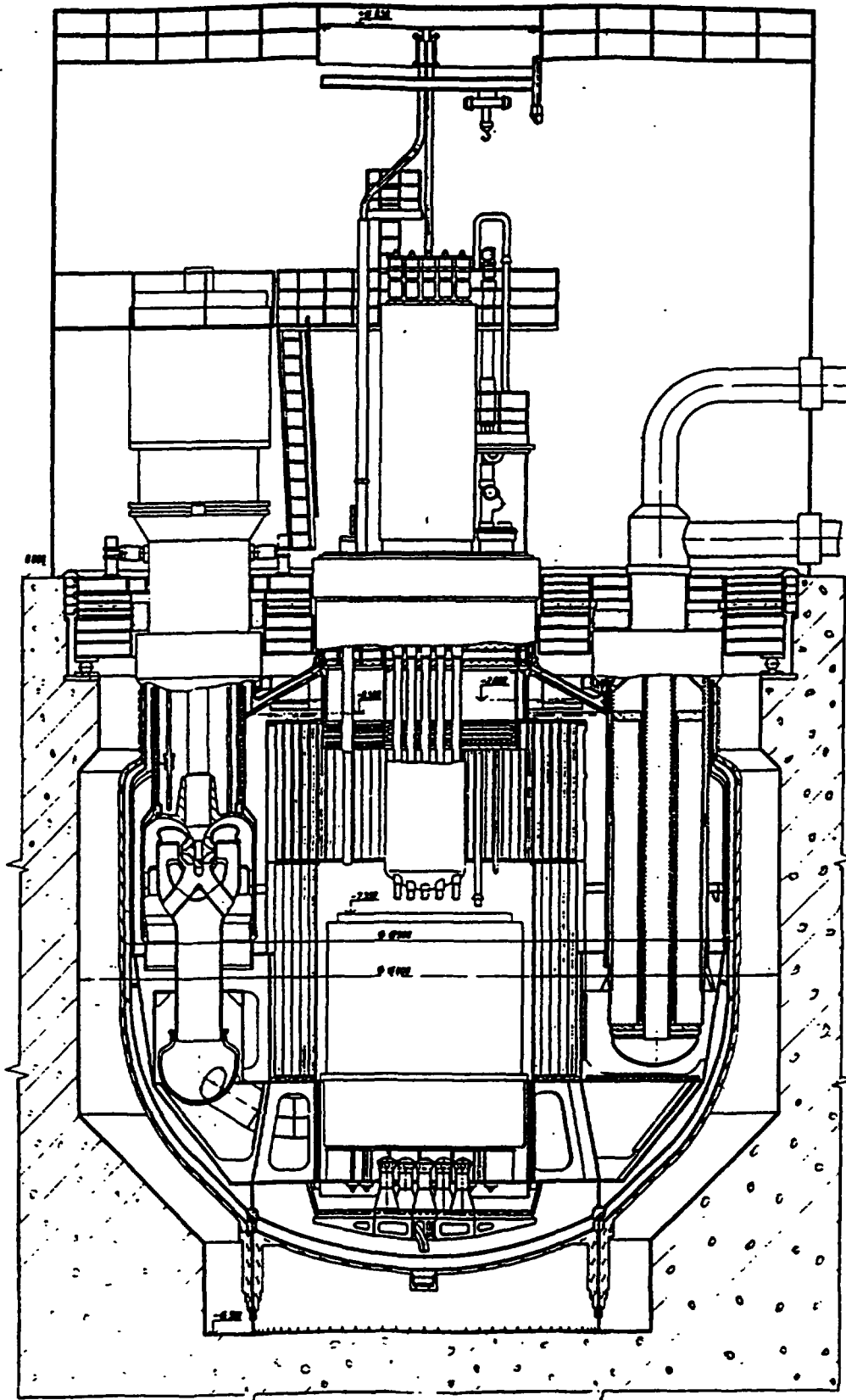


FIG.9.38. BN-600M Reactor unit cut-away view

The primary system comprises two reactor coolant pumps, four IHXs, pressure pipes and the reactor core. The secondary system consists of four loops (if vessel-type SGs are used), each including an IHX, steam generator, coolant pump and pipelines. If the development of a vessel-type SG is delayed sectional-modular SGs might be used instead. In this case the secondary system will be composed of two loops with circulating pumps of double capacity. In the event of loss of heat removal through the SGs the residual heat will be removed by the DHR system consisting of four independent channels. Each channel includes a sodium/sodium IHX built into the reactor, an air cooler, pipelines, damper, and stack. The heat removal capacity of one DHR channel is 15 MW, which allows the reactor to be cooled by two channels without exceeding the nominal working temperature of the primary sodium, and even by one channel without exceeding the allowable design limits for fuel integrity. To ensure seismic stability the reactor building with all the safety-related systems is erected on a single foundation plate. The reactor building functions as a containment providing protection for the reactor and safety systems against external impacts (air crash, tornado, shock waves).

The major portion of the refuelling mechanisms used in BN-600 and BN-800 has been borrowed for BN-600M. However the refuelling complex has been modernised to reduce the number and weight of equipment items. In particular the number of positions in the in-reactor spent fuel store has been increased to hold the FAs from two fuel cycles. This allows the FA residual power at unloading to be reduced to 1.5 kW, so that they can be transported for washing without additional delay in the external fuel storage drum used in BN-600 and BN-800. The drum itself is not required.

The main design data are given in Table 9.3. The correspondent characteristics for BN-600 are given for comparison.

9.4.4. Safety features

Safety is enhanced by implementing the following advanced design features (in contrast with BN-600): (1) Residual heat removal in loss-of-power accidents is provided by the DHR heat exchangers immersed in the reactor pool and by air coolers (the ultimate heat sink); (2) For reactor shutdown, besides traditional absorber rods with drive mechanisms, an additional group of passively-actuated absorber rods is provided, which are inserted into the core under gravity if the primary coolant flow is reduced to 50% of nominal value; (3) The reactor self-protection capability is improved by virtue of the negative sodium void reactivity effect. To eliminate the positive sodium void reactivity effect in a sodium-boiling accident a sodium layer has been introduced above the fuel and an upper primary shield made of boron carbide is incorporated in stead of the upper axial blanket used in BN-600; (4) Neutron flux measurement is improved by placing ionization chambers immediately in the reactor pool. (In BN-600 and BN-800 special neutron guides are provided to ensure sufficient neutron flux at the ionization chambers, which are arranged in a moderated box in the reactor well.); (5) Primary coolant pipes outside the reactor vessel are eliminated by placing the filter-traps in the reactor pool; (6) Seismic stability of the plant is ensured to magnitude 8 earthquake (MSK-64 scale) which is adopted as the maximum design earthquake; and (7) Protection of the reactor plant against external impacts is ensured by robust design of the containment building. The physical and technical features of BN-600M combine inherent safety with in-depth protection relying on passive safety systems to eliminate serious accident consequences. According to a preliminary assessment the probability of an accident with severe core damage is less than $1 \cdot 10^{-6}$ per reactor-year.

9.4.5. Improvement of economic performance

The economic efficiency of the BN-600M power unit has been improved by reducing all the power generating cost components: (1) Reduction in capital investment results from the smaller specific weight of the equipment items: the specific weight of the BN-600M reactor plant is 1.58 times less than that of BN-600 (for BN-600M with vessel-type SGs). According to this performance indicator BN-600M is close to an integral PWR of the VPBER-600 design now under development in Russia for the new generation of NPPs; (2) Reduction in the fuel cycle cost results from increasing the fuel burnup (the average burnup of the fuel is 80-100 MWd/kg); (3) Depreciation costs are reduced by improving equipment reliability and extending the service life to 60 years; and (4) Operating expenses are reduced because automation of technological processes and reduction in the number of refuelling and equipment replacement operations (due to improvement in reliability) allow staff numbers to be cut.

TABLE 9.3. BN-600M MAIN DESIGN DATA

Parameters		BN-600M	BN-600
1.	Reactor thermal output, MW	1520	1470
2.	Power unit output, MW(e)		
	- gross	647	613
	- nett	595	564
3.	Power unit thermal efficiency, brutto %	42.5	40.7
4.	Auxiliary power, % nominal	8	8
5.	Number of primary system main loops	2	3
6.	Primary coolant parameters:		
	- sodium temperature at core inlet, °C	382	377
	- sodium temperature at core outlet, °C	550	550
	- coolant flow, t/h	25590	24000
7.	Secondary system parameters:		
	- sodium temperature at SG inlet, °C	515	518
	- sodium temperature at SG outlet, °C	345	328
	- sodium flow, t/h	25300	21900
8.	Tertiary system parameters:		
	- superheated steam temperature, °C	495	505
	- feedwater temperature, °C	240	240
	- main steam pressure, MPa	3.7	13.7
	- steam flow, t/h	2411	1980
9.	Steam reheating	by steam	by Na
10.	Refuelling interval, ed	150	150-160
11.	Refuelling outage, day	12	12
12.	Design load factor, %	85	80
13.	Design lifetime, years	60	30
14.	Seismostability, units to MSK-64 scale	8	7
15.	Specific weight of reactor plant, t/MW(e)	8.23*	13.0**

Notes: * with vessel-type SG, ** with sectional-modular SG.

9.5. THE DEMONSTRATION FAST BREEDER REACTOR

9.5.1. Introduction

The FBR is being developed as a future alternative to light water reactors in Japan. The shift from LWRs to FBRs, which is expected to start around 2030, is the reactor strategy in the "Long-term Plan for the Development and Application of Nuclear Power" established by the Japan Atomic Energy Commission (JAEC).

The experimental FBR "Joyo" and the prototype FBR "Monju" were developed by the Power Reactor and Nuclear Fuel Development Corporation (PNC).

As a next step toward commercialization of the FBR, the demonstration FBR "DFBR" is planned to start construction in the first decade of the next century and utilities are expected to play a major role in its design, construction and operation. The Japan Atomic Power Co. (JAPC) is the principal organization responsible for the design, construction and operation of the DFBR for utility companies.

Research and development of the DFBR are being conducted by PNC, the Japan Atomic Energy Research Institute (JAERI), the Central Research Institute of Electric Power Industry (CRIEPI) and JAPC, who have established the Steering Committee for Coordinating FBR R&D.

Design studies for DFBR reactors of the top-entry loop and pool types have been conducted by JAPC since 1985. The top-entry arrangement, in which the reactor vessel, intermediate heat exchanger (IHX) vessels and pump vessels are connected by reverse-U shaped piping, was judged to give the most compact primary system for loop-type reactors. The study concluded that both loop and pool types could be operated commercially and each had its advantages and disadvantages. For the DFBR design study, which is an intermediate step between "Monju" and commercial reactors, the top-entry loop type reactor was selected as a consequence of the following considerations:

- (1) Over several years of operation a plant may encounter problems which require repairs to the primary system. In this case it is important to incorporate ease of access and maintainability of primary system equipment into the design of the plant.
- (2) System flexibility is important to allow stepwise accommodation of various innovative technologies necessary to achieve the goal of commercialization in the future.
- (3) Experience gained at the prototype "Monju" must be fully utilized and international cooperation can be expected to be supportive.

In the preliminary conceptual design phase from 1990 to 1991, the technical feasibility of the top entry loop type reactor was confirmed and the possibility of FBR commercialization was also envisioned. The conceptual design study of the DFBR was conducted for two years from 1992. The design of the DFBR is summarized below, along with the technical and cost evaluation results.

9.5.2. DFBR Plant design

General design considerations: The design targets of the DFBR are as follows: (a) Safety level equivalent to that of LWRs, (b) Economic feasibility of about 1.5 times the cost of

an LWR on a 1,000 MWe basis, (c) Reactor outlet temperature of 550°C to achieve high thermal efficiency, (d) High burnup and long operating cycle to reduce the cost of electricity generated, (e) Easier maintenance and repair taking advantage of distributed layout of equipment.

The "Guidelines on the Safety Design for the DFBR" and the "Elevated Temperature Structural Design Guide for the DFBR (DDS)" form the basis of the design. These guidelines are based on the guidelines for the design of "Monju", with recent R&D results incorporated.

Overall plant design: Table 9.4. lists major specifications of the plant, and Fig. 9.39 shows an overview of the nuclear steam supply system of the top entry loop type DFBR.

TABLE 9.4. PLANT MAJOR SPECIFICATIONS

Item	Specifications
1 Reactor type	Top entry loop type reactor
2 Thermal output	1,600 MWt (Electric output : 660MWe)
3 Number of loops	3 loops
4 Reactor outlet temperature	550 degree C
5 Main steam temperature and pressure	495 degree C / 169 atg
6 Core and fuel (1) Core type (2) Fuel (3) Burnup (4) Breeding ratio	Two homogeneous regions core Pu- U mixed oxide fuel 90,000 MWd/t (Initial phase core) 150,000 MWd/t (High burnup phase core) 1.2 (with radial blanket) 1.05 (without radial blanket)
7 Core support structure	Lateral support
8 Vessel wall thermal protection	Low temperature sodium circulation type
9 Upper internal structure	Single cylindrical
10 Intermediate heat exchanger	Primary sodium in tube side or primary sodium in shell side
11 Primary pump	Single suction, single stage
12 Steam generator	Integrated once-through type with helical coil heat transfer tubes
13 Reactor shutdown system	Two independent systems
14 Decay heat removal system	Direct reactor auxiliary cooling system (DRACS)
15 Reactor containment facility	Rectangular concrete structure with inner lining, with emergency gas treatment system
16 Fuel handling system	Double rotating plug, direct drive and manipulator type
17 Fuel transfer system	Rotating chamber and chute system
18 Spent fuel storage	Ex- vessel storage
19 Spent fuel cleaning	Dry cleaning
20 Reactor building	Aseismic building or seismically isolated building

The thermal output of the reactor is 1,600 MW, with three main cooling loops, to ensure investment costs and core characteristics similar to those of future large cores. The main steam conditions are 495°C and 169 atg, to attain higher thermal efficiency based on past experience and the results of recent R&D on steam generator (SG) design and materials.

The primary cooling system consists of a reactor vessel, three IHX vessels, three pump vessels and reverse-U shaped piping to connect these vessels. The reverse-U shaped piping reduces the required installation space. The vessels have free coolant surfaces and the cover gas is maintained at equal pressure by inter-connecting pipes. The coolant surface level in the IHX vessel during operation is lower than that in the reactor vessel due to the pressure loss in the hot leg piping. The cover gas pressure is about 0.9 atg in order to maintain positive pressure at the highest point of the primary piping.

The secondary cooling system consists of a secondary pump, a once-through SG and piping for each loop. The reactor has two shutdown systems, the primary reactor shutdown system and the backup reactor shutdown system. Either can stop the reactor rapidly independent of the other. The decay heat removal system has four independent loops and employs a direct reactor auxiliary cooling system (DRACS) to reduce the cost while maintaining reliability.

Core and fuel. Figure 9.40 shows the core configuration. The core is designed for two phases, an initial phase and a future high burnup phase, since great improvements in fuel design and materials are likely within the life of the plant. For example, cladding materials with good resistance to swelling, giving better burnup and longer operating cycle while still maintaining the reactor outlet temperature of 550°C, will probably be developed during the life of the plant. The initial phase core is designed to produce an average burnup of 90,000 MWd/t with an operating period of 13 to 15 months and a breeding ratio of 1.2 (with radial blanket) or 1.05 (without radial blanket), which provides flexibility to balance of the supply and demand of plutonium. The calculated void reactivity of the entire core is approximately 4\$ at the end of the equilibrium cycle.

The design targets for the high burnup phase core are average burnup of 150,000 MWd/t, and an operating cycle of 20 months. However, such issues as increased plutonium enrichment, increased control rod reactivity, maximum linear power density and control rod life, remain to be solved. Further study on the flattening of the power distribution is also required. Although advanced ferritic steel is a potential fuel cladding material, it is still in the stage of test production and its feasibility needs to be established by repeated irradiation tests.

The core has two homogeneous regions with different plutonium enrichments to flatten the power. The height and equivalent diameter of the core are 100 cm and 299 cm respectively. The maximum linear power density is 41 kW/m, based on local power peaking in the core. Advanced austenitic stainless steel (PNC1520) is used as the cladding material of the initial phase core fuel because of its high resistance to swelling deformation and fast neutron irradiation creep damage. A fuel pin of 8.5 mm diameter is used to achieve the burnup of 90,000 MWd/t and an operating cycle of 15 months.

The required control rod reactivity can be attained by 24 control rods in the initial phase core, but 30 control rods are provided for the high burnup phase core.

A sufficient margin for cladding creep damage is assured by extending the plenum length to 115 cm and by increasing the thickness of the cladding tube to 0.5 mm. These

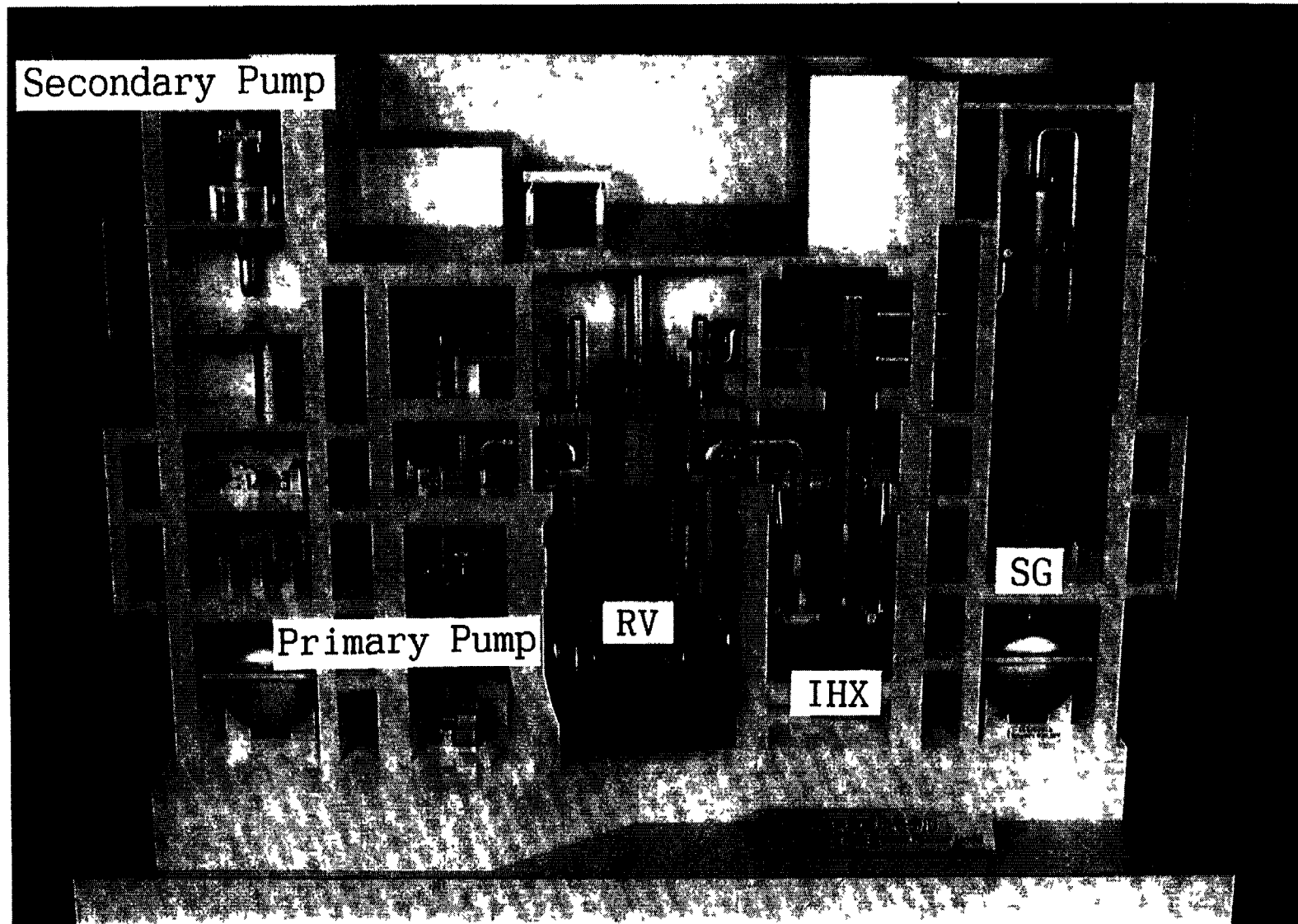
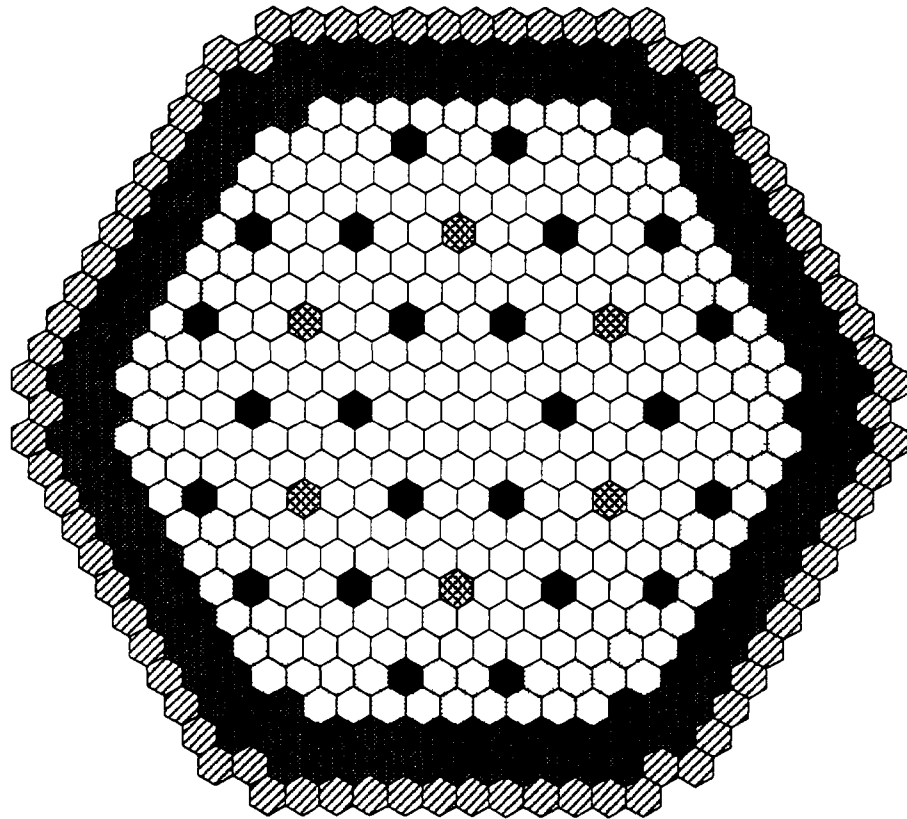


FIG 9 39 Nuclear steam supply system of top-entry loop type DFRBR



	Inner core fuel assemblies	199
	Outer core fuel assemblies	96
	Radial blankets	138
	Primary reactor control rods	24
	Back-up reactor control rods	6
	SUS shields	78

FIG. 9.40. Reactor core configuration

dimensions are based on evaluation of the fuel integrity, and the safety of the plant has been confirmed even in the event of a serious accident in the primary system.

The spent fuel assemblies are stored in an ex-vessel storage system with a single large tank or modular small tanks.

Reactor structure. Figure 9.41 shows the reactor structure. It consists of the reactor vessel, roof deck, double rotating plug, upper internal structure (UIS), reactor vessel thermal protection structure, core support structure and guard vessel. The main flow of coolant passes through the core support structure, core, and upper plenum and is discharged through the outlet piping. A part of the coolant branches off from the inlet plenum of the core support structure, flows over the reactor vessel wall to cool it, and exits to the upper plenum where it joins the main stream from the core.

The reactor vessel is 10.4 m diameter, 16 m high and 50 mm thick, made of modified SUS316 stainless steel for fast reactors (316FR) with high strength at elevated temperatures. The diameter is determined by the layout of components on the reactor top, chosen to

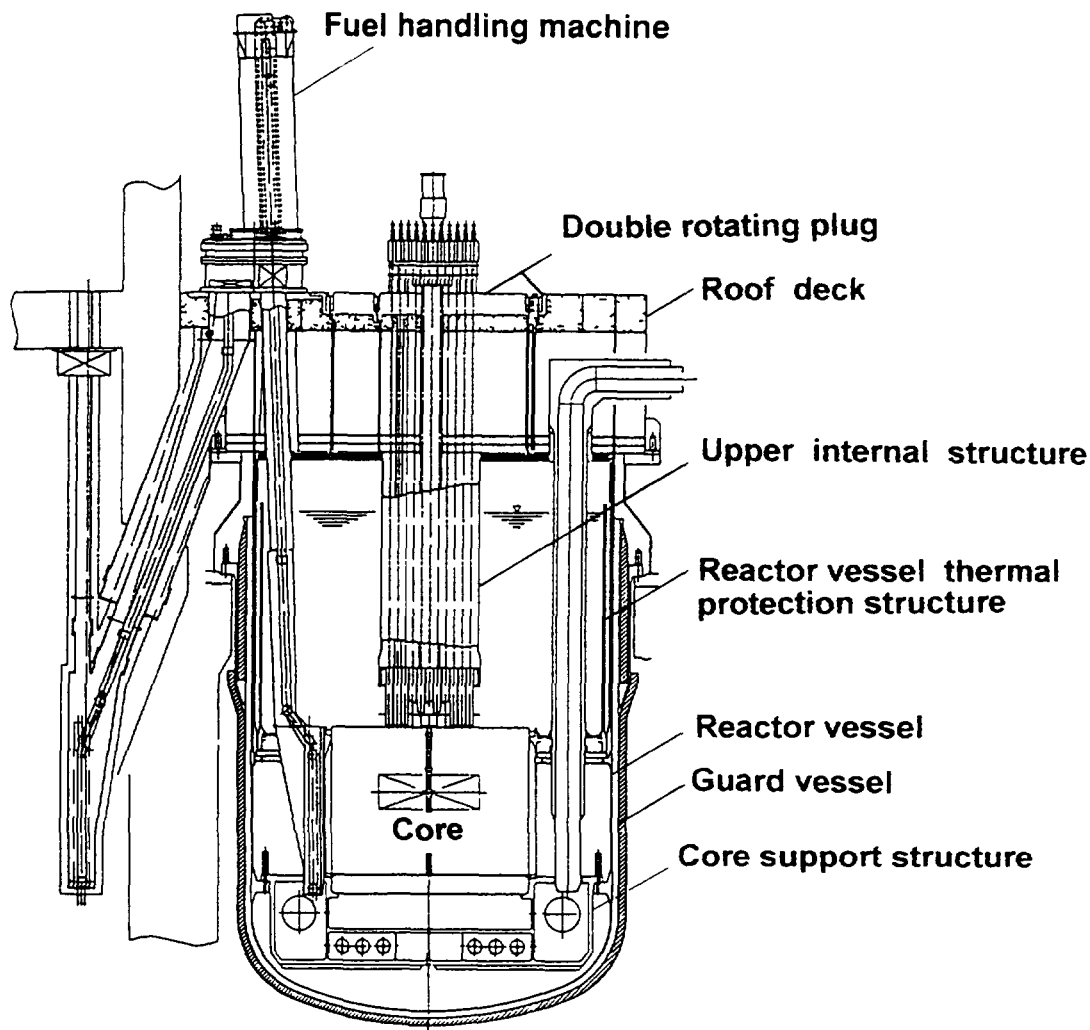


FIG 9 41 Reactor structure

minimize the diameter of the vessel. The height of the reactor vessel is set so that the fuel assemblies are submerged in coolant during transport. The thickness of the vessel wall is set to withstand both seismic forces and thermal stress.

The roof deck is a ribbed box structure, 13.0 m diameter, 6.2 m high with 60 mm thick plates, and is connected to the reactor vessel via a dissimilar material joint. The roof deck supports the reactor vessel, rotating plug, UIS, fuel handling machine, and the direct reactor heat exchangers (DHXs) of the decay heat removal system. Radiation shielding concrete is placed in the upper part of the roof deck, and it is cooled to about 60°C to ensure that electrical components such as the control rod driving mechanisms installed on the upper surface function properly. A piping chamber inside the roof deck houses the primary piping.

The UIS is a cylindrical structure located above the core. It supports the control rod guide tubes and instrument wells in the event of an earthquake. The cylindrical drum is made of 316FR with no vertical weld seam, to allow it to withstand the thermal stress due to the axial temperature distribution near the liquid surface, which changes as the liquid level changes. The surface of the UIS near the core outlet is covered with Alloy 718 as a measure against thermal striping, similar to the design of the prototype reactor "Monju".

The low temperature sodium circulation system protects the reactor vessel wall by keeping it cool. It utilises cold sodium taken from the inlet plenum of the core support structure to a liner with three cylindrical layers. The cooling sodium flows upward through the clearance between the reactor vessel wall and the outermost layer of the liner. It then flows over the top of the outer layer, descends through the clearance between the outer and middle layers, and finally discharges into the upper plenum. The inner layer is provided for the thermal protection of other layers. The flow rate of cooling sodium is about 3% of the primary coolant flow in order to keep the reactor vessel wall cool and also to prevent self-exciting vibration of the liners and uneven overflow. Each liner is made of 316FR and is thick enough to prevent buckling in the event of an earthquake. The low-temperature sodium discharge region is coated with Alloy 718 to prevent thermal stripping as the return stream of coolant mixes with the hot sodium in the upper plenum.

The core support is a box structure with ribs attached to the reactor vessel by a single plate flange. A backup structure prevents the core from falling in the event of damage to the single plate. The vertical rigidity of the core support structure is designed to withstand vertical seismic motion. The inlet piping is inserted via a slide joint in the top plate of the box structure to avoid restriction of the vertical displacement of the inlet piping due to thermal expansion.

The guard vessel surrounding the reactor vessel is supported independently from the roof deck so that it can control leakage from the reactor vessel, maintain the coolant inventory, and prevent common mode failure with the reactor vessel. The guard vessel is filled with a nitrogen atmosphere.

Main primary components. The design of the IHX is compact with enhanced performance to improve economy. Two types of IHX, primary sodium in the tube side or the shell side, were designed and compared, and the former was selected to reduce the construction cost due to the smaller heat transfer area. A gas dam structure is employed to decrease the thermal stress in the IHX vessel wall near the liquid surface. The structural concept of the IHX is shown in Fig. 9.42.

The primary pump is a single suction, single stage pump with simple structure and proven experience in previous reactors. A loose-part trap structure is provided on the discharge side of the pump to prevent loose parts, if any, from flowing into the core. The discharge piping runs through the upper plenum to help detect piping failures by monitoring the liquid level in the pump vessel. The structural concept of the primary pump is shown in Fig. 9.43.

The distinctive feature of the top entry loop type reactor is the primary piping design with its reverse-U shape to attain a compact primary system arrangement. The primary piping is shown in Fig. 9.44. The piping is supported by a deck seal via a Y-piece structure near the pipe opening so that the thermal expansion of the horizontal pipe can be absorbed by bending with an appropriate length of vertical pipe. The primary piping has a duplex construction with an outer pipe to detect any sodium leakage rapidly and, by restricting the free volume outside the primary piping, to help retain the minimum sodium level in the reactor vessel necessary for core cooling.

These primary components, including the reactor vessel, are made of 316FR to ensure the structural integrity of the system at high temperature.

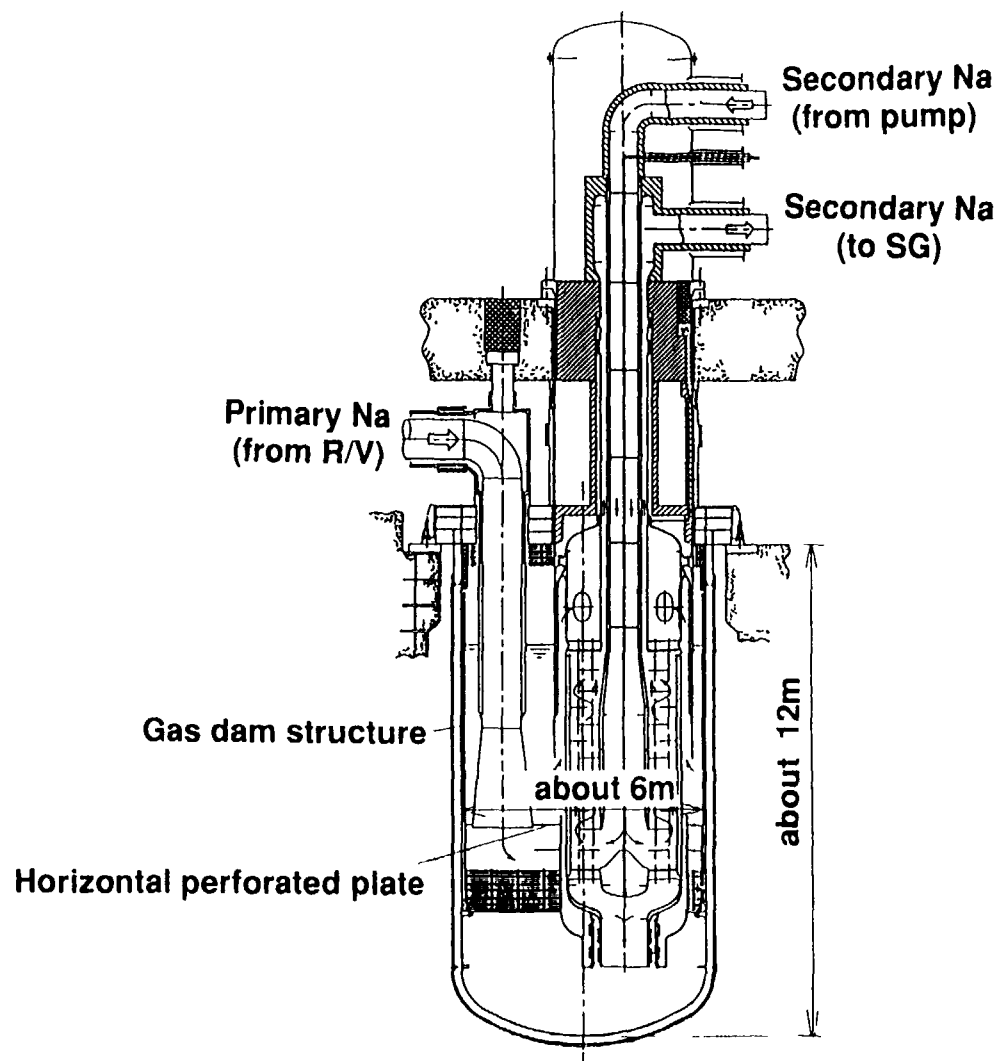


FIG 9 42 Intermediate heat exchanger

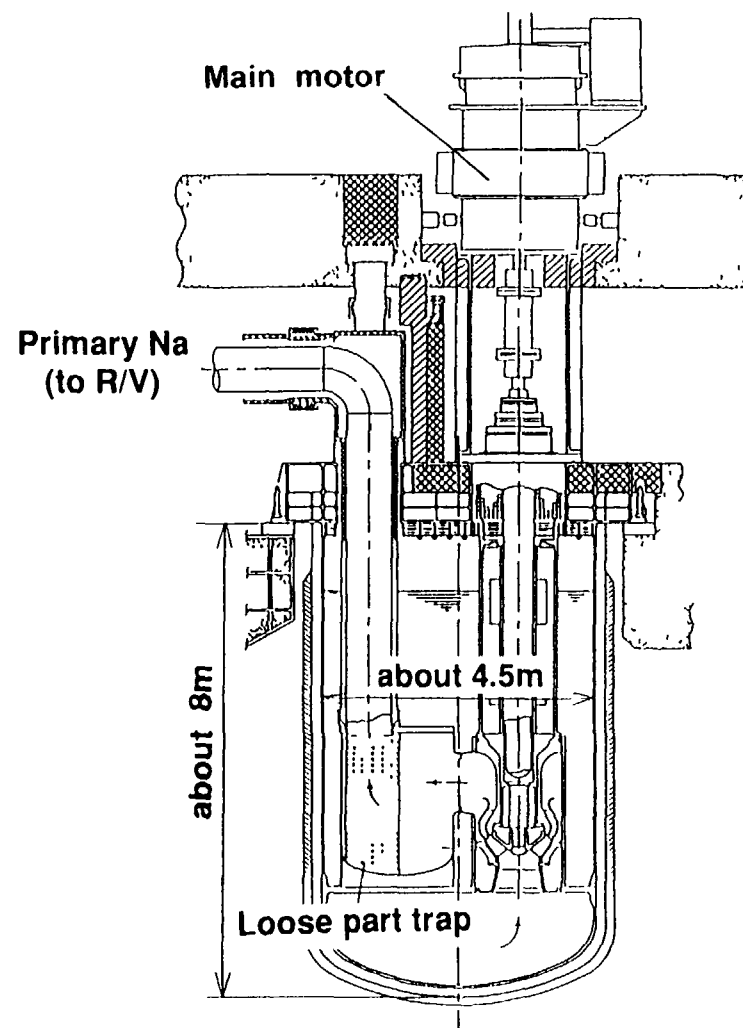


FIG 9 43 Primary pump

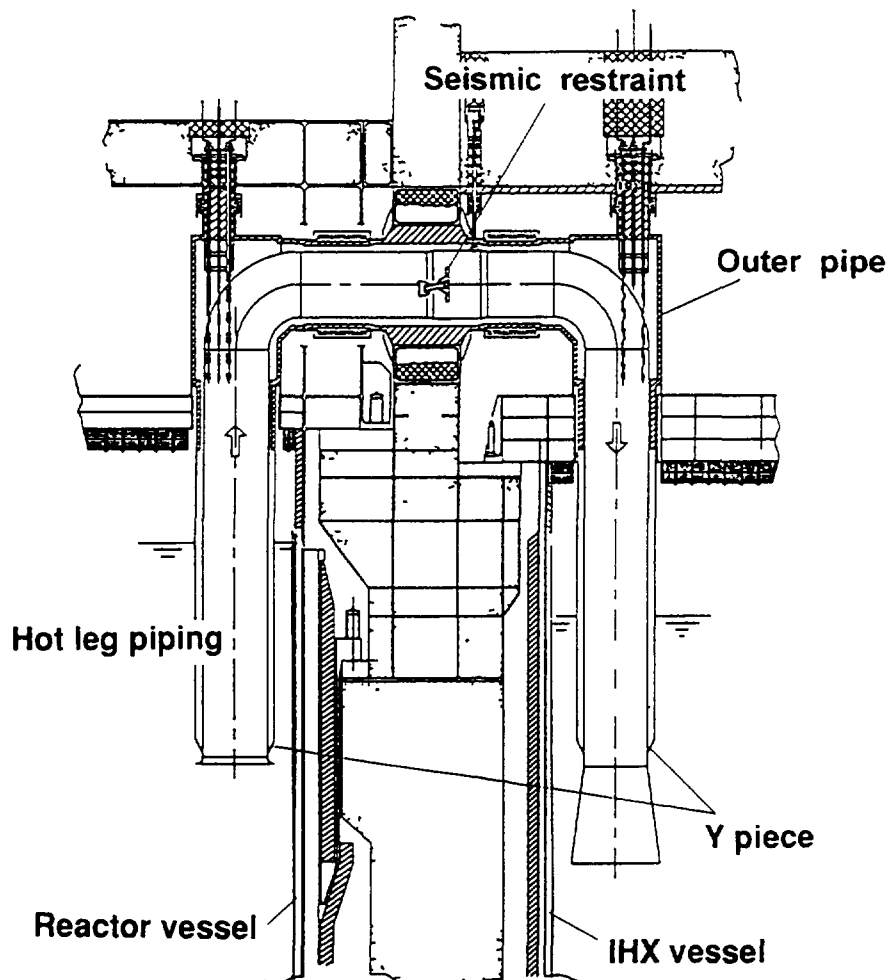


FIG 9 44 Primary piping

Main secondary components: The main secondary cooling system consists of the secondary pumps, steam generators and secondary piping

The steam generator is of an integrated once-through type with helical-coil heat transfer tubes, proven in the development of the prototype reactor "Monju". It is made of modified 9Cr-1Mo steel because of its superior strength at high temperature and resistance to stress-corrosion cracking. The diameter and thickness of the tubes is 31.8 mm and 3.9 mm to ensure adequate strength. The steam generator concept is shown in Fig 9 45.

Safety features. The reactor has two shutdown systems, the primary reactor shutdown system and the backup reactor shutdown system, either of which can stop the reactor rapidly independently of the other. The primary reactor shutdown system employs rigid control rods, while the backup reactor shutdown system employs articulated rods to ensure insertion during earthquakes. The backup reactor shutdown system is provided with a self-actuated shutdown mechanism to reduce the consequence of an anticipated transient without scram.

Decay heat removal is by a Direct Reactor Auxiliary Cooling System (DRACS) with heat exchangers immersed in the reactor vessel, which improves reliability by a combination of forced and natural circulation, and can remove decay heat without reliance on the outer

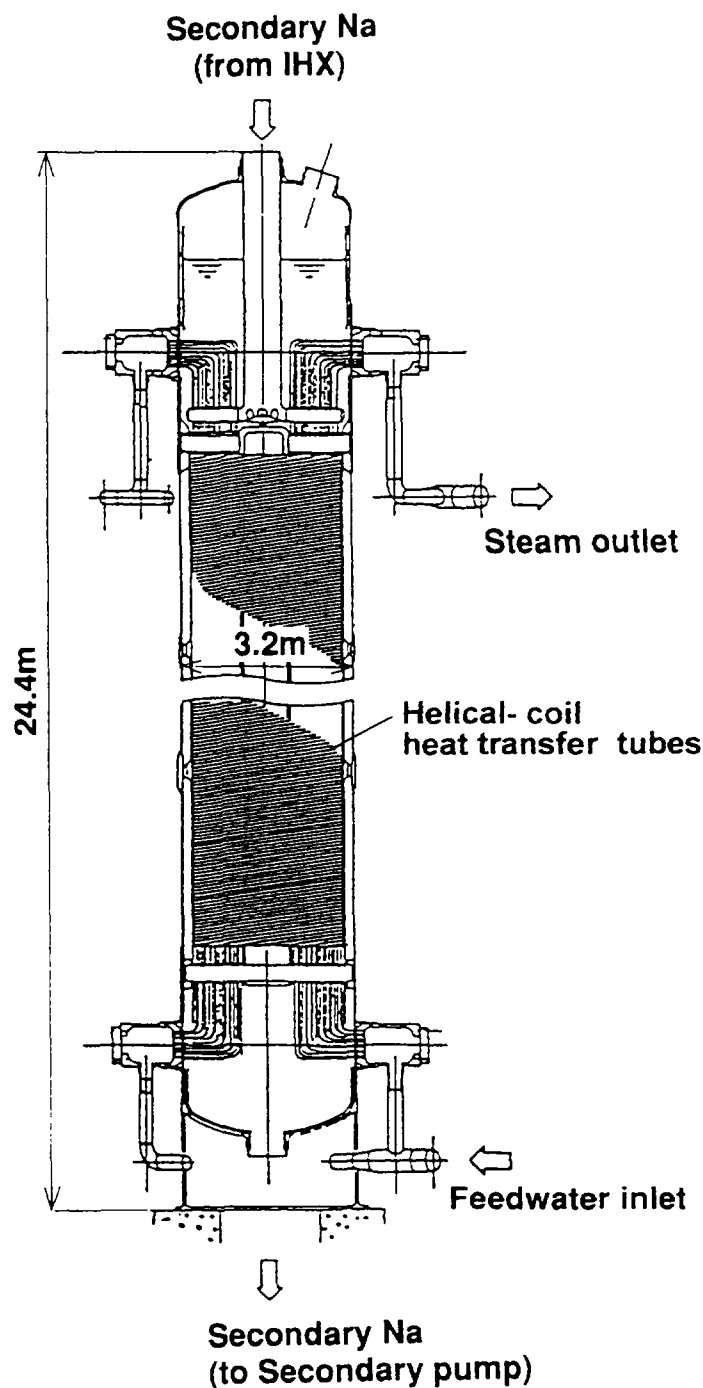


FIG. 9.45. Steam generator

primary loops in the extreme case. Four independent systems are installed to provide redundancy, and the heat removal capacity has been determined by various safety analyses. In the normal operational mode after a reactor trip decay heat is removed by the steam water system using the turbine bypass.

The containment facility is a rectangular concrete structure with an inner lining, integrated with the building for effective use of space and for economy. A secondary containment is provided, as for an LWR, for those areas with penetrating piping and cables,

and is maintained at negative pressure and provided with an emergency gas system to absorb radioactive substances. The design temperature and pressure are 150°C and 0.5 kg/cm² respectively, based on the result of safety analysis of an event in which sodium is ejected into the containment facility in the course of anticipated transients without scram (ATWS).

The emergency power supply system shuts the plant down safely in the event of loss of external power. Three independent emergency bus lines with proven diesel generators are provided to supply power to the emergency system.

The reactor protection system has "2 out of 4" logic design to improve reliability. Different designs are used for the operation of the primary reactor shutdown system and the backup reactor shutdown system, including the detectors and logic circuits, to reduce the probability of common mode failure.

Fuel handling system. The fuel handling system consists of the fuel exchange system, the fuel loading and unloading machine, and the fuel handling and storage system outside the reactor. The fuel exchange system charges fuel into the core and removes it from the core. This system is installed on a rotating plug and consists of direct lift and manipulator machines. Fuel assemblies around the centre of the core are transferred using the direct lift machine to the area which the manipulator machine can reach. This minimizes the average distance of horizontal travel of the fuel handling machine and reduces the diameter of the rotating plug. The fuel loading and unloading machine transfers fresh fuel assemblies into the reactor vessel and spent fuel from it. The rotating chamber and chute system accelerates the fuel transfer operation and greatly reduces the fuel exchange time.

Reactor building. Two types of reactor building were investigated. One is an anti-seismic structure embedded in rock, and the other is a seismically isolated structure to reduce seismic force applied to the building. The layout of all components has been analyzed in detail to secure efficient access and maintenance of components, and to reduce the size of the building. The aseismic reactor building is about 57 m x 58 m with a height of 65 m. Figure 9.46 shows the aseismic reactor building embedded in rock, and Fig. 9.47 shows the seismically isolated reactor building.

9.5.3. Technical and economic evaluation

Safety. In the safety evaluation, a number of typical accident events were analyzed to understand the consequences of abnormal plant conditions. The purpose is to ensure that accidents are prevented effectively and to minimize their consequences with an adequate margin. The safety evaluation events include: (a) Events that affect the core due to abnormal conditions in the core and primary cooling system, such as loss of external power supply, primary pump shaft seizure, primary piping break, accidental control rod withdrawal, and passage of a void through the core; (b) Events peculiar to the top-entry arrangement such as abnormal liquid level in the primary system and cover gas piping break; and (c) Events caused by the sodium coolant such as leakage of the secondary coolant and heat transfer tube failure in the steam generator.

Cooling core flow. In the events of loss of external power, primary pump shaft seizure and primary piping break, analyses show that the reactor trips automatically and the event is terminated safely in all cases. The maximum temperature of the fuel and fuel cladding remain within the limits with sufficient margins. In the event of one primary pump shaft seizing the

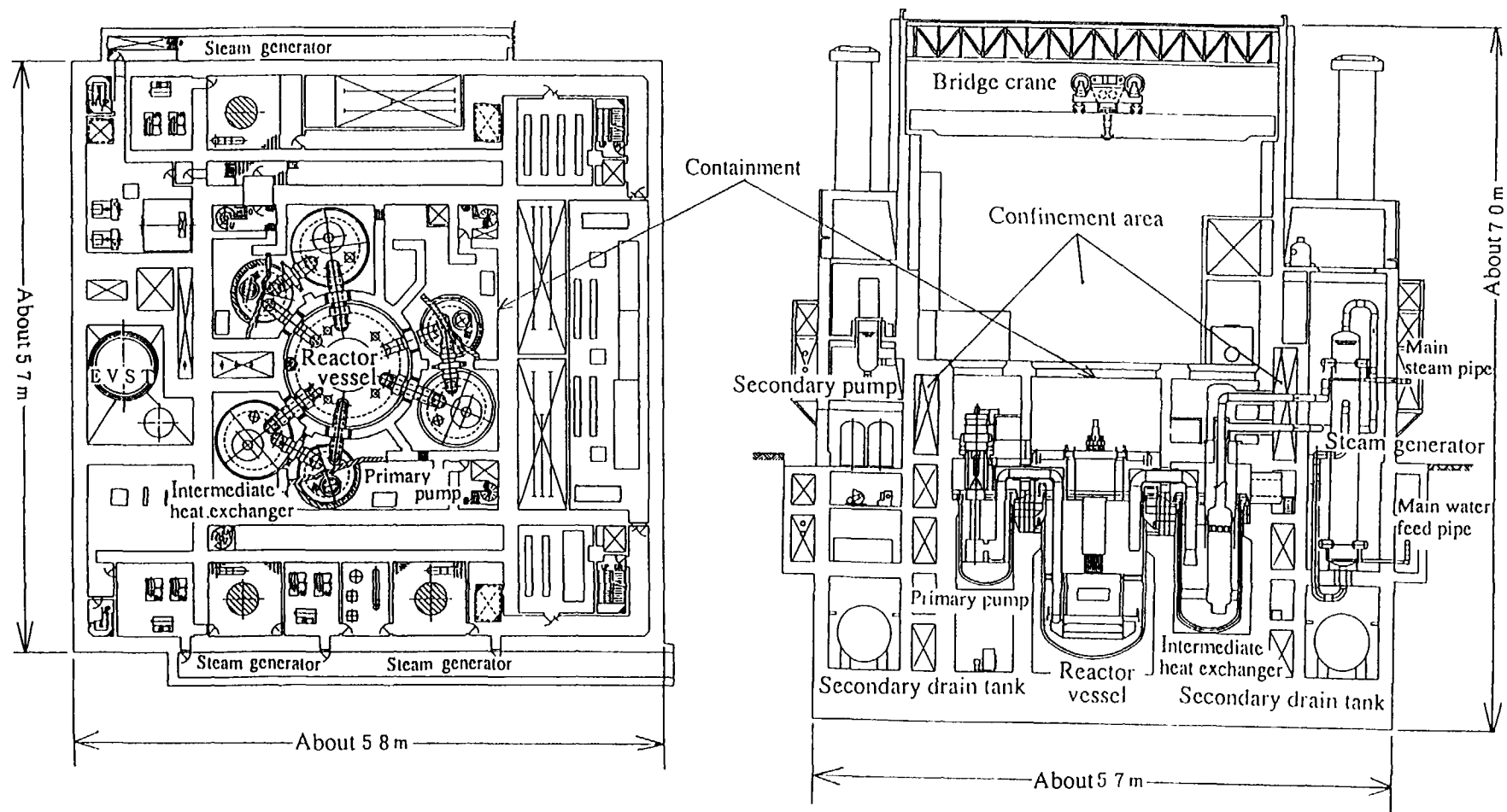


FIG. 9.46. Aseismic reactor building

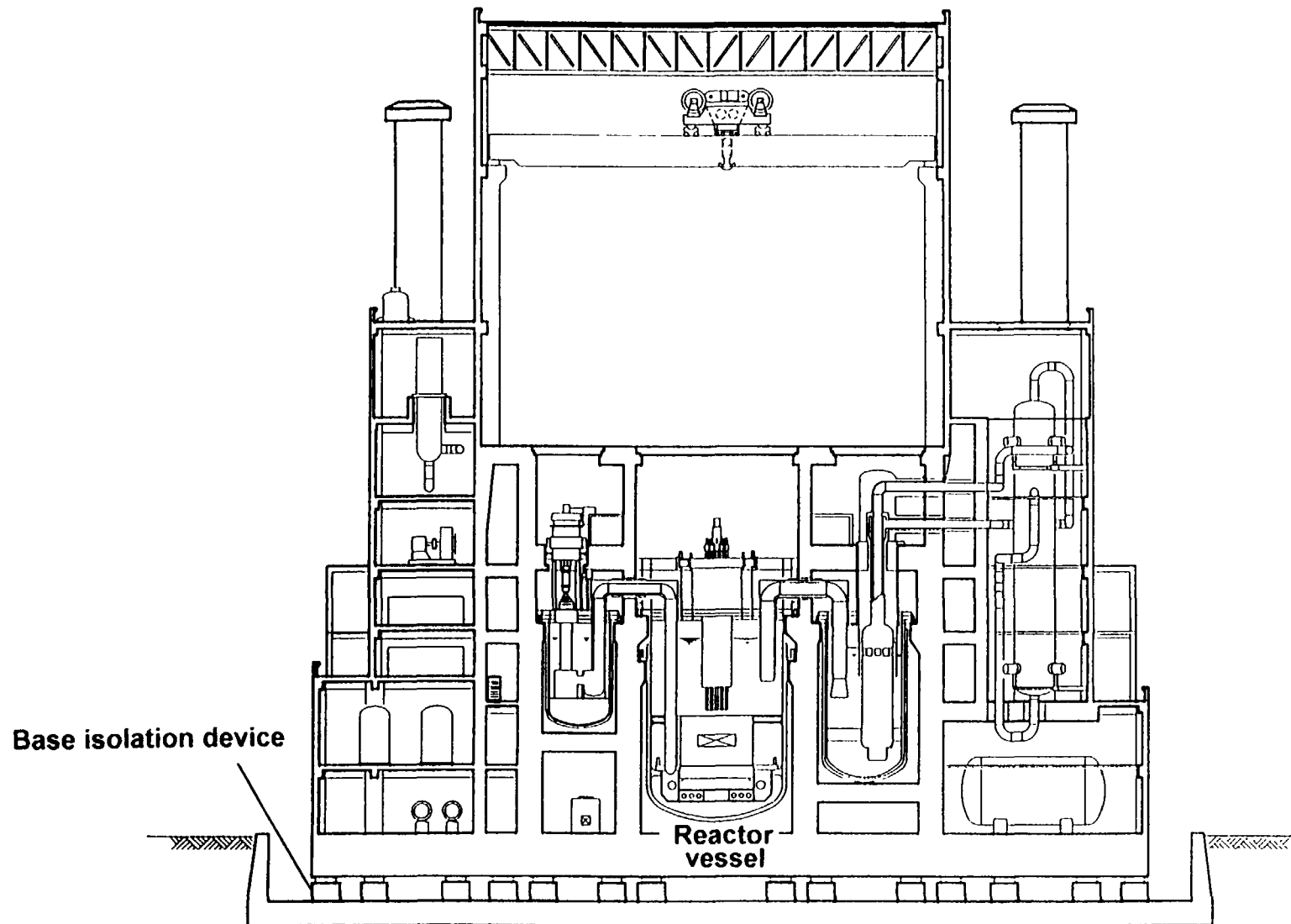


FIG. 9.47. Seismically isolated reactor building

pump is conservatively assumed to stop instantaneously and the reactor is assumed to scram after one second due to the signal of low rotating speed of the pump. The sound pumps trip automatically due to the scram signal but are delayed by about 0.1 - 2 seconds. Analysis of the effect of the pump trip delay on the maximum temperature of the fuel cladding shows that the temperature of the fuel cladding remains lower than the limit with sufficient margin for a one second trip delay as the power of the reactor begins to drop due to the scram.

Prevention of abnormal reactivity. Accidental withdrawal of control rods and passage of gas through the core during reactor operation were analyzed. In both events, the reactor automatically shuts down, the event terminates safely and the maximum temperature of the fuel and fuel cladding remains within the limits with sufficient margin.

Pipe break in the cover gas system. If a pipe of the cover gas system breaks, the liquid levels in the vessels may vary due to difference of the cover gas pressure between the vessels. Sodium leakage from the broken pipe and possible fires were analyzed. Any leakage of sodium from the break is controlled and sodium fires can be prevented by duplicate connecting pipes between vessels with double walls in the necessary portions and by a nitrogen atmosphere. This allows the liquid level to settle soon after any break.

Chemical reaction of sodium. In the event of coolant leakage caused by a secondary piping break, analyses confirm that buildings are safe since the pressure in the room and the temperature of the concrete wall do not exceed the limits.

In the event of instantaneous guillotine break of one tube in a steam generator with resultant fracture of three further tubes, analysis shows that the reactor shuts down and the event is terminated safely by several automatic operations. These include blowdown of the water in the steam generator and tripping of the secondary pump. The pressure generated in the secondary piping and the secondary side of the IHX is also kept below the structural integrity limit for these components.

Structural integrity. The structural integrity of the main components and structures in the primary system was analyzed, especially for different structures or load conditions from those of "Monju". The structural integrity was carefully examined for the reactor outlet temperature of 550°C. Elastic analysis was used to evaluate all parts of components and structures. The seismic conditions used to evaluate structural integrity were 3.2g in the horizontal direction (for 0.1 to 0.2 sec) and 1.9g in the vertical direction (for approx. 0.1 sec) on the floor supporting the reactor vessel. The thermal transient conditions are set by analysis of frequent events which cause significant hot or cold shocks. The frequency of such events is assumed to be the same as for "Monju". The number of normal startups is set to 427 with 120 normal shutdowns in accordance with the classification of operating conditions set by the government notification, and 300, 6 and 1 emergency shutdowns in operating conditions II, III and IV respectively.

Reactor structure. The seismic response of the reactor structure was analyzed using a 3-dimensional shell model with fluid-structure interaction. The structural integrity was confirmed without buckling of the reactor vessel or the vessel wall cooling liner, while ensuring that control rods can be inserted. Thermal stresses are especially severe on the reactor vessel wall near the liquid surface, the bottom plate of the UIS, and the inlet plenum of the core support structure. Thermal ratchetting and creep fatigue damage were evaluated at these locations by thermal stress analysis, confirming that the structural integrity is maintained by the

use of 316FR for those structures exposed to high temperatures and by cooling the reactor wall by the circulation of low temperature sodium.

Primary Piping. The seismic response of the primary piping was analyzed using a beam model. The seismic strength is maintained by installing a seismic restraint on the horizontal piping. The temperature distribution and thermal stress were also analyzed, and the thermal expansion stress and creep fatigue damage were evaluated, particularly for the thermal expansion of the entire piping system and for those parts with structural discontinuity subject to high thermal transient stresses, for example, the Y piece. Structural integrity is assured by using 316FR for high temperature components and installing a seismic restraint on the horizontal piping near the neutral point of thermal expansion.

IHX. The results of seismic response analysis using a 3-dimensional model of the interconnected system of vessel and IHX show that the integrity of the IHX is maintained without buckling. The temperature distribution and thermal stresses were analyzed, and thermal ratchet and creep fatigue damage were evaluated, particularly for those parts subject to high thermal stresses, for example, the IHX vessel wall near the liquid surface, the upper and lower tube sheet and the foot of the gas dam wall. Structural integrity is assured by using 316FR for high temperature components and by gas dam thermal protection of the vessel walls.

Steam generator. Seismic response analysis of the steam generator using a beam model shows that the seismic strength is maintained without buckling of the drum or supporting skirt. The temperature distribution and thermal stresses were analyzed and creep fatigue damage was evaluated for those parts with structural discontinuity subject to high thermal transient stress, for example, the steam outlet tube sheet. Structural integrity is assured by using Mod. 9Cr-1Mo steel and partitioned small tube sheets. Evaluation of the fatigue damage to the heat exchanger tubes by DNB oscillation in the boiling region shows that the damage is within the allowable limit.

Thermal hydraulics. Three kinds of thermal hydraulic tests were conducted to confirm the technical feasibility of the top entry loop type reactor: a natural circulation flow test, a multiple-surface sloshing test and a gas entrainment test. These tests were conducted with the cooperation of CRIEPI, PNC and various universities.

Natural circulation. A natural circulation water flow test simulated the operating conditions of the decay heat removal system (DHRS) for various events, varying the core flow rate, temperature change characteristics, and the type of DHRS. A 1/8 scale 3-loop model of the primary system of the actual plant was used, with water as the working fluid. Applicability of analytical codes was also evaluated. Three DHRSs were tested, an immersion type DRACS, a penetrating DRACS, and a primary reactor auxiliary cooling system (PRACS). Simulated events included loss of external power, loss of total power, and natural circulation in the reactor. These tests show that the core flow rate under steady-state natural circulation is 1.6% of the rated flow. The integrity of the fuel and structure during decay heat removal in the actual plant is assured.

Sloshing. Sloshing characteristics tests were conducted with a multiple liquid surface system simulating an earthquake to check that siphon break or large volume gas entrainment is not caused by sloshing of the multiple liquid surfaces. A 1/8 scale 3-loop model of the primary system of the actual plant was used, with water as the working fluid. Tests were conducted for a seismic vibration equivalent to the extreme design basis earthquake, and confirmed that the

lower end of the hot leg piping was not exposed to gas and a large volume of gas was not entrained.

Gas entrainment. Gas entrainment tests were conducted in order to develop a method to evaluate the gas entrainment limits in an actual plant and to check that no gas is entrained, particularly in the IHX vessel. Tests were conducted using four models of 1/10, 1/6, 1/3 and 1/1.6 scales as gas entrainment might depend on the scale of the model. It was found that reducing the flow speed at the free liquid surface will prevent gas entrainment due to broken or superimposed waves. A survey shows that gas entrainment can be suppressed by the introduction of measures such as a horizontal perforated plate or a perforated cylinder near the inlet nozzle.

Operability and maintainability. The control system of the plant was designed and checked for plant stability with no significant oscillation or deviation for 10% stepwise changes and 5% ramp changes in reactor power. ISI of the primary major components was implemented for the structural concept based on the ISI policy(draft) established for the DFBR. It is confirmed that the major components and main piping in the primary loop can be repaired and maintained. Maintenance methods and procedures were examined using 3-dimensional CAD simulation. It was confirmed that regular maintenance and inspection works can be carried out within 60 days.

Construction costs. Derived from the quantities of major materials calculated from the DFBR design, the construction cost was estimated by the "Command Cost Code" specially developed for the prediction of FBR construction cost. The evaluation shows that the construction cost of the 660 MWe DFBR is 130 if the cost of a 1000 MWe class LWR is 100 (the cost of a 1000 MWe class DFBR is 150), which meets the target of DFBR cost of about 1.5 times that of a LWR for a large scale reactor.

9.5.4. Prospects for FBR commercialization

The possibility of FBR commercialization and the targets of technological development have been established with the cooperation of JAPC and PNC. The key factors affecting the commercialization of FBR are as follows.

- (1) In order to utilize uranium resources effectively and to help protect the environment, FBRs need to be commercialized. However, commercialization will be possible only around the year 2020 to 2030 when the required innovative technologies have been developed.
- (2) Stricter safety standards will be required to gain public acceptance in order to introduce FBRs widely.
- (3) Since the economy and reliability of LWRs might also be improved, the economy and reliability of a commercial FBR must be improved still further by system simplification and rationalization.

To achieve these objectives, the following new innovative technologies and system improvements will be required for commercial FBRs:

- (1) Core design with enhanced safety and highly reliable reactor shutdown systems,
- (2) More reliable decay heat removal such as a passive system with natural circulation,
- (3) Simplification of the upper structure of the reactor vessel and the fuel handling system to avoid the need for rotating plugs,

- (4) Electromagnetic pumps for the primary and secondary cooling system to be combined with the IHXs and SGs,
- (5) Seismic isolation systems to reduce the quantity of structural materials and to standardize the plant design independent of site conditions,
- (6) Elimination of the intermediate heat transport system.

Combinations of these innovative technologies can bring about a substantial reduction in plant costs. Preliminary concepts of the commercial plant were drawn up assuming that all these innovative technologies will be available. Cost evaluation using "Command cost Code" has shown that economically competitive FBRs can be realized even compared to advanced LWRs in the future.

9.5.5. Conclusion

Design work is progressing in JAPC on the DFBR. The technical feasibility of the top entry loop type DFBR has been confirmed, and the economic targets fulfilled. The possibility of FBR commercialization and targets of technological development have been envisioned through the cooperation of JAPC and PNC.

Research and development of the DFBR are progressing with the cooperation of JAPC, PNC, JAERI, and CRIEPI, and the results of the R&D effort by individual organizations are being reflected in the design.

The Committees of JAEC are currently discussing ways to establish a revised "Long-term Plan for the Development and Application of Nuclear Power". A national consensus will then be reached in order to realize the DFBR in the near future.

9.6. PROTOTYPE FAST BREEDER REACTOR - DESIGN DESCRIPTION

9.6.1. Introduction

The Prototype Fast Breeder Reactor (PFBR) is a 1250 MWt, 500 MWe pool-type sodium-cooled reactor under design in India. This closely follows the successful construction and commissioning of the experimental reactor FBTR (40 MWt, 13,2 MWe). A brief design description of the various systems is given below. The main characteristics are given in Table 9.5. A schematic of the main heat transport system is given in Fig.9.48.

9.6.2. Reactor assembly

Fig. 9.49 shows a vertical section of the reactor assembly. Mixed oxides of plutonium and uranium ($\text{PuO}_2\text{-UO}_2$) is used as fuel and depleted uranium oxide as blanket. The entire primary sodium circuit consisting of the core, four intermediate heat exchangers (IHXs), two primary sodium pumps and the grid plate are, housed in the main vessel. The inner vessel divides the sodium pool into two parts viz hot pool and cold pool. A small quantity of primary sodium is taken out of the main vessel for purification and returned after purification. The main vessel is covered by the top shield consisting of a roof slab, rotatable plugs and control plug. Argon at 10 kPa pressure is used as the cover gas. A safety vessel is provided around the main vessel to contain sodium in the unlikely event of leakage from the main vessel. The entire reactor assembly is supported on the reactor vault by a conical support shell which is welded at the top to the roof slab. The reactor assembly is housed inside the reactor vault

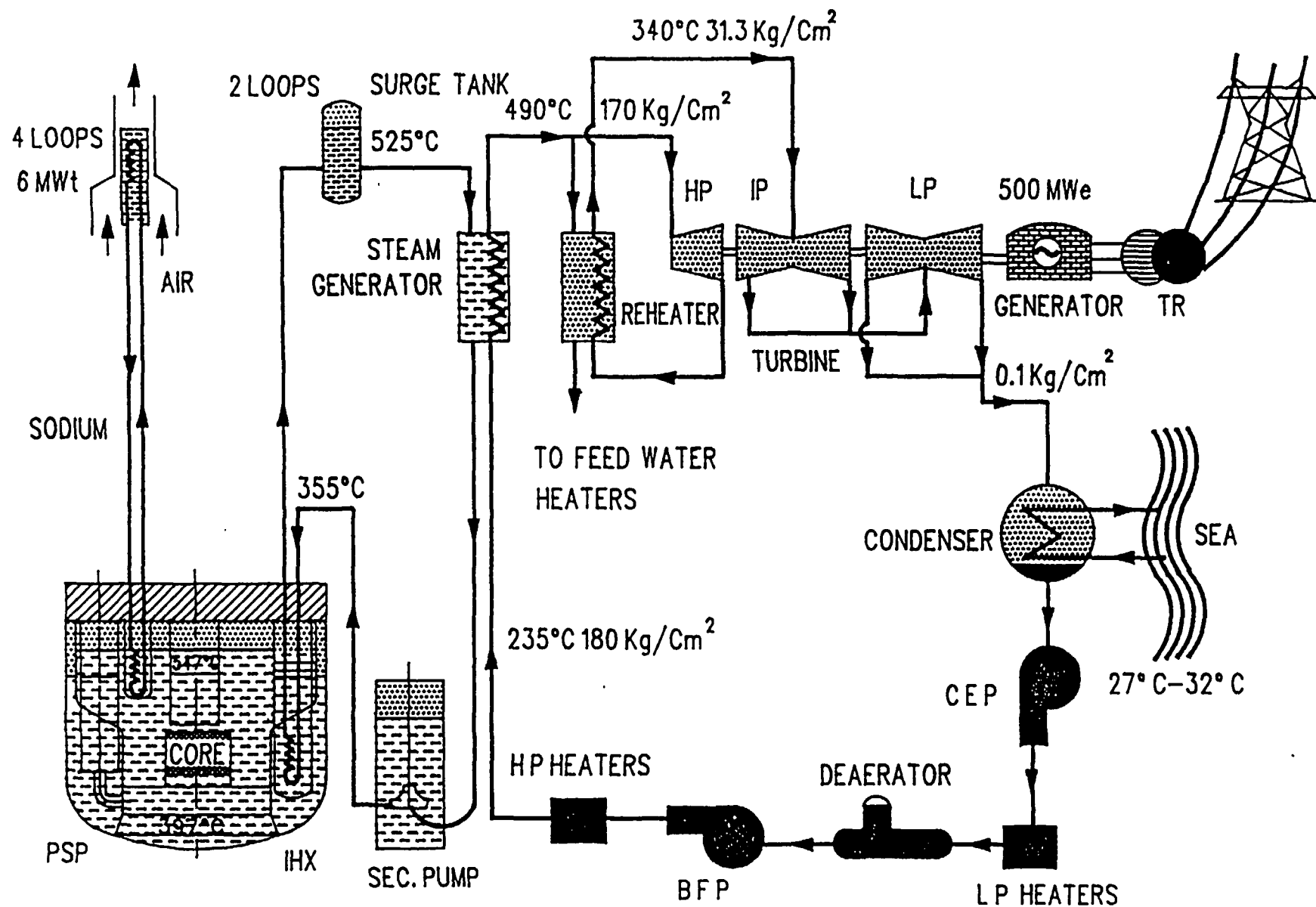
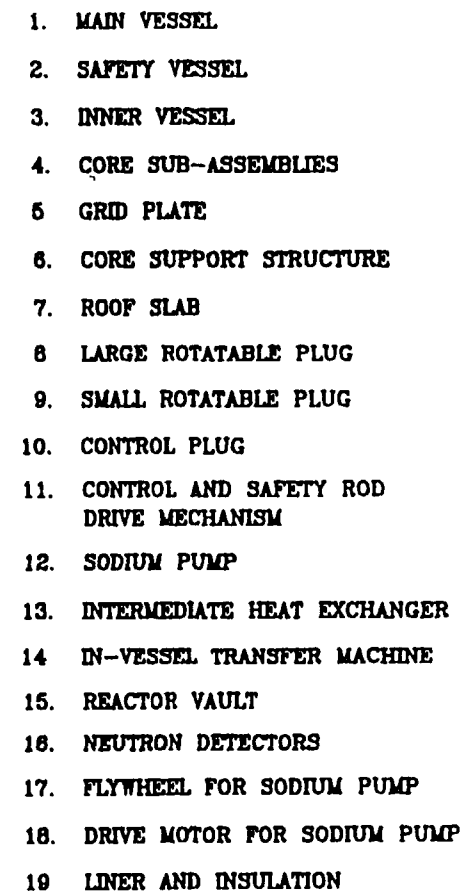


FIG. 9.48. Heat transport system



471

which is lined with carbon steel plates. Four sodium-sodium decay heat exchangers are placed in the hot pool to remove decay heat during loss of offsite power.

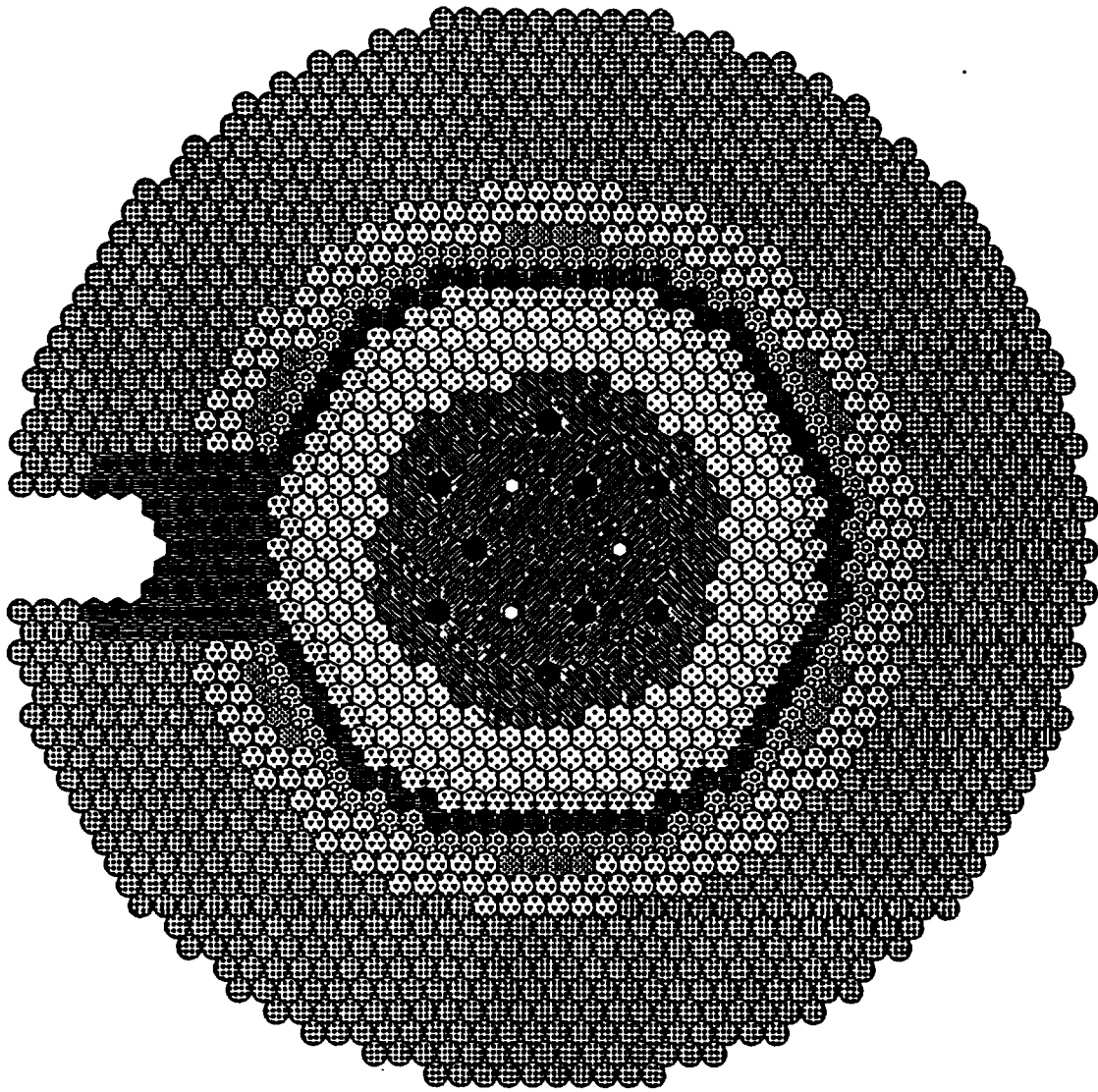
Core: Fig. 9.50 shows the core plan. The core is homogenous with a central fuel region surrounded by blanket subassemblies which are in turn surrounded by neutron shields. The fuel region is divided into two zones of different fissile enrichment. The inner core of 91 subassemblies has 21% PuO₂ while the outer core of 90 subassemblies has 28.4% PuO₂. Excess reactivity of 9000 pcm is built in to allow for reactivity loss on going from shutdown to full power, burnup, and control margin. The total control rod worth is estimated to be 10,900 pcm for 9 primary rods with 70 at % of B10. The worth of the 3 secondary rods, which are only used for shutdown purposes, is 3850 pcm. The neutron flux at core centre is 7.8×10^{15} n/cm²s and the design burnup is 100 MWd/kg (max). To limit the activation of the secondary sodium shielding is provided in both the axial and radial directions. The upper axial shield (Boron & stainless steel) is integral with the fuel subassembly. In the radial direction, 78 reflector, 78 inner boron carbide, 869 steel and 426 outer boron carbide assemblies are provided in a 13-row configuration to limit the sodium activity in the secondary sodium to 81 Bq/cc. For the shielding in the vault 180 cm of concrete is provided. Shielding against sodium 24 gammas is provided in the axial direction by the top shields. The fuel, blanket, reflector, inner boron carbide shielding and storage subassemblies are located on the main grid plate (637 subassemblies) and are provided with forced cooling. The rest of the steel and shielding subassemblies are located on the auxiliary grid plate. The profile of a fuel subassembly is shown in Fig. 9.51. The fuel pins are of 5.55 mm OD and there are 217 fuel pins in each subassembly. The active length is 1 m. The blanket assemblies have 61 pins. About 5.5% of the core flow leaks downwards past the foot of the subassemblies and is used to cool the main vessel.

Absorber rod drive mechanisms: There are 9 primary control and safety rods (CSR) which are used to raise or lower reactor power at a fixed speed. They are also used to shut the reactor down by continuous (automatic) lowering or gravity drop as necessitated by the reactor protection logic. To provide diversity and avoid common mode failures 3 diverse safety rods (DSR) are also provided. These rods are coupled to their drive mechanisms by electromagnets which are immersed in sodium. A Curie point magnetic switch is located in the mechanisms. In the unexpected event of failure of the reactor protection logic, the temperature of the sodium exiting from the fuel subassemblies rises as a result of overheating or undercooling to 600°C, and actuates the Curie point switch, thereby deenergising the electromagnet, leading to a gravity drop of the 3 DSRs into the core.

Grid plate: The grid plate is a box-type welded structure which consists of upper and lower plates interconnected by a number of tubes called sleeves and an outer cylindrical shell. The sleeves act as tie rods between the top and bottom plate and also supports for the subassemblies. Sodium enters the grid plate through four pipes connected to the discharge of the four primary pumps.

Core support structure: The grid plate is supported on the core support structure (CSS) which also supports the shielding subassemblies via the auxiliary grid plate and the inner vessel. It is a radially stiffened structure supported on the main vessel bottom by a cylindrical shell.

Roof slab: The roof slab forms a part of the primary containment boundary in addition to providing thermal & biological shielding and support for the major components viz. 2







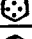







SYMBOL	TYPE OF SUBASSEMBLY	No.	MASS PER SUBASSY. IN Kg
	FUEL (INNER)	85	245
	FUEL (OUTER)	96	245
	CONTROL & SAFETY ROD	9	200
	DIVERSE SAFETY ROD	3	200
	BLANKET	186	320
	STEEL REFLECTOR (INNER)	72	355
	B ₄ C SHIELDING (INNER)	69	185
	STORAGE LOCATION	75	245
	RESERVE STORAGE LOCATION	24	355
	ENRICHED BORON SHIELDING	56	185
	STEEL SHIELDING (OUTER)	180	330
	B ₄ C SHIELDING (OUTER)	903	265

FIG. 9.50. Core configuration

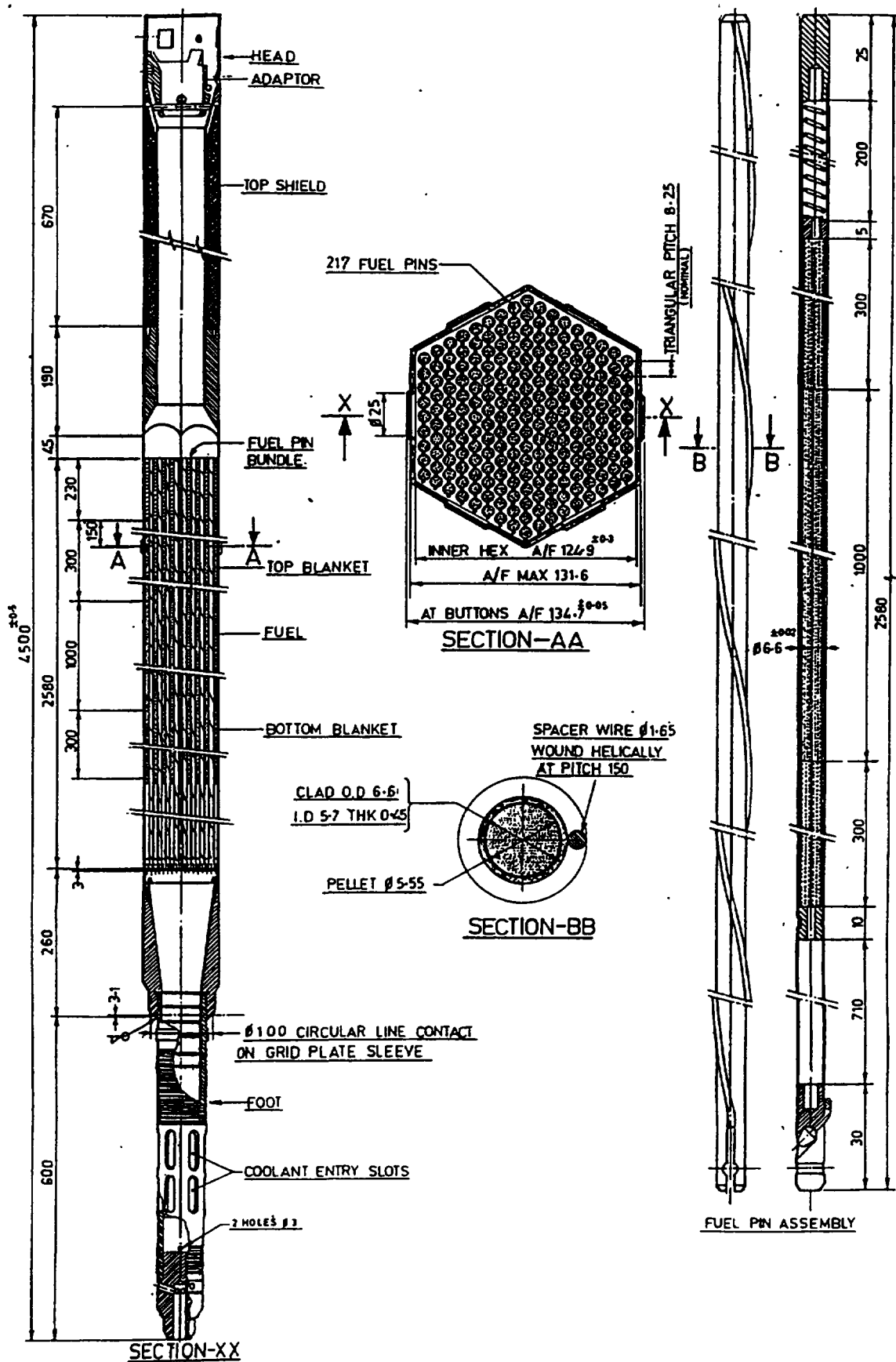


FIG 9 51. PFBR fuel subassembly

primary pumps, 4 IHXs, 4 DHXs etc. The main vessel with its internals is also supported from the roof slab. This is a box-type welded structure in carbon steel filled with high temperature heavy density concrete. In order to reduce the heat flux incident on its lower surface from the hot pool sodium a thermal baffle is provided below the bottom plate of the roof slab. The temperature of the bottom plate is maintained at 120°C by forced air cooling. To facilitate control of sodium fires on the roof slab, a cell type enclosure is provided which can be inerted with nitrogen in case of fire.

Rotatable plugs: Two rotatable plugs, the large plug concentric with the core and the small eccentric to core it, provide access to the core subassemblies for refuelling.

Control plug: The control plug houses the control rod drive mechanisms and the instruments for core surveillance. The heat flux is reduced and shielding is provided by stainless steel plates stacked at suitable elevations in the plug. Unlike the rotatable plugs, the control plug is not cooled.

Reactor vault: The reactor vault supports the entire load of the reactor assembly. The walls of the vault are lined with carbon steel plates to prevent direct contact between concrete and sodium in the most unlikely event of multiple barrier leaks. The steel liner is provided with thermal insulation. To cool the vault water is passed through pipes embedded in the concrete close to the steel liner.

9.6.3. Primary sodium system

The primary circuit consists of 2 pumps and 4 IHXs with one IHX on either side of each pump. The two IHXs on either side of a pump are linked to one secondary sodium loop. The primary sodium from the hot pool flows on the shell side while secondary sodium flows on the tube side of the IHX. The IHXs discharge primary sodium to the cold pool, from where it is pumped to the grid plate through a pump-grid plate pipe connection.

Primary sodium pumps: Each pump delivers 3636 kg/s flow and develops a head of about 75 m. It is a vertical submersible, centrifugal pump with free cover gas surface. It has a mechanical seal and thrust bearing at the top and a hydrostatic bearing at the bottom. At the top radiation shielding is provided and the pump is driven by a variable frequency synchronous motor. A flywheel mounted directly on the pump shaft is designed to provide a coastdown with a flow halving time of 8 s. A battery bank has been provided as a defence in depth, to supply the power to a pony motor that rotates the pump at 100 rpm for half an hour following a station blackout.

Intermediate heat exchanger (IHX): This is a vertical shell and tube counter-flow heat exchanger with no free sodium level. The tubes are straight with no expansion bends and the tube-to-tubesheet joint is rolled and welded. Thermal shields are provided to protect the bottom tubesheet from thermal transients. Antivibration belts surround the tube bundle to prevent vibration. A sleeve-type valve is used to isolate the IHX primary side when it is non-operational.

Primary sodium purification: Purification of the primary sodium is accomplished by two cold traps located outside the main vessel. Organic cooling with a NaK jacket is provided.

9.6.4. Secondary sodium system

There are two identical loops each comprising 2 IHXs, a pump, a surge tank and 3 steam generator modules. The pump is located on the cold leg, at the lowest elevation. It is similar in design to the primary pump. The secondary sodium piping inside the Reactor Containment Building (RCB) is provided with guard piping to minimise the effects of a sodium leak. The layout and location of the piping and components are optimised with a view to minimize the amount of piping.

Steam generator: Once through steam generators have been chosen and there are 4 steam generators (SG) in each loop. Each steam generator delivers superheated steam at 17 MPa and 766 °K (493°C). They are vertical shell and tube heat exchangers with sodium on the shell side and high pressure water/steam on the tube side. Differential thermal expansion between tubes and shell is accommodated by expansion bends in the tubes. The tube-to-tubesheet joints have internal bore welds with a raised spigots. The SG are provided with reverse buckling rupture discs on the sodium outlets and inlets of all the units to relieve the pressures generated in a large sodium water reaction. Isolation valves are provided on the sodium and water sides to allow operation with an isolated SG.

9.6.5. Fuel handling (Fig. 9.52)

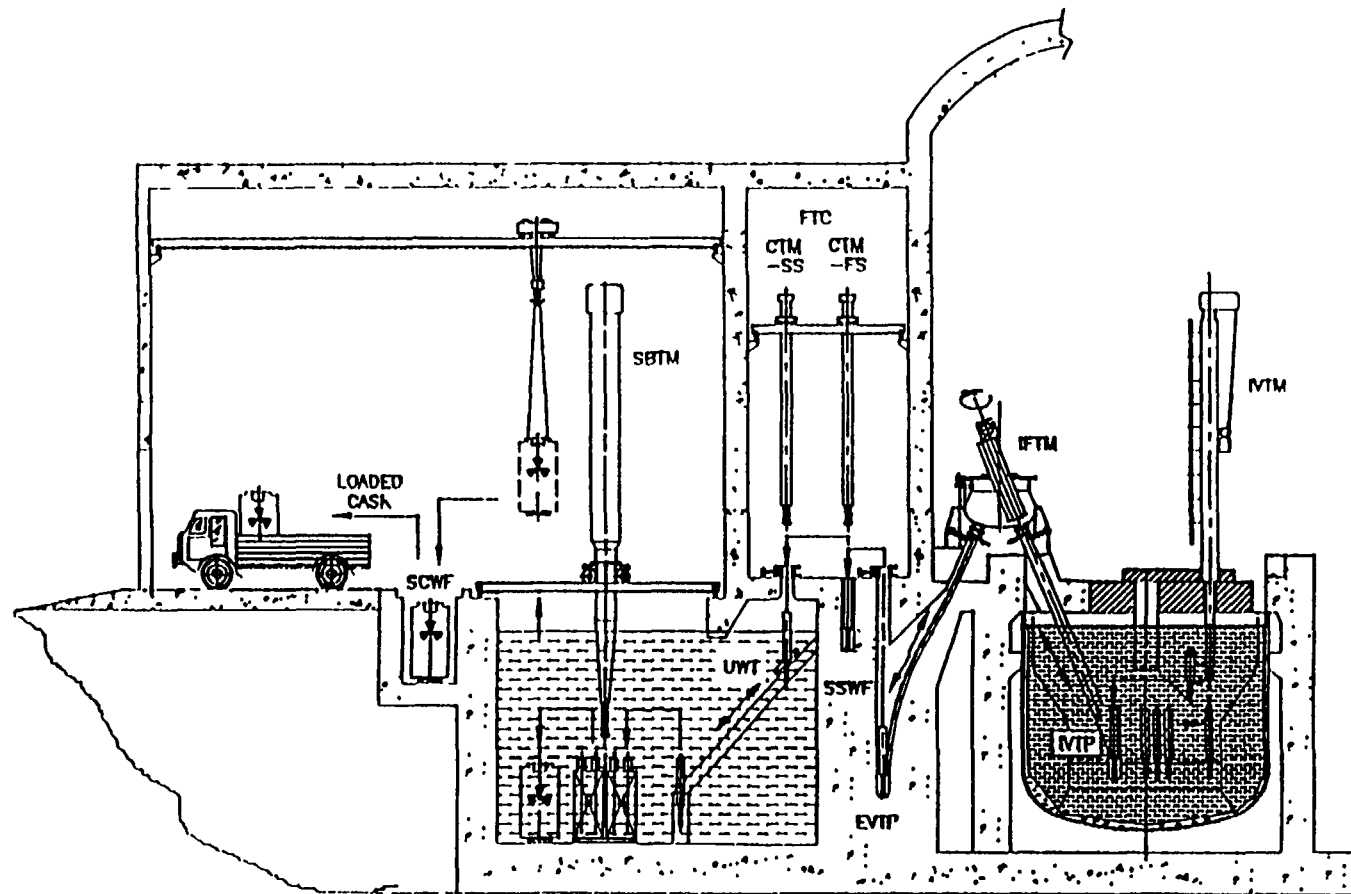
Fuel handling operations include charging of fresh subassemblies and removal of irradiated subassemblies from the reactor. After its desired burnup an irradiated fuel subassembly is moved to a storage location within the main vessel in the region beyond the neutron shields by a straight-pull in-vessel transfer machine (IVTM). It is kept in the vessel until the decay power is 5 kW. It is then taken to ex-vessel storage through an inclined fuel transfer mechanism (IFTM). After suitable washing and decontamination it is put in the spent fuel storage bay under water before it is sent for reprocessing.

9.6.6. Decay heat removal

If all main transport circuits and power are available the decay heat is removed via the normal path. In case of loss of offsite power or station blackout decay heat is removed via the 4 decay heat removal circuits in the hot pool. Each circuit has a Na/Na decay heat exchanger (DHX) immersed in the hot pool and linked to an air heat exchanger (AHX), and is rated for 6 MW decay heat removal based on 18 MW capacity and a single failure criterion. The sodium flows between the DHX and the AHX by natural convection, as a consequence of the temperature and elevation differences between the two. There are dampers on the air side of the AHX which have to be opened. Apart from the damper, the rest of the system is passive. The system is designed to sustain a delay of up to 30 min. in opening the dampers.

9.6.7. Materials

The fuel clad and wrapper are made from 20% CW D9. Most of the materials used in the primary and secondary components and pipelines, except for the steam generators, are of AISI 316LN/304 LN grade. The roof slab is made of A516 grade carbon steel. The steam generators are made of modified 9Cr-1Mo steel (Grade 91).



IVTM : INVESSEL TRANSFER MACHINE
 IFTM : INCLINED FUEL TRANSFER MECHANISM
 IVTP : INVESSEL TRANSFER POSITION
 EVIP : EX-VESSEL TRANSFER POSITION
 SSWF : SPENT SUBASSEMBLY WASHING FACILITY

CTM-FS : CELL TRANSFER MACHINE (Fresh Subassembly)
 CTM-SS : CELL TRANSFER MACHINE (Spent Subassembly)
 UWT : UNDER WATER TROLLEY
 SBTM : STORAGE BAY TRANSFER MACHINE
 SCWF : SHIPPING CASK WASHING FACILITY

FIG 9 52 Spent fuel handling

9.6.8. Instrumentation and control

PFBR is to be operated as a base load station. It has a main control room and an emergency control room as well as local control stations. Distributed control systems using microprocessors are used. Safety-related systems are provided with redundancy, diversity, on-line testability and maintainability.

Neutron flux monitoring: To cover the whole range of flux from shutdown to full power, 3 sets of detectors with overlapping ranges are provided. One set is placed within the core and is effective from mW to 100 W. The other two sets are located below the reactor. While the second set responds to the range from tens of watts to few MW, the third set covers the range from a few hundred kW to beyond rated power.

Failed fuel detection: Failed fuel is detected by sampling the cover gas and the sodium coolant. Sodium samples are taken from 4 locations in the hot pool. As this method cannot identify the failed fuel subassembly, 3 localization modules are provided and housed in the control plug. Samples of sodium from the top of the subassemblies are taken one by one by means of a selector valve and measured for delayed neutrons. The subassemblies are divided into three groups and each group has a localization module.

Core temperature monitoring: All the fuel subassemblies are provided with temperature measurement at the outlet by 2 Cr-Al thermocouples. The signals are scanned every second by 3 dedicated computers. The signals are processed to detect overheating due to global or individual subassembly loss of flow. Inlet flow to the core from the discharge of the 2 primary pumps is measured using eddy-current flowmeters.

Steam generator leak detection: Leakage of water into the sodium is monitored by leak detection systems in the sodium at the outlet of each SG, and in the pump cover gas. They are based on the diffusion of hydrogen through nickel membranes. Acoustic leak detectors are also provided for each SG.

Reactor protection system: The purpose of this system is to shut the reactor down and bring it to a safe condition when any of the safety thresholds are crossed. Two types of safety actions are planned viz. continuous lowering of all 9 CSR or gravity drop of all 9 rods. The diverse safety rods are designed for gravity drop. Both the primary and secondary shutdown systems receive all plant inputs required for safety. Redundancy and diversity is provided and 2/3 logic is followed.

9.6.9. Fire protection

The system is designed to USNRC and IAEA safety guidelines. The relevant IS and NFPA codes have been adopted in the design of individual systems and components. A balance is achieved between fire prevention, fire detection, fire suppression and damage limitation. The overall scheme makes use of fire water and carbon dioxide for electrical cables, diesel generator rooms etc.; Halon 130 for control and computer rooms; piped dry powder for areas housing sodium system; nitrogen flooding for inaccessible areas; foam for the diesel fuel storage area; and portable extinguishers for other areas. In many cases double-walled pipes are used with an inert atmosphere between the two walls. Leak-collection trays are provided below large sodium capacities.

9.6.10. Containment

A hypothetical core meltdown accident resulting from loss of flow and transient overpower has been analysed and the mechanical energy release is expected to be 200 MJ. Nevertheless as a defence in depth measure the main vessel and roof slab are designed to withstand an energy release of more than 200 MJ. For the design of the containment building it is assumed that 500 kg of primary sodium would escape from the reactor vessel during a HCDA, and the containment building is therefore designed to withstand an internal over-pressure of 250 mb.

9.6.11. Emergency control room

This is situated above the fuel handling building and houses the redundant control and safety related systems to monitor the plant under emergency conditions of a fire in main control room or under any other accidental condition. Adequate shielding has been provided to reduce occupational exposure to persons in the room.

9.6.12. Balance of plant (BOP)

The BOP comprises a conventional turbine of 500 MWe with its associated steam/water system. The steam pressure and temperature are 17.3 Mpa and 480°C. Steam at the HP turbine outlet is reheated by live steam to 340°C. There are six feedwater heaters, three low-pressure surface heaters, one deaerator and two high-pressure surface heaters. The low-pressure heaters are arranged in a single-train configuration, while the HP heaters are arranged in a two-train configuration. A 60 % bypass across the HP and IP/LP turbines is provided to facilitate normal startup and fast restart after a turbine trip. Three 50% capacity main boiler feed pumps, 2 turbo driven and one electrically driven, are provided for coolant circulation. Full-capacity on-line demineralisation is provided to maintain the water quality required for the once-through steam generators. The condenser is cooled by sea water pumped by 3x50% capacity cooling water pumps. The generated voltage of 21 kV is stepped up to 220 kV and linked to the state grid. There are interlinks with the grid at six points. For emergency power supply to essential components there are four diesel generators (50%) housed in two independent stations.

Non-interruptible instrumentation and control supply is provided to support all loads for 30 minutes after off-site power failure and thereafter to support essential loads for 8 h.

9.6.13. Present status

The conceptual design of PFBR has been completed. Detailed analysis, R&D and technology development for component manufacture are in progress.

9.7 ALMR TECHNOLOGY DEVELOPMENT

9.7.1. Introduction

The objective of this programme was to verify the performance, reliability, and safety of the ALMR design. The concept utilizes the wealth of safety and sodium components technology developed for U.S. reactors, including the EBR-II, FERMI reactor, Southeast Fast Oxide Reactor, Fast Flux Test Facility (FFTF), and Clinch River Breeder Reactor.

TABLE 9.5. PLANT DATA

Thermal Power	- 1250 MWt
Electrical Power Gross	- 500 MWe
Net	- 470 MWe
Primary sodium pumps	- 2
IHX	- 4
Primary temperatures	- 547/397 °C
Secondary loops	- 2
Secondary temperatures	- 525/355 °C
Steam generators	- 8
Steam conditions	- 16.7 MPa, 490 °C
Turbine generator	- 1
Fuel Pin dia.	- 6.60 mm
Clad thickness	- 0.45 mm
Fuel smeared density	- 85%
Max. liner heat rating	- 45 kW/m
Main vessel dia x height	- 12.9 x 13.2 m
Safety vessel dia x height	- 13.5 x 13.2 m
Grid plate dia x height	- 6.35 x 1.0 m
Roof slab dia x height	- 12.9 x 1.8 m
Spent fuel storage	- Water pool for 900 SAs
Primary sodium pump	- Centrifugal, free surface, single stage
Flow per pump	- 3.64 t/s
Head developed	- 75 m
Secondary sodium pump	- Centrifugal, free surface, single stage
Flow per pump	- 2.90 t/s
Head developed	- 60 mm
Feed water heaters	- 5 surface type + 1 deaerator
Condensate extraction pump	- 3 x 50% pumps
Boiler feed pumps	- 3 x 50% (2 turbo driven, 1 electrical)
Generation voltage	- 21 kV
Grid voltage	- 220 kV
Station loads main supply	- 6.6 kV, 415 V
DC supply	- 48 V, 220 V
Single phase AC supply	- 220 V
Decay heat removal system	- 4 x 8 MWt Na/Na HX Natural convection to atmospheric air

Supplementary development programmes were initiated in selected areas where innovations were introduced to further enhance reactor and plant safety, performance characteristics, reliability, and availability. Extensive use is made of the U.S. national laboratories and engineering test centers to establish the required data base.

Concurrent with the design development effort, technology development was scheduled to progress through several phases, including feasibility tests, key features tests, components tests, and systems tests to eventual safety testing of a prototype reactor module. Throughout each test phase, high emphasis has been given to assuring the structural integrity of components, to characterizing the reliability of safety components, and to establishing design margins and margins beyond the design basis, as required in support of licensing reviews.

The programme included demonstration of: (1) the design adequacy of sodium components such as the self-cooled electromagnetic pump, control drives, ultimate shutdown

system, in-vessel fuel transfer machine, and steam generator; (2) advanced instrumentation and controls concepts; (3) advanced technologies such as seismic isolation, life extension of structural materials, and thermal-hydraulics simulation testing; and (4) technologies for safety systems including the reactor vessel auxiliary cooling system, passive reactor shutdown features and containment design, backup, and ceramic fuel (oxide) development.

A self-cooled electromagnetic pump is included in the ALMR design, consistent with the hermetic sealing of the reactor during operation. The development programme objective was to sufficiently assure the goals of a 30-year lifetime and a performance capability of delivering 700 kg/s at 7.8 bars using reactor sodium for waste heat removal. This development was considered the next logical step in the development of sodium pumps. The expected reduction in maintenance work was estimated to provide a 2% improvement in plant availability on a plant-wide basis.

To accommodate the elevated temperatures associated with the use of reactor sodium as the heat sink, materials have been developed which show excellent long-term electrical insulation capability. Oven tests conducted with bar samples and coil show a consistent low leakage current. A series of stator segment tests are being performed at Argonne National Laboratory to verify the design adequacy of the stator segment, to evaluate fabrication techniques, and to establish the design performance in terms of mechanical performance of the coil restraint system. In the second testing phase, an improved coil constraint design was demonstrated to adequately accommodate the total number of expected reactor startup and shutdown cycles. In the Phase III test, the inner stator iron will be replaced by a second concentric coil (double-stator design) which will reduce the maximum coil temperature and enhance pump reliability and mechanical performance.

One ALMR control system design task is to develop the functional requirements for the Plant-Wide Integrated Environment Distributed on Workstations (Plant-Window) System. The Plant-Window System (PWS) is a distributed computing environment tailored to nuclear power plant operations. The PWS resides on workstation platforms distributed throughout an ALMR. Its purpose is to facilitate the access and functional integration of data and applications. Access integration gives plant personnel ready access to the plant systems and data needed to accomplish control, monitoring, and analysis activities. Functional integration allows applications and computer systems to cooperate in performing tasks for the utility user. The PWS serves as a common interface to plant instrumentation and control (I&C) systems and data networks and provides needed functional applications and software services to support the activities of operations, maintenance, and engineering personnel. The PWS will provide a consistent, flexible environment for operations, maintenance, and engineering activities in the plant. The PWS will provide a common computer environment in which to utilize analytic, diagnostic, and decision-aid tools and will act as an interface to the monitoring, control, and protection systems in the plant.

Another ALMR control system design task is to develop a control and communications architecture simulation capability to provide a software-based approach to test the ALMR control system architecture designs before implementation. The implementation of a plant architecture can be very costly. Therefore, it is important that the architecture implemented will support the plant's needs under all conditions. This simulator will allow potential architecture designs to be modeled. These models can then be tested under a variety of plant and information-flow conditions to assure that a vehicle for testing modifications to the architecture and new systems being implemented. This capability will discover architecture problems and facilitate fixing them before costly implementation expenditures.

Seismic isolation is included in the ALMR to decouple the reactor and its safety equipment from potentially damaging ground motions. Flexible isolation elements with high vertical and low horizontal stiffness are used between the building basement and the superstructure to transform high energy seismic input motions into harmonic response cycles with significantly reduced accelerations. This approach is well suited for the low pressure liquid metal reactor system, which has thin-walled components and structures. Some of these components are flexible in the horizontal direction, and reduced accelerations lead to reduced stresses and displacements or enhanced safety margins. The technology programme objective is to demonstrate that the seismic isolation elements perform during earthquakes as designed, with a high reliability throughout their 60-year design life.

A testing programme of variously sized seismic isolation bearings indicated that a consistently high horizontal displacement capability can be achieved, and that the bearings have substantial margins for accommodating earthquakes beyond the safety shutdown earthquake. Seismic isolation technology is relatively new to nuclear powerplants and has been used only in special, limited applications. The general technology is well understood, however, and the application of seismic isolation to buildings with sensitive contents is rapidly expanding.

The transport of heat from the reactor sodium systems to the conventional steam systems is a critical process. Several types of sodium-heated steam generators have been developed and tested in the U.S. Programme, including the helical coil, the hockey-stick or J-tube, and the double-walled tube steam generator. The ALMR programme has selected the helical coil steam generator for the reference design because of the expected capital cost and reliability advantages. The objectives of the development programme were to develop and qualify the steam generator for a cost target of US \$ 75/kWe, a high reliability (failure rate of $< 10^{-3}$ per unit year), and a long lifetime (60 years). The initial phase of performance testing a 76 MW helical coil steam generator unit was successfully completed at the Energy Technology Engineering Center, and post-test examination, which includes water and sodium side inspections and the cutting and plugging of a tube section, is in progress.

Research and development efforts were also directed at determining the performance of major auxiliary systems, including fuel handling, in-service inspection, sodium leak detection, and remote maintenance. Sufficient test and design verification data are needed so that these systems can be clearly specified and accurately costed. Research and development was directed at those critical features that differ significantly from FFTF or EBR-II operating systems and offer potential for significant future cost savings, improved reliability, and/or increases in plant availability.

Development of oxide fuel technologies has continued in the Consolidated Fuel Reprocessing Programme (CFRP) at the Oak Ridge national Laboratory (ORNL). The technologies developed have spanned a full range of reprocessing functions from receipt, handling, and storage of spent fuel assemblies to waste treatment and packaging. Both mechanical (fuel disassembly and shearing) and chemical processes have been developed.

Some fuel cycle facility technologies developed through the CFRP are currently being transferred to Japan's Power Reactor and Nuclear Fuel Development Corporation (PNC) for application in the Recycle Equipment Test Facility (RETF). This is being done through a jointly-funded collaborative agreement between the DOE and PNC. Additionally, both France and Great Britain have interest in specific elements of the technology through other international exchange agreements, although the agreements are not currently in force.

One of the early DOE objectives for the CFRP was to develop advanced technology which would substantially increase the overall availability (on-line time) of reprocessing facilities. Increased availability would allow annual throughput criteria to be met with smaller, less costly, hot-cell facilities and processes. This led to development of new technologies for remote operations, remote maintenance systems, remotely operable and maintainable in-cell equipment, in-cell equipment reliability, space-efficient in-cell equipment arrangements, hot-cell layouts, and facility layouts.

Many of these technologies are generally applicable to large hot-cell facility operations and can be applied beneficially regardless of the basis used for processing operations. Areas of technology which are generally applicable are:

- mechanical head-end operations (remote fuel handling, storage, disassembly, and shearing)
- design of in-cell equipment for remote maintenance
- in-cell equipment layout arrangement
- in-cell remote maintenance systems
- in-cell viewing systems
- in-cell microwave signal transmission
- in-cell process instrumentation/controls
- in-cell inert atmosphere ventilation system control
- waste treatment, packaging, and assay
- radiation-resistant components/equipment
- improved safeguards utilizing process instrumentation
- reliability, availability, and maintainability
- centrifugal contactor design and operating parameters
- remote sampling systems
- flow sheet optimization
- fluidic transfer devices
- continuous rotary dissolution system

ORNL has pioneered and developed the concept of totally remote operation and maintenance of mechanical and chemical process equipment in large hot-cell facilities. This technology has been demonstrated and tested in cold facilities and has been a key element in conceptual design studies involving evaluation of liquid metal reactor fuel cycles and in the design of the RETF in Japan.

Many of the concepts jointly developed by the CFRP and PNC are being incorporated into the reference design of the RETF. Hot testing of these concepts under prototypical conditions will provide the basis for a proven reprocessing facility with low capital and operating costs, minimal personnel exposure, improved effluent control, and increased safety and safeguard ability. Major DOE-developed components and systems currently under cold testing and evaluation include a laser disassembly machine, a robotic sampling system, a rotary dissolver, and centrifugal contactors for separation.

ORNL developed a remote maintenance system based on a mobile, highly dexterous, remotely maintainable, servomanipulator with television viewing. This system, the Advanced Integrated Maintenance System (AIMS), is well tested, demonstrated, and in use today to support activities with the DOE and other Federal agencies. The AIMS technology, as well as that of supporting systems, can be applied to IFR fuel processing facilities. Since the original

objective of this technology was to improve in-cell maintenance, and thus plant availability, this same benefit also applies to the IFR.

9.7.2 ALMR plant design

Advanced liquid metal reactor design description

ALMR plant: The reference ALMR commercial plant utilizes six below-grade 840 MWth reactor modules arranged in three identical 622 MWe power blocks for an overall plant net electrical rating of 1866 MWe. A power block includes two identical reactor modules, each with its own steam generator, that jointly supply steam to a single turbine generator (Figs.9.53, 9.54). The ALMR's modular design offers flexibility to utilities in meeting the need for incremental load growth by providing options for installing only one or two of the power blocks with a generating capacity of 622 or 1244 MWe.

The ALMR plant is controlled by an automated digital control system that is supervised from a single control center. The individual power blocks (one turbine each) are functionally independent of each other and are operated separately to provide power to the main bus. The two reactors in each power block generally will operate together as a unit for power generation and load following. However, they can be operated separately. This capability applies mainly to refuelling or maintenance operations in which one reactor is temporarily shut down, while the other continues to operate and supply steam to the power block turbine. The plant control system (PCS) adjusts the position of the control rods in each reactor to follow load demands and for startup and shutdown. Remote shutdown capability and post-accident monitoring equipment are provided at the reactor modules and in the reactor service building, as well as at the control center. Plant performance data are summarized in Table 9.6.

Nuclear steam supply system: Each reactor is coupled to a dedicated steam generator by a single nonradioactive secondary sodium loop. Steam lines from the two steam generators in each power block are manifolded together to supply a single turbine. An advantage of this arrangement is that, if one becomes inoperative, the other parallel power system will continue to supply steam to the turbine. This minimizes the impact on availability, reduces the need for a spinning reserve, and promotes high plant availability, which is presently predicted to exceed 85%. In general, large monolithic plants with multiple (N) heat transfer loops do not offer this flexibility, but may allow for N-1 loop operation.

Figure 9.55 shows the schematic of the nuclear steam supply system (NSSS). The NSSS includes the reactor module, the primary sodium system and its associated auxiliary equipment, the steam generator system, and the secondary, nonradioactive, intermediate heat transport system (IHTS) that circulates elevated temperature sodium (480°C) from intermediate heat exchangers (IHX) in the reactor to the steam generator. Sodium flow in the IHTS is provided by two 1700 kg/s electromagnetic pumps located in the steam generator building. The pump design is similar to that developed for the primary sodium pumps. The relative elevations of the reactor module and the steam generator are such that, during reactor shutdown conditions, the IHTS will naturally circulate sodium at a flow rate sufficient to remove decay heat from the reactor. The reactor module and the steam generator reside on a common, seismically isolated platform. With this arrangement, the seismic loading is minimized, and short, flexible sodium piping can be used. The IHTS includes a sodium leak detection system to provide early warning of any sodium leaks. Steel leak jackets on the IHTS piping, sodium catch pans and fire suppression decks in the IHTS pipe tunnel and steam

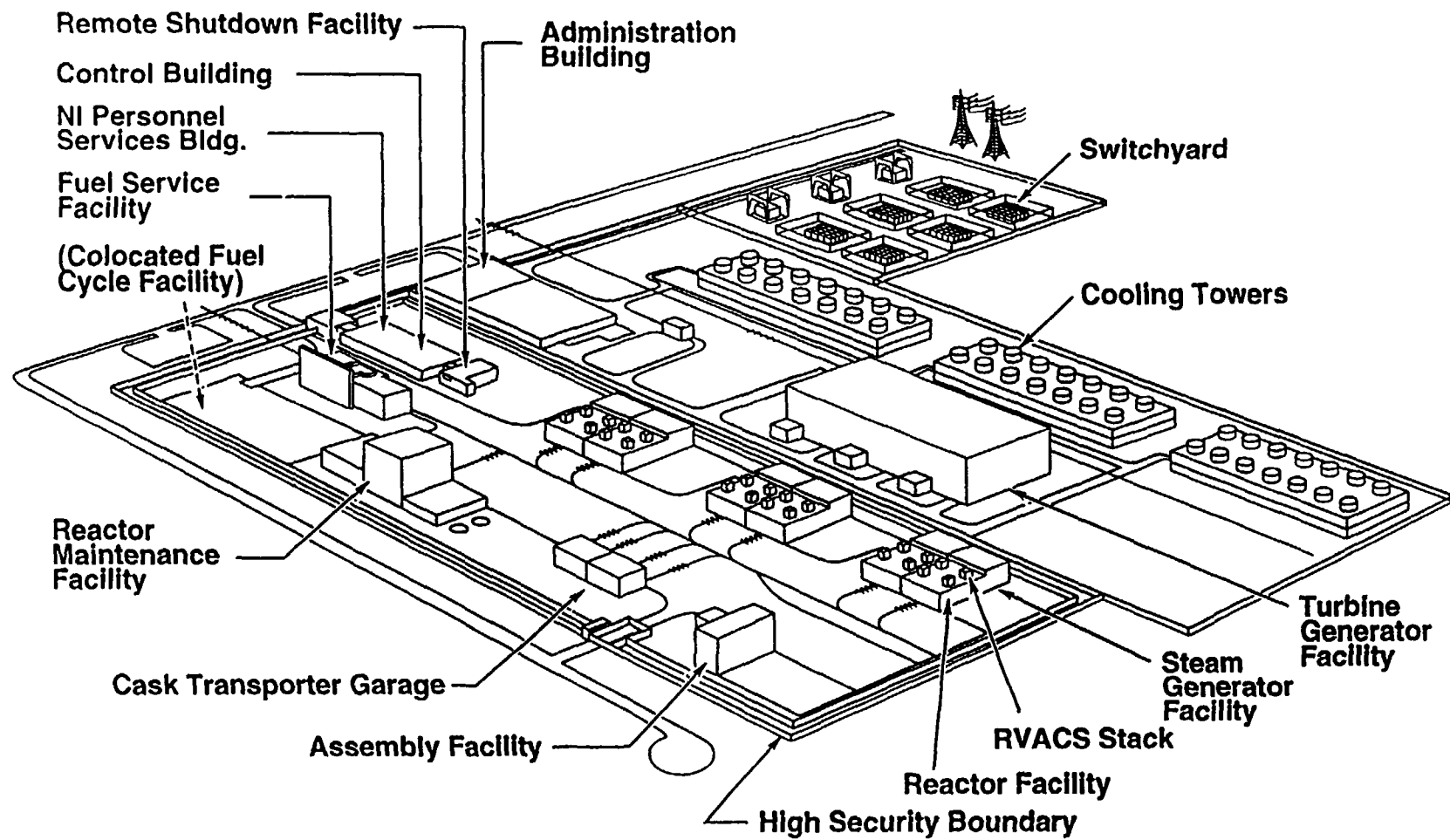


FIG 9 53. ALMR power plant (3 power blocks) - 1866 Mwe

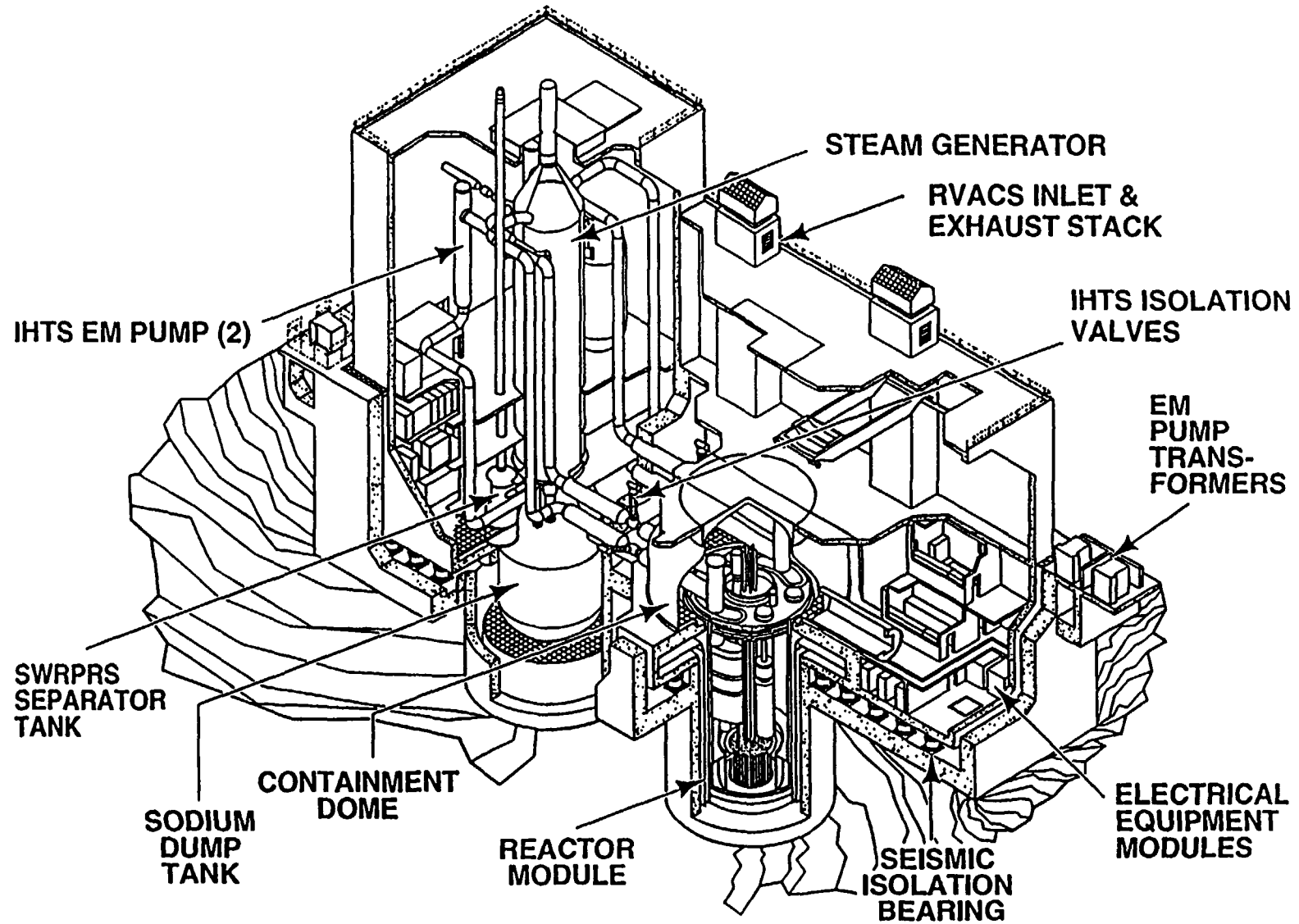


FIG 9.54 Reactor & steam generator facility general arrangement

TABLE 9.6. ALMR PERFORMANCE DATA

Number of reactors/power block	Two
Number of power blocks	One/two/three
Thermal reactor power	840 MWt
Electrical power for 1,2,3 power blocks	622/1244/1866 MWe
Net station efficiency	37%
Plant capacity factor	85%
Steam conditions (superheat)	14.8 MPa at 452°C
Primary sodium inlet/outlet temperature	360°C/500°C
Secondary sodium inlet/outlet temperature	327°C/477°C
Fuel	Metal
	(Uranium/0.23 Plutonium/0.1 Zirconium)
Average fuel burnup	106 MWd/kg
Average fuel linear power, BOL/EOL	20/18 kW/m
- Refuelling interval	23 months
- Breeding/Conversion Ratio Range for breakeven core/moderate burner	1.06/0.7
Containment dome leak rate	< 1 % (10 psig, 70°C)
Seismic isolation	
- Licensing requirements/design basis for SSE	0.3/0.5 g
- Horizontal/vertical frequency	0.7/21 Hz
- Lateral SSE displacement/gap	19/71 cm

generator silo, and a rapid IHTS drain system are provided to minimize the consequences of fires from a sodium leak. The portion of the IHTS piping in the head access area (HAA) above the reactor module is encased in guard piping to protect the reactor closure or HAA equipment from contact with sodium.

Reactor: The reactor module (Fig.9.56) is about 9.6 meters in diameter (31 ft. 1 in.) and 19.6 meters high (64 ft., 3 in.). The vessels, head closure, and permanent internal structures are fabricated in a factory and shipped as an assembled unit to the site. The shipping weight is about 1500 tons. Removable internal equipment is shipped separately and installed through the top head. The reactor vessel and all components are constructed of austenitic stainless steel (304SS and 316SS). The relatively tall, slender reactor geometry enhances the uniformity and stability of internal sodium flow distributions and natural circulation for shutdown heat removal.

There are two 420 MWt IHXs in the reactor to transfer heat from the primary sodium to the intermediate heat transport system. These are located above the reactor core in an annular region between the support cylinder and the reactor vessel wall. The IHX is designed to withstand, without breaching, the 7 MPa (1000 psi) steam pressure that could possibly be approached in the highly unlikely event of a severe sodium/water reaction.

Primary sodium is circulated in the reactor by four electromagnetic (EM) pumps. These pumps are self-cooled by the pumped sodium. This results in higher temperature for the electrical insulation material than for an arrangement with an external gas cooling system. However, suitable ceramic and mica-based materials have been developed and qualified for a life expectancy in excess of 30 years. The self-cooled EM pump simplifies the head

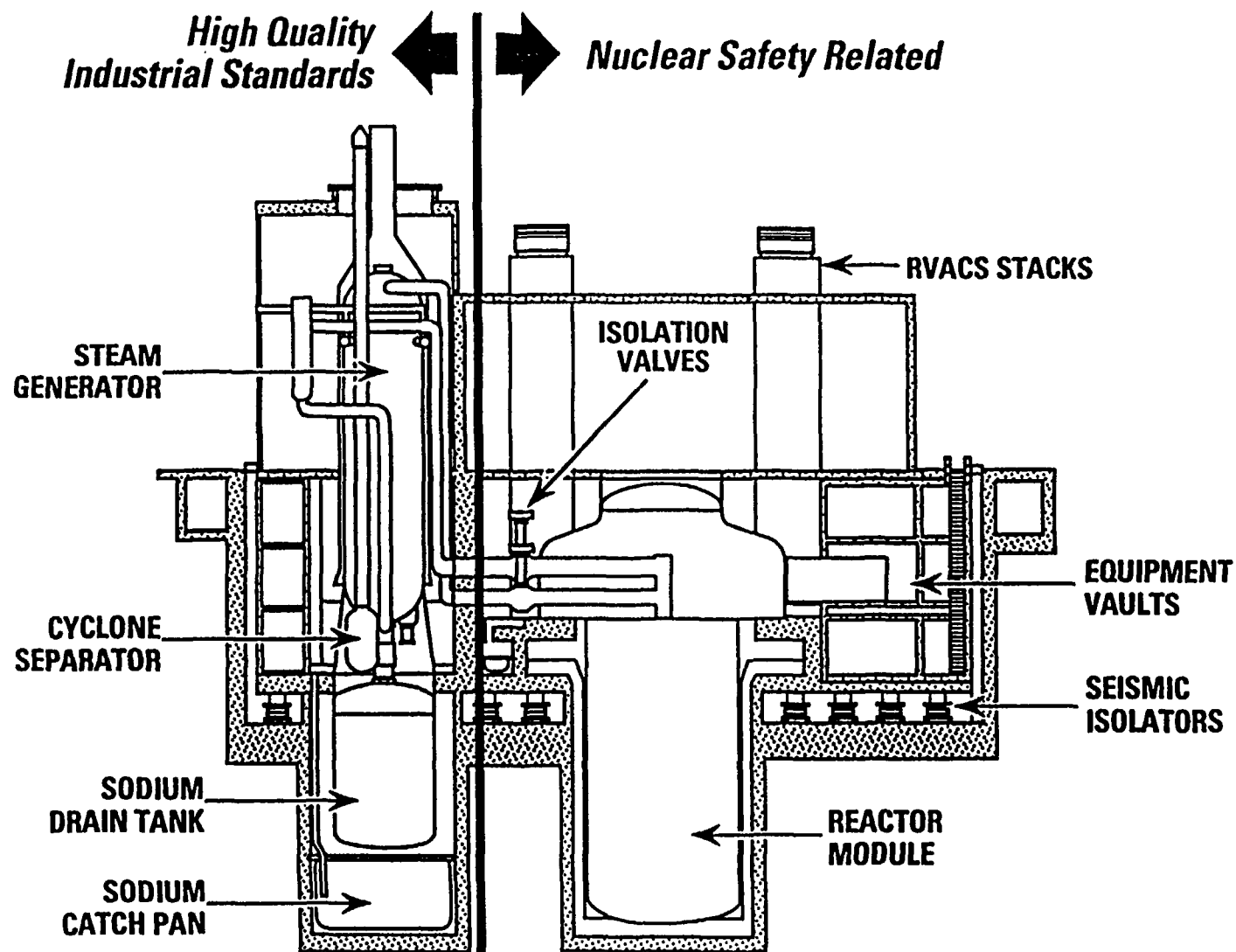


FIG. 9.55. Reactor steam supply system - Mod B

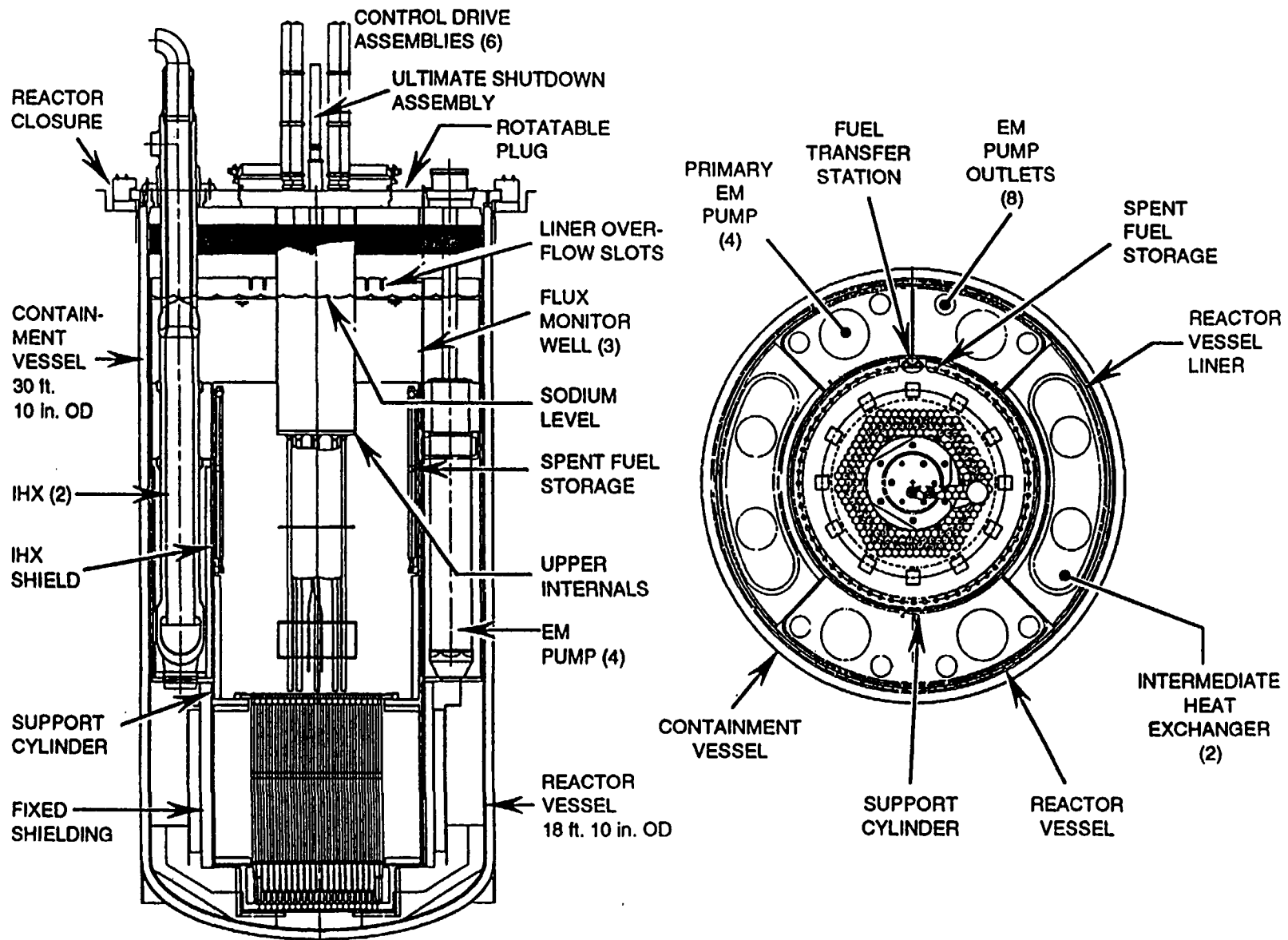


FIG. 9.56. ALMR Reactor module - Mod B

penetration, requiring only a pass-through for the power and instrumentation lines. Each EM pump is controlled by a solid-state power supply. Pump coastdown flow consistent with core power reductions or shutdown is provided by a synchronous converter that motors on the system during normal operation and also makes corrections for the system to counteract the inductive load of the EM pump. If loss of normal power occurs, the stored kinetic energy in the synchronous machine is utilized for pump coastdown. Substantial progress has been made in the development of the self-cooled EM pump, including life and irradiation testing of high temperature electrical insulation candidates at Argonne National Laboratory (ANL), fabrication of several full-scale, $\frac{1}{4}$ length segments of the pump stator by General Electric, and testing of these devices at full temperature by ANL. Additional tests are under preparation for prototypic flow and temperature tests of a stator segment from a double stator pump at the Energy Technology Engineering Center (ETEC), in collaboration with Japan Atomic Power Corporation (JAPC).

A pantograph-type, in-vessel transfer machine (IVTM) is used to transfer fuel and other core components between the core, storage racks, and the transfer station, where they are inserted or removed from the reactor by a shielded transfer cask. During operation, the IVTM is stored in-vessel in a retracted position near the transfer station. Refuelling machines of this type have been applied in the United Kingdom's Prototype Fast Reactor (PFR), Italy's PEC, and Japan's MONJU. The conceptual design of the ALMR transfer machine was provided by ANSALDO (Italy), and utilizes available technology.

Core design: One of the major attributes of a liquid metal-cooled fast reactor is the flexibility to adjust the core configuration within the reactor envelope to provide a range of fuel consumption/production rates at a given power level, depending on the selected design mission. However, for a specific mission, the fuel and fuel cycle qualification effort is substantial. Consistent with the objective of this report, only the light water reactor actinide recycle mission is addressed. As a representative configuration, a burner core with a conversion ratio of 0.72 was selected. In a typical burner core, the net consumption of transuranics can be achieved by minimizing the uranium inventory (e.g., eliminating blanket assemblies) and by reducing the core height (pancaking the core shape) to further reduce fissile material and to reduce the neutron capture probability by increasing leakage. To retain a high level of passive safety protection, the decrease of the core height is constrained. The selected nuclear performance limits were: (1) a burnup reactivity swing limited to \$10, (2) a peak fuel burnup limited to 150 MWd/kg, (3) the peak neutron fast fluence limited to 4.0×10^{23} n/cm², and a transuranic enrichment limited to 30 wt. percent of the ternary alloy (the range of the current metallic fuels database). A characteristic core design is shown in Figure 9.57.

The minimal core height is 66 cm, with a diameter of 358 cm, and includes a total of 192 fuel assemblies (Table 9.7). The small sodium void worth could be reduced by further pancaking the core, which would come at the expense of increases in the burnup reactivity loss. Initial evaluations of postulated accident sequences indicated attractive safety characteristics for the burner core, comparable to a conventional (breakeven) core design. Since the reactivity insertion from withdrawal of control rods is larger for the pancaked core, smaller incremental movements (rod stop adjustments) are required.

The actinide consumption rate for the burner core is 3.3% of the inventory per year. Calculations showed that the small burner destroyed approximately 315 kg of minor actinides (MA) and 2400 kg of transuranics (TRU) per core over 60 years.

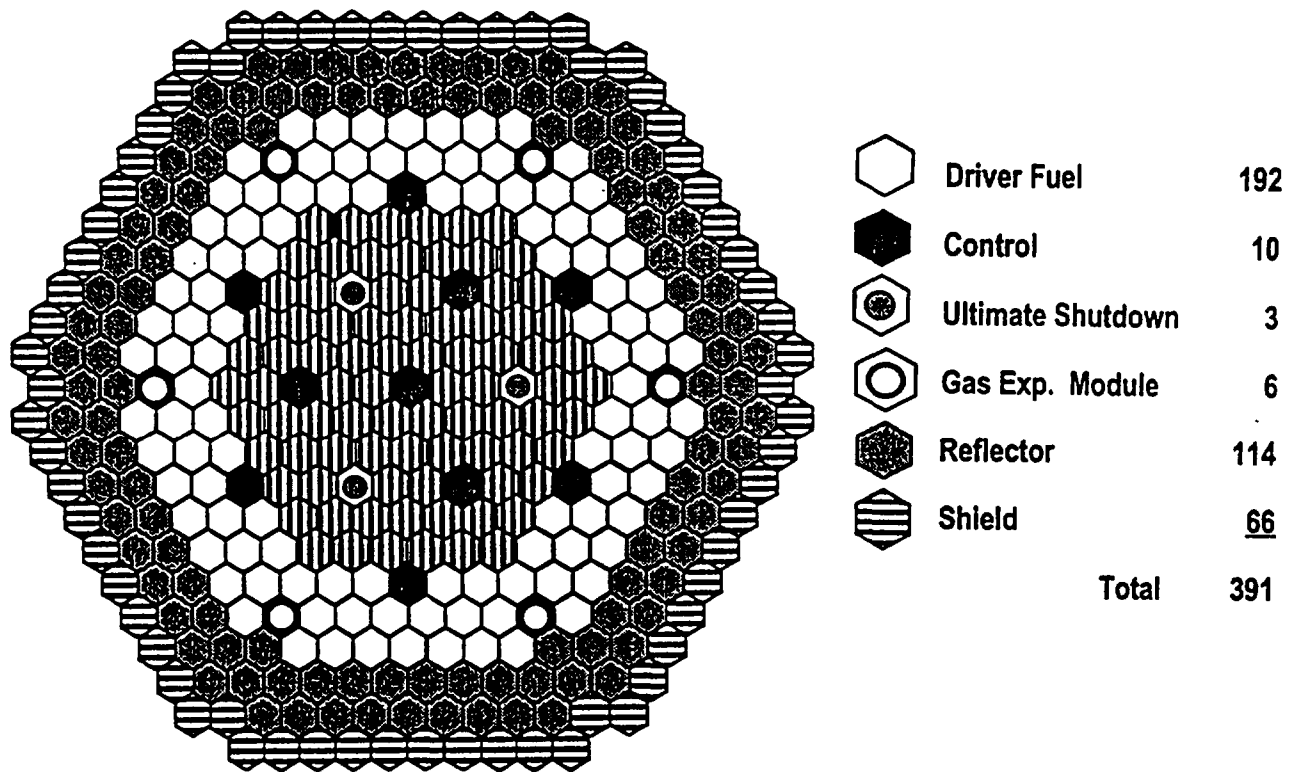


FIG. 9.57. ALARM 840 MWth burner core

TABLE 9.7. CORE NEUTRONIC CHARACTERISTICS

	Burner core
Core height	66
Core diameter (cm)	358
No. of fuel assemblies	192
No. of blanket assemblies	---
Conversion ratio	0.72
Cycle length (months)	12
Burnup reactivity swing (\$)	9.0
Peak linear power (kW/m)	34
Sodium void worth (\$)	~ 2.50
TRU enrichment (wt% in U-TRU-Zr)	1/23
TRU inventory (kg/core)	2554
TRU consumption rate	
- kg/year/core	83.2
- % inventory/year	3.3

More than 60 percent of the total TRU introduced to the burner ALMR is consumed during the reactor lifetime, as well as more than 60% of the MA introduced. In addition to the net consumption of TRU in the burner ALMR design, an additional benefit is gained from the storage of the working TRU inventory in the metal fuel cycle for the system lifetime. Evaluations of core designs with different core heights indicate that shorter cores both load and consume more TRU than the taller cores over the plant lifetime (due to the larger required makeup in the shorter cores). However, the larger cores require larger inventory at startup.

The crossover point where the additional makeup required by the shorter core is greater than the larger amount of TRU loaded into the taller core is reached at approximately 20 years. The lower conversion ratio of the shorter cores also leads to greater consumption amounts during the plant lifetime. However, in the case of a large burner (shorter core, larger diameter), the core requires larger makeup and consumes more TRU per year. The breakeven core is 106.7 cm (42 in) long and has 84 blanket (breeding) assemblies interspersed within 108 fuel assemblies. There are no upper or lower axial blankets in either core. Both cores include 6 gas expansion modules (GEMs), 10 control assemblies, and 3 ultimate shutdown assemblies. Surrounding the active cores are 114 reflector and 66 shield assemblies. The assembly pitch is 16.1 cm (6.35 in) and the core outer diameter (for all removable assemblies) is 358 cm (141 in).

ALMR safety features

Approach: The ALMR was designed to provide high reliability for the key safety functions, including reactor shutdown heat removal, and containment. These functions can be achieved by passive means without operator action. The key processes underlying these functions are governed by thermal expansion, temperature effects on neutron absorption, natural circulation of the sodium coolant, natural air circulation on the outer containment surface, and thermal radiation heat transfer, which becomes very effective at elevated temperatures. The ALMR design integrates all these effects into an efficient passive safety system, which allows the accommodation of anticipated transients without reactor scram, such as loss of primary coolant flow without scram (ULOF) or loss of heat removal by the intermediate transport system without scram (ULOHS), with benign consequences to the reactor core. Basically, the core can survive these severe scenarios with no damage. These passive safety features are provided as a backup in case the highly reliable active systems fail to perform their functions. They provide an additional, operator-independent level of defense against accident propagation.

Passive reactivity shutdown: The plant control system (PCS) causes the reactor to follow load demand, and normally will maintain the core outlet sodium temperature within specified limits. If an emergency event develops too rapidly for the PCS to control it, then the safety-grade reactor protection system (RPS), located at the reactor module, will independently respond by causing a reactor scram (rapid insertion of the nine control rods). The RPS includes substantial internal diversity and redundancy and is expected to be highly reliable with an estimated failure probability of less than 10^{-6} per demand. A testing programme is planned to confirm the response characteristics.

As a further safety backup, the core is designed to provide strong, inherent negative reactivity feedback with rising temperature. This feature, combined with the Reactor Vessel Auxiliary Cooling System (RVACS) heat removal capability, makes the ALMR capable of safely withstanding severe undercooling or over-power accidents without reactor scram, including (1) loss of all cooling by the IHTS from a full power condition (Fig.9.58), and (2) withdrawal of all control rods from a full power condition (Fig.9.59). For both these events, which envelope in their severity several other extremely low probability accidents, the system brings itself in a totally passive manner to a stable equilibrium state at a core outlet sodium temperature that is below the American Society of Mechanical Engineers (ASME) Code long-term structural design limit of 704°C (1300°F), or more than 290°C (525°F) below the sodium boiling point. This condition can be safely accommodated until corrective action can be taken to bring the reactor to cold, subcritical shutdown. Based on the results of on-going metal fuel

tests at ANL, it is expected that damage to the fuel during these transients will be minor, and no breach of fuel pin cladding will occur.

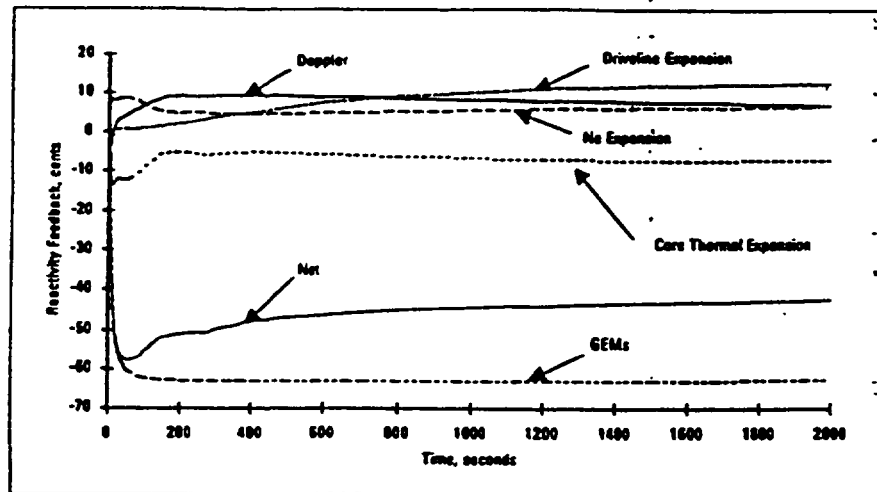
A landmark series of experiments was successfully completed in ANL-Idaho's Experimental Breeder Reactor-II (EBR-II) to demonstrate the capability of a metal-fueled reactor to accommodate severe accidents without scram with very benign consequences, i.e., no failure of fuel assemblies or core structures. In earlier designs, such event sequences were considered as potential, extremely low-probability initiating events leading to core disruption. Similar tests were performed in the Fast Flux Test Facility (FFTF) with an oxide fuel configuration.

To enhance the negative reactivity feedback at elevated temperatures, gas expansion modules (GEMs) were added at the core periphery to compensate for the large positive Doppler feedback associated with the decreasing fuel temperature of oxide cores during fission shutdown. The gas expansion modules have a vapour space which will expand with loss of core inlet pressure to increase the core neutron leakage.

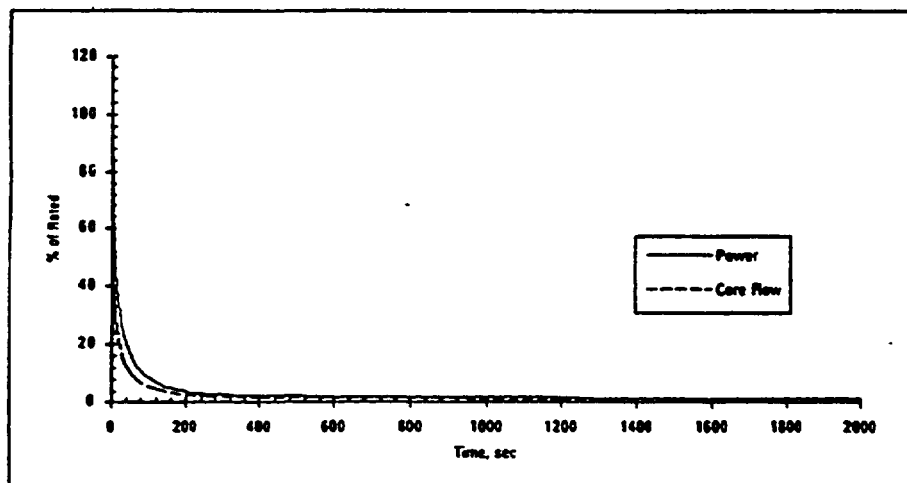
Shutdown heat removal: Normal reactor shutdown heat removal is through a single dedicated Intermediate Heat Transport System (IHTS). A passive, reliable safety-grade backup to the IHTS is provided by the reactor vessel auxiliary cooling system (RVACS) (Fig.9.60). In the rare event that the IHTS becomes unusable during power operation (for example, as in a sodium dump), the reactor will scram and the RVACS will automatically increase the naturally circulating air flow around the containment vessel with rising wall temperatures. The temperatures will rise until equilibrium between reactor heat generation and RVACS cooling is established. The core bulk outlet sodium temperature was predicted to peak at about 590°C (1094°F) after about 30 hours, with a substantial margin to structural limits and over 360°C (650°F) margin to boiling. RVACS is expected to be extremely tolerant to off-normal events, such as unlikely flow blockages and surface fouling, due to several factors: (1) redundancy of the air flow passages; (2) predominantly thermal radiation heat transfer, increases exponentially with rising temperatures; (3) natural air convection; and (4) substantial performance margins to structural temperature limits. For example, an unlikely blockage of 90% of the air ducting would still result in peak temperatures below the ASME Level D structural limit set for the design. An even more extreme case involving complete blockage of the air passages, which is essentially impossible apart from a short period of sabotage, could be accommodated without exceeding ASME level D limits for over ten hours, which should provide sufficient time to remedy the situation. A major testing programme to characterize the RVACS performance has been completed. Full-scale segment tests of the heated air riser adjacent to the containment vessel were performed at ANL, and the thermal emissivity of both unexposed and aged samples of the reactor vessel and containment vessel materials was determined at Purdue University. Earlier system tests with the air-cooling system of the FFTF Interim Decay Storage Tank provided data for a configuration similar to RVACS. The data from these tests have been correlated and are reflected conservatively in the RVACS performance predictions.

Containment: The primary containment comprises the containment vessel, the reactor head closure and fittings, and the intermediate heat exchangers (Fig. 9.61). There are no penetrations in the reactor vessel below the closure head. During power operation, the reactor is hermetically sealed, all sodium and cover gas service lines (in the head closure) are closed with double isolation valves, and all other penetrations are seal-welded. The pressure of the reactor cover gas is approximately atmospheric during normal power operation. The leak

ULOF - FEEDBACK



ULOF - POWER



ULOF - TEMPERATURE

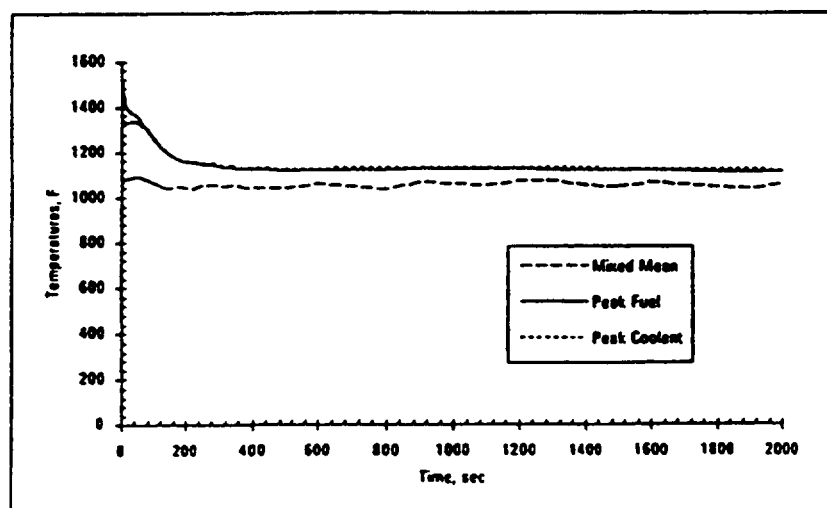
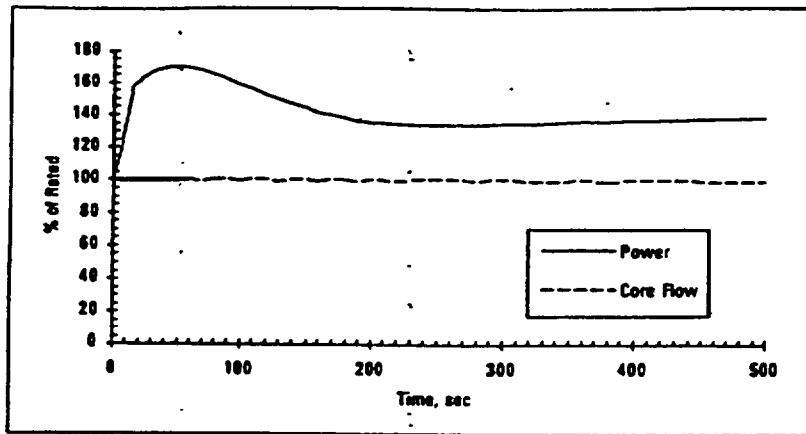
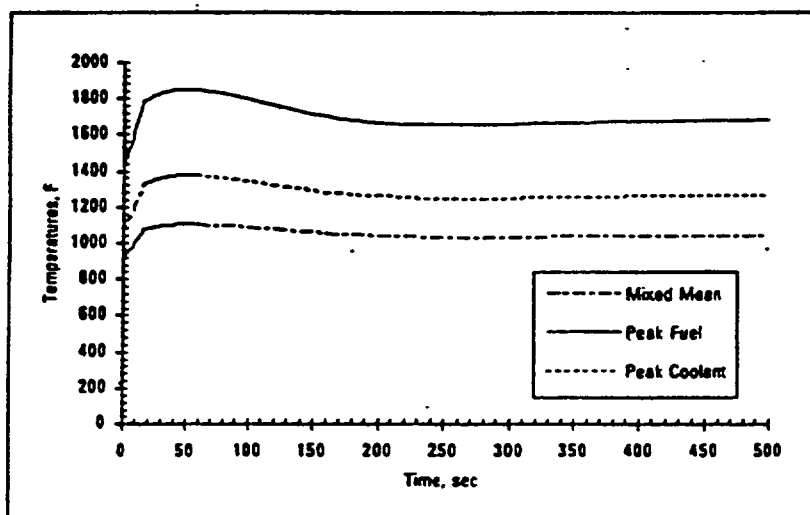


FIG. 9.58. MOD B fissile breakeven core ATWS performance - ULOF/LOHS

UTOP - POWER



UTOP - TEMPERATURE



UTOP - FEEDBACK

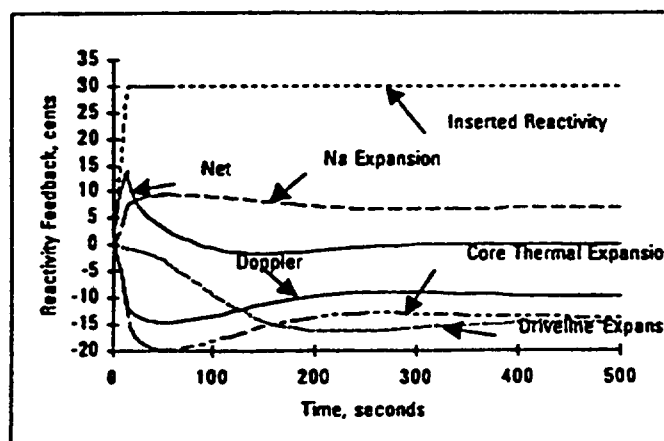


FIG. 9.59. MOD B fissile breakeven core ATWS performance UTOP

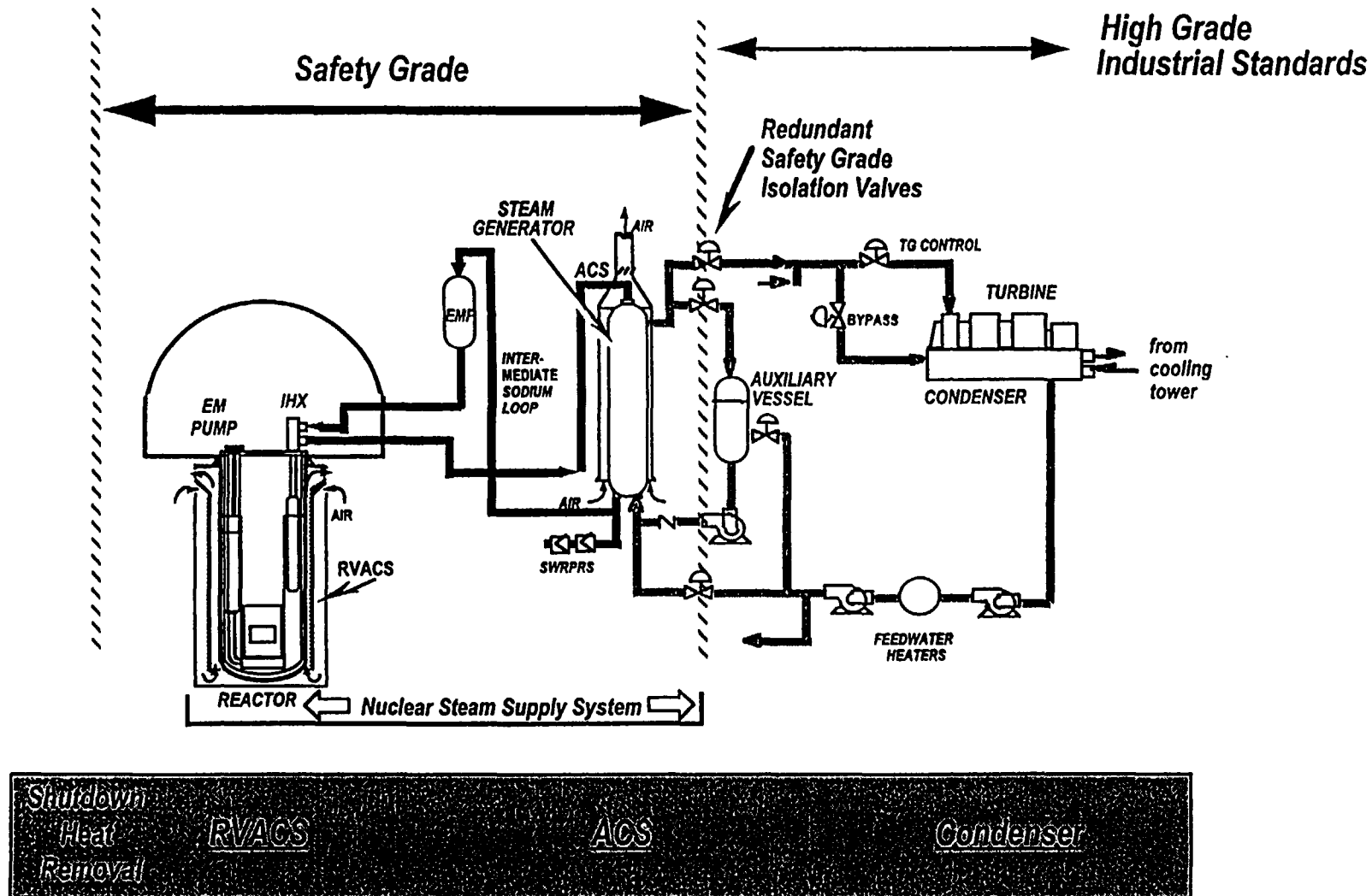
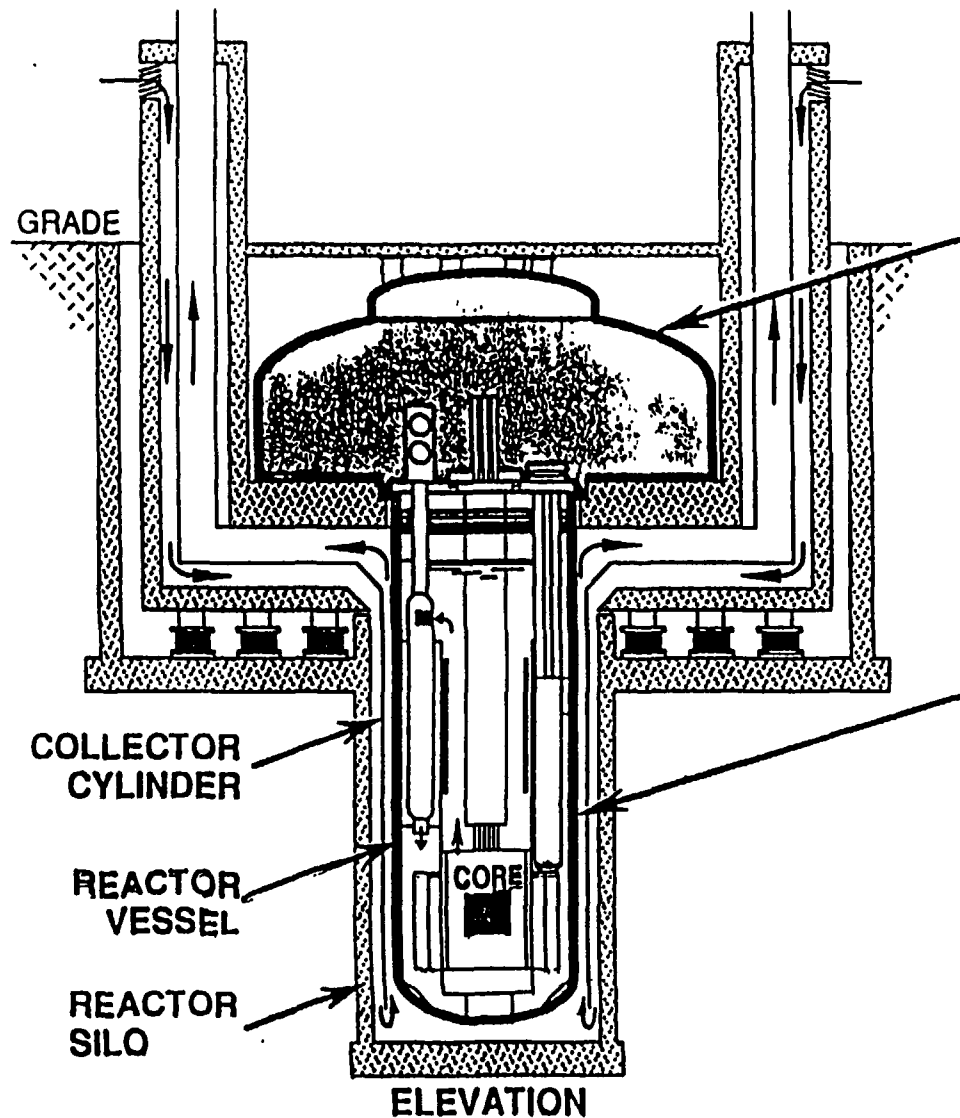


FIG. 9.60. ALMR power train



Containment Dome

- ASME Section III, Div. 1, Class MC
- Material – SA 516 Grade 70
- Design Requirements:
 $< 1\% / \text{day at } 25 \text{ psig}/700^\circ\text{F}$

Containment Vessel

- ASME Section III, Div. 1, Class MC
- Material – 2 1/4 Cr - 1 Mo
- Design Requirements:
 $\text{Zero Leak Rate at } 60 \text{ psig}/800^\circ\text{F}$

FIG. 9.61. Reactor containment

tightness of the head closure will be constantly monitored and maintained to assure that the maximum leakage rate will be less than 0.1% of the contained cover gas per day. Calculations show that, with this leak rate, even for a very severe low probability accident in which all of the fuel pins are assumed to be breached, the release of radioactivity will be well within the requirements of the Code of Federal Regulations (10CFR100).

The 127 mm (5 in.) argon-filled gap between the reactor vessel and the containment vessel is monitored continuously by pressure and sodium ionization detectors for early warning of any leak in either vessel. In addition, the weld regions will be inspected periodically with ultrasonic devices. If a leak in the reactor vessel should occur, the containment vessel will retain the primary sodium. The two vessels are sized such that the reactor core, the spent fuel stored in-vessel, and the inlets to the intermediate heat exchangers will always remain covered by sodium to cool the core assemblies. Extremely unlikely accidents that could challenge the containment have been evaluated on a probabilistic basis. These assessments indicate that the risk of a breach of the primary containment is extremely small, mainly due to the significant thermal and structural margins in the design, the invulnerability of the RVACS, the high reliability of the reactor protection system, and the inherent negative reactivity feedback characteristics of the metal core. In addition, the reactor silo and the refuelling enclosure above the vessel head access area will be optimized for mitigation of radioactive releases in the extremely unlikely case of a containment leak. Backup approaches have been identified.

Sodium/water reaction and sodium fire protection: Sodium is a reactive material in air and water, and special measures were taken to prevent reactions from occurring. In the unlikely event of such a reaction, additional measures are taken to prevent failure progression and to limit consequences. Significant expertise has been accumulated in the U.S. on sodium technology, and the major systems, including EBR-II, FFTF, and the major sodium components test facilities have operated flawlessly. The fact that recent experience with U.S. systems is better than that at comparable international facilities is attributable to the significant investment in the development of adequate structural materials, design rules, and procedures in the U.S.

The steam generator system includes leak detectors to provide early warning of any tube leak, a highly reliable isolation and blowdown system to rapidly remove the high pressure steam/water from the steam generator to limit sodium-water reaction damage after a tube leak, and an automatic (0.9 MPa rupture disc) sodium-side pressure relief system of huge capacity to protect the IHTS and intermediate heat exchangers (IHX) from excessive pressures in the unlikely event of concurrent tube leaks. Additionally, both the IHX and the IHTS piping have been designed, using ASME Level D (faulted) damage criteria, to withstand the full 7 MPa (1000 psi) steam pressure for at least one hour. The pressure relief system is sized to accommodate failure of all the steam generator tubes without exceeding the IHX and IHTS Level D design limit. These protective features, coupled with a highly reliable steam generator, provide excellent investment protection and a high assurance that the IHX, an element of the containment boundary, will not be breached in the unlikely event of a steam generator sodium/water reaction.

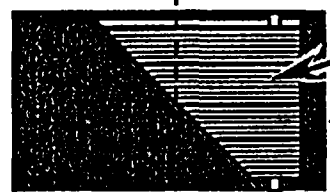
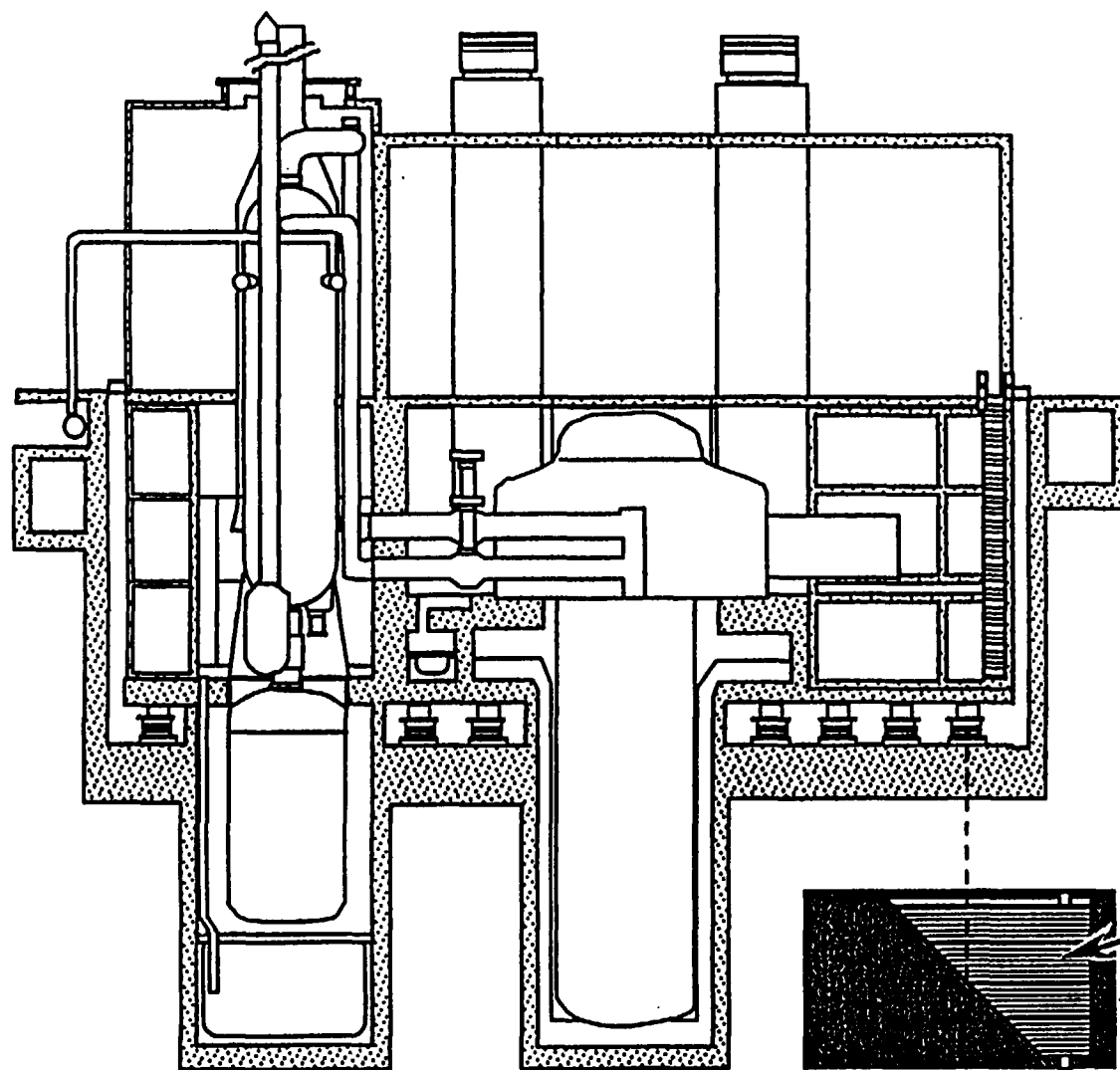
To avoid sodium fires inside the containment, all vessels and piping are double walled, with an inerted gap and leak monitoring capability. In general, sodium fire protection has matured considerably. Historically, the frequency of sodium leaks for various international LMRs has been in the range of 0.5 to 2.5 events/year, resulting in zero to seven sodium fires. In the U.S. the EBR-II and FFTF performance records are better.

Seismic isolation: (Fig 9 62) Horizontal seismic isolation has been adopted for the ALMR design to simplify the reactor and nuclear island design and the in-service inspection programme, and to enhance design margins for beyond-design basis earthquakes. An added economic and licensing benefit of seismic isolation is the ability to achieve reactor design standardization for site locations with different seismic conditions and soil properties. The seismic isolation system decouples the reactor, its safety equipment, and the intermediate heat transport system (including the steam generator) from potentially damaging ground motion by transforming high energy, high frequency seismic inputs into lower frequency response cycles with significantly reduced accelerations. This approach is well suited for the low pressure liquid metal reactor system, which has flexible components with relatively small wall thicknesses. The isolated system responds to horizontal ground motion essentially as a rigid body, with little amplification of the ground acceleration. This limits the inertial loads and increases the structural margins for critical components and structures. Also reduced are relative displacements between components. This is helpful for limiting the potential for seismic interference between the control drives and their guide elements, and for minimizing the forcing function for seismic core compaction.

The ALMR nuclear island is supported from a common, seismically isolated platform, with a horizontal isolation frequency of 0.7 Hz and a maximum displacement of 19 cm during a safe shutdown earthquake (SSE) with 0.3g Zero Period Acceleration (ZPA) ground acceleration. The design earthquake was specified to envelop the Nuclear Regulatory Commission's (NRC) Regulatory Guide 1.60 spectra. The selected criteria are expected to apply to over 80% of potential nuclear sites in the U.S., excluding California. Options for siting in seismic zones with higher ground accelerations were investigated and found acceptable. The seismically isolated ALMR system has the capability of accommodating at 0.5g ZPA earthquake. The isolation arrangement is shown in Figure 9.62. Sixty-six seismic isolators with access and space for in-service inspection and replacement, if necessary, are included. Each isolator is a composite of laminated steel plates and high damping rubber layers encased in rubber.

There is a substantial experience base for this isolator design. Performance testing of the isolator bearings has been underway at the University of California (Berkeley) Seismic Engineering Laboratory since 1984. A powerful testing machine with a horizontal dynamic load capability of 150t and a vertical capability of 750t was built at the Energy Technology Engineering Center. Tests performed with half-size bearings demonstrated a significant margin to failure (three to seven times the expected SSE displacement).

A seismic bearing qualification programme has been implemented. This includes (1) static and dynamic performance tests of bearings, (2) the evaluation of aging and environmental effects, such as temperature, gamma radiation, and ozone, and (3) seismic isolation system shake table tests to evaluate performance characteristics and margins. The vertically stiff reactor assembly places the vertical natural frequencies of critical structures well above the dominant ground motion frequencies, thereby providing sufficient vertical seismic margins without isolation. In cooperation with Italy's Agency for New Technologies, Energy, and Environment (ENEA), a proposal for seismic isolation design guidelines for seismically isolated nuclear power plants was developed. Extension of this work is intended to establish a framework of design rules accepted by the American Society of Civil Engineers (ASCE) and the NRC.



~4 ft. ϕ
Seismic Isolator (66)

Seismic Isolation System Characteristics

- Safe Shutdown Earthquake (SSE)
 - Licensing Basis 0.3g (ZPA)
 - Design Requirement 0.5g
- Lateral Displacement
 - at 0.3g 7.5 in.
 - Space Allowance
 - Reactor Cavity 20 in.
 - Remaining Structures 28 in.

FIG. 9.62. Seismic design

Modular construction approach

A modular construction approach is utilized to allow factory series fabrication and pre-assembly of components. Key construction modules will be installed in the field. By using this approach, a high quality product that is cost-competitive with an on-site constructed, large, monolithic power plant, is achievable. The plant facilities are divided into equipment and structural modules, which are factory fabricated, transported to the plant site, and connected together with limited field labor. The ALMR plant, with its replicated reactor and heat transport facilities, is well suited to modular construction. For a plant of three power blocks, some facilities are duplicated six times. Where multiple, identical modules are used, such as the IHXs, twelve components of one design are provided. Three types of plant facilities are being designed for modular construction: the reactor facility, the steam generator building, and the turbine building. The reactor silo, the steam generator silo, the head access area enclosure walls, and the equipment vaults, are constructed of reinforced concrete, which is slip-formed against excavated earth above basemats. The seismically isolated assembly consists of 44 structural modules.

There is one turbine for each power block. The turbine generator equipment is located in one turbine building. An estimate of the plant capital cost, using the modular construction approach, showed a small cost reduction when compared with conventional construction. Aside from any direct cost reduction, modular construction provides advantages such as greater control of plant capital cost and construction schedule and, hence, a reduced risk in these areas.

The size and weight of the reactor module, though large, are within the capacities of large road transporters. Shipping considerations are based on a maximum diameter of 9.6 m, an overall length, not including end shipping fixtures, of 19.6 m, and a shipping weight of 1500t (without shipping fixtures). The module can be shipped by barge or road transporters. Some of the smaller modules are designed for rail shipment. Most shipments will likely involve a combination of transport methods. The mix of methods will depend on the locations of the module manufacturing plant and the power plant sites. Barge shipment is generally the simplest and least expensive. Existing large barges are capable of carrying two reactor modules as one load. Multi-wheeled transporters provide access and route flexibility.

9.7.3. Integral fast reactor concept development

The Integral Fast Reactor (IFR) is a concept based on the integrated development of a power reactor and its entire fuel cycle. It is the first nuclear power concept to consider efficient resource utilization, proliferation resistance, public safety and protection of the environment (in particular, nuclear waste considerations) in the design. Development of this concept is intended to produce a straightforward, highly adaptable means of utilizing plutonium in a closed fuel cycle without the need to separate it. The goals of IFR technology development in the U.S. ALMR programme were to confirm metal fuel performance capabilities and to (1) establish the basis for manufacturing specifications; (2) establish and demonstrate a reference pyroprocessing method for recycle of metal fuel; (3) evaluate the practicality and benefits of actinide burning as part of an overall waste management strategy; (4) demonstrate reliable and transparent safeguards and accountancy techniques for the entire fuel cycle; (5) assess passive reactor safety characteristics; and (6) demonstrate fuel cycle economics. There is sufficient evidence to indicate that, when utilized in conjunction with advanced ALMR designs, metal fuel has the potential for very favourable economics, passive safety performance, and outstanding safeguards transparency.

The IFR fuel cycle is being designed to burn essentially all of the long-life actinides present in reactor spent fuel. The fuel cycle is extremely adaptable. After initial fueling, the IFR can accept depleted uranium as an adequate feed, or, if desired, consume scrap actinides separated from light water reactors (LWRs) or from other sources, including excess stocks of separated plutonium. By using seed plutonium as a catalyst, the system can effectively burn depleted uranium. These objectives have been successfully achieved. Continued development of this technology could be taken as a U.S. endorsement of the civilian use of plutonium; therefore the Administration has recommended to the Congress that this research be terminated. The IFR concept encompasses three major components which are currently at various stages of development: (1) the ALMR, characterized by liquid metal (sodium) cooling, a pool-type reactor configuration, and metallic fuel; (2) a fuel recycle capability based on high temperature, proliferation-resistant metals purification technology (pyrometallurgy) and electrorefining; and (3) a comprehensive waste processing technology that separately addresses gaseous, metallic, and other fission products. The waste processing technologies were to be designed to leave only trace amounts of transuranics, which would be alloyed with non-recovered metal fission products for disposal.

Integral fast reactor technology development

DOE's IFR technology programme included three elements: (1) Fuel Performance Testing and Demonstration, including fabrication, irradiation testing, performance evaluation, and modeling of metal fuel to demonstrate its performance under normal conditions and provide a basis for manufacturing specification, (2) Core Design R&D, including evaluation of major reactor design aspects for metal fueled cores and their influence on the passive safety response, and on performance and economics, and (3) Safety Tests and Analysis, including demonstration of IFR and metal fuel response to off-normal and accident situations, through testing in EBR-II and TREAT.

Fuel performance testing and demonstration: The primary objectives of metal fuel performance demonstration are to demonstrate, through irradiation of individual test assemblies and whole core loadings, the economic and safety performance potential of metallic fuels, and to develop a technology data base, as required, to support advanced reactor design and licensing processes. The demonstration includes the fabrication of fresh fuel and components for irradiation in the EBR-II. The basic physical properties of the ternary alloy IFR fuel and the fuel/cladding interactions over a broad range of compositions and operating conditions are being established.

Out-of-reactor experiments are underway to establish the compatibility of the metal fuel with advanced cladding materials, to characterize the distribution of the alloy elements within the fuel, to measure the thermal and physical properties of the fuel, and to validate calculational methods of modeling the fuel behaviour. The irradiation test programme covers a comprehensive range of design and operating parameters. The U-Pu-Zr fuel composition has varied from 0% Pu to 28% Pu, with zirconium variations from 2% to 14%. Three cladding materials have been used, including the two austenitic, materials 316 and D9, and the ferritic/martensitic alloys HT9 and HT9M. The plenum-to-fuel volume ratio, smear density, linear power, and fuel/cladding temperatures have cover a wide range. The maximum burnup achieved to date is 19.9 atom percent and, in general, the steady-state irradiation performance of the IFR fuel has been excellent.

The factor which limits the thermal performance of IFR fuel is the potential for clad wastage from interaction with fuel over an extended period at extreme conditions in a slowly

cooling accident. At sufficiently high temperatures, a eutectic type interaction between Pu and the Fe in the clad can thin the clad and also facilitate migration of fission products into the clad. No credible accidents have been identified that lead to rapidly progressing fuel/clad interaction. Inductively heated furnaces, the Fuel Behaviour Test Apparatus, and the Whole Pin Furnace are used to determine the limiting time and temperatures with respect to clad wastage and to validate calculational models.

IFR reactor core design research and development: The reference ALMR power plant described in Section 2 is a particularly well-developed adaptation of the IFR reactor technology. As noted, it incorporates a number of specific innovations and advances and is solidly based on liquid metal fast breeder reactor experience in the U.S., France and U.K. It also benefits from experience obtained in the former Soviet Union and from technology development in Japan, Italy, Germany, and many other countries. In addition, the IFR metal fuel benefits from years of experience with metallic fuel in the EBR-II, and incorporates fundamental advances in fuels technology.

Safety tests and analysis: The overall objective of the IFR safety analysis task is to develop understanding of the phenomenology which controls the safety performance of the IFR metallic fuel, to provide the experimental data to validate the unique safety features of the IFR, and to fully characterize the safety features associated with the IFR concept. Primary activities were:

- Analyses of reactor operational transients, anticipated-transient-without scram (ATWS) events, and local faults to establish margins of safety for metal-fueled IFRs;
- Out-of-reactor tests on both unirradiated and irradiated fuel to establish key fuel behaviour data under upset conditions;
- TREAT tests to establish the margins to failure for metal fuel and to validate the modelling and analysis of the transient behaviour of metallic fuel under severe accident conditions; and
- Analyses to demonstrate the safety margin of metallic fuel for a wide range of reactor sizes and to apply these analyses to the reference reactor concept.

Following the successful Inherent Safety Demonstration test series conducted at the EBR-II in 1986, a wide range of design basis accidents (including anticipated, unlikely, and extremely unlikely transients) have been evaluated for the IFR concept. These events were found to lead to consequences well within conservatively-interpreted acceptance guidelines. The improved passive safety capability of the pool configuration and the improved reactivity feedback response of metal fuel lead to the availability of large design margins of safety. In pool systems, the large heat capacity buffers the primary system so that no reactor scram is required for any combination of balance-of-plant (BOP) faults. In the metal-fueled IFR, the reactivity decrement associated with changing power level is small when compared to oxide-fueled reactors. These basic characteristics and the availability of large margins are being exploited to develop simplifications in the plant protection system and plant control system configurations, leading to the emergence of a new optimum control strategy that could reduce even frequencies and scram demands to provide robustness with respect to human error in maintenance or control.

Progress has also been made in the programme area focused on understanding metallic fuel performance under severe accident conditions. While no further TREAT tests have been performed during the past year, analyses of previous metal fuel tests show that transient

heating of the fuel under accident conditions produces cladding loadings which are dominated by the plenum pressure. The similarity of the thermal expansion of fuel and cladding and the compliant nature of the porous fuel lead to negligible Fuel-Cladding Mechanical Interaction (FCMI) damage to the cladding. Although the FCMI stresses in the cladding may be significantly early in the transient, little plastic strain accumulates before fuel creep relaxes the cladding loading to a hydrostatic state that follows the transient increase in plenum pressure.

Should the accident sequence proceed to fuel melting, high fuel porosity with entrained gas retention in the open porosity and a small decrease in fuel density on melting lead to little pressurization of the pin before the fuel melt zone extends to the top of the fuel column. This allows molten fuel to expand under the porosity-entrained gas pressure into the plenum region. Besides delaying fuel failure (to about four times normal power as measured in a number of TREAT eight-second period over power transients), this molten fuel extrusion can provide a significance source of negative reactivity feedback. Once clad failure does occur, that same entrained fission gas pressure leads to a dramatic dispersion of the liquid-phase fuel through the breach and out of the pin bundle.

Current activities in the severe accident domain are addressed by translating these understandings of phenomenology into their resultant safety implications and capturing this phenomenology in disruption models for the SAS4A severe accident analysis code.

Integral fast reactor fuel cycle technology development

A key element of the IFR concept is its unique fuel cycle, which is based on a combination of pyrometallurgical and electrochemical processing ("pyroprocessing"). This element of the IFR Programme deals with the development of a compact process for recovering uranium, plutonium, and other transuranic elements from irradiated metallic core fuel and blanket materials, for separating fission products from the actinides, and for re-enriching the core fuel with plutonium bred in the blanket. To accomplish this, major development efforts were directed toward flowsheet and process chemistry development, process equipment development, and engineering-scale demonstration of the pyroprocess, including waste treatment/management.

Pyroprocess development: This process is illustrated in Figure 9.63. The first step in the electrorefining process for separation and recovery of actinides consists of the batch dissolution of chopped fuel element segments. With the electrorefining cell operating at a temperature of 500°C, an oxidant such as CdCl_2 is added to convert most of the actinides, the sodium from the fuel element thermal bond, and active fission product metals to their chlorides. Various alternate oxidants have been evaluated to reduce the processing and recycle (and inevitable losses to a waste stream) of cadmium, a "hazardous" material. These chlorides are dissolved in the electrorefiner electrolyte, which is a mixture of LiCl and KCl . The remaining fuel is then anodically dissolved. A potential is then applied between the electrorefining cell anode and a solid cathode suspended in the electrolyte salt. Uranium is electrotransported to the cathode and adheres as a dendritic deposit. The electronegative fission products (noble metals, transition metals, and some rare earths) remain in the electrolyte salt. When an appropriate concentration of plutonium is achieved in the electrolyte, special liquid cadmium cathodes are installed in the electrolyte and the plutonium and remaining actinides, including an approximately equal amount of uranium, are deposited on the cadmium cathode.

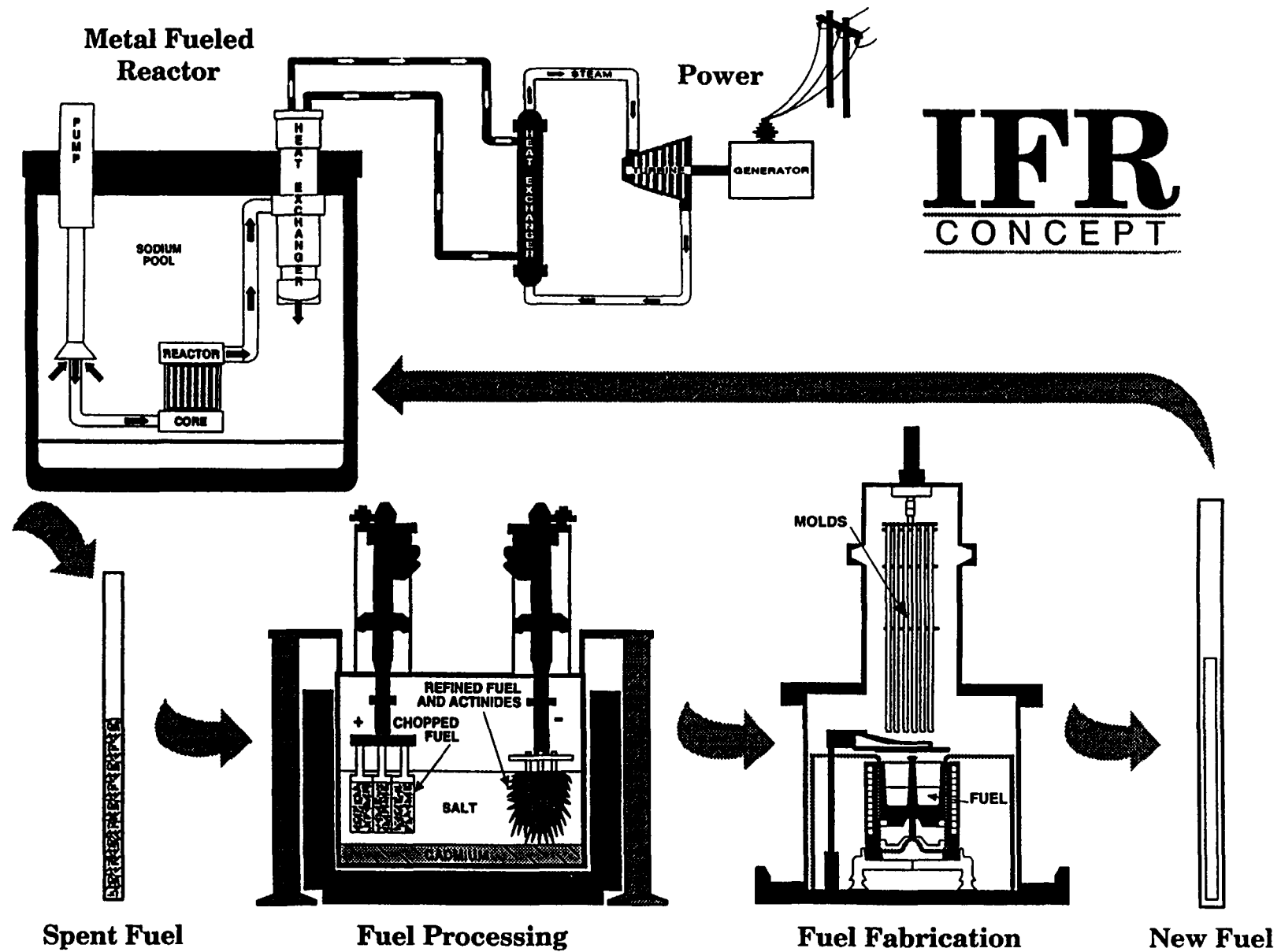


FIG. 9.63. The integral fast reactor (IFR) concept

The electrorefiner apparatus is pictured in Figure 9 64. A liquid cadmium cathode is utilized in the IFR pyroprocess for the recovery of plutonium and other minor actinides because of the much higher deposition rates available for these materials in liquid cadmium, as compared to the deposition rates on solid mandrel cathodes placed in the salt phase. Recent work on the liquid cadmium cathode concept has focused on development of the "pounder" cathode, a rotating plunger device that compresses the salt/cadmium interface. Results obtained to date with the pounder cathode indicate that it enables production of a metal ingot that is free of dendrites and salt. The pounder cathode is capable of a high loading of heavy metal and operates at virtually 100% collection efficiency. The cathode deposits are removed from the electrorefiner cell at the completion of the deposition process. Any occluded salt and

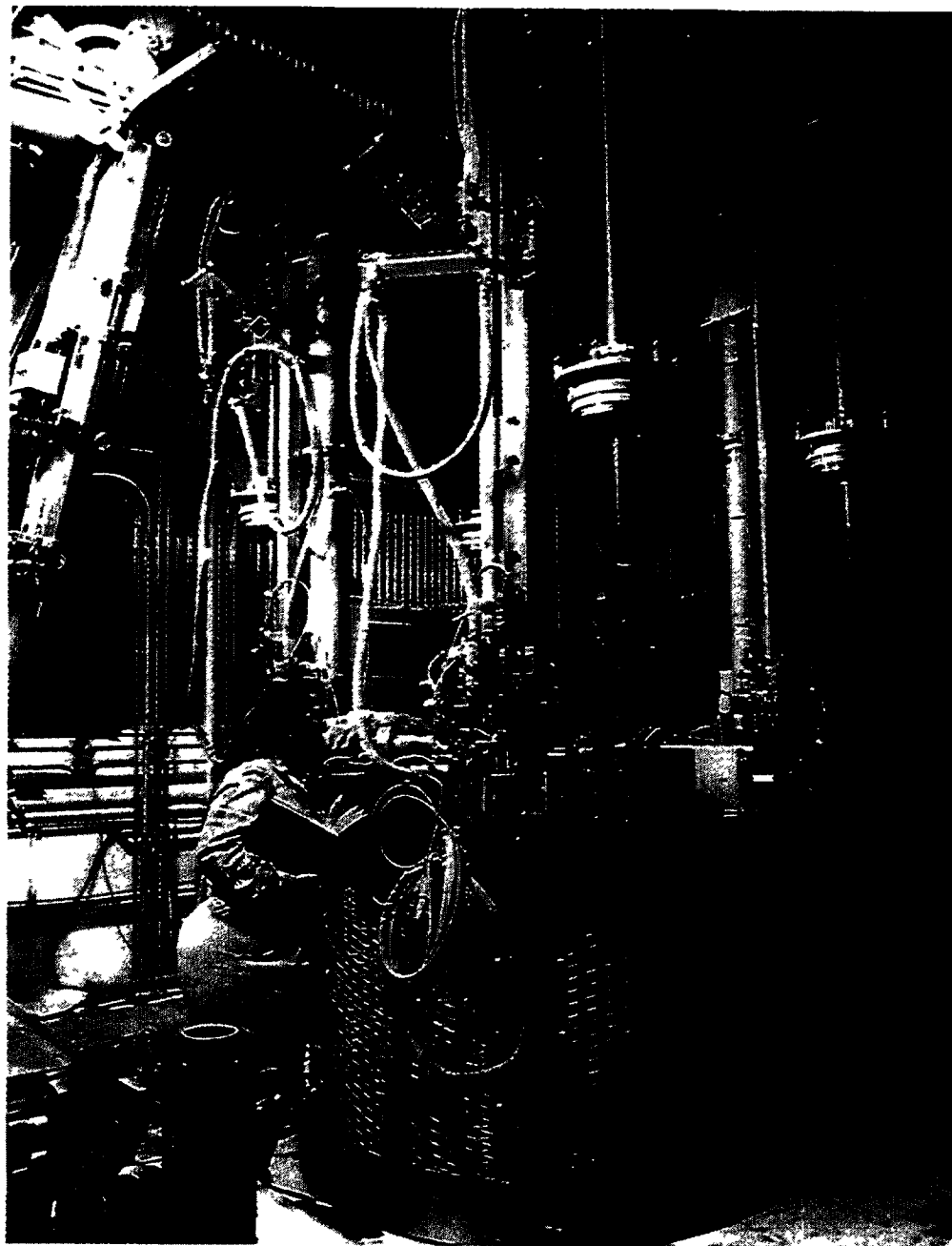


FIG 9 64 The IFR Electrorefiner undergoing final functional test at Argonne National Laboratory-West prior to placement into Fuel Cycle Facility

cadmium are separated from the actinides and recycled by retorting, and the uranium and U-Pu-TRU products are consolidated by melting (Figure 9 65) The consolidated fuel material ingots are then transferred to the injection casting system for fabrication of fuel rods

Fuel cycle technology demonstration: The objective of this programme element is to verify the operability of the pyrometallurgical and fabrication systems on a production scale, and to quantify the economic potential of the IFR metal fuel cycle Comprehensive demonstration of all aspects of the fuel cycle technology under simulated commercial conditions had been scheduled to be carried out in the refurbished FCF at the ANL-Idaho site between 1994 and 1996, using spent IFR fuel discharged from the EBR-II reactor This

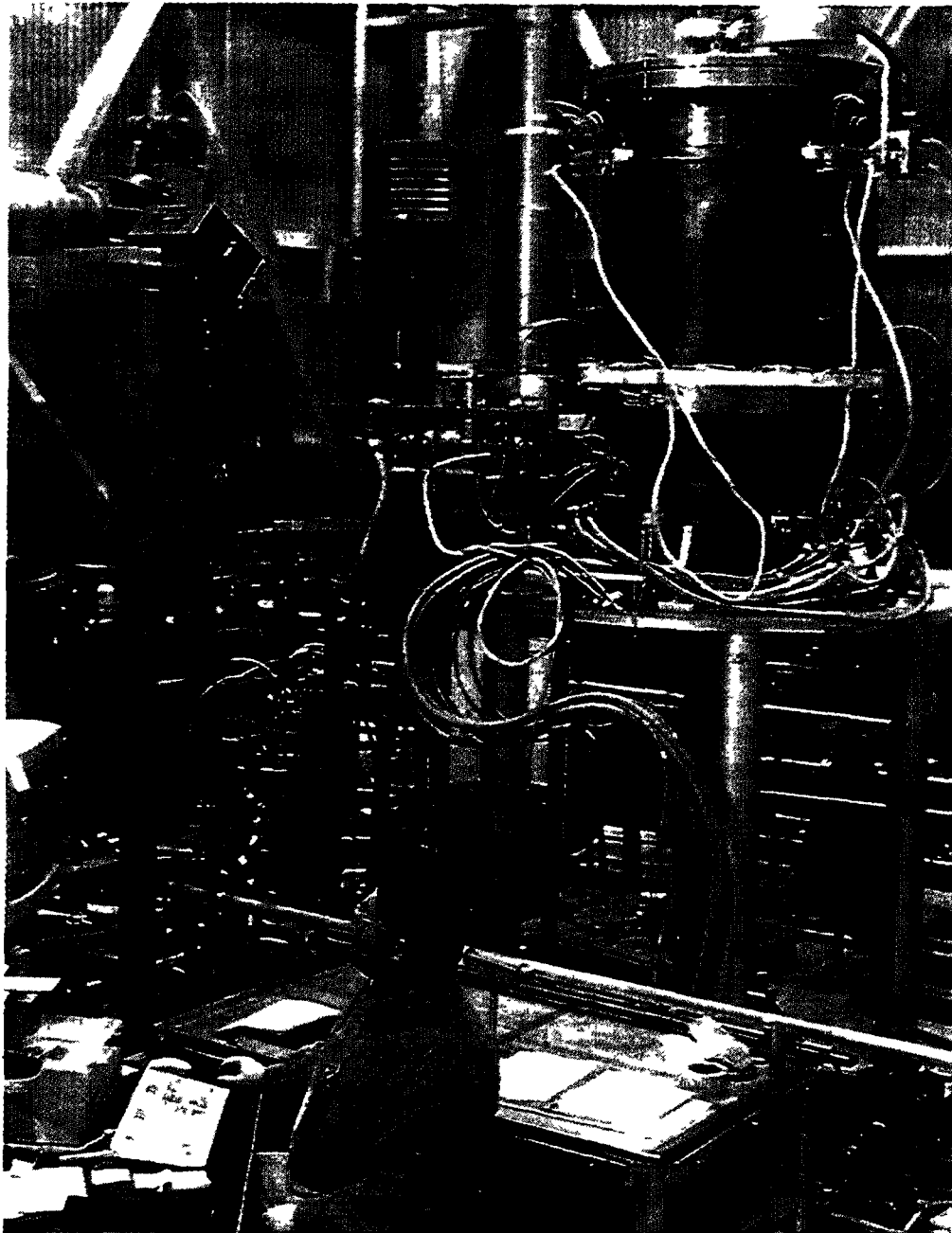


FIG 9 65 The IFR cathode processor (to purify 10 kg Ingots of fuel for recycle) undergoing finals tests at Argonne National Laboratory-West

facility is designed to provide complete fuel service to support EBR-II operation. Modifications to the FCF (formerly the Hot Fuel Examination Facility-South) to include installation of full-scale IFR pyroprocessing unit operations and component check-out have been completed. The pyroprocessing demonstration was planned on a scale and at a throughput rate that would facilitate reliable economic evaluation of the process. One in full hot operation, about 60 to 90 EBR-II fuel subassemblies could have been processed per year. Unit operations would have ranged from initial fuel subassembly breakdown to final waste treatment and packaging for disposal. During this time, the EBR-II complex was to have been in full operation as an IFR prototype, with fuel at goal burnup levels and fuel being recycled (i.e. processed and refabricated) to the reactor in a closed fuel cycle.

Limited operation of this facility will be required as part of the shutdown of the EBR-II reactor and the close-out of the IFR research programme. Considerable material is in process, including all of the EBR-II fuel and blanket material. The FCF facilities will be adapted to stabilize material from interim storage and may be used later for preparation of waste forms for final disposal. Naturally, all of the intermediate waste products which result from these processing operations will need to be prepared for disposal. Fortunately, much of the waste from development performed as part of the IFR programme is applicable and can be used in this mission.

Light water reactor actinide recovery: The success of pyrometallurgical recycle, in particular the extremely low loss of transuranics to the waste stream, has led to the suggestion that the same general concept could be used as a means of minimizing the actinide burden on the high-level nuclear waste repository. Basic work to date has been done on the assumption that the separated transuranics could be disposed of as fuel in an IFR. This symbiotic fuel cycle would not only have minimized the repository burden, but would have provided a means of rapidly eliminating excess stores of separated plutonium, eventually leading to the elimination of all excess stores of both separated and unseparated plutonium. By operating the IFR reactor in a burner mode (by designing to minimize the space available for external blankets) and using transuranics recovered from spent LWR fuel as make-up, a combined cycle with uranium as the only feed and recovered excess uranium set aside as the only output (other than electricity and fission products) can easily be assembled.

The particular case shown in Figure 9.66 is based on the Organization for Economic Cooperation and Development-Nuclear Energy Agency/International Atomic Energy Agency (OECD-NEA/IAEA) projections of nuclear power extended linearly to 2045, and constant thereafter. For simplicity, all once-through operation is assumed to be comparable to a 33,000 MWD/MTHM LWR. Thermal recycle is one-cycle only. Fast reactors assume total recycle of all transuranics (as with the IFR). Fast reactors are slowly introduced from 2010 to 2020, with all new construction after 2020 being fast reactors. The fast reactor plutonium regeneration rate is adjusted such that, after 2045, there is no excess world plutonium; it is being used for active power generation. While this case is idealized, it illustrates the concept of using plutonium management to limit world plutonium inventories to avoid inactive storage and to eliminate discharge of significant quantities of plutonium to wastes.

Several conceptual processes have been under development at Argonne National Laboratory for recovery of actinide elements from LWR spent fuel. High temperature processes ($\sim 800^{\circ}\text{C}$) based on work performed at ANL during the 1960s and 1970s are being evaluated. In these processes, the LWR oxide spent fuel is reduced by reaction with calcium metal in a two-phase (liquid metal and molten salt) system. The CaO formed during the

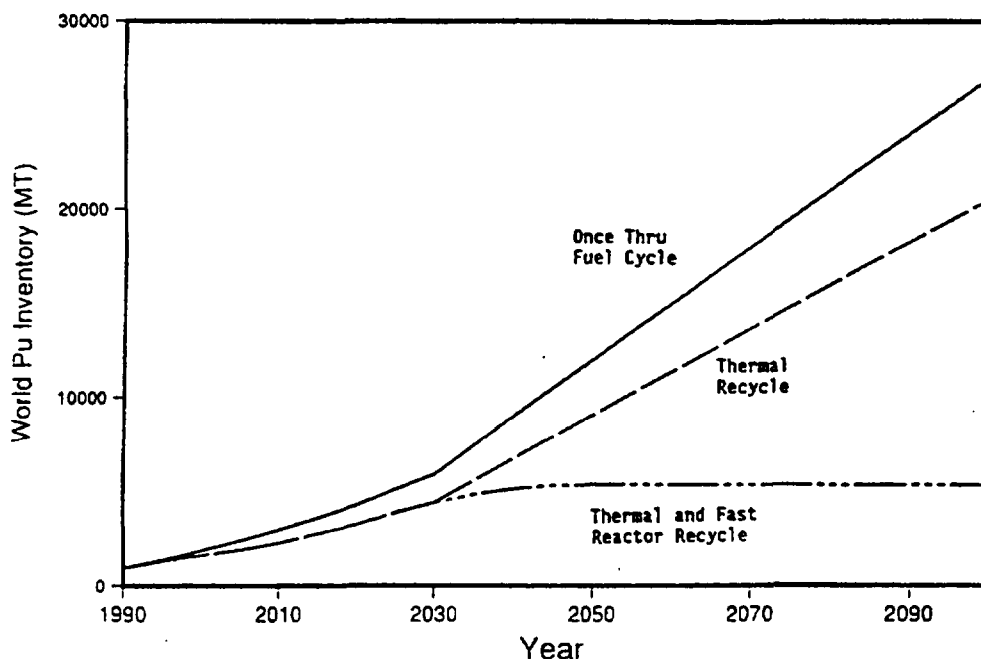


FIG. 9.66 The effect of recycle on world plutonium inventories

reduction process is soluble in the molten salt ($\text{CaCl}_2\text{-CaF}_2$), and the salt is recycled by electrochemically reducing the CaO to calcium metal. Oxygen is evolved as CO and CO_2 at a carbon anode. The actinide elements are extracted from the liquid metal phase and transferred to the IFR fuel cycle for further purification. The separated fission products will be prepared for final disposal as described below.

An alternative method which uses lithium is now the preferred process. The process operates at 550°C , a much easier engineering undertaking. Both processes have been shown to be effective in reducing LWR spent oxide fuel to a metallic form, but, in addition to the difference in operating temperature, there are differences in the course of the fission products. In either case, all of the transuranics (including Am, Np, and Cm) and all noble metals are reduced, yielding a product that is fully transparent to safeguarding and significantly self-protecting. In the calcium process, a large part of the rare earths also accompany the transuranics, providing an even higher degree of self-protection. These two processes were selected for their ease of recycle and introduction into the IFR fuel cycle with minimum waste.

Consideration has also been given, again incidental to IFR technology development, to the use of pyrometallurgical processing technologies such as these as means of treating other fuels and nuclear wastes which may not be suitable for direct disposal. In this instance, for fuels containing a substantial fissile content, there is advantage to retaining fission products for self-protection. The above products remain fully self-protecting during the lifetime of the retained noble metal and rare earth fission products (several years to a few decades), which is ample time for any realistic IFR-type fuel cycle. To extend self-protection to many decades, the process should also retain Cs and Sr.

Small-scale experiments are being conducted to develop unit operations for these processes. Containment vessel materials are being developed for use in the process steps, and testing is being conducted to determine their performance in the high temperature, corrosive environment. Experiments are also being done to develop methods for recycle of the

reductants to minimize waste streams. Processes developed in the small-scale experiments are being upgraded to "engineering-scale" (~2-kg batch size) for demonstration. The equipment and containment gloveboxes necessary to perform these demonstrations are being designed and fabricated.

Waste processing technology

Metallic fission products in the cadmium pool at the bottom of the electrorefiner are separated by drawing off the bulk of the cadmium and then retorting and recovering the cadmium for recycle to the electrorefiner. Any insoluble oxides or carbides (e.g, ZrC) are removed from the liquid cadmium by filtration. The metallic fission products and insolubles, together with the cladding, are then immobilized in a metal matrix using a material such as copper (other candidate matrix materials are also under investigation), thereby creating a stable waste form for geologic disposal.

The electrolyte salt is periodically withdrawn and treated to recover trace uranium and TRU elements by direct chemical reduction. A test apparatus has demonstrated highly effective extracting efficiency for uranium, transuranics, and rare earths for a pyrocontractor operating with molten cadmium and chloride salts at 500°C. The treated salt, a non-TRU waste material, is then immobilized by filtration through a zeolite column where the fission product cations are sorted by a highly effective ion exchange reaction. Salt molecules are also sorted by occlusion into a solid monolithic sodalite form, which produces a waste form which appears to be suitable for geologic disposal. Initial leach tests show more effective fission product retention for this sodalite form than for borosilicate glass.

Flowsheet variations are being tested with laboratory-scale electrorefining apparatus, and results are being compared against calculations based on an electrochemical model of the overall process. Agreement has been obtained between the measured and calculated composition of the salt and metal phases. An engineering-scale version of the electrorefiner, capable of handling cathode deposits of 10 kg, is being used for process development and system optimization.

The IFR waste treatment process flowsheet includes a salt-stripping step in which the TRU-free salt from the salt extraction step is treated with Li(Cd) to remove all residual uranium and rare earth fission products. Testing of the prototype salt-stripper vessel has begun.

9.8. BMN-170 MODULAR FAST NUCLEAR REACTOR

9.8.1. Design goals and status

BMN-170 power units are being developed as a new generation of universal power source for economic and effective production of electricity, process steam, fresh water and district heating (Fig.9.67). The nuclear power unit is based on the advanced 400 MWth sodium cooled fast nuclear reactor BMN-170. The capability of fast nuclear reactors to produce both electricity and heat in a safe and reliable manner has been confirmed convincingly by operating experience of NPPs with the BN-350 and BN-600 reactors. For large NPPs a 500 MWe power unit is proposed consisting of three BMN-170 reactors with standard steam turbines. A power unit with one BMN-170 reactor is capable of providing electricity, heat and potable water (using proven technology and available desalination facilities) for an industrial

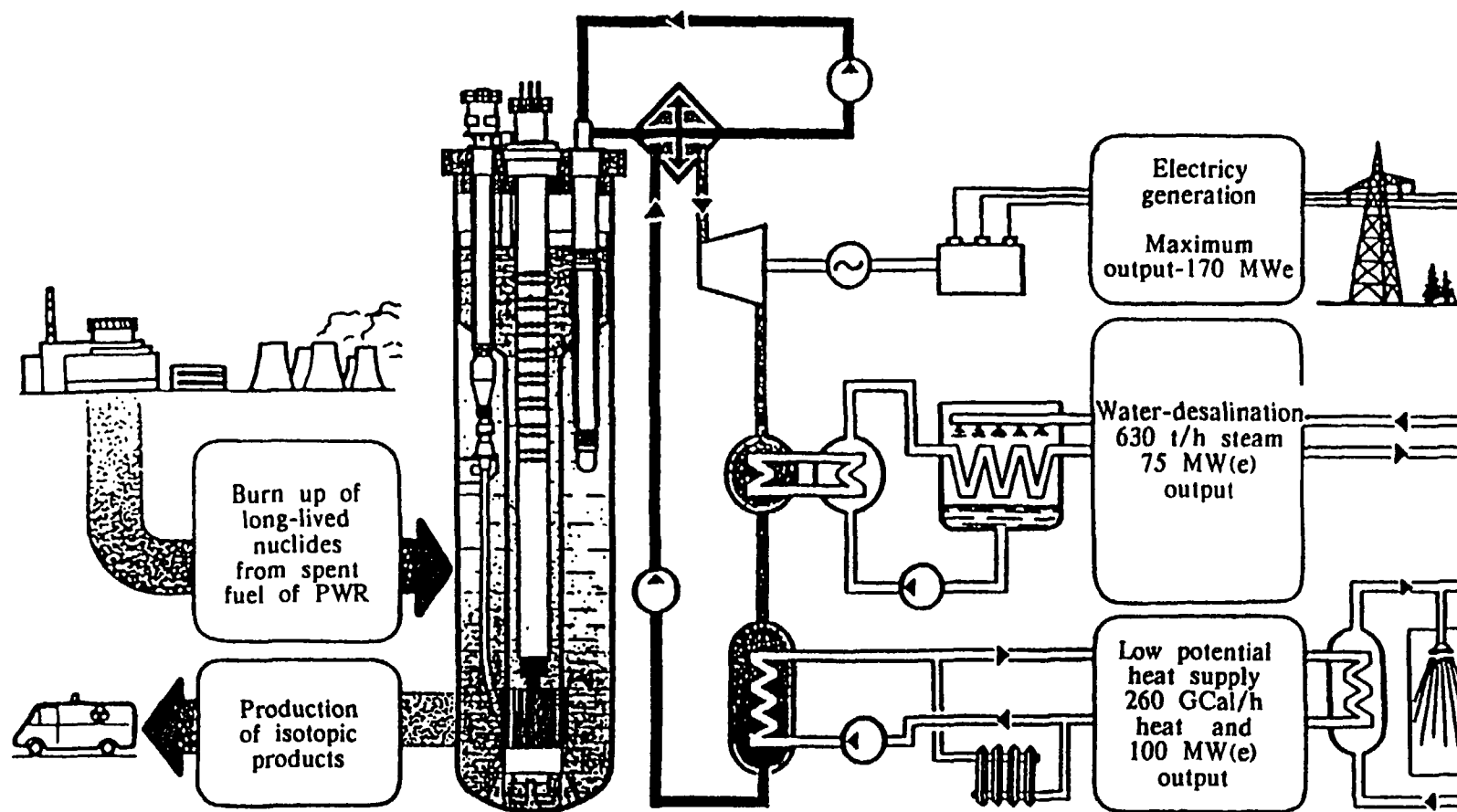


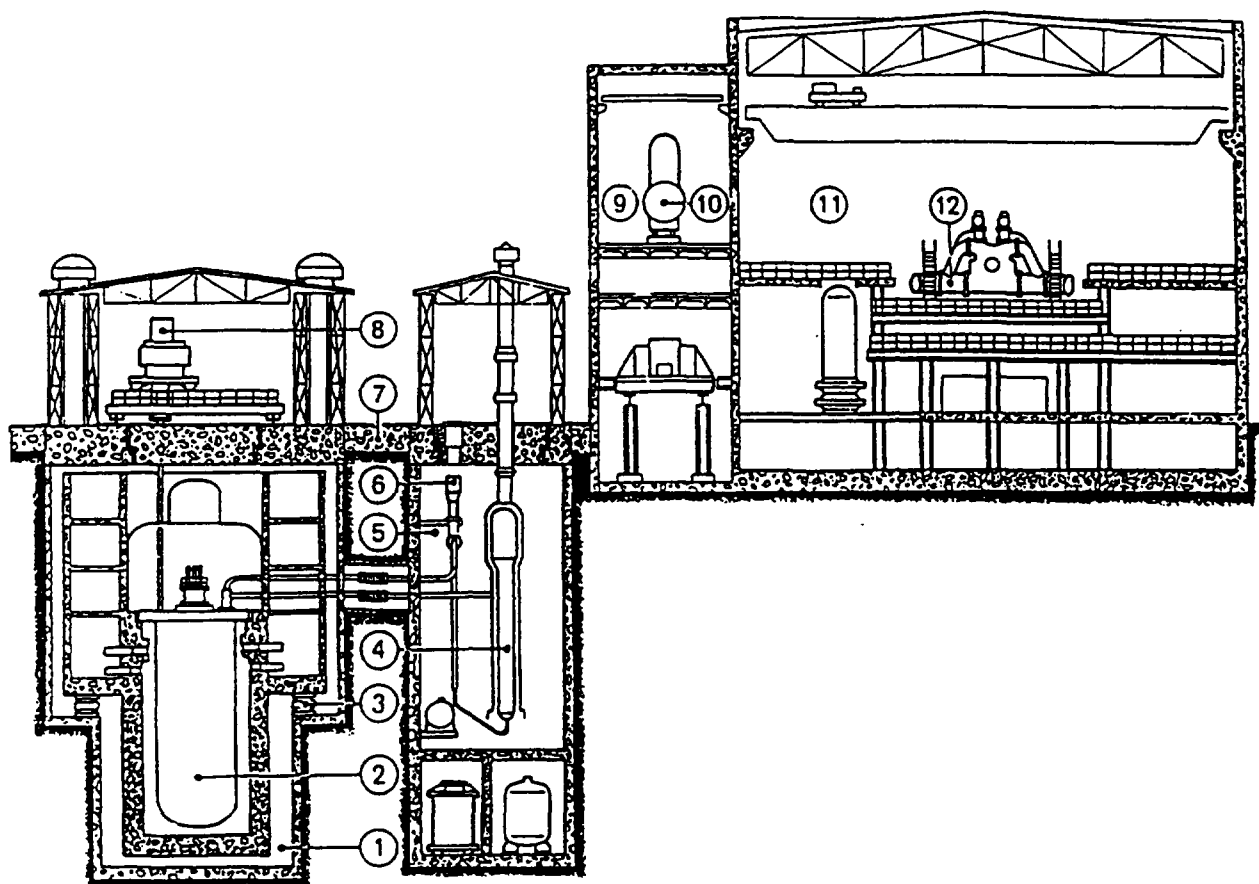
FIG. 9.67. BMN-170 Reactor Energy utilization options

town with around fifty thousand residents. The BMN-170 power unit is planned in particular to replace the BN-350 reactor plant after its lifetime has expired. A general view of the power unit is given in Fig. 9.68.

In 1990, preliminary development work had been carried out for the Conceptual Design of BMN-170, which included an assessment of promising technical and economic performance and a report "Safety concept for the reactor plant BMN-1700".

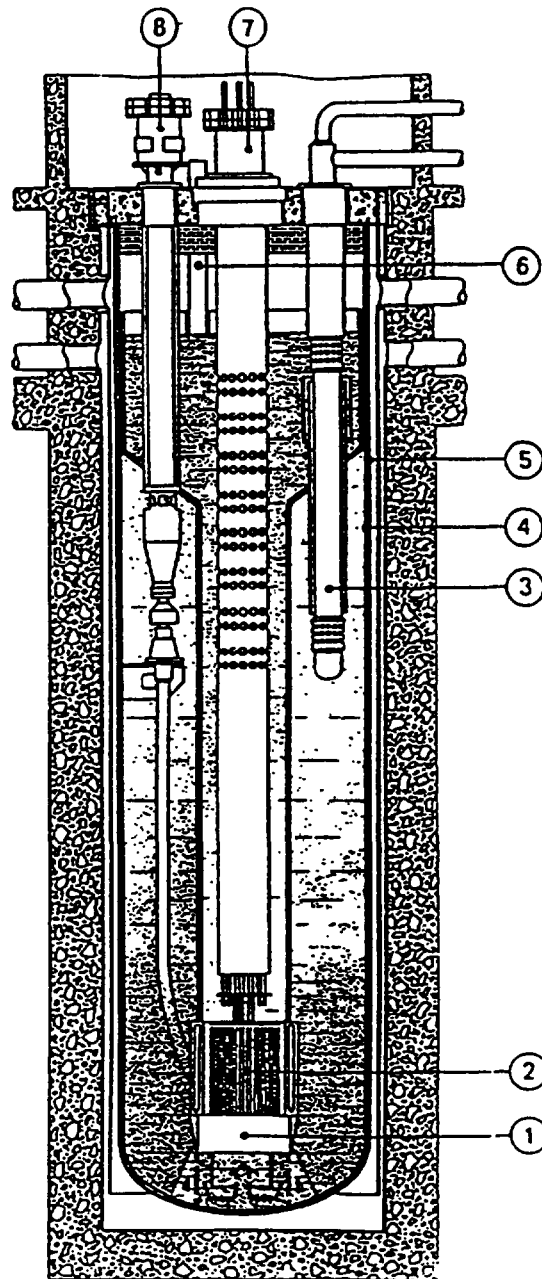
9.8.2. Design basis

The BMN-170 reactor plants have a typical three-circuit flow scheme. Integral layout of the reactor is adopted with all the primary components and systems and radioactive sodium in a single vessel (Fig. 9.69). This feature in combination with simplification of the safety systems provides maximum compactness and safety of the reactor itself and the plant as a whole. The reactor vessel is a long cylindrical steel tank with an ellipsoidal bottom confined in a close fitting guard vessel up to the elevation of the maximum possible level of coolant in the reactor (allowing for accidental draining of a secondary loop into the reactor). The reactor core and diagrid, and a catcher to localise and cool core debris in the case of a beyond-design accident, are installed on the reactor vessel bottom. Each reactor coolant pump is connected to the core diagrid by a pressure pipe. "Cold" and "hot" sodium plena in the reactor pool are



1 - reactor compartment, 2 - reactor, 3 - shock absorber, 4 - steam generator, 5 - SG compartment, 6 - secondary pump, 7 - protective concrete slab, 8 - refuelling machine, 9 - deaerator stand, 10 - deaerator, 11 - turbine building, 12 - turbogenerator.

FIG. 9.68. BMN-170 Power plant arrangement



1 - core diagrid, 2 - reactor core, 3 - intermediate heat exchanger,
4 - reactor vessel, 5 - guard vessel, 6 - cold filter-trap, 7 - control rod
drive mechanisms, 8 - reactor coolant pump

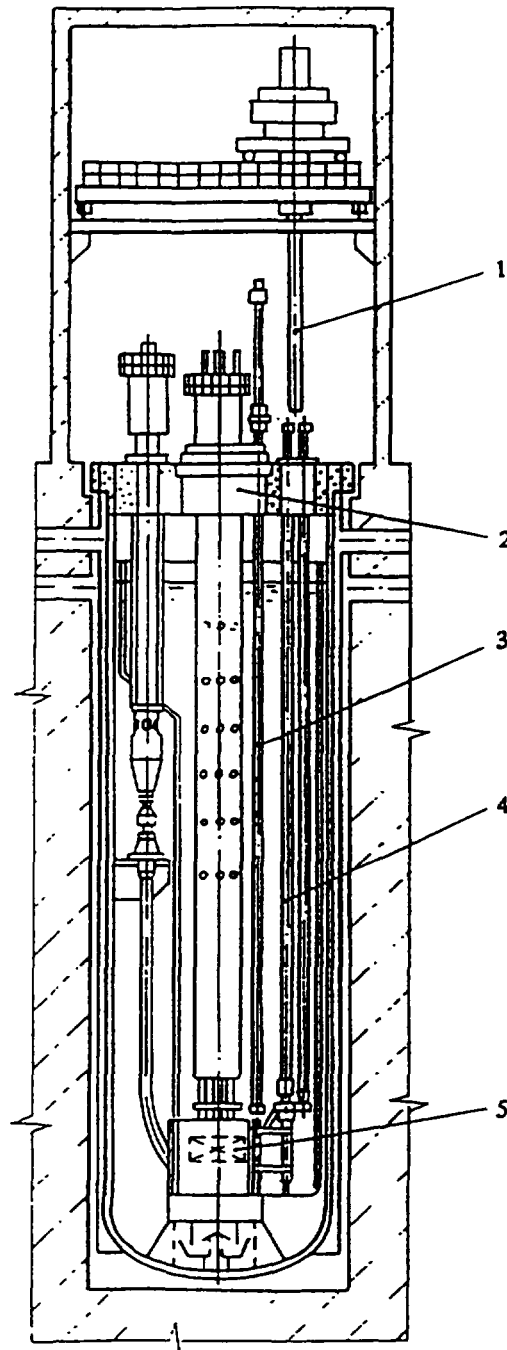
FIG.9.69. BMN-170 Reactor unit

separated by a baffle. The core is assembled from hexagonal fuel assemblies (FAs) 96 mm width across flats, which gives the possibility of unifying not only the fuel design but also certain refuelling equipment items with those for the BN-350, BN-600 and BN-800 reactors.

Two design options are being considered for the ex-reactor portion of the refuelling system. The first design uses a loading/unloading machine (Fig 9.68) comprising a self-moving remotely-controlled leak-tight cell with a refuelling mechanism and fuel drums for provisional storage of new and spent FAs, installed on a rail truck. This design is suitable for the case of several reactors deployed on one site. The hazard of leakage of radioactive gas from the connections between the machine and the reactor interior and the external spent fuel store are

considered to be the main disadvantage of the design. The second design consists of a stationary refuelling cell (Fig. 9.70) and utilizes the traditional and proven designs used in the BN-350, BN-600, BN-800 and BN-1600M reactors.

Enhanced immunity of the power unit to external impact (aircraft crash, shock wave) is provided by location of the reactor and the related safety systems in protected rooms below ground level (Fig. 9.68). Enhanced seismic stability of the unit is provided by the use of shock



1 - refuelling machine, 2- rotating shield plug, 3 - refuelling mechanism,
4 - elevator, 5 - reactor core

FIG. 9.70. BMN-170 Reactor with refueling machine

absorbing supports for the reactor equipment and the safety-related systems. The reactor plant remains operable at magnitude 7 earthquake (to MSK-64 scale) and its safety is ensured at magnitude 8 earthquake. The reactor plant makes use of equipment items used in operating fast reactors, of which prototypes have already been fabricated by the home industry. The main problems of structural materials, sodium coolant technology, nuclear fuel and maintenance during operation have been solved.

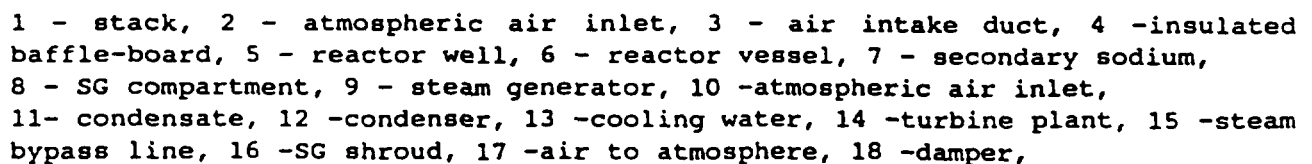
TABLE 9.8. BMN-170 BASIC DESIGN DATA

Parameter		Value
1.	Reactor thermal power, MW	400
2.	Primary sodium flowrate, t/h	7300
3.	Primary sodium temperature, °C:	
	- core inlet	395
	- core outlet	550
4.	Pressure in reactor gas plenum MPa	0.04
5.	Secondary sodium temperature, °C:	
	- steam generator inlet	530
	- steam generator outlet	350
6.	Fuel	(U, Pu)O ₂
7.	Fuel inventory in the core, t	4.65
8.	Core lifetime, year	4
9.	Refuelling interval year	1
10.	Breeding ratio	1.1...1.3
11.	Sodium void reactivity effect, % Dk/k	-0.15
12.	Reactor specific metal weight, t/MW(th)	1.68

9.8.3. Reactor safety features

The enhanced safety features which are intrinsic to fast nuclear reactors in general have been developed to the maximum feasible extent in the BMN-170 design. The possibility of uncontrolled excursion of the reactor power accompanied by increasing coolant temperature is completely excluded by virtue of the zero or negative void reactivity coefficient. The reactivity margin for fuel burnup is small. Reactor shut down and residual heat removal systems based on the passive principle of operation have been incorporated. They help to keep the reactor in a safe state independent of the operability of the supporting systems (power and compressed gas supply, etc.) and of operator actions. To shut the reactor down additional control rods are provided which are inserted into the core under gravity in the case of sudden loss of coolant flow or sodium temperature rise. This system shuts the reactor down independently of the automatic emergency protection system.

The passive residual heat removal system removes heat from the core to the ambient air in accidents involving complete loss of feedwater supply to the steam generators (Fig. 9.71). In such an event the residual heat is removed by air cooling of the reactor vessel driven by a chimney effect. Air passes through a cooling duct in the reactor well. Flowing down a gap between the well liner and a baffle the air protects the well concrete from overheating, and in the upward-flowing section between the baffle and the guard vessel the air removes heat from the reactor. It then passes to the atmosphere through stacks. There is no thermal insulation on the surface of the guard vessel to ensure the required emergency cooling.



Heat removal from the surface of the steam generators by air flow under natural convection improves thermal conditions in loss-of-cooling accidents and preserves the operability of reactor equipment. This system operates continuously and does not require any actions for initiation.

516

By virtue of the physical properties and design decisions adopted for BMN-170 this reactor is able to limit its power in emergency situations and even to shut down and cool down over an unlimited period, and to confine radioactive releases within the passive protective barriers. Fast power transients, large coolant losses, and overheating or melting of the fuel are physically excluded. The assessed probability of severe beyond-design accidents potentially leading to damage to the reactor core is considerably lower for BMN-170 than for reactors now in operation: it is less than 1 E-6 per reactor-year, which meets up-to-date safety requirements and international recommendations for new generation nuclear power reactors.

9.8.4. Radiological safety

Operation of fast reactor NPPs confirms that their radiation impact on the environment is small. Ventilation discharges from operating reactors contain only noble radioactive gases (xenon, krypton and argon), iodine being virtually absent. In normal operation of a BN-500 power unit with three BMN-170 reactors the dose to an individual of the local population would not exceed fractions of a percent of the natural radiation background (0.008 mSv/year in comparison with 2 mSv/year from natural factors). In the event of extremely improbable severe accidents the protective barriers provided for BMN-170 mitigate the radioactive releases to a level which is not dangerous to the local population. There are no BMN-170 accidents which require the population to be evacuated for radiological reasons.

9.8.5. Economics

The BMN-170 power units have some positive features allowing the capital cost to be decreased and the economic efficiency of energy production to be improved. They are:

- the possibility of series fabrication of the modular reactors in a factory and delivery ready-made to site, which reduces labour-consuming erection works at site and cuts construction time and expense including interest payments,
- the use of the self-protection principle and passive systems for residual heat removal allow the number of both auxiliary and safety systems to be reduced and the classification of power unit equipment to be lowered,
- the use of standardized steam turbine and condensate equipment fabricated in accordance with the rules established for conventional power engineering,
- the high efficiency of the steam cycle,
- minimum heat discharge to the environment and consequently minimum requirements for condenser cooling water,
- the potential to connect various heat consumers to the power unit, which gives an additional increase to its thermal and total economic efficiency, and
- increase in the reactor plant and power unit lifetime to 60 years.

Standardization of the reactor unit simplifies the licensing procedure significantly. For these reactors an R&D programme may be needed only for the pilot plant, while for the subsequent plants a standard license would be issued.

The relatively small unit power of the BMN-170 reactors allows construction and operation in sequence in a flow construction scheme to provide a NPP of any required total power.

9.9.1. Introduction

The development process for large, expensive and complicated equipment of commercial importance is generally divided into several stages in order to reduce the investment risk. For example theory and physical principles are validated first, and then, after engineering analysis, a prototype component is designed, built and tested. Finally products are acceptance tested and are then ready for commercialization.

Such being the case for an individual item of equipment, it is the more so for a complete engineering system. Fast reactors constitute such a system. According to experience in many countries, a complete fast reactor development procedure can be characterized by the following phases.

- Basic research, especially on fast reactor physics, thermohydraulics, fuels and materials, sodium technology, components and safety is undertaken. This phase implies the construction and operation of numerous experimental facilities, such as a fast zero-power critical facility, sodium loops with various types of test sections, a fuel laboratory, and materials test facilities. Study of fast reactor development strategy has to be included in this phase.
- The knowledge and results gained from the basic research programme are used to design, construct and operate an experimental fast reactor (or more than one) of modest size (generally 10 to 100 MW(th)).
- Based on experience of constructing and operating the experimental fast reactor a prototype power reactor of 100 to 500 MW(e) will be built and operated.
- Having accumulated experience of reliable operation of the prototype, the commercial demonstration fast reactor plant will be built and operated, the components of which are scaled up from the prototype reactor.
- With further improvement the commercial fast reactor plant is ready for deployment.

This section describes a second-phase experimental fast reactor. The purposes, developments and achievements of experimental fast reactor throughout the world are summarized. In addition a brief presentation of the Chinese Experimental Fast Reactor (CEFR) is given.

9.9.2. History and achievements

Since the inauguration of the world's first experimental fast reactor Clementine in the United States of America this type of reactor has about 50 years of history during which 15 experimental fast reactors with different power and technical characteristics have been constructed and operated in 7 countries. About 200 reactor years' operating experience has been accumulated worldwide. The general characteristics of the experimental fast reactors built and designed are given in Table 9.9.

9.9.2.1. Purposes of experimental fast reactors

The design and construction of an experimental fast reactor is the first engineering accomplishment of FBR development. It requires compromises with respect to core neutronics, thermohydraulics, fuel pin and fuel assembly design, materials, components

TABLE 9.9. GENERAL CHARACTERISTICS OF EXPERIMENTAL FAST REACTORS IN THE WORLD

Reactor	Country	Power thermal/ electric (MW)	Coolant	Fuel	Operation		Purposes ²	
					A	B	C	D
Clementine	USA	0.025/0	Hg	Pu	1946-52			•
EBR-I	USA	1.2/0.2	NaK	U, Pu	1951-63	•		•
BR-2	Russia	0.1/0	Hg	Pu	1956-57		•	•
BR-5/10	Russia	5~10/0	Na	PuO ₂	1958--		•	•
DFR	UK	72/15	NaK	U-alloy	1959-77	•	•	
LAMPRE	USA	1/0	Na	Pu-Fe alloy	1961- 65			•
EBR-II	USA	62.5/20	Na	U alloy	1963 --		•	
EFFBR	USA	200/66	Na	U alloy	1963 - 72	•		•
Rapsodie	France	20~40/0	Na	PuO ₂ -UO ₂	1967 - 83	•	•	
BR-60	Russia	60/12	Na	(Pu, U) O ₂	1969 --	•	•	
SEFOR	USA, Germany	20/0	Na	(Pu, U) O ₂	1969 - 72			•
KNK-II	DeBeNeD	60/21.4	Na	PuO ₂ -UO ₂	1977 - 92	•	•	
JOYO	Japan	100/0	Na	(Pu, U) O ₂	1977 --	•	•	
FFTF	USA	400/0	Na	(Pu, U) O ₂	1980 --		•	
FBTR	India	42/12.5-15	Na	(Pu, U) C	1985 --	•	•	
PEC	Italy	123/0	Na	(Pu, U) O ₂			•	
CEFR	China	65/25	Na	(Pu, U) O ₂		•	•	

1) Germany, Belgium and the Netherlands

2) A: Demonstration of fast power reactor operation

B: Fuel and materials irradiation

C: Science demonstration (breeding, Safety,...)

D: Demonstration of large scale fast reactor operation, electricity generation.

previously selected, and the initial design specifications. It is therefore an important step in the fast reactor development procedure.

Looking back on the development the main purpose of some earlier experimental fast reactors can be seen to have been scientific demonstration. For example, Clementine, EBR-I and SEFOR in the United States of America and BR-2 in Russia were designed, constructed and operated to study neutronics, and to demonstrate breeding and safe control of a fast reactor. The study of molten Pu alloy fuel was the unique purpose of LAMPRE in the USA.

Since the middle of the 60s it appears that the scientific demonstration of fast reactors has been completed. Based on economic consideration for commercial fast reactors, fuel burnup is the most important factor in decreasing the fuel cycle cost and it is evident that the development of fuels and materials needs a fast neutron flux facility. In fact, almost all subsequent experimental fast reactors have had the same purposes:

- to provide experience in design, construction and operation of fast reactors, and
- to serve as an irradiation facility for the development of fuel and structural materials.

9.9.2.2. Coolant

As shown in Table 9.9., Hg and NaK were chosen as the primary coolant for some early experimental fast reactors because they have high atomic weight, are liquid at room temperatures and are easily obtained. But Mercury needs a high pumping power, about 14 times that for sodium, and has a low boiling point, 357°C under atmospheric pressure. In addition it is extremely toxic. NaK, the eutectic alloy of sodium and potassium, has higher cost and a relatively high neutron absorption cross section, which outweighs the advantage of using a material which is liquid at low temperature.

From the early 60s to the present sodium has been chosen as the primary coolant for all fast reactors. Its relatively low absorption cross section coupled with its low cost makes it highly attractive. Furthermore sodium has some outstanding features which make it very suitable for fast reactors at high temperature:

- good corrosion compatibility with structural materials up to a temperature of 700°C;
- high thermal conductivity, high heat capacity and good fluidity which provide good conditions for natural convection and natural circulation.

So far, there has been satisfactory experience in the use of sodium as fast reactor coolant in the fields of purification, analysis, leak detection, early diagnostics of sodium-water reactions, extinguishing of sodium fires, etc.

9.9.2.3. Fuel and burn-up

At the beginning of world fast reactor development great importance was attached to breeding so that metal or alloy fuels were emphasized because a hard neutron spectrum, and therefore a high breeding ratio, could be obtained. High burn-up, or more precisely long fuel subassembly life, is a very important factor in the economy of the fast reactor fuel cycle. Unfortunately metal or alloy fuels could not attain high burn-up because of excessive swelling. When the commercialization of fast reactors was taken into account economic considerations became predominant (after safety had been assured). For this reason, the selection of fuel was reoriented towards ceramics, i.e. plutonium-uranium mixed dioxide. In some cases mixed

plutonium-uranium carbide has been used for experimental fast reactors, and at the Argonne National Laboratory in the United States of America the development of alloy fuel has been pursued and, with technological improvements, high burn-up has been achieved.

According to design studies in Europe and Japan, the fuel burn-up target for commercial fast reactors should be 200,000 MWd/t and the irradiation dose target for cladding and wrapper materials should not be less than 180 dpa. The relevant experience obtained so far from experimental fast reactors is shown in Table 9.10.

Safety and reliability: Table 9.11. shows the operating records of some experimental fast reactors, indicating that high reliability and safety have been gained. It appears that the good operational results of experimental fast reactors are due to the following main reasons:

- sodium technology has been mastered, including sodium quality control, operation and maintenance of sodium systems, cleaning of equipment and removal sodium residues;
- the inherently safe features of sodium-cooled fast reactors are unique, i.e. low operating pressure of the primary system, high boiling temperature, large thermal inertia and the possibility of natural convection and natural circulation of the coolant; and
- sufficiently large design margins have been taken in the most of the experimental fast reactors.

Very important transient experiments have been performed in some experimental fast reactors. A loss-of-flow without scram at a nominal power of 22.4 MWth was performed at Rapsodie on 15 April 1983. In this test the maximum fissile subchannel temperature rose to 800°C, while the nuclear power decreased continuously without any intervention from the

TABLE 9.10. MAXIMUM BURN-UP AND DOSE IRRADIATION REACHED AT VARIOUS EXPERIMENTAL FAST REACTORS

Reactor	Up to year	Maximum burn-up	Maximum dose (dpa)
Rapsodie	1983	200000 MWd/t	135
DFR	1977	20%	
KNK-II	1992	175000 MWd/t	
EBR-II	1992	19.2%	
FFTF	1992	238000 MWd/t	100
BOR-60	1994	26%	
BR-10	1990	8.2%	
JOYO	1990	70800 MWd/t	

TABLE 9.11. OPERATING RECORDS

Reactor	Period	Availability factor (%)	Capacity factor (%)	Operation hours (hr)
BOR-60	1970-1991	60	60.5	50373
EBR-II	1970-1984	63.9		
FFTF	1982-1991	63.8		
JOYO	1978-1993			

reactor control systems. Also transient experiments such as loss-of-flow without scram and loss-of-heat sink without scram were performed at EBR-II in 1985-1986. The results were that the reactor was shut down by its reactivity negative feedback and the outlet temperature was finally no more than 400°C for LOHSWS and less than 700°C for LOFWS.

Rapsodie and EBR-II are respectively MOX-fueled loop-type, and metal-fueled pool-type, reactors. Thus these dramatic transient experiments have shown that advanced fast reactors can be designed with passive safety properties.

9.9.3. Trends of experimental fast reactors

In view of more than 40 years of worldwide fast reactor development experience, from experimental and prototype reactors up to economic demonstration, with very comprehensive international cooperation, it is not obvious that every country developing the technology in the future should without exception start by building an experimental fast reactor. On the other hand the development, design, construction and operation of an experimental fast reactor of a suitable power is necessary to decrease the economic risk of development.

Based on the extensive experience from the fast reactor family, successor fast reactor developers can avoid detours in the main technical choices. An experimental fast reactor has a higher value for demonstration purposes if the main technical selections, including primary circuit arrangement (pool or loop), are consistent between experimental, prototype and commercial demonstration reactors. The most important demonstration missions are the design features and, especially, the safety features of the reactor.

9.9.4. CEFR-25 design

Main purposes and demands: As the first step of FBR technology development in China, it is planned to design and construct the CEFR-25, the main purpose of which is to enable the nation to master the methodology of FBR design, including the establishment of data library, computer codes and more important experience in harmonizing neutronics, thermohydraulics, mechanics, fuel element design, etc. within the boundary conditions of the general requirements for the reactor; to master the fabrication of components under the appropriate standards and criteria of quality control and assurance; and to accumulate experience on operating a FBR as a generation plant.

The second purpose is to make the reactor available as a fast neutron irradiation facility for the development of fuels and materials.

The requirements for CEFR-25 have been specified as follows:

- a) the main technical selections should be consistent with the world trends of FBR technology development,
- b) the basic thermodynamic parameters of commercial fast reactors should be adopted,
- c) the design is required to have a self-stable reactor core and a passive decay heat removal system,
- d) the systems and components should be as simple as possible to achieve high reliability and economy, and

- e) the safety rules, regulations and codes promulgated by the China National Nuclear Safety Administration, and the environment impact limitations issued by the China National Environment and Protection Administration and by the Local Environment and Protection Administration, should be obeyed.

Main technical selections and design conditions: The main technical selections and design conditions for CEFR-25 were decided in 1988 as follows:

- a) reactor power 65MWth matched with a 25MWe turbo-generator
- b) (Pu-U)O₂ as fuel and 316 (Ti) stainless steel as core structure material
- c) sodium pool primary coolant circuit arrangement
- d) maximum fuel pin linear power, 43 kW/m
- e) core outlet temperature, 530°C
- f) maximum permitted cladding temperature, 700°C
- g) maximum burn-up of the fuel, 50,000MWD/t
- h) steam temperature, 480°C ~ 490°C, pressure ~ 10.0 MPa
- i) primary storage of spent fuel at the core periphery
- j) straight lift fuel handling machine with double rotating plugs, with transport of new and spent fuel subassemblies through a fixed port
- k) two coolant circuits,
- l) two independent shutdown systems, and primary systems entirely within the containment.

Reactor core and subassembly design: The core of CEFR-25 is shown in Fig. 9.72. It is composed of 82 fuel subassemblies, 158 blanket subassemblies, 378 radial reflector subassemblies, 2 safety rods, 6 control rods and 54 spent fuel storage positions, surrounded by shielding subassemblies. The nominal subassembly lattice pitch is 61.5 mm.

Each fuel subassembly is composed of 61 fuel pins 6 mm in diameter, positioned by wire wraps. It has a hexagonal tube 58.5 mm wide across flats, and a tube foot for positioning and sodium inlet. Each fuel pin contains a 500 mm fuel pellet column with 300 mm upper and lower depleted UO₂ axial blankets.

The fuel is plutonium uranium mixed dioxide with 27.2% weight percentage of PuO₂. The uranium will be enriched to 30%.

There are two active shut-down systems. The first has 6 control rods of which 1 is used for temperature compensation, 3 for burn-up compensation, and 2 for regulation. The second shut down systems has 2 safety rods. These two shut-down systems can scram automatically or by manual operation if necessary. The rod-drop times are designed to be 1.2 ~ 1.5s and 0.7s respectively.

The power generation in different regions is given in Table 9.12. To facilitate the arrangement of the reactor core, all subassemblies have the same lattice pitch. This allows the possibility of replacing the first row of the radial blanket by fuel so that the reactor core could be enlarged in future.

Reactor block: The reactor block is of pool type design as shown in Fig 9.73. The entire primary circuit is contained in the main sodium vessel, which is about 8m in diameter, 8m deep, and 25/50 mm in thickness. It is surrounded by the guard vessel which is designed so

TABLE 9.12. BREAKDOWN OF POWER GENERATION (MWth)

Region	Initial loading	Equilibrium loading
Fuel	61.5	60.2
Blanket	2.6	3.9
Control rods	0.43	0.43
Reflector	0.27	0.27
Shielding	0.23	0.23

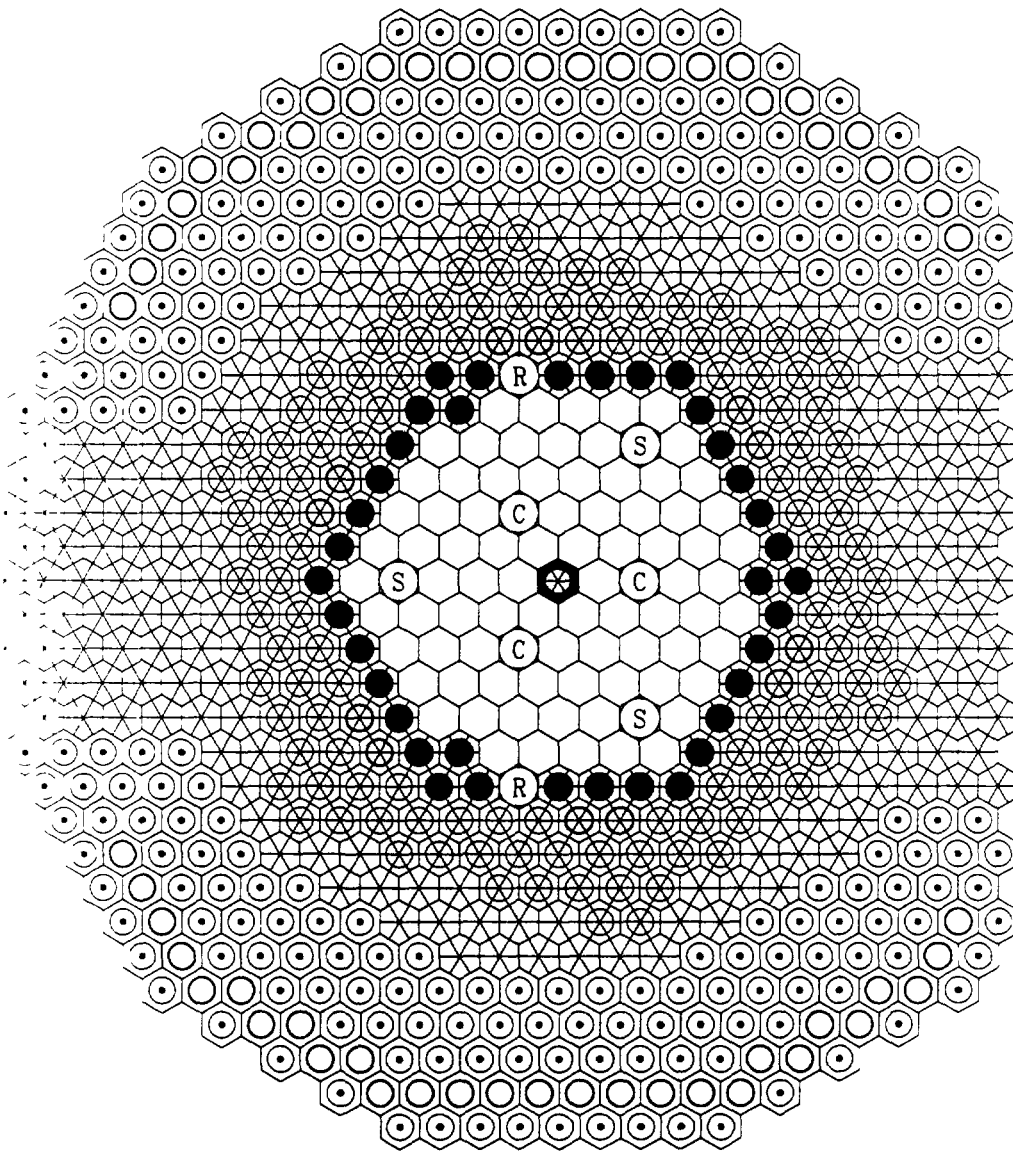
that natural convection in the three decay heat removal systems, of which the Na-Na heat exchangers are situated in the main sodium vessel, is possible even in an accident involving leakage of the main vessel.

Argon gas from an auxiliary argon circuit covers the sodium surface to prevent any contact with air. The sodium contained in the primary vessel is operated at a pressure slightly higher than atmospheric. The "hot" and "cold sodium" pools are separated by an inner vessel. An upper core structure is suspended from the small rotating plug and contains control rod guide ducts and thermocouples.

Main heat transport systems: The primary circuit consists of two primary pumps and four intermediate heat exchangers. There are two secondary sodium circuits and two tertiary water-steam circuits, but only one turbo-generator. The main features of the heat transfer system are shown in Fig. 9.74. Sodium from the primary pumps enters the core at 360°C, flowing upwards, and leaves the core at 530°C to pass to the intermediate heat exchangers. Allowing for other cooling requirements apart from the core the nominal flow rate of each pump is 713 t/h. The secondary sodium is heated from 310°C to 495°C in the tube side of the intermediate heat exchangers. It passes to the superheaters and then to the evaporators. These produce 95.44 t/h of steam at 480°C and 10.0 MPa which passes to the turbine at 470°C and 8.82 MPa. Normally CEFR-25 will be operating as an experimental reactor rather than a nuclear power station, so 80% of the thermal power can be dumped to the condenser. It is also intended to test its load following properties.

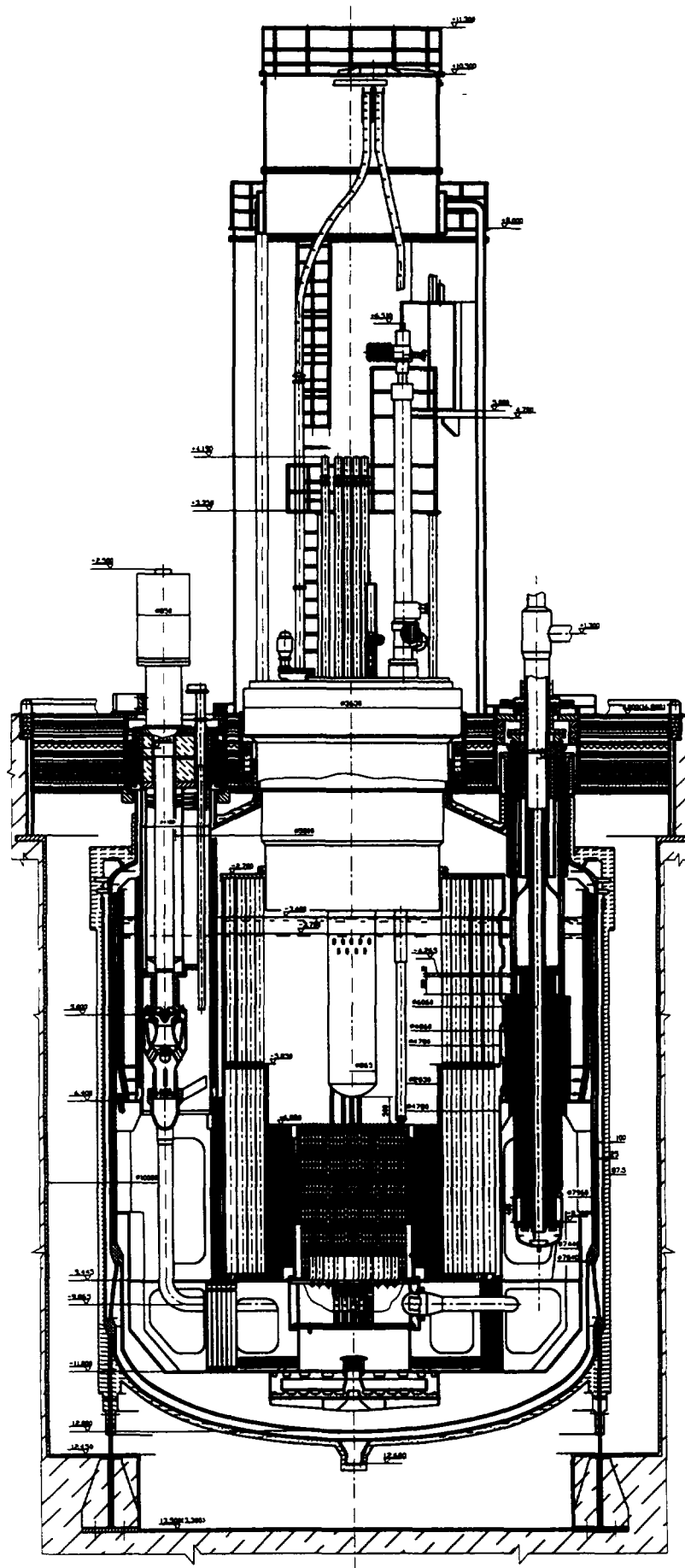
Fuel handling systems: In the conceptual design, double rotating plugs with a straight lift fuel handling machine are selected for in-core loading and unloading operations. At each refuelling, after about 3 days shutdown and cooling, spent fuel subassemblies at about 2~3 kW residual power will be moved from the core to the one of the primary storage positions. After 6 months' decay they will be transferred through a fixed port in the reactor roof to a fuel handling cell by the in-core handling machine and a fuel transfer machine. They will then be moved to a washing station by a rotating drum. After washing and inspection they will be put in a water storage pool. After inspection new fuel subassemblies will be transferred by the drum, preheated by hot argon gas to about 200°C, and moved into the core in the reverse direction by the fuel transfer machine and the in-core handling machine.

Auxiliary systems: The auxiliary systems of CEFR-25 include the sodium purification systems and the primary and secondary argon cover gas systems. The primary sodium purification system is composed of an electro-magnetic pump, two cold traps (one as standby), an economizer, and plugging meter, filter, storage tank and valves, is located in a shielded cell.



	Fuel subassembly	81
	Stainless steel rod	1
	Stainless steel reflector subassembly	37
	Stainless steel reflector rod 1	132
	Stainless steel reflector rod 2	167
	Shielding subassembly	230
	Storage position for spent fuel subassembly	56
	Safety subassembly	3
	Regulation subassembly	2
	Compensation subassembly	3

FIG. 9.72. CEFR-25 Core



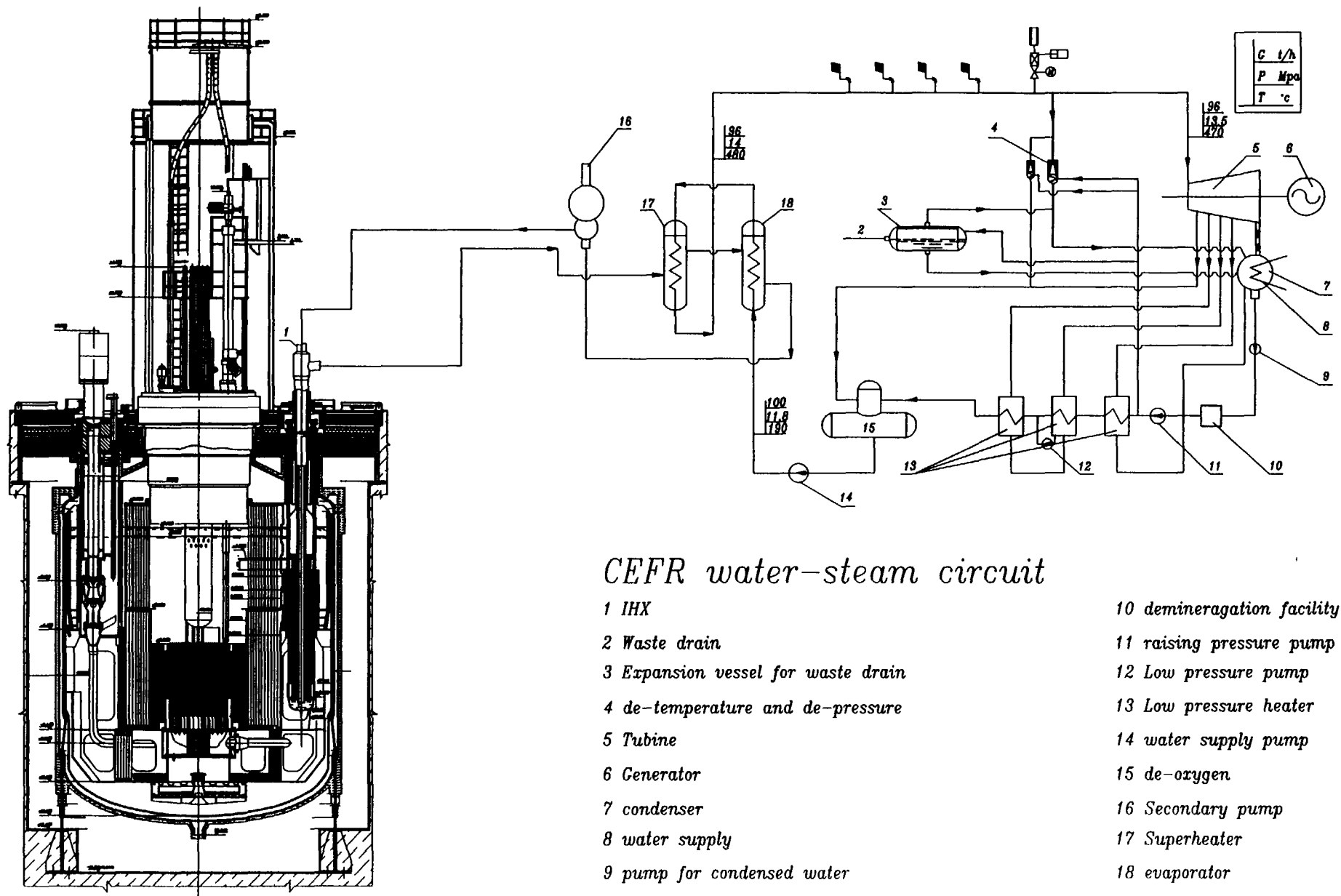


FIG. 9.74. Water-steam circuit of CEFR

The system is connected to the primary circuit by pipes and can be isolated by two stop valves. With this system the primary sodium can be kept below following impurity concentrations: oxygen 10 ppm, hydrogen 0.5 ppm and carbon 20 ppm. The primary cover gas system serves as an isolation between the atmosphere and the sodium, and as a buffer for the reactor vessel, reactor roof and mechanism seals. The system is composed of a vapour trap, filters, decay tank, cesium trap, and compressor. The sodium purification and argon cover gas systems for the secondary sodium are similar to those for the primary sodium, but there is no cesium trap in the purification system or decay tank in the cover gas system.

There is a sodium supply system which will purify the commercial grade sodium to reactor grade, the specification of which is as follows:

0 < 30 ppm, C < 30 ppm, B < 5 ppm, Cd < 5 ppm
Halogen < 30 ppm, Ca < 10 ppm, Li < 10 ppm
K < 200 ~ 1000 ppm.

The sodium supply system consists of an electro-magnetic pump with a flow rate of 8 m³/h, a cold trap and a storage tank.

Parameters: The main design parameters of CEFR-25 are summarized in Table 9.13.

9.9.5. Site work

The CEFR-25 will be located at the boundary of the China Institute of Atomic Energy, 40 km from Beijing City. In accordance with the code on the safety of nuclear power plant siting issued by the China National Nuclear Safety administration, detailed exploration of the site, including geology, earthquakes, meteorology, hydrological characteristics, and topographic features, has been completed. Important data concerning external events, such as floods, water waves, tornados, tropical cyclones, aircraft crashed, chemical explosions etc.,

TABLE 9.13.: CEFR-25 MAIN PARAMETERS

Thermal power	MW	65.5
Electric power (turbogenerator)	MW	25
Electric power, net	MW	20
Reactor type	pool, sodium coolant	
Fuel	(Pu,U)O ₂	
loading Pu total	kg	121.6
Pu-239	kg	93.2
U-235	kg	97.6
Enrichment, U-235	%	30
Linear power, max.	kW/m	43
Burn-up, max.	MWD/t	50,000
Outlet/inlet temp. of the core	°C	530/360
No of fuel subassemblies		82
No of fuel pins per S.A.		61
Steam temp.	°C	480
Steam pressure	MPa	10.0

* First loading - UO₂ with 257 kg of U-235 at 60.5% enrichment

have been collected. After detailed analysis by the National Earthquake Administration, a safe operation earthquake dynamic parameter of 0.107g (SL1) and a safe shutdown earthquake dynamic parameter of 0.214 (SL2) have been set and approved by the National Earthquake Intensity Evaluation Committee.

The site work has shown that the site would be suitable for this experimental reactor.

9.9.6. Nuclear licensing system in China

The China National Nuclear Safety Administration (CNNSA) was established in October 1984. It is an independent governmental organization functioning under the State Council through the State Science and Technology Commission, and is responsible for surveillance and control of nuclear safety matters for all civilian nuclear installations and nuclear materials in China.

Safety reviews and safety inspections are implemented step by step. There are five phases; siting, construction, commissioning, operation and decommissioning; covering the whole life of a nuclear installation. Five kinds of licences with defined requirements and conditions relate to the five phases; site approval, construction permit, fuel loading approval, operation licence and decommissioning approval. The CNNS also issues operator licences to the key operators of nuclear installations. Apart from above procedure, as a national project, nuclear or non-nuclear, it has to be approved by the State planning Commission (SPC). Before approval is given the environment impact of the project has to be reviewed and approved by the China National Environment and Protection Administration and the Local Environment and Protection Administration. It is certain that CEFR-25 is and will be obeying each step of all the licensing procedures currently in force in China, and adopting the nuclear safety and environment codes, regulations and standards issued by the appropriate administrations.

9.9.7. Safety features

Great attention has been paid to the safety features of the reactor. There are two independent shut down systems. Each can bring the reactor to cold shutdown, even if the rod with maximum reactivity worth in the system is stuck. The two systems together can reach a shut down reactivity of -6.71% Dk/k according to the design. In addition the reactor will have a strong negative reactivity feedback from sodium density, the Doppler effect, expansion and core deformation, so it would shut itself down independently of the active shutdown systems in any credible transient incident. In normal circumstances the residual heat will be rejected by the main heat transport system with the pumps at low speed. In accidents such as loss of off-site power or failure of the emergency power or main heat transport systems, the residual heat will be dispersed by one of the three decay heat removal systems, consisting of Na-Na heat exchangers immersed in the main sodium vessel and Na-air coolers with high stacks, working by natural convection and circulation. There is a very large quantity of sodium in the main vessel in relation to the reactor power, so CEFR-25 has a large thermal inertia which contributes strongly to the inherent safety properties of the reactor. Concerning radiological safety, the guard vessel is designed to protect against sodium leakage from the primary system, and the whole primary vessel is contained in a reinforced concrete pit with a leaktight steel liner. A leaktight steel dome will cover the reactor top to protect the parts susceptible to leakage.

A cylindrical concrete containment about 30m in diameter will be the last barrier against radioactive leakage to the environment. The parts of the primary or secondary sodium pipes within the containment are all provided with a leaktight jacket to avoid the possibility of a sodium fire. The cells and chambers containing radioactive sodium are all shielded and gastight, and protected by steel liners. Thus it is envisaged that the safety properties of CEFR-25 will be acceptable and the impact on the environment will be negligible.

CEFR-25 is still in the design phase, so some systems, structures and parameters may be changed in the future. But the main technical choices and designs, especially the safety features will be retained.

BIBLIOGRAPHY

Mitenkov, F.M., et al., BN-1600 Reactor Plant Main Decisions and Characteristics, Int. Conf. on Fast Reactors and Related Fuel Cycles, FR'91, Oct. 28 - Nov. 1, 1991, Kyoto, Japan.

Vasilyev, V.A., et al., Heterogeneous Modular Core of BN-1600 Reactor, Ibid.

Kirushin, A.I., et al., Concept Development of BN-1600 Reactor Core, 4-th Annual Scientific & Technical Conf. of the Nuclear Society "Nuclear Energy and Human Safety, NE-93", 28 June - July 2, 1993, Nizhny Novgorod, Russia (in Russian).

Kirushin, A.I., et.al., Safety Concept for BN-1600M Reactor Plant, (in Russian). Ibid.

Usynin, G.B., et al., Study of Processes Occuring in Case of FEs Overheating Using Their Models, Sv. Atomnaya Energia, 61(5), 1986, p. 347 (in Russian).

Usynin, G.B., et al., Estimation of Pressure Impulse at Corium-Coolant Interaction in Fuel Assembly, Sov. Atomnaya Energia, 67(6), 1989, p. 378 (in Russian).

Usynin, G.B., et al., Study of Fuel Rods Melting on Simulators with Fuel Composition, Sov. Atomnaya Energia, 70(2), 1991, p. 108 (in Russian).

Bagdasarov, Yu. E., et al., BN-800 Reactor is a New Phase in Development of Fast Nuclear Reactors, Int. Symp. on Fast Breeder Reactors - Experience and Future Trends, Lyons, France, July 22-26, 1985, IAEA-SM-284/41.

Mitenkov, F.M. and Kirushin, A.I., Advanced Commercial Fast Reactor, Int. Conf. on Design and Safety of Advanced Nuclear Power Plants (ANP'92), Oct. 25-29, 1992 Tokyo, Japan.

Kirushin, A.I., et al., BN-600M - Fast Reactor Plant of New Generation, 4-th Annual Scientific & Technical Conf. of the Nuclear Society "Nuclear Energy and Human Safety, NE-93", 28 June - 2 July, 1993, Nizhny Novgorod, Russia (in Russian).

Sinelnik, S.I., et al., Enhanced Safety Power Units for NPP with Fast Reactors, Bulletin of Public Information Center on Nuclear Power, pp. 24-31, Moscow, 1993.

Kirushin, A.I., et al., Enhanced Safety Nuclear Power Units with BMN-170 Fast Modular Reactor, Scientific-Technical Conf. "Nuclear Power in the Republic of Kazkhstan" Concept of Development, Substantiation, Safety", Semipalatinsk, Sept., 1993.

Serpante, J.P. et.al., The EFR Primary System Design; Advances and Improvements. Proc. Int. Conference on Fast Reactor and Related Fuel Cycles, Kyoto, Japan, 28 October - 1 November 1991.

Manget, C., Girloy, J., Advanced Steam Generator for EFR. Ibid.

Balz, W., Chazzat, J.C., Perspectives for Fast Reactors in the European Community. Ibid.

Hennies, H.H., Development of Fast Reactor in Europe. Ibid.

Clamand, D., et al., Assessment of the Physics of Shielding for EFR. Ibid.

Rosen, S., Weber, C.E., The ALMR as a Future Energy Source for the United States. Proc. Int. Conference and Fast Reactor and Related Fuel Cycles, Kyoto, Japan, 28 October - 1 November, 1991.

Gluekler, E.L., Quinn, J.E., Advanced Liquid Metal Reactor (LMR) R&D Program - Focus on Innovation. Ibid

Inagaki, T., et al., Development of the Demonstration Fast Breeder Reactor in Japan. Proc. Int. Conference on Future Nuclear Systems (Global '97). Pacifico Yokohama, Yokohama, Japan, 5-10 October, 1997.

Nakagawa, H., et al., Design Studies and R&D Activities for DFBR Evaluation. Proc. Int. Conference on Fast Reactor and Related Fuel Cycles. Kyoto, Japan, 28 October - 1 November, 1991.

Miuro, M., Present Status of the DFBR Conceptual Design Studies. Ibid.

Kondo, S., Design Trends and Major Technical Issues of Advanced Non-water-cooled Nuclear Reactors. Proc. Series of an IAEA Symposium on Advanced Nuclear Power Systems: Design, Technology, Safety and Strategies for their Development, Seoul, 18-22 October 1993. IAEA, Vienna, 1994.

Xu, M., Chinese FBR Programme and its First FR Conceptual Design. Proc. Int. Conference on Fast Reactor and Related Fuel Cycles. Kyoto, Japan, 28 October - 1 November 1991.

Dayuan, M., The Role of FBR in Nuclear Energy Development of China. Ibid.

International Atomic Energy Agency publications:

Status of National Programmes of Fast Reactors
IAEA-TECDOC-741, 1994

Status of Liquid Metal Fast Reactor Development
IAEA-TECDOC-791, 1995

Progress in Liquid Metal Fast Reactor Technology
IAEA-TECDOC-876, 1996

Advances in Fast Reactor Technology
IAEA-TECDOC-1015, 1998

Conceptual Designs of Advanced Fast Reactor
IAEA-TECDOC-907, 1996

Fast Reactor Fuel Failures and Steam Generator Leaks: Transient and Accident Analysis Approaches
IAEA-TECDOC-908, 1996

Chapter 10

SUMMARY AND FUTURE TRENDS

10.1. INTRODUCTION

In the period since 1985 the prospects for the development of fast reactors have changed substantially. The change can easily be illustrated by reference to the corresponding chapter to this in the 1985 Status Report. There are two outstanding differences. Firstly the 1985 chapter refers throughout to "LMFBR" development making no reference to the use of fast reactors other than as breeders. Secondly it expects accelerating development, speaking of "Designing, building and commissioning about three or four large commercial-size plants within the already-established European co-operation and in the USSR by the year 2000, and somewhat later in Japan and the USA."

By now the situation has changed in several respects. The purpose of fast reactors and their place in the totality of the exploitation of nuclear power has changed as more possibilities for their use become potentially attractive. As the nuclear industry has become more mature fast reactors are seen more and more as one component in a varied and flexible energy industry embracing the whole fuel cycle from extraction to waste disposal, with overall objectives of safety, environmental impact and cost. Fast reactors are likely to fulfil several roles in this emerging structure.

For economical and political reasons the pace of development has reduced in Europe and the USA. The 1985 Status Report speaks of liquid fossil energy reserves being depleted "sometime early in the twenty-first century". This is no longer accurate: the fossil fuel shortage is unlikely before the second quarter of the approaching century, and development timescales have lengthened accordingly.

The 1985 Report devotes only 3 pages to Indian fast reactors and 10 to those of Japan. The contrast with the present report illustrates another change of major importance in the decade: the increasing role of Asian countries in fast reactor development. In 1985 there was no mention of China or the Republic of Korea. By now it has become clear that these and other Asian countries where rapid economic growth is planned for will play a very large role in the future.

The following paragraphs summarise the likely developments, as far as they can be foreseen, to be expected in the next decade.

10.2. TECHNOLOGY TRENDS

10.2.1. Fast reactors as burners of plutonium

There is no change in the view that the ultimate role of fast reactors is to make available the very large reserves of U-238 and other fertile isotopes, and by means of the breeding process to turn them into fissile isotopes such as Pu-239 and then fission them to generate useful energy in the form of heat. However in the medium term, before the breeding role is economically demanding, fast reactors have other purposes. One of these is to consume plutonium.

At present there are large stocks of plutonium in several countries. These have arisen from two sources. Firstly commercial thermal power reactors have produced large amounts of plutonium. In some countries this plutonium lies in the unprocessed fuel in spent fuel stores: in others, where the spent fuel has been reprocessed, it has been separated and stored. Secondly significant quantities of plutonium have been released by the decommissioning of nuclear weapons. The relaxation of the "cold war" in the last decade has seen a substantial reduction in the stockpiles of nuclear warheads held by nuclear weapons states, particularly the USA and the former USSR. The fissile material from these warheads is now also in store.

As explained in Chapter 1 plutonium stocks from both these sources are seen in some quarters as constituting a danger, because they could in principle give rise to further proliferation of weapons. It is felt that as long as the plutonium is present there is a danger that it could be used for military purposes again, either, in the event of some future political catastrophe, by governmental agencies, or illicitly by terrorist or criminal groups.

At present this possibility is guarded against quite adequately by keeping plutonium, especially when it is chemically separated from irradiated fuel, under high security, but this is costly. An alternative is to use it as a nuclear fuel, and this may be attractive in both economic and political terms. Plutonium is nowhere as well protected as when it is in the core of a reactor.

Plutonium can be used as a fuel in thermal reactors, and in some countries this is being done. Mixed UO_2/PuO_2 fuel ("MOX") is commonly used in some PWR power reactors. However there are limits to the extent to which plutonium can be recycled in this way. Firstly in most existing PWR reactors the amount of MOX fuel which can be incorporated in the core is limited, typically to about 30%. At higher MOX loadings the effectiveness of the control rods would be unacceptably reduced, and the negative temperature coefficient of reactivity would be reduced by the effect of the fission resonance in Pu-239 at 0.3 eV. Secondly there is a limit to the number of times plutonium can be recycled in and LWR because of the build-up of Pu-240 and higher isotopes, which makes the coolant void coefficient of reactivity more positive. Thus although the amount of plutonium in store can be reduced by recycle in thermal reactors the overall effect on the total inventory is small and it cannot be destroyed entirely.

In a fast reactor, on the other hand, the greater reactivity allows these limitations to be avoided. In principle plutonium can be recycled indefinitely and the overall inventory can be reduced to a low level. For this reason there is interest in fast "burner" reactors (as opposed to "breeders") in several countries.

The activities undertaken so far have served to indicate the great flexibility of fast reactors, which can be used either to consume plutonium or to generate it, and can utilise plutonium with a wide range of isotopic composition, from weapons-grade material which is high in Pu-239 to plutonium which has been recycled several times in thermal or fast reactors and contains more than 50% of the non-fissile isotopes Pu-240 and Pu-242. During the next decade further work to optimise the performance of burner reactors can be expected. Some of the outstanding questions are as follows.

The core of a fast burner reactor inevitably has a low, or possibly zero, uranium content compared with a breeder. As a result the reactivity parameters, notably the Doppler coefficient and the sodium void reactivity, are different. However the reduction or

elimination of the uranium content provides the opportunity to incorporate new materials, such as moderators or absorbers, in its place, and these can be used to influence the reactivity parameters. There is therefore scope to optimise the composition to give acceptable performance in normal operation and accident conditions.

When internal breeding in the core is suppressed the change in reactivity with burnup is increased. Either the worth of the control absorbers has to be increased to compensate, the refuelling interval has to be decreased, or burnable poisons have to be used. A balance giving operational flexibility, adequate safety margins and acceptable costs has to be found.

Mixed oxide fuel becomes insoluble in nitric acid if the plutonium content exceeds about 45%. This places a lower bound on the uranium content, and therefore an upper bound on the net plutonium consumption rate of about 75 kg per TWh of electricity produced, if the fuel is to be oxide and is to be reprocessed by the Purex route. It remains to be determined whether the advantages of higher plutonium consumption, towards the theoretical maximum of about 110 kg per TWh, are sufficient to make alternative fuels, such as nitride, or alternative reprocessing routes attractive.

In addition to these theoretical questions experimental investigations will be needed. The performance of mixed-oxide fuel with plutonium contents up to 45% under irradiation to high burnup will have to be determined. Reactor physics calculation methods suitable for burner cores will have to be validated by comparison with data from critical assemblies. There may also be a need for experimental work on the thermal hydraulic performance of heterogeneous cores containing both fuel and diluent material.

The CAPRA ("Consommation Accrue de Plutonium dans les reacteurs Rapides") project in Western Europe is aimed at the utilisation of plutonium stocks arising from the operation of commercial thermal reactors. The project was initiated by the French CEA and several research laboratories and design companies are co-operating in the studies, in particular in the UK, Germany and Switzerland. There are also close links with related research projects in Japan and Russia.

The project has established that a dilute EFR core using 45 % MOX fuel and consuming around 70 kg of Pu per TWh of electricity generated appears to be entirely feasible, subject to the practical demonstration of the performance of the fuel and its ability to reach high burnup, preferably in excess of 20 %.

The reduced fuel content of the dilute core is achieved in the following ways.

- The fuel pellets have a large central hole to reduce the fuel "smear" density.
- Each subassembly contains a large number of small diameter pins about 2/3 of which contain fuel and the remaining 1/3 an inert material. These latter pins allow the reactor to be converted into a breeder if required.
- About 15 % of the core subassemblies are diluents containing no fuel at all. By interchanging diluent subassemblies containing neutron absorbers or transparent materials flexibility in controlling reactivity is provided.

In an alternative "poisoning" approach an absorber, such as B_4C , is introduced in the diluent subassemblies. However, the reactivity coefficients and reactivity control are less favourable.

The diluent pins and subassemblies provide potential sites for minor actinide transmutation.

The feasibility of fabricating fuel using the traditional methods of powder metallurgy, blending the UO_2 and PuO_2 , milling, pressing and sintering has been demonstrated up to 65 % Pu. The chemical and physical properties are similar to those of the classical MOX fuel with enrichment up to 30 % Pu. Care has to be taken to avoid pellet cracking. Dissolution in nitric acid is thermodynamically possible up to 55 % Pu but above 50 % Pu it is very slow. The conclusion is that 45 % Pu fuel is likely to be satisfactory for Purex reprocessing, with some margin above this value.

10.2.2. Fast reactors as incinerators of nuclear waste

Another role which fast reactors may be called upon to fulfil is that of waste reduction. Long-lived radioactive materials are produced by the operation of reactors of all types and, with the exception of the few that have commercial applications, have to be treated as waste. The most intensely radioactive are the "high-level wastes" (HLW) from irradiated fuel - either the spent fuel itself if it is not reprocessed, or the waste streams from the reprocessing plant. The main contributors to the high radioactivity are the fission products and the isotopes of elements beyond uranium in the periodic table (apart from plutonium). The latter are often referred to as "minor actinides" (MAs). The long-lived fission products and minor actinides set severe demands on the arrangements for safe waste disposal, in that it is necessary to ensure that they are kept isolated until they have decayed to activity levels at which they pose no danger to the health of people and other living organisms. In some cases this requires secure containment for many millennia.

By 2010 it is estimated that there will be more than 300,000 tons of spent fuel, including 3,000 tons of plutonium and of the order of 100 tons of Np-237 and of americium (the amounts depending on the decay times). There will also be about 250 tons of Tc-99, 90 tons of Cs-135 and 60 tons of I-129.

In most countries the policy is to construct waste repositories, which will ensure the adequate protection of the environment for the foreseeable future, but in some quarters the opinion that it is not right to impose on future generations the obligation to care for the waste products of the present day is gaining in influence. If it is eventually decided that it would be better to destroy (or "incinerate") the HLW rather than store it fast reactors will play an important part.

MA isotopes can be transmuted more efficiently in fast reactors than thermal because most have a lower ratio of capture to fission for fast neutrons. However, for the efficient transmutation of fission product isotopes a soft spectrum is required, so moderating assemblies situated around the core of a fast reactor are favoured.

The materials of greatest importance are the long-lived isotopes of neptunium, americium and curium, Np-237, Am-241, Am-243, Cm-242 and Cm-244. Neptunium can be

eliminated by recycling it with the plutonium. In fact, Np-237 is a good burnable poison, and including 2.5 % of it in the fuel of a fast reactor has only small effects on the Doppler coefficient and the sodium void reactivity. In the reprocessing plant it would not be separated but would pass out in the plutonium stream and incorporated in mixed Np-Pu-U fuel elements.

Americium, on the other hand, has such high gamma activity that it could not be made into new fuel in the normal fabrication plant. It would have to be separated in the reprocessing plant and fabricated into separate fuel elements or "targets", which would be irradiated in the radial blanket. Studies have been made of subassemblies containing 40 % by weight of Am in the form of oxide in a matrix of Al_2O_3 . It is estimated that, if the neutron damage dose to the structural components of the subassemblies is limited to 200 dpa, 63 % of the Am can be transmuted.

The transmutation products would include a high percentage of Pu-238 and Cm-244. A limit has to be placed on the Pu-238 concentration if the irradiated targets are to be reprocessed by the Purex process because its high alpha activity degrades the reprocessing solvent.

The "SPIN" programme in France and the "OMEGA" programme in Japan are addressed to MA destruction, but so far none of the processes of separation, fabrication, or irradiation has been implemented on a commercial scale, and indeed there are significant problems, particularly in separation of americium and making it into targets for irradiation. In the next decade, therefore, it is likely that there will be extensive work on these aspects of MA destruction, and on the performance of fast reactors with a significant MA loading. This will include test irradiations of MA fuel assemblies.

The destruction of radioactive fission products is more difficult because the neutron cross-sections are lower and they cannot be fissioned. As a result even in a fast reactor there are not enough excess neutrons to destroy fission products at a greater rate than they are being produced. However it may be possible to reduce the quantities of some of the longest-lived fission products, such as I-129, Cs-135, Kr-93 and Tc-99, by irradiation in fast reactors. This would reduce the long-term demands on waste repositories. Because absorption cross sections are greater for thermal neutrons than fast the long-lived fission products are best incinerated in special moderating subassemblies placed in the radial blanket. The next decade may see irradiation testing of targets containing long-lived fission products.

An important feature of the above potential uses of fast reactors is that in all cases the reactor cannot be considered separately from the entire nuclear fuel cycle. In any future developments the technology of the fabrication and reprocessing of the fuel and the treatment of the waste will interact with that of the reactor, and the economics and environmental impact of the whole fuel cycle, not just the reactor, will determine commercial exploitation. The Japanese "Self-Consistent Nuclear Energy System" (SCNES) illustrates this approach. The objective of the SCNES is a nuclear power facility, incorporating reactors and fuel cycle plants, which consumes nothing but U-238 and emits nothing but electric power, waste heat, and useful radioactive materials. This is a vision for the middle of the next century at the earliest, but in the nearer future ideas of this type are likely to become increasingly influential.

10.2.3. Design styles

In the past the development of fast reactors has been characterised by the convergence of most but not all programmes to a single design style, that of the large oxide-fuelled reactor with a pool layout of the primary circuit typified by BN-600 and Super-Phenix. It seemed probable that the proponents of alternative styles, and in particular the use of metal fuel, small modular reactors and loop primary circuits, would eventually capitulate to the majority trend.

This now seems less likely. While the majority style is secure in Western Europe and Russia, and has been adopted in India for the PFBR, developments in Japan are firmly centred on loop reactors. Metal fuel and modular reactors have long been advocated in the USA and have now been adopted in the Republic of Korea, and in Kazakhstan the modular system is seen as having advantages. The Chinese programme is starting with a small oxide-fuelled pool reactor, but modular reactors are planned. It seems likely that there will not be any further convergence, and that in future several design styles will be available to be chosen by utilities making use of their relative advantages according to the specific circumstances.

Lead or lead-bismuth alloy can be used as alternatives to sodium as coolant. They have the advantages of higher boiling point and a coolant void reactivity which is much less positive than that of sodium, or even negative. They also lack the high gamma activity of Na-24, and as they are also inflammable in air or water a reactor cooled with Pb or Pb-Bi would not have to have an intermediate circuit between the primary coolant and the steam.

There are however significant disadvantages. During irradiation radioactive polonium Po-210 is produced by neutron capture in Bi-209 or two successive captures in Pb-208. Po-210 is alpha active. It is volatile, so that any leakage from the cover gas poses a hazard to the plant operators and the environment. In addition lead is corrosive to stainless steel, and the heavy metals can damage high-speed components such as pump impellers by erosion.

Techniques to counter these disadvantages have been developed particularly in Russia, but in spite of this work and the apparent disadvantages of sodium, the consensus in favour of sodium remains strong. This is demonstrated by the fact that in the last few years sodium has been chosen in both Korea and China, two countries in which a new departure would have been feasible without abandoning large investments. This is a significant endorsement of sodium as the best coolant, re-emphasising that its considerable advantages outweigh its drawbacks.

While oxide fuel is favoured in most countries for breeders it may not be the optimum for burners. If burning of plutonium acquires high priority nitride fuel may be needed. This is compatible with Purex reprocessing but allows much higher plutonium enrichment, and therefore burning rates, than oxide. It would probably require the use of nitrogen enriched in N-15, to avoid the production of C-14 (an unwanted radioactive waste product) by the (n,p) reaction in N-14. This in turn may require a modification of the reprocessing route to avoid loss of N-15.

The use of nitride allows the possibility of pure plutonium fuel without uranium diluent. The thermal rating of such fuel would be very high, which means either that some other diluent material must be found, or the design of the fuel elements must be altered radically. Whichever direction is chosen the design will be different from the familiar pins

with diameters in the range 5 - 7 mm. typical of oxide fuel, and the subassembly design may also be changed.

10.2.4. Safety

There has always been a trend to improve the safety of nuclear reactors, and this has been intensified by the accident at Chernobyl. Fast reactors will undoubtedly be subject to continuing efforts to make them safer, even though it has been demonstrated that they are quite well able to meet contemporary safety standards (see Chapter 1 above).

There are two features of contemporary fast reactors which have attracted particular attention on the grounds of safety: core disruptive accidents (CDAs) caused by positive reactivity transients which may be exacerbated by the fact that coolant void coefficient of reactivity is under some circumstances positive (if the coolant is sodium); and sodium fires. There is no doubt that there will be continuing work during the coming decade to improve safety in both of these areas.

Since the earliest days of fast reactors there have never been any accidents in which the positive reactivity change caused by loss of sodium from the centre region of the core has been a contributing factor. There have, however, been minor unexplained reactivity changes, notably in Phenix, which serve as reminders that the possibility of a reactivity accident must always be guarded against. The contribution of the positive coolant void reactivity effect to the Chernobyl accident has reinforced this concern. As a result there have been several attempts to design a reactor core in which the sodium void reactivity is either considerably reduced or if possible made negative.

One approach to this problem is to provide a volume of sodium, or plenum, immediately above the core. This has the effect that, in the event of an accident in which the sodium is overheated, boiling in the core generates vapour which expands rapidly and voids not only the core where it causes a positive reactivity change, but also the plenum where it causes a negative change so that the overall change is less positive or even negative. This approach has been adopted in the BN-600M and BN-1600M designs.

Another way to reduce the sodium void reactivity is to increase the neutron leakage by reducing the height of the core or by incorporating a layer of neutron absorbing material (which may be fertile) at the core mid-plane. In the past this has been seen as disadvantageous because it tends to reduce the breeding ratio. However, now that breeding is for the time being less important (or in the case of burner reactors actually a disadvantage) this approach is more attractive. To reduce the void reactivity the BN-1600M design has a flattened or "pancake" core in which the ratio of core diameter to height is 5.7. In the EFR design, of comparable power, this ratio is 4.1.

It is not universally accepted that a negative sodium void reactivity is necessary. Provided the Doppler effect gives adequate reliable prompt negative feedback, it is held that the reactor can meet all necessary safety criteria even with a positive void reactivity. There will probably be further developments in this area in the coming decade.

Even if the problem of positive void reactivity could be eliminated there would remain the fact that the reactivity of the core can in principle be increased by rearranging the materials in a compact form. As a result in the event of a CDA in which the structure of the

core is destroyed it is difficult to prove that a prompt-critical excursion, caused by motion of the core materials after the initiating event is over, is completely impossible. This possibility is known as "recriticality". Particularly in Japan there is a continuing search for a reliable means of preventing recriticality by ensuring that, in the event of a CDA, a route is available for the core material to be relocated into a safe configuration. Such a system would provide a degree of absolute safety and remove a feature of fast reactors which, in spite of technical arguments to the contrary, continues to attract criticism.

In contrast to the absence of reactivity accidents there have been several instances of sodium fires. None of these has caused injury to personnel, but the event at the MONJU plant caused a serious interruption to reactor operation. For this reason there will undoubtedly be important efforts to reduce the incidence of sodium leaks and to improve the protection against the consequences of fires.

The number of leaks will be reduced by improvement of the design methods for sodium systems taking account of the peculiar conditions to which the materials are subject, particularly high and fluctuating secondary stresses, high-cycle fatigue, and prolonged exposure to high temperatures which can cause degradation of the properties of some austenitic steels. Improved methods of estimating stresses and improved design codes appropriate to thin-walled vessels and pipework are to be expected.

Additional protection will be afforded by improved methods of non-destructive in-service inspection to demonstrate the integrity of sodium vessels and pipework, and to detect incipient defects so that they can be repaired before they grow to cause leaks. Ultrasonic methods for inspecting welds in austenitic steels, and transition welds between steels of different composition, have been improved and further improvement can be expected. Components will increasingly be designed to facilitate in-service inspection.

In addition there will be greater acceptance of the "leak-before-break" approach to protecting against major failure and large leaks. This requires close attention to the reliable detection of small leaks at an early stage, before they can give rise to significant fires. There will also probably be developments in the field of protection against the effects of fires, by means of improved segregation and protection of essential equipment and services, faster sodium dump systems, better methods of extinguishing sodium fires, and enhanced protection from damage by sodium smoke.

10.3. THE PROGRAMME

The programme of development in Western Europe, Russia and the USA which was envisaged in the 1985 Status Report will not be met. In Western Europe the next advance foreseen in the construction of a demonstration reactor based on the EFR design starting no earlier than 2010. Such a reactor will probably incorporate the capability to burn plutonium and minor actinides.

In Russia continued operation of BN-600 will demonstrate the reliability of the system for a prolonged lifetime. This sound technology base should be exploited by the completion of BN-800, and steps to meet enhanced safety and economic objectives can be expected. In Kazakhstan a replacement for BN-350 is under consideration.

In all of these countries the principle constraint on development will be financial, both in terms of the availability of capital funds for investment, and the return to be earned from the investment. New plants will be built when there is money to build them, and money will be forthcoming when there is confidence that the return will be commercially attractive compared with other competing ventures.

In Japan the same considerations apply but a longer-term view is taken. Continued investment is to be expected on the grounds that it will pay back on a timescale of decades. The Japanese programme has suffered a delay as a result of the MONJU fire, but it is unlikely that the event will alter the long-term objectives or the commitment to fast reactors. Thus the construction of demonstration reactors is to be expected in the first decades of the next century.

The Indian programme continues to advance and in view of the energy needs of that country and the rate of economic development steady movement towards the construction of the PFBR is expected.

The arguments for the necessity of fast reactors in India apply with even more force in China, and although the Chinese are late into the fast reactor community a development programme of increasing strength is to be expected, based on the imminent construction of the CEFR.

The need for fast reactors is also great in the Republic of Korea and construction of the KALIMER modular reactor is expected in the first decade of the new century. This makes use of some aspects of the American ALMR technology.

Further significant investment in fast reactors by American utilities depends on a political change in the United States in favour of reprocessing and the commercial utilisation of plutonium. The same is true of Germany and Italy.

10.4. CONCLUSION

The technology of fast reactors, and in particular the technology of sodium coolant, has been mastered. It has taken longer than originally expected, but in retrospect this was to have been expected in view of the novelty of so many of its aspects. There are of course still developments and improvements to be made, as there are in any technology, but it has been shown conclusively that it is possible to build and operate a fast reactor power station reliably and safely. The technology is available.

It has been shown that the technology can reach acceptable safety standards. There are always opportunities to improve safety, and improvements will continue to be made. It is becoming increasingly clear that safety and economics are not incompatible: a reactor which is built and operated to high safety standards tends to be a reliable reactor which earns a good income. Fast reactors with sodium coolant have intrinsic safety advantages which already show in terms of low radiation doses to the operating staff.

Development has been slow in several countries characterised by advanced market economies, relatively slow economic growth and ready availability of fossil fuel reserves. This is due to financial reasons given more prominence by political changes such as the move to privatisation of utilities which were formerly publicly owned. On the other hand in

countries with more rapid growth and less fossil fuel development continues and in some cases is accelerating.

There is widespread agreement that fast reactor technology will eventually be needed to provide abundant energy free from pollution. The only possible alternative to breeder fission power, on a timescale of centuries, is fusion, and even the most favourable view of the prospects has to concede that there is a large chance that fusion will not be available in time to meet the energy needs, particularly of the rapidly developing nations of Asia and South America. The need for breeding on a large scale will become pressing within 50 years or so.

The development of the breeder has been delayed, but in due course, when it is economically necessary, fast reactors will almost certainly make the major contribution to the world's energy supplies. There will undoubtedly be further improvements of the technology before then, and fast reactors will be exploited as a growing component of a complex nuclear energy industry which will achieve the highest standards of safety, environmental protection, and economy.

CONTRIBUTORS TO DRAFTING AND REVIEW

Bagdasarov, Yu.	Institute of Physics and Power Engineering, Russian Federation
Broomfield, A.	AEA Technology, UK
Bhoje, S.B.	Indira Gandhi Centre for Atomic Research, India
Bramman, J.I.	AEA Technology, UK
Fink, Ph.	Centre d'Etudes de Cadarache, France
Heusener, G	Forschungszentrum Karlsruhe Technik and Umwelt, Germany
Hofmann, F.	Forschungszentrum Karlsruhe Technik and Umwelt, Germany
Horton, K.	US Department of Energy, USA
Judd, A.	British Nuclear Fuels, UK
Kamaev, A.	Institute of Physics and Power Engineering, Russian Federation
Korobejnikov, V.	Institute of Physics and Power Engineering, Russian Federation
Kiryushin, A.	OKB Mechanical Engineering, Russian Federation
Kostin, V.	OKB Mechanical Engineering, Russian Federation
Kremeser, J.	Centre d'Études de Cadarache, France
Kupitz, J.	International Atomic Energy Agency
Kusmartsev, E.	OKB Mechanical Engineering, Russian Federation
Lefevre, J.C.	FRAMATOME-NOVATOME, France
Mesnager, B.	Centrale, Super-Phénix France
Mitenkov, F.	OKB Mechanical Engineering, Russian Federation
Miura, M.	Japan Atomic Power Company, Japan
Moisset, J.-C.	Centre d'Etudes de Cadarache, France
Moreau, J.	Centre d'Etudes de Cadarache, France
Morgenstern, F.	Siemens, AG-KWU, Germany
Novinsky, E.	OKB Mechanical Engineering, Russian Federation

Pages, P.	Centre d'Etudes de Cadarache, France
Poplvasky, V.	Institute of Physics and Power Engineering, Russian Federation
Rinejski, A.	International Atomic Energy Agency
Rowlands, J.L.	AEA Technology, UK
Xu, Mi	China Atomic Energy Institute, China
Yarovitsin, V.	Institute of Physics and Power Engineering, Russian Federation
Zabudko, L.	Institute of Physics and Power Engineering, Russian Federation